

Design and Synthesis of Small Molecule Inhibitors of Zinc Metalloenzymes

A Dissertation
Presented to
The Academic Faculty

By

Vishal Patil

In Partial Fulfillment of the Requirements for the Degree
Doctor of Philosophy in Chemistry

School of Chemistry and Biochemistry
Georgia Institute of Technology, Atlanta, GA 30332
December 2011

Design and Synthesis of Small Molecule Inhibitors of Zinc Metalloenzymes

Approved by:

Dr. Adegboyega (Yomi) Oyelere, Advisor
School of Chemistry & Biochemistry
Georgia Institute of Technology

Dr. Stefan France
School of Chemistry & Biochemistry
Georgia Institute of Technology

Dr. Niren Murthy
Department of Biomedical Engineering
Georgia Institute of Technology

Dr. James Powers
School of Chemistry & Biochemistry
Georgia Institute of Technology

Dr. Laren Tolbert
School of Chemistry & Biochemistry
Georgia Institute of Technology

Date approved: August 25, 2011

Dedicated to my mother, Asha.

ACKNOWLEDGEMENTS

This acknowledgement is my sincere effort to thank those who have helped me directly and indirectly during my pursuit of doctoral degree. I owe my most sincere gratitude to my advisor, Dr. Adegboyega (Yomi) Oyelere for providing me platform to launch my scientific career. I will be forever indebted for his encouragement and support during all these years. I have immensely benefited from his talk on science, life and ethics. His mentoring will be missed in the future but his teachings will always remain with me.

I would also like to thank my committee members Dr. Stefan France, Dr. Niren Murthy, Dr. James Powers and Dr. Laren Tolbert for their valuable time and guidance to complete this thesis research. I would also like to acknowledge our collaborators Dr. Babu Tekwani, Dr. Reinhard Luhrmann, Dr. Milan Mrksich for sharing their expertise and enhance our understanding of the projects undertaken. Additionally, I want to acknowledge Dr. Chiaolong Hsiao for sharing his molecular docking expertise and augmenting my troubleshooting skills to perform computational studies.

Oyelere Research Group has grown a lot in very small time. I have been very fortunate to have good mentors, colleagues, and great friends among them. I wholeheartedly thank Dr. Bob Chen for providing me synthetic training and help during initial years of my PhD. I would also like to thank Josh Canzoneri, William Guerrant, Dr. Celinah Mwakwari, Quoavi Sodji, Arren Washington, Imani Jones, Michelle Razumov, Bryan Moskowitz, Daniel Yao, Rebecca Hood, Dr. Subhasish Tapadar for their friendship and help during all these years. Special thanks to Berkley Gryder for his time to help me with scientific writings and discussions. I would like to remember

contributions from late Derek Benicewicz. He was always there to help and contributed immensely to the lab. He will always be missed. I would also like to thank my friends from Murthy lab for their friendship and assistance in lab work. Special thanks to Dr. Kousik Kundu, Dr. Madhuri Dasari, Scott Wilson, and Dr. Xinghai Ning.

Graduate student life can be daunting at times and you need someone who can listen and give you good advice. I am lucky to have great friends with whom I can always share my joy and sorrow. I will always be thankful to Satyajeet Ojha, Shreyas Athavale, Dadasaheb Patil, Prashant Chopade, Arshad Sayyad, Yogini Bhavsar, Sandip Patil, Amrendra Kumar, Dhaval Bhandari, Subodh Jagtap, Rakesh Nambiar, Manoj Agrawal, Vijay Suryawanshi, Deepak Patil for being there, encouraging me when I was down, and making me laugh.

I would like to thank my brother Prashant, sister Madhuri and my grandparents who have made my journey possible to GeorgiaTech. They all have supported me from childhood and helped me grow as a better person. Prashant stood by me all these years and importantly during my time abroad as life away from family was distressing at a time. I want to extend my special thanks to my wife Gayatri. She has been truly supportive and caring all this time. Her loving and comforting nature has made final year of PhD very bearable. I can't thank her enough for her love, support and understanding.

Last but not the least; I reserve my special thanks to my mother Asha. Her boundless love and countless sacrifices have enabled me to pursue my dreams. She has nurtured me delicately during toughest time. Her life is an inspiration to me and I will always strive to make her proud. It is to her, I dedicate this thesis.

TABLE OF CONTENTS

ACKNOWLEDGEMENT.....	iv
LIST OF TABLES.....	x
LIST OF FIGURES.....	xi
LSIT OF SYMBOLS AND ABBREVIATIONS.....	xvi
SUMMARY.....	xxii
CHAPTER 1. INTRODUCTION.....	1
1.1 Histone Deacetylases (HDACs).....	1
1.2 HDAC Isoforms and Inhibition.....	2
1.3 HDAC Inhibitors.....	7
1.4 Bifunctional Inhibitors.....	9
1.4.1 Dual -acting topoisomerase-HDAC inhibitors.....	10
1.4.2 Anthracyclines (Topoisomerase II inhibitor).....	11
1.4.3 Camptothecins (Topoisomerase I inhibitor).....	12
1.5 Stalling Spliceosome Assembly with Zinc Chelators.....	14
1.6 Novel Zinc Binding Group for HDAC Inhibition.....	17
1.7 Antileishmanial Agents.....	18
1.8 References.....	19
CHAPTER 2. SAHA-LIKE ARYLTRIAZOLYLHYDROXAMATES.....	24
2.1 Introduction.....	24
2.2 Design of SAHA-like Aryltriazolyhydroxamates.....	25
2.3 SAR Studies of Triazole-linked Simple HDAC Inhibitors.....	26

2.4 Molecular Docking Analysis.....	30
2.5 Cell Growth Inhibition Studies of Triazole-linked Simple HDACi.....	32
2.6 Conclusions.....	33
2.7 General Procedures and Experimental.....	33
2.8 References.....	53

CHAPTER 3. MOLECULAR ARCHITECTURE OF ZINC CHELATING

SPLICEOSOME ASSEMBLY INHIBITORS.....	56
3.1 Alternative Splicing.....	56
3.2 Screening of HDACi as Splicing Assembly Inhibitors.....	59
3.3 Structure-Activity Relationship (SAR) of Splicing Inhibition.....	65
3.4 Conclusion.....	74
3.5 General Procedure & Experimental.....	74
3.6 References.....	93

CHAPTER 4. DUAL ACTING HDAC – TOPOISOMERASE (TOPO) INHIBITORS.....

4.1 Introduction.....	96
4.2 HDAC – Topoisomerase (TOPO II) Inhibitors.....	98
4.2.1 Design of HDAC & Topoisomerase II Conjugates.....	99
4.2.2 Synthesis of HDAC & Topoisomerase II Conjugates.....	100
4.2.3 <i>In vitro</i> HDAC Inhibition of HDAC & Topoisomerase II Conjugates.....	103
4.2.4 Molecular Docking Analysis of HDAC & Topoisomerase II Conjugates.....	105
4.2.5 Biological Activities.....	108
4.3 Topoisomerase I (TOPO I) Inhibitors.....	109

4.3.1 Design of HDAC & Topoisomerase I Conjugates.....	110
4.3.2 Synthesis of HDAC & Topoisomerase I Conjugates.....	111
4.3.3 <i>In vitro</i> HDAC Inhibition of HDAC & Topoisomerase I Conjugates.....	112
4.3.4 <i>In vitro</i> Topo I Inhibition.....	114
4.4 Conclusion.....	116
4.5 General Procedures & Experimental.....	116
4.5.1 General Procedures.....	116
4.5.2 HDAC & Topoisomerase II Conjugates Experimental.....	118
4.5.3 HDAC & Topoisomerase I Conjugates Experimental.....	130
4.6 References.....	136
 CHAPTER 5. IDENTIFICATION OF NOVEL ZINC BINDING GROUP (ZBG) FOR HDAC INHIBITION.....	 142
5.1 Introduction.....	142
5.2 Fragment-based Approach for Identification of Novel ZBG.....	146
5.3 Design of 1 st Generation Novel ZBG in HDACi Design.....	147
5.4 Synthesis of 1 st Generation Novel HDACi.....	156
5.5 <i>In vitro</i> HDAC Inhibition of 1 st Generation HDACi.....	158
5.6 Further Molecular Docking Analysis on 1 st generation HDACi.....	161
5.7 Design of 2 nd Generation 3-HPT based HDACi.....	162
5.8 Synthesis of 2 nd generation 3-HPT based HDACi.....	163
5.9 <i>In vitro</i> HDAC Inhibition of 2 nd Generation 3-HPT based HDACi.....	165
5.10 Design of 3 rd Generation 3-HPT based HDACi.....	167
5.11 Synthesis of 3 rd Generation 3-HPT based HDACi.....	167
5.12 <i>In Vitro</i> HDAC inhibition of 3 rd Generation 3-HPT based HDACi.....	168
5.13 Molecular Docking Analysis of 3 rd Generation 3-HPT based HDACi.....	170

5.14 Conclusion.....	174
5.15 General Procedures and Experimental.....	175
5.16 References.....	223
CHAPTER 6 – LEISHMANOLYSIS (GP63) AS AN ANTI-LEISHMANIAL TARGET.....	228
6.1 Leishmaniasis.....	228
6.2 Leishmanolysin (gp63).....	231
6.3 Comparison of HDAC8 and gp63 enzyme active site.....	232
6.4 Design of 1 st Generation GP63 Inhibitors by Molecular Docking Analysis.....	233
6.5 Whole Cell Activities of 1 st Generation Antileishmanials.....	237
6.6 Structure-Activity Relationship (SAR) of antileishmanial activity of HDAC8 Selective HDACi (2 nd Generation Antileishmanials).....	241
6.7 Conclusion.....	245
6.8 References.....	245
APPENDIX A.....	247
APPENDIX B.....	286
APPENDIX C.....	322
APPENDIX D.....	349
APPENDIX E.....	353
VITA.....	455

LIST OF TABLES

Table 2-1	<i>In vitro</i> Inhibition Data for Arytriazolylhydroxamates.....	28
Table 2-2	Cell growth inhibitory data for lead compounds.....	32
Table 3-1	HDACi Library Screened for pre-mRNA Splicing Inhibition.....	60
Table 3-2	Structure activity relationship study of the splicing inhibition activities of 6-methoxynaphthalen-2-yl hydroxamates.....	71
Table 4-1	<i>In vitro</i> HDAC Inhibition.....	105
Table 4-2	<i>In vitro</i> HDAC inhibition activity of novel HDAC/Topo I inhibitors...	114
Table 5-1	3-HPT fragment activities.....	152
Table 5-2	<i>In vitro</i> HDAC inhibition of 1 st generation HDACi.....	159
Table 5-3	<i>In vitro</i> HDAC Inhibition of 2 nd Generation Compounds.....	165
Table 5-4	<i>In vitro</i> HDAC inhibition of 3 rd vGeneration 3-HPT based HDACi.....	169
Table 6-1	Preliminary Whole cell activity against the promastigote and amastigote form of <i>L. donovani</i>	239
Table 6-2	Whole cell activity against the promastigote and amastigote form of <i>L. Donovan</i> i.....	242

LIST OF FIGURES

Figure 1-1	Acetylation switch.....	2
Figure 1-2	(A) HDAC1 homology model and (B) HDAC8 crystal structure as viewed in PYMOL. Zinc ion is shown as white sphere.....	3
Figure 1-3	Mesh representation of the (A) HDAC1 homology and (B) HDAC8 tunnel-like active site viewed in PYMOL. Zinc ion is shown as white sphere.....	5
Figure 1-4	Pharmacophoric Model of HDACi. Representation of HDAC.....	6
Figure 1-5	The proposed mechanism for the deacetylation of acetylated lysine residue at HDAC active site	7
Figure 1-6	Representative Examples of HDACi a) Simple hydroxamates such as SA & SAHA; short chain fatty acids and benzamides; b) Macrocyclic HDACi.....	8
Figure 1-7	Representative Structures of Anthracycline Antibiotics.....	11
Figure 1-8	Representative topoisomerase I inhibitors.....	13
Figure 1-9	Steps involved in splicing Mechanism.....	15
Figure 1-10	Structure of SAHA and TSA.....	17
Figure 2-1	Pharmacophoric Model of HDACi.....	24
Figure 2-2	Synthesis of SAHA-like aryltriazolyldruxamate 4a-d	25
Figure 2-3	Synthesis of aryltriazolyldruxamates 7 for SAR studies.....	26
Figure 2-4	Molecular docking Analysis of 7o,7p,7u and SAHA to HDLP using Autodock 3.05 and viewed in PYMOL.....	31
Figure 3-1	Steps involved in splicing Mechanism.....	57
Figure 3-2	Structures of HDACi which stalled the spliceosome assembly at A-like complex.....	59
Figure 3-3	Effects of HDACi on Splicing Activity.....	64

Figure 3-4	Concentration dependence of splicing inhibition by hit compounds 24 , 25 and 56	64
Figure 3-5	Synthesis of 67a-67d	65
Figure 3-6	Synthesis of 71a-71d	67
Figure 3-7	Synthesis of 74a-74b	67
Figure 3-8	Synthesis of 79a-79b	69
Figure 3-9	Standard <i>in vitro</i> splicing test with radioactively labeled MINX pre-mRNA.....	70
Figure 4-1	SAHA pharmacophoric model showing proposed modification at cap group.....	98
Figure 4-2	Representative Structures of Anthracycline Antibiotics.....	99
Figure 4-3	Design of dual-acting Topo II-HDAC inhibitors.....	100
Figure 4-4	Synthesis of the SAHA-based dual-acting Topo II-HDAC inhibitor.....	102
Figure 4-5	Synthesis of the SAHA-like, triazole-based Topo II-HDACi.....	103
Figure 4-6	Docked structure of Topo II-HDACi conjugates at HDAC 1 active site.(a) Superposition of low energy conformations of 12a and 12c (b) Overlap of low energy conformations of 12c and 7	107
Figure 4-7	(a) Docked structure of compound 12a (b) Orientation of compound 12a near catalytic zinc at active site.....	107
Figure 4-8	(a) Docked structure of compound 12c (b) Orientation of compound 12c near catalytic zinc at active site.....	108
Figure 4-9	(a) Docked structure of compound 7 (b) Orientation of compound 7 near catalytic zinc at active site.....	108
Figure 4-10	Representative HDAC and Topo I inhibitors.....	110
Figure 4-11	Designed dual-acting Topo I-HDAC inhibitors.....	111
Figure 4-12	Synthesis of dual acting Topoisomerase I-HDAC inhibitors.....	112
Figure 4-13	Topoisomerase I-Induced Plasmid Relaxation Assay.....	115

Figure 5-1	Prototypical HDACi – SAHA fits into classical pharmacophoric model of HDACi.....	143
Figure 5-2	Heterocyclic aromatic ZBGs.....	145
Figure 5-3	Monodentate ZBGs.....	145
Figure 5-4	Docked fragments a) 3-hydroxy pyridin-2-thiones (3-HPT) a ; b) 3-hydroxypyridin-4-thiones b ; c) 1-hydroxypyridin-2-thione c	148
Figure 5-4	(i) HDAC1 active site (homology model); (ii) Docked fragment 3-hydroxypyridin-2-thiones (3-HPT; a) against HDAC1; (iii) Docked fragment 3-hydroxypyridin-4-thiones (b) against HDAC1; (iv) Docked fragment 1-hydroxypyridin-2-thione (c) against HDAC1.....	149
Figure 5-5	(i) HDAC8 active site (homology model); (ii) Docked fragment 3-hydroxypyridin-2-thiones (a) against HDAC8.....	150
Figure 5-6	(ii) Docked fragment 3-hydroxypyridin-4-thiones (b) against HDAC8;(iv) Docked fragment 1-hydroxypyridin-2-thione (c) against HDAC8.....	150
Figure 5-7	(a) Structure of 1-methyl-3-hydroxypyridin-2-thiones (a) Surface View of docked orientation 1-methyl-3-hydroxypyridin-2-thiones at HDAC8;(b) Amino acid residues around docked fragment within 5 Å distance.....	152
Figure 5-8	Proposed fragments for development of lead against HDAC8 Selective inhibitors.....	153
Figure 5-9	(a) Docked structure of 1 against HDAC8 (b) Docked structure of 2 against HDAC8. (c) Docked structure of 3 against HDAC8.....	154
Figure 5-10	AA residues surrounding 2 nd phenyl ring of docked compound Against HDAC8.....	155
Figure 5-11	Proposed 1 st generation compounds.....	155
Figure 5-12	Synthesis of the 3-DHP based ZBG HDACi - I.	156
Figure 5-13	Synthesis of the 3-DHP based ZBG HDACi - II.....	157
Figure 5-14	Synthesis of the 3-DHP based ZBG HDACi – III.....	157

Figure 5-15	(a) Docked structure of 12d against HDAC8 (b) Docked structure of 12d interacting with key AA residues near Zn ²⁺ active site (c) Overlap of ortho, meta and para-methyl substituted compounds...161
Figure 5-16	Synthesis of 2 nd generation 3-HPT based HDACi.....164
Figure 5-17	Design of 3 rd Generation 3-HPT-based HDACi.....167
Figure 5-18	Synthesis of 3 rd Generation HDACi.....168
Figure 5-19	(a) Docked structure of 25d against HDAC8 (b) Docked structure of 25d against HDAC8 showing key AA residues forming deep pocket around phenyl cap group.....171
Figure 5-20	(a) Overlap of docked structure of 25d and 25e ; (b) Docked structure of 25e against HDAC8 showing key AA residues forming deep pocket around phenyl cap group.....172
Figure 5-21	(a) Docked structure of 30d ; (b) Docked structure of 30d against HDAC8 showing key AA residues forming deep pocket around phenyl cap group.....173
Figure 5-22	(a) Docked structure of 12d against HDAC1. (b) Docked structure of 12d against HDAC8.....173
Figure 6-1	Leishmania life cycle.....229
Figure 6-2	Leishmania worldwide endemics.....230
Figure 6-3	The Surface of the Promastigote Form of <i>Leishmania</i> is covered With Leishmanolysin (gp63).....231
Figure 6-4	(a) Enzyme active site of HDAC8 (b) Enzyme active site of gp63.....232
Figure 6-5	GP63 crystal structure.....233
Figure 6-6.	(a) Structures of first generation molecules based on 3-hydroxypyridin-2(1H)-one skeleton. (b) Docked structures of 3-hydroxypyridin-2(1H)-one 1a and triazole-linked 3-hydroxypyridin-2-ones 2a and 3a at the active site of gp63.....235

Figure 6-7	(a) Representative structures of gp63-binding small molecules used in molecular docking analysis. Docked structures of (b) p-dimethylamino substituted biphenyl compound 6a	236
Figure 6-8	Docked structure of p-pyridinylbenzyl compound 7a a) space filling model b) Cartoon model with compound 7a making key interactions at active site.....	237

LIST OF SYMBOLS AND ABBREVIATIONS

α	alpha
β	beta
δ	delta
3-HPT	3-hydroxypyridin-2-thione
Ala	alanine
Å	angstrom
ACS	American Chemical Society
app	apparent
Arg	arginine
Asp	aspartic acid
BBr ₃	boron tribromide
br	broad
BSA	bovine serum albumin
Bn	benzyl
C	carbon
CDCl ₃	deuterated chloroform
CD ₃ OD	deuterated methanol
Cys	cysteine
°C	degrees Centigrade
CH ₂ Cl ₂	dichloromethane
CHCl ₃	chloroform

cm^{-1}	reciprocal centimeter (SI unit for wavenumber)
Cu	copper
CuI	copper (I) iodide
d	doublet
DAU	daunorubicin
dd	doublet of doublets
DIPEA	<i>N,N</i> -diisopropylethylamine (Hunig's base)
DMAP	<i>N,N</i> -dimethylaminopyridine
DMF	<i>N,N</i> -dimethylformamide
DMSO	dimethylsulfoxide
DNA	deoxyribonucleic acid
EC_{50}	half maximal effective concentration
EDCI	1-ethyl-3-(3-dimethylaminopropyl)carbodiimide
	hydrochloride
ESI	electrospray ionization
EI	electron impact ionization
Et_3N	triethylamine
EtOAc	ethyl acetate
FAB	fast-atom bombardment
g	gram
GLY	glycine
H^+	proton
h	hour

Ile	isoleucine
H ₂ O	water
HAT	histone acetyltransferase
HCl	hydrochloric acid
HDACi	histone deacetylase inhibitors
HDAC	histone deacetylase
HDLP	histone deacetylase-like protein
HIS	histidine
HOBT	hydroxylbenzyltriazole
HPLC	high performance liquid chromatography
HRMS	high resolution mass spectroscopy
Hz	hertz
IC ₅₀	half maximal inhibitory concentration
<i>J</i>	coupling constant
KBr	potassium bromide
KCN	potassium cyanide
K ₂ CO ₃	potassium carbonate
Leu	leucine
LiOH•H ₂ O	lithium hydroxide hydrate
M	molar concentration
m	multiple, multiplet
MALDI	matrix-assisted laser desorption/ionization
Me	methyl

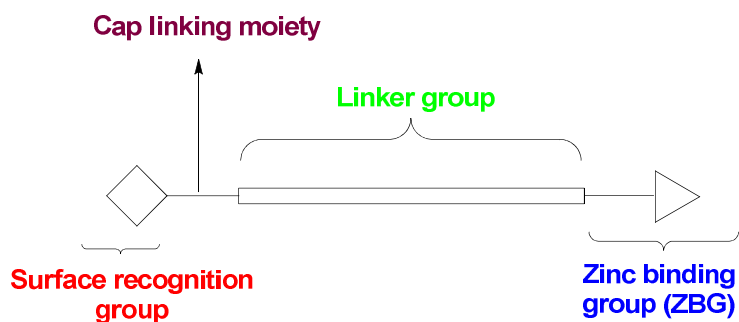
MeOH	methanol
mg	milligram
MIC	minimal inhibitory concentration
min	minutes
mL	milliliter
mmol	millimole
MS	mass spectroscopy
Ms	mesylate, mesyl
MsCl	methanesulfonyl chloride
N ₃	azide or azido
Na	sodium
NaH	sodium hydride
NaN ₃	sodium azide
NaNO ₂	sodium nitrite
NaOAc	sodium acetate
Nap	naphthalyl
NH ₄ OAc	ammonium acetate
NH ₂ OH	hydroxylamine
NH ₄ OH	ammonium hydroxide
nm	nanometer
nM	nanomolar
NMM	<i>N</i> -methylmorpholine
NMR	nuclear magnetic resonance

P ₄ S ₁₀	phosphorus pentasulfide
PEG	poly-ethylene glycol
Ph	phenyl
Phe	phenylalanine
PK	pharmacokinetic
ppm	parts per million
prep TLC	preparatory thin-layer chromatography
Pro	proline
Py	pyridyl
q	quartet
RNA	ribonucleic acid
rpm	revolution per minute
rt	room temperature
s	singlet
S	sulfur
SAHA	suberoylanilide hydroxamic acid
SAMDI	self-assembled monolayers for MALDI
SAR	structure activity-relationship
t	triplet
Thr	threonine
TBAF	tetrabutylammonium fluoride
TBTA	tris-(benzyltriazolylmethyl)amine
<i>t</i> -BuPh ₂ SiCl	tert-butyl diphenylsilyl chloride

TFA	trifluoroacetic acid
TfN ₃	triflic azide
THF	tetrahydrofuran
TIPS	triisopropylsilane
TLC	thin-layer chromatography
TMSCl	trimethylsilyl chloride
TOF	time of flight
Topo	topoisomerase
Tol	tolyl
Trp	tryptophan
TSA	trichostatin A
Tyr	tyrosine
μg	microgram
μM	micromolar
μm	micromole
UV-vis	ultraviolet-visible spectroscopy
ZBG	zinc binding group
Zn ²⁺	zinc(II) metal ion

SUMMARY

Histone deacetylases (HDACs) are a class of enzymes that play a crucial role in DNA expression by removing an acetyl group from the ϵ -N-acetyl lysine residue on histone proteins. Out of 18 isoforms of HDAC enzymes which are classified into 4 classes, only 11 of them are metalloenzymes that require zinc for its catalytic activity. HDACs are considered promising target for drug development in cancer and other parasitic diseases due to their role in gene expression. Histone deacetylase inhibitors (HDACi) can cause cell cycle arrest, and induce differentiation or apoptosis. While HDACi shows promising antitumor effects, their mechanism of action and selectivity against cancer cells have not been adequately defined yet. In addition, low oral bioavailability, short half-life time, bone marrow toxicity, and cardiotoxicity limit their use in clinic. Therefore, there is considerable interest in developing compounds with selectivity and specificity towards individual family members of HDACs. The prototypical pharmacophore for HDAC inhibitors consist of a metal-binding moiety that coordinates to the catalytic metal ion within the HDAC active site, a capping group that interacts with the residues at the entrance of the active site and a linker that appropriately positions the metal-binding moiety and capping group for interactions in the active site. It has been shown that modification of cap, cap linking moiety, linker or zinc binding group (ZBG) shows promises of superior potency and isoform selectivity. My thesis research involves manipulating different aspects of the pharmacophoric model to yield not only more potent, selective, and effective drugs but also to help understand the biology of zinc metalloenzymes such as HDAC isoforms, gp63 and spliceosome associated zinc-metalloenzymes.



Pharmacophoric Model of HDACi

In the quest of effective chemotherapy, we modified the cap group to introduce an additional anticancer drug (warhead) in the HDACi design to combat cancer effectively. As many essential enzymes are overexpressed in cancer cells, multi-targeting therapy might be more beneficial, not only to eliminate cancer cells but also to combat the emergence of drug resistance. To explore the prospect in cancer therapy of a bivalent agent that combines two complimentary chemo-active groups within a single molecular architecture, we have synthesized bifunctional HDAC - topoisomerase II (topo II) and HDAC – topoisomerase I (topo I) inhibitors. We have identified single agents that simultaneously inhibit topoisomerase and HDAC activities for the first time. Moreover, they potently inhibit the proliferation of representative cancer cell lines.

In a class of these dual acting agents, the topoisomerase inhibiting moieties were connected to the HDACi pharmacophore through a cap linking moiety. One of the most commonly employed cap linking moiety in HDACi design is the amide group. We have introduced 1,2,3-triazole as an alternative cap group linking moiety. Simple hydroxamates containing triazole linking moiety have enhanced HDACi activities. This

development simplified our compound design and facilitated facile synthesis of numerous novel and structurally diverse HDACi.

Another important biological phenomenon thought to be regulated by HDACs is the pre-mRNA splicing catalyzed by the spliceosome. We have screened our triazole based HDACi library for their effect on splicing reaction in an *in vitro* system in collaboration with Prof. Reinhard Luhrmann of the Max Planck Institute, Germany. We have indentified molecular architecture of a novel class of zinc chelating agents with splicing inhibitory activities. Interestingly however there is no correlation between HDAC and spliceosome inhibiting activities of these compounds. This result suggests that these compounds may be inhibiting the functional role of Zn-ion in splicing since only a subset of them, with well defined structure, is active.

In concluding part of my thesis research, I undertook the challenge of identifying a non-hydroxamate ZBG in HDACi design. Even though hydroxamic acids are widely used as ZBG, they suffer from many drawbacks such as poor *in vivo* stability, low oral bioavailability, generation of harmful unwanted metabolites, low isoform selectivity among others. I have explored heterocyclic aromatic functional groups as potentially more stable, less-toxic, potent alternatives to hydroxamate ZBG. Using the tools of structure-based drug design, fragment-based drug discovery and *in vitro* biological screening, I have successfully identified 3-hydroxypyridin-2-ones as novel ZBG in HDAC inhibitor design. Additionally, structure activity relationship (SAR) studies through structural optimization of linker region and surface recognition cap group have yielded small molecules with HDAC8 selectivity relative to HDAC1. These isoform selective inhibitors could be ideal chemical tools to elucidate the individual functions of each HDAC isoform. Such selective inhibitors could be critical in deciphering the roles of HDAC isoforms in cancer etiology and possibly provide

more effective chemotherapy compared to nonselective inhibitors. Molecular docking analysis revealed structural basis of selectivity and was attributed to the effective accommodation of the inhibitors at the shallow active site of HDAC8 enzyme in comparison to HDAC1. This prompted us to investigate other zinc-metalloenzymes with similar active site attributes, such as HDAC8-Leishmanolysin (gp63), a zinc metalloprotease found on cell surface of *Leishmania* species, with a shallow active site similar to HDAC8. It is well established that gp63 is essential for the degradation of host proteins and it is an attractive target for the development of anti-leishmanial chemotherapeutics. Leishmaniasis is a tropical/sub-tropical parasitic disease caused by protozoan parasites of the genus *Leishmania*. Although it affects about 2 million people per year, there is a dearth of effective treatment modalities for this fatal disease. Despite the attractiveness of gp63 as an anti-leishmanial target, there are currently no efficient, non-toxic inhibitors of gp63. Using a molecular docking analysis, I found that the 3-hydroxypyridin-2-one based HDAC8 inhibitors adopted docked poses on gp63 that were similar to those they adopted on HDAC8. Subsequent whole cell assay reveal that these compounds are potent inhibitors of the promastigote and amastigote forms of *L. donovani* with IC₅₀ comparable to Miltefosine, the only clinically approved oral drug against visceral leishmaniasis. Ongoing efforts are on identifying the intracellular target(s) that confers anti-leishmanial activity to these 3-hydroxypyridin-2-one based HDACi.

Overall, my thesis research aims at better understanding biology of zinc metalloenzymes by developing potent and selective small molecule inhibitors. This will aid in improvement of existing therapeutics for treatment of cancer, leishmania, malaria and other genetic disorders.

CHAPTER 1

INTRODUCTION

1.1 Histone Deacetylases (HDACs)

In eukaryotes, DNA is wrapped tightly around histone and non-histone proteins to form higher order structure called chromatin. Chromatin consists of basic repeating units called nucleosome which consists of approximately 146 bp of DNA tightly wrapped around histone octamers. There are two copies of each of the four core histones, H2A, H2B, and H3 and H4 in each nucleosome.¹⁻⁴ Histones are small globular proteins with more flexible and charged NH₂-terminus (histone tails) that protrudes from the nucleosome. Post-translational modifications of histones such as acetylation of lysines, methylation of lysines and arginines, phosphorylation of serines, and ubiquitination and sumoylation of lysines constitute a “histone code” that ultimately regulates gene expression by modulating the unwinding of DNA and recruitment of binding partners.^{1,2} Transcriptionally active genes associate with hyperacetylated chromatin, whereas transcriptionally silent genes associate with hypoacetylated chromatin. Chromatin acetylation is controlled by the opposite effects of two families of enzymes, histone acetyltransferases (HATs) and histone deacetylases (HDACs). HATs catalyze the addition of acetyl groups on the ϵ -amino groups of lysine residues in the amino terminal tails of core histones. HDACs remove the acetyl group from the acetylated lysines in histones (Figure 1-1).^{3,4} Increased acetylation has been correlated with increased gene expression, and decreased acetylation has been correlated with transcriptional repression.⁴ A controlled equilibrium between HAT and HDAC activity is required for

normal cell growth.¹ Aberrant HDAC function has been linked to cancer development and maintenance, which could be attributed to abnormal silencing of the expression of gene.⁴ HATs and HDACs also target non-histone protein substrates, in particular transcriptional factors such as p53, GATA-1, E2F, estrogen receptor (ER), and various cell-cycle regulatory proteins with variable functional consequences.⁵

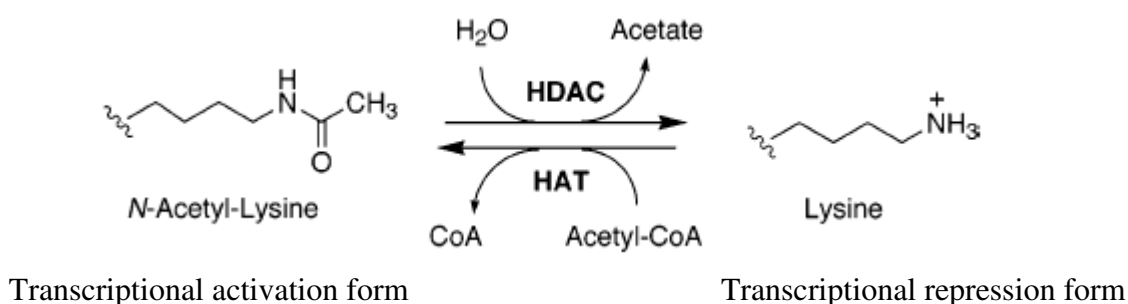


Figure 1-1. Acetylation switch^{16b}

1.2 HDAC Isoforms and Inhibition

There are four subclasses of HDACs in humans. They are classified on the basis of on their size, cellular localization, number of catalytic active sites, and homology to yeast HDAC proteins. Class I includes HDAC1, HDAC2, HDAC3, HDAC8. Class II includes HDAC4, HDAC5, HDAC6, HDAC7, HDAC9, HDAC10. Class II has been further subdivided into IIa (HDAC4, HDAC5, HDAC7, HDAC9) and IIb (HDAC6, HDAC10) because of their single and double catalytic active sites respectively. HDAC11 is the only member of class IV. Class I, II and IV operate by metal (Zn^{2+}) ion dependent mechanism. In contrast, Class III (Sirtuins) operate by NAD^+ dependent mechanism and are unrelated to other class of HDAC enzymes.^{6,10a} Class I, II and IV HDACs have been intensively scrutinized in recent years because of their role in cancer pathogenesis, as

well as several other diseases.^{4,7} Classes I and IV HDACs are primarily found in the nucleus with the exception of HDAC3 which is also found in cytoplasm in addition to nuclear localization. Class I and IV HDACs are expressed in many cell types, while the expression of class II HDACs, which are able to shuttle in and out of the nucleus, are restricted to some tissues.⁸ HDAC6 in particular is a cytoplasmic and microtubule associated enzyme.^{8c} Because of their crucial role in a plethora of biological events including gene expression, cell development, differentiation and apoptosis, various HDAC isoforms are associated with different basic cellular events and disease conditions. For example, HDAC 1, 6, and 8 are crucial for breast cancer; HDAC 1-3 are overexpressed in ovarian cancers; HDAC 1 and 3 are implicated in lung cancers, HDAC2 associated with gastric cancers; and there is possible correlation between HDAC8 overexpression and acute myeloid leukemia (AML).⁹ While different HDAC isoforms are linked to cancer formation, the exact cellular function of HDACs is still far from being completely elucidated. Particularly, the molecular mechanism connecting aberrant HDAC activity to cancer formation is not well understood.

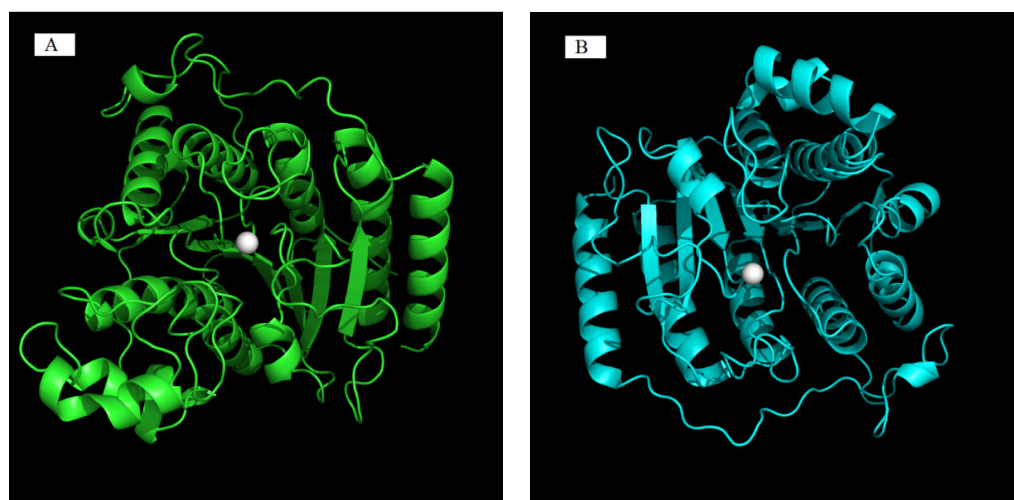


Figure 1-2. (A) HDAC1 homology model and (B) HDAC8 crystal structure as viewed in PYMOL. Zinc ion is shown as white sphere.

Structural information essential for rational design of isoform selective class I and II HDACs inhibitors is scarce. To date, only the crystal structure of HDAC-like protein (HDLP, bacterial homologue to human class I HDAC), HDAC2, HDAC7, and human HDAC8 are available (Figure 1-2).¹⁰ However, HDAC1 homology model built from human HDAC2 X-ray crystal structure with 3MAX coordinates has found useful applications in literature to understand HDAC1 enzyme structural attributes.¹¹ Overall the architecture of HDAC1 and HDAC8 active site is conserved relative to other class I and II HDACs. In HDAC1, the active site is composed of a hydrophobic tunnel approximately 14 Å deep (Figure 1-3). The amino acid residues, Pro29, Phe150, Phe205, Leu271, His178, Tyr204, Gly149, and Tyr303, formed the wall of the tunnel. The Zn²⁺ ion at the base of the tunnel is coordinated with adjacent amino acid residues (Asp176, His140, and Asp264) and water molecules to hydrolyze the acetylated lysine of the *N*-terminal tail of core histones.^{10a} In HDAC8, the only architectural difference is the replacement of leucine with methionine among the amino acid residues that constructed the wall of the active site. In addition, the HDAC8 active site adopts a different shape and is only 12 Å deep, a distinction that can be exploited in the design of isoform structure HDAC inhibitors (HDACi) (Figure 1-3).¹²

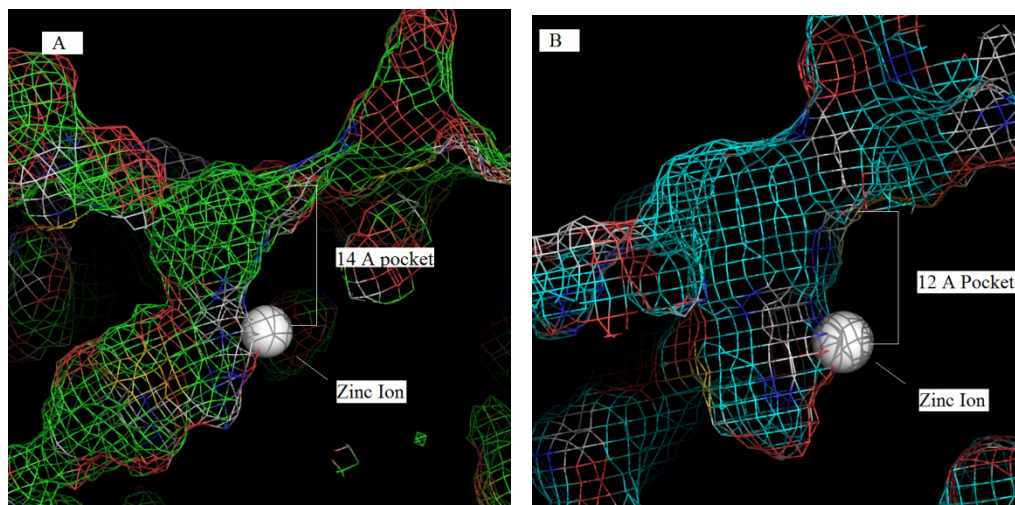


Figure 1-3. Mesh representation of the (A) HDAC1 homology and (B) HDAC8 tunnel-like active site viewed in PYMOL. Zinc ion is shown as white sphere.

HDACi generally conforms to a three-motif pharmacophoric model consisting of a zinc binding group (ZBG), a hydrophobic linker chain, and a surface recognition group (consisting of cap linking moiety and a cap group).¹³ The recognized mode of HDAC inhibition involves ZBG interaction with the catalytic zinc ion at the base of the active site while the linker efficiently positions the cap group to make interactions with amino acid residues on the surface of the enzyme.^{10a} Most HDACi chelate the active site Zn^{2+} using the hydroxamate moiety as a ZBG.^{13,14}

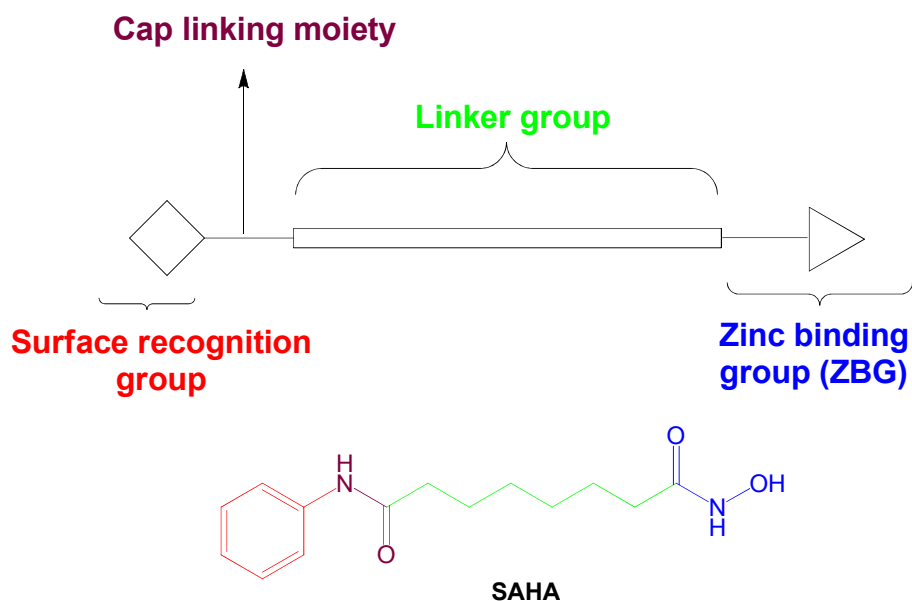


Figure 1-4: Pharmacophoric Model of HDACi. Representation of HDAC inhibitor SAHA (suberoylanilide hydroxamic acid) in pharmacophoric model.

The mechanism of action of these zinc metalloenzyme involves the removal of the acetyl group of lysine residues via charge relay system consisting of two adjacent histidine residues, two aspartate residues, and one tyrosine residue. Mechanism involves coordination of the carbonyl group of the *N*-acetyl lysine residue to the Zn^{2+} ion. The Zn^{2+} ion polarizes the carbonyl group making the carbonyl carbon more electrophilic.¹⁰ This coordination brings the acetylated lysine in close proximity with the water molecule which interacts with histidine and Zn^{2+} ions making it more nucleophilic. This leads to the hydrolysis of the carbonyl carbon to form a tetrahedral oxyanion intermediate. The intermediate is stabilized by two oxygen-zinc interactions and hydrogen bonding to the hydroxyl group of a tyrosine residue. During next step, the oxyanion restores its charges by forming a carbonyl group leading to the cleavage of the carbon nitrogen bond of the intermediate.¹⁰ The free nitrogen then accepts a proton from histidine yielding the free

lysine residue and the acetate group (Figure 1-5). Binding of HDACi often results in the displacement of the Zn^{2+} ion thereby making charge-relay system dysfunctional.¹⁰ Understanding the overall structure and mechanism of the class I and II HDACs active site has led to the development of many HDACi with few in clinical trials. In fact, HDACi have drawn much interest and research efforts have culminated in the validation of HDAC inhibition as a clinically viable approach for cancer treatment with the approval of SAHA and Romidepsin (FK-228) for the treatment of cutaneous T-cell lymphoma.¹⁵

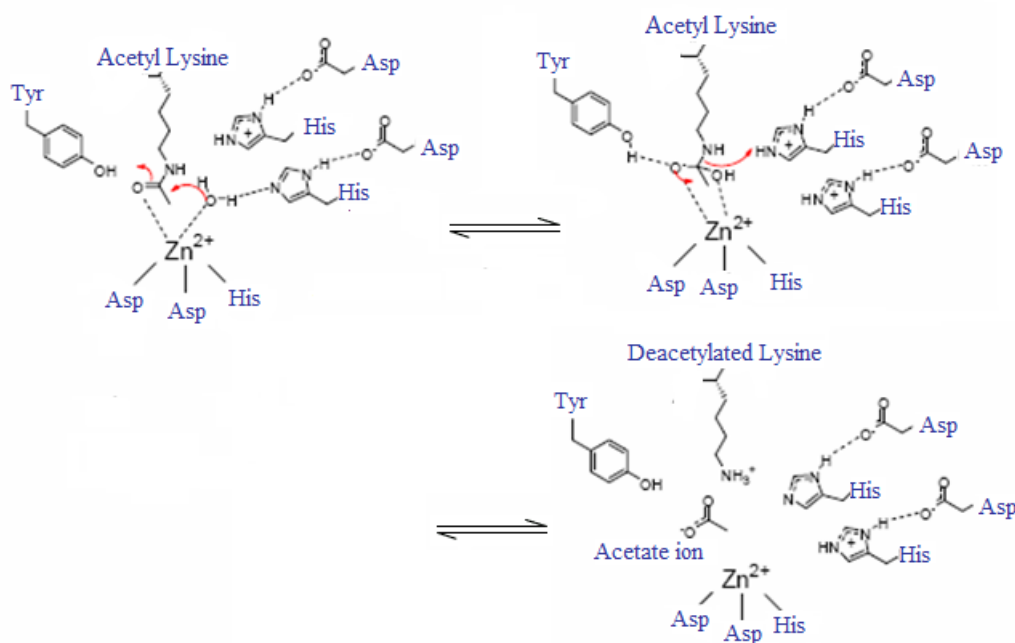


Figure 1-5. The proposed mechanism for the deacetylation of acetylated lysine residue at HDAC active site.¹⁰

1.3 HDAC Inhibitors

Inhibition of HDAC activity has emerged as a promising approach for reversing the anomalous epigenetic states associated with cancer and other chronic diseases, because of their role in fundamental cellular processes.^{1-3,7} Majority of HDACi are relatively less toxic to normal cells while broad variety of transformed cells are more

sensitive to HDACi.^{4b} HDACi show promising antitumor effects however their mechanism of action and selectivity against cancer cells have not yet been adequately defined. Most HDACi are global, non-selective inhibitors of various HDAC isoform.⁴ Their low isoform selectivity does not differentiate the relevant HDACs that regulate proliferation, apoptosis or angiogenesis.

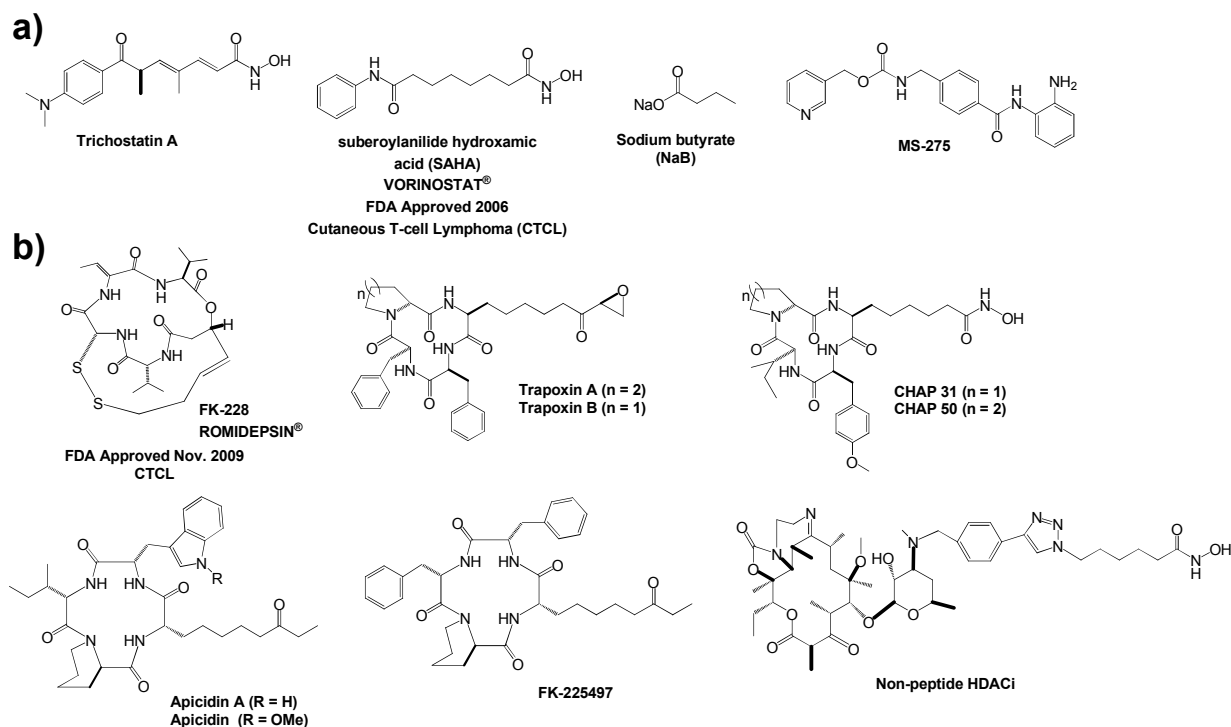


Figure 1-6: Representative Examples of HDACi a) Simple hydroxamates such as TSA & SAHA; short chain fatty acids and benzamides; b) Macrocyclic HDACi

In addition, low oral bioavailability, short half-life time, bone marrow toxicity, and cardiotoxicity are limiting the clinical use of current HDACi.^{2b} Therefore, there is considerable interest in developing compounds with selectivity towards individual family members of HDACs.

My thesis research work centers around addressing important drawbacks of current generation HDACi to generate more potent, selective drugs as well as design

novel molecules that will aid in our understanding of the biology of these important zinc metalloenzymes. Most of the current HDACi fits into pharmacophoric model depicted in Figure 1-4 which has been extensively used to design and SAR studies on existing HDACi with the goal of improving potency, selectivity, and pharmacokinetic profiles.^{13,14}

To address some of the major drawbacks that have limited the progress of current HDACi, I have worked on the HDACi pharmacophoric model in this thesis. I have designed new surface recognition groups (chapter 4), new cap linking moiety (chapter 2), investigated SAR of the linker group and identified a new ZBG compatible with HDAC inhibition (chapter 5). Some of the important outcomes of the studies disclosed in this thesis are the identification of a new class of HDAC-topo inhibitors, the introduction of 1,2,3-triazole as a new cap linking moiety and 3-hydroxypyridin-2-one as a new HDACi ZBG. Several of the HDACi disclosed in this thesis have anticancer, anti-malarial, and anti-leishmanial activity. I have also used several of these molecules as tools to probe the role of Zn-metalloenzyme in pre-mRNA splicing.

1.4 Bifunctional Inhibitors

Currently a “one drug, one target” paradigm is the dominant approach to drug discovery in pharmaceutical industry. This approach has yielded many blockbuster drugs and will continue to dominate the future drug discovery efforts. Despite this, there are lots of disease conditions which are inadequately treated. Therefore developing agents that can modulate multiple targets simultaneously with combination of drugs or bifunctional agents which can enhance efficacy could be a useful approach. Many essential enzymes are overexpressed in cancer cells and are responsible for maintenance

of the transformed state of human tumors.¹⁸ Therefore multi-targeting therapy might be more beneficial, not only to eliminate cancer cells but also to combat the emergence of drug resistance.¹⁹ Despite promising clinical reports and low toxicity, HDACi have proven difficult as a sole agent to improve the cancer chemotherapy outcome, partly due to reversible cell cycle arrest by HDACi.²⁰ Therefore, many HDACi including SAHA have been shown to increase the efficiency of several anticancer drugs that target DNA.^{21,22} However combination therapies are often scheduling dependent and often associated with dose dependant toxic side effects not seen with individual drugs.²³ Additionally, multiple drug therapy is often complicated by the inherent pharmacokinetic disadvantage of separate drugs, drug-drug interactions, and the possibility of additive toxicity. Therefore a single molecule containing a dual warhead of combination therapy could be useful. Such compounds may lead to agents that require only low doses to elicit antiproliferative activities, thereby minimizing dose dependent side effects of combination therapy. These dual acting inhibitors are expected to act across various stages of cancer cell cycle, thereby targeting larger population of cells, resulting in superior cytotoxicity.^{21,22}

1.4.1 Dual -acting topoisomerase-HDAC inhibitors

DNA topoisomerases (Topo) are essential human enzymes that alter the supercoiling of DNA. They are classified as topo I and topo II depending on whether they induce a DNA single and double strand break respectively. DNA topoisomerases aids in the transcription and replication of DNA.²³

DNAs do not exist as naked structures; they are locked up in complexes with histone proteins. Agents, such as HDAC*i*, that induce hyperacetylation of histone^{2b} proteins complexed with DNA could unlock these complexes. The unlocking of the DNA histone complexes could increase the accessibility of cellular DNA within chromatin and thus potentiate the activities of DNA targeting, Topo II- and Topo I-inhibiting anticancer agents.

1.4.2 Anthracyclines (Topoisomerase II inhibitor) –

Anthracyclines (Figure 1-7) rank among the most effective anticancer drugs and are effective against more types of cancer than any other class of chemotherapy agents. They act primarily by stabilizing the intermediate of Topo II-DNA reaction, the cleavage complex, through the formation of a ternary complex. The tetracyclic ring of anthracyclines intercalates DNA while the sugar moiety functions as a DNA minor groove binder.²⁵

The clinical use of anthracyclines is limited by the occurrence of both chronic and acute cardiotoxicity that can often lead to cardiomyopathy, myocardial infarction, and congestive heart failure.²⁶

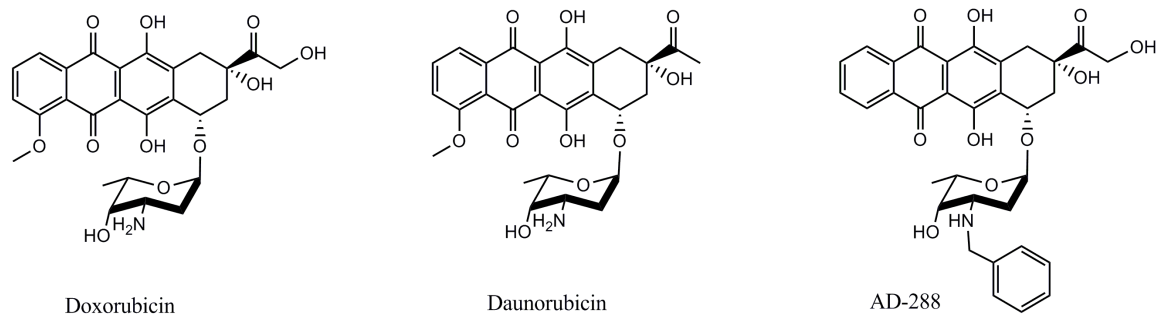


Figure 1-7. Representative Structures of Anthracycline Antibiotics

Several preclinical reports have shown that HDACi act synergistically with Topo II inhibitor such as anthracyclines to enhance apoptosis.²⁷ The HDACi-induced structural changes of chromatin may render the DNA more accessible and HDACi may therefore be used to potentiate DNA damaging agents such as topo II inhibitors. However such combination therapies are often sequence and dose dependent, complicated by the inherent pharmacokinetic disadvantages of individual drugs. Therefore development of single molecule containing "combination therapy" potential will harness the positive attributes of multiple drug therapy while eliminating or minimizing its shortcomings.¹⁹ We have designed novel single agents that simultaneously inhibit Topo II and histone deacetylase (HDAC) activities. We found that many of these conjugates potently inhibit HDAC and Topo II activities comparable to that of SAHA and daunorubicin, standard HDACi and Topo II inhibitors, respectively. Additionally, these compounds exhibited potent whole cell antiproliferative activities against representative breast, lung and prostate cell lines.

1.4.3 Camptothecins (Topoisomerase I inhibitor) –

Camptothecin is a naturally occurring Topo I inhibitor. It acts by stabilizing the intermediate of the Topo I-DNA reaction, the cleavage complex, through the formation of ternary complex. Camptothecins penetrate vertebrate cells readily and target Topo I within minutes of exposure. Therefore camptothecins are efficacious due to their selectivity rather than potency. However camptothecins have some limitations such as prolonged exposure to maintain persistent cleavage complex and deleterious side effects that limit the dose that can be safely administered.²⁸

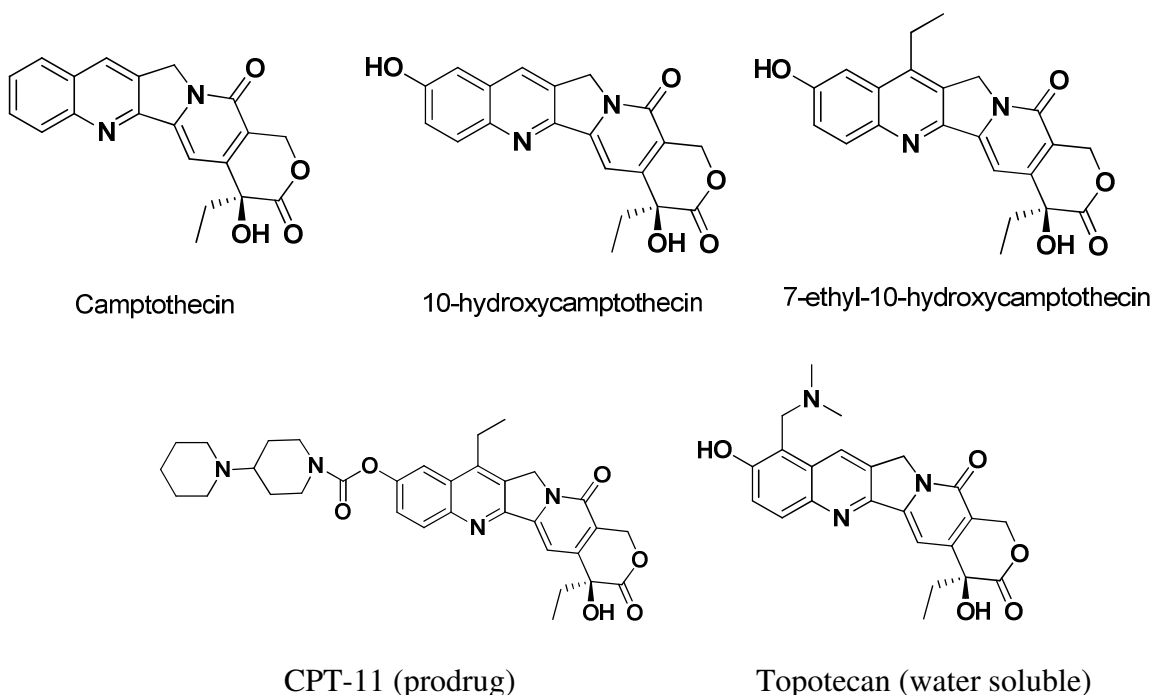


Figure 1-8. Representative topoisomerase I inhibitors.²⁹

It has been shown that HDACi facilitate the cytotoxic effectiveness of the topoisomerase I inhibitor camptothecin in the killing of tumor cells.^{20a} Effectiveness of such therapy is sequence, scheduling and dose dependent in much the same way as the effect of HDACi on topo II inhibitor potency.^{20a} In our efforts to design multifunctional compounds, we have synthesized range of compounds containing a HDACi moiety coupled with camptothecin templates. We anticipate that the individual anticancer moieties within these dual acting compounds would synergistically inhibit tumor cell proliferation with fewer off-target effects than the individual parent compounds. We propose that the HDACi will characteristically relax DNA-histone interactions, thereby allowing the better access to the camptothecin analog hence markedly increasing the efficacy of the compound. Additionally, while coupling a camptothecin analog to another active moiety may decrease the efficacy of topoisomerase poisoning, a decrease in the

off-target effects inherent with treatment of camptothecin alone could be a balancing benefit.

Classical examples of HDACi such as SAHA and TSA include either a keto or amide group as a cap linking moiety. We incorporated an amide group as cap linking moiety in 1st generation conjugates. However synthesis of these conjugates suffered a low overall yield. In order to address this issue, we proposed 1,2,3-triazole as an alternative, more synthetically tractable cap linking moiety for HDACi. A successful implementation of this proposal also helped in simplifying SAR study of 1st generation bifunctional conjugates.

In a related study, we investigated the consequence of incorporation of 1,2,3-triazole moiety into the pharmacophore of SAHA-based simple aliphatic hydroxamates.³⁰ Our study on simple HDACi showed that triazole incorporation enhanced HDACi activities by several fold compared to control compound SAHA *in vitro*. An additional SAR study on cap group and linker region revealed cap group dependent preference for either five- or six- methylene spacer groups. A subset of these compounds potently inhibited the proliferation of representative cancer lines.³⁰

1.5 Stalling Spliceosome Assembly with Zinc Chelators

Splicing is a major source of proteomic diversity in humans. The splicing reaction is a 2-step transesterification reaction which excises the introns and ligates the exons.³¹ This exceedingly complex process recruits spliceosomes, a large and dynamic ribonucleo-particle consisting of 5 small nuclear RNAs (snRNAs) and close to 150 proteins. In the first step, the 2'-OH of adenosine from the branch site nucleophilically

attacks the phosphodiester bond at the 5'-splice site forming the lariat intermediate. During the second step, the 3'-OH of the released 5' exon then performs nucleophilic attack at the 3' splice site, releasing the intron lariat. The process is tightly controlled by intricate interplays between RNA-protein, RNA-RNA and protein-protein which ultimately determine the identity of the protein formed from a pre-mRNA (Figure1-9).³² Understanding the splicing mechanism is of prime importance as many human genetic conditions, such as β -thalassemia, inherited breast cancer and many types of neurological diseases, are associated with aberrant pre-mRNA splicing.³³

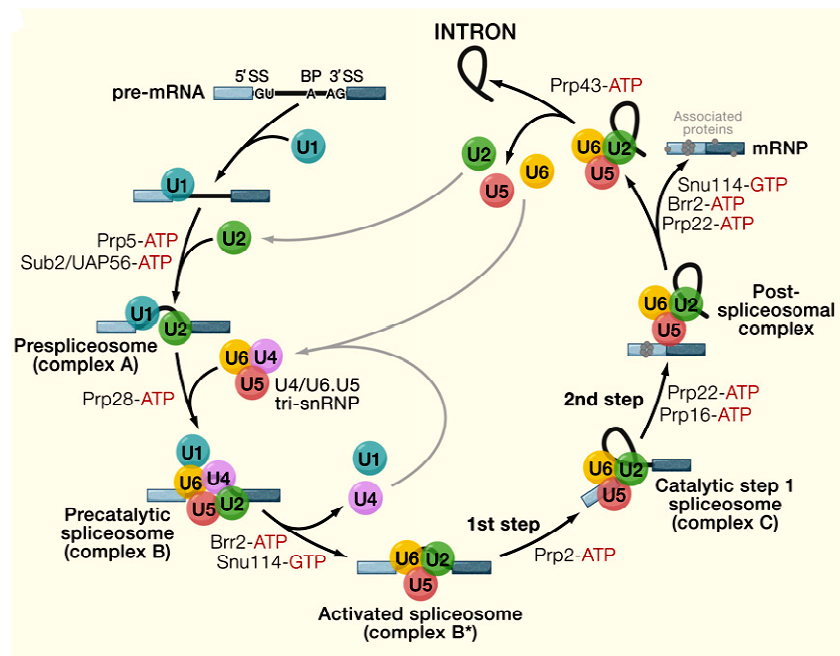


Figure 1-9: Steps involved in splicing mechanism³⁶

Spliceosome formation proceeds through coordinated assemblies of complexes – A, B, B* and C (Figure 1-9). The detail of molecular interactions between the five small nuclear ribonucleoproteins (snRNPs - U1, U2, U4, U5 & U6) and proteins in the spliceosome continues to be a subject of intense research. Remarkable advances have

been made in the characterization and structural elucidation of the various spliceosome complexes.³⁴ These studies have furnished exquisite information about spliceosome assembly at the RNA level. With the increased number of known splicing factors, we are now gaining an appreciation that the dynamic nature of the spliceosome is much more complex than simple addition and release of individual snRNPs proteins. However, the order of recruitment, interaction between these splicing factors, and signals that trigger their addition and release from the spliceosome remained poorly understood.³⁵ Additionally, little is known about the mechanism of catalysis and the trigger for the global conformational changes which ensure the fidelity of splicing. The availability of agents which perturb splicing at specific stages will greatly enhance our understanding of the workings of the spliceosome.

HDACs have been shown to be closely associated with spliceosome complexes, although their precise functions in splicing process are not clear. In order to gain more knowledge about spliceosome assembly and its function, we screened library of aryltriazolylhydroxamates HDACi to check their effect on splicing.

In collaboration with Prof. Reinhard Luhrmann of the Max Planck Institute, we have elucidated the molecular architecture that confer splicing inhibition to zinc chelating agents with HDAC inhibition activities. Characterization of the splicing complexes that accumulated on native gels, demonstrated that these agents specifically stalled the spliceosome assembly at A-like complex. However, there was no correlation between HDAC and splicing inhibition activities of these compounds. Therefore we conclude that the primary target(s) of the splicing inhibition activities of these

aryltriazolyl hydroxamates are not HDACs. This study has aided our understanding of splicing mechanism by shedding light on the role of zinc metalloenzyme/s in splicing.

1.6 Novel Zinc Binding Group for HDAC Inhibition –

The classic pharmacophore for HDACi consists of a metal-binding moiety that coordinates to the catalytic metal ion within the HDAC active site and a capping group that interacts with the residues at the entrance of active site. A linker appropriately positions the metal-binding moiety and capping group for interactions in the active site.¹³

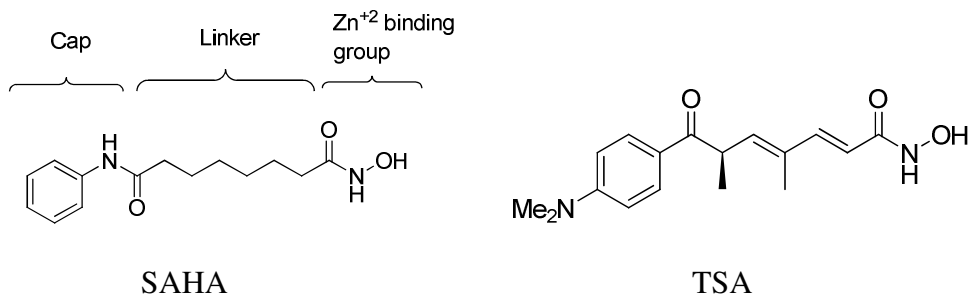


Figure 1-10. Structure of SAHA and TSA

Though hydroxamic acids are frequently employed as ZBG, they are often associated with poor pharmacokinetics and severe toxicity. Susceptibility to *in vivo* hydrolysis and metabolic transformations are some of the drawbacks which necessitate the identification of novel ZBG with better potency and less toxicity.³¹ In addition, hydroxamic acids do not discriminate well among the HDAC subtypes. However, non-hydroxamates such as benzamide have shown subtype selectivity.^{38,39} Therefore identification of non-hydroxamate ZBG may lead to potent HDACi with low toxicity. Towards this end, we have established 3-hydroxypyridin-2-thione (3-HPT) as a novel ZBG for HDAC inhibition. Preliminary biological studies on these compounds reveal

isoform selectivity for HDAC8 relative to HDAC1. Extensive SAR study on linker region confirms that either aromatic phenyl or aliphatic methylene linker are compatible with HDAC inhibition activity of these 3-HPT HDACi. Five methylene space shows optimum activity however other linkers such as one and seven methylene linkers showed respectable biological activities as well. For phenyl linker compounds, hydrophobic substitution on the aromatic surface cap group shows enhanced activity. We however found that a similar substitution on the five methylene linked compounds, is not compatible with HDAC inhibition. Molecular docking analysis reveals the important disparity between HDAC1 and HDAC8 active site that confers HDAC8 selectivity. HDAC8 active site is apparently shallower and therefore more easily accessible to 3-HPT based compounds. Based on this observation, we surveyed the possibility of interaction of 3-HPT based HDACi with gp63, another Zn-metalloenzyme which shared similar active site attributes with HDAC8.

1.7 Antileishmanial Agents

Visceral leishmaniasis is parasitic disease that is caused by the bite of female sandfly. Out of four known clinical forms, visceral leishmaniasis is most deadly form if left untreated.⁴⁰ It is caused by parasite *Leishmania donovani* and it shuttles between promastigote and amastigote forms during leishmania life cycle that includes transition from sandfly and mammalian host and vice versa.^{41,42} Leishmaniasis is contributing to significant morbidity and mortality worldwide. It has an estimated incidence of 500,000 new cases and 60,000 deaths each year, a death toll that is highest among all the parasitic diseases except malaria.⁴³ Human leishmaniasis is distributed worldwide, but mainly

concentrated in tropics and sub-tropics. The majority of deaths occur in developing countries such as Bangladesh, Brazil, Ethiopia, India, Nepal and Sudan.⁴⁴

The major surface zinc-metalloenzyme leishmanolysin (gp63) is highly expressed on the surface of the promastigote form of *Leishmania*, where it is enzymatically active, prototypically cleaving several host defensive enzymes.⁴⁵ Gp63 has been established as a virulence factor in leishmaniasis.⁴⁶ With the aid of other major cell surface components such as the lipophosphoglycans (LPGs) and glycoinositolphospholipid (GIPL), gp63 enables promastigotes to reach and infect sufficient macrophages to establish an infection.⁴⁵ Despite the attractiveness of gp63 as an anti-leishmanial target, there are currently no efficient, non-toxic inhibitors of gp63. Using a molecular docking analysis, I found that the 3-hydroxypyridin-2-one based HDAC8 inhibitors adopted docked poses on gp63 that were similar to those they adopted on HDAC8. Subsequent whole cell assay reveal that these compounds are potent inhibitors of the promastigote and amastigote forms of *L. donovani* with IC₅₀ comparable to Miltefosine, the only clinically approved oral drug against visceral leishmaniasis. Ongoing efforts are on identifying the intracellular target(s) that confers anti-leishmanial activity to these 3-hydroxypyridin-2-one based HDACi.

1.8 References

- 1 Jenuwein, T.; Allis C. D. *Science* **2001**, 1074.
- 2 (a) Grewal, S. I.; Jia, S. *Nat Rev Genet.* **2007** 8(1), 35-46. (b) Minucci, S.; Pelicci P. G.; *Nat Rev Cancer* **2006**, 6, 38.
- 3 (a) Grozinger, C. M.; Schreiber, S. L. *Chem. Biol.* **2002** 9(1), 3-16. (b) Kouzarides, T.; *Curr. Opin. Genet. Dev.* **1999**, 9, 40. (c) Taunton, J. ; Hassig, C. A. ; Schreiber, S. L. *Science* **1996**, 272, 408.
- 4 a) Sambucetti, L. C. ; Fischer, D. D. ; Zabudoff, S. ; Kwon, P. O. ; Chamberlin, H. ; Trogani, N. ; Xu, H.; Cohen, D. *J. Biol. Chem.* **1999**, 274, 34940. b) Martinez-Iglesias, O. ; Ruiz-Llorente, L. ; Sanchez-Martinez, R. ; Garcia, L. ; Zambrano, A. ; Aranda, A. *Clin. Transl. Oncol.* **2008**, 10, 395.
- 5 Mai, A.; Massa, S.; Rotili, D.; Cerbara, I.; Valente, S.; Pezzi, R.; Simeoni, S.; Ragno, R. *Med. Res. Rev.* **2005**, 25, 261–309.
- 6 (a) Marks, P. A. ; Miller, T. ; Richon, V. M. *Curr. Opin. Pharmacol.* **2003**, 3, 344. (b) Gray, S. G. ; Ekstrom, T. J. ; *Exp. Cell. Res.* **2001**, 262, 75 (c) Blander, G. ; Guarente L. ; *Annu. Rev. Biochem.* **2004**, 73, 417. (c) Gregoret, I. ; Lee, Y. M. ; Goodson, H. V. *J. Mol. Biol.* **2004**, 338, 17.
- 7 (a) Cardinale, J. P.; Sriramula, S.; Pariaut, R.; Guggilam, A.; Mariappan, N.; Elks, C. M.; Francis, J. *Hypertension* **2010**, 56, 437–444. (b) Dietz, K. C.; Casaccia, P.; *Pharmacol. Res.* **2010**, 62, 11–17. (c) Patil, V.; Guarrant, W.; Chen, P. C.; Gryder, B.; Benicewicz, D. B.; Khan, S. I.; Tekwani, B. L.; Oyelere, A. K. *Bioorg. Med. Chem.* **2010**, 18, 415–425. (d) Wang, L.; de Zoeten, E. F.; Greene, M. I.; Hancock, W. W. *Nat. Rev. Drug Discovery* **2009**, 8, 969–98. (e) Welberg, L., *Nature Rev. Drug Discovery* **2009**, 8, 538–539. (f) Kazantsev, A. G.; Thompson, L. M.; *Nature Rev. Drug Discovery* **2008**, 7, 854–868. (g) Meinke, P.T.; Liberator, P.; *Curr. Med. Chem.* **2001**, 8(2), 211-235.
- 8 (a) de Ruijter A. J. ; van Gennip A. H.; Caron, H. N.; Kemp, S.; van Kuilenburg A. B.; *Biochem. J.* **2003**, 370 (Pt 3): 737–49. (b) Longworth, M. S.; Laimins, L. A.; *Oncogene* **2006**, 25 (32): 4495–500 (c) Alenzuela-Fernández, A.; Cabrero, J. R.; Serrador, J. M.; Sánchez-Madrid, F.; *Trends Cell. Biol.* **2008**, 18 (6): 291–7.
- 9 (a) Khabele, D.; Son, D. S.; Parl, A. K.; Goldberg, G. L.; Augenlicht, L. H.; Mariadason J. M.; Rice, V. M. *Cancer Biol. Ther.* **2007**, 6, 795. (b) Song, J.; Noh, J. H.; Lee, J. H.; Eun, J. W.; Ahn, Y. M.; Kim, S. Y.; Lee, S. H.; Park, W. S.; Yoo, N. J.; Lee, J. Y.; Nam, S. W. *APMIS* **2005**, 113, 264. (c) Bartling, B.; Hofmann, H. S.; Boettger, T.; Hansen, G.; Burdach, S.; Silber R. E.; Simm, A. *Lung Cancer* **2005**, 49(2), 145. (d) KrennHrubec, K.; Marshall, B. L.; Hedglin, M.; Verdin, E.; Ulrich, S. M. *Bioorg. Med. Chem. Lett.* **2007**, 17, 2874. (e) Saji, S.; Kawakami, M.; Hayashi, S.;

Yoshida, N.; Hirose, M.; Horiguchi, S. I.; Itoh, A.; Funata, N.; Schreiber, S. L.; Yoshida, M.; Toi, M. *Oncogene* **2005**, 24, 4531.

- 10 (a) Finnin, M. S.; Donigian, J. R.; Cohen, A.; Richon, V. M.; Rifkind, R. A.; Marks, P. A.; Breslow, R.; Pavletich, N. P. *Nature* **1999**, 401, 188. (b) Somoza, J. R.; Skene, R. J.; Katz, B. A.; Mol, C.; Ho, J. D.; Jennings, A. J.; Juong, C.; Arvai, A.; Buggy, J. J.; Chi, E.; Tang, J.; Sang, B.C.; Verner, E.; Wynands, R.; Leahy, E. M.; Fougan, D. R.; Snell, G.; Navre, M.; Knuth, M. W.; Swanson, R. V.; McRee, D. E.; Tari, L.W. *Structure* **2004**, 12, 1325. (c) Schuetz, A.; Min, J.; Allali-Hassani, A.; Schapira, M.; Shuen, M.; Loppnau, P.; Mazitschek, R.; Kwitkowski, N. P.; Lewis, T. A.; Maglathin, R. L.; McLean, T. H.; Bochkarev, A.; Plotnikov, A. N.; Vedadi, M.; Arrowsmith, C.H. *J. Biol. Chem.* **2008**, 283, 11355. (d) Bressi, J. C.; Jennings, A. J.; Skene, R.; Wu, Y.; Melkus, R.; De Jong, R.; O'Connell, S.; Grimshaw, C.E.; Navre, M.; Gangloff, A.R. *Bioorg.Med.Chem.Lett.* **2010**, 20, 3142-3145.
- 11 Estiu, G.; Wiest, O. HDAC1 homology model. Personal communication.
- 12 Vannini, A.; Volpari, C.; Filocamo, G.; Casavola, E. C.; Brunetti M.; Renzoni, D.; Chakravarty, P.; Paolini, C.; De Francesco, R.; Gallinari, P.; Steinkühler, C.; Di Marco, S. *Proc Natl Acad Sci U S A.* **2004**, 101(42), 15064.
- 13 Miller, T. A.; Witter, D. J.; Belvedere, S. *J. Med.Chem.* **2003**, 46, 5097.
- 14 Bieliauskas, A. V.; Pflum, M. K. H. *Chem. Soc. Rev.* **2008**, 37, 1402.
- 15 (a) Paris, M.; Porcelloni, M.; Binaschi, M.; Fattori, D. *J. Med. Chem.* **2008**, 51, 1505. (b) Deal watch: Celgene acquires Gloucester Pharmaceuticals, gaining approved HDAC inhibitor. *Nat. Rev. Drug Discovery* **2010**, 9, 94. (c) Grant, S.; Easely, C.; Kirkpatrick, P. *Nat. Drug Discovery Rev.* **2007**, 6, 21–22.
- 16 (a) Wong, J.; Hong, R.; Schreiber, S. *J. Am. Chem. Soc.* **2003**, 125, 5586–5587. (b) Haggarty, S. J.; Koeller, K. M.; Wong, J. C.; Grozinger, C. M.; Schreiber, S. L. *Proc. Natl. Acad. Sci. U.S.A.* **2003**, 100, 4389–4394.
- 17 (a) Meutermans, W. D.; Bourne, G. T.; Golding, S. W.; Horton, D. A.; Campitelli, M. R.; Craik, D.; Scanlon, M.; Smythe, M. L. *Org. Lett.*, **2003**, 5, 2711. (b) Glenn, M. P.; Kelso, M. J.; Tyndall, J. D.; Fairlie, D. P. *J. Am. Chem. Soc.*, **2003**, 125, 640. (c) Shivashimpi, G. M.; Amagai, S.; Kato, T.; Nishino, N.; Maeda, S.; Nishino, T. G.; Yoshida, M. *Bioorg. Med. Chem.* **2007**, 15, 7830. (d) Deshmukh, P. H.; Schulz-Fademrecht, C.; Procopiou, P. A.; Vigushin, D. A.; Coombes, R. C.; Barrett, A. G.; M. *Adv. Synth. Catal*, **2007**, 349, 175. (e) Oyelere, A. K.; Chen, P. C.; Guerrant, W.; Mwakwari, S. C.; Hood, R.; Zhang, Y.; Fan, Y. *J. Med. Chem.*, **2009**, 52(2), 456.
- 18 Hanahan D.; Weinberg R. A. *Cell* **2000**, 100(1), 57.
- 19 Sarkar F. H.; Li Y. *Acta Pharmacol Sin*, **2007**, 28, 1305.

- 20 (a) Bevin, R. L.; Zimmer S. G. *Cancer Res* **2005**, 65(15), 6957 (b) Kelly W. K.; Richon V. M.; O'Connor O.; *et al*, *Clin cancer res*, **2003**, 9, 3578 (c) Chobanian N. H.; Greenberg V. L.; Gass J. M.; Desimone C. P.; Van-Nagell, J. R.; Zimmer, S. G.; *Anticancer Res.* **2004**, 24, 539.
- 21 (a) Kim M. S.; Blake M.; Baek J. H.; Baek J. H.; Kohlhagen G.; Pommier Y.; Carrier F. *Cancer Res* **2003**, 63, 7291 (b) Castro-Galache M. D.; Ferragut J. A.; Barbera V. M.; *et al*, *Int J Cancer* **2003**, 104, 579.
- 22 Carew J. S.; Giles F. J.; Nawrocki S. T. *Cancer Lett.* **2008**, 269, 7.
- 23 Huston, T. E.; Vukelja S.; Atienza D.; *et al Invest. New Drugs*, **2008**, 26, 151.
- 24 Champoux J. J., *Annu rev. biochem*, **2001**, 70, 369.
- 25 Minotti, G.; Menna, P.; Salvatorelli, E., Cairo, G.; Gianni, L. *Pharmacol. Rev.* **2004**, 56, 185.
- 26 (a) Singal P.; Iliskovic, N. *N. Engl. J. Med.* **1998**, 339, 900 (b) Thorburn, A.; Frankel, A. *Mol. Cancer Ther.* **2006** 5,197 (c) Jones, R.; Swanton, C.; Ewer, M. *Expert Opin. Drug Saf.* **2006**, 5,791.
- 27 Johnson C. A.; Padget, K.; Austin C. A.; Turner B. M. *J. Biol. Chem.* **2001**, 276, 4539.
- 28 (a) Pommier Y. *Nat. Rev. Cancer* **2006**, 6, 789. (b) Minnotti, G.; Menna, P.; Salvatorelli, E.; Cairo, G.; Gianni, L. *Pharmacol. Rev.* **2004**, 56, 185 (c) Fischer, B.; Constantino, J.; Wickerham D.; *et al. J. Natl. Cancer Inst.* **1998**, 90, 1371 (d) Davis T., Kennedy, C.; Chiew, Y.; Clarke, C.; DeFazio, A. *Cancer Res.* **2000**, 6, 4334.
- 29 Pommier Y. *Curr Med Chem Anticancer Agents.* **2004**, 4(5), 429-34
- 30 Chen, P.C.; Patil, V.; Guerrant, W.; Green, P.; Oyelere, A. K. *Bioorg. Med. Chem.* **2008**, 16, 4839.
- 31 Nilsen, T.W. *Molecular Cell* **2002**, 9, 8-9.
- 32 Jurica, M. S. *Curr. Opin. Struct. Biol.* **2008** 18, 315–320
- 33 (a) Disney, M. D. *Nat. Chem. Biol.* **2008**, 4, 723-724. (b) Teraoka, S. N.; Telatar, M.; Becker-Catania, S.; Liang, T.; Onengut, S.; Tolun, A.; Chessa, L.; Sanal, O.; Bernatowska, E.; Gatti, R. A.; Concannon, P. *Am. J. Hum. Genet.* **1999**, 64, 1617. (c) Meshorer, E.; Soreq, H. *Trends Neurosci.* **2006**, 29, 216-224.
- 34 (a) Will, C. L.; Lührmann, R. *Spring Harb. Perspect. Biol.* **2011**, 3, a003707. (b) Jurica, M. S.; Licklider, L. J.; Gygi, S. R.; Grigorieff, N.; Moore, M. J. *RNA* **2002**, 8, 426. (c) Boehringer, D.; Makarov, E. M.; Sander, B.; Makarova, O. V.; Kastner, B.; Luhrmann, R.; Stark, H. *Nat. Struct. Mol. Biol.* **2004**, 11, 463. (d) Bessonov, S.;

- Anokhina, M.; Will, C. L.; Urlaub, H.; Luhrmann, R. *Nature* **2008**, 452, 846. (e) Pomeranz Krummel, D. A.; Oubridge, C.; Leung, A. K.; Li, J.; Nagai, K. *Nature* **2009**, 458, 475.
- 35 Jurica, M.S.; Moore, M. J. *Mol. Cell* **2003**, 12, 5–14.
- 36 Wahl, M. C.; Will, C. L.; Luhrmann, C. L. *Cell* **2009**, 136, 701-718.
- 37 (a) Jones, P.; Altamura, S.; Chakravarty, P. K.; Cecchetti, O.; De Francesco, R.; Gallinari, P.; Ingenito, R.; Meinke, P. T.; Petrocchi, A.; Rowley, M.; Scarpelli, R.; Serafini, S.; Steinkuehler, C. *Bioorg. Med. Chem. Lett.* **2006**, 16, 5948. (b) Suzuki, T.; Miyata, N. *Curr. Med. Chem.* **2006**, 13, 935. (c) Dehmelt, F.; Ciossek, T.; Maier, T.; Weinbrenner, S.; Schmidt, B.; Zoche, M.; Beckers, T.; *Bioorg. Med. Chem. Lett.* **2007**, 17, 4746. (d) Chen, B.; Petukhov, P. A.; Jung, M.; Velená, A.; Eliseeva, E.; Dritschilo, A.; Kozikowski, A. P. *Bioorg. Med. Chem. Lett.* **2005**, 15, 1389. (e) Suzuki, T.; Matsuura, A.; Kouketsu, A.; Hisakawa, S.; Nakagawa, H.; Miyata, N. *Bioorg. Med. Chem.* **2005**, 13, 4332. (f) Vasudevan, A.; Ji, Z.; Frey, R. R.; Wada, C. K.; Steinman, D.; Heyman, H. R.; Guo, Y.; Curtin, M. L.; Guo, J.; Li, J.; Pease, L.; Glaser, K. B.; Marcotte, P. A.; Bouska, J. J.; Davidsen, S. K.; Michaelides, M. R. *Med. Chem. Lett.* **2003**, 13, 3909. (g) Moradei, O.; Maroun, C. R.; Paquin, I.; Vaisburg, A. *Curr. Med. Chem.: Anti-Cancer Agents* **2005**, 5, 529. (h) Hanessian, S.; Vinci, V.; Auzzas, L.; Marzi, M.; Giannini, G. *Bioorg. Med. Chem. Lett.* **2006**, 16, 4784.
- 38 Wong, J. C.; Hong, R.; Schreiber, S. L. *J. Am. Chem. Soc.* **2003**, 125, 5586.
- 39 Beckers, T.; Burkhardt, C.; Wieland, H.; Gimmnich, P.; Ciossek, T.; Maier T.; Sanders, K. *Int. J. Cancer* **2007**, 121, 1138.
- 40 Akopyants, N. S.; Kimblin, N.; Secundino, N.; Patrick, R.; Peters, N.; Lawyer, P.; Dobson, D. E.; Beverley, S. M.; Sacks, D. L. *Science* **2009**, 324, 265.
- 41 Rogers, M.; Kropf, P.; Choi, B. S.; Dillon, R.; Podinovskaia, M.; Bates, P.; Muller, I.; *PLoS Pathog.* **2009**, 5, e1000555.
- 42 Sharma, U.; Singh, S. *Indian J. Exp. Biol.* **2009**, 47, 412.
- 43 WHO Report, Available at: <http://www.who.int/leishmaniasis/burden/en>.
- 44 Chappuis, F.; Sundar, S.; Hailu, A.; Ghalib, H.; Rijal, S.; Peeling, R. W.; Alvar, J.; Boelaert, M.; *Nat. Rev. Microbiol.* **2007**, 5(11), 873-82.
- 45 (a) Russell, D. *Eur. J. Biochem.* **1987**, 164, 213. (b) Puentes, S.; Dwyer, D. M.; Bates, P. A.; Joiner K. A. *J. Immunol.* **1989**, 143, 3743.
- 46 Pandey, S.; Chakraborti, P.; Sharma, R.; Bandyopadhyay, S.; Sarkar, D.; Adhya, S. *J. Biosci.* **2004** 29(1), 15.

CHAPTER 2

SAHA-like Aryltriazolyhydroxamates

2.1 Introduction

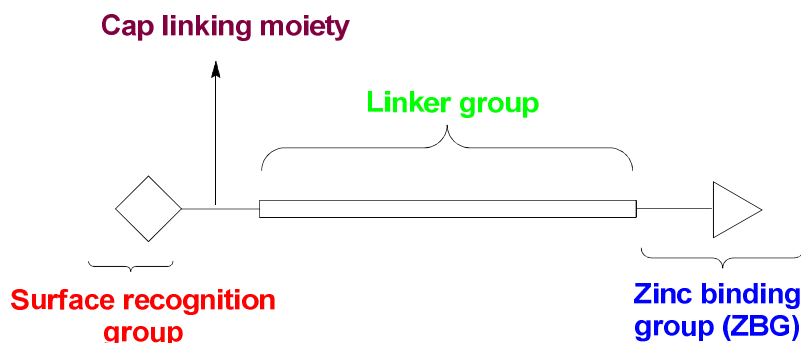


Figure 2-1: Pharmacophoric Model of HDACi.

HDACi generally conforms to a pharmacophoric model consisting of a zinc binding group (ZBG), a hydrophobic linker chain and a surface recognition group (which comprises cap-linking moiety and a cap group) (Figure 2-1).¹ ZBG interacts with a Zn^{2+} ion at the base of a tunnel-like active site. The linker region efficiently presents the ZBG in the vicinity of Zn^{2+} ion by filling the channel while the cap-group at the other end interacts with amino acid residues at the surface of the enzyme.²⁻⁴

The most commonly used ZBG in HDACi is the hydroxamic acid. Attempts to incorporate non-hydroxamate based ZBG in HDACi have been modestly successful.^{1,2,5,6} On the contrary, modulation of cap group have yielded many potent and more selective HDACi.^{7,8} For example, studies by Schreiber and coworkers have led to the identification of cap group-modified agents that display isoform selectivity for different HDACs.^{9,10} In order to connect these cap groups with rest of the pharmacophoric model of HDACi, either hydrogen bond accepting or donating groups such as keto- and amide- groups

(Figure 2-1) are used as the cap-linking moiety. We hypothesize that a 1,2,3-triazole ring could act as an HDACi cap-linking moiety. If successful, the proposed modification will simplify design and synthesis of complex HDACi due to the synthetic tractability and favorable pharmacokinetic profile of the triazole moiety.

2.2 Design of SAHA-like Aryltriazolyldihydroxamates

To commence this study, we initially undertook the synthesis of SAHA-like aryltriazolyldihydroxamates **4a-d** (Figure 2-2), which linked the aromatic surface recognition cap group to the aliphatic zinc binding hydroxamate moiety via a 1,2,3-triazole ring. In the first step, alkyne intermediate **1** was cyclized with azidomethylesters **2a-d** using Cu(I) catalyzed Huisgen cycloaddition reaction (click chemistry) to afford compounds **3a-d**.^{11,12, 13-15} The utility of this chemistry was popularized by Sharpless and Meldal labs,¹² and it has become a tool for synthesizing various complex macromolecules and rapid identification of small molecules that possess interesting biological activity.¹²

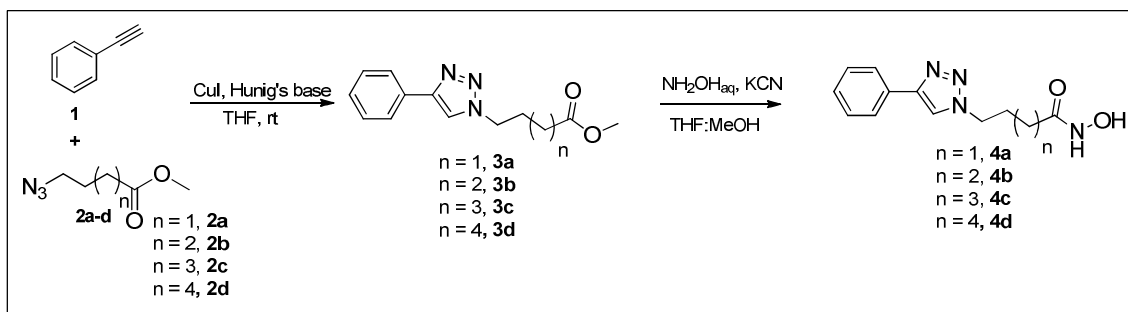


Figure 2-2. Synthesis of SAHA-like aryltriazolyldihydroxamate **4a-d**.

Treatment of the intermediate esters **3a-d** with 50% aqueous hydroxylamine¹⁶ furnished the desired hydroxamic acids **4a-d** in good to excellent yields (Figure 2-2).

Similarly, the synthesis of analogs with other aromatic surface recognition cap groups is achieved starting from the corresponding aryl alkynes and azido esters (Figure 2-2).

To further explore the SAR of this class of HDACi, we synthesized various analogs incorporating assorted surface recognition group using similar chemistry worked out for the synthesis of **4a-d**. The requisite aryl alkynes, **5g**, **5i**, **5j**, **5l**, **5p**, and **5q**, that were not commercially available were synthesized from the corresponding aldehydes and carboxylic acids (through the intermediacy of aldehyde) using the Bestmann-Ohira Reagent.¹⁷⁻¹⁹ Coupling of these alkynes with appropriate azidomethylesters, following by treatment of the intermediate esters with 50% aqueous hydroxylamine gave the desired aryltriazolyhydroxamates **7a-y** (Figure 2-3).

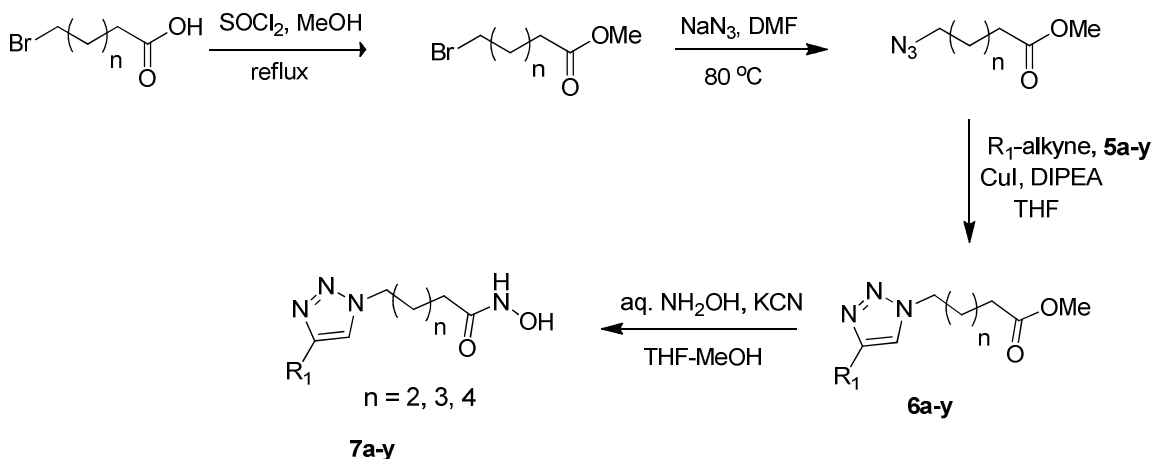


Figure 2-3. Synthesis of aryltriazolyhydroxamates **7** for SAR studies. For R₁ structures refer Table 1-2.

2.3 SAR Studies of Triazole-linked Simple HDAC Inhibitors

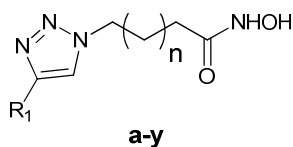
Initially, we synthesized hydroxamates **4a-d** to allow head to head comparison of their HDAC inhibition activity with SAHA. and conclude any advantage of triazole ring (or lack thereof) on potency. Analysis of the HDAC inhibition activity of **4a-d** against

HeLa nuclear extract (mixture of HDAC1 and HDAC1), using the standard *Fluor de lys* assay²⁰ revealed an interesting linker length dependency. Compound **4a**, the analog with the shortest methylene linker didn't show any detectable activity. However, **4b-d** displayed linker-length dependence with five and six methylene linkers being the most potent (Table 2-1). This study is in good accord with the optimum linker for SAHA and TSA like compounds.^{1,21} More importantly, we observed that compounds **4c-d**, the closest analogs to SAHA, are 4-fold more active than SAHA. This suggests that the replacement of HDACi amide cap linking moiety with triazole enhanced the anti-HDAC activities of the resulting aryltriazolyhydroxamates.

Further SAR study on cap group for five to six methylene spacer reveal that there is no clear trend in five- or six-methylene spacer regions. For example, for phenyl substituted compounds, the six-methylene linked compound **4d** is slightly more active than the five-methylene compound **4c** (Table 2-1). However, the introduction of *N, N*-dimethylamino moiety to the *para* position of the phenyl group for five methylene linker, led to 25-fold more active analog than the corresponding six-methylene compound (Table 2-1, compare **7a** and **7b**). Due to this cap group dependent potency for five- and six-methylene spacer group, we prepared a series of aromatic and heteroaromatic derivatives consisting of either spacer group in order to flush out the SAR of these compounds. Relative to compounds **4c** and **4d**, nitrogen substitution into the phenyl ring (pyridine) did not improve the potency (Table 2-1, compounds **7c-f**). However, the position of pyridine nitrogen affects the potency with the 2-pyridyl derivative **7e** being more active than the corresponding 3-pyridyl and 4-pyridyl analogs **7c** and **7d** respectively. Additionally, pyridine based simple HDACi analogs **7e** and **7f**, which differ by a

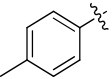
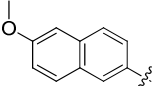
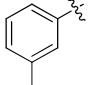
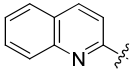
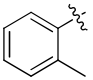
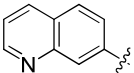
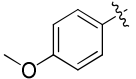
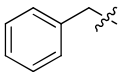
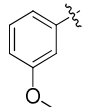
methylene group, show a chain length dependency similar to that observed with **4c** and **4d**. Similarly, among methyl-substituted compounds **7g-i** *ortho*-substitution is more favorable. However, *para*-substitution is preferred for methoxy group substitution (Table 2-1, compare compounds **7j-l** with **7g-i**).

Table 2-1. *In vitro* inhibition data for arytriazolylhydroxamates^a



Compounds	R ₁	n	IC ₅₀ ^b (nM)	Compounds	R ₁	n	IC ₅₀ ^b (nM)
4a [*]		1	N.D. ^b	7l		3	76.0
4b [*]		2	110.0	7m ⁺		3	315.9
4c [*]		3	14.2	7n ⁺		3	31.7
4d		4	9.6	7o ⁺		3	52.4
7a ⁺		3	4.3	7p ⁺		3	1.9
7b		4	106.1	7q		4	5.4
7c		3	287.2	7r ⁺		3	162.6
7d		3	112.5	7s		3	2.3
7e		3	67.6	7t		4	16.6
7f		4	23.9	7u ⁺		3	1.8

Table 2-1 continued.

7g		3	43.4	7v		4	15.3
7h		3	31.9	7w		3	2.1
7i		3	17.4	7x		3	151.5
7j		3	2.09	7y		2	N.D. ^c
7k		3	13.9		SAHA		65

^aPo-Chih Chen and Patience Green also contributed in synthesis of compound **7**. ^bData represent mean values of at least three-independent experiments in *Fluor-de Lys* assay; performed by William Guerrant. ^cNot determinable. ^{*}Compounds made by Patience Green [†]Compounds made by Po-Chih Chen, included here to clarify SAR studies. For details, refer to Chen et al, *Bioorg. & Med. Chem.*, **2008**, 16, 4839-4853.

There is a precedence that *para*-substitution has been preferred for methoxy-substituted SAHA-like HDACi in which cap linking moiety was ketone instead of triazole.²² The enhanced steric bulkiness of the methoxy moiety relative to methyl group may be responsible for the observed *para*-position preference. To investigate this prospect, we synthesized the 2,6-dimethoxy substituted compound **7m**. We observed a drop in activity for compound **7m** compared to **7l**. This result confirmed that steric repulsion at the ortho position influenced compound anti-HDAC activity. The 2-quinoline analog **7w**, in similar manner to the pyridine analogs **7c-e**, is more active than the 7-quinoline analog **7x**. We observed enhanced potency for the five-methylene linker compounds compared to six-methylene analogs. For example, 6-methoxynaphthalene capped compound **7u** showed enhanced activity relative to a corresponding six-methylene analog **7v**. Furthermore, biphenyl compounds **7o-t** showed preference for the *meta*-placement of the triazole ring and a five-methylene spacer (Table 2-1, compare

compounds **7o-r**). Finally, to the importance of placement of triazole ring in compound design was confirmed by the disparity between the anti-HDAC activities of **4c** and **7y**, two analogs which have the same number of carbon atoms separating the cap group and the ZBG. Compound **4c** contains triazole ring directly attached to the phenyl cap group and is several fold more potent than **7y** whose triazole ring is separated from the cap group by a methylene group. This result supports the hypothesis that the triazole ring is indeed contributing to the interaction of this class of compound with the HDAC active site.

2.4 Molecular Docking Analysis

In order to gain insight on structural basis for the observed disparity in the anti-HDAC activities of these aryltriazolyhydroxamates HDACi, we performed molecular docking analyses using a validated molecular dock program (AutoDock)²³⁻²⁵ We chose to perform docking studies on histone deacetylase-like protein (HDLP)² because it shared conserved active site residues with class I HDACs. Moreover, docking on HDAC1 homology model built from the same HDLP structure also concurred with experimentally obtained data. Both approaches have been used in literature to validate the HDAC inhibition data.²⁴ We used AutoDock 3.05 as described by Lu *et al.*²⁵ Independent docking of SAHA, **4c**, **7o**, **7p**, and **7u** into HDLP revealed that these compounds bind to two different binding pockets at the protein surface (Figure. 2-4). It has been shown earlier that there are four pockets on HDLP surface where HDACi tend to bind.²⁴ Compounds **7o** and **7u** bind within the binding pocket designated as pocket 1 while SAHA, **4c** and **7p** bind within pocket 2. The 1,4-biphenyl ring of **7o** adopts a co-planar

geometry to orient in pocket 1. This is due to the stacking interactions in pocket 1 that favor a co-planar orientation of the cap group, an inference that may be supported by the binding of **7u**, an analog with a flat fused six-six ring, within pocket 1. To adopt the observed conformation, a sharp twist is introduced into the methylene linker portion of **7o**. The resulting twist in **7o** pulls off the hydroxamate moiety thereby reducing Zn^{2+} binding of hydroxamate, compared to that of **7p** and SAHA. This might cancel out any positive effects derived from the cap group interaction with pocket 1 and may explain the reduced potency of **7o** compared to structurally similar **7p**. Unlike **7o**, the 1,3-biphenyl ring of **7p** preferred a non-planar geometry with the biphenyl ring projecting deeper into the binding pocket 2 where it interacted hydrophobically further with the pocket residues. This extra interaction could explain the higher potency of **7p** compared to **4c** and SAHA.

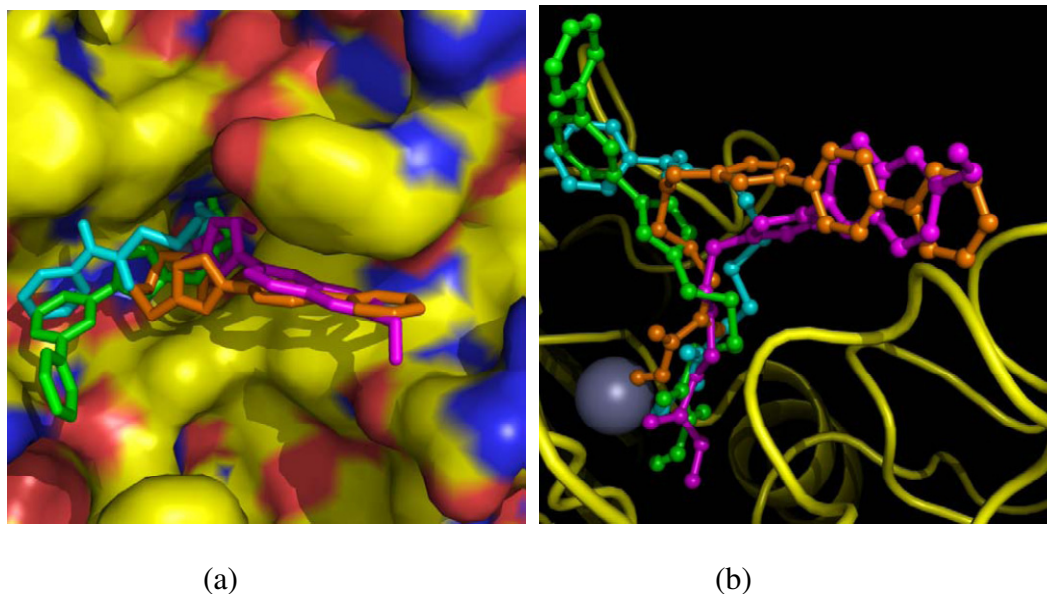


Figure 2-4. Molecular docking analysis^a **7o** (orange), **7p** (green), **7u** (magenta), and SAHA (cyan) to HDLP using Autodock 3.05¹⁹⁻²¹ and viewed in PYMOL. (a) Surface presentation of HDLP near the active site; (b) side view of the triazolylhydroxamates **7o**, **7p**, **7u**, and SAHA coordinating to zinc with amino acid residues in and near the active sites.¹⁹⁻²¹

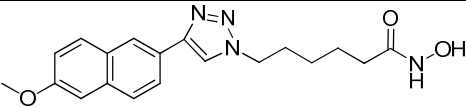
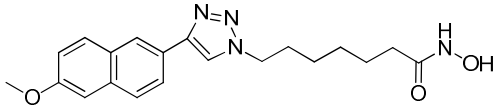
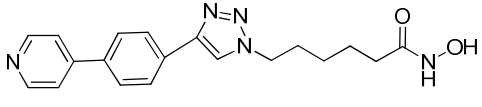
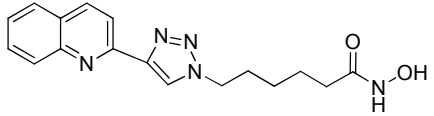
^aMolecular docking analysis performed by Po-Chih Chen. Presented here to explain SAR disparity. For details, refer to Chen et al, *Bioorg. & Med. Chem.*, **2008**, *16*, 4839-4853.

2.5 Cell Growth Inhibition Studies of Triazole-linked Simple HDACi

To determine whole cell activity of these compounds against cancer cell line, we treated representative compounds with DU-145 cell line.²⁶ We investigated compounds **7s**, **7u**, **7v** and **7w** with SAHA as a control, using both the MTS test (a colorimetric method) and trypan blue exclusion.^{27,28}

SAHA exhibited EC₅₀ value of 2.12 μ M which is in close agreement with the reported value in literature.²⁹ Compounds **7s**, **7u**, **7v** and **7w** also inhibited the proliferation of DU-145 in a dose-dependent manner, with EC₅₀ values ranging from 2.2 to 8.0 μ M (Table 2-2). These results validated the suitability of the triazole moiety as a linking moiety in the design of SAHA-like HDACi.

Table 2-2. Cell growth inhibitory data for lead compounds

Aryltriazolyhydroxamates 7	IC ₅₀ (nM)	EC ₅₀ ^a (μ M)	EC ₅₀ ^b (μ M)
 7u	1.8	3.95	2.6
 7v	15.3	7.76	3.99
 7s	2.3	4.72	3.07
 7w	2.1	2.25	2.46
SAHA	65.0	2.12	2.11

SAHA was used as a control for these experiments. EC₅₀ values were determined from ^atrypan blue exclusion data and ^bMTS assay (Progmega), in DU-145 prostate cancer cell line, performed by William Guerrant. ^cCompound made by Bob Chen. These are included to clarify the SAR. See Chen et al, *Bioorg. & Med. Chem.*, **2008**, *16*, 4839-4853 for detailed synthetic protocol.

2.6 Conclusions

We have demonstrated the suitability of 1,2,3-triazole ring as a cap group-linking moiety in SAHA-like HDAC inhibitors. This study showed that the anti-HDAC activities of the resulting triazole-linked hydroxamates followed a cap group dependent preference for five- and six- methylene linkers. We have identified compounds that are several folds more potent than SAHA. A subset of these compounds also inhibited the proliferation of DU-145 cells. These triazole based compounds are expected to simplify SAR study for more complex HDACi by facilitating easy synthetic access to connect linker and cap group.

2.7 General Procedure and Experimental

4-bromobutyric acid, 5-bromovaleric acid, 6-bromohexanoic acid, and 7-bromoheptanenitrile were purchased from Sigma Aldrich. Anhydrous solvents and other reagents were purchased and used without further purification. Analtech silica gel plates (60 F₂₅₄) were used for analytical TLC, and Analtech preparative TLC plates (UV 254, 2000 μm) were used for purification. UV light was used to examine the spots. 200-400 Mesh silica gel was used in column chromatography. NMR spectra were recorded on a Varian-Gemini 400 magnetic resonance spectrometer. ¹H NMR spectra are recorded in parts per million

(ppm) relative to the peak of CDCl₃, (7.24 ppm), CD₃OD (3.31 ppm), or DMSO-*d*₆ (2.49 ppm). ¹³C spectra were recorded relative to the central peak of the CDCl₃ triplet (77.0 ppm), CD₃OD (49.0 ppm), or the DMSO-*d*₆ septet (39.7 ppm), and were recorded with complete hetero-decoupling. Multiplicities are described using the abbreviation s, singlet; d, doublet; t, triplet; q, quartet; m, multiplet; and app, apparent. High-resolution mass spectra were recorded at the Georgia Institute of Technology mass spectrometry facility in Atlanta. Methyl bromoalkanoates **1a-d** and azido alkylesters **2a-d** were synthesized by adapting literature protocol.^{13-16,30} The Bestmann-Ohira reagent was prepared as described by Ghosh *et al.*¹⁸ Alkynes that we could not obtain from commercial sources were synthesized using the Bestmann-Ohira reagent as described before.²⁹

Representative procedure for Cu(I)-catalyzed cycloaddition reaction

Methyl 7-(phenyl)triazolylheptanoate (3d).

Methyl 4-azidobutanoate **2d** (0.15 g, 0.81 mmol) and phenylacetylene (182 mg, 1.78 mmol) were dissolved in anhydrous THF (10 mL) and stirred under argon at room temperature. Copper (I) iodide (0.011 g, 0.07 mmol) and Hunig's base (0.1 mL) were then added to the reaction mixture, and stirring continued for 24 h.³¹ The reaction mixture was diluted with CH₂Cl₂ (20 mL) and washed with 1:4 NH₄OH/saturated NH₄Cl (3 x 30 mL) and saturated NH₄Cl (30 mL). The organic layer was dried over Na₂SO₄ and concentrated *in vacuo*. The crude product was purified by flash chromatography (silica, gradient 2:1; 3:2 Hexane/EtOAc) to give 151 mg (65%) of **3d** as white solid. ¹H NMR (CDCl₃, 400 MHz) δ 1.35 (4H, p, *J* = 7.3, 3.5 Hz), 1.57-1.64 (2H, m), 1.89-1.96 (2H, m),

2.28 (2H, t, $J = 7.3$ Hz), 3.63 (3H, s), 4.36 (2H, t, $J = 7.1$ Hz), 7.30 (1H, t, $J = 7.2$ Hz), 7.39 (2H, t, $J = 7.3$ Hz), 7.72 (1H, s), 7.80 (2H, d, $J = 7.1$ Hz); ^{13}C NMR (CDCl_3 , 100 MHz) δ 24.7, 26.2, 28.5, 30.2, 33.9, 50.2, 51.5, 119.2, 125.5, 127.9, 128.6, 130.5, 147.5, 173.7; HRMS (FAB, thioglycerol) calcd for $[\text{C}_{16}\text{H}_{21}\text{N}_3\text{O}_2 + \text{H}]^+$ 288.1712, found 288.1711.

Methyl 7-(4-anilyl)triazolyheptanoate (6b). Reaction of methyl 7-azidoheptanoate **2d** (0.15 g, 0.81 mmol) and 4-ethynyl-*N,N*-dimethylaniline **5a** (127 mg, 0.87 mmol) within 24 h as described for the synthesis of **3d**, followed by flash chromatography (silica, 3:2 Hexane/EtOAc) gave 165 mg (62%) of **6b** as colorless oil. ^1H NMR (CDCl_3 , 400 MHz) δ 1.34-1.37 (4H, m), 1.58-1.64 (2H, m), 1.92 (2H, m), 2.28 (2H, t, $J = 7.3$ Hz), 2.97 (6H, s), 3.64 (3H, s), 4.34 (2H, t, $J = 7.1$ Hz), 6.75 (2H, d, $J = 8.9$ Hz), 7.58 (1H, s), 7.65-7.69 (2H, m); ^{13}C NMR (CDCl_3 , 100 MHz) δ 25.0, 26.5, 28.8, 30.5, 34.1, 40.8, 50.4, 51.7, 112.6, 118.1, 119.1, 126.7, 148.2, 150.4, 174.0; HRMS (FAB, thioglycerol) calcd for $[\text{C}_{18}\text{H}_{26}\text{N}_4\text{O}_2 + \text{H}]^+$ 331.2134, found 331.2150.

Methyl 6-(3-pyridyl)triazolyhexanoate (6c). Reaction of methyl 6-azidohexanoate **2c** (0.2 g, 1.17 mmol) and 3-ethynylpyridine **5b** (180 mg, 1.74 mmol) within 24 h as described for the synthesis of **3d**, followed by flash chromatography (silica, 3:2 Hexane/EtOAc) gave 294 mg (92%) of **6c** as colorless oil. ^1H NMR (CDCl_3 , 400 MHz) δ 1.34-1.41 (2H, m), 1.67 (2H, m), 1.93-2.01 (2H, m), 2.30 (2H, t, $J = 7.2$ Hz), 3.63 (3H, s), 4.41 (2H, t, $J = 7.1$ Hz), 7.34 (1H, q, $J = 7.9, 4.8$ Hz), 7.85 (1H, s), 8.18 (1H, d, $J = 7.9$ Hz), 8.54 (1H, d, $J = 4.3$ Hz), 8.97 (1H, d, $J = 2.1$ Hz); ^{13}C NMR (CDCl_3 , 100 MHz) δ

24.1, 25.9, 30.0, 33.6, 50.2, 51.5, 119.7, 123.5, 126.6, 132.7, 144.4, 146.8, 148.9, 173.4; HRMS (FAB, thioglycerol) calcd for $[C_{14}H_{18}N_4O_2 + H]^+$ 275.1508, found 275.1491.

Methyl 6-(4-pyridyl)triazolylhexanoate (6d). Reaction of methyl 6-azidohexanoate **2c** (0.2 g, 1.17 mmol) and 4-ethynylpyridine **5c** (180 mg, 1.74 mmol) within 24 h as described for the synthesis of **3d**, followed by flash chromatography (silica, 3:2 Hexane/EtOAc) gave 288 mg (90%) of **6d** as colorless oil. 1H NMR ($CDCl_3$, 400 MHz) δ 1.30-1.38 (2H, m), 1.64 (2H, m), 1.90-1.99 (2H, m), 2.28 (2H, t, $J = 7.2$ Hz), 3.6 (3H, s), 7.39 (2H, t, $J = 7.1$ Hz), 7.67 (2H, dd, $J = 4.5, 1.5$ Hz), 7.90 (1H, s), 8.6 (2H, dd, $J = 4.5, 1.5$ Hz); ^{13}C NMR ($CDCl_3$, 100 MHz) δ 24.1, 25.8, 29.9, 33.5, 50.2, 51.5, 119.7, 120.9, 137.7, 145.1, 150.1, 173.4; HRMS (FAB, thioglycerol) calcd for $[C_{14}H_{18}N_4O_2 + H]^+$ 275.1508, found 275.1512.

Methyl 6-(2-pyridyl)triazolylhexanoate (6e). Reaction of methyl 6-azidohexanoate **2c** (0.2 g, 1.17 mmol) and 2-ethynylpyridine **5d** (180 mg, 1.74 mmol) within 24 h as described for the synthesis of **3d**, followed by flash chromatography (silica, 3:2 Hexane/EtOAc) gave 269 mg (84%) of **6e** as colorless oil. 1H NMR ($CDCl_3$, 400 MHz) δ 1.31-1.39 (2H, m), 1.65 (2H, m), 1.94 (2H, m), 2.27 (2H, t, $J = 7.3$ Hz), 3.62 (3H, s), 4.39 (2H, t, $J = 7.1$ Hz), 7.17-7.20 (1H, m), 7.71 (1H, m), 8.09 (1H, s), 8.13 (1H, d, $J = 7.9$ Hz), 8.52-8.54 (1H, m); ^{13}C NMR ($CDCl_3$, 100 MHz) δ 24.6, 26.3, 30.3, 34.0, 50.5, 51.8, 120.3, 121.9, 122.9, 137.0, 148.4, 149.4, 150.4, 173.7; HRMS (FAB, thioglycerol) calcd for $[C_{14}H_{18}N_4O_2 + H]^+$ 275.1508, found 275.1518.

Methyl 7-(2-pyridyl)triazolylheptanoate (6f). Reaction of methyl 7-azidoheptanoate **2d** (0.225 g, 1.21 mmol) and 2-ethynylpyridine **5d** (134 mg, 1.30 mmol) within 24 h as described for the synthesis of **3d**, followed by flash chromatography (silica, 3:2 Hexane/EtOAc) gave 271 mg (78%) of **6f** as colorless oil. ¹H NMR (CDCl₃, 400 MHz) δ 1.35-1.39 (4H, m), 1.58-1.68 (2H, m), 1.92-1.99 (2H, m), 2.29 (2H, t, *J* = 7.4 Hz), 3.65 (3H, s), 4.42 (2H, t, *J* = 7.1 Hz), 7.21-7.24 (1H, m), 7.75-7.79 (1H, m), 8.14 (1H, s), 8.17 (1H, d, *J* = 7.9 Hz), 8.56-8.58 (1H, m); ¹³C NMR (CDCl₃, 100 MHz) δ 24.5, 26.0, 28.3, 29.9, 33.7, 50.2, 51.3, 119.8, 121.5, 122.5, 136.6, 147.9, 148.9, 149.9, 173.5; HRMS (EI) calcd for [C₁₅H₂₀N₄O₂ + H]⁺ 289.1664, found 289.1665.

Methyl 6-(4-tolyl)triazolylhexanoate (6g). Reaction of methyl 6-azidohexanoate **2c** (0.2 g, 1.17 mmol) and 4-ethynyltoluene **5m** (204 mg, 1.76 mmol) within 24 h as described for the synthesis of **3d**, followed by flash chromatography (silica, 3:2 Hexane/EtOAc) gave 287 mg (85%) of **6g** as colorless oil. ¹H NMR (CDCl₃, 400 MHz) δ 1.18-1.26 (2H, m), 1.53 (2H, m), 1.79 (2H, m), 2.17 (2H, t, *J* = 7.3 Hz), 2.24 (3H, s), 3.52 (3H, s), 4.21 (2H, t, *J* = 7.1 Hz), 7.09 (2H, t, *J* = 7.9 Hz), 7.60 (2H, t, *J* = 8.0 Hz), 7.67 (1H, s); ¹³C NMR (CDCl₃, 100 MHz) δ 20.9, 23.9, 25.6, 29.6, 33.3, 49.6, 51.1, 118.9, 125.0, 127.4, 128.9, 137.2, 147.0, 173.1; HRMS (EI) calcd for [C₁₆H₂₁N₃O₂ + H]⁺ 288.1712, found 288.1732.

Methyl 6-(3-tolyl)triazolylhexanoate (6h). Reaction of methyl 6-azidohexanoate **2c** (0.2 g, 1.17 mmol) and 3-ethynyltoluene **5n** (204 mg, 1.76 mmol) within 24 h as described for the synthesis of **3d**, followed by flash chromatography (silica, 3:2 Hexane/EtOAc) gave

287 mg (84%) of **6h** as colorless oil. ^1H NMR (DMSO- d_6 , 400 MHz) δ 1.33-1.40 (2H, m), 1.63-1.70 (2H, m), 1.95 (2H, m), 2.30 (2H, t, $J = 7.3$ Hz), 2.38 (3H, s), 4.38 (2H, s, $J = 7.1$ Hz), 7.11-7.13 (1H, m), 7.28 (1H, t, $J = 7.6$ Hz), 7.55-7.59 (1H, m), 7.67 (1H, d, $J = 0.5$ Hz), 7.72 (1H, s); ^{13}C NMR (CDCl $_3$, 100 MHz) δ 21.9, 24.5, 26.2, 30.3, 33.9, 50.3, 51.8, 119.8, 122.8, 126.4, 128.8, 128.9, 130.6, 138.5, 147.8, 147.8; HRMS (EI) calcd for $[\text{C}_{16}\text{H}_{21}\text{N}_3\text{O}_2 + \text{H}]^+$ 288.1752, found 288.1744.

Methyl 6-(2-tolyl)triazolylhexanoate (6i). Reaction of methyl 6-azidohexanoate **2c** (0.2 g, 1.17 mmol) and 2-ethynyltoluene **5o** (204 mg, 1.76 mmol) within 24 h as described for the synthesis of **3d**, followed by flash chromatography (silica, 3:2 Hexane/EtOAc) gave 287 mg (60%) of **6i** as colorless oil. ^1H NMR (DMSO- d_6 , 400 MHz) δ 1.25-1.33 (2H, m), 1.58 (2H, m), 1.87 (2H, m), 2.22 (2H, t, $J = 7.3$ Hz), 2.37 (3H, s), 3.56 (3H, s), 4.30 (2H, t, $J = 7.1$ Hz), 7.16 (2H, d, $J = 3.1$ Hz), 7.62 (1H, s), 7.66-7.70 (1H, s); ^{13}C NMR (DMSO- d_6 , 100 MHz) δ 21.1, 23.9, 25.7, 29.7, 33.3, 49.6, 51.1, 121.4, 125.5, 127.5, 128.2, 129.5, 130.3, 134.9, 146.3, 173.1; HRMS (EI) calcd for $[\text{C}_{16}\text{H}_{21}\text{N}_3\text{O}_2 + \text{H}]^+$ 288.1712, found 288.1709.

Methyl 6-(4-anisyl)triazolylhexanoate (6j). Reaction of methyl 6-azidohexanoate **2c** (0.2 g, 1.17 mmol) and 4-ethynylanisole **5r** (0.232 mg, 1.75 mmol) within 24 h as described for the synthesis of **3d**, followed by flash chromatography (silica, 3:2 Hexane/EtOAc) gave 347 mg (98%) of **6j** as colorless oil. ^1H NMR (CDCl $_3$, 400 MHz) δ 1.29-1.37 (2H, m), 1.63 (2H, p, $J = 15.0, 7.3$ Hz), 1.91 (2H, p, $J = 15.0, 7.3$ Hz), 2.27 (2H, t, $J = 7.3$ Hz), 3.61 (3H, s), 3.79 (3H, s), 4.33 (2H, t, $J = 7.1$ Hz), 6.88- 6.92 (2H, m),

7.64 (1H, s), 7.69-7.72 (2H, m); ^{13}C NMR (CDCl_3 , 100 MHz) δ 24.2, 25.9, 30.1, 33.6, 44.9, 51.5, 55.2, 114.0, 118.5, 123.2, 126.7, 147.3, 159.2, 173.4; HRMS (EI) calcd for $[\text{C}_{16}\text{H}_{21}\text{N}_3\text{O}_3 + \text{H}]^+$ 304.1661, found 304.1685.

Methyl 6-(3-anisoyl)triazolylhexanoate (6k). Reaction of methyl 6-azidohexanoate **2c** (0.2 g, 1.17 mmol) and 3-ethynylanisole **5s** (0.232 g, 1.75 mmol) within 24 h as described for the synthesis of **3d**, followed by flash chromatography (silica, 3:2 Hexane/EtOAc) gave 301 mg (85%) of **6k** as colorless oil. ^1H NMR ($\text{DMSO}-d_6$, 400 MHz) δ 1.18-1.26 (2H, m), 1.52 (2H, p, $J = 14.9$, 7.4 Hz), 1.84 (2H, p, $J = 7.0$, 14.3 Hz), 1.93 (2H, t, $J = 7.2$ Hz), 3.79 (3H, s), 4.36 (2H, t, $J = 6.9$ Hz), 6.86-6.89 (1H, m), 7.33 (1H, app. t), 7.39-7.41 (2H, m), 8.58 (1H, s), 8.67 (1H, s), 10.33 (1H, s); ^{13}C NMR ($\text{DMSO}-d_6$, 100 MHz) δ 24.5, 25.4, 29.3, 32.0, 49.3, 55.0, 110.1, 113.3, 117.2, 121.2, 129.8, 131.9, 145.9, 159.3, 168.6; HRMS (EI) calcd for $[\text{C}_{16}\text{H}_{20}\text{N}_3\text{O}_3 + \text{H}]^+$ 304.1661, found 304.1688.

Methyl 6-(2-anisoyl)triazolylhexanoate (6l). Procedure: Reaction of methyl 6-azidohexanoate **2c** (0.2 g, 1.17 mmol) and 2-ethynylanisole **5t** (0.232 mg, 1.75 mmol) within 24 h as described for the synthesis of **3d**, followed by flash chromatography (silica, 3:2 Hexane/EtOAc) gave 336 mg (95%) of **6l** as colorless oil. ^1H NMR (CDCl_3 , 400 MHz) δ 1.41-1.21 (2H, m), 1.47 (2H, p, $J = 15.1$, 7.4 Hz), 1.75 (2H, p, $J = 14.8$, 7.2 Hz), 2.11 (2H, t, $J = 7.42$ Hz), 3.47 (3H, s), 3.73 (3H, s), 4.18 (2H, t, $J = 7.1$ Hz), 6.79 (1H, d, $J = 8.3$ Hz), 6.89 (1H, t, $J = 7.4$ Hz), 7.09-7.13 (1H, m), 8.21 (1H, dd, $J = 7.6$, 1.5 Hz); ^{13}C NMR (CDCl_3 , 100 MHz) δ 23.8, 25.4, 29.5, 33.1, 49.3, 50.9, 54.8, 110.2, 118.8,

120.1, 122.4, 126.6, 128.1, 142.1, 154.8, 172.8; HRMS (FAB, thioglycerol) calcd for $[\text{C}_{16}\text{H}_{21}\text{N}_3\text{O}_3 + \text{H}]^+$ 304.1661, found 304.1676.

Methyl 7-(3-biphenyl)triazolylheptanoate (6q). Reaction of methyl 7-azidoheptanoate **2d** (0.184 g, 1.03 mmol) and 3-ethynylbiphenyl **5i** (185 mg, 1.03 mmol). within 24 h as described for the synthesis of **3d**, followed by flash chromatography (silica, 3:2 Hexane/EtOAc) gave 201 mg (54%) of **6q** as colorless oil. ^1H NMR (CDCl_3 , 400 MHz) δ 1.32-1.35 (4H, m), 1.59 (2H, p, $J=14.72$, 7.36), 1.91 (2H, m), 2.26 (2H, t, $J=7.4$ Hz), 3.62 (3H, s), 4.35 (2H, t, $J=7.1$ Hz), 7.31-7.35 (1H, m), 7.39-7.44 (2H, m), 7.46 (1H, dd, $J=7.6$, 0.4 Hz), 7.51-7.54 (1H, m), 7.60-7.63 (2H, m), 7.73-7.78 (1H, m), 7.79 (1H, s), 8.05-8.06 (1H, m); ^{13}C NMR (CDCl_3 , 100 MHz) δ 24.6, 26.1, 28.4, 30.1, 33.8, 50.2, 51.4, 119.4, 124.2, 124.3, 126.9, 127.2, 128.5, 129.0, 129.3, 130.9, 140.5, 141.5, 147.3, 173.6; HRMS (EI) calcd for $[\text{C}_{22}\text{H}_{25}\text{N}_3\text{O}_2 + \text{H}]^+$ 364.2025, found 364.2045.

Methyl 6-(4-pyridylphenyl)triazolylhexanoate (6s). Reaction of methyl 6-azidohexanoate **2c** (0.2 g, 1.17 mmol) and 4-(4-ethynylphenyl)-pyridine **5l** (0.232 g, 1.76 mmol) within 24 h as described for the synthesis of **3d**, reaction followed by flash chromatography (silica, 1:3 Hexane/EtOAc) gave 274 mg (67%) of **6s** as colorless oil. ^1H NMR (CDCl_3 , 400 MHz) δ 1.32-1.40 (2H, m), 1.62-1.70 (2H, m), 1.91-2.00 (2H, m), 2.29 (2H, t, $J=7.42$), 3.62 (3H, s), 4.38 (2H, t, $J=7.1$ Hz), 7.49-7.50 (2H, m), 7.67 (2H, d, $J=8.3$ Hz), 7.82 (1H, s), 7.91-7.93 (2H, m), 8.61-8.63 (2H, m); ^{13}C NMR (CDCl_3 , 100 MHz) δ 24.0, 25.7, 29.8, 33.4, 50.0, 51.4, 119.8, 121.2, 126.1, 127.2, 127.8, 128.5, 128.9,

131.3, 137.4, 146.8, 147.5, 150.1, 173.6. HRMS (FAB) calcd for $[C_{20}H_{22}N_4O_2 + H]^+$ 351.1821, found 351.1844.

Methyl 7-(4-pyridylphenyl)triazolylheptanoate (6t). Reaction of methyl 7-azidoheptanoate **2d** (0.17 g, 0.91 mmol) and 4-(4-ethynylphenyl)-pyridine **5l** (163 mg, 0.91 mmol) within 24 h as described for the synthesis of **3d**, reaction followed by flash chromatography (silica, 3:2 Hexane/EtOAc) gave 231 mg (70%) of **6t** as colorless oil. 1H NMR ($CDCl_3$, 400 MHz) δ 1.28-1.32 (4H, m), 1.51- 1.58 (2H, m), 1.85-1.92 (2H, m), 2.21 (2H, app. q), 3.58 (3H, s), 4.33 (2H, t, $J = 7.2$ Hz), 7.42-7.46 (2H, m), 7.62 (2H, d, $J = 8.3$ Hz), 7.78 (1H, s), 7.84-7.90 (2H, m), 8.58 (2H, d, $J = 5.4$ Hz); ^{13}C NMR ($CDCl_3$, 100 MHz) δ 24.8, 26.4, 28.6, 30.3, 34.0, 50.5, 51.7, 119.9, 121.3, 126.3, 127.4, 131.5, 137.4, 146.8, 147.5, 150.2, 173.8; HRMS (FAB, MNBA) calcd for $[C_{21}H_{24}N_4O_2 + H]^+$ 365.1977, found 365.1982.

Methyl 7-(6-methoxynaphthyl)triazolylheptanoate (6v). Reaction of methyl 7-azidoheptanoate **2d** (0.15 g, 0.81 mmol), and 2-ethynyl-6-methoxy-naphthalene **5f** (162 mg, 0.89 mmol) within 24 h as described for the synthesis of **3d**, followed by flash chromatography (silica, 6:1:1 Hexane/Acetone/Dichloromethane) gave 202 mg (68%) of **6v** as colorless oil. 1H NMR ($CDCl_3$, 400 MHz) δ 1.45-1.49 (4H, m), 1.72 (2H, m), 2.02-2.07 (2H, m), 2.39 (2H, t, $J = 7.3$ Hz), 3.75 (3H, s), 4.01 (3H, s), 4.42 (2H, t, $J = 7.1$ Hz), 7.20-7.27 (2H, m), 7.87 (2H, app. t), 4.48 (2H, t, $J = 7.1$ Hz), 7.23-7.26 (2H, m), 7.86 (2H, dd, $J = 8.5, 1.9$ Hz), 7.90 (1H, s), 7.98 (1H, dd, $J = 8.4, 1.5$ Hz), 8.34 (1H, s); ^{13}C NMR ($CDCl_3$, 100 MHz) δ 24.6, 26.2, 28.5, 30.1, 33.8, 50.2, 51.5, 55.3, 105.6, 119.11,

119.17, 124.0, 124.2, 125.7, 127.1, 128.8, 129.4, 134.1, 147.7, 157.6, 173.7; HRMS (FAB, MNBA) calcd for $[\text{C}_{21}\text{H}_{25}\text{N}_3\text{O}_3 + \text{H}]^+$ 368.1974, found 368.1977.

Methyl 6-(2-quinolyl)triazolylhexanoate (6w). Reaction of methyl 6-azidoheptanoate **2c** (0.13 g, 0.76 mmol) and 2-ethynylquinoline **5p** (0.09 g, 0.58 mmol) within 24 h as described for the synthesis of **3d**, followed by flash chromatography (silica, 3:2 Hexane/EtOAc) gave 167 mg (68%) of **6w** as colorless oil. ^1H NMR (CDCl_3 , 400 MHz) δ 1.25-1.33 (2H, m), 1.58 (2H, p, $J = 15.0, 7.3$ Hz), 1.89 (2H, p, $J = 14.9, 7.3$ Hz), 2.22 (2H, t, $J = 7.3$ Hz), 3.57 (3H, s), 4.34 (2H, t, $J = 7.1$ Hz), 7.39-7.43 (1H, m), 7.59-7.63 (1H, m), 7.71 (1H, d, $J = 8.0$ Hz), 7.98 (1H, d, $J = 8.4$ Hz), 8.13 (1H, d, $J = 8.6$ Hz), 8.24-8.28 (2H, m); ^{13}C NMR (CDCl_3 , 100 MHz) δ 24.0, 25.7, 29.7, 33.4, 50.0, 51.3, 118.2, 122.3, 125.9, 127.3, 127.4, 128.5, 129.3, 136.4, 147.5, 148.1, 150.1, 173.5; HRMS (FAB, thioglycerol) calcd for $[\text{C}_{18}\text{H}_{20}\text{N}_4\text{O}_2 + \text{H}]^+$ 325.1624, found 325.1621.

Methyl 6-(7-quinolyl)triazolylhexanoate (6x). Reaction of methyl 6-azidoheptanoate **2c** (0.184 g, 1.07 mmol) and 7-ethynylquinoline **5q** (0.15 g, 0.98 mmol) within 24 h as described for the synthesis of **3d**, followed by flash chromatography (silica, 1:4 Hexane/EtOAc) gave 209 mg (60%) of **6x** as colorless oil. ^1H NMR (CDCl_3 , 400 MHz) δ 1.20-1.28 (2H, m), 1.53 (2H, p, $J = 15.0, 7.3$ Hz), 1.79-1.88 (2H, m), 2.16 (2H, t, $J = 7.2$ Hz), 3.49 (3H, s), 4.27 (2H, t, $J = 7.0$ Hz), 7.19-7.23 (1H, m), 7.70 (1H, d, $J = 8.4$ Hz), 7.81 (1H, s), 7.97 (1H, d, $J = 8.0$ Hz), 8.02 (1H, d, $J = 8.4$ Hz), 8.26 (1H, s), 8.75 (1H, d, $J = 4.1$ Hz); ^{13}C NMR (CDCl_3 , 100 MHz) δ 24.1, 25.8, 29.9, 33.5, 50.0, 51.4, 120.2,

120.8, 124.2, 125.1, 127.6, 128.1, 131.5, 135.5, 146.7, 148.0, 150.6, 173.3; HRMS (FAB, thioglycerol) calcd for $[C_{18}H_{20}N_4O_2 + H]^+$ 325.1704, found 325.1697.

Methyl 5-(benzyl)triazolypentanoate (6y). Reaction of methyl 5-azidopentanoate **2b** (0.2 g, 1.27 mmol) and 3-phenyl-1-propyne **5k** (221 mg, 1.91 mmol) within 24 h as described for the synthesis of **3d**, followed by flash chromatography (silica, 3:2 Hexane/EtOAc) gave 287 mg (87%) of **6y** as colorless oil. 1H NMR (DMSO- d_6 , 400 MHz) δ 1.56-1.63 (2H, m), 1.84-1.91 (2H, m), 2.30 (2H, t, $J = 7.2$ Hz), 3.62 (3H, s), 4.05 (2H, s), 4.26 (2H, t, $J = 7.1$ Hz), 7.14 (1H, s), 7.17- 7.29 (5H, m); ^{13}C NMR (DMSO- d_6 , 100 MHz) δ 21.7, 29.5, 32.2, 33.1, 49.7, 51.5, 121.0, 126.2, 128.4, 138.8, 147.3, 172.9; HRMS (FAB, thioglycerol) calcd for $[C_{15}H_{19}N_3O_2 + H]^+$ 274.1555, found 274.1558.

Representative Procedure for Conversion of Methyl Ester to Hydramic Acid.

7-(phenyl)triazolylheptahydroxamic acid (4d).

To a solution of methyl 7-(phenyl)triazolyl-heptanoate **3d** (0.1 g, 0.35 mmol) in 1:1 THF (1.5 mL) and methanol (1.5 mL) was added aqueous hydroxylamine (0.23 mL, 3.74 mmol) and KCN (0.004 g, 0.062 mmol), and the stirring continued for 24 h. The reaction was diluted with EtOAc (30 mL) and washed with saturated $NaHCO_3$ (2 x 30 mL) and saturated brine (30 mL). The organic layer was dried over Na_2SO_4 and concentrated *in vacuo* to give 73 mg (73%) of **4d** as white solid. 1H NMR (DMSO- d_6 , 400 MHz) δ 1.22-1.27 (4H, m), 1.43-1.51 (2H, m), 1.84 (2H, m), 1.92 (2H, t, $J = 7.2$ Hz), 4.36 (2H, t, $J = 7.0$ Hz), 7.31 (1H, t, $J = 7.2$ Hz), 7.43 (2H, t, $J = 7.5$ Hz), 7.82 (2H, d, $J = 7.1$ Hz), 8.56 (1H, s), 8.63 (1H, s), 10.31 (1H, s); ^{13}C NMR (DMSO- d_6 , 100 MHz) δ 24.9, 25.5, 27.9,

29.5, 32.1, 49.4, 120.9, 124.8, 127.5, 128.6, 130.6, 145.9, 168.6; HRMS (FAB, thioglycerol) calcd for $[C_{15}H_{20}N_4O_2 + H]^+$ 289.1664, found 289.1612.

7-(4-anilyl)triazolylheptahydroxamic acid (7b). Reaction of methyl 7-(4-anilyl)-triazolylheptanoate **6b** (0.128 g, 0.38 mmol) and aqueous hydroxylamine (0.25 ml, 4.07 mmol) within 32 h as described for the synthesis of **4d**, gave 95 mg (76%) of **7b** as white solid. 1H NMR (CD_3OD , 400 MHz) δ 1.23-1.36 (4H, m), 1.52-1.59 (2H, m), 1.84-1.91 (2H, m), 2.02 (2H, t, $J = 7.2$ Hz), 2.91 (6H, s), 4.33 (2H, t, $J = 6.9$ Hz), 6.75 (2H, d, $J = 8.5$ Hz), 7.58 (2H, d, $J = 8.5$ Hz), 8.05 (1H, s); ^{13}C NMR (CD_3OD , 100 MHz) δ 26.5, 27.1, 29.4, 31.1, 33.6, 40.7, 51.2, 113.6, 119.6, 120.4, 127.3, 149.2, 151.8, 172.5; HRMS (FAB, thioglycerol) calcd for $[C_{17}H_{25}N_5O_2 + H]^+$ 332.2086, found 332.2071.

6-(3-pyridyl)triazolylhexahydroxamic acid (7c). Reaction of methyl 6-(3-pyridyl)-triazolylhexanoate **6c** (0.14 g, 0.51 mmol) and aqueous hydroxylamine (0.33 ml, 5.37 mmol) within 32 h as described for the synthesis of **4d**, gave 103 mg (74%) of **7c** as white solid. 1H NMR ($CDCl_3$, 400 MHz) δ 1.19-1.30 (2H, m), 1.54 (2H, m), 1.85 (2H, m), 1.96 (2H, t, $J = 7.2$ Hz), 4.34 (2H, t, $J = 7.0$ Hz), 7.28 (1H, q, $J = 7.6, 4.9$ Hz), 8.13 (1H, d, $J = 7.9$ Hz), 8.36-8.38 (2H, m), 8.86 (1H, s); ^{13}C NMR ($CDCl_3$, 100 MHz) δ 26.0, 26.9, 30.8, 33.4, 51.3, 122.9, 125.4, 128.5, 134.7, 146.9, 149.2, 173.2; HRMS (FAB, thioglycerol) calcd for $[C_{13}H_{17}N_5O_2 + H]^+$ 276.1460, found 276.1478.

6-(4-pyridyl)triazolylhexahydroxamic acid (7d). Reaction of methyl 6-(4-pyridyl)-triazolylhexanoate **6d** (0.14 g, 0.51 mmol) and aqueous hydroxylamine (0.33 ml, 5.37 mmol) within 32 h as described for the synthesis of **4d**, gave 96 mg (69%) of **7d** as white

solid. ^1H NMR (DMSO- d_6 , 400 MHz) δ 1.18-1.25 (2H, m), 1.51 (2H, m), 1.85 (2H, m), 1.92 (2H, t, J = 7.2 Hz), 4.40 (2H, t, J = 6.9 Hz), 7.78 (2H, d, J = 5.6 Hz), 8.60 (2H, d, J = 5.5 Hz), 8.78 (1H, s), 10.35 (1H, s); ^{13}C NMR (DMSO- d_6 , 100 MHz) δ 24.5, 25.4, 29.3, 32.1, 49.6, 54.9, 119.3, 123.1, 137.8, 143.7, 150.1, 168.9, 184.0; HRMS (FAB, thioglycerol) calcd for $[\text{C}_{13}\text{H}_{17}\text{N}_5\text{O}_2 + \text{H}]^+$ 276.1460, found 276.1469.

6-(2-pyridyl)triazolylhexahydroxamic acid (7e). Reaction of methyl 6-(2-pyridyl)-triazolylhexanoate **6e** (0.14 g, 0.51 mmol) and aqueous hydroxylamine (0.33 ml, 5.37 mmol) within 32 h as described for the synthesis of **4d**, gave 89 mg (64%) of **7e** as white solid. ^1H NMR (DMSO- d_6 , 400 MHz) δ 1.17-1.25 (2H, m), 1.51 (2H, m), 1.82-1.89 (2H, m), 1.92 (2H, t, J = 7.2 Hz), 4.40 (2H, t, J = 6.9 Hz), 7.30-7.34 (1H, m), 7.85-7.89 (1H, m), 7.99-8.02 (1H, m), 8.56-8.58 (1H, m), 8.60 (1H, s), 10.32 (1H, s); ^{13}C NMR (DMSO- d_6 , 100 MHz) δ 24.5, 25.4, 29.3, 32.0, 49.4, 119.1, 122.6, 122.9, 136.9, 146.9, 149.3, 149.8, 168.5; HRMS (FAB, thioglycerol) calcd for $[\text{C}_{13}\text{H}_{17}\text{N}_5\text{O}_2 + \text{H}]^+$ 276.1460, found 276.1457.

7-(2-pyridyl)triazolylheptahydroxamic acid (7f). Reaction of methyl 7-(2-pyridyl)-triazolylheptanoate **6f** (0.1 g, 0.35 mmol) and aqueous hydroxylamine (0.2 ml, 3.26 mmol) within 32 h as described for the synthesis of **4d**, gave 57 mg (57%) of **7f** as white solid. ^1H NMR (CD $_3$ OD, 400 MHz) δ 1.36-1.40 (4H, m), 1.61 (2H, m), 1.96 (2H, m), 2.07 (2H, t, J = 7.5 Hz), 4.47 (2H, t, J = 7.0 Hz), 7.34-7.37 (1H, m), 7.88-7.92 (1H, m), 8.05 (1H, d, J = 7.9 Hz), 8.40 (1H, s), 8.56 (1H, d, J = 4.4 Hz); ^{13}C NMR (CD $_3$ OD, 100

MHz) δ 26.5, 27.1, 29.4, 31.1, 33.6, 51.4, 121.3, 123.9, 124.3, 138.6, 148.3, 150.8, 150.9, 172.5; HRMS (EI) calcd for $[\text{C}_{14}\text{H}_{19}\text{N}_5\text{O}_2 + \text{H}]^+$ 290.1617, found 290.1590.

6-(4-tolyl)triazolylhexahydroxamic acid (7g). Reaction of methyl 6-(4-tolyl)-triazolylhexanoate **6g** (0.15 g, 0.52 mmol) and aqueous hydroxylamine (0.34 ml, 5.54 mmol) within 32 h as described for the synthesis of **4d**, gave 94 mg (63%) of **7g** as white solid. ^1H NMR ($\text{DMSO-}d_6$, 400 MHz) δ 1.18-1.26 (2H, m), 1.48-1.55 (2H, m), 1.80-1.89 (2H, m), 1.92 (2H, app. t), 2.31 (3H, s), 4.35 (2H, t, $J = 7.4$ Hz), 7.23 (2H, d, $J = 7.5$ Hz), 7.71 (2H, d, $J = 7.8$ Hz), 8.50 (1H, s), 10.31 (1H, s); ^{13}C NMR ($\text{DMSO-}d_6$, 100 MHz) δ 20.8, 24.5, 25.4, 29.3, 32.0, 49.3, 120.6, 124.8, 127.8, 29.2, 136.8, 146.0, 168.5; HRMS (FAB, MNBA) calcd for $[\text{C}_{15}\text{H}_{20}\text{N}_4\text{O}_2 + \text{H}]^+$ 289.1664, found 289.1636.

6-(3-tolyl)triazolylhexahydroxamic acid (7h). Reaction of methyl 6-(3-tolyl)-triazolylhexanoate **6h** (0.15 g, 0.52 mmol) and aqueous hydroxylamine (0.34 ml, 5.54 mmol) within 32 h as described for the synthesis of **4d**, gave 115 mg (77%) of **7h** as white solid. ^1H NMR ($\text{DMSO-}d_6$, 400 MHz) δ 1.17-1.24 (2H, m), 1.44-1.57 (2H, m), 1.83 (2H, p, $J = 14.4, 7.1$ Hz), 1.92 (2H, t, $J = 7.2$ Hz), 2.33 (3H, s), 4.35 (2H, t, $J = 6.9$ Hz), 7.11 (1H, d, $J = 7.5$ Hz), 7.29 (1H, t, $J = 7.6$ Hz), 7.60 (1H, d, $J = 7.2$ Hz), 7.65 (1H, s), 8.52 (1H, s); ^{13}C NMR ($\text{DMSO-}d_6$, 100 MHz) δ 21.1, 24.5, 25.5, 29.3, 32.0, 49.3, 120.9, 122.0, 125.4, 128.2, 128.5, 130.5, 137.5, 146.1, 168.6; HRMS (EI) calcd for $[\text{C}_{15}\text{H}_{20}\text{N}_4\text{O}_2 + \text{H}]^+$ 289.1664, found 289.1684.

6-(3-tolyl)triazolylhexahydroxamic acid (7i). Reaction of methyl 6-(3-tolyl)-triazolylhexanoate **6i** (0.15 g, 0.52 mmol) and aqueous hydroxylamine (0.34 ml, 5.54 mmol) within 32 h as described for the synthesis of **4d**, gave 116 mg (78%) of **7i** as white solid. ¹H NMR (DMSO-*d*₆, 400 MHz) δ 1.21-1.29 (2H, m), 1.52 (2H, m), 1.82-1.89 (2H, m), 1.93 (2H, t, *J* = 7.9 Hz), 2.41 (3H, s), 4.38 (2H, t, *J* = 6.9 Hz), 7.23-7.28 (3H, m), 7.70-7.73 (1H, m), 8.36 (1H, s); ¹³C NMR (DMSO-*d*₆, 100 MHz) δ 21.2, 24.5, 25.5, 29.4, 32.0, 49.2, 122.9, 125.7, 127.4, 127.9, 129.9, 130.6, 134.6, 145.2, 168.5; HRMS (EI) calcd for [C₁₅H₂₀N₄O₂ + H]⁺ 289.1664, found 289.1681.

6-(4-anisoly)triazolylhexahydroxamic acid (7j). Reaction of methyl 6-(4-anisoly)-triazolylhexanoate **6j** (0.15 g, 0.52 mmol) and aqueous hydroxylamine (0.34 ml, 5.2 mmol) within 32 h as described for the synthesis of **4d**, gave 99 mg (60%) of **7j** as white solid. ¹H NMR (DMSO-*d*₆, 400 MHz) δ 1.18-1.26 (2H, m), 1.52 (2H, p, *J* = 14.5, 6.9 Hz), 1.83 (2H, p, *J* = 14.5, 7.1 Hz), 1.93 (2H, t, *J* = 7.3 Hz), 4.34 (2H, t, *J* = 7.0 Hz), 6.99 (2H, d, *J* = 7.9 Hz), 7.74 (2H, d, *J* = 7.9 Hz), 8.44 (1H, s), 10.31 (1H, s); ¹³C NMR (DMSO-*d*₆, 100 MHz) δ 24.5, 25.4, 29.3, 32.0, 49.2, 55.0, 114.0, 120.0, 123.2, 126.2, 145.4, 158.6, 168.5; HRMS (FAB, thioglycerol) calcd for [C₁₅H₂₀N₄O₃ + H]⁺ 305.1613, found 305.1629.

6-(3-anisoly)triazolylhexahydroxamic acid (7k). Reaction of methyl 6-((3-anisoly)triazolylhexanoate **6k** (0.15 mg, 0.52 mmol) and aqueous hydroxylamine (0.34 ml, 5.2 mmol) within 32 h as described for the synthesis of **4d**, gave 75 mg (50%) of **7k** as white solid. ¹H NMR (DMSO-*d*₆, 400 MHz) δ 1.18-1.26 (2H, m), 1.52 (2H, p, *J* =

15.0, 7.4 Hz), 1.84 (2H, p, $J = 14.4, 7.0$ Hz), 1.93 (2H, t, $J = 7.2$ Hz), 3.79 (3H, s), 4.36 (2H, t, $J = 6.9$ Hz), 6.86-6.89 (1H, m), 7.33 (1H, app. t), 7.39-7.41 (2H, m), 8.59 (1H, s), 10.3 (1H, s); ^{13}C NMR (DMSO- d_6 , 100 MHz) δ 24.5, 25.4, 29.3, 32.0, 49.3, 55.0, 110.1, 113.3, 117.2, 121.2, 129.8, 131.9, 145.9, 159.3, 168.5; HRMS (FAB, thioglycerol) calcd for $[\text{C}_{15}\text{H}_{20}\text{N}_4\text{O}_3 + \text{H}]^+$ 305.1613, found 305.1633.

6-(2-anisoly)triazolyhexahydroxamic acid (7l). Reaction of methyl 6-(2-anisoly)triazolyhexanoate **6l** (0.15 mg, 0.52 mmol) and aqueous hydroxylamine (0.34 ml, 5.2 mmol) within 32 h as described for the synthesis of **4d**, gave 82 mg (55%) of **7l** as white solid. ^1H NMR (DMSO- d_6 , 400 MHz) δ 1.41-1.21 (2H, m), 1.19-1.26 (2H, m), 1.52 (2H, p, $J = 15.0, 7.5$ Hz), 1.80-1.88 (2H, m), 1.93 (2H, t, $J = 7.3$ Hz), 3.90 (3H, s), 4.38 (2H, t, $J = 7.0$ Hz), 7.03 (1H, app. t), 7.11 (1H, d, $J = 8.2$ Hz), 7.28-7.33 (1H, m), 8.12 (1H, dd, $J = 7.6, 1.7$ Hz), 8.36 (1H, s), 10.23 (1H, s); ^{13}C NMR (DMSO- d_6 , 100 MHz) δ 24.5, 25.5, 29.5, 32.0, 49.1, 55.3, 111.4, 120.3, 123.7, 126.2, 128.5, 141.4, 155.0, 168.5; HRMS (FAB, MNBA) calcd for $[\text{C}_{15}\text{H}_{20}\text{N}_4\text{O}_3 + \text{H}]^+$ 305.1673, found 305.1576.

7-(3-biphenyl)triazolyheptahydroxamic acid (7q). Reaction of methyl 7-(3-biphenyl)triazolyheptanoate **6q** (0.1 g, 0.27 mmol) and aqueous hydroxylamine (0.2 ml, 3.26 mmol) within 32 h as described for the synthesis of **4d**, gave 47 mg (48%) of **7q** as white solid. ^1H NMR (CD_3OD , 400 MHz) δ 1.18-1.21 (4H, m), 1.39-1.49 (2H, m), 1.72-1.80 (2H, m), 1.90 (2H, t, $J = 7.5$ Hz), 2.02 (2H, t, $J = 7.5$ Hz), 4.21-4.25 (2H, m), 7.14-7.18 (1H, m), 7.24-7.28 (2H, m), 7.31 (1H, d, $J = 7.6$ Hz), 7.39-7.41 (1H, m), 7.47-7.50 (2H, m), 7.58-7.61 (1H, m), 7.91 (1H, d, $J = 1.6$ Hz), 8.19 (1H, d, $J = 6.1$ Hz). ^{13}C NMR

(CD₃OD, 100 MHz) δ 26.5, 27.1, 29.4, 31.0, 33.6, 51.3, 122.2, 124.9, 125.3, 127.6, 127.8, 128.4, 129.7, 130.3, 132.0, 141.7, 142.9, 148.5, 172.8. HRMS (EI) calcd for [C₂₁H₂₄N₄O₂ + H]⁺ 365.1977, found 365.1954.

6-(4-pyridylphenyl)triazolylhexahydroxamic acid (7s). Reaction of methyl 6-(4-pyridylphenyl)triazolylhexanoate **6s** (0.1 g, 0.28 mmol) and aqueous hydroxylamine (0.2 ml, 2.7 mmol) within 32 h as described for the synthesis of **4d**, gave 54 mg (54%) of **7s** as white solid. ¹H NMR (DMSO-*d*₆, 400 MHz) δ 1.24-1.33 (2H, m), 1.50-1.58 (2H, m), 1.83-1.98 (4H, m), 4.39 (2H, t, *J* = 7.3 Hz), 7.75-7.76 (2H, m), 7.90 (2H, d, *J* = 8.3 Hz), 7.98 (2H, d, *J* = 8.3 Hz), 8.64 (1H, s), 8.66-8.68 (2H, m), 10.34 (1H, s). ¹³C NMR (DMSO-*d*₆, 100 MHz) δ 24.5, 25.4, 29.3, 32.0, 49.4, 120.8, 121.5, 125.5, 127.1, 131.5, 135.9, 145.3, 146.0, 149.9, 168.5. HRMS (FAB, thioglycerol) calcd for [C₁₉H₂₁N₅O₂ + H]⁺ 352.1773, found 352.1756.

7-(4-pyridylphenyl)triazolylheptahydroxamic acid (7t). Reaction of methyl 7-(4-pyridylphenyl)triazolylheptanoate **6t** (0.1 g, 0.27 mmol) and aqueous hydroxylamine (0.2 ml, 3.26 mmol) within 32 h as described for the synthesis of **4d**, followed by prep TLC (silica, 91:9 Dichloromethane/MeOH) gave 54 mg (55%) of **7t** as white solid. ¹H NMR (DMSO-*d*₆, 400 MHz) δ 1.24-1.33 (4H, m), 1.44-1.50 (2H, m), 1.83-1.87 (2H, m), 2.18 (2H, t, *J* = 7.3 Hz), 4.39 (2H, t, *J* = 7.3 Hz), 7.74-7.76 (2H, m), 7.90 (2H, d, *J* = 8.3 Hz), 7.98 (2H, d, *J* = 8.3 Hz), 8.63 (2H, d, *J* = 4.4 Hz), 8.69 (1H, s), 10.34 (1H, s); ¹³C NMR (DMSO-*d*₆, 100 MHz) δ 24.3, 25.6, 27.9, 29.4, 33.5, 49.5, 120.7, 121.5, 125.5, 127.1,

131.5, 135.9, 145.3, 146.0, 149.9, 174.0; HRMS (FAB, thioglycerol) calcd for $[\text{C}_{20}\text{H}_{23}\text{N}_5\text{O}_2 + \text{H}]^+$ 366.1930, found 365.1942.

7-(6-methoxynaphthalyl)triazolylheptahydroxamic acid (7v). Reaction of methyl 7-(6-methoxynaphthalyl)triazolylheptanoate **6v** (0.217 g, 0.59 mmol) and aqueous hydroxylamine (0.4 ml, 6.52 mmol) within 32 h as described for the synthesis of **4d**, gave 110 mg (51%) of **7v** as white solid. ^1H NMR (DMSO- d_6 , 400 MHz) δ 1.26-1.28 (4H, m), 1.43-1.53 (2H, m), 1.82-1.89 (2H, m), 1.92 (2H, t, $J = 7.2$ Hz), 3.87 (3H, s), 4.39 (2H, t, $J = 7.0$ Hz), 7.17 (1H, dd, $J = 8.9, 2.5$ Hz), 7.33 (1H, d, $J = 2.3$ Hz), 7.85-7.93 (3H, m), 8.30 (1H, s), 8.63 (1H, s), 8.66 (1H, s), 10.35 (1H, s); ^{13}C NMR (DMSO- d_6 , 100 MHz) δ 24.9, 25.6, 28.0, 29.5, 32.1, 49.4, 55.1, 105.8, 118.9, 120.9, 123.1, 123.9, 125.8, 127.1, 128.3, 129.2, 133.6, 146.2, 157.1, 168.7; HRMS (EI) calcd for $[\text{C}_{20}\text{H}_{24}\text{N}_4\text{O}_3 + \text{H}]^+$ 369.1926, found 369.1900.

6-(2-quinolyl)triazolylhexahydroxamic acid (7w). Reaction of methyl 6-(2-quinolyl)-triazolylhexanoate **6w** (0.129 g, 0.39 mmol) and aqueous hydroxylamine (0.26 ml, 3.9 mmol) within 32 h as described for the synthesis of **4d**, gave 77 mg (60%) of **7w** as white solid. ^1H NMR (DMSO- d_6 , 400 MHz) δ 1.24 (2H, app. p), 1.53 (2H, p, $J = 14.7, 7.1$ Hz), 1.86-1.95 (4H, m), 4.45 (2H, t, $J = 7.0$ Hz), 7.56-7.60 (1H, m), 7.75-7.79 (1H, m), 7.98 (2H, d, $J = 8.4$ Hz), 8.21 (1H, d, $J = 8.5$ Hz), 8.45 (1H, d, $J = 8.5$ Hz), 8.65 (1H, s), 8.81 (1H, s), 10.32 (1H, s); ^{13}C NMR (DMSO- d_6 , 100 MHz) δ 24.5, 25.4, 29.3, 32.0, 49.5, 117.9, 123.7, 126.1, 127.0, 127.8, 128.2, 129.8, 136.9, 146.9, 147.2, 150.0, 168.6; HRMS (FAB, thioglycerol) calcd for $[\text{C}_{17}\text{H}_{19}\text{N}_5\text{O}_2 + \text{H}]^+$ 326.1576, found 326.1572.

6-(7-quinolyl)triazolylhexahydroxamic acid (7x). Reaction of methyl 6-(7-quinolyl)-triazolylhexanoate **6x** (0.1 g, 0.31 mmol) and aqueous hydroxylamine (0.2 ml, 3.1 mmol) within 32 h as described for the synthesis of **4d**, followed by prep TLC (9 % MeOH in Dichloromethane) gave 66 mg (66%) of **7x** as white solid. ^1H NMR (DMSO- d_6 , 400 MHz) δ 1.21-1.29 (2H, m), 1.50-1.57 (2H, m), 1.84-1.95 (4H, m), 4.41 (2H, t, $J = 7.3$ Hz), 7.50 (1H, q, $J = 8.4, 4.3$ Hz), 8.04 (1H, d, $J = 8.5$ Hz), 8.10 (1H, dd, $J = 8.5, 1.6$ Hz), 8.33-8.36 (1H, m), 8.44 (1H, s), 8.61-8.64 (1H, m), 8.82 (1H, s), 8.90 (1H, q, $J = 4.2, 4.1$ Hz), 10.31 (1H, s); ^{13}C NMR (DMSO- d_6 , 100 MHz) δ 26.0, 26.9, 30.9, 33.4, 51.3, 122.4, 123.1, 124.8, 125.6, 129.8, 129.3, 133.3, 137.9, 147.6, 148.7, 151.6, 172.3; HRMS (EI) calcd for $[\text{C}_{17}\text{H}_{19}\text{N}_5\text{O}_2 + \text{H}]^+$ 326.1617, found 326.1646.

5-(benzyl)triazolylpentahydroxamic acid (7y). Reaction of methyl 5-(benzyl)triazolylpentanoate **6y** (0.15 g, 0.52 mmol) and aqueous hydroxylamine (0.5 ml, 8.15 mmol) within 32 h as described for the synthesis of **4d**, gave 111 mg (78%) of **7y** as white solid. ^1H NMR (DMSO- d_6 , 400 MHz) δ 1.38-1.45 (2H, m), 1.71-1.77 (2H, m), 1.95 (2H, t, $J = 7.28$), 3.96 (2H, s), 4.27 (2H, t, $J = 7.10$), 7.16-7.29 (5H, m), 7.81 (1H, s), 8.67 (1H, s), 10.34 (1H, s); ^{13}C NMR (DMSO- d_6 , 100 MHz) δ 22.1, 29.3, 31.3, 31.5, 48.8, 122.1, 125.8, 128.1, 128.2, 139.4, 145.6, 168.3; HRMS (FAB, thioglycerol) calcd for $[\text{C}_{14}\text{H}_{18}\text{N}_4\text{O}_2 + \text{H}]^+$ 275.1508, found 275.1506.

Representative Procedure for the Alkyne Transformation Reaction.

4-(4-Ethynylphenyl)pyridine (**5l**):

Reaction of 4-(4-formylphenyl)pyridine (0.3 g, 1.64 mmol), anhydrous K₂CO₃ (0.679 g, 4.92 mmol) and Bestmann-Ohira reagent (0.627 g, 3.27 mmol) within 24 h followed by flash chromatography (silica gel, 2:1 Hexane/EtOAc) gave 261 mg (89%) of **5l** as a white solid. ¹H-NMR (CDCl₃, 400MHz) δ 3.16 (1H, s), 7.47 (2H, d, *J* = 6.4 Hz), 7.59 (4H, s), 8.66 (2H, d, *J* = 6.4Hz). HRMS (EI) calc for [C₁₃H₉N] 179.0735, found 179.0746.

2-Ethynylquinoline (**5p**):

The required quinoline-2-carboxaldehyde was synthesized from the corresponding 2-methylquinoline through selenium dioxide oxidation.³¹ Quionline-2-carboxyladehyde (0.21 g, 1.33 mmol), anhydrous K₂CO₃ (0.551 g, 3.99 mmol) and Bestmann-Ohira reagent (513 mg, 2.67 mmol) gave 153 mg (73%) of **5p** as white solid. ¹H NMR (CDCl₃, 400 MHz) δ 3.20 (1H, s), 7.43-7.48 (2H, m), 7.62-7.66 (1H, m), 7.69 (1H, d, *J* = 8.1 Hz), 8.01-8.04 (2H, m). ¹³C NMR (CDCl₃, 100 MHz) δ 76.9, 82.6, 123.2, 126.4, 126.5, 126.6, 128.5, 129.2, 135.4, 141.4, 147.1

7-Ethynylquinoline (**5q**):

The required quinoline-7-carboxaldehyde was synthesized from the corresponding 7-methylquinoline through selenium dioxide oxidation.³¹ Quionline-7-carboxyladehyde (0.21 g, 1.33 mmol), anhydrous K₂CO₃ (0.551 g, 3.99 mmol) and Bestmann-Ohira reagent (513 mg, 2.67 mmol) gave 163 mg (78%) of **5q** as white solid. ¹H NMR (CDCl₃,

400 MHz) δ 3.16 (1H, s), 7.21 (1H, q, J = 8.28, 4.23), 7.41 (1H, dd, J = 8.4, 1.5 Hz), 7.56 (1H, d, J = 8.38), 7.91-7.94 (2H, m), 8.76 (1H, dd, J = 4.2, 1.7 Hz) ^{13}C NMR (CDCl_3 , 100 MHz) δ 79.1, 83.0, 121.5, 126.1, 127.7, 126.6, 129.1, 129.4, 133.1, 135.6, 150.9.

2.7 REFERENCES

1. Miller, T. A.; Witter, D. J.; Belvedere, S. *J. Med. Chem.* **2003**, 46, 5097.
2. Finnin, M. S.; Donigian, J. R.; Cohen, A.; Richon, V. M.; Rifkind, R. A.; Marks, P. A.; Breslow, R.; Pavletich, N. P. *Nature* **1999**, 401, 188.
3. Suzuki, T.; Matsuura, A.; Kouketsu, A.; Nakagawa, H.; Miyata, N. *Bioorg. Med. Chem. Lett.* **2005**, 15, 331.
4. Samoza, J. R.; Skene, R. J.; Katz, B. A.; Mol, C.; Ho, J. D.; Jennings, A. J.; Luong, C.; Arvai, A.; Buggy, J. J.; Chi, E.; Tang, J.; Sang, B. C.; Verner, E.; Wynands, R.; Leahy, E. M.; Dougan, D. R.; Snell, G.; Navre, M.; Knuth, M. W.; Swanson, R. V.; McRee, D. E.; Tari, L. W. *Structure* **2004**, 12, 1325.
5. Vannini, A.; Volpari, C.; Filocamo, G.; Casavola, E. C.; Brunetti, M.; Renzoni, D.; Chakravarty, P.; Paolini, C.; De Francesco, R.; Gallinari, P.; Steinkuhler, C.; Di Marco, S. *Proc. Natl. Acad. Sci. U.S.A.* **2004**, 101, 15064.
6. Monneret, C. *Eur. J. Med. Chem.* **2005**, 40, 1.
7. Bieliauskas, A. V.; Pflum, M. K. H. *Chem. Soc. Rev.* **2008**, 37, 1402.
8. Mwakwari, S.C.; Patil, V.; Guerrant, W., Oyelere, A.K. *Curr. Top. Med. Chem.* **2010**, 10, 1423.
9. Wong, J.; Hong, R.; Schreiber, S. *J. Am. Chem. Soc.* **2003**, 125, 5586.
10. Haggarty, S. J.; Koeller, K. M.; Wong, J. C.; Grozinger, C. M.; Schreiber, S. L. *Proc. Natl. Acad. Sci. U.S.A.* **2003**, 100, 4389.
11. Numerous examples of Cu(I) catalyzed Huisgen cycloaddition reaction have appeared in the literature (A comprehensive list is available at <http://www.scripps.edu/chem/sharpless/click.html>). Cited here are two pioneering examples: (a) Rostovtsev, V. V.; Green, L. G.; Fokin, V. V.; Sharpless, K. B. *Angew. Chem., Int. Ed.* **2002**, 41, 2596 (b) Tornøe, C. W.; Christensen, C.; Meldal, M. *J. Org. Chem.* **2002**, 67, 3057.

12. For reviews on application of click chemistry see: (a) Kolb, H. C.; Sharpless, K. B. *DDT* **2003**, 8, 1128–1137; (b) Bock, V. D.; Hiemstra, H.; van Maarseveen, J. H. *Eur. J. Org. Chem.* **2006**, 51.
13. Savariar, E. N.; Aathimanikandan, S. V.; Thayumanavan, S. *J. Am. Chem. Soc.* **2006**, 128, 16224.
14. Heine, H. W.; Becker, E. B.; Lane, J. F. *J. Am. Chem. Soc.* **1953**, 75, 4514.
15. (a) Collman, J. P.; Devaraj, N. K.; Chidsey, C. E. *D. Langmuir* **2004**, 20, 1051–1053 (b) Shon, Y.; Kelly, K. F.; Halas, N. J.; Lee, T. R. *Langmuir* **1999**, 15, 5329.
16. Ho, C. Y.; Strobel, E.; Ralbovsky, J.; Galemme, R. A. *J. Org. Chem.* **2005**, 70, 4873.
17. Quesada, E.; Taylor, R. J. K. *Tetrahedron Lett.* **2005**, 6, 6473.
18. Ghosh, A. K.; Bischoff, A.; Cappiello, J. *J. Eur. Org. Chem.* **2003**, 821.
19. (a) Anhoury, M. L.; Arickx, M.; Crooy, P.; De Neys, R.; Eliaers, J. *J. Chem. Soc. Perkin 1* **1974**, 191; (b) Callant, P.; D’Haenens, L.; Vandewalle, M. *Synth. Commun.* **1984**, 14, 155.
20. HDAC Fluorimetric Assay/Drug Discovery Kit—AK-500 Manual. Fluorescent Assay System (BIOMOL - International, Plymouth Meeting, PA), **2005**.
21. Breslow, R.; Belvedere, S.; Gershell, L. *Helv. Chim. Acta* **2000**, 83, 1685.
22. Woo, S. H.; Frechette, S.; Abou Khalil, E.; Bouchain, G.; Vaisburg, A. *et al. J. Med. Chem.* **2002**, 45, 2877.
23. Morris, G. M.; Goodsell, D. S.; Halliday, R. S.; Huey, R.; Hart, W. E.; Belew, R. K.; Olson, A. J. *J. Comput. Chem.* **1998**, 19, 1639.
<http://www.scripps.edu/pub/olsonweb/doc/autodock>
24. Wang, D. F.; Wiest, O.; Helquist, P.; Lan-Hargest, H. Y.; Wiech, N. L. *J. Med. Chem.* **2004**, 47, 3409.
25. Lu, Q.; Wang, D. S.; Chen, C. S.; Hu, Y. D.; Chen, C. S. *J. Med. Chem.* **2005**, 48, 5530.
26. Butler, L. M.; Agus, D. B.; Scher, H. I.; Higgins, B.; Rose, A.; Cordon-Cardo, C.; Thaler, H. T.; Rifkind, R. A.; Marks, P. A.; Richon, V. M. *In Vivo Cancer Res.* **2000**, 60, 5165.
27. Mosmann, T. J. *Immunol. Methods* **1983**, 65, 55.
28. Freshney, R. *New York, NY: Alan R. Liss, Inc.*, **1987**, p. 117.

29. Suzuki, T.; Nagano, Y.; Kouketsu, A.; Matsuura, A.; Maruyama, S.; Kurotaki, M.; Nakagawa, H.; Miyata, N. *J. Med. Chem.* **2005**, 48, 1019.
30. Chen, P. C.; Emrich, R. E.; Patel, P. A.; Oyelere, A. K. *Bioorg. Med. Chem.* **2007**, 15, 7288.
31. The reaction could also be catalyzed by the addition of Cu-chelating ligand called tris-(benzyltriazolylmethyl) amine (TBTA).

CHAPTER 3

MOLECULAR ARCHITECTURE OF ZINC CHELATING SPLICEOSOME ASSEMBLY INHIBITORS

3.1 Alternative Splicing –

Maturation of the eukaryotic precursor messenger RNA (pre-mRNA) is catalyzed by the spliceosome, a large and dynamic ribonucleo-particle consisting of 5 small nuclear RNAs (snRNAs) and close to 150 proteins. The splicing reaction is a 2-step transesterification reaction which excises the introns and ligates the exons.¹ In first step, the 2'-OH of adenosine from the branch site nucleophilically attacks the phosphodiester bond at the 5'-splice site forming the lariat intermediate. During second step, the 3'-OH of the released 5' exon then performs nucleophilic attack at the 3' splice site, releasing intron lariat. The process is tightly controlled by intricate interplays between RNA-protein, RNA-RNA and protein-protein which ultimately determine the identity of the protein formed from a pre-mRNA.² Understanding the splicing mechanism is of prime importance as many human genetic conditions, such as β -thalassemia, inherited breast cancer and many types of neurological diseases, are associated with aberrant pre-mRNA splicing.³⁻⁵ Spliceosome formation proceeds through coordinated assemblies of complexes – A, B, B* and C (Figure 3-1). The detail of molecular interactions between the five small nuclear ribonucleoproteins (snRNPs - U1, U2, U4, U5 & U6) and proteins in the spliceosome continues to be a subject of intense research. Remarkable advances have been made in the characterization and structural elucidation of the various spliceosome complexes.⁶⁻¹⁶ These studies have furnished exquisite information about the

spliceosome assembly at the RNA level. With the increased number of known splicing factors, we are now gaining an appreciation that the dynamic nature of the spliceosome is much more complex than simple addition and release of individual snRNPs proteins. However, the order of recruitment, interaction between these splicing factors, and signals that trigger their addition and release from the spliceosome remains poorly understood.¹⁷ Additionally, little is known about the mechanism of catalysis and the trigger for the global conformational changes which ensure the fidelity of splicing. The availability of agents which perturb splicing at specific stages will greatly enhance our understanding of the workings of the spliceosome.

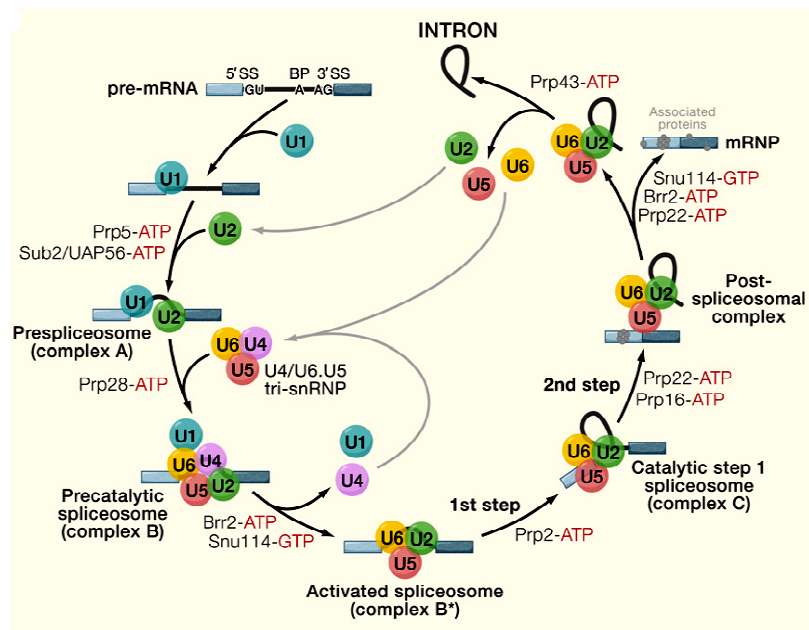


Figure 3-1: Steps involved in splicing mechanism.¹⁸

Several small molecules which inhibit splicing have been identified. Examples of small molecule splicing inhibitors include: antitumor drugs such as pladienolide B, FR901464 and spliceostatin A;^{19,20} antibiotics such as tetracyclines, neomycin and streptomycin;²¹ isoginkgetin²² and selected histone deacetylases and histone

acetyltransferases inhibitors.²³⁻²⁹ The specific spliceosome targets of a subset of these compounds have been elucidated; however, targets for several of these compounds remain unknown. With few exceptions,³⁰ the structural attributes which conferred splicing inhibition on most of these compounds are yet to be elucidated. This lack of clear understanding may be partly due to the structural complexities of many of these compounds.

Several spliceosome associated proteins possess potential enzymatic activities whose purpose in splicing reaction remain unclear.^{25,31} Specifically, many of these spliceosomal proteins possess zinc binding motifs, suggesting that zinc metal may have functional and/or structural roles in splicing. Additionally, histone deacetylases (HDACs), classic Zn-metallo-proteases, have been shown to be closely associated with spliceosome complexes, although their precise functions in splicing process are not clear.^{24,32,33} In fact, zinc depletion by the random Zn-chelator 1,10-phenanthroline (1,10-PHE), has been shown to inhibit the second step of splicing.³⁴ We have shown previously that specific zinc chelating agents that perturb the protein acetylation state, through inhibition of HDAC activity, blocked splicing cycle at distinct stages.²⁵ The exact relationship between zinc chelation, protein acetylation state and splicing reaction integrity was not clear from this study as limited set of HDACi were screened. We sought to clarify this relationship by screening a more structurally diverse HDACi library.³⁵⁻⁴⁰ We report herein the elucidation of unique molecular features that confer splicing inhibition to zinc chelating agents with HDAC inhibition activities. Characterization of the splicing complexes that accumulate on native gels, demonstrates that these agents specifically stalled the spliceosome assembly at A-like complex. Because there is no

correlation between HDAC and splicing inhibition activities of these compounds, we conclude that the primary target(s) of their splicing inhibition are not HDACs.

3.2 Screening of HDACi as Splicing Assembly Inhibitors

Premised on earlier work that demonstrated close association of HDACs with mixed population of spliceosome,^{32,33,41} we have previously investigated the prospect of splicing inhibition by selected HDACi – hydroxamate based drugs SAHA, scriptaid, and trichostatin A (TSA); and non-hydroxamate MS-275 (Figure 3-2). These HDACi stalled the spliceosome assembly at A-like complex with sub-micromolar IC₅₀ (concentration giving 50% inhibition).²⁵ However, there is no clear evidence linking the effects of these HDACi on splicing with HDAC inhibition as their splicing IC₅₀ are several orders of magnitude higher than the reported values for HDAC inhibition.

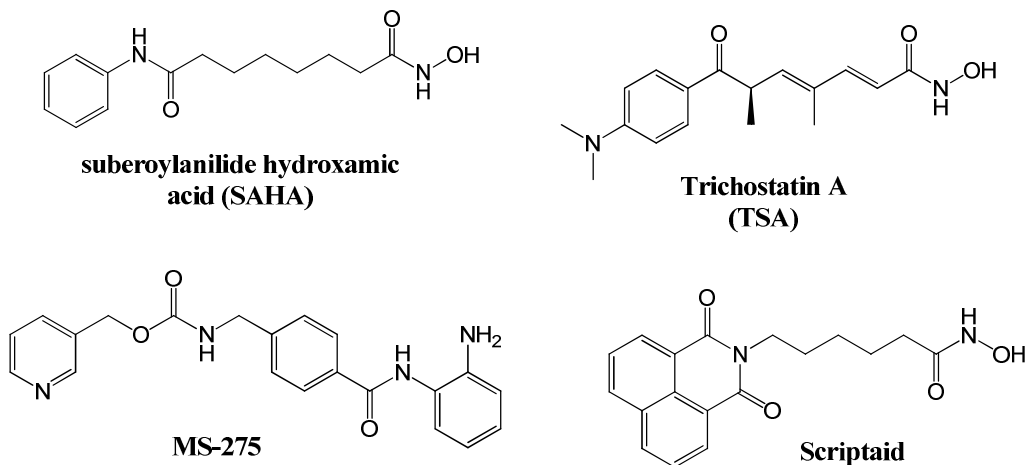


Figure 3-2. Structures of HDACi which stalled the spliceosome assembly at A-like complex.

HDAC has 18 known isoforms, organized into four different classes. Classes I, II, and IV depend on a catalytic zinc ion and differ by cellular localization, while Class III HDACs require NAD⁺.⁴² The prototypical pharmacophore for HDACi consists of three

distinct structural motifs: a recognition cap group, a hydrophobic linker, and the zinc binding group (ZBG).^{38,43} The HDACi recognition cap group moieties make interactions with amino acid residues on the surface of HDACs and present excellent opportunities for the selective modulation of their biological activities.³⁸ We surmised that profiling the splicing inhibition activities of HDACi with diversity within their three distinct structural motifs will unravel the links between HDAC inhibition and splicing fidelity. Toward this end, we first screened a small (63-member), yet structurally diverse HDACi library (Figure 3-3) for their effect on splicing at 50 μ M. The activity of HDACi in the screened library, against HDAC1 and HeLa cell nuclear extract HDACs, ranges from single digit- to mid-nanomolar.^{35-37,39,40} Despite their potency, these HDACi did not broadly inhibit splicing.

Table 3-1: HDACi Library Screened for pre-mRNA Splicing Inhibition

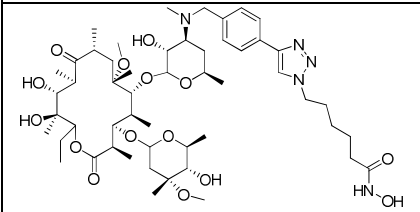
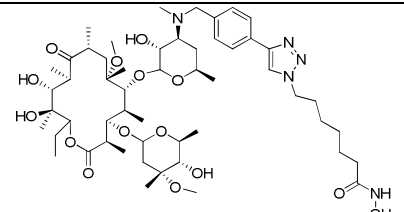
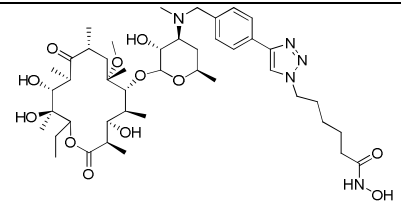
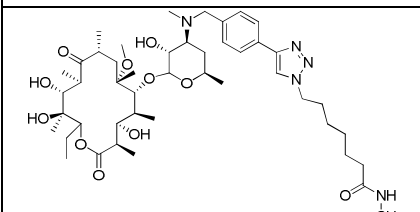
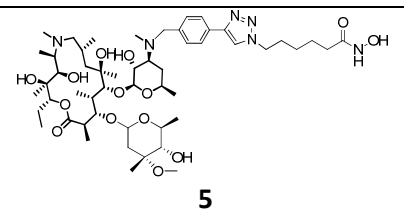
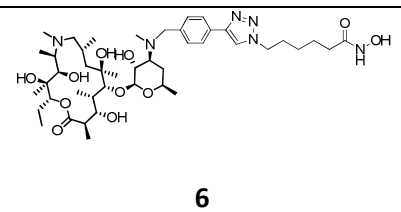
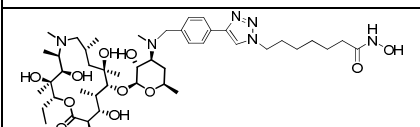
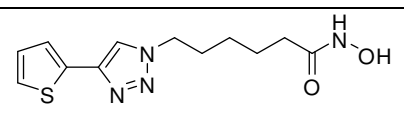
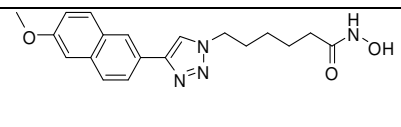
Structure	Structure	Structure
 1	 2	 3
 4	 5	 6
 7	 8	 9

Table 3-1 continued.

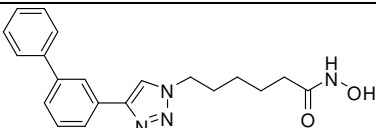
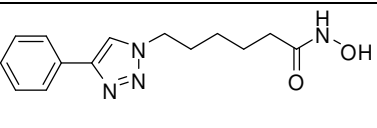
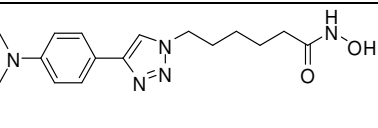
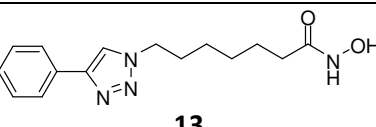
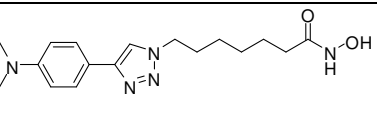
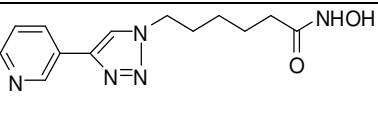
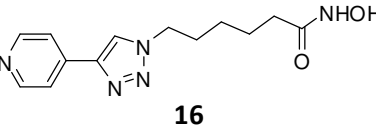
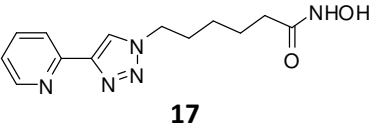
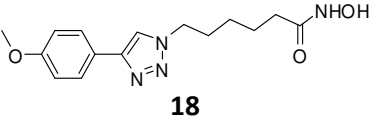
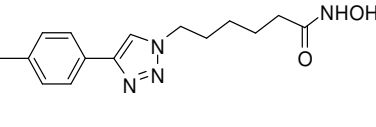
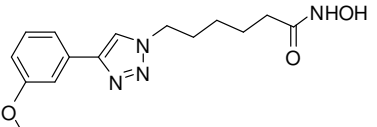
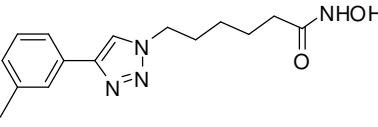
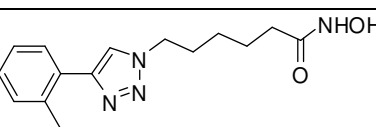
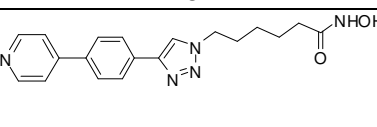
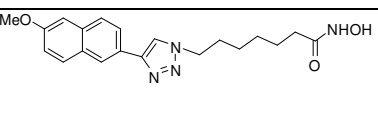
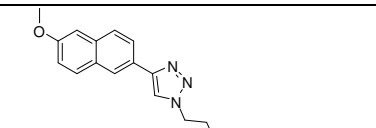
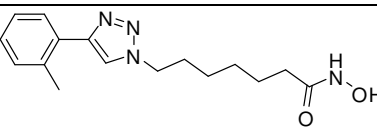
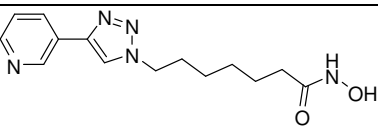
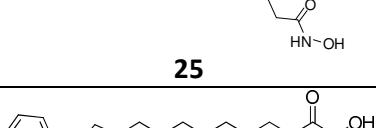
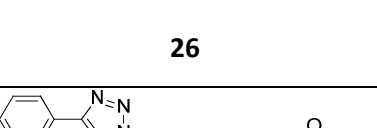
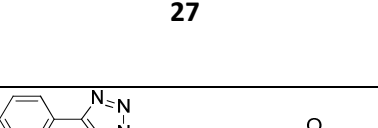
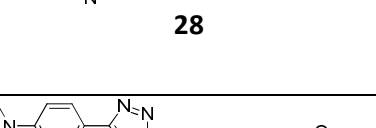
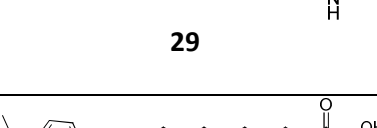
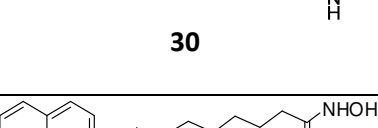
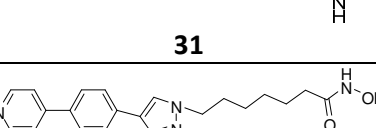
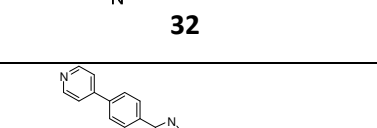
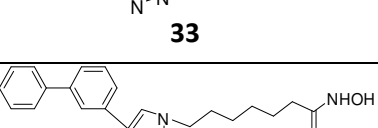
 10	 11	 12
 13	 14	 15
 16	 17	 18
 19	 20	 21
 22	 23	 24
 25	 26	 27
 28	 29	 30
 31	 32	 33
 34	 35	 36

Table 3-1 continued.

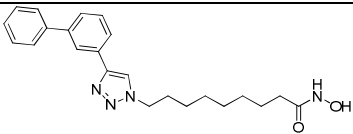
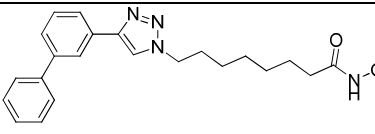
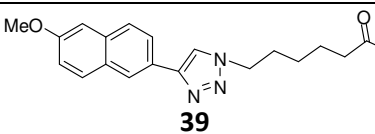
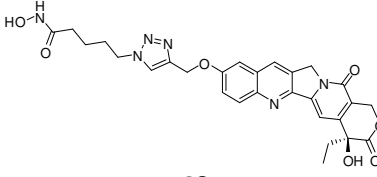
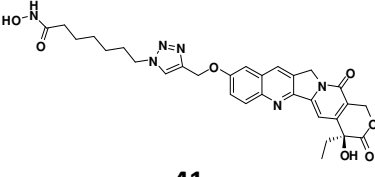
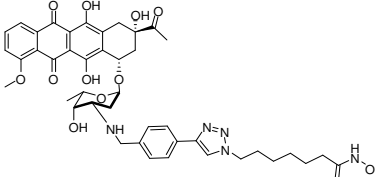
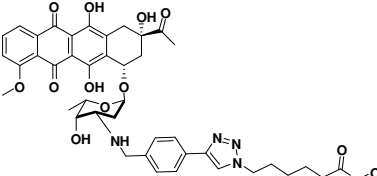
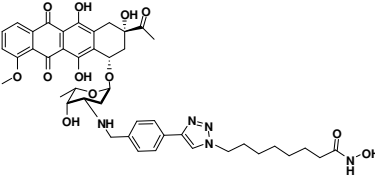
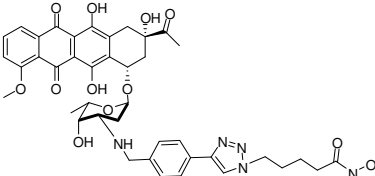
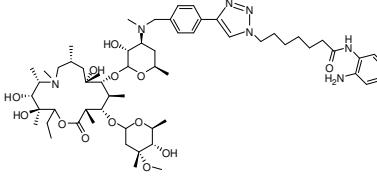
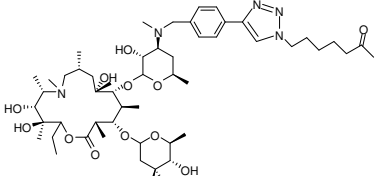
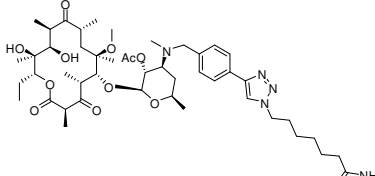
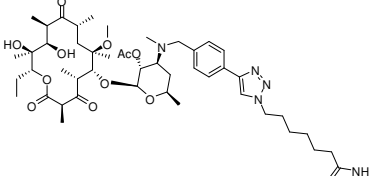
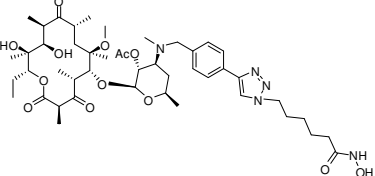
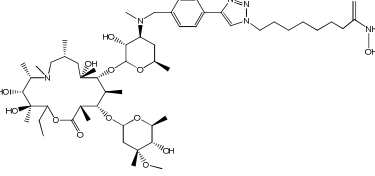
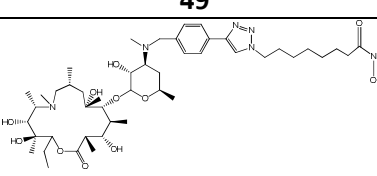
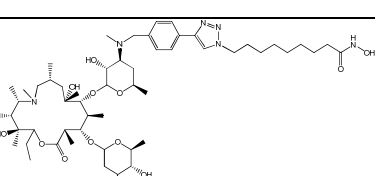
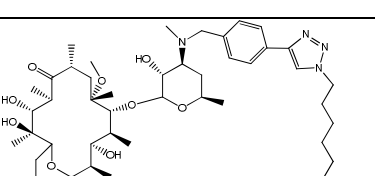
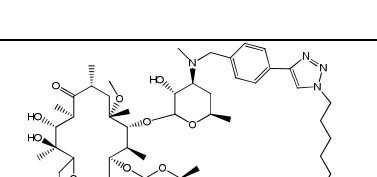
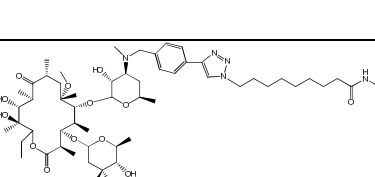
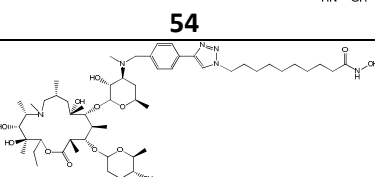
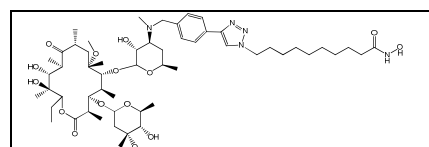
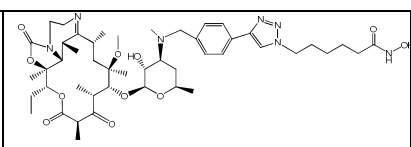
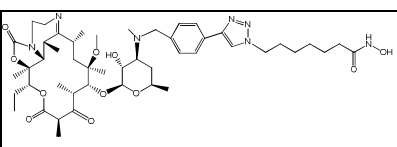
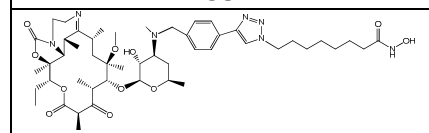
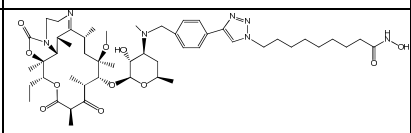
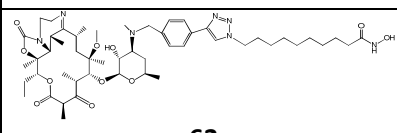
 <p>37</p>	 <p>38</p>	 <p>39</p>
 <p>40</p>	 <p>41</p>	 <p>42</p>
 <p>43</p>	 <p>44</p>	 <p>45</p>
 <p>46</p>	 <p>47</p>	 <p>48</p>
 <p>49</p>	 <p>50</p>	 <p>51</p>
 <p>52</p>	 <p>53</p>	 <p>54</p>
 <p>55</p>	 <p>56</p>	 <p>57</p>

Table 3-1 continued.

 <p style="text-align: center;">58</p>	 <p style="text-align: center;">59</p>	 <p style="text-align: center;">60</p>
 <p style="text-align: center;">61</p>	 <p style="text-align: center;">62</p>	 <p style="text-align: center;">63</p>

We identified only three compounds – **24**, **25** and **56** – which strongly inhibit splicing at 50 μ M (Figure 3-3a). Subsequent analysis revealed that structurally related **24** and **25** inhibit splicing in a concentration dependent manner while **56** lacked such concentration dependence (Figure 3-4). Both **24** and **25** stalled the spliceosome assembly at A-like complex to about the same extent despite over 15-fold difference in their anti-HDAC activities (in favor of **24**).⁴⁰ Intriguingly, compound **25** (Figure 3-3), a single methylene chain deletion analog of **24** which is over 8-fold stronger HDACi than **24**,³⁶ is devoid of any splicing inhibition activity. Another interesting fallout from this initial screening is the fact that the substitution of the anilide amide of SAHA with HDAC inhibition enhancing triazole ring³⁶ abrogated splicing inhibition at 50 μ M (see Figure for SAHA analog compound **13**). All together, these data suggest that the target(s) of splicing inhibition by these compounds may not be HDACs.

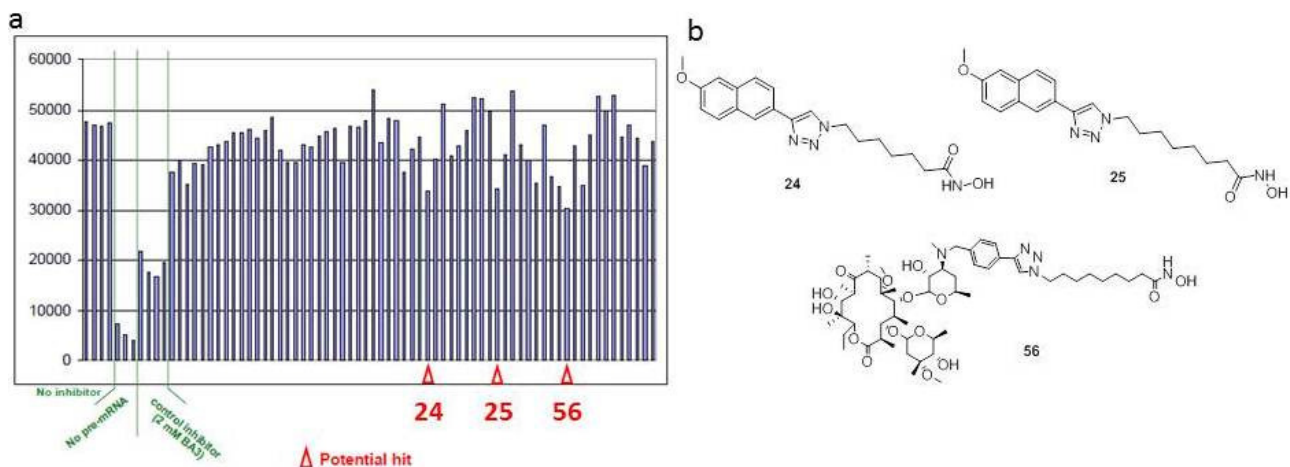


Figure 3-3 Effects of HDACi on splicing activity. (a) Screening of HDACi library at 50 μ M, probing for the incorporation of abstrakt protein into the spliceosome on PM5 pre-mRNA, revealed three hits compounds (b) Structures of hit compounds **24**, **25** and **56**.

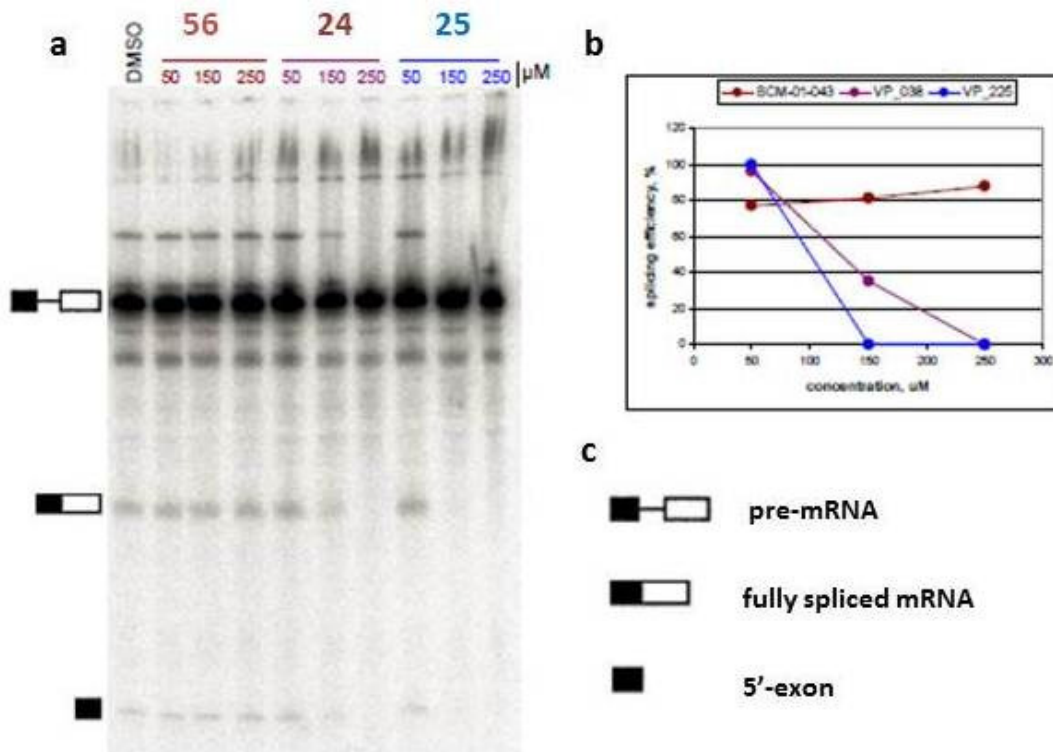


Figure 3-4. Concentration dependence of splicing inhibition by hit compounds **24**, **25** and **56**. (a) Increasing concentrations of compounds **24**, **25**, and **56** were tested for their effect on the splicing of 32 P-labeled MINX pre-mRNA. After splicing, the radiolabeled RNA was analyzed by denaturing PAGE followed by autoradiography. Shown on the leftmost lane is the DMSO control

experiment. Compound numbers are shown on the top panel while drug concentrations tested are shown just below the compound numbers. Analysis revealed that structurally related **24** and **25** inhibit splicing in a concentration dependent manner while **56** lacked such concentration dependence. (b) Quantification of mRNA splicing product bands. (c) Illustrations of the RNA splicing states.

3.3 Structure-Activity Relationship (SAR) of Splicing Inhibition

The screening of HDACi library for splicing inhibition furnished 6-methoxynaphthalen-2-yl hydroxamate **24** and **25** as small molecules which inhibit splicing in a specific context. Both **24** and **25** stalled the spliceosome assembly at the A-like complex to about the same extent, with IC_{50} 130 μ M and 100 μ M respectively (Table 3-1)^{36,40}

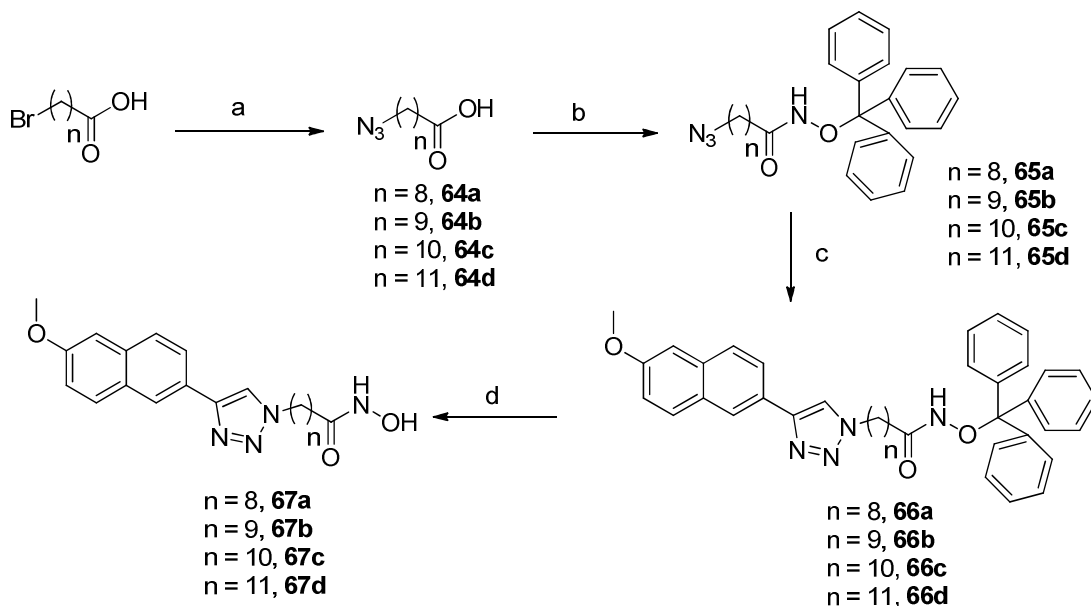


Figure 3-5. Synthesis of **67a-67d**. a) NaN_3 , DMF, 75 °C; b) NH_2 -O-trityl; Isobutyl Chloroformate, *N*-methylmorpholine, THF; c) 2-ethynyl-6-methoxynaphthalene, CuI, DIPEA, THF:DMSO d) Trifluoroacetic acid, Triisopropylsilane, DCM

To establish the structure activity relationship (SAR) of these compounds, we synthesized a series of structural analogs of **24** and **25** (Figure 3-5) by adapting similar synthetic procedure as depicted in Figure 2-3 (Chapter 2) and investigated their effect on the splicing of ^{32}P -labeled MINX pre-mRNA as well as their HDAC inhibition activity against representative class I and Class II HDAC isoforms – HDAC1, HDAC6 and HDAC8. This exercise resulted in compounds that display varying splicing inhibition which trends with the changes to the compounds' three distinct structural motifs – the substituent on the naphthalene, the methylene linker and the ZBG (Table 3-1). Relative to compound **25**, a single methylene chain extension (in **67a**) abolished splicing inhibition while a 2-methylene extension (in **67b**) enhanced the splicing inhibition activity by more than 3-fold. Further increase in methylene chain length in **67c** and **67d** did not improve splicing inhibition; in fact, such increase compromised splicing inhibition as IC_{50} increased to the levels of the lead compounds **24** and **25**. Additionally, we observed that these compounds preferentially inhibited the HDAC isoform tested. Compounds **67a** and **67b** inhibited HDAC1 and HDAC6 with sub-nanomolar IC_{50} and completely inactive against HDAC8; while **67c** potently inhibited HDAC6 and HDAC8 and somewhat inactive against HDAC1. Compound **67d**, although an equally effective splicing inhibitor as the lead compounds **24** and **25**, interestingly, has the poorest HDAC inhibition activity – inactive against HDAC1 and HDAC6 and weakly active against HDAC8.

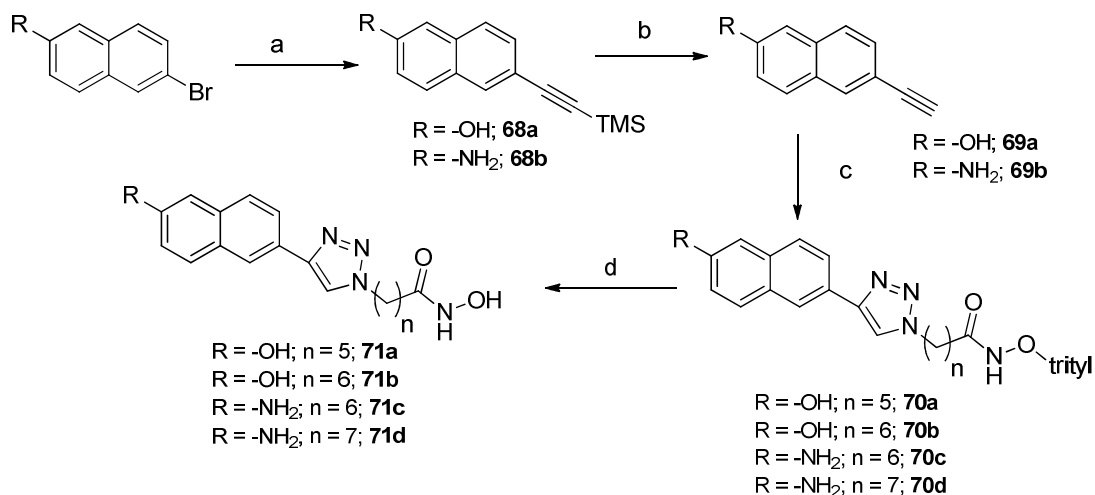


Figure 3-6 Synthesis of **71a-71d** a) TMS-acetylene, $\text{PdCl}_2(\text{PPh}_3)_2$, CuI, triethylamine; b) TBAF, THF; c) **69a/69b**, CuI, DIPEA, THF:DMSO d) Trifluoroacetic acid, Triisopropylsilane, DCM

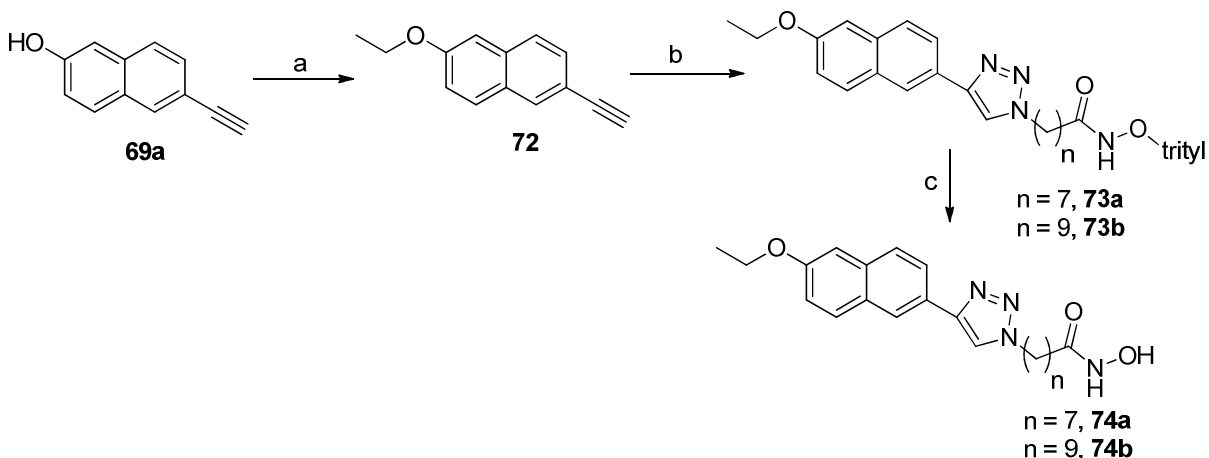


Figure 3-7 Synthesis of **74a-74b**. a) Ethylbromide, K_2CO_3 ; THF, 60 °C; b) **72**, CuI, DIPEA, THF:DMSO; c) Trifluoroacetic acid, Triisopropylsilane, DCM

The substitution of the naphthalene cap group 6-methoxy moiety by protic electron donating groups such as OH and NH_2 is detrimental to function as these changes abolished splicing inhibition activity (Table 3-1, comparing **71b** and **71c** with **24**; and **71d** with **25**). Synthesis of compounds **71a-d** is depicted in Figure 3-6. Synthesis

involves making of alkyne intermediates **69a-b** from 6-bromo-2-naphthol and 6-bromonaphthalen-2-amine using Sonogashira coupling with TMS-acetylene to give silyl intermediate **68a-b** followed by TBAF deprotection of silyl group to give desired alkyne intermediate **69a-b**. Corresponding hydroxamates **71a-d** were prepared using chemistry described in chapter 2. Similarly compounds **74a-b** (Figure 3-7) and compounds **79a-b** (Figure 3-8) were synthesized. In contrast, compounds **71b**, **71c** and **71d** are broadly active against the HDAC isoform tested, with single digit to sub-nanomolar IC₅₀ against HDAC1 and HDAC6. The consequence of the replacement of the naphthalene cap group 6-methoxy moiety with azide group on splicing inhibition activity is however closely linked to the length of the methylene chain of the molecule. The 6-methylene compound **79a**, an azido analog of **24** is inactive while the 7-methylene linked compound **79b** is twice as potent as its direct congener, compound **25**. The extension of the naphthalene cap 6-methoxy group by an additional carbon chain is tolerable but not beneficial to the splicing inhibition attributes of the resulting compounds **74a** and **74b**, relative to the corresponding 6-methoxy compounds **25** and **67b** respectively. Synthesis of compounds **74a** and **74b** is depicted in Figure 3-7. Again, there is no correlation between HDAC inhibition and splicing inhibition activities of these compounds as they maintained potent activity against HDAC isoforms tested, particularly HDAC1 and HDAC6 (Table 3-2).

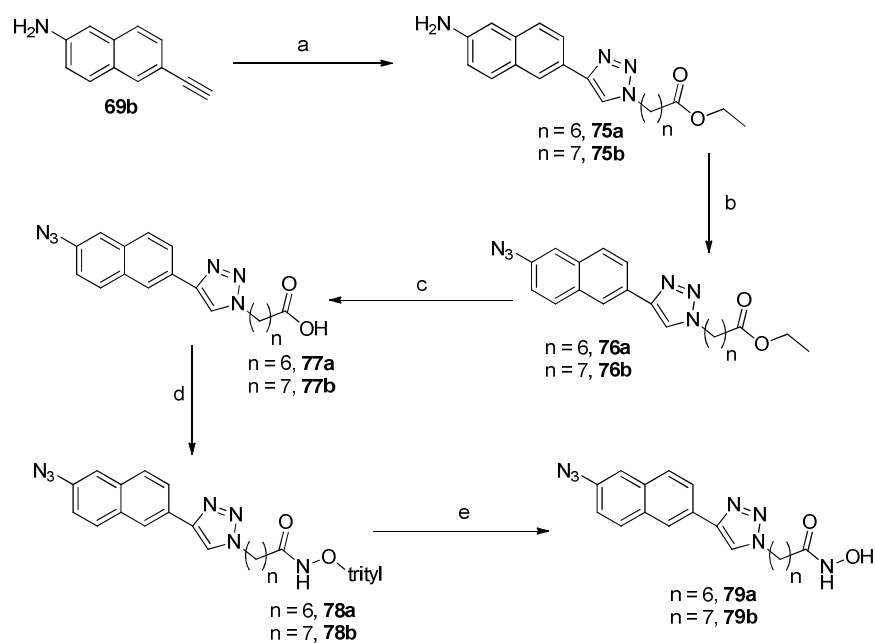


Figure 3-8. Synthesis of **79a-79b** a) **69b**, CuI, DIPEA, THF:DMSO; b) NaNO₂, NaN₃, HCl/H₂O, 0 °C c) LiOH, THF/H₂O; d) NH₂-O-trityl; TBTU, DIPEA, DMF; e) Trifluoroacetic acid, Triisopropylsilane, DCM.

To confirm the role of zinc chelation in the splicing inhibition activities of these naphthalen-2-yl hydroxamates, we synthesized methyl ester **80** and **81**, carboxylic acid **82**, and carboxamide **83**.^{36,40} These compounds are derivatives of most active hydroxamates **24**, **25** and **67b**. Expectedly, all of these non-hydroxamate analogs lacked HDAC inhibition activity. More importantly however, they did not perturb the splicing of MINX pre-mRNA (Table 3-1). This data suggests a role for zinc chelation in the mechanism of splicing inhibition by these hydroxamates. Additionally, the results herein presented further highlight the importance Zn-ion in pre-mRNA splicing.

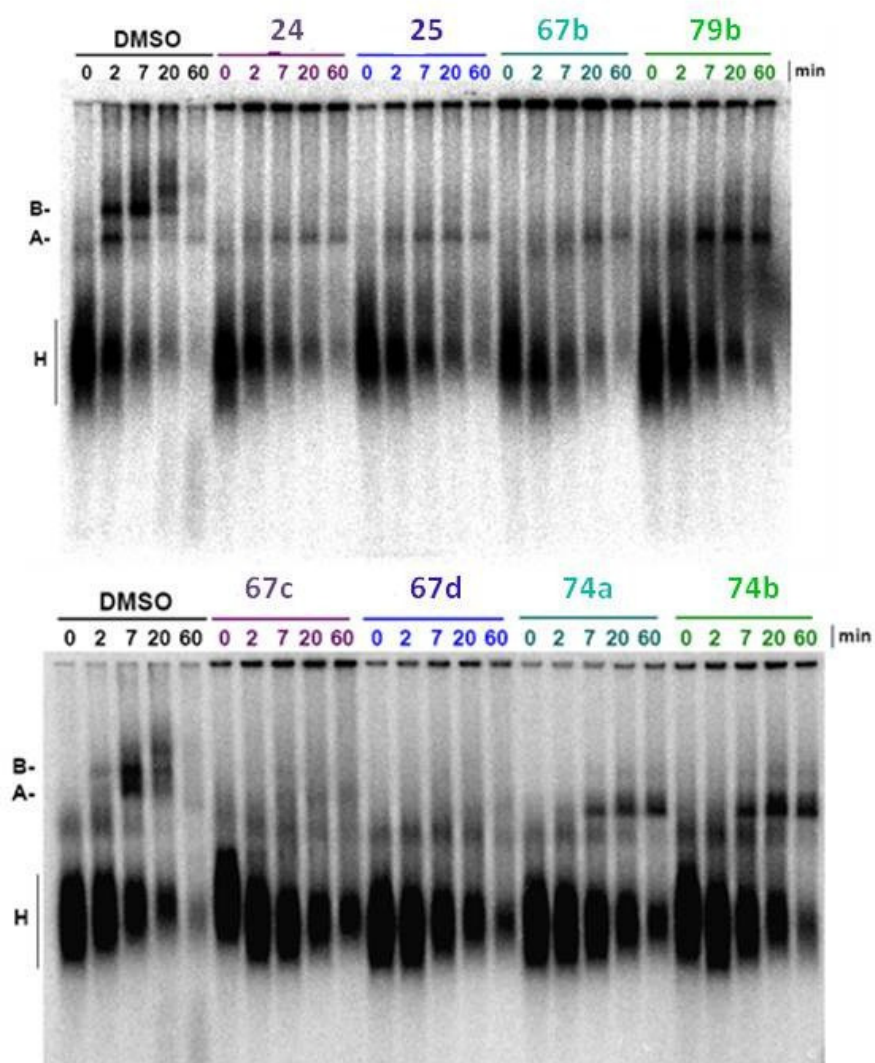


Figure 3-9. Standard *in vitro* splicing test with radioactively labeled MINX pre-mRNA^a

^aPre-mRNA splicing activities determined by Dr. Timur Samatov from Dr. Reinhard Luhrmann lab at Max Plack Institute of biophysical chemistry, Germany.

Table 3-2: Structure-activity relationship study of the splicing inhibition activities of 6-methoxynaphthalen-2-yl hydroxamates.^a

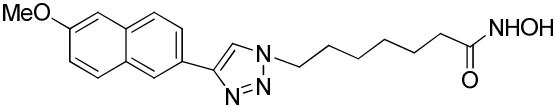
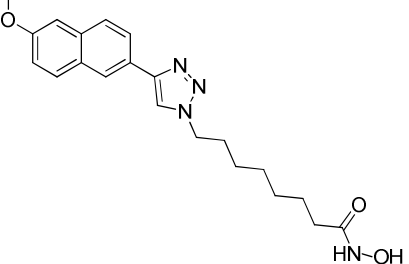
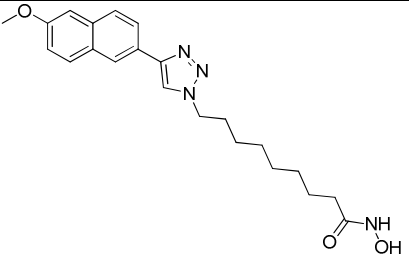
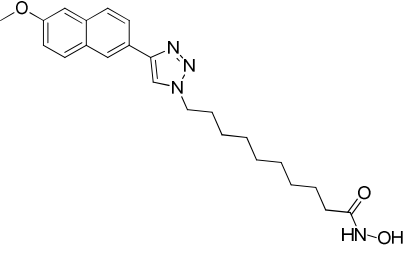
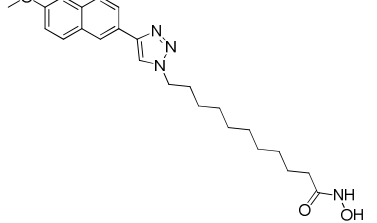
Compounds	IC ₅₀			
	HDAC1	HDAC6	HDAC8	pre-mRNA splicing ^b
 <p>24^a</p>	15.3 nM ^a	NT	NT	130 μM
 <p>25^a</p>	226.1 nM ^a	NT	NT	100 μM
 <p>67a</p>	55 ± 4 nM	93 ± 7 nM	NI	NI
 <p>67b</p>	155 ± 17 nM	212 ± 26 nM	NI	< 50 μM
 <p>67c</p>	9298 ± 1453 nM	400 ± 29 nM	245 ± 18 nM	100 μM

Table 3-2 continued.

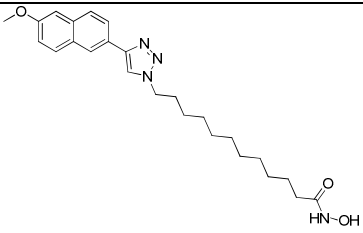
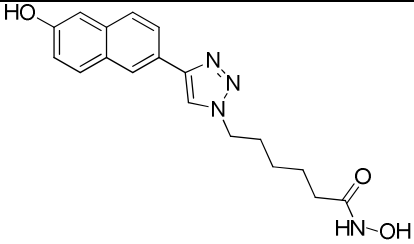
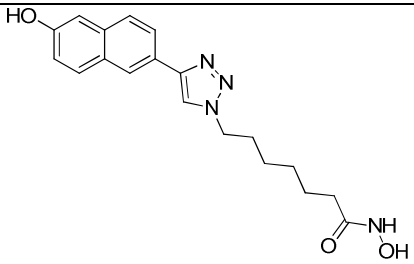
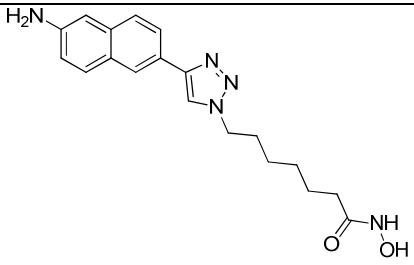
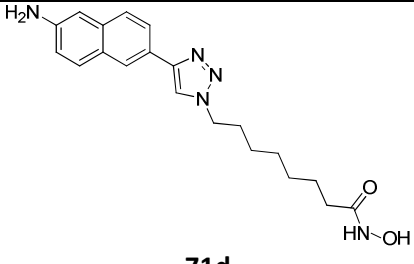
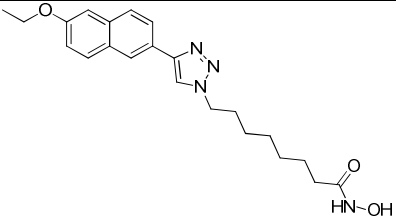
 <p>67d</p>	28%	5390 ± 734 nM	NI	120 μM
 <p>71a</p>	6.0 ± 0.4 nM	7.0 ± 0.5 nM	1300 ± 128 nM	NI
 <p>71b</p>	1.0 ± 0.1 nM	2.0 ± 0.1 nM	252 ± 28 nM	NI
 <p>71c</p>	1.0 ± 0.1 nM	5.0 ± 0.6 nM	810 ± 158 nM	NI
 <p>71d</p>	5.0 ± 0.4 nM	49.0 ± 2.6 nM	2300 ± 540 nM	NI
 <p>74a</p>	25 ± 2 nM	47 ± 4 nM	5292 ± 605 nM	130 μM

Table 3-2 continued.

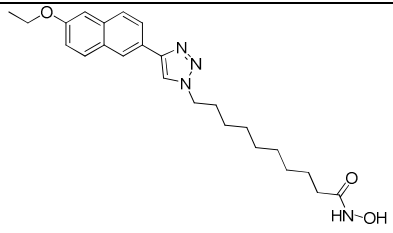
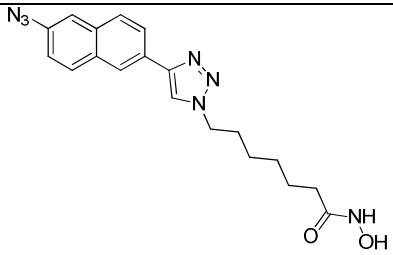
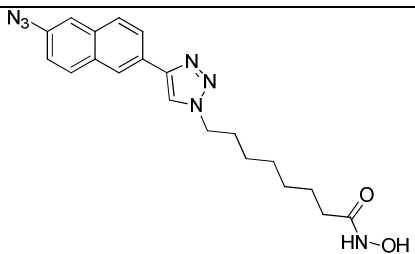
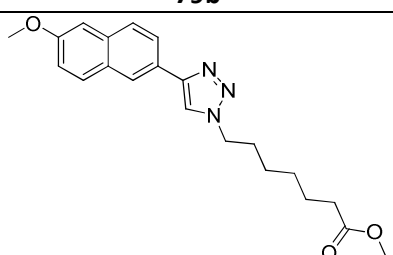
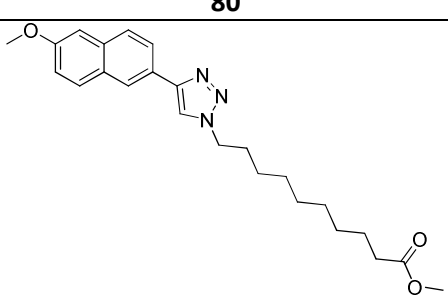
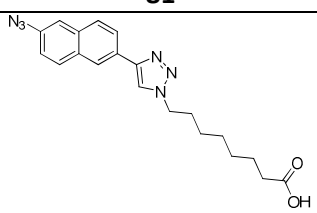
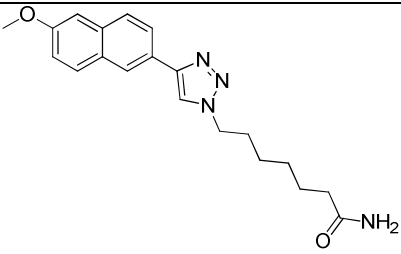
 <p>74b</p>	311 ± 32 nM	25 ± 26 nM	4706 ± 561 nM	50 μM
 <p>79a</p>	3.0 ± 0.1 nM	9.0 ± 0.6 nM	3000 ± 509 nM	NI
 <p>79b</p>	16.0 ± 0.2 nM	45 ± 3 nM	4000 ± 501 nM	< 50 μM
 <p>80</p>	NT	NT	NT	NI
 <p>81</p>	NT	NT	NT	NI
 <p>82</p>	NT	NT	NT	NI

Table 3-2 continued.

 83	NI	22%	27%	NI
--	----	-----	-----	----

^aCited from refs 36,40 – activities against HeLa nuclear extract (HDAC 1 & 2).

^bPre-mRNA splicing activities determined by Dr. Timur Samatov from Dr. Reinhard Luhrmann lab at Max Plack Institute of biophysical chemistry, Germany. Included here to clarify SAR

NT – Not Tested

NI – No significant Inhibition (below 20% Inhibition)

% inhibitions of the compounds at 10 μ M are given if the IC₅₀ was above 10 μ M.

3.4 Conclusion

The precise role of Zn-ion in splicing is not yet well understood. It is known that several spliceosomal proteins possess zinc binding motifs which could play both structural and functional roles. Additionally, zinc metalloenzymes such as HDACs are known to closely associate with mixed population of spliceosome. The study herein presented has revealed molecular architecture of a novel class of zinc-chelating agents with splicing inhibitory activities. An interesting aspect of this data suggests that these compounds may be inhibiting the functional role of Zn-ion in splicing since only a subset of them, with well-defined structure, is active. Ongoing efforts are on identifying the spliceosome associated target(s) of these compounds using pull down approaches.

3.5 General Procedure & Experimental

Bromoalkanoic acid, 2-ethynyl-6-methoxynaphthalene and 6-bromo-2-naphthol were purchased from Sigma–Aldrich. 6-bromonaphthalen-2-amine was purchased from

Astatech, Inc. Anhydrous solvents and other reagents were purchased and used without further purification. Analtech silica gel plates (60 F254) were used for analytical TLC, and Analtech preparative TLC plates (UV 254, 2000 μm) were used for purification. UV light was used to examine the spots. Silica gel (200–400 Mesh) was used in column chromatography. NMR spectra were recorded on a Varian-Gemini 400 magnetic resonance spectrometer. ^1H NMR spectra were recorded in parts per million (ppm) relative to the peak of CDCl_3 (7.24 ppm), CD_3OD (3.31 ppm), or $\text{DMSO}-d_6$ (2.49 ppm). ^{13}C spectra were recorded relative to the central peak of the CDCl_3 triplet (77.0 ppm), CD_3OD (49.0 ppm), or the $\text{DMSO}-d_6$ septet (39.7 ppm), and were recorded with complete heterodecoupling. Multiplicities are described using the abbreviation s, singlet; d, doublet; t, triplet; q, quartet; m, multiplet; and app, apparent. High-resolution mass spectra were recorded at the Georgia Institute of Technology mass spectrometry facility in Atlanta. Azidoalkanoic acids **64a-64d** and 6-azido-*O*-tritylhexahydroxamate, 7-azido-*O*-tritylheptahydroxamate, 8-azido-*O*-trityloctahydroxamate and 9-azido-*O*-tritylnonahydroxamate were synthesized according to literature protocol.⁴⁰

Representative Procedure for coupling of trityl protected hydroxylamine with azidoalkanoic acid –

10-Azido-*O*-trityldecahydroxamate (65b)

Carboxylic acid **64b** (1.50 g, 6.98 mmol) was dissolved in anhydrous THF (35 mL). *N*-methylmorpholine (0.21 mL, 6.98 mmol) was added to the solution. The reaction mixture was then cooled down to $-15\text{ }^\circ\text{C}$ and stirred for 5 min. Isobutylchloroformate

(0.91 mL, 6.98 mmol) was added and the mixture was stirred for 10 min at -15 °C. *O*-tritylhydroxylamine (1.92 g, 6.98 mmol) was added followed by 2 more equivalents of *N*-methylmorpholine. Stirring continued for 15 min at -15 °C and 2 h at room temperature. Afterwards the mixture was poured into CH₂Cl₂ (90 mL) and water (90 mL). Organic layer was separated and extracted 3 times (60 mL) in each case with water, sodium bicarbonate solution (5%) and water. After washing with brine (1 X 50 mL) and drying over Na₂SO₄, solvent was evaporated *in vacuo*. Column chromatography with eluent system CH₂Cl₂-acetone (step gradient from 0-12% of acetone) gave 2.55 g of compound **65b** (78 %) as a white solid. ¹H NMR (400 MHz, CDCl₃) δ 7.34 (m, 17H), 3.25 (t, *J* = 6.9 Hz, 2H), 1.59 (m, 4H), 1.23 (m, 12H). ¹³C NMR (100 MHz, CDCl₃) δ 128.98, 128.90, 128.80, 127.92, 127.44, 127.34, 126.95, 126.85, 51.29, 29.06, 28.96, 28.90, 28.66, 26.52.

11-Azido-*O*-tritylundecahydroxamate (65c) –

Reaction of carboxylic acid **64c** (4.50 g, 19.82 mmol), *N*-methylmorpholine (6.51 mL, 59.46 mmol), Isobutylchloroformate 2.59 mL, 19.82 mmol), and *O*-tritylhydroxylamine (5.45 g, 19.82 mmol) within 2h as described for the synthesis of **65b** gave compound **65c** (6.87 g, 74%) as a white solid. ¹H NMR (400 MHz, DMSO) δ 10.11 (s, 1H), 7.27 (m, 15H), 3.27 (t, *J* = 6.9 Hz, 2H), 1.76 (m, 2H), 1.49 (m, 2H), 1.16 (m, 14H) ¹³C NMR (100 MHz, DMSO) δ 170.88, 142.95, 129.41, 127.90, 105.12, 92.18, 51.08, 32.48, 29.32, 29.20, 29.11, 28.98, 28.70, 26.59, 25.21.

12-Azido-*O*-trityldodecahydroxamate (65d) –

Reaction of carboxylic acid **64d** (2.20 g, 9.12 mmol), *N*-methymorpholine (3.00 mL, 27.36 mmol), isobutylchloroformate (1.19 mL, 9.12 mmol), and *O*-tritylhydroxylamine (2.51 g, 9.12 mmol) within 2h as described for the synthesis of **65b** gave compound **65d** (3.51 g, 80%) as a white solid. ¹H NMR (400 MHz, DMSO) δ 10.11 (s, 1H), 7.26 (m, 15H), 3.28 (t, *J* = 6.9 Hz, 2H), 1.50 (m, 2H), 1.12 (m, 16H). ¹³C NMR (100 MHz, DMSO) δ 170.33, 142.45, 128.91, 127.40, 127.30, 104.63, 91.65, 50.58, 31.98, 28.85, 28.77, 28.64, 28.49, 28.30, 28.20, 26.10, 24.72.

Representative Procedure for Cu(I)-catalyzed cycloaddition reaction –

***O*-Trityl-6-methoxynaphthyltriazolynonahydroxamate (66a) –**

2-ethynyl-6-methoxynaphthalene (0.08 g, 0.44 mmol) and **65a** (0.24 g, 0.53 mmol) were dissolved in anhydrous THF:DMSO (8mL:8 mL) and stirred under argon at room temperature. Copper (I) iodide (0.011 g, 0.07 mmol) and Hunig's base (0.16 mL) were then added to the reaction mixture, and stirring continued for 12 h. The reaction mixture was diluted with CH₂Cl₂ (40 mL) and washed with 1:4 NH₄OH/saturated NH₄Cl (3 x 30 mL) and saturated NH₄Cl (30 mL). The organic layer was dried over Na₂SO₄ and concentrated *in vacuo*. Crude product was purified by prep-TLC (Eluent - CH₂Cl₂:Acetone:MeOH:EtOH (25:1:0.2:0.2)) to give **66a** (0.16 g, 59%) as white solid.

***O*-Trityl-6-methoxynaphthyltriazolyldecahydroxamate (66b) –**

Reaction of 2-ethynyl-6-methoxynaphthalene (0.07 g, 0.38 mmol) and **65b** (0.21 g, 0.45 mmol) within 12 h as described for synthesis of **66a** gave compound **66b** (0.14 g, 60%)

as a white solid. ^1H NMR (400 MHz, CDCl_3) δ 8.24 (s, 1H), 7.88 (dd, $J = 8.5, 1.5$ Hz, 1H), 7.76 (m, 3H), 7.33 (m, 15H), 7.14 (m, 2H), 4.34 (t, $J = 7.1$ Hz, 2H), 3.90 (s, 3H), 1.81 (m, 4H), 1.21 (m, 14H). ^{13}C NMR (100 MHz, CDCl_3) δ 157.71, 147.67, 140.99, 134.14, 129.50, 128.86, 128.83, 127.93, 127.18, 125.81, 124.25, 124.05, 119.28, 119.08, 105.66, 93.17, 77.31, 76.99, 76.67, 55.15, 50.43, 50.23, 30.13, 28.90, 28.74, 26.28.

***O*-Trityl-6-methoxynaphthyltriazolylundecahydroxamate (66c) –**

Reaction of 2-ethynyl-6-methoxynaphthalene (0.06 g, 0.34 mmol) and **65c** (0.20 g, 0.41 mmol) within 12 h as described for synthesis of **66a** gave compound **66c** (0.14 g, 63%) as a white solid. ^1H NMR (400 MHz, $\text{DMSO}-d_6$) δ 10.09 (s, 1H), 8.61 (s, 1H), 8.28 (s, 1H), 7.88 (m, 3H), 7.23 (m, 21H), 4.39 (t, $J = 7.0$ Hz, 2H), 3.87 (s, 3H), 1.85 (m, 2H), 1.74 (t, $J = 6.6$ Hz, 2H), 1.18 (m, 14H). ^{13}C NMR (100 MHz, CDCl_3) δ 157.70, 147.67, 140.94, 134.13, 129.51, 128.87, 128.82, 127.94, 127.18, 125.83, 124.25, 124.04, 119.25, 119.10, 105.62, 104.83, 55.16, 50.25, 31.04, 30.19, 29.56, 29.07, 28.83, 26.32, 23.30.

***O*-Trityl-6-methoxynaphthyltriazolyldodecahydroxamate (66d) –**

Reaction of 2-ethynyl-6-methoxynaphthalene (0.06 g, 0.33 mmol) and **65d** (0.20 g, 0.40 mmol) within 12 h as described for synthesis of **66a** gave compound **66d** (0.21 g, 91%) as a white solid. ^1H NMR (400 MHz, dmso) δ 10.10 (s, 1H), 8.62 (s, 1H), 8.29 (s, 1H), 7.88 (m, 3H), 7.32 (m, 17H), 7.18 (dd, $J = 9.0, 2.5$ Hz, 1H), 4.39 (t, $J = 7.0$ Hz, 2H), 3.88 (s, 3H), 1.87 (m, 2H), 1.73 (m, 2H), 1.12 (dd, $J = 71.8, 64.7$ Hz, 17H). ^{13}C NMR (100 MHz, CDCl_3) δ 157.70, 147.65, 134.13, 129.49, 128.86, 127.91, 127.16, 125.85, 124.25, 124.03, 119.24, 119.07, 105.65, 55.14, 50.24, 30.17, 29.15, 29.02, 28.83, 26.33.

Representative Procedure for Deprotection of Trityl Group –

9-(6-Methoxynaphthyl)triazolynonahydroxamic acid (**67a**) –

To a solution of **66a** (0.12 g, 0.19 mmol) in CH₂Cl₂ (7 ml) was added triisopropylsilane (0.2 mL) and trifluoroacetic acid (TFA) (0.15 mL) dropwise at room temperature. Additional triisopropylsilane was added till reaction mixture became colorless. After 15 min of stirring at RT, solvent was evaporated and thick brown-black liquid was treated with petroleum ether (~15 mL) to give yellowish suspension. Suspension was filtered and residue was again washed with petroleum ether (~30 mL) then with CH₂Cl₂:petroleum ether (1:1) mixture (~30 mL), followed by more washing with CH₂Cl₂ (~50 mL) to give 65 mg (83%) of pure **67a** as a white solid. ¹H NMR (400 MHz, dmsO) δ 10.30 (s, 1H), 8.64 (m, 2H), 8.29 (s, 1H), 7.89 (dd, *J* = 22.1, 9.3 Hz, 3H), 7.32 (m, 1H), 7.17 (d, *J* = 8.8 Hz, 1H), 4.39 (t, *J* = 7.0 Hz, 2H), 3.87 (s, 3H), 1.88 (m, 2H), 1.48 (m, 2H), 1.18 (m, 10H).). ¹³C NMR (100 MHz, DMSO-*d*₆) δ 157.25, 146.25, 133.61, 129.14, 128.37, 126.97, 126.00, 123.90, 123.14, 120.70, 118.64, 106.07, 54.99, 49.29, 41.21, 29.26, 28.19, 27.96, 25.57. HRMS (EI) calcd for C₂₂H₂₈N₄O₃ [M]⁺ 396.2161 found 396.2170.

10-(6-Methoxynaphthyl)triazolyldecahydroxamic acid (**67b**) –

Reaction of **66b** (0.05 g, 0.076 mmol) with triisopropylsilane (0.4 ml) & TFA (0.15 ml) in CH₂Cl₂ (7 ml) at RT within 15 min as described for the synthesis of **67a**, gave 28 mg (90%) of **67b** as a white solid. ¹H NMR (400 MHz, DMSO-*d*₆) δ 10.30 (s, 1H), 8.63 (s, 1H), 8.30 (s, 1H), 7.89 (dd, *J* = 23.0, 9.6 Hz, 3H), 7.32 (d, *J* = 2.3 Hz, 1H), 7.17 (dd, *J* = 9.0, 2.5 Hz, 1H), 4.39 (t, *J* = 7.1 Hz, 2H), 3.87 (s, 3H), 1.89 (dd, *J* = 15.5, 7.9 Hz, 4H),

1.45 (d, $J = 6.6$ Hz, 2H), 1.24 (d, $J = 20.6$ Hz, 10H). ^{13}C NMR (100 MHz, DMSO- d_6) δ 169.12, 157.42, 146.49, 133.85, 129.51, 128.56, 127.35, 126.12, 124.13, 123.33, 121.14, 119.13, 106.02, 55.23, 49.55, 32.26, 29.65, 28.76, 28.66, 28.55, 28.39, 25.88, 25.11. HRMS (EI) calcd for $\text{C}_{23}\text{H}_{30}\text{N}_4\text{O}_3$ $[\text{M}]^+$ 410.2318 found 410.2322.

11-(6-Methoxynaphthyl)triazolylundecahydroxamic acid (67c) –

Reaction of **66c** (0.15 g, 0.22 mmol) with triisopropylsilane (0.4 ml) & TFA (0.15 ml) in CH_2Cl_2 (7 ml) at RT within 15 min as described for the synthesis of **67a**, gave 72 mg (76%) of **67c** as a white solid. ^1H NMR (400 MHz, DMSO) δ 10.54 (s, 1H), 8.62 (s, 1H), 8.28 (s, 1H), 7.88 (m, 3H), 7.31 (s, 1H), 7.16 (d, $J = 7.9$ Hz, 1H), 4.38 (t, $J = 7.0$ Hz, 2H), 3.86 (s, 3H), 1.87 (m, 4H), 1.47 (m, 2H), 1.21 (m, 12H). ^{13}C NMR (100 MHz, $\text{CDCl}_3 + \text{CD}_3\text{OD}$) δ 157.79, 134.25, 129.48, 128.79, 127.30, 125.27, 124.18, 124.07, 119.68, 119.14, 105.61, 92.65, 55.12, 50.40, 30.03, 29.47, 29.00, 28.65, 26.17. HRMS (MALDI) calcd for $\text{C}_{24}\text{H}_{33}\text{N}_4\text{O}_3$ $[\text{M} + \text{H}]^+$ 425.2553 found 425.2550.

12-(6-Methoxynaphthyl)triazolyldecadecahydroxamic acid (67d) –

Reaction of **66d** (0.18 g, 0.26 mmol) with triisopropylsilane (0.4 ml) & TFA (0.15 ml) in CH_2Cl_2 (7 ml) at RT within 15 min as described for the synthesis of **67a**, gave 78 mg (66%) of **67d** as a white solid. ^1H NMR (400 MHz, DMSO) δ 10.28 (s, 1H), 8.62 (s, 1H), 8.29 (s, 1H), 7.89 (m, 3H), 7.32 (s, 1H), 7.17 (d, $J = 6.7$ Hz, 1H), 4.39 (t, $J = 7.0$ Hz, 2H), 3.87 (s, 3H), 1.89 (m, 4H), 1.43 (m, 2H), 1.24 (m, 14H). ^{13}C NMR (100 MHz, DMSO) δ 157.24, 146.26, 133.62, 129.19, 128.75, 128.37, 128.02, 127.01, 125.99, 123.91, 123.13,

120.78, 118.72, 106.03, 55.02, 49.32, 29.31, 28.57, 28.51, 28.42, 28.10, 25.62, 24.79.

HRMS (MALDI) calcd for $C_{25}H_{35}N_4O_3$ $[M+H]^+$ 439.2709 found 439.2715.

6-((Trimethylsilyl)ethynyl)-2-naphthol (68a) –

Dry round bottom flask was charged with 6-bromo-2-naphthol (0.20 g, 0.89 mmol) and triethylamine (3 mL) under inert atmosphere and the solution was stirred for 5 min at RT. Following addition of $PdCl_2(PPh_3)_2$ (20 mg, 0.028 mmol) & CuI (6 mg, 0.031 mmol), the solution was degassed. Under slow flow of argon TMS-acetylene was added quickly and reaction mixture was heated overnight at 80 °C. The reaction mixture was slowly cooled at RT and dry THF was added and stirred at room temperature for 1 h. The mixture was concentrated in vacuo, diluted with CH_2Cl_2 , organic layers were combined and dried over Na_2SO_4 . Column chromatography with gradient Hexane:EtOAc (step gradient, 20-33 % of EtOAc) gave 0.193 g, 90% of pure **68a** as brown solid. 1H NMR (400 MHz, $CDCl_3$) δ 7.99 (s, 1H), 7.68 (d, J = 8.8 Hz, 1H), 7.52 (m, 2H), 7.15 (m, 2H), 0.38 (s, 9H). ^{13}C NMR (100 MHz, $CDCl_3$) δ 154.11, 134.13, 131.85, 129.70, 129.07, 128.11, 126.31, 118.42, 117.74, 109.61, 105.92, 93.86, -0.02.

6-((Trimethylsilyl)ethynyl)-naphthalen-2-amine (68b) –

Reaction of 6-bromonaphthalen-2-amine (1.00 g, 4.50 mmol), triethylamine (15 mL), $PdCl_2(PPh_3)_2$ (100 mg, 0.14 mmol), CuI (30 mg, 0.16 mmol), TMS-acetylene (0.66 g, 6.75 mmol) as described for synthesis of **68a**, gave 0.64 g (60%) of **68b** as a brown solid. 1H NMR (400 MHz, $CDCl_3$) δ 7.86 (s, 1H), 7.57 (d, J = 8.5 Hz, 1H), 7.47 (d, J = 8.5 Hz, 1H), 7.40 (dd, J = 8.5, 1.3 Hz, 1H), 6.89 (m, 2H), 3.87 (s, 2H), 0.28 (s, 9H). ^{13}C NMR

(100 MHz, CDCl₃) δ 145.05, 134.53, 131.94, 129.16, 129.07, 127.11, 125.63, 118.59, 116.50, 108.18, 106.10, 93.06, 0.07.

6-Ethynyl-2-naphthol (69a) –

To a stirring reaction mixture of **68a** (1.85 g, 7.72 mmol) in THF (10 mL), 1M TBAF in THF (9.26 mL) was added dropwise. After 45 min stirring at room temperature, reaction mixture was diluted with EtOAc (80 mL) and washed with water (80 mL). Aqueous layer was washed with EtOAc (2 X 60 mL). Combined organic layer was washed with brine (1 x 50 mL) and dried over Na₂SO₄. Column chromatography with hexane:ether (2:1), gave 1.07 g (83%) pure **69a** as brown solid. ¹H NMR (400 MHz, CDCl₃) δ 7.95 (m, 1H), 7.67 (m, 1H), 7.55 (d, *J* = 8.6 Hz, 1H), 7.47 (m, 1H), 7.14 (m, 2H), 6.33 (s, 1H), 3.16 (s, 1H). ¹³C NMR (100 MHz, CDCl₃) δ 154.58, 134.46, 132.27, 129.90, 129.25, 128.21, 126.54, 118.82, 116.88, 109.83, 84.37, 77.45. HRMS (EI) calcd for C₁₂H₈O [M]⁺ 168.0575 found 168.0574.

6-Ethynyl-naphthalen-2-amine (69b) –

Reaction of **68b** (0.46 g, 1.92 mmol), 1M TBAF in THF (2.31 mL) as described for synthesis of **69a**, gave 0.23 g (72%) of **69b** as a dark orange solid. ¹H NMR (400 MHz, CDCl₃) δ 7.87 (s, 1H), 7.54 (d, *J* = 8.8 Hz, 1H), 7.42 (m, 2H), 6.90 (dd, *J* = 8.7, 2.3 Hz, 1H), 6.85 (d, *J* = 2.3 Hz, 1H), 4.02 (s, 2H), 3.14 (s, 1H). ¹³C NMR (100 MHz, CDCl₃) δ 145.34, 134.52, 132.01, 128.88, 128.75, 126.73, 125.63, 118.69, 114.98, 107.83, 84.50, 76.24. HRMS (EI) calcd for C₁₂H₉N [M]⁺ 167.0735 found 167.0732.

***O*-Trityl-6-hydroxynaphthyltriazolyhexahydroxamate (70a) –**

Reaction of 6-ethynyl-2-naphthol (0.12 g, 0.72 mmol) and 6-azido-*O*-tritylhexahydroxamate (0.25 g, 0.60 mmol) within 12 h as described for synthesis of **66a** gave compound **70a** (0.30 g, 86%) as a white solid. ¹H NMR (400 MHz, DMSO) δ 10.16 (s, 1H), 9.78 (s, 1H), 8.55 (s, 1H), 8.24 (s, 1H), 7.80 (m, 3H), 7.28 (m, 15H), 7.10 (m, 2H), 4.30 (t, *J* = 7.0 Hz, 2H), 1.75 (m, 4H), 1.25 (m, 2H), 0.99 (m, 2H). ¹³C NMR (100 MHz, DMSO) δ 155.99, 152.20, 147.06, 142.89, 134.59, 129.99, 129.39, 128.18, 127.95, 127.08, 125.69, 124.34, 123.81, 121.32, 119.61, 109.21, 92.19, 49.76, 32.19, 29.75, 25.68, 24.58.

***O*-Trityl-6-hydroxynaphthyltriazolyheptahydroxamate (70b) –**

Reaction of 6-ethynyl-2-naphthol (0.19 g, 1.12 mmol) and 7-azido-*O*-tritylheptahydroxamate (0.40 g, 0.93 mmol) within 12 h as described for synthesis of **66a** gave compound **70b** (0.53 g, 95%) as a white solid. ¹H NMR (400 MHz, DMSO – *d*₆) δ 10.15 (s, 1H), 9.78 (s, 1H), 8.58 (s, 1H), 8.24 (s, 1H), 7.80 (m, 3H), 7.31 (m, 15H), 7.11 (m, 2H), 4.34 (t, *J* = 6.9 Hz, 2H), 1.76 (m, 4H), 1.07 (m, 6H). ¹³C NMR (100 MHz, DMSO) δ 155.99, 151.74, 147.07, 146.89, 142.92, 134.59, 129.99, 129.39, 128.18, 127.92, 127.82, 127.08, 125.70, 124.34, 123.82, 121.33, 119.61, 109.20, 100.43, 92.16, 50.00, 32.36, 29.91, 28.17, 26.00, 25.02.

***O*-Trityl-6-aminonaphthyltriazolyheptahydroxamate (70c) –**

Reaction of 6-ethynyl-naphthalen-2-amine (0.10 g, 0.60 mmol) and 7-azido-*O*-tritylheptahydroxamate (0.26 g, 0.60 mmol) within 12 h as described for synthesis of **66a**

gave compound **70c** (0.24 g, 67%) as a dark orange solid. ^1H NMR (400 MHz, DMSO – d_6) δ 10.16 (s, 1H), 8.51 (s, 1H), 8.09 (s, 1H), 7.66 (m, 3H), 7.31 (m, 15H), 6.94 (d, J = 8.8 Hz, 1H), 6.81 (s, 1H), 5.45 (s, 2H), 4.32 (t, J = 6.6 Hz, 2H), 1.76 (m, 4H), 1.12 (m, 6H). ^{13}C NMR (100 MHz, DMSO) δ 146.87, 144.63, 142.46, 134.60, 128.94, 127.49, 126.25, 123.69, 123.45, 120.43, 118.90, 105.80, 91.73, 49.42, 31.89, 29.49, 27.74, 25.56, 24.63.

O-Trityl-6-aminonaphthyltriazolyloctahydroxamate (70d) –

Reaction of 6-ethynylnaphthalen-2-amine (0.10 g, 0.60 mmol) and 8-azido-*O*-trityloctahydroxamate (0.26 g, 0.60 mmol) within 12 h as described for synthesis of **66a** gave compound **70d** (0.22 g, 59%) as a dark orange solid. ^1H NMR (400 MHz, DMSO) δ 10.13 (s, 1H), 8.52 (s, 1H), 8.08 (s, 1H), 7.66 (m, 3H), 7.29 (m, 15H), 6.93 (dd, J = 8.7, 2.1 Hz, 1H), 6.80 (d, J = 1.9 Hz, 1H), 5.44 (s, 2H), 4.35 (t, J = 7.0 Hz, 2H), 1.77 (m, 4H), 1.07 (m, 8H). ^{13}C NMR (100 MHz, CDCl_3) δ 148.04, 144.45, 140.99, 134.60, 129.47, 128.95, 128.05, 127.81, 126.29, 124.61, 124.31, 124.29, 119.05, 118.65, 108.36, 104.75, 50.68, 50.27, 31.04, 30.16, 28.56, 26.18, 23.23.

6-(6-hydroxynaphthyl)triazolylohexahydroxamate (71a) –

Reaction of **70a** (0.11 g, 0.19 mmol) with triisopropylsilane (0.4 ml) & TFA (0.15 ml) in CH_2Cl_2 (7 ml) at RT within 15 min as described for the synthesis of **67a**, gave 55 mg (86%) of **71a** as a white solid. ^1H NMR (400 MHz, DMSO) δ 10.33 (s, 1H), 8.60 (s, 1H), 8.24 (s, 1H), 7.80 (m, 3H), 7.11 (m, 2H), 4.39 (t, J = 6.9 Hz, 2H), 1.91 (m, 4H), 1.54 (m, 2H), 1.24 (m, 2H). ^{13}C NMR (100 MHz, DMSO) δ 168.98, 155.60, 146.67, 136.69,

134.19, 129.60, 127.77, 126.69, 125.25, 123.93, 123.43, 120.97, 119.21, 108.79, 49.44, 32.08, 29.40, 25.51, 24.55. HRMS (MALDI) calcd for $C_{18}H_{21}N_4O_3$ $[M+H]^+$ 341.1614 found 341.1633.

7-(6-hydroxynaphthyl)triazolylheptahydroxamate (71b) –

Reaction of **70b** (0.09 g, 0.15 mmol) with triisopropylsilane (0.4 ml) & TFA (0.15 ml) in CH_2Cl_2 (7 ml) at RT within 15 min as described for the synthesis of **67a**, gave 48 mg (92%) of **71b** as a white solid. 1H NMR (400 MHz, DMSO) δ 10.32 (s, 1H), 9.79 (s, 1H), 8.65 (s, 1H), 8.60 (s, 1H), 8.23 (s, 1H), 7.80 (m, 3H), 7.09 (m, 2H), 4.38 (t, J = 7.0 Hz, 2H), 1.88 (m, 4H), 1.47 (m, 2H), 1.27 (m, 4H). ^{13}C NMR (100 MHz, DMSO) δ 155.57, 146.65, 134.16, 129.58, 127.74, 126.67, 125.24, 123.92, 123.40, 120.94, 119.19, 108.77, 49.49, 32.17, 29.54, 28.00, 25.62, 24.95. HRMS (MALDI) calcd for $C_{19}H_{23}N_4O_3$ $[M+H]^+$ 355.1774 found 355.1770.

7-(6-aminonaphthyl)triazolylheptahydroxamate (71c) –

Reaction of **70c** (0.065 g, 0.15 mmol) with triisopropylsilane (0.4 ml) & TFA (0.15 ml) in CH_2Cl_2 (7 ml) at RT within 15 min as described for the synthesis of **67a**, gave 32 mg (quantitative) of **71c** as an off white solid. 1H NMR (400 MHz, DMSO) δ 10.35 (s, 1H), 8.68 (s, 1H), 8.37 (s, 1H), 7.97 (m, 3H), 7.63 (s, 1H), 7.35 (dd, J = 8.8, 1.4 Hz, 1H), 4.39 (t, J = 7.0 Hz, 2H), 1.89 (m, 4H), 1.47 (m, 2H), 1.27 (m, 4H). ^{13}C NMR (100 MHz, DMSO) δ 169.12, 158.62, 158.26, 146.21, 132.83, 129.81, 127.82, 124.72, 123.39, 121.60, 121.22, 117.15, 48.62, 32.18, 29.55, 28.01, 25.63, 24.97. HRMS (MALDI) calcd for $C_{19}H_{24}N_5O_2$ $[M+H]^+$ 354.1930 found 354.1889.

8-(6-aminonaphthyl)triazolyloctahydroxamate (**71d**) –

Reaction of **70d** (0.05 g, 0.15 mmol) with triisopropylsilane (0.4 ml) & TFA (0.15 ml) in CH₂Cl₂ (7 ml) at RT within 15 min as described for the synthesis of **67a**, gave 27 mg (90%) of **71d** as a off white solid. ¹H NMR (400 MHz, DMSO) δ 8.67 (s, 1H), 8.37 (s, 1H), 8.29 (d, *J* = 1.2 Hz, 2H), 7.97 (m, 3H), 7.61 (s, 1H), 7.35 (d, *J* = 8.8 Hz, 1H), 4.40 (t, *J* = 6.9 Hz, 2H), 1.89 (m, 4H), 1.46 (m, 2H), 1.25 (m, 6H). HRMS (MALDI) calcd for C₂₀H₂₆N₅O₂ [M+H]⁺ 368.2087 found 368.2039.

6-Ethoxy-2-ethynylnaphthalene (**72**) –

In a sealed pressure tube 6a (0.10 g, 0.59 mmol), ethylbromide (0.19 g, 1.78 mmol), K₂CO₃ (0.24 g, 1.78 mmol) were dissolved in THF (10 mL). Reaction mixture was stirred overnight at 60 °C. Reaction mixture was then quenched with water (40 mL) and CH₂Cl₂ (50 mL). Organic layer was washed subsequently with water (2X30 mL) and brine (1X30 mL) and dried over Na₂SO₄. Column chromatography with Hexane:EtOAc (4:1) gave pure **72** (0.07 g, 57%) as brown solid. ¹H NMR (400 MHz, CDCl₃) δ 7.93 (s, 1H), 7.66 (m, 2H), 7.48 (dd, *J* = 8.5, 1.6 Hz, 1H), 7.15 (dd, *J* = 8.9, 2.5 Hz, 1H), 7.07 (d, *J* = 2.4 Hz, 1H), 4.12 (q, *J* = 7.0 Hz, 2H), 3.11 (s, 1H), 1.47 (t, *J* = 7.0 Hz, 3H). ¹³C NMR (100 MHz, CDCl₃) δ 157.75, 134.39, 132.02, 129.22, 129.02, 128.17, 126.74, 119.71, 116.77, 106.45, 84.22, 63.48, 14.71. HRMS (EI) calcd for C₁₄H₁₂N₅O [M]⁺ 196.0888 found 196.0891.

***O*-Trityl-6-ethoxynaphthyltriazolyloctahydroxamate (73a) –**

Reaction of **72** (0.063 g, 0.32 mmol) and 8-azido-*O*-trityloctahydroxamate (0.17 g, 0.39 mmol) within 12 h as described for synthesis of **66a** gave compound **73a** (0.15 g, 72%) as a white solid. ¹H NMR (400 MHz, DMSO) δ 10.13 (s, 1H), 8.61 (s, 1H), 8.29 (s, 1H), 7.89 (m, 3H), 7.30 (m, 16H), 7.15 (m, 1H), 4.37 (t, *J* = 6.7 Hz, 2H), 4.13 (q, *J* = 6.9 Hz, 2H), 1.79 (m, 3H), 1.38 (t, *J* = 7.0 Hz, 4H), 1.04 (m, 8H). ¹³C NMR (100 MHz, CDCl₃) δ 176.99, 157.02, 147.67, 141.74, 140.90, 134.16, 129.45, 128.85, 128.72, 127.95, 127.14, 125.68, 124.16, 124.01, 119.35, 119.25, 106.35, 93.15, 63.31, 51.21, 50.16, 30.90, 30.05, 28.58, 26.05, 23.12, 14.66. HRMS (MALDI) calcd for C₄₁H₄₂N₄O₃ [M+Na]⁺ 661.3149 found 661.3099.

***O*-Trityl-6-ethoxynaphthyltriazolyldecahydroxamate (73b) –**

Reaction of **72** (0.066 g, 0.34 mmol) and 10-azido-*O*-trityldecahydroxamate (0.17 g, 0.37 mmol) within 12 h as described for synthesis of **66a** gave compound **73b** (0.13 g, 56%) as a white solid. ¹H NMR (400 MHz, DMSO) δ 10.11 (s, 1H), 8.62 (s, 1H), 8.28 (s, 1H), 7.87 (m, 3H), 7.29 (m, 16H), 7.15 (dd, *J* = 9.0, 2.2 Hz, 1H), 4.38 (t, *J* = 7.0 Hz, 2H), 4.13 (q, *J* = 7.0 Hz, 2H), 1.77 (m, 4H), 1.38 (t, *J* = 6.9 Hz, 3H), 1.12 (m, 14H). ¹³C NMR (100 MHz, CDCl₃) δ 157.03, 147.69, 141.77, 140.92, 134.18, 129.46, 128.86, 128.74, 127.95, 127.58, 127.14, 125.68, 124.17, 124.03, 119.36, 119.25, 106.36, 63.33, 50.46, 50.23, 31.02, 30.77, 30.15, 28.94, 26.29, 14.67. HRMS (MALDI) calcd for C₄₃H₄₆N₄O₃ [M+Na]⁺ 689.3462 found 689.3473.

8-(6-Ethoxynaphthyl)triazolyloctahydroxamic acid (74a) –

Reaction of **73a** (0.09 g, 0.15 mmol) with triisopropylsilane (0.4 ml) & TFA (0.15 ml) in CH₂Cl₂ (7 ml) at RT within 15 min as described for the synthesis of **67a**, gave 48 mg (92%) of **74a** as a white solid. ¹H NMR (400 MHz, DMSO) δ 10.32 (s, 1H), 8.65 (s, 1H), 8.62 (s, 1H), 8.28 (s, 1H), 7.87 (m, 3H), 7.30 (d, *J* = 2.3 Hz, 1H), 7.15 (dd, *J* = 8.9, 2.4 Hz, 1H), 4.38 (t, *J* = 7.0 Hz, 2H), 4.13 (q, *J* = 7.0 Hz, 2H), 1.88 (m, 5H), 1.37 (m, 10H). ¹³C NMR (100 MHz, DMSO) δ 169.12, 156.68, 146.53, 133.90, 129.52, 128.50, 127.36, 126.06, 124.09, 123.34, 121.15, 119.35, 106.66, 63.19, 49.55, 32.24, 29.65, 28.43, 28.14, 25.81, 25.06, 14.68. HRMS (MALDI) calcd for C₂₂H₂₉N₄O₃ [M+H]⁺ 397.2234 found 397.2229.

10-(6-Ethoxynaphthyl)triazolyldecahydroxamic acid (74b) –

Reaction of **73b** (0.12 g, 0.18 mmol) with triisopropylsilane (0.4 ml) & TFA (0.15 ml) in CH₂Cl₂ (7 ml) at RT within 15 min as described for the synthesis of **67a**, gave 63 mg (83%) of **74b** as a white solid. ¹H NMR (400 MHz, DMSO) δ 10.29 (s, 1H), 8.61 (s, 1H), 8.28 (s, 1H), 7.87 (m, 3H), 7.30 (s, 1H), 7.16 (d, *J* = 9.0 Hz, 1H), 4.38 (t, *J* = 7.1 Hz, 2H), 4.14 (q, *J* = 6.9 Hz, 2H), 1.89 (m, 4H), 1.34 (m, 15H). ¹³C NMR (100 MHz, DMSO) δ 169.44, 156.63, 146.48, 133.85, 129.46, 128.46, 127.29, 126.04, 124.05, 123.29, 121.08, 119.29, 106.64, 63.14, 49.53, 32.24, 29.61, 28.72, 28.63, 28.52, 28.36, 25.85, 25.07, 14.62. HRMS (MALDI) calcd for C₂₄H₃₃N₄O₃ [M+H]⁺ 425.2547 found 425.2525.

Ethyl 7-(6-amino-2-naphthyl)triazolyheptanoate (75a) –

Reaction of **69b** (0.20 g, 1.19 mmol) and Ethyl 7-azidoheptanoate (0.36 g, 1.79 mmol) within 12 h as described for synthesis of **66a** gave compound **75a** (0.34 g, 77%) as a dark orange solid. ¹H NMR (400 MHz, CDCl₃) δ 8.12 (s, 1H), 7.74 (dd, *J* = 8.5, 1.4 Hz, 1H), 7.66 (s, 1H), 7.59 (d, *J* = 9.3 Hz, 1H), 7.52 (d, *J* = 8.5 Hz, 1H), 6.87 (m, 2H), 4.21 (t, *J* = 7.2 Hz, 2H), 3.98 (m, 4H), 2.20 (t, *J* = 7.4 Hz, 2H), 1.80 (m, 2H), 1.53 (m, 2H), 1.21 (m, 7H). ¹³C NMR (100 MHz, CDCl₃) δ 173.32, 147.72, 144.61, 134.42, 129.13, 127.44, 126.02, 124.29, 124.03, 123.99, 119.03, 118.53, 107.93, 59.95, 49.87, 33.80, 29.77, 28.13, 25.83, 24.35, 13.97.

Ethyl 8-(6-amino-2-naphthyl)triazolyloctanoate (75b) –

Reaction of **69b** (0.20 g, 1.19 mmol) and Ethyl 8-azidooctanoate (0.38 g, 1.79 mmol) within 12 h as described for synthesis of **66a** gave compound **75b** (0.31 g, 73%) as a dark orange solid. ¹H NMR (400 MHz, CDCl₃) δ 8.13 (d, *J* = 1.2 Hz, 1H), 7.75 (dd, *J* = 8.5, 1.7 Hz, 1H), 7.70 (s, 1H), 7.63 (m, 1H), 7.55 (d, *J* = 8.6 Hz, 1H), 6.89 (m, 2H), 4.26 (t, *J* = 7.2 Hz, 2H), 4.08 (q, *J* = 7.1 Hz, 2H), 3.96 (s, 2H), 2.23 (t, *J* = 7.5 Hz, 2H), 1.87 (m, 2H), 1.55 (m, 2H), 1.21 (m, 9H). ¹³C NMR (100 MHz, CDCl₃) δ 173.55, 147.80, 144.56, 134.46, 129.23, 127.54, 126.10, 124.38, 124.10, 124.07, 119.02, 118.56, 108.06, 60.00, 50.06, 33.99, 30.00, 28.61, 28.42, 26.06, 24.56, 14.04. HRMS (EI) calcd for C₂₂H₂₈N₄O₂ [M]⁺ 380.2212 found 380.2213.

Ethyl 7-(6-azido-2-naphthyl)triazolyheptanoate (76a) –

The amine **75a** (0.33 g, 0.9 mmol) was suspended in HCl/H₂O (1:1; 14 mL) and cooled to 0 °C. An aqueous solution of NaNO₂ (0.08 g, 1.13 mmol) was added dropwise and then reaction mixture was stirred for 1h. An aqueous solution of NaN₃ (0.18 g, 2.70 mmol) was added dropwise. The reaction mixture was stirred at RT for another 3h and extracted with EtOAc (3X30 mL). The organic layers were washed with brine (2 X 30 mL), dried over Na₂SO₄ and concentrated under vacuo to give 0.31 g (86%) of pure **76a** as brown solid. ¹H NMR (400 MHz, CDCl₃) δ 8.28 (d, *J* = 0.9 Hz, 1H), 7.91 (dd, *J* = 8.5, 1.7 Hz, 1H), 7.79 (m, 3H), 7.40 (d, *J* = 2.2 Hz, 1H), 7.13 (dd, *J* = 8.7, 2.3 Hz, 1H), 4.38 (t, *J* = 7.2 Hz, 2H), 4.10 (q, *J* = 7.1 Hz, 2H), 2.26 (t, *J* = 7.5 Hz, 2H), 1.93 (m, 2H), 1.58 (m, 2H), 1.30 (m, 5H), 1.22 (t, *J* = 7.1 Hz, 3H). ¹³C NMR (100 MHz, CDCl₃) δ 173.61, 147.34, 137.58, 133.49, 130.99, 130.04, 127.59, 127.47, 124.90, 124.10, 119.60, 119.20, 115.59, 60.12, 50.32, 34.10, 30.16, 28.73, 28.55, 26.20, 24.66, 14.15. HRMS (EI) calcd for C₂₂H₂₆N₆O₂ [M]⁺ 406.2117 found 406.2118.

Ethyl 8-(6-azido-2-naphthyl)triazolyloctanoate (76b) –

Reaction of amine **75b** (0.30 g, 0.82 mmol), NaNO₂ (0.07 g, 1.02 mmol), NaN₃ (0.16 g, 2.46 mmol) in HCl/H₂O (1:1; 14 mL) within 4h as described for synthesis of **76b** gave compound **13b** (0.29 g, 74%) as a brown solid. ¹H NMR (400 MHz, CDCl₃) δ 8.29 (d, *J* = 0.9 Hz, 1H), 7.92 (dd, *J* = 8.5, 1.7 Hz, 1H), 7.84 (m, 2H), 7.78 (m, 1H), 7.42 (d, *J* = 2.2 Hz, 1H), 7.15 (dd, *J* = 8.7, 2.3 Hz, 1H), 4.40 (t, *J* = 7.2 Hz, 2H), 4.10 (q, *J* = 7.1 Hz, 2H), 2.27 (t, *J* = 7.5 Hz, 2H), 1.96 (m, 2H), 1.59 (m, 2H), 1.33 (m, 6H), 1.23 (t, *J* = 7.1 Hz, 3H).

7-(6-azido-2-naphthyl)triazolylheptanoic acid (77a) –

To a stirring reaction mixture of ester **76a** (0.20 g, 0.51 mmol) in THF:water (3:1; 12 mL) was added LiOH:H₂O (0.11 g, 2.55 mmol). After overnight stirring at RT, reaction mixture was quenched with addition of water (35 mL) and was extracted with EtOAc (2X30 mL). Aqueous layer was isolated and 1N HCl was added to bring pH ~ 2. Aqueous layer was extracted with EtOAc (3X30 mL). Combined organic layer was washed with water (1X35 mL), brine (1X30 mL), dried over Na₂SO₄ to give **77a** (0.17 g) as a crude off white solid which was used for next step without further purification.

8-(6-azido-2-naphthyl)triazolyloctanoic acid (77b) –

Reaction of ester **76b** (0.20 g, 0.49 mmol), LiOH:H₂O (0.10 g, 2.46 mmol) within 12h as described for synthesis of **77a** gave compound **77b** (0.17 g) as a crude off white solid which was used for next step without further purification.

O-Trityl-6-azido-2-naphthyltriazolylheptahydroxamate (78a) –

Carboxylic acid **77a** (92 mg, 0.25 mmol) was dissolved in anhydrous DMF (8 mL). Diisopropylethylamine (65 mg, 0.50 mmol), TBTU (162 mg, 0.50 mmol) and finally *O*-tritylhydroxylamine (91 mg, 0.32 mmol) was added sequentially. After 2 h of stirring reaction mixture was poured into CH₂Cl₂ (50 mL) and water (50 mL). Organic layer was separated and extracted 3 times in each case with water, sodium bicarbonate solution (5%) and water. After washing with brine and drying over Na₂SO₄, solvent was evaporated *in vacuo*. Column chromatography with eluent system CH₂Cl₂-acetone (step gradient, 0-12% of acetone) gave 0.13 mg of compound **78a** (85%) as a white solid. ¹H

NMR (400 MHz, DMSO) δ 10.15 (s, 1H), 8.66 (s, 1H), 8.39 (s, 1H), 8.00 (m, 3H), 7.68 (d, J = 2.3 Hz, 1H), 7.29 (m, 15H), 4.36 (t, J = 7.0 Hz, 2H), 1.78 (m, 4H), 1.08 (m, 6H). ^{13}C NMR (100 MHz, DMSO) δ 146.09, 142.43, 137.02, 133.07, 130.78, 130.15, 128.91, 127.94, 127.68, 127.45, 124.71, 123.30, 121.53, 119.44, 115.78, 91.68, 54.82, 49.50, 31.90, 29.41, 27.68, 25.51.

***O*-Trityl-6-azido-2-naphyltriazolyloctahydroxamate (78b) –**

Reaction of carboxylic acid **77b** (0.30 g, 1.07 mmol), DIPEA (0.10 mL, 0.58 mmol), TBTU (0.19 g, 0.58 mmol), and *O*-tritylhydroxylamine (0.10 g, 0.35 mmol) within 2h as described for the synthesis of **78a** gave compound **78b** (0.15 g, 82%) as a white solid. ^1H NMR (400 MHz, CDCl_3) δ 8.29 (s, 1H), 7.92 (dd, J = 8.5, 1.7 Hz, 1H), 7.83 (m, 2H), 7.77 (d, J = 8.6 Hz, 1H), 7.41 (m, 3H), 7.27 (m, 12H), 7.14 (dd, J = 8.7, 2.3 Hz, 1H), 4.36 (t, J = 7.1 Hz, 2H), 1.86 (m, 2H), 1.55 (m, 2H), 1.21 (m, 6H), 1.03 (m, 2H). ^{13}C NMR (100 MHz, CDCl_3) δ 171.16, 147.32, 140.97, 137.58, 133.50, 131.01, 130.04, 128.90, 127.98, 127.60, 127.46, 124.91, 124.12, 119.62, 119.18, 115.60, 60.27, 50.29, 30.07, 28.48, 26.08, 24.59, 20.92, 14.09.

7-(6-Azido-2-naphyl)triazolylheptahydroxamic acid (79a) –

Reaction of **78a** (0.065 g, 0.10 mmol) with triisopropylsilane (0.2 mL) & TFA (0.10 mL) in CH_2Cl_2 (7 mL) at RT within 15 min as described for the synthesis of **67a**, gave 27 mg (70%) of **79a** as a white solid. ^1H NMR (400 MHz, DMSO) δ 10.31 (s, 1H), 8.68 (s, 1H), 8.64 (s, 1H), 8.39 (s, 1H), 7.99 (m, 3H), 7.68 (d, J = 2.3 Hz, 1H), 7.28 (dd, J = 8.8, 2.3 Hz, 1H), 4.41 (t, J = 7.0 Hz, 2H), 1.90 (m, 4H), 1.48 (m, 2H), 1.28 (m, 4H). ^{13}C NMR

(100 MHz, dmso) δ 168.98, 146.10, 137.06, 133.08, 130.78, 130.16, 127.96, 127.69, 123.32, 121.57, 119.45, 115.78, 105.85, 49.52, 32.13, 29.47, 27.95, 25.57, 24.89.

8-(6-Azido-2-naphyl)triazolyloctahydroxamic acid (79b) –

Reaction of **78b** (0.04 g, 0.063 mmol) with triisopropylsilane (0.2 ml) & TFA (0.10 ml) in CH₂Cl₂ (7 ml) at RT within 15 min as described for the synthesis of **67a**, gave 24 mg (quantitative) of **79b** as a white solid. ¹H NMR (400 MHz, DMSO) δ 10.31 (s, 1H), 8.69 (s, 1H), 8.64 (s, 1H), 8.39 (s, 1H), 7.99 (m, 3H), 7.69 (s, 1H), 7.28 (dd, J = 8.8, 2.3 Hz, 1H), 4.41 (t, J = 7.0 Hz, 2H), 1.90 (m, 4H), 1.46 (m, 2H), 1.24 (m, 6H). ¹³C NMR (100 MHz, DMSO) δ 169.06, 146.09, 137.04, 133.09, 130.79, 130.17, 127.94, 127.69, 124.72, 123.32, 121.59, 119.45, 115.79, 49.54, 32.19, 29.56, 28.37, 28.07, 25.74, 24.98.

3.6 REFERENCES

1. Nilsen, T. W. *Molecular Cell* **2002**, 9, 8.
2. Jurica, M. S. *Curr. Opin. Struct. Biol.* **2008**, 18, 315.
3. Disney, M. D. *Nat. Chem. Biol.* **2008**, 4(12), 723.
4. Meshorer E.; Soreq, H. *Trends Neurosci.* **2006**, 29 (4), 216.
5. Teraoka, S. N.; Becker-Catania, S. T. M.; Liang, T.; Onengüt, S.; Tolun, A.; Chessa, L.; Sanal, O.; Bernatowska, E.; Gatti, R. A.; Concannon, P. *Am. J. Hum. Genet.* **1999**, 64(6), 1617.
6. Deckert, J.; Hartmuth, K.; Boehringer, D.; Behzadnia, N.; Will, C.L.; Kastner, B.; Stark, H.; Urlaub, H.; Lührmann, R. *Mol. Cell Biol.* **2006**, 26(14), 5528.
7. Behzadnia, N.; Golas, M.; Hartmuth, K.; Sander, B.; Kastner, B.; Deckert, J.; Dube, P.; Will, C. L.; Urlaub, H.; Stark, H.; Lührmann, R. *EMBO J.* **2007**, 26(6), 1737.

8. Bessonov, S.; Anokhina, M.; Will, C. L.; Urlaub, H.; Lührmann, R. *Nature Chemical Biology* **2008** ,452(7189), 846.
9. Boehringer, D.; Makarov, E. M.; Sander, B.; Makarova, O. V.; Kastner, B.; Lührmann, R.; Stark, H. *Nat. Struct. Mol. Biol.* **2004**, 11(5), 463.
10. Häcker, I.; Sander, B.; Golas, M. M.; Wolf, E.; Karagöz, E.; Kastner, B.; Stark, H.; Fabrizio, P.; Lührmann, R. *Nat. Struct. Mol. Biol.* **2008** , 15(11), 1206.
11. Jurica, M. S.; Licklider, L.; Gygi, S. R.; Grigorieff, N.; Moore, M. J. *RNA* **2002**, 8(4), 426.
12. Jurica, M. S.; Sousa, D.; Moore, M. J.; Grigorieff, N. *Nat. Struct. Mol. Biol.* **2004**, 11(3), 265.
13. Pomeranz Krummel, D. A.; Oubridge, C.; Leung, A. K.; Li, J.; Nagai, K.; *Nature Chemical Biology* **2009** , 458(7237), 475.
14. Sander, B.; Golas, M.; Makarov, E. M.; Brahms, H.; Kastner, B.; Lührmann R.; Stark, H. *Mol. Cell.* **2006** , 24(2), 267.
15. Spadaccini, R.; Reidt, U.; Dybkov, O.; Will, C.; Frank, R.; Stier, G.; Corsini, L.; Wahl, M. C.; Lührmann, R.; Sattler, M. *RNA.* **2006**, 12(3), 410.
16. Will, C. L.; Lührmann, R. *Cold Spring Harb Perspect Biol.* **2011**, 3(7), a003707.
17. Jurica, M. S.; Moore, M. J. *Mol. Cell* **2003** , 12(1), 5.
18. Wahl, M. C.; Will, C. L.; Lührmann, R. *Cell* **2009**, 136(4), 701.
19. Kaida, D.; Motoyoshi, H.; Tashiro, E.; Nojima, T.; Hagiwara, M.; Ishigami, K.; Watanabe, H.; Kitahara, T.; Yoshida, T.; Nakajima, H.; Tani, T.; Horinouchi, S.; Yoshida, M. *Nat. Chem. Biol.* **2007**, 3(9), 576.
20. Kotake, Y.; Sagane, K.; Owa, T.; Mimori-Kiyosue, Y.; Shimizu, H.; Uesugi, M.; Ishihama, Y.; Iwata, M. and Mizui, Y. *Nature Chemical Biology* **2007**, 3, 570.
21. Aukema, K. G.; Chohan, K.; Plourde, G. L.; Reimer, K. B.; Rader, S. D. *ACS Chem. Biol.* **2009** , 4(9), 759.
22. O'Brien, K.; Matlin, A.; Lowell, A. M.; Moore, M. J. *J. Biol. Chem.* **2008**, 283(48), 33147.
23. Ajuh, P.; Lamond, A. *Nucleic Acids Res.* **2003**, 31(21), 6104.
24. Hnilicová, J. H. S.; Dušková, E.; Icha, J.; Tománková, T.; Staněk, D. *PLoS One* **2011**, 6(2), e16727

25. Kuhn, A. N.; van Santen, M. A.; Schwienhorst, A.; Urlaub, H. and Luhrmann, R. *RNA* **2009**, 15, 153.
26. Lu, Y.; Qian, X.; Krug, R. M. *Genes Dev.* **1994**, 8(15), 1817.
27. Mermoud, J. E.; Cohen, P. T.; Lamond, A. I. *EMBO J.* **1994**, 13(23), 5679.
28. Parker, A. R.; Steit, J. A. *RNA* **1997**, 3(11), 1301.
29. Zhou, H. L.; Lou, H. *Mol. Cell Biol.* **2008**, 28(17), 5507.
30. Fan, L.; Lagisetti, C.; Edwards, C. C.; Webb, T. R.; Potter, P.M. *ACS Chem. Biol.* **2011**, 6(6), 582.
31. Staley, J. P.; Guthrie, C. *Mol. Cell.* **1999**, 3(1), 55.
32. Rappsilber, J.; Ryder, U.; Lamond, A.I.; Mann, M. *Genome Res.* **2002** , 12(8), 1231.
33. Zhou, Z.; Licklider, L.; Gygi, S. P.; Reed, R. *Nature* **2002**, 419(6903), 182.
34. Shomron, N.; Malca, H., Vig, I.; Ast, G. *Nucleic Acids Res.* **2002** , 30(19), 4127.
35. Canzoneri, J.C.; Chen, P. C.; Oyelere, A. K. *Bioorg Med. Chem. Lett.* **2009**, 19(23), 6588.
36. Chen, P. C.; Patil, V.; Guerrant, W.; Green, P.; Oyelere, A. K. *Bioorg Med. Chem.* **2008**, 16(9), 4839.
37. Mwakwari, S.C.; Guerrant, W.; Patil, V.; Khan, S. I.; Tekwani, B.L.; Gurard-Levin, Z. A.; Mrksich, M.; Oyelere, A. K. *J. Med. Chem.* **2010**, 53(16), 6100.
38. Mwakwari, S. C.; Patil, V.; Guerrant, W.; Oyelere, A. K. *Curr. Top Med. Chem.* **2010**, 10(14), 1423.
39. Oyelere, A. K.; Chen, P.; Guerrant, W.; Mwakwari, S. C.; Hood, R.; Zhang, Y.; Fan, Y. *J. Med. Chem.* **2009**, 52(2), 456.
40. Patil, V.; Guerrant, W.; Chen, P. C.; Gryder, B.; Benicewicz, D. B.; Khan, S. I.; Tekwani, B. L.; Oyelere, A. K. *Bioorg Med. Chem.* **2010**, 18(1), 415.
41. Gunderson, F. Q.; Merkhofer, E.; Johnson, T. L. *Proc Natl. Acad Sci. U S A.* **2011**, 108(5), 2004.
42. Ropero, S.; Estellar, M. *Mol. Oncol.* **2007**, 1(1), 19.
43. Miller, T. A.; Witter, D. J.; Belvedere, S. *J. Med. Chem.* **2003**, 46(24), 5097.

CHAPTER 4

DUAL ACTING HDAC – TOPOISOMERASES (TOPO) INHIBITORS

4.1 INTRODUCTION

Several rational pharmacological strategies, including vaccination, gene therapy, immunotherapy, and new target identification and validation, have emerged for the treatment of metastatic diseases. Despite these advances, chemotherapy remains the primary treatment of choice for most cancer cases.¹ However, almost all chemotherapeutic agents suffer from severe toxicities and other undesirable side-effects. To address these problems, the ideal chemotherapeutics will incorporate, within a single molecule, elements that allow for simultaneous targeting of multiple cancer-fighting targets while maintaining lower side effects.^{1c,2,3} This realization has spawned immense efforts in the literature. Studies aimed at identifying multivalent ligands as promising pharmacological tools, that may be more efficacious for various human diseases than highly selective single-target drugs, are ongoing in several academic and pharmaceutical labs.⁴⁻⁷ A subset of these studies has revealed that balanced modulation of a small number of targets may have superior efficacy and fewer side effects than single-target treatments.^{1c,7,8}

Epigenetic control has become widely accepted as a mechanism for cell regulation.⁹⁻¹¹ Specifically, HDAC is a class of epigenetic enzymes that has generated much interest in cancer therapeutics literature. HDACs are known to associate with many oncogenes and tumor suppressors, leading to altered expression patterns, and have consequently become attractive targets for small-molecule inhibition.^{12,13} HDACi have

been shown to cause growth arrest, differentiation, and apoptosis in tumor cells and in animal models by inducing histone hyperacetylation and p21^{waf1} expression.¹⁴⁻¹⁷ Additionally, modulation of activities of HDACs alters the activity of a diverse range of proteins, many of which are attractive therapeutic targets themselves, including p53, E2F, tubulin, and Hsp90.¹⁸⁻²² HDAC inhibition has been clinically validated as a therapeutic strategy for cancer treatment with the FDA approvals of suberoylanilide hydroxamic acid (SAHA) and romidepsin (FK-228) for treatment of cutaneous T cell lymphoma.²³⁻²⁵ However, a large number of the currently known HDACi have elicited only limited *in vivo* antitumor activities and have not progressed beyond preclinical characterizations.²⁶⁻²⁸ HDACi that modulate the functions of additional intracellular targets, other than the various HDAC isoforms, may be able to ameliorate many of the shortcomings of current inhibitors.

We modified the cap group to introduce additional warhead in HDACi design to combat cancer effectively. As many essential enzymes are overexpressed in cancer cells, multi-targeting therapy might be more beneficial, not only to eliminate cancer cells but also to combat the emergence of drug resistance. To explore the prospect in cancer therapy of a bivalent agent that combines two complimentary chemo-active groups within a single molecular architecture, we have synthesized dual-acting HDAC - Topoisomerase II (Topo II) and HDAC – Topoisomerase I (Topo I) inhibitors. We have identified single agents that simultaneously inhibit topoisomerase and HDAC activities for the first time. Moreover, they potently inhibit the proliferation of representative cancer cell lines.

4.2 HDAC – TOPOISOMERASE II (TOPO II) INHIBITORS

Due to the presence of large hydrophobic patches at the HDAC surface rim,^{29,30} it is conceivable that appropriate conjugation of the surface recognition group of a prototypical HDACi (Figure 4-1) to other hydrophobic anti-tumor pharmacophores could furnish a new class of bifunctional agents. To date, there exist only a few examples of this subtype of bifunctional HDACi derived compounds.³¹ Expansion of the repertoire of such bifunctional compounds could lead to broad acting, therapeutically-viable anti-cancer agents.

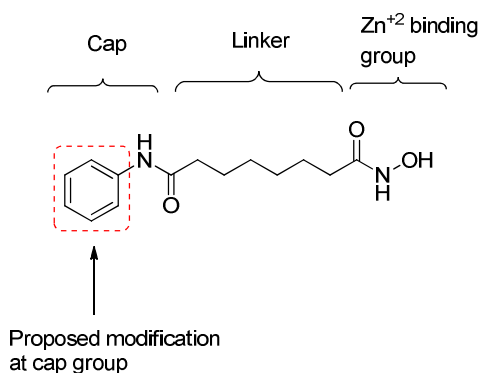


Figure 4-1. SAHA pharmacophoric model showing proposed modification at cap group.

An attractive starting point for a secondary target is the topoisomerase class of enzymes (Topo I and Topo II), which are validated targets for many small molecule inhibitors including clinically useful anthracyclines, such as doxorubicin (DOX) and daunomycin (DAU) (Figure 4-2), and camptothecins such as irinotecan and topotecan.³² Topo inhibitors elicit anticancer activities primarily by stabilizing the DNA-enzyme cleavable complex through intercalation between DNA base pairs. However, DNA does not exist as a naked structure in the nucleus. It is non-covalently associated with histones to form the nucleosomes which make up chromatin subunits. Agents, such as HDACi,

that induce hyperacetylation of histone proteins complexed with DNA could increase the accessibility of DNA within chromatin and consequently potentiate the anticancer activities of Topo inhibitors.^{33,34} Moreover, recent observations have shown that HDAC1, HDAC2 and Topo II co-localize *in vivo* as part of functionally coupled complexes.^{35,36} This evidence suggests simultaneous Topo and HDAC inhibition could be a viable alternative approach in cancer therapy.

4.2.1 Design of HDAC-Topoisomerase II Conjugates

Anthracyclines are one of the most thoroughly studied classes of anticancer agents with copious structure activity relationship (SAR) data to aid the design and characterization of new anthracycline-containing compounds.^{37-39,40,41}

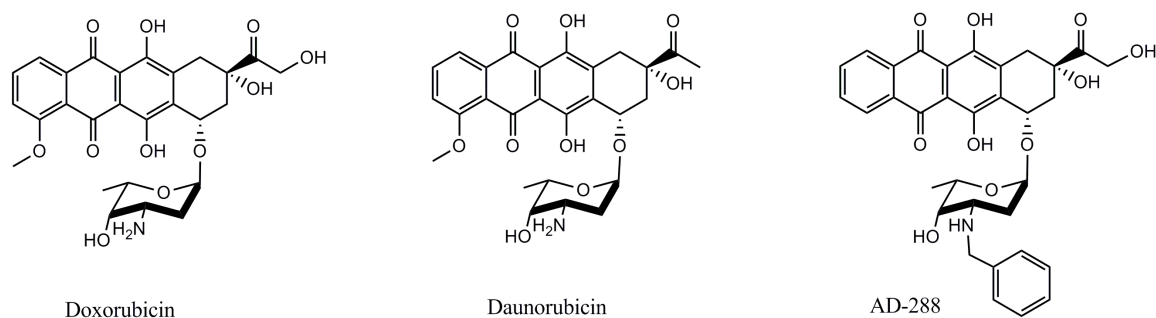


Figure 4-2. Representative Structures of Anthracycline Antibiotics

Specifically, *N*-benzylated anthracyclines such as **AD-288** (Figure 4-2) have enhanced Topo II inhibitory activities, reduced cardiotoxicity activity, and reduced susceptibility to the p-gp mediated multidrug resistance.⁴²⁻⁴⁶ We postulated that introduction of the HDACi via *N*-benzylation of the DAU amino group would be compatible with Topo II inhibition and possibly engender the positive attributes of **AD-288** to the resulting conjugates. In turn, the anthracycline moiety could serve two other purposes: i) as a

surface recognition cap group, allowing favorable orientation of hydroxamic acid within the zinc binding pocket of HDAC, and ii) as a delivery vehicle, since the transport of the anthracycline via proteasome could facilitate nuclear accumulation of HDACi.⁴¹ Based on the former, we designed two classes of conjugates - a direct DAU-SAHA conjugate and DAU-triazolylaryl hydroxamate conjugates (Figure 4-3). The later conjugates were inspired by our previous studies which revealed that the triazole moiety could be incorporated in lieu of an amide bond as a surface recognition connecting group in prototypical HDACi.⁴⁷

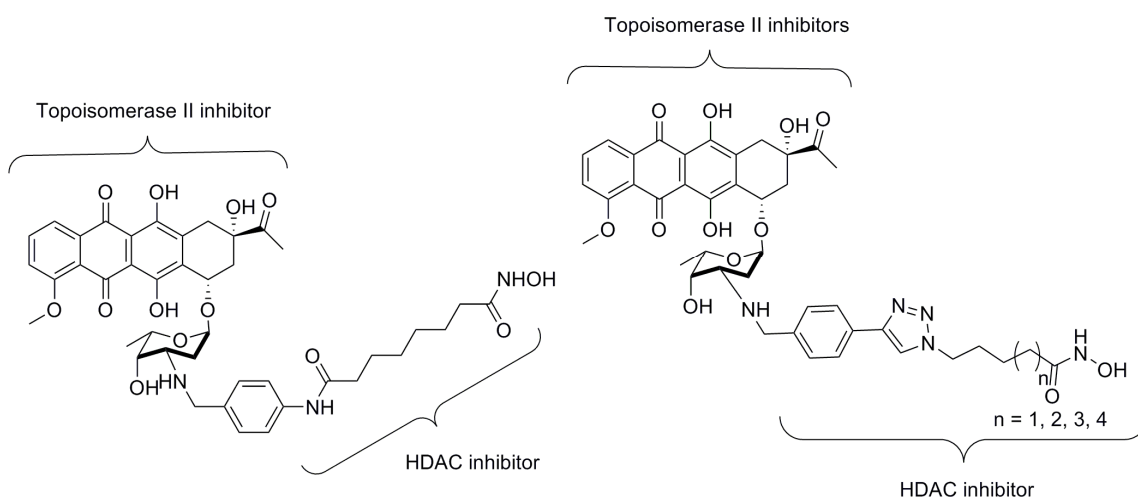


Figure 4-3. Design of dual-acting Topo II-HDAC inhibitors.

4.2.2 Synthesis of HDAC-Topoisomerase II Conjugates

Crucial to the successful synthesis of all the conjugates described in this report is the reductive amination reaction between DAU and appropriate aldehyde intermediates **5** and **10a-d** (Figure 4-4 and 4-5). Synthesis of aldehyde intermediate **5** started with the coupling of 4-aminobenzyl alcohol **1** to suberic anhydride **2** to give benzyl alcohol **3**. In order to assess the suitable oxidizing agent for conversion of alcohol **3** to aldehyde **4**, we

employed MnO_2 , PCC and Dess-Martin periodinane (DMP) oxidation. All yielded the desired aldehyde, with DMP giving the optimum yield among them. To synthesize the protected hydroxamate **5**, we coupled **4** to *O*-trityl hydroxylamine using standard EDC coupling chemistry. Interestingly, the amide bond of compound **4** was also susceptible to nucleophilic attack and led to a substantially lower yield under this condition. Using TBTU as coupling reagent resulted in the same outcome. Gratifyingly, the use of isobutylchloroformate (IBCF), as a coupling reagent gave coupled requisite product **5** in 66% yield within 2 h. Longer reaction times didn't improve the yield and led to degradation of product. Reductive amination with DAU hydrochloride was the major hurdle in making the DAU-SAHA conjugate. Initial investigation with NaBH_3CN as a reducing agent with acetonitrile–water solvent system at room temperature led to a complex reaction mixture. Employing a non-aqueous solvent system, as well as a milder reducing agent such as $\text{NaBH}(\text{OAc})_3$, didn't produce any detectable amount of product. Previous studies in the literature indicated that generation of free amine by addition of base and elevated temperature might promote the imine formation.^{48,49} Indeed, adding Hunig's base to the reductive amination reactions between DAU and aldehyde **5** in the presence of NaBH_3CN at 70 °C, gave the desired coupled product **6**, albeit in low yield. Reducing the reaction temperature to 50 °C and below worsened the yield, as did employing $\text{NaBH}(\text{OAc})_3$ as a reducing agent. The deprotection of the acid sensitive trityl group of compound **6** was accomplished by treatment with the Lewis acid boron trifluoride etherate.⁵⁰ This led to the removal of the trityl group to give the desired conjugate **7** in good yield without any need for further purification.

Similar chemistry was applied for the synthesis of triazole-based conjugates. The synthesis of the requisite aldehydes **10a-d** started with Cu(I)-catalyzed cycloaddition of 4-ethynylbenzaldehyde **8** with trityl-protected azido hydroxamates **9a-d** (Figure 4-5). Reductive amination of triazole aldehydes **10a-d** with DAU proceeds readily at room temperature in CH₃CN:H₂O (3:1) to give the triazole-based conjugates **11a-d** in slightly improved yields compared to conjugate **6**. Boron trifluoride etherate promoted deprotection of the trityl group of **11a-d** yielded the desired triazole-based conjugates **12a-d** in good to excellent yields.

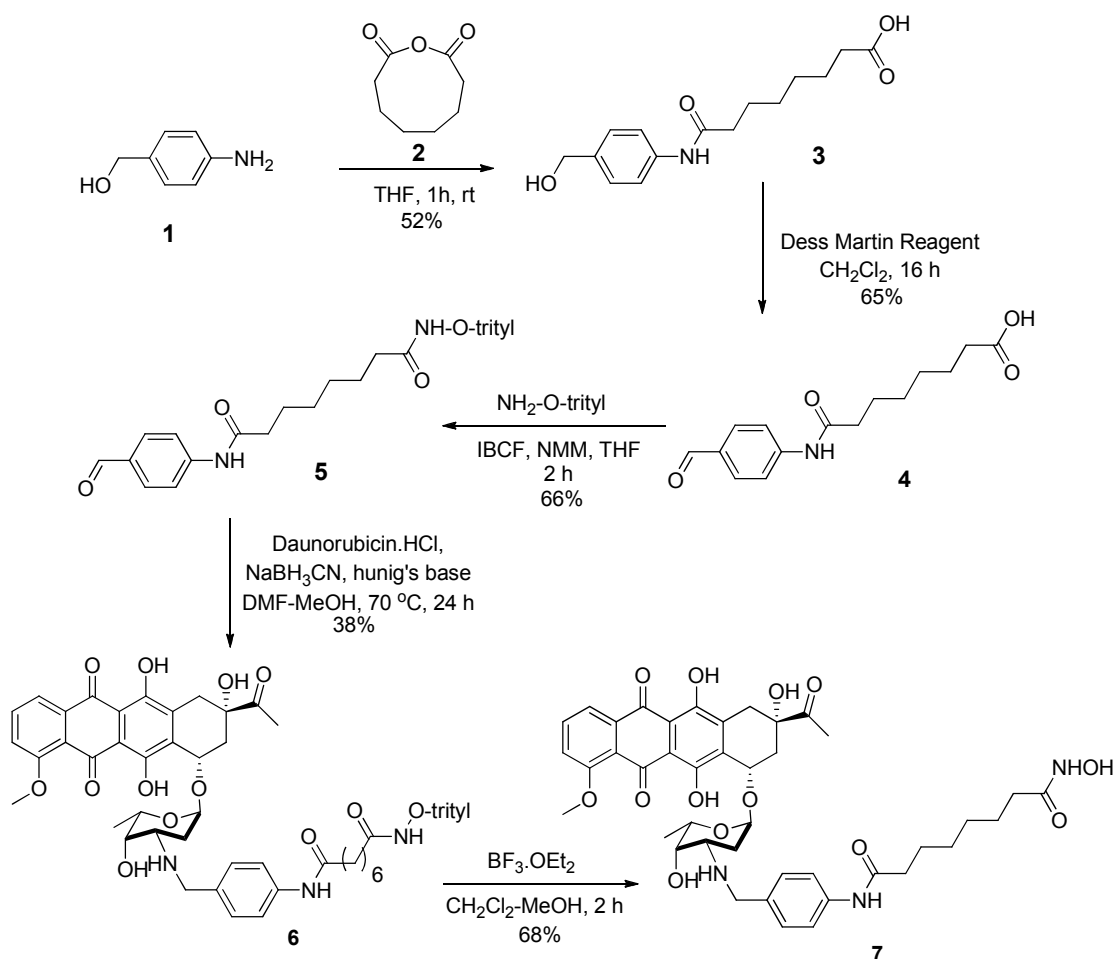


Figure 4-4. Synthesis of the SAHA-based dual-acting Topo II-HDAC inhibitor.

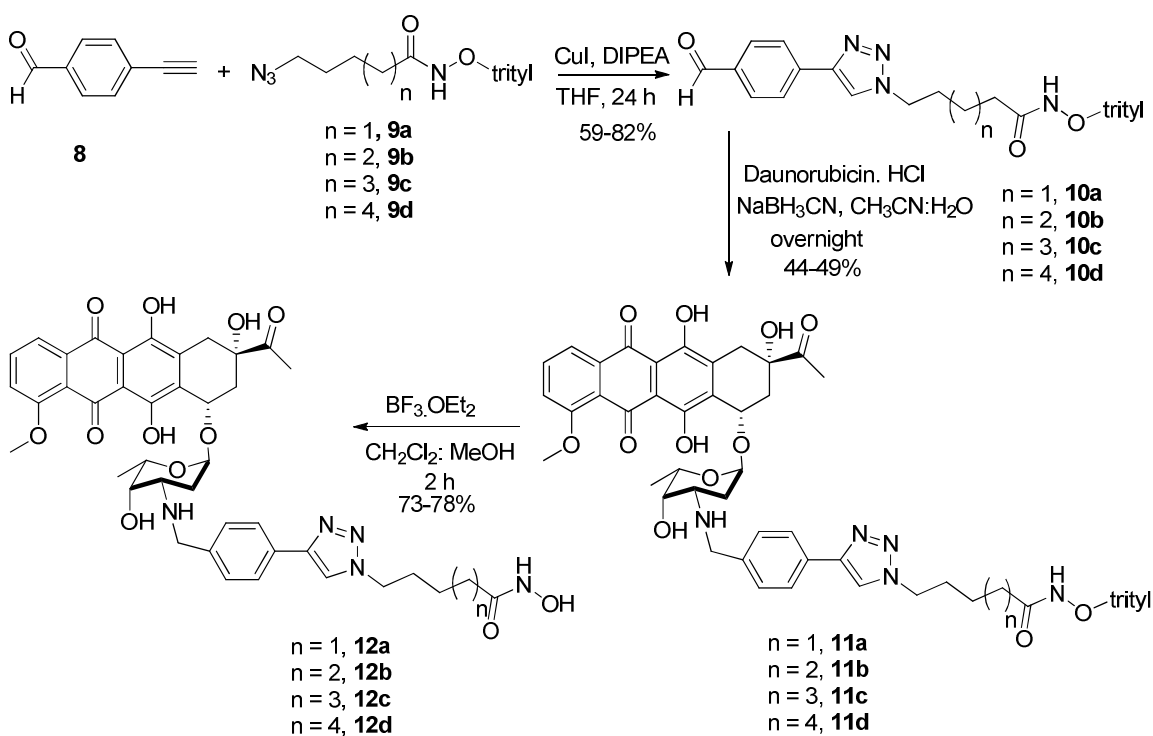


Figure 4-5. Synthesis of the SAHA-like, triazole-based Topo II-HDACi.

4.2.3 *In vitro* HDAC Inhibition of HDAC & Topoisomerase II Conjugates

We first tested the HDAC inhibition activity of compounds **7** and **12a-d** against crude HeLa cell nuclear extract HDACs using a cell free assay (*Fluor de Lys*) as previously described.⁴⁷ Overall, these compounds showed inhibition activities against HeLa cell nuclear extract HDACs which are comparable to or exceed that of the standard SAHA (Table 4-1). It is particularly interesting that **7** has identical anti-HDAC activity to SAHA. This result suggests that the attachment of DAU does not impair the interaction between the HDACi component of the conjugate and the HDAC enzyme outer surface residues. It is also conceivable that the conjugate may adopt a conformation whereby the anthracycline moiety can contribute positively to the interaction with the crucial active site or surface residues. All triazole-linked conjugates potently inhibit

HeLa cell nuclear extract HDACs with IC_{50} in the low to mid-nanomolar range. Among these conjugates, **12a** is the least active, closely followed by **12d**, which is about 20-fold more potent. Compounds **12b** and **12c** have the most potent anti-HDAC activity, with a slight preference for the six methylene-linked **12c**. Interestingly, the triazole-linked compound **12b** is 40-fold more potent than the amide-linked **7**, despite their similar linker length. Relative to the standard SAHA, **12c**, the most potent compound in this series, is 70-fold more potent (Table 4-1). The foregoing results showed that these conjugates followed a trend similar to that which we noted for the previously reported, structurally unrelated, triazole-based HDACi.⁴⁷

To obtain evidence for the HDAC isoform selectivity, we tested these dual acting Topo II –HDACi conjugates against selected recombinant HDACs – HDAC 1, HDAC 6 and HDAC 8. The pattern of the anti-HDAC activities of these compounds against HDAC 1 and HDAC 6 is similar to what we observed for the HeLa cell nuclear extract HDACs with few exceptions. Specifically, compounds **7** and **12b** have indistinguishable activity against HDAC 1 and HDAC 6 (Table 4-1). Additionally, **12a** which has mid-nanomolar IC_{50} against HeLa cell nuclear extract HDACs is almost inactive against HDAC 1 ($IC_{50} = 4.6 \mu M$) while it maintains decent activity against HDAC 6 ($IC_{50} = 0.6 \mu M$). We are not exactly sure of the cause of this disparity. In general, these compounds are weaker inhibitors of HDAC 8 with the exception of **7**, whose anti-HDAC 8 activity is only 2-fold less than its anti-HDAC 1 activity (Table 4-1). These data suggest that **7** is a more indiscriminate inhibitor of these sets of HDACs while the rest of the conjugates are more selective.

Table 4-1. *In vitro* HDAC Inhibition.

Compound	n	HDAC 1/2 IC ₅₀ (nM) ^a	HDAC 1 IC ₅₀ (nM) ^b	HDAC 6 IC ₅₀ (nM) ^b	HDAC 8 IC ₅₀ (nM) ^b
SAHA	-	65.0	38+/- 2	27+/- 2	294+/- 35
DAU	-	N.D.	N.T.	N.T.	N.T.
7	-	64.7	47+/- 3	20+/- 1	87+/- 6
12a	1	89.9	4,600+/- 240	555+/- 36	N.D.
12b	2	1.6	54+/- 3	30+/- 2	2000+/- 243
12c	3	0.9	8+/- 0.4	20+/- 0.4	674+/- 81
12d	4	4.2	11+/- 0.4	19+/- 1	294+/- 14

^aInhibition was assayed using the Biomol HDAC Fluorimetric Assay/Drug Discovery Kit by William Guerrant. ^bData obtained through contract arrangement with BPS Bioscience (San Diego, USA; www.bpsbioscience.com).

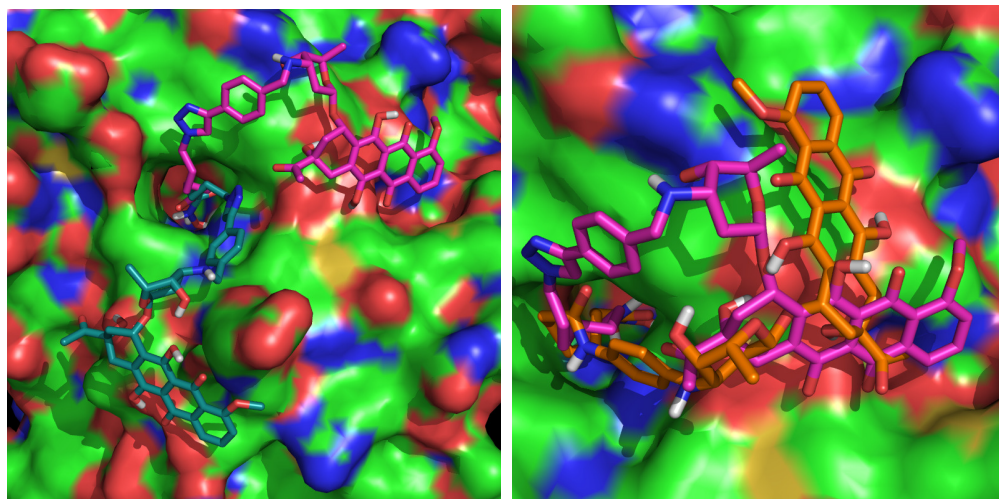
4.2.4 Molecular Docking Analysis of HDAC & Topoisomerase II Conjugates

To obtain information on the structural basis of the observed disparity in the HDAC inhibitory activity of these compounds, we performed molecular docking using a validated molecular dock program (AutoDock)^{47,51} Docking analysis was performed on a HDAC 1 homology model built from human HDAC 2 X-ray structure 3MAX coordinates.⁵² We chose to dock the compound which had the least HDAC inhibitory activity (**12a**) and the compound which had the best HDAC inhibitory activity (**12c**) to delineate the basis of the ~600 fold activity difference between the two. Additionally, we performed docking on compound **7** because of its distinct structural feature compared to **12a-12c**.

Interestingly, compound **12a** and **12c**, differing only in linker length, do not bind to the same pocket, but instead localize to two different pockets (Figure 4-6a). For the six methylene-linked compound **12c**, the hydroxyl group of the daunosamine sugar could

potentially make hydrogen bonding contact with the guanidinium group of Arg270 and the linker region could facilitate the presentation of the hydroxamic acid to the catalytic zinc by entering through the top of the hydrophobic channel that leads to the active site (Figure 4-6a, 4-7c, 4-7d). In addition, two of the hydroxyl groups from the anthracycline ring of **12c** could take part in the H-bonding interaction with the backbone carbonyl group of Arg270 and the N-H group of Gly272. Possibly to accommodate the shorter linker length, **12a** loses the H-bonding interaction between the hydroxyl group of its daunosamine sugar and the enzyme's Arg270. Though other hydroxyl groups of the **12a** anthracycline ring make potentially compensatory H-bonding contacts with the phenolic group of Tyr201 and the backbone carbonyl groups of Gly207 and Pro206 (See Figure 4-7a, 4-7b), its binding pocket is more solvent-exposed, compared to the binding pocket of **12c** (Figure 4-6a).

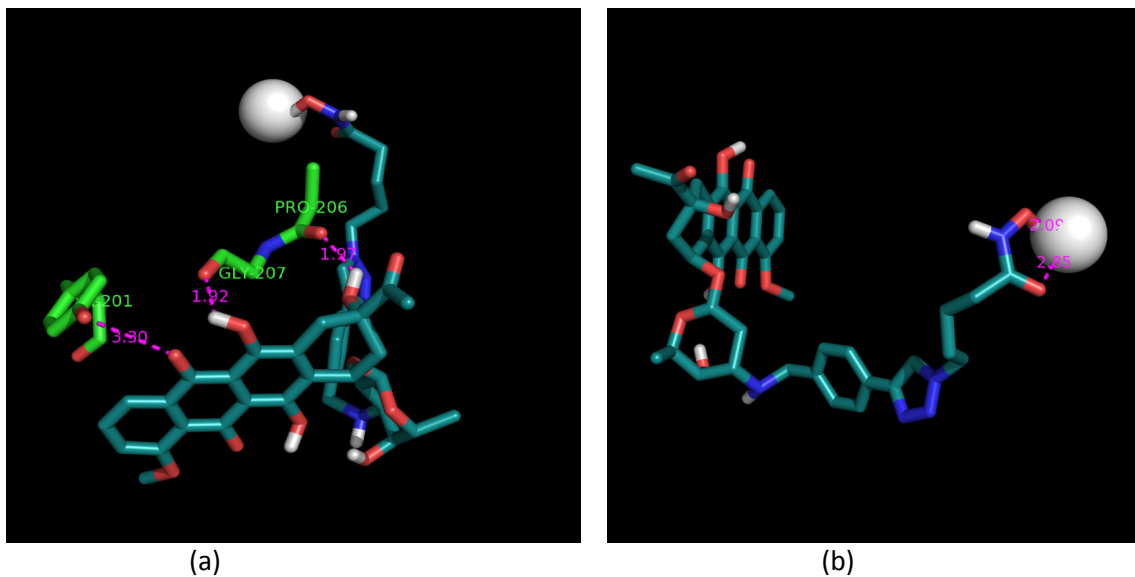
Compound **7** binds close to the same pocket as **12c**; it however derives its binding affinity through different sets of interactions. Unlike **12c** which enters the active site associating with the top of the hydrophobic channel, **7** traverses the same channel more closely associated with residues on the opposite side of the channel (Figure 4-6b). Consequently, the daunosamine hydroxyl group of **7** could not interact with Arg270 in a similar way as that of **12c**. In lieu of this interaction, the anthracycline ring of **7** may engage in other H-bonding interactions with the backbone carbonyl groups of Gly272, Gly268, and Thr304 on the enzyme surface rim (Figure 4-6, Figure 4-7, Figure 4-8 and 4-9). These apparent differences in the binding orientation at the enzyme surface rim could account for the disparity in the potency of compounds **7**, **12a** and **12c** against HDAC1.



(a)

(b)

Figure 4-6. Docked structure of Topo II-HDACi conjugates at HDAC 1 active site. (a) Superposition of low energy conformations of **12a** (teal) and **12c** (pink) (b) Overlap of low energy conformations of **12c** (pink) and **7** (orange).



(a)

(b)

Figure 4-7. (a) Docked structure of compound **12a** reveals H-bonding interaction between anthracycline ring and Gly207, Pro206, Tyr201 (b) Orientation of compound **12a** near catalytic zinc at active site.

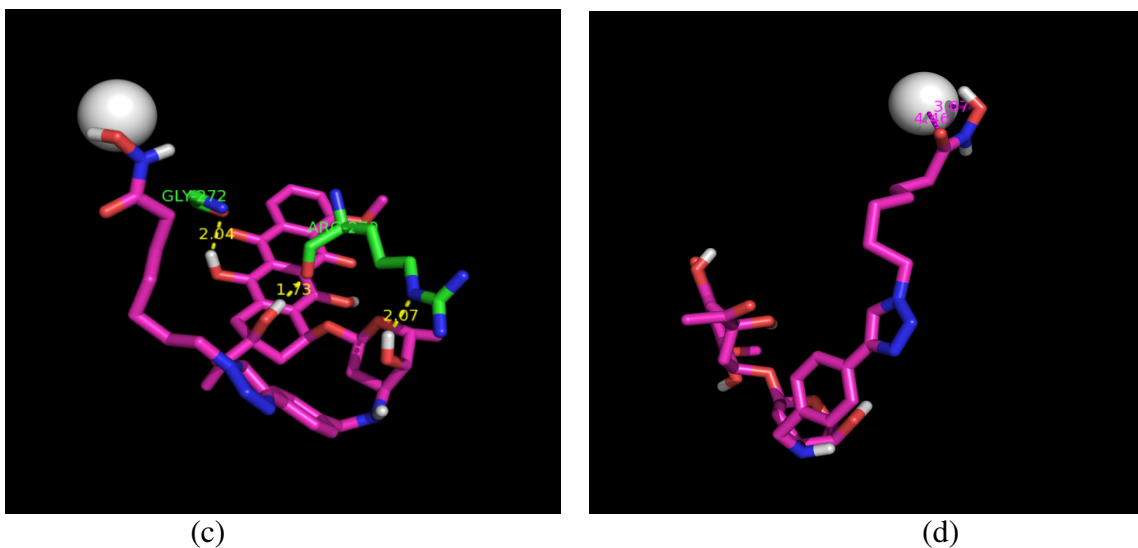


Figure 4-8. (a) Docked structure of compound **12c** reveals H-bonding interaction between anthracycline ring and Arg270 and Gly272 (b) Orientation of compound **12c** near catalytic zinc at active site.

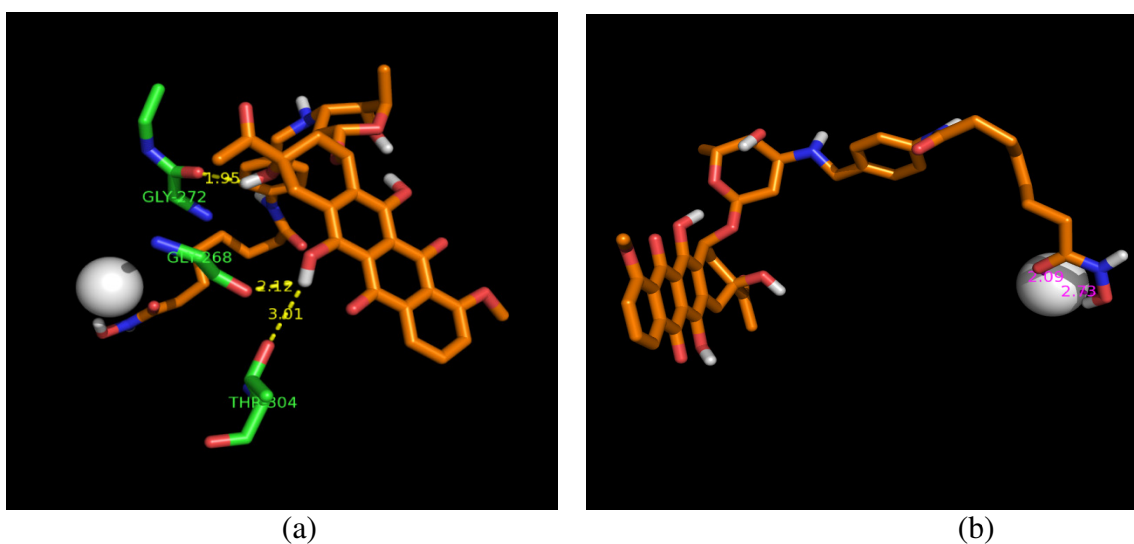


Figure 4-9. (a) Docked structure of compound **7** reveals H-bonding interaction between anthracycline ring and Gly272, Gly268, Thr304 (b) Orientation of compound **7** near catalytic zinc at active site.

4.2.5 Biological Activities

These dual acting inhibitors were subjected to topoisomerase II decatenation analysis to determine topoisomerase II inhibition signature of these compounds.

Conjugate **12b** and **7** inhibited Topo II activity at comparable levels to that of daunorubicin at the same drug concentration while **12c** showed enhanced topo II inhibition activity relative to daunorubicin. In addition, a subset of these compounds potently inhibits the proliferation of representative cancer cell lines. Josh Canzoneri and William Guerrant will present details of these biological experiments in their respective theses soon.

4.3 HDAC – Topoisomerase I (TOPO I) Inhibitors

Another proven anticancer target is topoisomerase I (topo I). Topo I enzymes relieve the torsional strain on DNA during DNA replication by cutting one strand of the DNA double helix and passing one strand over the other.^{53,54} Due to the inherent need for rapid replication in cancer, inhibitors of topoisomerases result in DNA double strand breaks, cell cycle arrest, and apoptosis.⁵⁵⁻⁵⁹ Many small molecule inhibitors of topo I have proven clinically effective and are currently FDA approved for cancer chemotherapy.⁵⁷ Since both HDAC and topo I enzymes are localized to the nucleus, the opportunity for dual inhibition from a single agent is a promising possibility.

Creating a dual-acting HDAC-Topo I inhibitor could prove beneficial for many reasons. First, HDACi have been shown to act synergistically with topo I inhibitors, resulting in enhanced apoptosis in cancer.^{60,61} Also, since both enzymes are nuclear localized, dual-targeted agents may have better therapeutic indices. As a follow-up to our work on dual-acting HDAC-topo II inhibitors, we have designed and synthesized dual-acting HDAC-Topo I inhibitors derived from the camptothecin ring system and the linker region of SAHA-like HDACi. We present evidence here that these compounds retain

inhibitory activities against both target enzymes and potently inhibit the proliferation of selected cancer cell lines.

4.3.1 Design of HDAC-Topoisomerase I Conjugates

We chose 10-hydroxycamptothecin and 7-ethyl-10-hydroxycamptothecin (SN-38) (Figure 4-10) as the topo I inhibiting templates for the design of the proposed topo I-HDAC inhibitors due to their promising activity against a range of tumor types and the presence of functionalizable phenolic group at their C-10 position. Also, both inhibitors have demonstrated more potency and less toxicity than camptothecin.⁶²⁻⁶⁴ From SAR

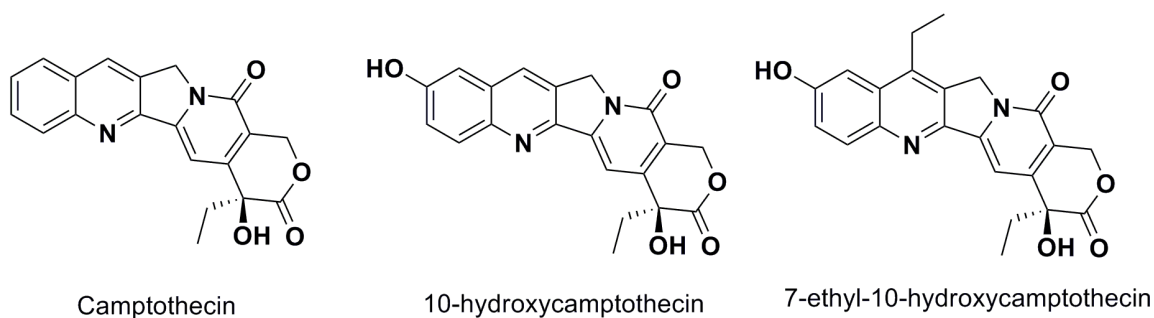


Figure 4-10. Representative HDAC and Topo I inhibitors.

studies on camptothecins, substitution at the 10-hydroxy group has been found to be tolerable.⁶⁵ We have already reported the suitability of the 1,2,3-triazole ring as a surface recognition cap group-linking moiety in SAHA-like HDAC inhibitors.⁶⁶ These studies showed cap group-dependent preference for five- to six- methylene linkers. In the designed dual acting compounds, the linker region of SAHA-like HDACi is coupled through a triazole moiety to the camptothecin template, which in turn is anticipated to act as an aromatic surface recognition cap group essential for HDAC inhibition that also retains its topo I inhibition activity (Figure 4-11). We introduced variations into the linker

region to test the linker length-dependent potency of these dual inhibitors. Additionally, incorporation of the triazole ring into the compound design helps to simplify synthesis and SAR studies of these dual topo I-HDAC inhibitors.

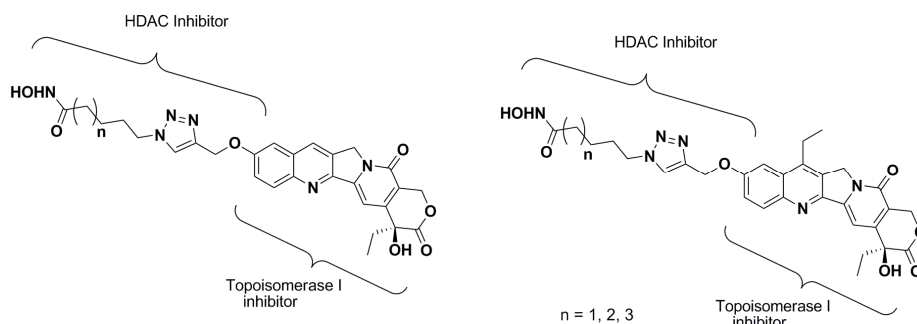


Figure 4-11. Designed dual-acting Topo I-HDAC inhibitors

4.3.2 Synthesis of HDAC-Topoisomerase I Conjugates

The reaction route to all the designed compounds is shown in Figure 4-12. The phenolic OH-group of 10-hydroxycamptothecin and 7-ethyl-10-hydroxycamptothecin was alkylated with propargyl bromide to yield the alkyne intermediate **14a-b**. Cu-catalyzed Huisgen cycloaddition⁶⁷ with known azido intermediates **15a-e**⁶⁸ afforded trityl protected compounds **16a-h**. TFA deprotection of **16a-h** yielded the desired compounds **17a-h** in good yields with minimal purification required.

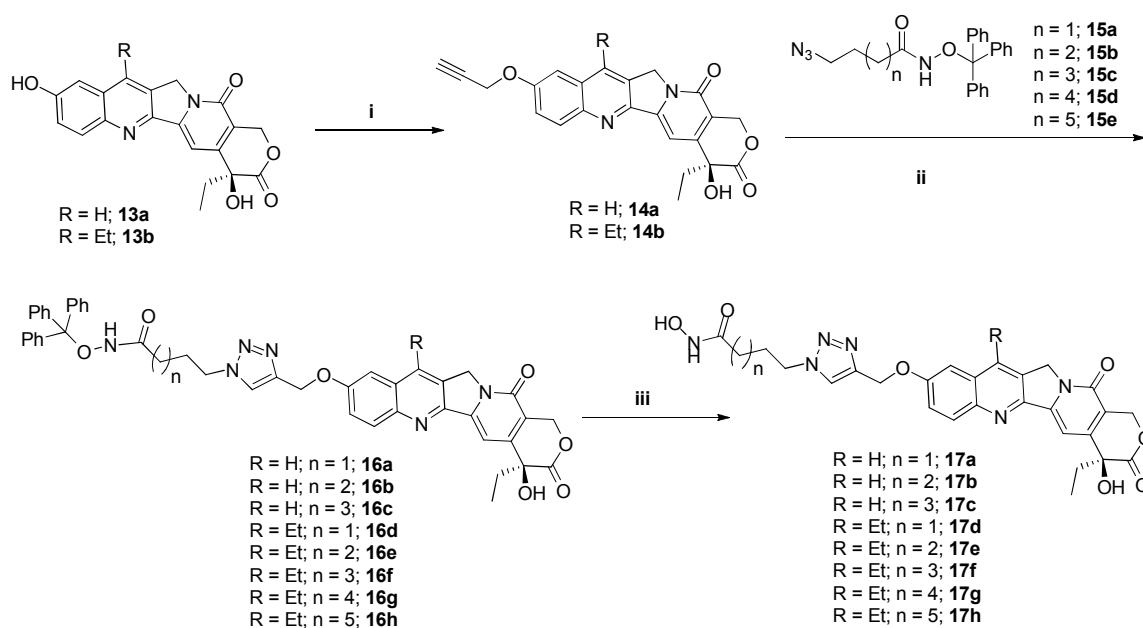


Figure 4-12. Synthesis of dual acting Topoisomerase I-HDAC inhibitors. Reagents and conditions: (i) propargyl bromide, K_2CO_3 , DMSO, rt, 48 h (ii) **15a-15e**, CuI, THF:DMSO:Hunig's base 10:1:0.1 (iii) TFA, thioanisole, CH_2Cl_2 , 0 °C.

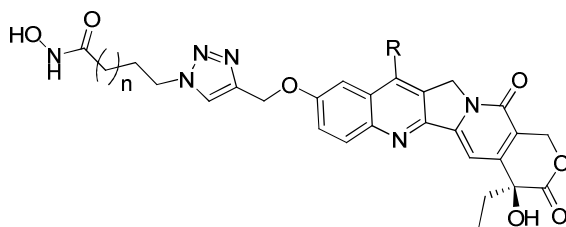
4.3.3 *In vitro* HDAC Inhibition of HDAC & Topoisomerase I Conjugates

Building on our previous observations about the linker length-dependent potency of aryltriazolyl HDACi,^{66,68} we first synthesized and evaluated the anti-HDAC activity of 7-ethylcamptothecin derived compounds **17d-h** against HeLa cell nuclear extract HDACs as described previously with slight modification.⁶⁶ Camptothecin has a fluorescence emission close to the wavelength (460nm) of the fluorescence generated by the HDAC enzyme cleavage of its substrate. To circumvent this potential interference, controls containing the same concentration of the test compound without the enzyme were used, and the background fluorescence of these controls were subtracted from the experimental fluorescence readings. Compound **17d**, an analog with three methylene spacers separating the triazole ring and the hydroxamate moiety, has no measurable anti-HDAC

activity at concentrations greater than 10 μ M. The inactivity of **17d** may be due to the fact that its linker region is too short to effectively position its hydroxamate moiety within the active site while maintaining the crucial surface residue contacts. Conversely, compounds **15e-h** displayed spacer-length dependent HDAC inhibitory activities with compound **17g**, an analog with six methylene linkers, having inhibition activities comparable to **SAHA** (Table 4-2). The anti-HDAC activities of these compounds followed linker length-dependence similar to what we observed for other aryltriazolyl HDACi.

To test the influence of the ethyl group at the C-7 of 7-ethylcamptothecin on HDAC inhibition activity, we synthesized camptothecin derived compounds **17a-c**, analogs with four, five and six methylene linkers respectively. Our choice of this linker range is based on the forgoing observation that this range conferred the optimum activity to the 7-ethylcamptothecin derived compounds **17e-g**. A comparison of the anti-HDAC activities of **17a-c** and **17e-g**, against the HeLa cell nuclear extract HDACs, reveals that pairs with the same linker length have nearly identical HDAC inhibition activity (Table 4-2). These results suggest that the presence or lack thereof of the ethyl group at the C-7 of camptothecin ring system has no significant effect on inhibition HeLa cell nuclear extract HDACs. As expected, **SN-38** has no measurable HDAC inhibition activity.

To obtain additional evidence for HDAC isoform selectivity, we tested selected compounds against pure HDAC1, HDAC6 and HDAC8.



Compound	n	R	HDAC 1/2 IC ₅₀ (nM)	HDAC 1 IC ₅₀ (nM)	HDAC 6 IC ₅₀ (nM)	HDAC 8 IC ₅₀ (nM)
17a	2	-H	144.5	116+/- 40	260+/- 40	ND
17b	3	-H	112.2	NT	NT	NT
17c	4	-H	56.2	37+/-7	81+/- 26	1046+/- 316
17d⁺	1	-CH ₂ CH ₃	ND	ND	85+/- 34	1726+/- 577
17e⁺	2	-CH ₂ CH ₃	155.4	NT	NT	NT
17f⁺	3	-CH ₂ CH ₃	120.7	129+/- 33	42+/- 6	ND
17g⁺	4	-CH ₂ CH ₃	64.65	50+/- 7	36+/- 5	ND
17h⁺	5	-CH ₂ CH ₃	212.3	369+/- 111	75+/- 34	2599+/- 475
SN-38	-	-	ND	NT	NT	NT
SAHA	-	-	65.0	38+/- 2	27+/- 2	294+/- 35

Table 4-2. *In vitro* HDAC inhibition activity of novel HDAC/Topo I inhibitors. N.D. – Nondeterminable within tested range; 1 nM – 10 μ M; NT – Not tested.

4.3.4 *In vitro* Topo I Inhibition^a

Topo I inhibition was then quantified via a plasmid relaxation assay to ensure the dual-targeted inhibitors retained Topo I inhibition activity.⁶⁹ **SN-38** was used as a positive control for Topo I inhibition. Compounds **17a-c** inhibited Topo I function, as shown by both the reduction of relaxed plasmid and increase in nicked plasmid compared to the control, while there was a slight preference for **17b** (Figure 4-13). 7-Ethyl compounds **17d-h** also inhibited Topo I with no apparent drop in activity compared to **SN-38** (Figure 4-13b). This result, taken together with the HDAC inhibition result, showed that these dual-targeted inhibitors can function to inhibit either target enzyme *in vitro* and conjugation of the two inhibitors did not appreciably decrease activity.

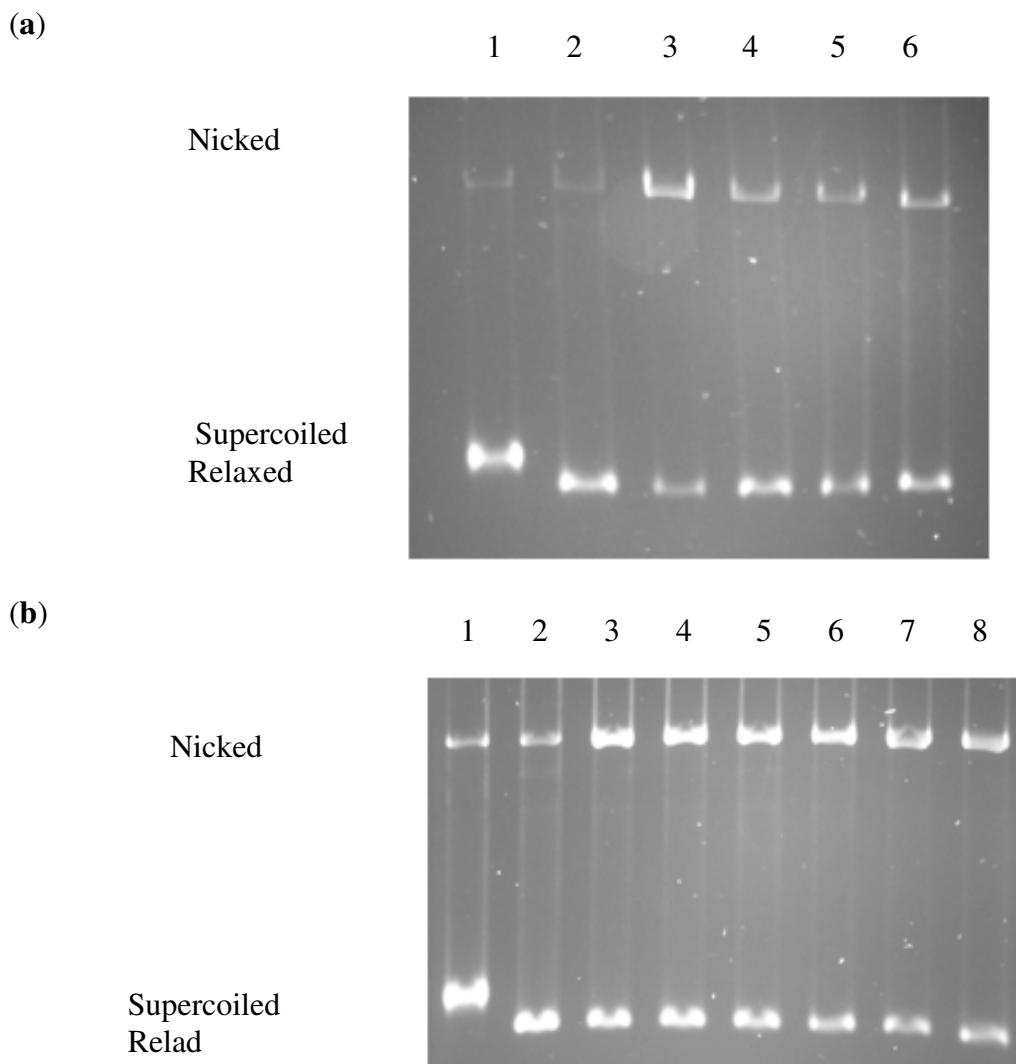


Figure 4-13 – Topoisomerase I-Induced Plasmid Relaxation Assay. (a) (1) PBR322 Plasmid DNA, (2) DNA and Topo I, (3-8) DNA, Topo I, and 50 μ M: (3) **SN-38**, (4) **17a**, (5) **17b**, (6) **17c**. (b) (1) PBR322 Plasmid DNA, (2) DNA and Topo I, (3-8) DNA, Topo I, and 50 μ M: (3) **SN-38**, (4) **17d**, (5) **17e**, (6) **17f**, (7) **17g**, (8) **17h**.

^aStudies performed by Josh Canzoneri.

4.4 Conclusion

To critically delineate the benefits of simultaneous topoisomerase and HDAC inhibition in cancer therapy, it will be of interest to identify agents that possess topoisomerase and HDAC inhibition activities within a single molecule. Toward this end, we have created dual-acting topoisomerase I & II/HDAC inhibitors. A subset of these compounds potently inhibits the proliferation of representative cancer cell lines. When subjected to target-specific screening, these agents present both HDAC and topoisomerase inhibition signatures under cell-free conditions and intracellularly. This observation suggests that the cytotoxic activities and potency of these dual-acting compounds could be dictated by either of the two anti-tumor pharmacophores.

Overall, these compounds show promise as potent dual-targeted agents against cancer. Their demonstrated ability to inhibit HDAC and topoisomerases has the potential to broadly arrest cancer by inhibiting essential enzymes. Future work will undoubtedly lead to a better understanding of both the specific mechanism of action and the interesting pharmacokinetic properties observed with this bifunctional class of compounds.

4.5 General Procedures and Experimental

4.5.1 General Procedures

Suberic acid, 4-aminobenzyl alcohol, 4-ethynylbenzyl alcohol, ω -bromoalkanoic acids, 7-bromoheptane nitrile, propargyl bromide were purchased from Sigma–Aldrich. 10-hydroxy camptothecin and 7-ethyl-10-hydroxycamptothecin were purchased from Shilpa Medicare Ltd and GreenField Chemical Inc respectively. Anhydrous solvents and other reagents were purchased and used without further purification. Analtech silica gel plates

(60 F254) were used for analytical TLC, and Analtech preparative TLC plates (UV 254, 2000 μm) were used for purification. UV light was used to examine the spots. Silica gel (200–400 Mesh) was used in column chromatography. NMR spectra were recorded on a Varian-Gemini 400 magnetic resonance spectrometer. ^1H NMR spectra were recorded in parts per million (ppm) relative to the peak of CDCl_3 , (7.24 ppm), CD_3OD (3.31 ppm), or $\text{DMSO}-d_6$ (2.49 ppm). ^{13}C spectra were recorded relative to the central peak of the CDCl_3 triplet (77.0 ppm), CD_3OD (49.0 ppm), or the $\text{DMSO}-d_6$ septet (39.7 ppm), and were recorded with complete heterodecoupling. Multiplicities are described using the abbreviation s, singlet; d, doublet, t, triplet; q, quartet; m, multiplet; and app, apparent. High-resolution mass spectra were recorded at the Georgia Institute of Technology mass spectrometry facility in Atlanta. HPLC analyses were performed on a Beckman Coulter instrument using a Phenomenex RP C-18 column (250 mm x 4.6 mm), eluting with solvent A (0.1% formic acid/water) and solvent B (0.1% formic acid/acetonitrile) at a gradient of 5-50% over 30 min, with detection at 498 nm and a flow rate of 1 mL/min. Sample concentrations were 250 μM , injecting 50 μL . *O*-Trityl-protected hydroxamates **9a-d**,^{66,68} 4-ethynylbenzaldehyde **8**,⁷⁰ and suberic anhydride **2**⁷¹ were prepared according to literature protocol. 5-Azidopentanoic acid was prepared by adapting literature protocol.⁴⁴

4.5.2 HDAC & Topoisomerase II Conjugates Experimental

8-(4-(hydroxymethyl)phenylamino)-8-oxooctanoic acid (**3**) –

To a stirring solution of suberic anhydride **2** (1.0 g, 6.40 mmol) in THF (15 mL), was added (4-aminophenyl)methanol **1** (0.78 g, 6.34 mmol) and resulting mixture was stirred at room temperature for 1 h. Ethyl acetate was added (60 mL) followed by washing with water (2 x 50 mL), brine (1 x 40 mL). Organic layer dried on Na₂SO₄ and solvent evaporated under reduced pressure to give crude compound **2** which was purified by column chromatography (silica, CH₂Cl₂:MeOH (step gradient, 0-10% methanol) to give 0.92 g of compound **3** (52 %). ¹H NMR (DMSO-*d*₆, 400 MHz) δ 1.25-1.32 (4H, m), 1.49-1.61 (4H, m), 2.21 (2H, t, *J* = 7.2 Hz), 2.29 (2H, t, *J* = 8.0 Hz), 4.42 (2H, s), 5.10 (1H, s), 7.23 (2H, d, *J* = 8.4 Hz), 7.54 (2H, d, *J* = 8.8 Hz), 9.84 (1H, s), 12.0 (1H, s). ¹³C NMR (DMSO-*d*₆, 100 MHz) δ 24.4, 25.0, 28.3, 28.4, 33.6, 36.3, 62.5, 118.5, 126.6, 136.7, 137.7, 170.7, 174.1. HRMS (MALDI) calcd for C₁₅H₂₁NO₄Na [M + Na]⁺ 302.1363 found 302.1343.

8-((4-formylphenyl)amino)-8-oxooctanoic acid (**4**)

To a stirring solution of alcohol **3** (1.71 g, 6.13 mmol) in CH₂Cl₂, was added Dess Martin reagent (3.898 g, 9.19 mmol) at 0 °C. The reaction mixture was stirred for the next 16 h at room temperature. The reaction was quenched by adding an aqueous solution of saturated sodium bicarbonate and saturated sodium thiosulfate (1:1, 40 mL) with stirring for 15 min. Methanol/CH₂Cl₂ 1:9 (70 mL) was added after the cessation of bubbling.

The organic layer was isolated, washed subsequently with sodium bicarbonate-sodium thiosulfate mixture (1:1, 40 mL), brine (40 mL) and dried on Na₂SO₄. Solvent was evaporated under reduced pressure and the crude product was purified by column chromatography using CH₂Cl₂: methanol (step gradient, 0-12% methanol) to give 1.10 g of compound **4** (65 %). ¹H NMR (DMSO-*d*₆, 400 MHz) δ 1.24-1.30 (4H, m), 1.47 (2H, p, *J* = 7.2, 15.6 Hz), 1.56 (2H, p, *J* = 7.2, 14.0 Hz), 2.17 (2H, t, *J* = 7.6 Hz), 2.33 (2H, t, *J* = 7.2 Hz), 7.77-7.83 (4H, m), 9.84 (1H, s), 10.28 (1H, s), 11.99 (1H, s). ¹³C NMR (DMSO-*d*₆, 100 MHz) δ 24.3, 24.7, 28.3, 28.4, 33.6, 36.4, 118.6, 130.8, 131.0, 144.8, 172.0, 174.4, 191.5. HRMS (EI) calcd for C₁₅H₁₉NO₄ [M + H]⁺ 277.1314 found 277.1315.

***N*-(4-formylphenyl)-*N*-(trityloxy)octanediarnide (**5**)**

Carboxylic acid **4** (0.30 g, 1.07 mmol) was dissolved in anhydrous THF. *N*-methylmorpholine (0.12 mL, 1.07 mmol) was added to the solution. The reaction mixture was then cooled down to -15 °C and stirred for 5 min. Isobutylchloroformate (0.14 mL, 1.07 mmol) was added and the mixture was stirred for 10 min at -15 °C. *O*-tritylhydroxylamine (0.29 g, 1.07 mmol) was added followed by 2 more equivalents of *N*-methylmorpholine. Stirring continued for 15 min at -15 °C and 2 h at room temperature. Afterwards the mixture was poured into CH₂Cl₂ (50 mL) and water (50 mL). Organic layer was separated and extracted 3 times in each case with water, sodium bicarbonate solution (5%) and water. After washing with brine and drying over Na₂SO₄, solvent was evaporated *in vacuo*. Column chromatography with eluent system CH₂Cl₂-acetone (step

gradient, 0-12% acetone) gave 0.37 g of compound **5** (66 %) as a white solid. ^1H NMR (DMSO- d_6 , 400 MHz) δ 1.10-1.21 (4H, m), 1.44-1.51 (2H, m), 1.73-1.77 (2H, m), 7.23-7.35 (15H, m), 7.78-7.84 (4H, m), 9.84 (1H, s), 10.16 (1H, s), 10.29 (1H, s). ^{13}C NMR (DMSO- d_6 , 100 MHz) δ 24.7, 28.3, 31.9, 36.4, 55.1, 91.5, 118.6, 127.4, 128.9, 130.9, 142.6, 144.6, 170.4, 172.1, 191.2. HRMS (ESI) calcd for $\text{C}_{34}\text{H}_{34}\text{N}_2\text{O}_4\text{Na}$ $[\text{M} + \text{Na}]^+$ 557.2207 found 557.2219.

Daunorubicin-*N*-benzyl-4-amino-8-oxo-*N*-(trityloxy)octanediamide (6)

A solution of daunorubicin (0.07 g, 0.12 mmol), aldehyde **5** (0.07 g, 0.12 mmol) and diisopropylethylamine (0.03 mL, 0.25 mmol) in DMF (2.5 mL) and MeOH (2.5 mL) was heated at 70 °C for 3 h and then allowed to cool to room temperature. Sodium cyanoborohydride (0.03 g, 0.50 mmol) was added and stirring was continued at 70 °C for additional 24 h and allowed to cool at ambient temperature. The reaction was partitioned between CH_2Cl_2 (30 mL) and 5 % NaHCO_3 (25 mL). The two layers were separated and the aqueous layer was extracted with CH_2Cl_2 (2 X 30 mL). The combined organic layer was washed with water (2 X 30 mL), brine (1X 20 mL) and dried over Na_2SO_4 . Solvent was evaporated off and crude was purified on preparative TLC plates, eluting with mixture of $\text{CH}_2\text{Cl}_2/\text{MeOH}$ (12:1) to give 0.05 g of compound **6** (38%). ^1H NMR (DMSO- d_6 , 400 MHz) δ 0.93-0.98 (3H, m), 1.04-1.21 (8H, m), 1.38-1.53 (4H, m), 1.60-1.64 (2H, m), 1.71-1.75 (2H, m), 2.06-2.18 (4H, m), 2.24 (3H, s), 2.80-2.98 (3H, m), 3.15 (1H, d, $J = 4.4$ Hz), 3.57 (1H, s), 3.67-3.70 (1H, m), 4.05 (1H, q, $J = 6.4, 12.8$ Hz), 4.91 (1H, t, $J = 4.4$ Hz), 5.21 (1H, s), 5.42 (1H, s), 7.17 (2H, d, $J = 8.4$ Hz), 7.25-7.34 (15H, m), 7.42 (2H, d, $J = 8.0$ Hz), 7.58-7.62 (1H, m), 7.85-7.87 (2H, m), 9.70 (1H, s), 10.12

(1H, s). ^{13}C NMR (CD_3OD , 100 MHz) δ 17.0, 24.7, 25.1, 25.5, 28.4, 29.6, 30.0, 30.9, 33.1, 34.8, 37.2, 49.7, 52.5, 56.5, 66.6, 66.7, 67.9, 69.7, 100.8, 111.1, 111.3, 118.3, 119.6, 119.8, 120.7, 127.7, 128.0, 128.6, 128.9, 134.2, 134.3, 135.3, 135.6, 137.2, 141.0, 155.7, 156.3, 160.9, 171.5, 186.5, 186.8, 211.8. HRMS (MALDI) calcd for $\text{C}_{61}\text{H}_{64}\text{N}_3\text{O}_{13}$ [$\text{M} + \text{H}$] $^{+}$ 1046.4439 found 1046.4415.

Daunorubicin-*N*-benzyl-4-amino-8-oxooctahydroxamic Acid (7)

To a solution of trityl-protected compound **6** (0.025 g, 0.024 mmol) in CH_2Cl_2 – MeOH (1:1, 4 mL) was added $\text{BF}_3\cdot\text{OEt}_2$ (0.05 mL) at room temperature. The reaction mixture stirred for 30 min at room temperature. Reaction was quenched by addition of water (25 mL) and 10% MeOH in CH_2Cl_2 (30 mL). Aqueous layer was isolated and its pH was adjusted to 8-9 by addition of sat. NaHCO_3 . This aqueous layer was then extracted with 10% MeOH in CH_2Cl_2 (3 X 30 mL). Combined organic layer was washed with sat. brine, dried over Na_2SO_4 and solvent was evaporated under reduced pressure. Trituration of crude product with CH_2Cl_2 (20 mL) gave pure 0.013 g of **7** (68 %) as red solid. Retention time 6.46 min (Solvent Gradient: 5% - 60% solvent B over 20 min); ^1H NMR (CD_3OD , 400 MHz) δ 1.28-1.33 (9H, m), 1.50-1.60 (4H, m), 1.79-1.85 (1H, m), 1.93-1.94 (1H, m), 2.04-2.12 (2H, m), 2.23-2.30 (3H, m), 2.34 (3H, s), 2.85-3.08 (5H, m), 3.69-3.83 (3H, m), 3.97 (3H, s), 4.18-4.23 (1H, m), 5.04 (1H, s), 5.40 (1H, s), 7.22 (2H, d, J = 7.6 Hz), 7.39 (2H, d, J = 8.4), 7.47 (1H, d, J = 8 Hz), 7.74 (1H, t, J = 8 Hz), 7.82 (1H, d, J = 7.2 Hz). ^{13}C NMR (CDCl_3 with drops of CD_3OD , 100 MHz) δ 17.2, 24.7, 26.2, 26.3, 29.5, 29.6, 30.4, 33.2, 33.5, 36.4, 37.6, 53.3, 54.4, 57.0, 67.5, 68.2, 71.1, 77.2,

101.7, 111.8, 112.1, 115.3, 119.8, 120.3, 121.0, 121.2, 128.3, 130.1, 135.3, 135.4, 136.0, 136.8, 139.2, 155.9, 157.1, 162.0, 172.5, 174.1, 187.3, 187.7, 213.5. HRMS (MALDI) calcd for $C_{42}H_{50}N_3O_{13}$ $[M + H]^+$ 804.3343 found 804.336 and calcd for $[M + Na]^+$ 826.3163, found 826.3153.

Representative Procedure for Cu(I)-catalyzed Cycloaddition Reaction. *O*-Trityl-4-formylphenyltriazolypentahydroxamate (10a)

5-Azido-*O*-tritylpentahydroxamate **9a** (0.15 g, 0.37 mmol) and 4-ethynylbenzaldehyde **8** (0.06 g, 0.49 mmol) were dissolved in anhydrous THF (10 mL) and stirred under argon at room temperature. Copper (I) iodide (9 mg, 0.05 mmol) and Hunig's base (0.1 mL) were then added to the reaction mixture, and stirring continued for 24 h. The reaction mixture was diluted with CH_2Cl_2 (30 mL) and washed with 1:4 NH_4OH /saturated NH_4Cl (3 X 30 mL) and saturated NH_4Cl (30 mL). The organic layer was dried over Na_2SO_4 and concentrated *in vacuo*. The crude product was purified by flash chromatography (CH_2Cl_2 :Acetone, gradient 12:1, 10:1, 8:1) to give 0.16 g of **10a** (82%) as a white solid. 1H NMR ($DMSO-d_6$, 400 MHz) δ 1.13-1.20 (2H, m), 1.49-1.56 (2H, m), 1.82 (2H, t, J = 7.2), 4.27 (2H, t, J = 6.8 Hz), 7.24-7.28 (15H, m), 7.97 (2H, d, J = 8.8 Hz), 8.05-8.07 (2H, d, J = 8.4 Hz), 8.68 (1H, s), 9.99 (1H, s), 10.23 (1H, s). ^{13}C NMR ($CDCl_3$, 100 MHz) δ 20.0, 29.2, 30.1, 50.0, 93.4, 120.8, 125.8, 127.7, 128.0, 128.8, 130.2, 135.5, 136.3, 140.8, 146.1, 176.2, 191.6. HRMS (MALDI) calcd for $C_{33}H_{30}N_4O_3Na$ $[M + Na]^+$ 553.2210, found 553.2191.

***O*-Trityl-4-formylphenyltriazolylhexahydroxamate (10b)**

Reaction of 6-azido-*O*-tritylhexahydroxamate **9b** (0.24 g, 0.58 mmol) and 4-ethynylbenzaldehyde **8** (0.09 g, 0.69 mmol) as described for the synthesis of **10a**, followed by purification using column chromatography (CH₂Cl₂:Acetone, gradient 12:1, 10:1, 8:1) gave 0.19 g of **10b** (61 %) as a white solid. ¹H NMR (DMSO-*d*₆, 400 MHz) δ 0.92-0.99 (2H, m), 1.19-1.26 (2H, m), 1.70-1.78 (4H, m), 4.30 (2H, t, *J* = 6.8), 7.26-7.29 (15H, m), 7.96 (2H, d, *J* = 8.0 Hz), 8.05 (2H, d, *J* = 8.4 Hz), 8.72 (1H, s), 9.99 (1H, s), 10.15 (1H, s). ¹³C NMR (CDCl₃, 100 MHz) 22.2, 25.5, 29.6, 30.7, 49.9, 93.1, 120.8, 125.7, 127.6, 127.9, 128.8, 130.1, 135.4, 136.3, 140.7, 141.6, 146.0, 176.5, 191.5.

***O*-Trityl-4-formylphenyltriazolylheptahydroxamate (10c)**

Reaction of 7-azido-*O*-tritylheptahydroxamate **9c** (0.30 g, 0.70 mmol) and 4-ethynylbenzaldehyde **8** (0.09g, 0.70 mmol) as described for the synthesis of **10a**, followed by purification using column chromatography (CH₂Cl₂:Acetone, gradient 12:1, 10:1, 8:1) gave 0.25 g of **10c** (65 %) as a white solid. ¹H NMR (DMSO-*d*₆, 400 MHz) δ 0.96-1.17 (6H, m), 1.71-1.78 (4H, m), 4.34 (2H, t, *J* = 7.2 Hz), 7.24-7.34 (15H, m), 7.96 (2H, d, *J* = 7.6 Hz), 8.06 (2H, d, *J* = 8.0 Hz), 8.75 (1H, s), 9.99 (1H, s), 10.14 (1H, s). ¹³C NMR (CDCl₃, 100 MHz) δ 22.8, 25.8, 28.0, 29.7, 30.7, 50.1, 93.2, 120.7, 125.7, 127.9, 128.8, 130.1, 135.4, 136.3, 140.8, 141.7, 146.1, 176.8 191.5.

***O*-Trityl-4-formylphenyltriazolyloctahydroxamate (10d)**

Reaction of 8-azido-*O*-trityloctahydroxamate **9d** (0.25 g, 0.57 mmol) and 4-ethynylbenzaldehyde **8** (0.07g, 0.57 mmol) as described for the synthesis of **10a**, followed by purification using column chromatography (CH₂Cl₂:Acetone, gradient 12:1, 10:1, 8:1) gave 0.19 g of **10d** (59 %) as a white solid. ¹H NMR (DMSO-*d*₆, 400 MHz) δ 0.85-0.93 (2H, m), 1.08-1.17 (6H, m), 1.72-1.80 (4H, m), 4.38 (2H, t, *J* = 7.2), 7.24-7.28 (15H, m), 7.96 (2H, d, *J* = 7.6 Hz), 8.06 (2H, d, *J* = 8.0 Hz), 8.77 (1H, s), 9.99 (1H, s), 10.13 (1H, s). ¹³C NMR (CDCl₃, 100 MHz) δ 23.0, 26.0, 28.3, 28.5, 30.0, 30.8, 50.3, 93.1, 120.7, 125.8, 127.9, 128.8, 130.2, 135.4, 136.3, 140.8, 141.7, 146.1, 176.9, 191.5. HRMS (MALDI) calcd for C₃₆H₃₆N₄O₃Na [M + Na]⁺ 595.2679, found 595.2609.

Daunorubicin-*N*-benzyl-4-triazolyl-*O*-tritylpentahydroxamate (11a)

A solution of daunorubicin hydrochloride (0.08 g, 0.14 mmol) and **10a** (0.15 g, 0.28 mmol) in acetonitrile (9 mL) and water (3 mL) was stirred at room temperature for 30 min. A suspension of sodium cyanoborohydride in THF was added within 1 min and stirring continued overnight at room temperature during which all of the starting material got consumed. The reaction mixture was partitioned between CH₂Cl₂ (30 mL) and water (30 mL), and the two layers separated. The aqueous layer was extracted with CH₂Cl₂ (30 mL), and the combined organic layer was dried over Na₂SO₄. Solvent was removed under reduced pressure and the crude was purified by preparative TLC, eluting with 12:1 CH₂Cl₂/MeOH to give 0.065 g of **11a** (44%) as red solid. ¹H NMR (DMSO-*d*₆, 400

MHz) 1.23-1.27 (5H, m), 1.36 (3H, d, $J = 6.4$ Hz), 1.60-1.68 (5H, m), 1.76-1.83 (2H, m), 2.10-2.15 (1H, m), 2.34-2.39 (1H, m), 2.88-2.93 (1H, m), 2.99-3.03 (1H, m), 3.21-3.26 (1H, m), 3.64 (1H, s), 3.67-3.70 (1H, m), 3.79-3.83 (1H, m), 3.97 (1H, q, $J = 6.4$ Hz), 4.06 (3H, s), 4.16-4.19 (2H, m), 4.73 (1H, s), 4.76 (1H, s), 5.30 (1H, s), 5.51 (1H, d, $J = 3.2$ Hz), 7.26-7.33 (15H, m), 7.36-7.42 (3H, m), 7.64 (1H, s), 7.71 (2H, d, $J = 8.0$ Hz), 7.76 (1H, t, $J = 8.4$ Hz), 8.01 (1H, d, $J = 7.2$ Hz). ^{13}C NMR (CDCl_3 , 100 MHz) δ 17.4, 20.4, 29.7, 29.9, 30.4, 34.2, 35.7, 50.2, 50.3, 52.5, 56.9, 65.7, 67.0, 67.1, 69.5, 101.0, 111.6, 111.7, 118.6, 119.6, 120.0, 121.1, 126.0, 127.4, 128.1, 128.4, 128.7, 129.2, 129.9, 133.8, 134.0, 135.7, 136.0, 139.6, 141.1, 155.9, 156.4, 161.3, 186.9, 187.3, 213.9. HRMS (ESI) calcd for $\text{C}_{60}\text{H}_{60}\text{N}_5\text{O}_{12}$ $[\text{M} + \text{H}]^+$ 1042.4233 found 1042.4189.

Daunorubicin-*N*-benzyl-4-triazolyl-*O*-tritylhexahydroxamate (11b**)**

Reaction of daunorubicin hydrochloride (0.055 g, 0.097 mmol) with **10b** (0.159 g, 0.29 mmol) and sodium cyanoborohydride (0.018 g, 0.29 mmol) in acetonitrile-water solvent system, as described in the synthesis of **11a**, gave 0.05 g of **11b** (49%) as red solid. ^1H NMR ($\text{DMSO}-d_6$, 400 MHz) 1.23-1.28 (5H, m), 1.38 (3H, d, $J = 6.4$ Hz), 1.56-1.60 (3H, m), 1.66-1.85 (6H, m), 2.12-2.17 (1H, m), 2.35-2.41 (1H, m), 2.91-2.94 (1H, m), 2.99-3.04 (1H, m), 3.23-3.28 (1H, m), 3.66-3.72 (2H, m), 3.81-3.84 (1H, m), 3.99 (1H, q, $J = 6.8$ Hz), 4.07 (3H, s), 4.28 (2H, t, $J = 7.6$ Hz), 4.74 (1H, s), 4.78 (1H, s), 5.29-5.32 (1H, m), 5.53 (1H, d, $J = 2.8$ Hz), 7.30-7.35 (15H, m), 7.37-7.45 (3H, m), 7.67 (1H, s), 7.73-7.80 (3H, m), 8.02 (1H, d, $J = 7.2$ Hz). ^{13}C NMR (CDCl_3 , 100 MHz) δ 17.1, 22.5, 25.7, 29.6, 29.8, 30.2, 30.7, 33.9, 35.4, 49.9, 50.0, 52.3, 56.6, 65.4, 66.7, 66.8, 69.3, 100.8,

111.3, 111.5, 118.4, 119.4, 119.8, 120.8, 125.8, 127.8, 128.1, 128.4, 128.9, 129.7, 133.5, 133.8, 135.4, 135.7, 139.5, 141.1, 147.3, 155.6, 156.2, 161.0, 186.7, 187.0, 213.7.
HRMS (ESI) calcd for $C_{61}H_{62}N_5O_{12}$ $[M + H]^+$ 1056.4389 found 1056.4440.

Daunorubicin-*N*-benzyl-4-triazolyl-*O*-tritylheptahydroxamate (11c)

Reaction of daunorubicin hydrochloride (0.055 g, 0.097 mmol) with **10c** (0.162 g, 0.29 mmol) and sodium cyanoborohydride (0.018 g, 0.29 mmol) in acetonitrile-water solvent system, as described in the synthesis of **11a**, gave 0.05 g of **11c** (48%) as a red solid. 1H NMR (DMSO- d_6 , 400 MHz) δ 0.99-1.07 (2H, m), 1.13-1.25 (6H, m), 1.36 (3H, d, $J = 6.4$ Hz), 1.52-1.57 (2H, m), 1.70-1.83 (5H, m), 2.02-2.10 (2H, m), 2.14 (1H, s), 2.33 (1H, s), 2.85-2.88 (1H, m), 2.93 (1H, s), 2.97-3.00 (1H, s), 3.14-3.19 (1H, m), 3.67-3.70 (2H, m), 3.80-3.83 (1H, m), 4.04 (3H, s), 4.28 (3H, t, $J = 6.8$ Hz), 4.66-4.69 (1H, m), 5.24 (1H, s), 5.50 (1H, d, $J = 3.2$ Hz), 7.26-7.30 (15H, m), 7.34-7.43 (3H, m), 7.63 (1H, s), 7.66-7.79 (3H, m), 7.97 (1H, d, $J = 7.6$ Hz). ^{13}C NMR (CDCl $_3$, 100 MHz) δ 17.1, 23.1, 24.8, 25.9, 28.2, 29.7, 30.0, 30.9, 30.9, 33.2, 34.9, 49.9, 50.2, 52.3, 56.6, 66.6, 66.7, 69.9, 100.6, 111.3, 111.5, 118.4, 119.4, 119.9, 120.9, 125.7, 127.8, 128.1, 128.4, 128.9, 129.9, 134.2, 134.2, 135.4, 135.7, 139.5, 141.1, 147.3, 155.6, 156.2, 161.0, 186.7, 187.1, 212.0.
HRMS (ESI) calcd for $C_{62}H_{64}N_5O_{12}$ $[M + H]^+$ 1070.4546 found 1070.4508.

Daunorubicin-*N*-benzyl-4-triazolyl-*O*-trityloctahydroxamate (**11d**)

Reaction of daunorubicin hydrochloride (0.055 g, 0.097 mmol) with **10d** (0.166 g, 0.29 mmol) and sodium cyanoborohydride (0.018 g, 0.29 mmol) in acetonitrile-water solvent system, as described in the synthesis of **11a**, gave 0.048 g of **11d** (46%) as a red solid. ¹H NMR (DMSO-*d*₆, 400 MHz) δ 0.98-1.06 (2H, m), 1.19-1.24 (8H, m), 1.37 (3H, d, *J* = 6.4 Hz), 1.53-1.58 (2H, m), 1.69-1.85 (5H, m), 2.07-2.10 (2H, m), 2.35 (1H, s), 2.88-2.92 (1H, m), 2.96-2.99 (1H, m), 3.15-3.20 (1H, m), 3.67-3.70 (2H, m), 3.79-3.83 (1H, m), 4.05 (3H, s), 4.31 (3H, t, *J* = 6.8 Hz), 4.68 (1H, s), 5.25 (1H, s), 5.50 (1H, s), 7.27-7.31 (15H, m), 7.35-7.47 (3H, m), 7.66 (1H, s), 7.69-7.77 (3H, m), 7.98 (1H, d, *J* = 7.6 Hz). ¹³C NMR (CDCl₃, 100 MHz) δ 17.0, 23.1, 24.8, 26.1, 28.5, 29.6, 30.1, 30.2, 31.0, 33.2, 34.8, 50.0, 50.2, 52.5, 56.6, 66.5, 66.7, 69.8, 100.9, 111.1, 111.2, 118.3, 119.2, 119.7, 120.7, 125.7, 127.8, 128.0, 128.4, 128.9, 129.6, 134.2, 134.3, 135.4, 135.6, 139.5, 141.0, 147.3, 155.7, 156.3, 160.9, 186.5, 186.8, 211.8. HRMS (ESI) calcd for C₆₃H₆₆N₅O₁₂ [M + H]⁺ 1084.4702 found 1084.4657.

Daunorubicin-*N*-benzyl-4-triazolylpentahydroxamic Acid (**12a**)

Reaction of **11a** (0.05 g, 0.048 mmol) and BF₃·OEt₂ (0.1 mL in CH₂Cl₂/MeOH (4 mL/4 mL) within 2 h, as described for the synthesis of **7**, followed by preparative TLC (eluent, CH₂Cl₂/MeOH 7:1) to give 0.028 g of **12a** (73%) as red solid. Retention time 15.06 min (Solvent Gradient: 0% - 100% solvent B over 30 min); ¹H NMR (DMSO-*d*₆, 400 MHz) δ 1.11-1.21 (7H, m), 1.42-1.50 (4H, m), 1.74-1.80 (2H, m), 1.96 (2H, t, *J* = 7.6 Hz), 2.06-2.22 (5H, m), 2.84-2.97 (3H, m), 3.63-3.80 (1H, m), 3.96 (3H, s), 4.07-4.09 (1H, m), 4.33

(2H, t, $J = 6.8$ Hz), 4.91 (1H, m), 5.22 (1H, s). 5.47 (1H, s), 7.37 (2H, d, $J = 8.0$ Hz), 7.61-7.63 (1H, m), 7.69-7.71 (2H, d, $J = 8.0$ Hz), 7.87-7.92 (2H, m), 8.46 (1H, s), 10.37 (1H, s). ^{13}C NMR (CDCl_3 with drops of CD_3OD , 125 MHz) δ 15.1, 22.5, 24.1, 24.2, 27.3, 27.4, 28.3, 31.0, 31.3, 34.2, 35.4, 51.1, 52.2, 54.8, 65.4, 66.1, 68.9, 75.1, 99.5, 109.7, 109.9, 113.1, 117.6, 118.2, 118.8, 119.0, 126.3, 127.9, 133.1, 133.2, 133.8, 134.7, 137.0, 153.7, 154.9, 159.8, 170.4, 172.0, 185.1, 185.5, 211.1. HRMS (ESI) calcd for $\text{C}_{41}\text{H}_{46}\text{N}_5\text{O}_{12} [\text{M} + \text{H}]^+$ 800.3137 found 800.3088.

Daunorubicin-*N*-benzyl-4-triazolylhexahydroxamic Acid (12b)

Reaction of **11b** (0.05 g, 0.047 mmol) and $\text{BF}_3\cdot\text{OEt}_2$ (0.1 mL) in $\text{CH}_2\text{Cl}_2/\text{MeOH}$ (4 mL/4 mL) within 2 h, as described for the synthesis of **7**, followed by preparative TLC (eluent, $\text{CH}_2\text{Cl}_2/\text{MeOH}$ 7:1) gave 0.028 g of **12b** (76%) as red solid. Retention time 15.20 min (Solvent Gradient: 0% - 100% solvent B over 30 min); ^1H NMR ($\text{CDCl}_3+\text{CD}_3\text{OD}$, 400 MHz) δ 0.74-0.84 (2H, m), 1.25-1.31 (7H, m), 1.54-1.62 (3H, m), 1.72-1.73 (2H, m), 1.83-1.93 (2H, m), 1.99 (1H, t, $J = 7.6$ Hz), 2.03-2.08 (1H, m), 2.19-2.33 (2H, m), 3.57-3.60 (5H, m), 3.68-3.73 (2H, m), 4.00 (3H, s), 4.30 (2H, q, $J = 7.2$ Hz), 4.65-4.66 (1H, m), 5.22-5.23 (1H, m), 5.44 (1H, s), 7.24-7.25 (1H, m), 7.34 (2H, d, $J = 8.4$ Hz), 1.61-1.65 (2H, m), 7.70-7.72 (1H, m), 7.74-7.75 (1H, m), 7.95 (1H, d, $J = 7.6$ Hz). ^{13}C NMR (CDCl_3 with drops of CD_3OD , 100 MHz) δ 16.8, 22.5, 24.3, 25.4, 29.5, 30.7, 32.2, 33.6, 35.3, 50.0, 50.1, 51.9, 56.5, 65.0, 67.0, 67.2, 69.0, 100.6, 111.3, 111.4, 118.4, 119.7, 119.9, 125.7, 127.8, 128.6, 129.1, 133.7, 133.8, 135.3, 135.7, 147.3, 160.9, 170.2, 186.7, 187.1, 213.5. HRMS (ESI) calcd for $\text{C}_{42}\text{H}_{48}\text{N}_5\text{O}_{12} [\text{M} + \text{H}]^+$ 814.3294 found 814.3323.

Daunorubicin-*N*-benzyl-4-triazolylheptahydroxamic Acid (**12c**)

Reaction of **11c** (0.05 g, 0.047 mmol) and BF₃·OEt₂ (0.1 mL) in CH₂Cl₂/MeOH (4 mL/4 mL) within 2 h, as described for the synthesis of **7**, followed by preparative TLC (eluent, CH₂Cl₂/MeOH 7:1) gave 0.030 g of **12c** (78%) as red solid. Retention time 16.98 min (Solvent Gradient: 5% - 60% solvent B over 20 min); ¹H NMR (DMSO-*d*₆, 400 MHz) δ 1.17-1.26 (8H, m), 1.37-1.49 (3H, m), 1.70-1.83 (5H, m), 1.89-1.92 (1H, m), 1.99 (1H, t, *J* = 7.2 Hz), 2.09-2.23 (5H, m), 2.83-2.99 (4H, m), 3.63-3.84 (2H, m), 3.92-3.96 (3H, m), 4.08 (1H, t, *J* = 6.8 Hz), 4.31 (2H, t, *J* = 6.8 Hz), 4.93-4.96 (1H, m), 5.25 (1H, s), 5.34 (1H, s), 7.36 (2H, d, *J* = 8.0 Hz), 7.53-7.60 (1H, m), 7.70 (2H, d, *J* = 8.0 Hz), 7.79-7.80 (1H, m), 7.85-7.86 (1H, m), 8.41 (1H, s), 10.21 (1H, s). ¹³C NMR (DMSO-*d*₆, 100 MHz) δ 17.7, 24.6, 25.5, 25.8, 26.1, 26.2, 27.2, 28.4, 28.6, 28.6, 30.1, 32.4, 32.8, 37.0, 50.1, 57.3, 67.4, 70.7, 76.1, 101.2, 111.5, 119.8, 120.6, 120.9, 121.8, 125.6, 128.6, 129.0, 129.5, 135.6, 136.4, 136.9, 146.8, 155.2, 155.9, 161.7, 186.8, 212.0. HRMS (ESI) calcd for C₄₃H₅₀N₅O₁₂ [M + H]⁺ 828.3450 found 828.3407.

Daunorubicin-*N*-benzyl-4-triazolyl-octahydroxamic Acid (**12d**)

Reaction of **11d** (0.05 g, 0.046 mmol) and BF₃·OEt₂ (0.1 mL) in CH₂Cl₂/MeOH (4 mL/4 mL) within 2 h, as described for the synthesis of **7**, followed by preparative TLC (eluent, CH₂Cl₂/MeOH 7:1) gave 0.028 g of **12d** (73%) as red solid. Retention time 16.93 min (Solvent Gradient: 5% - 60% solvent B over 20 min); ¹H NMR (DMSO-*d*₆, 400 MHz) δ 1.15-1.20 (8H, m), 1.41-1.44 (2H, m), 1.64-1.67 (2H, m), 1.77-1.80 (2H, m), 1.88 (2H, t, *J* = 7.6), 1.95-1.20 (2H, m), 2.23-2.24 (3H, m), 2.80-2.94 (3H, m), 3.60-3.67 (2H, m),

3.76-3.79 (1H, m), 3.89-3.94 (3H, m), 4.05-4.10 (1H, m), 4.30 (2H, t, $J = 7.2$), 4.88-4.91 (1H, m), 5.21 (1H, m), 5.42 (1H, s), 7.33-7.35 (2H, m), 7.57-7.59 (1H, m), 7.65-7.73 (2H, m), 7.83-7.86 (2H, m), 8.44 (1H, s), 10.29 (1H, m). ^{13}C NMR (DMSO- d_6 , 125 MHz) δ 17.2, 24.0, 24.8, 25.5, 27.9, 29.4, 30.8, 31.5, 32.1, 36.2, 48.4, 49.3, 51.8, 54.8, 56.5, 66.8, 70.0, 75.1, 75.2, 100.6, 110.5, 110.6, 118.8, 119.5, 119.9, 120.8, 124.9, 128.3, 129.1, 134.4, 134.6, 135.5, 136.1, 146.2, 154.1, 155.8, 160.6, 169.0, 186.3, 211.5. HRMS (ESI) calcd for $\text{C}_{44}\text{H}_{50}\text{N}_5\text{O}_{12} [\text{M} + \text{H}]^+$ 842.3607 found 842.3626.

4.5.3 HDAC & Topoisomerase I Conjugates Experimental

Representative procedures for *O*-alkylation reactions.

10-(Prop-2-ynyloxy) camptothecin (14a) –

To a stirring solution of **1a** (1.00 g, 2.75 mmol), K_2CO_3 (0.61 g, 4.4 mmol) in DMSO (15 mL), propargyl bromide (0.51 g, 3.44 mmol) was added dropwise. Reaction mixture was stirred for 24 h at room temperature and then diluted with 10 % MeOH in CH_2Cl_2 (80 mL). The resulting suspension was filtered and the residue was washed with 10 % MeOH in CH_2Cl_2 (~ 20 mL). The filtrate was washed sat. K_2CO_3 (2 x 50 mL), sat. brine (1 x 40 mL) and dried on Na_2SO_4 . Solvent was evaporated off to 1/10th of volume. Hexane:EtOAc (1:1 ratio, 60 mL) was added to reaction mixture. Suspension was filtered and washed again with hexane:EtOAc (1:1 ratio, 40 mL) to give pure pale yellow solid **2** (0.75 g, 68%). ^1H NMR (DMSO- d_6 , 400 MHz) δ 0.87 (3H, t, $J = 7.2$ Hz), 1.78-1.92 (2H, m), 3.65 (1H, s), 4.96-4.99 (2H, m), 5.17 (2H, s), 5.39 (2H, s), 6.50 (1H, s), 7.22 (1H, s), 7.44-7.55 (2H, m), 8.01 (1H, d, $J = 9.2$ Hz), 8.46 (1H, s); ^{13}C NMR (DMSO- d_6 , 100

MHz) δ 7.79, 30.2, 50.1, 55.9, 65.2, 93.9, 96.1, 107.6, 118.4, 122.8, 128.9, 130.0, 130.5, 144.0, 145.5, 150.0, 155.8, 156.7, 172.5. HRMS (FAB, m/ba) calcd for $[\text{C}_{23}\text{H}_{18}\text{N}_2\text{O}_5 + \text{H}]^+$ 403.1294, found 403.1289.

7-ethyl-10-(Prop-2-ynyloxy) camptothecin (14b) –

Reaction of **1b** (1.00 g, 2.55 mmol) with propargyl bromide (0.36 mL, 3.21 mmol) within 24 h as described for synthesis of **2a** gave 0.84 g (77%) of product as white brown solid.

^1H NMR ($\text{DMSO}-d_6$, 400 MHz) δ 0.86 (3H, t, $J = 7.2$ Hz), 1.30 (3H, t, $J = 7.6$ Hz), 1.79–1.90 (2H, m), 3.15 (2H, q, $J = 7.6$ Hz), 3.65 (1H, t, $J = 2.4$ Hz), 5.03 (2H, d, $J = 2.8$ Hz), 5.25 (2H, s), 5.40 (2H, s), 6.50 (1H, s), 7.24 (1H, s), 7.48–7.51 (1H, dd, $J = 2.4, 9.2$ Hz), 7.57 (1H, d, $J = 2.8$ Hz), 8.06 (1H, d, $J = 9.2$ Hz). ^{13}C NMR ($\text{DMSO}-d_6$, 100 MHz) δ 7.8, 13.5, 22.3, 30.2, 49.4, 55.9, 65.2, 72.3, 78.7, 95.9, 103.8, 118.1, 122.0, 127.3, 128.1, 131.2, 143.6, 144.2, 145.9, 149.5, 149.7, 155.5, 156.5, 172.2.

Experimental procedure for 5-azido-*O*-tritylpentahydroxamate (15a) –

5-azidopentanoic acid –

To a stirred solution of 5-bromo pentanoic acid (5.00 g, 27.6 mmol) in DMF (20 mL) was added sodium azide (5.74 g, 88.4 mmol), and the reaction mixture was heated at 85 °C overnight. The reaction mixture was diluted with CH_2Cl_2 , and was washed with 0.1 N aq. HCl. The organic layer was dried over anhydrous Na_2SO_4 , filtered, and concentrated

under reduced pressure to give 5-azido pentanoic acid (3.10 g, 79%) as colorless oil, which was used without further purification.

5-azido-*O*-tritylpentahydroxamate (15a) –

5-azidopentanoic acid (1.10 g, 7.69 mmol) was dissolved in anhydrous THF. *N*-methylmorpholine (0.84 mL, 7.69 mmol) was added to the solution. The reaction mixture was then cooled down to -15 °C and stirred for 5 min. Isobutylchloroformate (1.00, 7.69 mmol) was added and the mixture was stirred for 10 min at -15 °C. *O*-tritylhydroxylamine (2.11 g, 7.69 mmol) was added followed by 2 more equivalents of *N*-methylmorpholine. Stirring continued for 15 min at -15 °C and 2 h at room temperature. Afterwards the mixture was poured into 2M HCl and extracted 3 times in each case with water, sodium bicarbonate solution (5%) and water. After washing with brine and drying over Na₂SO₄, solvent was evaporated *in vacuo* to yield compound **15a** (2.78 g, 90%) as a white solid with no further purification required. ¹H NMR (DMSO-*d*₆, 400 MHz) δ 1.17-1.25 (4H, m), 1.79 (2H, t, *J* = 5.8 Hz), 3.15 (2H, t, *J* = 6.1 Hz), 7.27-7.31 (15H, m), 10.22 (1H, s); ¹³C NMR (CDCl₃, 100 MHz) δ 20.1, 27.7, 30.1, 50.6, 93.0, 127.8, 128.6, 140.6, 176.0.

Representative Procedure for Cu(I)-catalyzed Cycloaddition Reaction. *O*-trityl-10-hydroxycamptothecinriazolylpentahydroxamate (16a).

5-Azido-*O*-tritylpentahydroxamate **15a** (0.116 g, 0.29 mmol) and 10-(Prop-2-ynyloxy) camptothecin (**14a**) (0.09 g, 0.22 mmol) were dissolved in anhydrous THF:DMSO(10:1

mL) and stirred under argon at room temperature. Copper iodide (0.009 g, 0.048 mmol) and Hunig's base (0.1 mL) were then added to the reaction mixture, and stirring continued for 24 h. The reaction mixture was diluted with CH₂Cl₂ (30 mL) and washed with 1:4 NH₄OH/saturated NH₄Cl (3 x 30 mL) and saturated NH₄Cl (30 mL). The organic layer was dried over Na₂SO₄ and concentrated in vacuo. The crude product was purified by preparative TLC (silica, 14:1 CH₂Cl₂:MeOH) to give 0.131 g (73 %) of **16a** as a pale yellow solid. ¹H NMR (DMSO-*d*₆, 400 MHz) δ 0.86 (3H, t, *J* = 7.2 Hz), 1.12-1.19 (2H, m), 1.48 (2H, p, *J* = 7.6 Hz), 1.80-1.90 (4H, m), 4.23 (2H, t, *J* = 7.2 Hz), 5.26 (2H, s), 5.33 (2H, s), 5.41 (2H, s), 6.51 (1H, s), 7.26-7.29 (15H, m), 7.52 (1H, dd, *J* = 2.8, 8.8 Hz), 7.71 (1H, d, *J* = 2.4 Hz), 8.07 (1H, d, *J* = 9.2 Hz), 8.23 (1H, s), 8.54 (1H, s), 10.24 (1H, s); ¹³C NMR (CDCl₃, 100 MHz) δ 7.80, 20.1, 29.4, 30.3, 31.5, 50.0, 62.3, 66.3, 72.7, 77.1, 97.4, 106.7, 118.0, 122.8, 123.7, 128.1, 128.9, 129.0, 129.3, 129.6, 131.2, 140.8, 145.1, 146.6, 150.1, 150.3, 157.4, 157.6, 173.9. HRMS (ESI) calcd for [C₄₇H₄₂N₆O₇ + H]⁺ 803.3187, found 803.3227.

***O*-trityl-10-hydroxycamptothecin triazolylhexahydroxamate (16b) –**

Reaction of 6-Azido-*O*-tritylhexahydroxamate **15b** (0.120 g, 0.29 mmol) and 10-(Prop-2-ynyloxy) camptothecin (**14a**) (0.09 g, 0.22 mmol) within 24 h as described for synthesis of **16a**, followed by preparative TLC (silica, eluent 19:1 CH₂Cl₂:MeOH) gave 0.131g (72 %) of compound **16b** as pale yellow solid. ¹H NMR (DMSO-*d*₆, 400 MHz) δ 0.86 (3H, t, *J* = 7.2 Hz), 0.92-0.96 (2H, m), 1.18-1.23 (2H, m), 1.65-1.69 (2H, m), 1.75 (2H, t, *J* = 7.2 Hz), 1.80-1.90 (2H, m), 4.26 (2H, t, *J* = 7.2 Hz), 5.25 (2H, s), 5.31 (2H, s), 5.41 (2H,

s), 6.51 (1H, s), 7.27-7.30 (15H, m), 7.51 (1H, dd, $J = 2.8, 9.2$ Hz), 7.70 (1H, d, $J = 2.8$ Hz), 8.06 (2H, d, $J = 9.2$ Hz), 8.28 (1H, s), 8.53 (1H, s), 10.17 (1H, s); ^{13}C NMR (CDCl_3 , 100 MHz) δ 7.79, 22.4, 25.7, 29.8, 31.5, 40.9, 50.0, 62.2, 66.2, 72.7, 77.1, 97.4, 106.6, 118.0, 122.9, 123.5, 128.1, 128.9, 129.0, 129.2, 129.6, 131.1, 140.9, 143.1, 144.9, 146.4, 150.1, 150.2, 157.3, 157.5, 173.8. HRMS (ESI) calcd for $[\text{C}_{48}\text{H}_{44}\text{N}_6\text{O}_7 + \text{H}]^+$ 817.3344, found 817.3415.

***O*-trityl-10-hydroxycamptothecin triazolylheptahydroxamate (**16c**) –**

Reaction of 7-Azido-*O*-tritylheptahydroxamate **15c** (0.124 g, 0.29 mmol) and 10-(Prop-2-ynyloxy) camptothecin (**14a**) (0.09 g, 0.22 mmol) within 24 h as described for synthesis of **16a**, followed by preparative TLC (silica, eluent 19:1 CH_2Cl_2 :MeOH) gave 0.143 g (77 %) of compound **16c** as pale yellow solid. ^1H NMR ($\text{DMSO}-d_6$, 400 MHz) δ 0.86 (3H, t, $J = 7.2$ Hz), 0.92-0.98 (2H, m), 1.03-1.16 (4H, m), 1.66-1.76 (4H, m), 1.81-1.88 (2H, m), 4.31 (2H, t, $J = 6.8$ Hz), 5.26 (2H, s), 5.32 (2H, s), 5.41 (2H, s), 7.28-7.30 (15H, m), 7.52 (1H, dd, $J = 2.8, 9.6$ Hz), 7.71 (1H, d, $J = 2.4$ Hz), 8.06 (1H, d, $J = 9.2$ Hz), 8.30 (1H, s), 8.53 (1H, s); ^{13}C NMR (CDCl_3 , 100 MHz) δ 8.06, 30.1, 31.8, 41.1, 50.2, 50.5, 62.5, 66.5, 73.0, 77.4, 97.7, 107.0, 118.3, 123.0, 123.9, 128.3, 129.2, 129.3, 129.5, 129.8, 131.4, 143.4, 145.2, 146.7, 150.4, 157.6, 157.8, 174.1. HRMS (ESI) calcd for $[\text{C}_{49}\text{H}_{46}\text{N}_6\text{O}_7 + \text{H}]^+$ 831.3500, found 831.3567.

Representative procedure for conversion of *O*-tritylhydroxamate to hydroxamic acid.

5-(10-hydroxycamptothecin)triazolypentahydroxamic acid (17a).

To a solution of *O*-trityl-10-hydroxycamptothecin triazolypentahydroxamate **16a** (0.09 g, 0.11 mmol) in CH₂Cl₂ (7 ml) was added trifluoroacetic acid (TFA) (0.2 mL) and thioanisole (0.2 mL) dropwise at 0 °C. After 2 h stirring at 0 °C, solvent was evaporated and thick brown-black liquid was treated with Et₂O (~15 mL) to give yellowish suspension. Suspension was filtered and residue was washed with cold Et₂O (~30 mL) then with CH₂Cl₂:Et₂O (1:1) mixture (~30 mL), followed by more washing with CH₂Cl₂ (~100 mL) to give 0.042 g (67%) of pure **17a** as a yellow solid. ¹H NMR (DMSO-*d*₆, 400 MHz) δ 0.86 (3H, t, *J* = 7.6 Hz), 1.43-1.49 (2H, m), 1.75-1.88 (4H, m), 1.97 (2H, t, *J* = 6.8 Hz), 4.37 (2H, t, *J* = 7.2 Hz), 5.27 (2H, s), 5.32 (2H, s), 5.41 (2H, s), 7.27 (1H, s), 7.53 (1H, d, *J* = 9.2 Hz), 7.71 (1H, s), 8.07 (1H, d, *J* = 9.2 Hz), 8.31 (1H, s), 8.54 (1H, s), 10.37 (1H, s); ¹³C NMR (DMSO-*d*₆, 100 MHz) δ 7.78, 22.1, 29.3, 30.2, 30.7, 31.5, 49.1, 50.2, 61.6, 65.2, 72.4, 96.1, 107.4, 118.4, 123.1, 124.7, 129.2, 130.2, 130.5, 142.0, 144.0, 145.7, 150.0, 150.2, 156.8, 168.7, 172.5. HRMS (ESI) calcd for [C₂₈H₂₈N₆O₇ + H]⁺ 561.2092, found 561.2123.

6-(10-hydroxycamptothecin)triazolylhexahydroxamic acid (17b).

Reaction of *O*-trityl-10-hydroxycamptothecin triazolylhexahydroxamate **16b** (0.075 g, 0.09 mmol) with TFA (0.2 ml) and thioanisole (0.2 ml) in CH₂Cl₂ (7 ml) at 0 °C within 2 h as described for the synthesis of **17a**, gave 0.036 g (68 %) of **17b** as a yellow solid. ¹H NMR (DMSO-*d*₆, 400 MHz) δ 0.86 (3H, t, *J* = 7.2 Hz), 1.07 (2H, t, *J* = 7.2 Hz), 1.17-

1.24 (2H, m), 1.46-1.53 (2H, m), 1.78-1.93 (4H, m), 4.36 (2H, t, $J = 7.2$ Hz), 5.25 (2H, s), 5.32 (2H, s), 5.41 (2H, s), 7.27 (1H, s), 7.52 (1H, d, $J = 8.8$ Hz), 7.70 (1H, s), 8.06 (1H, d, $J = 9.2$ Hz), 8.32 (1H, s), 8.53 (1H, s), 10.33 (1H, s); ^{13}C NMR (DMSO- d_6 , 100 MHz) δ 7.7, 24.4, 25.3, 29.3, 30.1, 31.9, 49.2, 50.1, 61.5, 65.1, 72.3, 96.0, 107.3, 118.3, 123.0, 124.5, 128.8, 129.2, 130.0, 130.2, 130.4, 142.0, 143.9, 145.6, 149.9, 150.2, 156.7, 168.8, 172.4. HRMS (EI) calcd for $[\text{C}_{29}\text{H}_{30}\text{N}_6\text{O}_7 + \text{H}]^+$ 575.2254, found 575.2216.

7-(10-hydroxycamptothecin)triazolylheptahydroxamic acid (17c).

Reaction of *O*-trityl-10-hydroxycamptothecin triazolylheptahydroxamate **16c** (0.09 g, 0.108 mmol) with TFA (0.2 ml) and thioanisole (0.2 ml) in CH_2Cl_2 (7 ml) at 0 °C within 2 h as described for the synthesis of **17a**, gave 0.041 g (65 %) of **17c** as a yellow solid. ^1H NMR (DMSO- d_6 , 400 MHz) δ 0.85 (3H, t, $J = 7.2$ Hz), 1.18-1.26 (4H, m), 1.39-1.47 (2H, m), 1.77-1.91 (6H, m), 4.34 (2H, t, $J = 6.8$ Hz), 5.20 (2H, s), 5.29 (2H, s), 5.39 (2H, s), 7.24 (1H, s), 7.47 (1H, d, $J = 8.8$ Hz), 7.65 (1H, s), 8.02 (1H, d, $J = 9.2$ Hz), 8.30 (1H, s), 8.49 (1H, s), 10.33 (1H, s); ^{13}C NMR (DMSO- d_6 , 100 MHz) δ 7.7, 24.9, 25.5, 27.9, 29.6, 30.2, 32.1, 49.4, 50.2, 61.6, 65.2, 72.4, 96.1, 107.4, 118.4, 123.1, 124.6, 129.2, 130.0, 130.2, 130.5, 142.1, 144.0, 145.6, 150.0, 150.2, 156.8, 172.5. HRMS (ESI) calcd for $[\text{C}_{30}\text{H}_{32}\text{N}_6\text{O}_7 + \text{H}]^+$ 589.2405, found 589.2418.

4.6 References

- 1.) (a) Papac, R. J. *Yale J. Biol. Med.* **2001**, 74 (6), 391. (b) Buzdar, A. U. *Cancer* **2007**, 110 (11), 2394. (c) Morphy, R.; Kay, C.; Rankovic, Z. *Drug Discov. Today* **2004**, 9, 641.
- 2.) Morphy, R.; Rankovic, Z. *J. Med. Chem.* **2005**, 48, 6523.
- 3.) Frantz, S. *Nature* **2005**, 437, 942.
- 4.) Roth, B. L.; Sheffler, D. J.; Kroeze, W. K. *Nat. Rev. Drug Discov.* **2004**, 3, 353.
- 5.) Hopkins, A. L.; Mason, J. S.; Overington, J. P. *Curr. Opinion Struct. Biol.* **2006**, 16, 127.
- 6.) Cmeserly, P.; Agoston, V.; Pongor, S. *Trends Pharmacol. Sci.* **2005**, 26, 178.
- 7.) Fray, M. J.; Bish, G.; Brown, A. D.; Fish, P. V.; Stobie, A.; Wakenhut, F.; Whitlock, G.A. *Bioorg. Med. Chem. Lett.* **2006**, 16, 4345.
- 8.) (a) Neumeyer, J. L.; Peng, X.; Knapp, B. I.; Bidlack, J. M.; Lazarus, L. H.; Salvadori, S.; Trapella, C.; Balboni, G. *J. Med. Chem.* **2006**, 49, 5640. (b) Meutermans, W. D.; Bourne, G. T.; Golding, S. W.; Horton, D. A.; Campitelli, M. R.; Craik, D.; Scanlon, M.; Smythe, M. L., *Org. Lett.*, **2003**, 5, 2711-2714. (c) Glenn, M. P.; Kelso, M. J.; Tyndall, J. D.; Fairlie, D. P. *J. Am. Chem. Soc.* **2003**, 125, 640. (d) Shivashimpi, G. M.; Amagai, S.; Kato, T.; Nishino, N.; Maeda, S.; Nishino, T. G.; Yoshida, M. *Bioorg. Med. Chem.* **2007**, 15, 7830. (e) Deshmukh, P. H.; Schulz-Fademrecht, C.; Procopiou, P. A.; Vigushin, D. A.; Coombes, R. C. *Barrett Catal.* **2007**, 349, 175. (f) Oyelere, A. K.; Chen, P. C.; Guerrant, W.; Mwakwari, S. C.; Hood, R.; Zhang, Y.; Fan, Y. *J. Med. Chem.* **2009**, 52(2), 456.
- 9.) Jones, P. A.; Baylin, S. B. *Cell.* **2007**, 128, 683.
- 10) Kouzarides, T. *Cell.* **2007**, 128, 693.
- 11) Shilatifard, A. *Ann. Rev. Biochem.* **2006**, 75, 243.
- 12) Ropero, S.; Esteller, M. *Mol. Oncol.* **2007**, 1, 19.
- 13) Marks, P. A.; Richon, V. M.; Rifkind, R. A. *J. Natl. Cancer Inst.* **2000**, 92, 1210.
- 14) Saito, A.; Yamashita, T.; Mariko, Y.; Nosaka, Y.; Tsuchiya, K.; Ando, T.; Suzuki, T.; Tsuruo, T.; Nakanishi, O. *PNAS.* **1999**, 96, 4592.
- 15) Glick, R. D.; Swindemen, S. L.; Coffey, D. C.; Rifkind, R. A.; Marks, P. A.; Richon, V. M.; La Quaglia, M. P. *Cancer Res.* **1999**, 59, 4392.

- 16) Butler, L. M.; Agus, D. B.; Scher, H. I.; Higgins, B.; Rose, A.; Cordon-Cardo, C.; Thaler, H. T.; Rifkind, R. A.; Marks, P.A.; Richon, V.M. *Cancer Res.* **2000**, 60, 5165.
- 17) Oyelere, A. K.; Chen, P. C.; Guerrant, W.; Mwakwari, S. C.; Hood, R.; Zhang, Y.; Fan, Y. *J. Med. Chem.* **2009**, 52, 456.
- 18) Gu, W and Roeder, R. G. *Cell* **1997**, 90, 595.
- 19) Martinez-Balbás, M. A.; Bauer, U. M.; Nielsen, S. J.; Brehm, A.; Kouzarides, T. *EMBO J.* **2000** 19, 662.
- 20) Marzio, G.; Wagener, C.; Gutierrez, M. I.; Cartwright, P.; Helin, K.; Giacca, M. *J. Biol. Chem.* **2000** 275, 10887.
- 21) Hubbert, C.; Guardiola, A.; Shao, R.; Kawaguchi, Y.; Ito, A.; Nixon, A.; Yoshida, M.; Wang, X. F.; Yao, T. P. *Nature.* **2002**, 417, 455.
- 22) Kovacs, J. J.; Murphy, P. J.; Gaillard, S.; Zhao, X.; Wu, J. T.; Nicchitta, C. V.; Yoshida, M.; Toft, D. O.; Pratt, W. B.; Yao, T. P. *Mol. Cell.* **2005**, 18, 601.
- 23) Mann, B. S.; Johnson, J. R.; Cohen, M. H.; Justice, R.; Padzur, R. *Oncologist.* **2007**, 12, 1247.
- 24) Grant, C.; Rahman, F.; Piekarz, R.; Peer, C.; Frye, R.; Robey, R. W.; Gardner, E. R.; Figg, W. D.; Bates, S. E. *Expert Rev. Anticancer Ther.* **2010**, 10, 997.
- 25) Mwakwari, S. C.; Patil, V.; Guerrant, W.; Oyelere, A. K. *Curr. Top. Med. Chem.* **2010**, 10, 1423-1440.
- 26) Kelly, W. K.; O'Connor, O. A.; Marks, P. A. *Expert. Opin. Investig. Drug* **2002**, 11, 1695-1713.
- 27) Rosato, R. R.; Grant, S. *Expert Opin. Invest. Drugs* **2004**, 13, 21-38.
- 28) Yoo, C. B.; Jones, P. A. *Nature Rev. Drug Discov.* **2006**, 5, 37-50.
- 29) Finnin, M. S.; Donigian, J. R.; Cohen, A.; Richon, V. M.; Rifkind, R. A.; Marks, P. A.; Breslow, R.; Pavletich, N. P. *Nature* **1999**, 401, 188.
- 30) Wang, D. F.; Wiest, O.; Helquist, P.; Lan-Hargest, H. Y.; Wiech, N.L. *J. Med. Chem.* **2004**, 47, 3409.
- 31) Chen, L.; Wilson, D.; Jayaram, H. N.; Pankiewicz, K.W. *J. Med. Chem.* **2007**, 50, 26, 6685.
- 32) Piccart-Gebhart, M. J. *N. Engl. J. Med.* **2006**, 354, 2177.

- 33) Kim, M. S.; Blake, M.; Baek, J. H.; Kohlhagen, G.; Pommier, Y.; Carrier, F. *Cancer Res.* **2003**, 63, 7291.
- 34) Catalano, M. G.; Fortunati, N.; Pugliese, M.; Poli, R.; Bosco, O.; Mastrocola, R.; Aragno, M.; Bocuzzi, G. *J. Endocrinol* **2006**, 191, 2, 465.
- 35) Johnson, C.A.; Padget, K.; Austin, C.A.; Turner, B.M. *J. Biol. Chem.* **2001**, 276, 7, 4539.
- 36) Marchion, D. C.; Bicaku, E.; Daud, A. I.; Richon, V.; Sullivan, D. M.; Munster, P. N. *J. Cell Biochem.* **2004**, 92, 2, 223.
- 37) Tewey, K. M.; Rowe, T. C.; Yang, L.; Halligan, B. D.; Liu, L. F. *Science* **1984**, 226, 466.
- 38) Binaschi, M.; Bigioni, M.; Cipollone, A.; Rossi, C.; Goso, C.; Maggi, C.A.; Capranico, G.; Animati, F. *Curr. Med. Chem. Anticancer Agents* **2001**, 1, 2, 113.
- 39) Pommier, Y.; Schwartz, R. E.; Kohn, K. W.; Zwelling, L.A. *Biochemistry* **1984**, 23, 3194.
- 40) Kiyomiya, K.; Matsuo, S.; Kurebe, M. *Life Sci.* **1998**, 62, 20, 1853-1860.
- 41) Kiyomiya, K.; Matsuo, S.; Kurebe, M., *Cancer Res.* **2001**, 61, 2467.
- 42) Castro-Galache, M. D.; Ferragut, J. A.; Barbera, V. M.; Martín-Orozco, E.; Gonzalez-Ros, J. M.; Garcia-Morales, P.; Saceda, M. *Int. J. Cancer* **2003**, 104, 579.
- 43) Martín, B.; Vaquero, A.; Priebe, W.; Portugal, J. *Nucleic Acids Res.* **1999**, 27, 3402.
- 44) Lothstein, L.; Israel, M.; Sweatman, T. W. *Drug Resist. Updat.* **2001**, 4, 169.
- 45) Gate, L.; Couvreur, P.; Nguyen-Ba, G.; Tapiero, H. *Biomed & Pharmacotherapy* **2003**, 57, 301.
- 46) Tong, G. L.; Wu, H. Y.; Smith, T. H.; Henry, D. W. *J. Med. Chem.* **1979**, 22, 912.
- 47) (a) Mwakwari, S. C.; Guerrant, W.; Patil, V.; Khan, S. I.; Tekwani, B. L.; Gurard-Levin, Z. A.; Mrksich, M.; Oyelere, A. K. *J. Med. Chem.* **2010**, 53, 6100; (b) Chen, P. C.; Patil, V.; Guerrant, W.; Green, P.; Oyelere, A. K. *Bioorg. Med. Chem.* **2008**, 16, 4839.
- 48) Lu, J.; Yoshida, O.; Hayashi, S.; Arimoto, H. *Chem. Commun.* **2007**, 251.

- 49) Preobrazhenskaya, M. N.; Olsufyeva, E. N.; Solovieva, S. E.; Tevyashova, A. N.; Reznikova, M. I.; Luzikov, Y. N.; Terekhova, L. P.; Trenin, A. S.; Galatenko, O. A.; Treshalin, I. D.; Mirchink, E. P.; Bukhman, V. M.; Sletta, H.; Zotchev, S. B. *J. Med. Chem.* **2009**, 52, 189.
- 50) Yang, S.; Lagu, B.; Wilson, L. *J. Org. Chem.* **2007**, 72(21), 8123.
- 51) Morris, G. M.; Goodsell, D. S.; Halliday, R. S.; Huey, R.; Hart, W. E.; Belew, R. K.; Olson, A. J. *J. Comput. Chem.* **1998**, 19, 1639.
- 52) Estiu G.; Wiest, O.; HDAC1 homology model, Personal Communication.
- 53) Wang, J. C. *Annu. Rev. Biochem.* **1985**, 54, 665.
- 54) Champoux, J. J. *Annu. Rev. Biochem.* **2001**, 70, 369.
- 55) Chen, A. Y. and Liu, L. F. *Annu. Rev. Pharmacol. Toxicol.* **1994**, 34, 191.
- 56) Froelich-Ammon, S. J. and Osheroff, N. *J. Biol. Chem.* **1995**, 270, 21429.
- 57) Pommier, Y. *Chem. Rev.* **2009**, 109, 2894.
- 58) Hsiang, Y. H.; Lihou, M. G.; Liu, L.F. *Cancer Res.* **1989**, 49, 5077.
- 59) Matsukawa, Y.; Marui, N.; Sakai, T.; Satomi, Y.; Yoshida, M.; Matsumoto, K.; Nishino, H.; Aoike, A. *Cancer Res.* **1993**, 53, 1328.
- 60) Johnson, C. A.; Padget, K.; Austin, C. A.; Turner, B. M. *J. Biol. Chem.* **2001**, 276, 4539.
- 61) Kawato, Y.; Aonuma, M.; Hirota, Y.; Kuga, H.; Sato, K. *Cancer Res.* **1991**, 51, 4187.
- 62) Zhang, R.; Li, Y.; Cai, Q.; Liu, T.; Sun, H.; Chambless, B. *Cancer Chemother. Pharmacol.* **1998**, 41, 257.
- 63) Chen, Z. S.; Furukawa, T.; Sumizawa, T.; Ono, K.; Ueda, K.; Seto, K.; Akiyama, S. I. *Mol. Pharmacol.* **1999**, 55, 921.
- 64) Sugimori, M.; Ejima, A.; Ohsuki, S.; Uoto, K.; Mitsui, I.; Matsumoto, K.; Kawato, Y.; Yasuoka, M.; Sato, K.; Tagawa, H.; Terasawa, H. *J. Med. Chem.* **1994**, 37, 3033.
- 65) (a) Leu, Y. L.; Chen, C. S., Wu Y. J.; Chern J. W. *J. Med. Chem.* **2008**, 51, 1740.
(b) Toki, B. E.; Cervený, C. G.; Wahl, A. F.; Senter, P. D. *J. Org. Chem.* **2002**, 67, 1866.
- 66) Chen, P. C.; Patil, V.; Guarrant, W.; Green, P.; Oyelere, A. K. *Bioorg. Med. Chem.* **2008**, 16, 4839.

- 67) (a) Rostovtsev, V. V.; Green, L. G.; Fokin, V. V.; Sharpless, K. B. A. *Angew. Chem. Int. Ed.* **2002**, 41, 2596–2599; (b) Tornøe, C. W.; Christensen, C.; Meldal, M. *J. Org. Chem.* **2002**, 67, 3057.
- 68) Patil, V.; Guarrant, W.; Chen, P. C.; Gryder, B.; Benicewicz, D.; Khan, S.; Tekwani, B.; Oyelere, A. K. *Bioorg. Med. Chem.* **2010**, 18(1), 415.
- 69) Madhavaiah, C.; Sandeep Verma *Bioorg. & Med. Chem. Lett.* **2003**, 13, 923.
- 70) Oyelere, A. K.; Chen, P.C.; Guarrant, W.; Mwakwari, S. C.; Hood, R.; Zhang, Y.; Fan, Y. *J. Med. Chem.* **2009**, 52, 456.
- 71) Mai, A.; Esposito, M.; Sbardella, G.; Massa, S. *Org. Prep. Proced. Int.* **2001**, 33, 4, 391.
- 72) Grandjean, C.; Boutonnier, A.; Guerreiro, C.; Fournier, J.; Mulard, L. *J. Org. Chem* **2005**, 70, 7123.

CHAPTER 5

IDENTIFICATION OF NOVEL ZINC BINDING GROUP (ZBG) FOR HDAC INHIBITION

5.1 Introduction

Effect of global acetylation of histones and non histone proteins by HDAC inhibitors is so vast and complex that inhibiting multiple isoforms of HDAC can undermine their use in treating disease conditions due to deleterious side effects.¹⁻¹⁰ Therefore, significant efforts are directed towards developing isoform selective inhibitors to understand the roles of the eighteen HDAC isoforms. These HDAC isoforms are implicated in cell cycle regulation, cell proliferation, development of human diseases including cancer, cardiovascular diseases, neurological diseases, inflammatory, and parasitic conditions.¹¹ Research over the years has developed our understanding of relationship between each HDAC isoform and their role in specific disease condition. For example, HDAC 1, 6, and 8 are crucial for breast cancer; HDAC 1-3 are overexpressed in ovarian; HDAC 1 and 3 are implicated in lung cancers, HDAC 2 is associated with gastric cancer; there is possible correlation between HDAC8 and acute myeloid leukemia (AML).¹²⁻¹⁶ Despite this progress, exact cellular function of HDAC isoforms are still not clearly understood due to lack of molecular reagents that exhibit selectivity for individual isoforms.

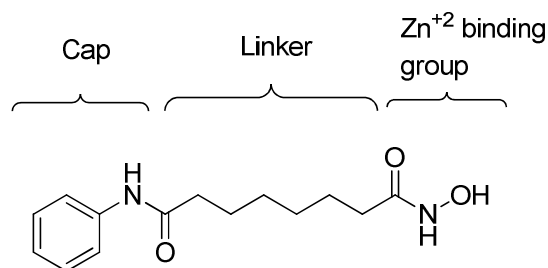


Figure 5-1. Prototypical HDACi – SAHA fits into classical pharmacophoric model of HDACi

The classical pharmacophoric model of HDAC inhibitor consists of zinc binding group (ZBG) which interacts at active site of enzyme. Linker region and surface recognition cap group provides support for placing zinc binding group at appropriate position for optimum chelation with zinc metal ion (Figure 5-1).¹⁷ Earlier chapter focused on SAR studies of surface recognition cap group, cap linking moiety and optimization of linker region for effective HDACi design to generate more potent HDACi. In this chapter, emphasis will be on development of novel ZBG for HDAC inhibition.

ZBG is crucial for binding to catalytic zinc active site thereby rendering HDAC enzymes inactive.¹⁸ Hydroxamic acid has been widely used in the literature as a ZBG of choice owing to its strong chelation to Zn²⁺ metal ion.¹⁹⁻²⁰ Despite strong Zn²⁺ metal ion chelation, hydroxamic acid presents metabolic and pharmacokinetic issues such as glucuronidation, sulfation, and enzymatic hydrolysis.²¹ For example, hydroxamic acid can readily hydrolyze into carboxylic acid *in vivo*, therefore the *in vivo* activities doesn't compare to *in vitro* potencies. In addition, most of the hydroxamates have poor bioavailability.²¹ Furthermore, hydroxamic acids have binding affinities for other biological relevant metals such as iron (III), copper (II) that are similar or exceed those measured for Zn²⁺ ion.²² Extensive reports have been published to improve the HDAC

inhibition profile by manipulating the surface recognition cap group and linker region while keeping hydroxamic acid as ZBG intact. Indeed, many of these efforts have resulted in compounds showing nanomolar or even subnanomolar activities *in vitro*.²³⁻²⁴ In some cases, isoform-selectivity was achieved.²⁴ However, significantly fewer efforts have focused on replacement of hydroxamic acids as ZBG to gain isoform selectivity.^{17,25} Many of the HDAC inhibitors which contain hydroxamates as ZBG show pan-inhibition of HDAC isoforms. For example, SAHA and TSA which have hydroxamic acid as ZBG are generally pan-inhibitors.²⁶ However, when hydroxamic acid moiety of SAHA was replaced with benzamide zinc binding group class I selectivity was seen.²⁷ Moreover, benzamide based HDACi MS-275 displayed class I selectivity with at least 135-fold HDAC1 preference over HDAC1 vs HDAC6 and HDAC8.²⁸ It has been suggested that benzamide may take advantage of sequence difference in the region adjacent to the catalytic zinc ion by positioning itself favorably within 14 Å internal cavity.²⁸ In lieu of liabilities seen in hydroxamate based compounds and to expand library of potential ZBG, we started exploring other functional groups that can serve as effective ZBGs in HDACi design.

Cohen *et al* have reported novel heterocyclic zinc binding fragments (Figure 5-2), which are more potent and selective than acetohydroxamic acid (AHA) tested against matrix metalloproteins (MMPs).²⁹

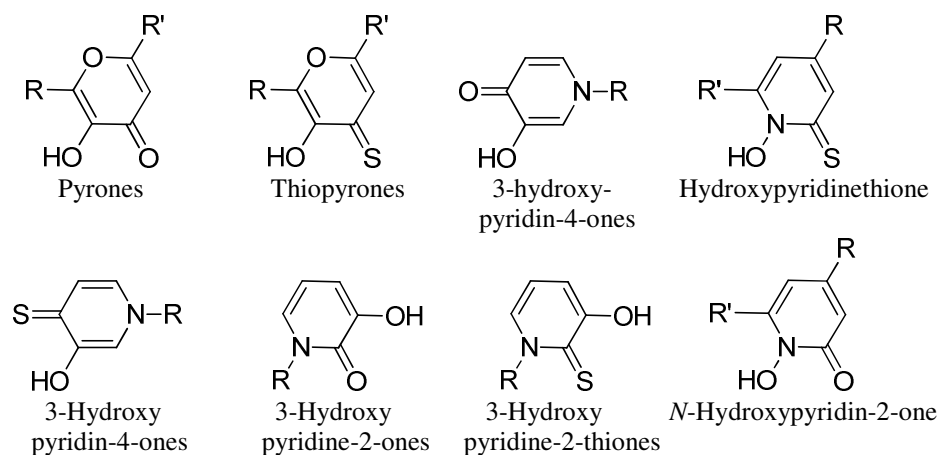


Figure 5-2. Heterocyclic aromatic ZBGs^{29a}

Monodentate ZBGs (Figure 5-3) generally exhibit weaker binding affinity for Zn^{2+} ion and therefore, are less likely to be effective chelators than hydroxamic acid. Several bidentate ZBGs containing heterocyclic aromatic fragments such as hydroxypyrones, hydroxypyridinones and their thione derivatives were shown to be more potent inhibitors of MMPs than corresponding hydroxamic acid fragment (acetohydroxamic acid).³⁰

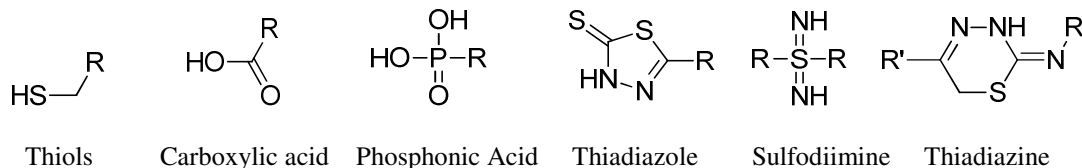


Figure 5-3. Monodentate ZBGs^{29a}

However, these ZBGs showed relatively low toxicities against MMPs in cell studies.³⁰ The thione derivatives such as thiopyrones and hydroxypyridinethiones exhibited significant increase in potency likely due to apparent thiophilicity of these chelators to

Zn²⁺ ion.³¹ Therefore we decided to test feasibility of these heterocyclic aromatic ZBG for incorporation into HDACi design.

5.2 Fragment-based Approach for Identification of Novel ZBG

Fragment based lead design (FBLD) is relatively new concept for designing small molecule inhibitors. It employs relatively small fragment library for screening against target protein to identify lead fragments.^{32,33} Knowledge of exactly how the fragments bind to the protein target allows the hits to be optimized by growing the fragments or by combining and linking different fragments. FBLD offers two unique advantages over traditional high throughput screening – First, smaller fragments explore chemical space more effectively and hence more likely to generate novel compounds. Secondly, the small size of the fragments (usually less than 250 Daltons) makes optimization relatively easier by decreasing the synthetic efforts since only the selected fragments need to be assembled and tested with the target protein(s).³²⁻³⁵

Several studies have shown successful implementation FBLD for the development of novel inhibitors of zinc metalloenzymes.^{29a,30a,36} However, these approaches used either X-ray crystallography or NMR-based screening for evaluation of fragment screening. These methods typically require large quantities of protein and time-consuming data analysis, and therefore may not be necessary for ZBG fragment screening.^{32,34,36} Recently, Li and coworkers successfully employed multiple ligand simultaneous docking to screen fragments to generate novel STAT3 inhibitor with improved potency and ADMET profiles.³⁷ We have explored a standard molecular docking approach and *in vitro* screening to test fragments against HDAC isoforms. We

have focused on pyridinone and their thione analogs as potential ZBG in HDACi design. In addition to their superior IC₅₀ values compared to acetohydroxamic acid fragments, pyridinones were chosen for this study because – i) these fragments are monoanionic ligands that are expected to bind the zinc ion in a bidentate fashion similar to hydroxamic acid; ii) their proven biocompatibility in biological systems;²⁹ iii) ubiquity of synthetic procedures for pyridinones^{36,38,54} modifications that will enable easy incorporation into HDACi design. A fragment based approach coupled with structure-based drug design as described here is expected to provide novel and selective HDAC inhibitors.

5.3 Design of 1st Generation Novel ZBG in HDACi Design

In order to test the feasibility of pyridinone fragments in HDACi design, fragments were docked against HDAC crystal structures using validated molecular dock program (AutoDock 4.2) as previously described.³⁹ We selected representative pyridinone fragments 3-hydroxypyridin-2-thiones; 3-hydroxypyridin-4-thiones and 1-hydroxypyridin-2-thione to dock against HDAC macromolecules. We postulated that N-1 position of 3-hydroxypyridin-2-thiones & 3-hydroxypyridin-4-thiones can be modified to include prototypical HDACi linker region coupled to surface recognition cap group. Small fragments tend to have lower binding energy and non-specific interaction at the surface. These problems were addressed by – i) selecting compact grid size around the Zn²⁺ active site. ii) Selecting thione analogs of pyridinone fragments which is expected to bind more tightly with Zn²⁺ metal ion than their carbonyl counterpart thereby improving binding energy.³¹

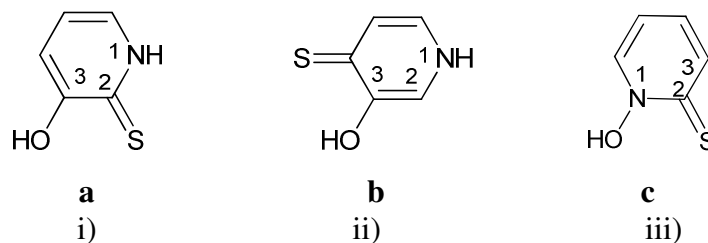


Figure 5-4. Docked fragments a) 3-hydroxy pyridin-2-thiones (3-HPT) **a**; b) 3-hydroxypyridin-4-thiones **b**; c) 1-hydroxypyridin-2-thione **c**.

We chose to dock these fragments against class I HDAC enzymes HDAC1 and HDAC8. Both the isoforms are phylogenetically similar⁹ yet there are distinct structural differences at the Zn^{2+} active site. Any evidence of isoform selectivity against any one of them should establish broader isoform profile. Docking analyses were performed on a HDAC 1 homology model built from human HDAC 2 X-ray structure 3MAX coordinates,⁴⁰ while HDAC8 crystal structure (PDB code: 1VKG)⁴¹ has been solved and was used to obtain in silico data for fragment interaction at active sites. Preliminary docking analysis against HDAC1 and HDAC8 revealed that 3-hydroxypyridin-2-thiones (3-HPT) (**a**), 3-hydroxypyridin-4-thiones (**b**) and 1-hydroxypyridin-2-thione (**c**) bound to vicinity of Zn^{2+} ion at active sites of HDAC1 and HDAC8, confirming our hypothesis that pyridinones can very well be tolerated in HDACi design.

Closer analyses of docked structure revealed that the orientation of N-1 position of 3-hydroxypyridin-4-thione is pointing towards the base of the active site pocket instead of pointing toward surface as seen with 3-HPT (Figure 5-5 and Figure 5-6; comparing b and c). Although, 1-hydroxypyridin-2-thione bound very well in vicinity of Zn^{2+} ion (Figure 5-5d and Figure 5-6d), substitution on the aromatic ring to introduce the

linker region can be synthetically challenging. Therefore, we focused on the 3-hydroxypyridin-2-ones fragment for further investigation.

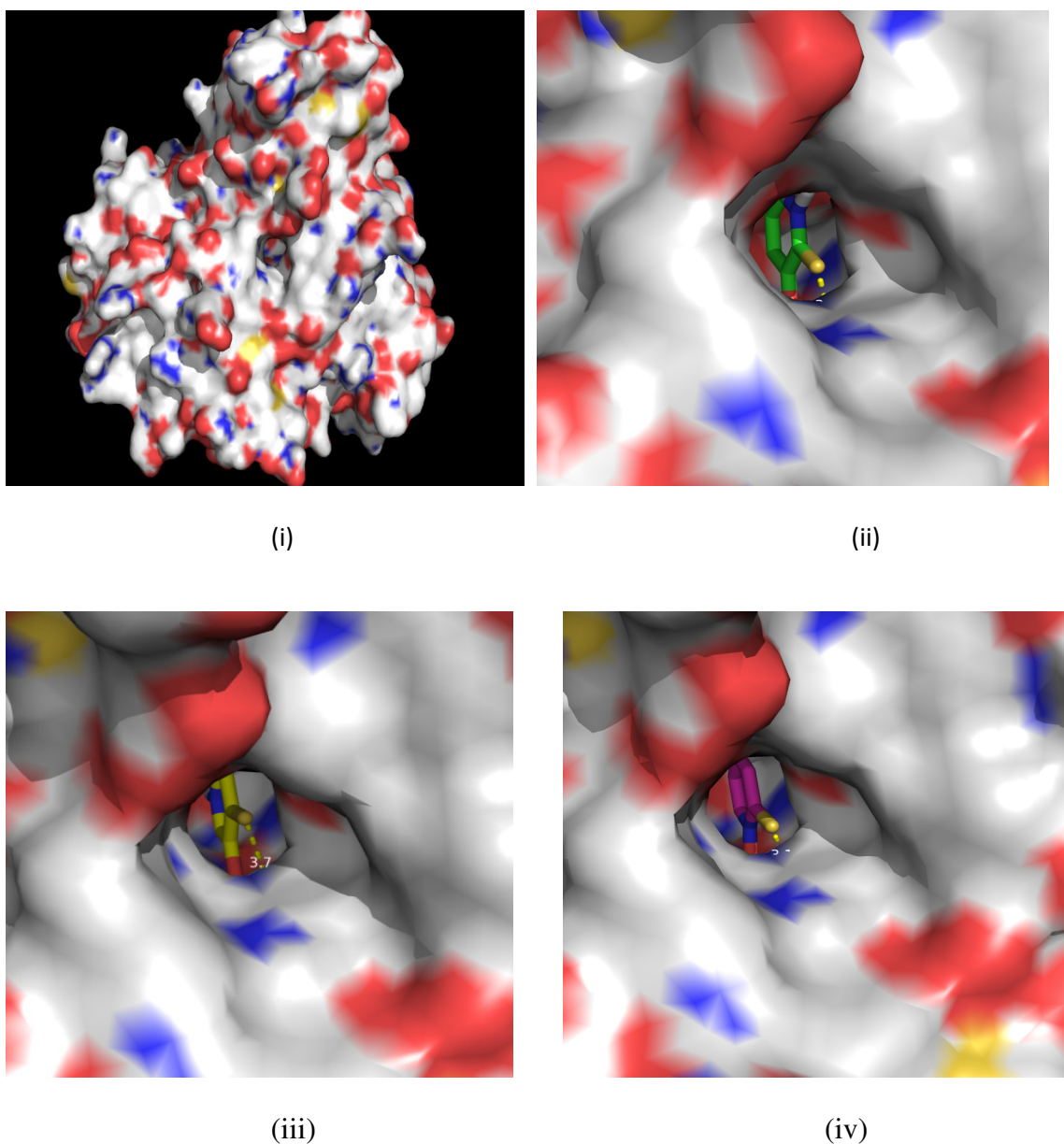
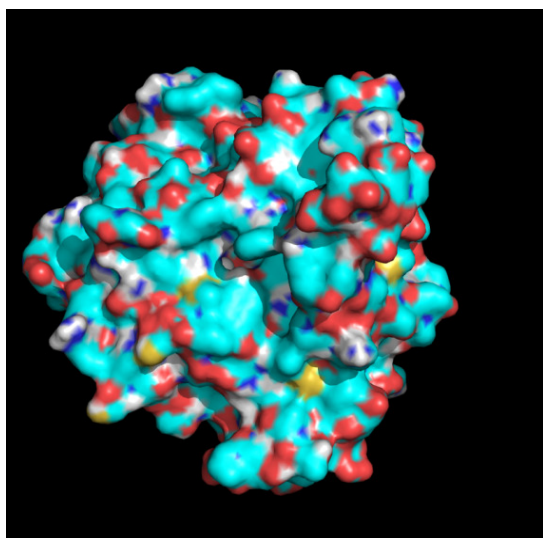
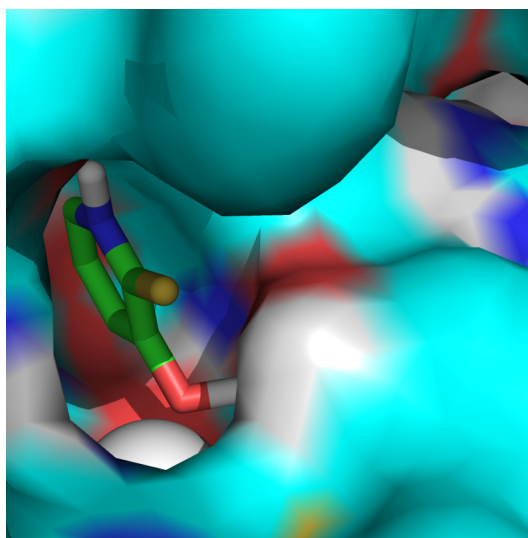


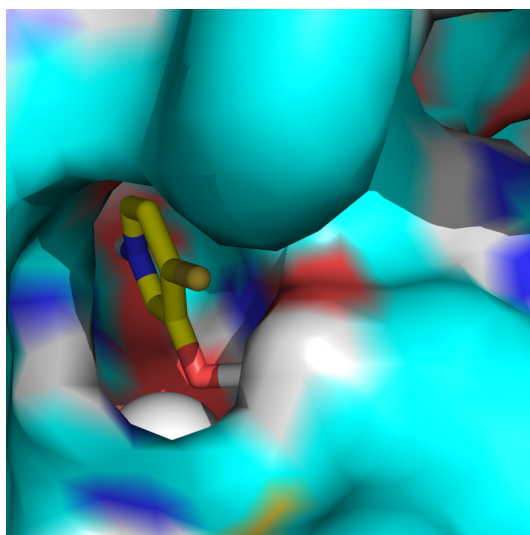
Figure 5-4. (i) HDAC1 active site (homology model); (ii) Docked fragment 3-hydroxypyridin-2-thiones (3-HPT; **a**) against HDAC1; (iii) Docked fragment 3-hydroxypyridin-4-thiones (**b**) against HDAC1; (iv) Docked fragment 1-hydroxypyridin-2-thione (**c**) against HDAC1.



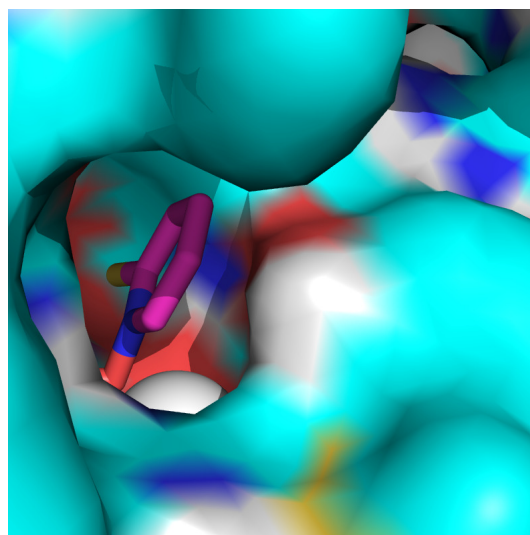
(i)



(ii)



(iii)



(iv)

Figure 5-5. (i) HDAC8 active site (homology model); (ii) Docked fragment 3-hydroxypyridin-2-thiones (**a**) against HDAC8; **Figure 5-6.** (iii) Docked fragment 3-hydroxypyridin-4-thiones (**b**) against HDAC8; (iv) Docked fragment 1-hydroxypyridin-2-thione (**c**) against HDAC8.

To further verify our docking results, we subjected these fragments to HDAC inhibition assay to determine their effect on enzyme activity. HDAC inhibition was assayed initially using cell free assay (*Fluor de Lys*) as previously described.⁴² However

there were discrepancies in data obtained when we tried to reproduce the data using fluorescence based analysis (data not shown). There is precedence that fluorescently labeled substrates can perturb enzyme activity and the effect of inhibitors. Trypsin inhibition can also lead to false positive signal. In one example, the discovery that resveratrol and various analogues activate the deacetylase sirtuin 1 (SIRT1) was found to be an artifact of the fluorescent assay.⁴³ Indeed, many recommended *Fluor de Lys* substrates have been shown not to be active toward their corresponding enzymes, including HDAC8, in the absence of fluorophore.^{44,45} Additionally, these fragments are highly colored solids and might lead to false positive signal. Mindful of these observations, we sought to validate these data using the label-free SAMDI (self-assembled monolayers for MALDI) mass spectrometry assay.⁴⁶

The SAMDI technique, wherein self-assembled monolayers (SAM) of alkanethiolates on gold are analyzed by matrix assisted laser desorption/ionization (MALDI) mass spectrometry, has been used to characterize many biochemical activities, including the deacetylase enzyme family.⁴⁵⁻⁴⁷ The SAMDI assay is also amenable to analysis of homogeneous reactions, as the substrates are immobilized to the SAMs after the reaction has been terminated.⁴⁸ We employed the SAMDI technique to measure the inhibition constant (K_i) of fragments against HDAC1 and HDAC8 using a previously identified preferred HDAC substrate.⁴⁵ Interestingly, 3-hydroxypyridin-2-one was found to be inactive against the two HDAC isoforms. However, thione derivative showed low micromolar IC_{50} values against the HDAC8 isoform and inactive against HDAC1 (Table 5-1). After this promising result which showed a glimpse of isoform selectivity, we focused on building the lead 3-HPT from N-1 nitrogen to investigate if the linker

substitution at this position can be tolerated. Accordingly, we substituted the 3-HPT *N*-1 hydrogen with methyl group and docked the resulting 1-methyl-3-hydroxypyridin-2-thione against HDAC8. We focused on HDAC8 due to the observed evidence of compounds selectivity for this HDAC isoform (Table 5-1).

Table 5-1. 3-HPT fragment activities*

Compounds	IC ₅₀ (nM)	
	HDAC1	HDAC8
	NI	NI
	32%	3650

*Activities determined by SAMDI analysis by James Kornacki from Dr. Milan Mrksich lab at University of Chicago. SAHA is used for a positive control.

NI – No significant Inhibition (below 20% Inhibition)

% inhibitions of the compounds at 10 μ M are given if the IC₅₀ was above 10 μ M.

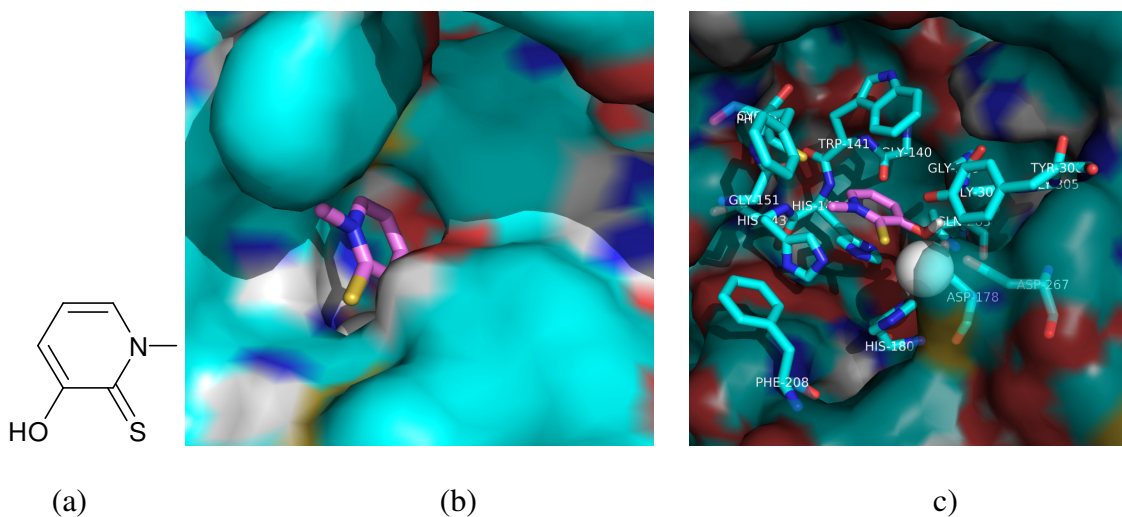


Figure 5-7 (a) Structure of 1-methyl-3-hydroxypyridin-2-thiones (a) Surface view of docked orientation 1-methyl-3-hydroxypyridin-2-thiones at HDAC8; (b) Amino acid residues around docked fragment within 5 Å distance.

Substitution with *N*-methyl group didn't alter the docked pose of 3-HPT fragment (Figure 5-7). We analyzed amino acid residues surrounding the docked structure of 1-methyl-3-hydroxypyridin-2-thiones to further refine our design of the linker region. The 12 Å hydrophobic tunnel which joins the ZBG active site to the surface consists of amino acid (AA) residues Phe152, Phe208, Tyr306, Trp141, His180, Asp267. Moreover, hydrophobic aromatic AA residues Phe152, Phe208, Tyr306, Trp141 are placed in close proximity of *N*-methyl group of docked 1-methyl-3-hydroxypyridin-2-thiones structure (Figure 5-7c). Therefore, we hypothesized that aromatic linkers such as phenyl, biphenyl or triazole rings might contribute to pi-stacking interactions with Phe152, Phe208 thereby reduce binding energy and improve compounds' affinity for HDAC8. Based on this rationale, we proposed the following structures and studied their orientation at the active site by performing another set of docking experiments.

Figure 5-8. Proposed fragments for development of lead against HDAC8 selective inhibitors.

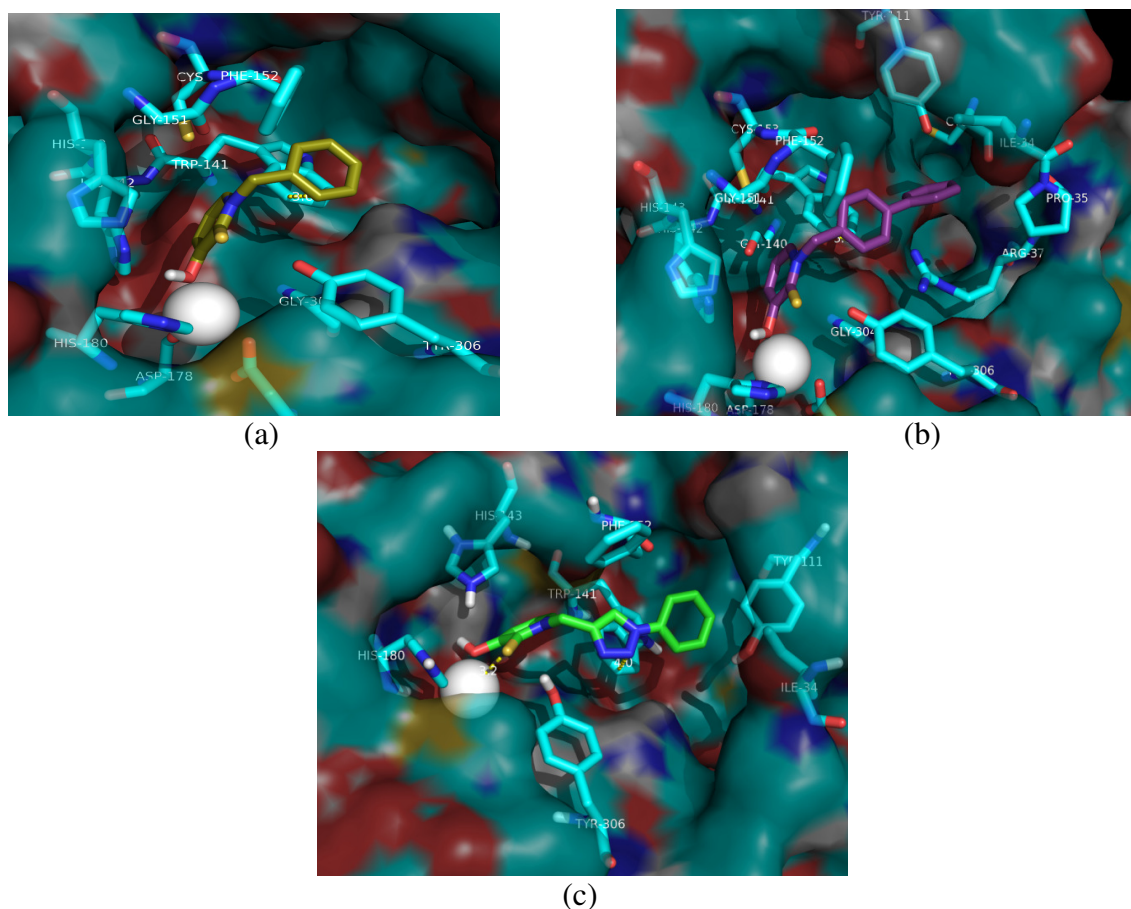


Figure 5-9. (a) Docked structure of **1** against HDAC8 (b) Docked structure of **2** against HDAC8. (c) Docked structure of **3** against HDAC8.

Analysis of the docked poses of **1**, **2** and **3** revealed that indeed the phenyl ring (Figure 5-9) and the triazole group made fruitful pi-stacking interaction with aromatic AA Trp141. In compound **2** containing a biphenyl substitution, the 1st phenyl ring adjacent to ZBG maintained its pi-stacking interaction with Trp141 and 2nd phenyl ring orients in deep subpocket near active site, albeit without any significant interaction (Figure 5-9 b). A closer look at docked structure **2** revealed that Pro35, Ile34, Cys28, Tyr111 are present surrounding 2nd phenyl ring compound **2** (Figure 5-10). Therefore we envisioned that the substitution on the 2nd phenyl ring with hydrogen bonding or hydrophobic groups might lower binding energy and improve potency.

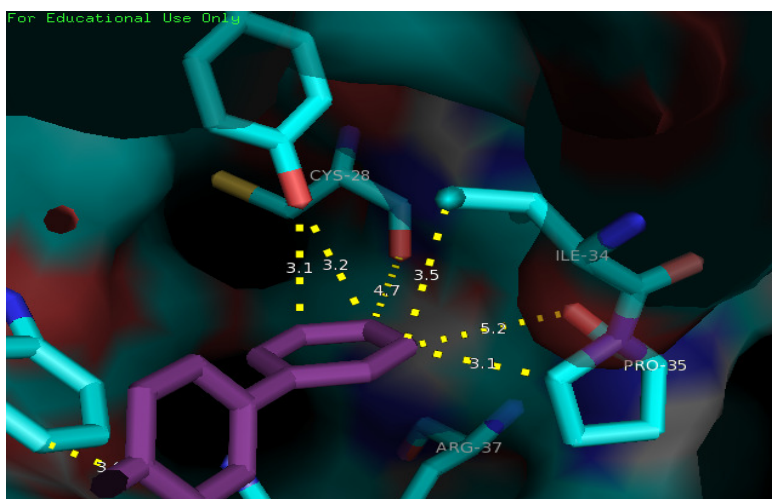


Figure 5-10. AA residues surrounding 2nd phenyl ring of docked compound against HDAC8.

To investigate the effect of incorporation of functional groups on the 2nd phenyl group of compound **2** and thus to flush out rest of SAR we proposed compounds as shown in Figure 5-11. The proposed modifications can take part in hydrogen bonding as well as hydrophobic interactions with AA residues surrounding the 2nd phenyl group of **2**.

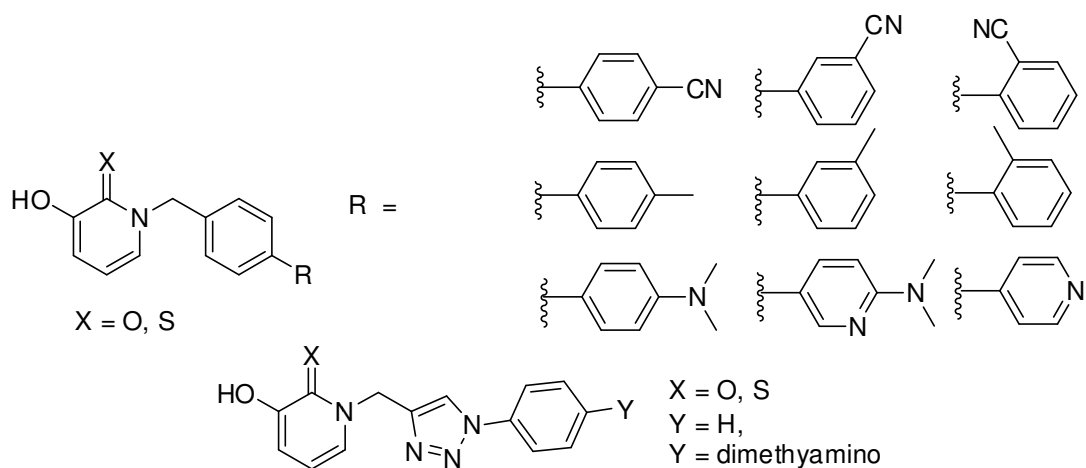


Figure 5-11. Proposed 1st generation compounds.

5.4 Synthesis of 1st Generation Novel HDACi

Initial fragments **5a-5c** and **7a-7c** were synthesized within 2 to 3 steps as indicated in Figure 4-12. Synthesis involved coupling of methyl iodide and corresponding benzyl bromides with commercially available 3-methoxypyridin-2-one to give the *O*-methyl protected intermediates **4a-4c**. Thione intermediates were synthesized from their carbonyl precursors using lawesson's reagent chemistry.⁴⁹ Finally, deprotection of *O*-methyl group by lewis acid BBr₃ gave the desired products **5a-5c** and **7a-7c**.

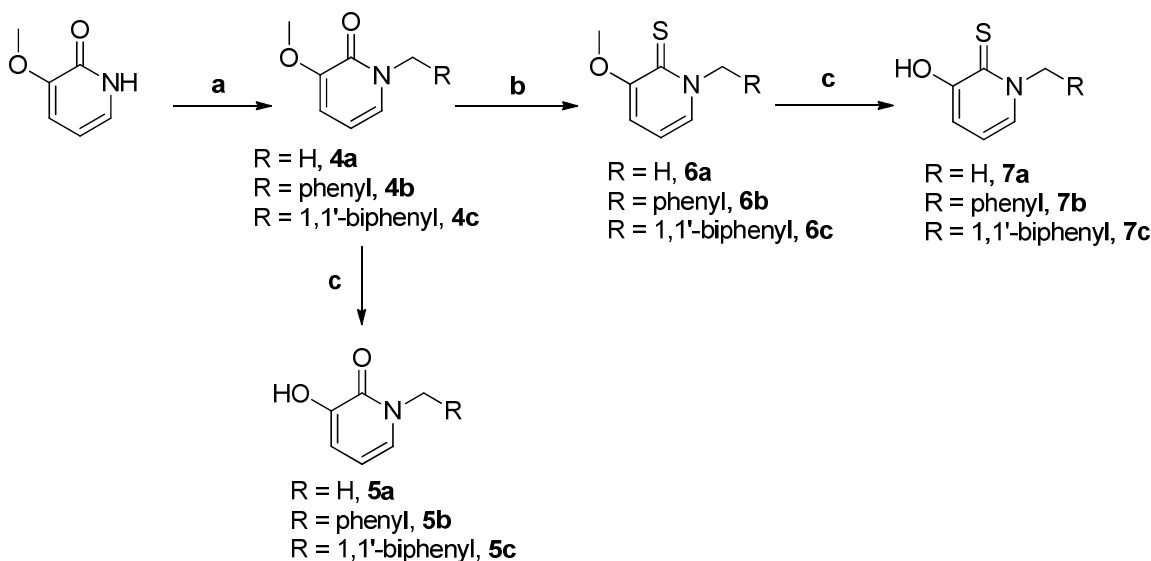


Figure 5-12. Synthesis of the 3-DHP based ZBG HDACi. For **4a** a) MeI, KOH, MeOH; For **4b**, **4c**; a) R-CH₂Br, K₂CO₃, DMF, 100 °C. b) Lawesson's reagent, toluene, reflux. c) BBr₃, CH₂Cl₂.

The proposed routes to the biphenyl fragments require crucial intermediate **8** which was obtained by coupling of 4-bromobenzylbromide with 3-methoxypyridin-2-ones (Figure 5-13). Standard Suzuki coupling⁵⁰ with corresponding boronic acids gave intermediates **9a-9i**. Similarly, Lawesson's chemistry⁴⁹ was used to prepare thione intermediates. Deprotection of the *O*-methyl group yielded the final biphenyl compounds **11a-11i** and **12a-12i** (Figure 5-13). Synthesis of triazole based compounds **16a-16b** and

17a-17b is shown in Figure 5-14. It involves the intermediacy of terminal alkyne **13**, by *N*-alkylation reaction of 3-methoxypyridin-2-one with propargyl bromide. Cu(I)-catalyzed Huisgen cycloaddition⁵¹ gave the cyclized product **14a-14b**. Lawesson's chemistry was again used to gain access to thiolated analogs. Deprotection of *O*-methyl group was achieved by reaction with BBr₃ (Figure 5-14).

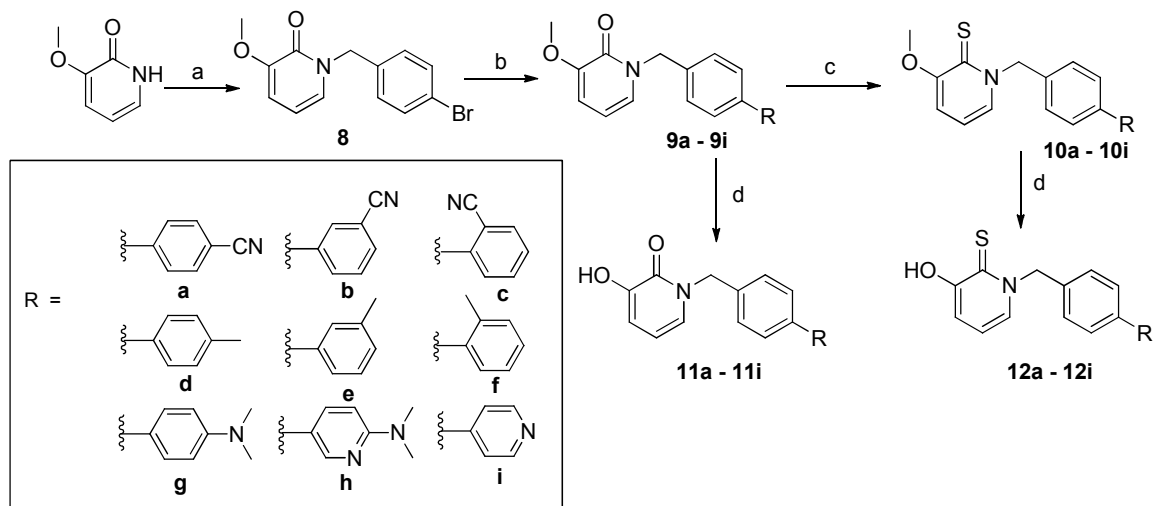


Figure 5-13. Synthesis of the 3-DHP based ZBG HDACi - I. (a) 4-bromobenzylbromide, K₂CO₃, THF, reflux b) R-B(OH)₂, Pd(PPh₃)₄, K₂CO₃, toluene:ethanol:H₂O; 80 °C c) Lawesson's reagent, toluene, reflux; d) BBr₃, CH₂Cl₂

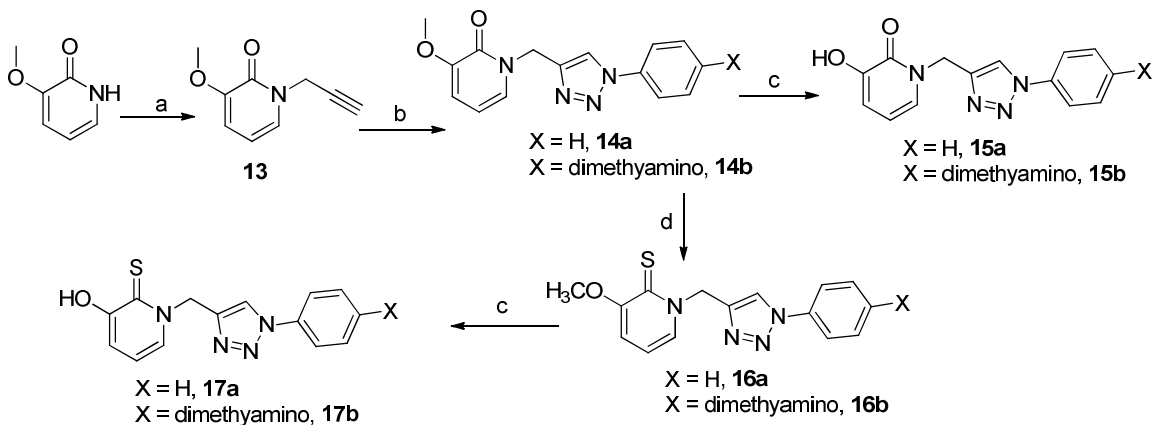


Figure 5-14. Synthesis of the 3-DHP based ZBG HDACi - II. (a) propargyl bromide, K₂CO₃, THF, reflux b) azido intermediates (phenyl azide, 4-azido-*N,N*-dimethylaniline), CuI, DIPEA, THF; c) BBr₃, CH₂Cl₂; d) Lawesson's reagent, Toluene, reflux

5.5 *In vitro* HDAC Inhibition of 1st Generation HDACi

With the compounds in hand, we tested them against SAMDI analysis as previously described.⁴⁶ There is clear distinction in the HDAC inhibition activities of the carbonyl and thione analogs with the latter showing higher potency (Table 5-2). The enhanced anti-HDAC activity of the thione analogs could be attributed to thiophilicity which favors Zn²⁺ binding.³¹ Most of the compounds in this series showed distinct selectivity towards HDAC8 compared to HDAC1. A head to head comparison of HDAC8 inhibition showed that compound **7b** which contains one phenyl ring has better activity than biphenyl compound **7c**. This observation is consistent with the docking result as the 2nd phenyl ring doesn't take part in any meaningful interactions with residues on HDAC8 outer rim (Figure 5-9). However, replacement of the 2nd phenyl ring of compound **7c** with a 4-pyridyl ring results in better activity (**7c** IC₅₀ = 4.28 μM Vs **12i** IC₅₀ = 2.78 μM against HDAC8) indicating that para-pyridine substitution contributed to lowering binding energy and hence better interaction than **7c** with AA residues on surface. Substitution of 2nd phenyl ring with electron donating *N,N*-dimethylamino group at para position (in **12g**) has similar effect as the para-pyridine substitution (in **12i**) (Table 5-2). However combination of pyridine and *N,N*-dimethylamine substitutions in compound **12h** is not comparable with HDAC8 inhibition. Incorporation of methyl group, another electron donating group, at the para position (in **12d**) resulted in the best IC₅₀ value (800 nM) in this series (Table 5-2). However *meta*- (compound **12e**) and *ortho*- (compound **12f**) methyl substitution did not surpass the activity of **12d**. This trend in HDAC8 inhibition did not hold for electron withdrawing cyano group. *Meta*- and *ortho*- substituted compounds **12b** and **12c** respectively showed better potency when

compared to *para*- substituted compound **12a**. Interestingly triazole substituted compounds **17a** was found to be more active than corresponding biphenyl compound **7c**. However a *para*-*N,N*-dimethylamino substitution of **17a** which resulted in compound **17b** was not beneficial. This is contrary to the effect of a similar substitution on the biphenyl compound (Table 5-2, comparing **7c** and **12g**; **17a** and **17b**).

Table 5-2. *In-vitro* HDAC inhibition of 1st generation HDACi

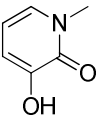
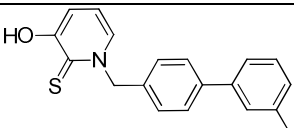
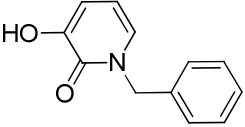
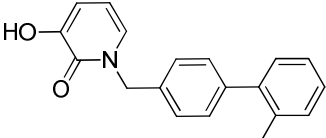
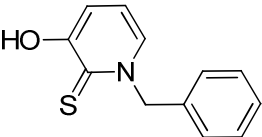
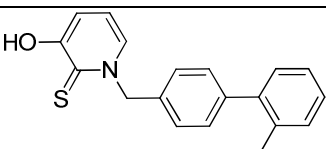
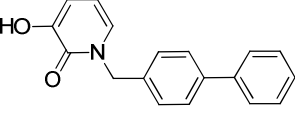
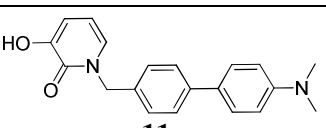
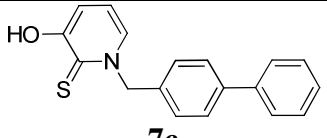
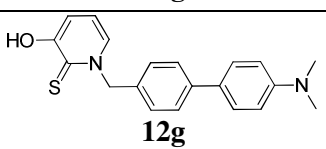
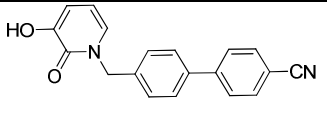
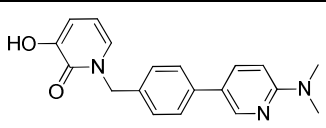
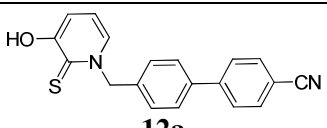
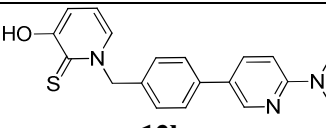
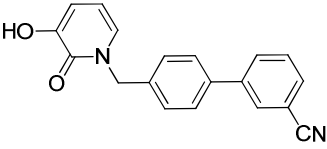
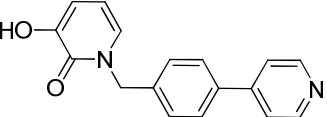
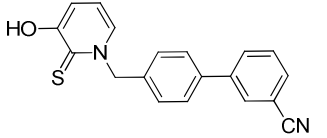
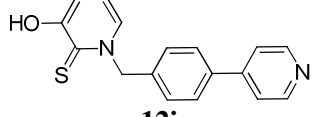
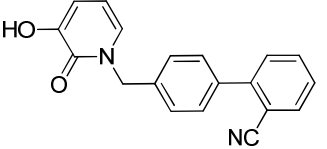
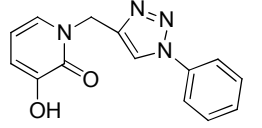
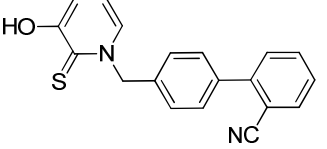
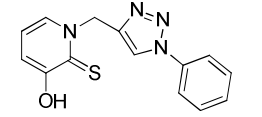
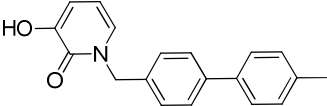
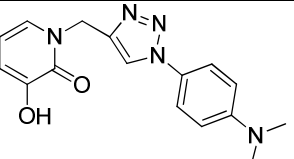
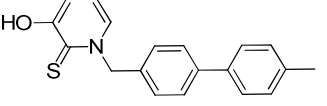
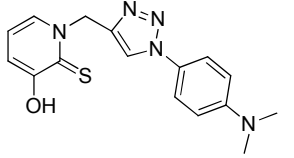
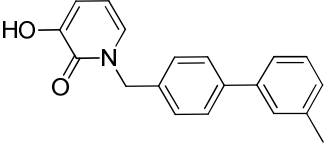
COMPOUNDS	IC ₅₀ (nM)*		COMPOUNDS	IC ₅₀ (nM)*	
	HDAC1	HDAC8		HDAC1	HDAC8
 5a	NI	8%	 12e	NI	2496±1180
 5b	NI	8%	 11f	NI	9%
 7b	NI	1272±200	 12f	NI	3105±1649
 5c	NI	8%	 11g	NI	35%
 7c	NI	4283±1548	 12g	NI	2858±944
 11a	NI	16%	 11h	NI	37%
 12a	NI	2075±459	 12h	NI	34%

Table 5-2 continued.

 <p>11b</p>	NI	9%	 <p>11i</p>	NI	16%
 <p>12b</p>	NI	1701±717	 <p>12i</p>	NI	2780±323
 <p>11c</p>	NI	9%	 <p>15a</p>	NI	17%
 <p>12c</p>	NI	1907±771	 <p>17a</p>	NI	1570±1067
 <p>11d</p>	NI	25%	 <p>15b</p>	NI	8%
 <p>12d</p>	NI	800±304	 <p>17b</p>	NI	1868±723
 <p>11e</p>	NI	NI	SAHA	38+/- 2	232±19

SAHA is used for a positive control.

NI – No significant Inhibition (below 20% Inhibition)

% inhibitions of the compounds at 10 μ M are given if the IC₅₀ was above 10 μ M.

5.6 Further Molecular Docking Analysis on 1st generation HDACi

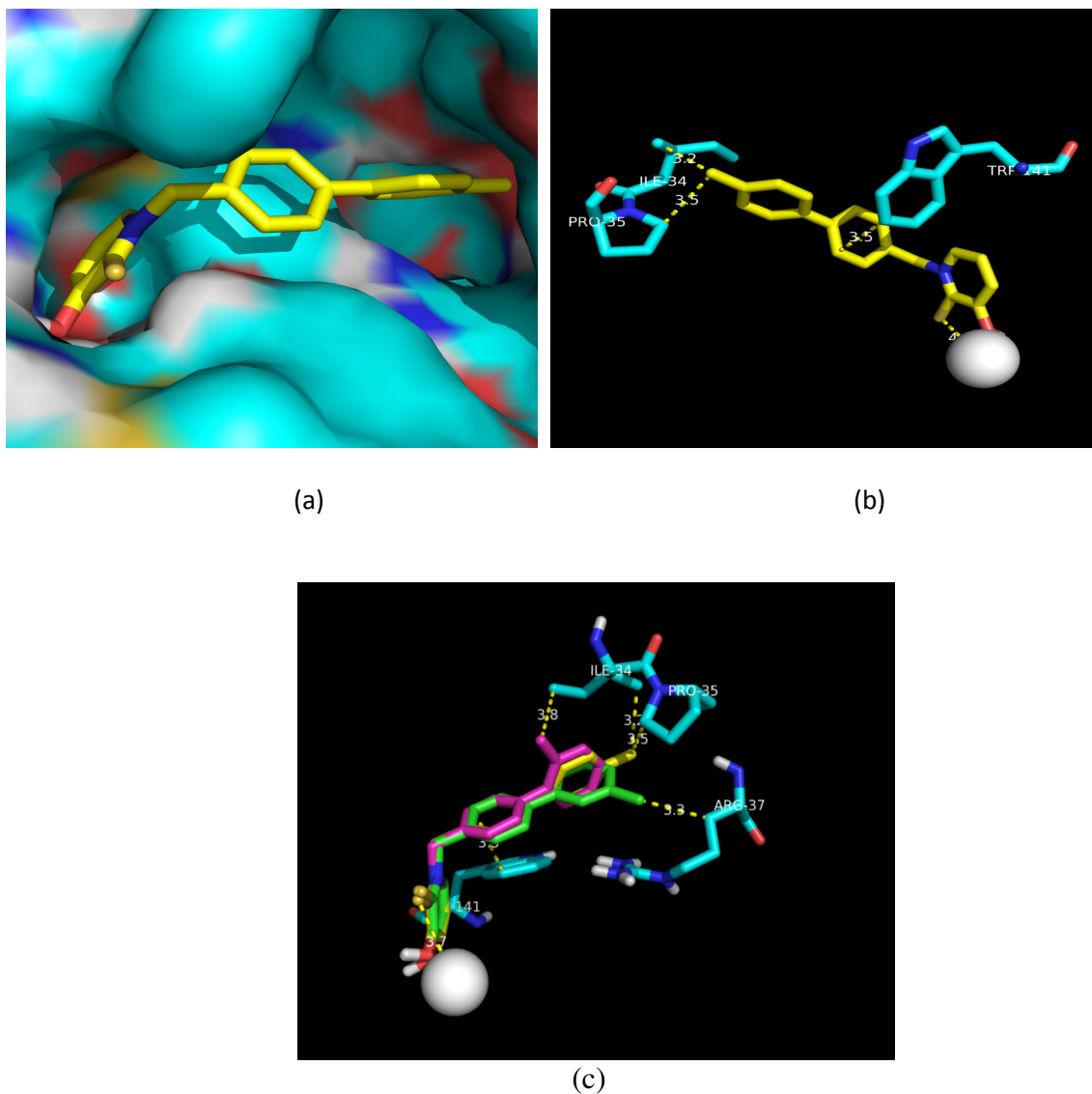


Figure 5-15. (a) Docked structure of **12d** against HDAC8 (b) Docked structure of **12d** interacting with key AA residues near Zn^{2+} active site (c) Overlap of *ortho*-, *meta*- and *para*-methyl substituted compounds (comparing **12d**, **12e**, **12f**)

Most of the biphenyl compounds with 3-HPT as ZBG shows biological activity in the range of 0.8-4 μM . We decided to dock representative structure of 1st generation compound to gain better understanding in binding mode of these compounds.

We chose to dock compound **12d-f** and **12a-c** which showed substitution pattern dependent HDAC8 inhibition activities. Results for this experiment are shown in Figure 5-15. Interestingly, the head groups of all these inhibitors are directed towards a second subpocket which is minimally solvent exposed near the zinc active site pocket. AA residues near the aromatic head group formed a second subpocket consisting of hydrophobic residues such as ILE34 and PRO35 (see Figure 5-15b) which interact with *para*-methyl substitution on head group of compound **12d**. However when methyl group substitution moves to *meta* position, there is lost interaction with Ile34 and Pro35, however it still manages a hydrophobic interaction with Arg37 (Figure 5-15c). Ortho substitution doesn't indulge in any hydrophobic interactions similar to *para* and *meta* position. However, *ortho* position manages to interact with ILE34. Therefore movement of methyl substitution on aromatic head group from *para* to *meta* to *ortho*, resulted in drop off in the activity.

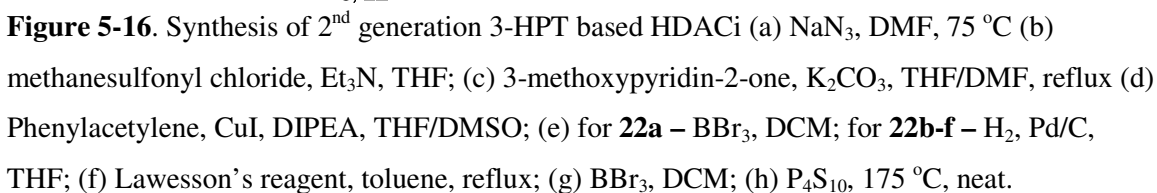
5.7 Design of 2nd Generation 3-HPT based HDACi

An important conclusion from the experiments described above is that isoform selectivity in favor of HDAC8 over HDAC1 was achieved by using heterocyclic aromatic ZBG. This finding provides 3-hydroxypyridin-2-thione as an alternative which might address the pharmacokinetic issues of hydroxamic acids. However there is room for the enhancement of compound potency since the best compound is still less active compared to prototypical hydroxamate based HDACi. Towards improving potency, we further explored the SAR around the linker region. The common linker moiety of HDACi consists of aliphatic methylene group which traverses the hydrophobic tunnel to present the cap group on surface. We investigated the consequences of the substitution of the

aromatic linker with methylene group on the HDAC inhibition activities of these 3-HPT HDACi. We synthesized and tested compounds with variable methylene group linker length –from one (as seen in compound **17a**) to seven (as seen in SAHA).

5.8 Synthesis of 2nd generation 3-HPT based HDACi

Synthesis of 2nd generation 3-HPT based compounds is depicted in Figure 5-16. The crucial azidoalkyl methanesulfonates are synthesized in two steps. The reaction of corresponding bromoalkanols with sodium azide furnished azidoalkanols **18a-18f** which were subsequently mesylated to give methanesulfonate intermediates **19a-19f** in almost quantitative yields. As described earlier, *N*-alkylation of *O*-methyl or *O*-benzyl protected 3-hydroxypyridin-2-one with the mesylate intermediates gave azido intermediates **20a-20f** in moderate to good yields. Aromatic surface recognition cap group was linked to these azido intermediates via 1,2,3-triazole ring. Cu(I)-catalyzed Huisgen cycloaddition⁵¹ between phenylacetylene and azido intermediates **20a-20f**, followed by deprotection of methyl ether by Lewis acid BBr₃ furnished the desired compounds in good to excellent yields. All the higher linker thione compounds were synthesized from their carbonyl counterparts by using P₄S₁₀ chemistry as previously reported.⁵² However 2 methylene linker compound **22a** did not tolerate the rigorous temperature conditions and was degraded to complex reaction mixture within 2 hrs. Therefore we modified the synthetic scheme as shown in Figure 5-16. Incorporation of *O*-methyl protected intermediate **21a** allowed us to use milder Lawesson's reaction chemistry⁴⁹ to gain access to final thione compound **24** (Figure 5-16).



5.9 *In vitro* HDAC Inhibition of 2nd Generation 3-HPT based HDACi

Activities of 2nd generation compounds also were consistent for HDAC8 selectivity over HDAC1 and thione compounds always outperformed their corresponding carbonyl compounds. For thione analogs, increase in methylene spacer by 1-carbon to compound **17a** shows significant loss of activity (comparing **17a** and **24** in Table 5-2 and Table 5-3). Gradual increase in methylene spacer length from 3-carbon to 5-carbon shows improvement in activity with 5-carbon linker shows optimum activity (compound **25d**, IC₅₀ = 917 nM). However, one additional carbon linker again results in drop of activity with 7-fold difference (Table 5-3; comparing **25d** and **25e**). Interestingly, 7-carbon linker compound **25f** showed superior activity than **25e** however it still didn't surpass the activity of **25d**.

This SAR study established that 5-carbon methylene chain is optimum linker in HDACi design containing 3-HPT as ZBG. In addition to five methylene spacer, one and seven methylene spacer showed comparable activities and should be viable leads as well.

Table 5-3. *In vitro* HDAC Inhibition of 2nd Generation Compounds

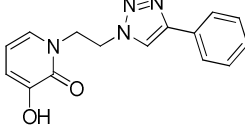
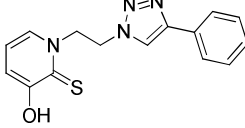
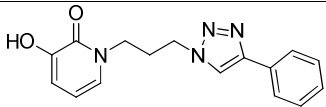
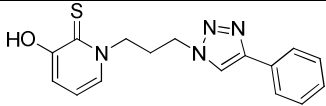
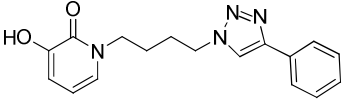
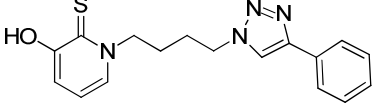
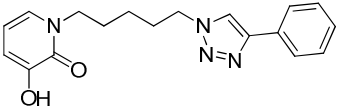
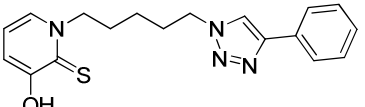
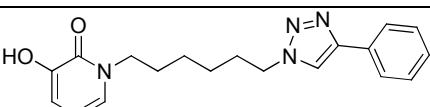
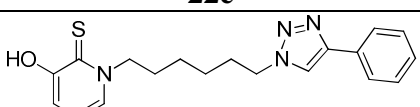
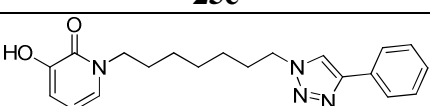
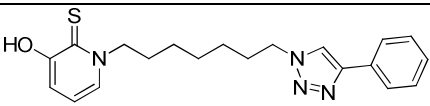
COMPOUNDS	IC ₅₀ (nM)	
	HDAC1	HDAC8
 22a	12%	15%
 24	21%	56%

Table 5-3 continued.

 <p>22b</p>	8%	47%
 <p>25b</p>	27%	63%
 <p>22c</p>	15%	10%
 <p>25c</p>	ND	3303±260
 <p>22d</p>	43%	30%
 <p>25d</p>	30%	917+/-139
 <p>22e</p>	12%	5%
 <p>25e</p>	23%	6791±910
 <p>22f</p>	2%	42%
 <p>25f</p>	35%	1377±205
SAHA	38+/- 2	232±19

SAHA is used for a positive control.

NI – No significant Inhibition (below 20% Inhibition)

% inhibitions of the compounds at 10 μ M are given if the IC₅₀ was above 10 μ M.

5.10 Design of 3rd Generation 3-HPT based HDACi

As demonstrated in section 5.9, we have established that 5-carbon methylene spacer traverses hydrophobic tunnel optimally to present 3-HPT in the vicinity of the active site zinc for tighter binding. We then undertook SAR study on surface recognition cap group with specific focus on the 5-carbon methylene spacer in the hope that such exercise will furnish more potent compounds. Based on our previous study on SAR studies on triazole based simple HDAC compounds⁴² and on 1st generation 3-HPT based HDACi, we proposed a distinct set of cap groups which could shed light on cap group orientation at the enzyme orientation (Figure 5-17).

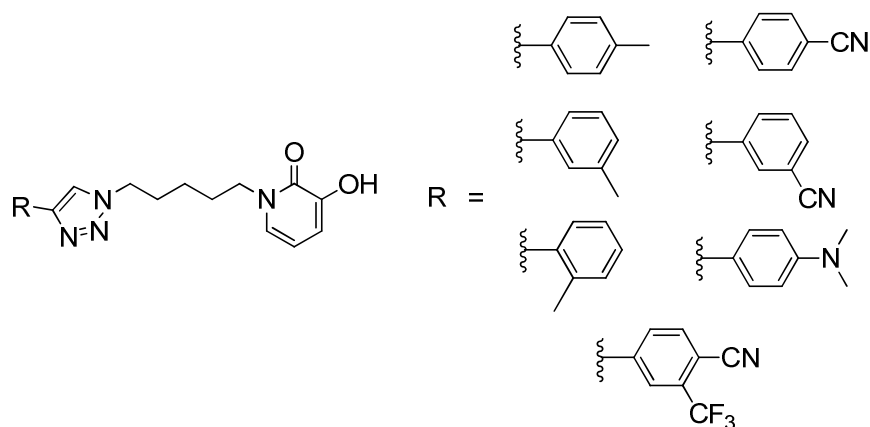


Figure 5-17. Design of 3rd Generation 3-HPT-based HDACi

5.11 Synthesis of 3rd Generation 3-HPT based HDACi

The synthetic route to the 3rd generation compounds is identical to that described for the 2nd generation compounds. The new surface cap recognition cap groups were coupled to ZBG modified linker using Cu(I)-catalyzed Huisgen cycloaddition⁵¹ to give intermediates in good to excellent yields. As described earlier, Lawessons' chemistry⁴⁹ followed by deprotection with BBr₃ resulted in desired compounds **29a-29g** and **30a-30g**.

Carbonyl derivatives were also synthesized using similar deprotection chemistry (Figure 5-18).

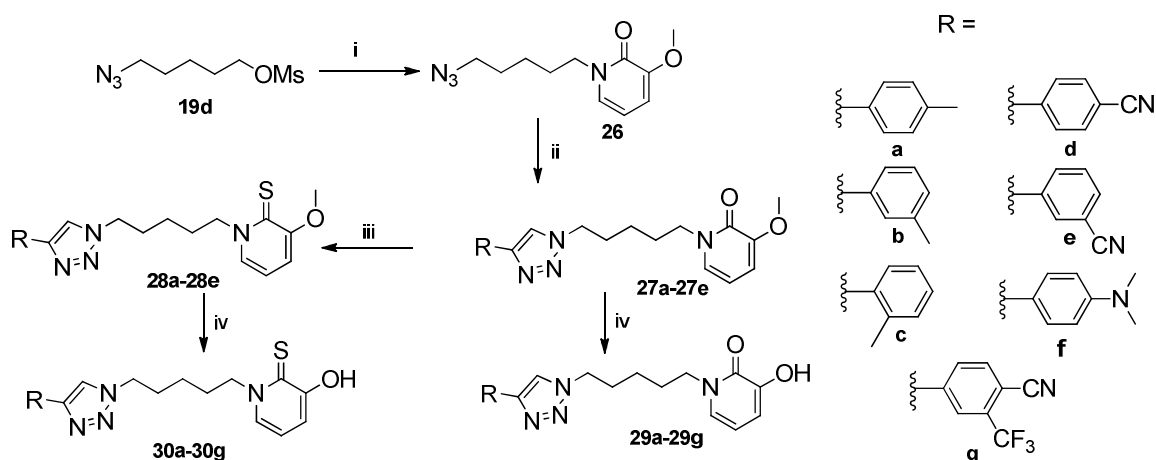


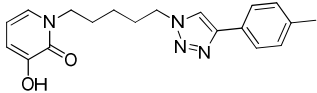
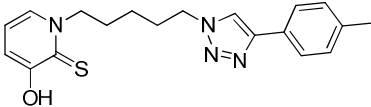
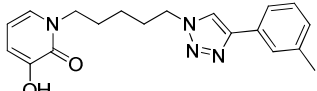
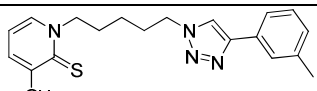
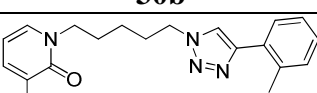
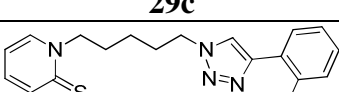
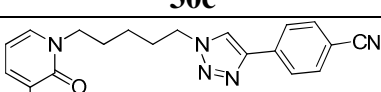
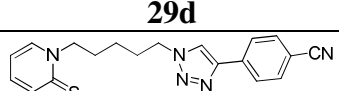
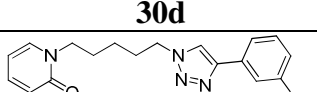
Figure 5-18. Synthesis of 3rd Generation HDACi i) 3-methoxypyridin-2-one, K₂CO₃, THF, reflux; ii) R-alkynes, CuI, DIPEA, DMSO:THF; iii) Lawesson's reagent, Toluene, reflux; iv) BBr₃, DCM. Compounds **26**, **27a-27e** synthesized by Quaovi Sojdi. Included here to show complete synthetic scheme.

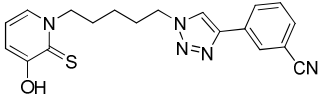
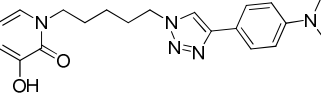
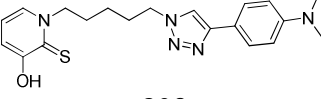
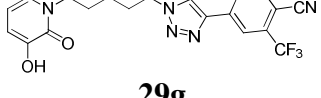
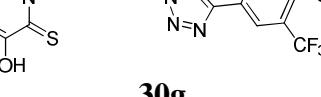
5.12 *In Vitro* HDAC inhibition of 3rd Generation 3-HPT based HDACi

The 3rd generation compounds in 3-HPT series were tested against HDAC1 & HDAC8 using the label-free SAMDI mass spectrometry assay as previously described.⁴⁶ The trend in HDAC inhibition activity was very similar to that observed in the early generation compounds with the thione compounds showing superior activity compared to the carbonyl derivatives. In contrast to what was obtained for the 2nd generation compounds, the results from this study indicate that substitution on the phenyl ring as cap group is not helpful for anti-HDAC activity. Almost all of the cap groups other than simple phenyl ring failed to improve compound potency. In order to gain additional insight into binding interactions of 2nd and 3rd generation of compounds at the enzyme

active site, we performed docking analyses on the best compounds in this series against HDAC8.

Table 5-4. *In Vitro* HDAC inhibition of 3rd Generation 3-HPT based HDACi^a

COMPOUNDS	IC ₅₀ (nM)	
	HDAC1	HDAC8
 29a	66%	15%
 30a	31%	2533+/-823
 29b	88%	NI
 30b	19%	1660+/-416
 29c	NT	4%
 30c	NT	2402 +/- 263
 29d	70%	26%
 30d	33%	1465+/-217
 29e	71%	NI

 <p>30e</p>	ND	2831+/-520
 <p>29f</p>	59%	28%
 <p>30f</p>	28%	1482+/-389
 <p>29g</p>	71%	14%
 <p>30g</p>	55%	2258+/-1005
SAHA	38+/- 2	232±19

SAHA is used for a positive control.

NI – No significant Inhibition (below 20% Inhibition)

% inhibitions of the compounds at 10 μ M are given if the IC₅₀ was above 10 μ M.

^aQuaovi Sodji contributed partly for synthesis of **29a-29g** and **30a-30g**.

5.13 Molecular Docking Analysis of 3rd Generation 3-HPT based HDACi

Compound **25d** adopts a docked pose at HDAC8 active site which presents the phenyl cap group into a deep, non-solvent exposed hydrophobic pocket (Figure 5-19), while the 5-carbon methylene spacer optimally fills the connecting the hydrophobic pocket to the Zn²⁺ active site. The ideal spacer length of the 5-carbon methylene group facilitates a proper presentation off the 3-HPT ZBG to the active site Zn²⁺. The deep pocket where the phenyl ring orients consists of Tyr111, Ala112, Leu155, Tyr154 AA residues. Two tyrosine residues are within 3.5 Å of the phenyl cap group of compound **25d** and are ideally suited for pi-stacking interaction. Tyr154 is expected to have stronger

pi-stacking interaction since plane of its ring is parallel to the phenyl cap group of compound **25d**. However, Tyr111 will contribute less to the pi-stacking interaction because the edge of its phenol ring is oriented toward the plane of the cap group **25d**. Other AA residues such as Leu115 and Ala112 are within 3.5 Å and contribute to the overall hydrophobicity of the pocket into which the phenyl cap group of compound **25d** is bound (Figure4-19). This might lead to lower binding energy conformation and hence better IC₅₀ value for this 2nd generation compound.

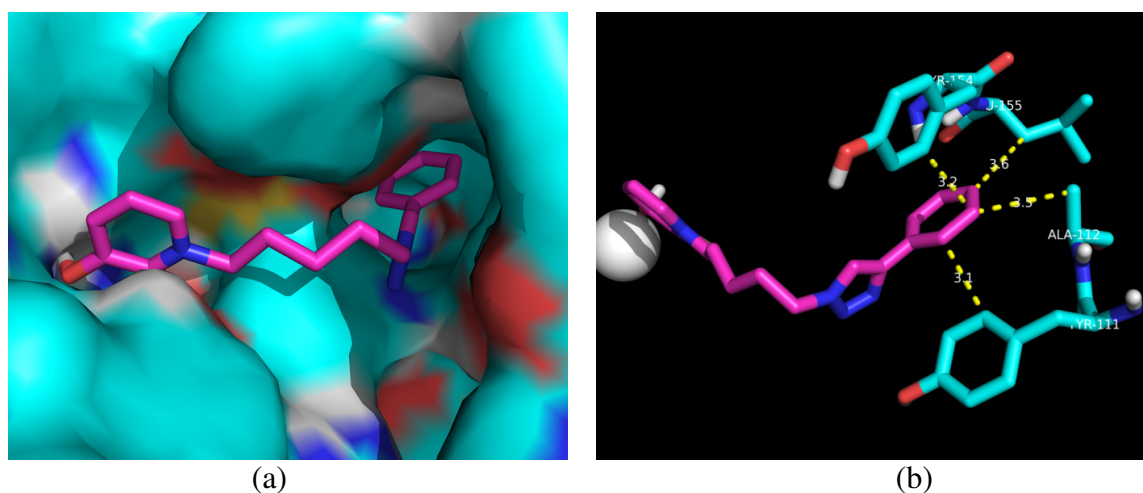


Figure 5-19. (a) Docked structure of **25d** against HDAC8 (b) Docked structure of **25d** against HDAC8 showing key AA residues forming deep pocket around phenyl cap group.

Figure 5-20 shows an overlay of the docked structures of **25d** and six methylene linker compound **25e**. Both compounds bind to the same pocket and adopt almost the similar orientation, except for slight kinks, at the methylene groups. The major difference between the docked poses of **25d** and **25e** is at their phenyl cap group which is slightly pushed outside of pi-stacking interaction with Tyr154 in compound **25e** and thus

abolishing this important interaction. This could be the reason that there is almost 7-fold activity difference between **25d** and **25e**.

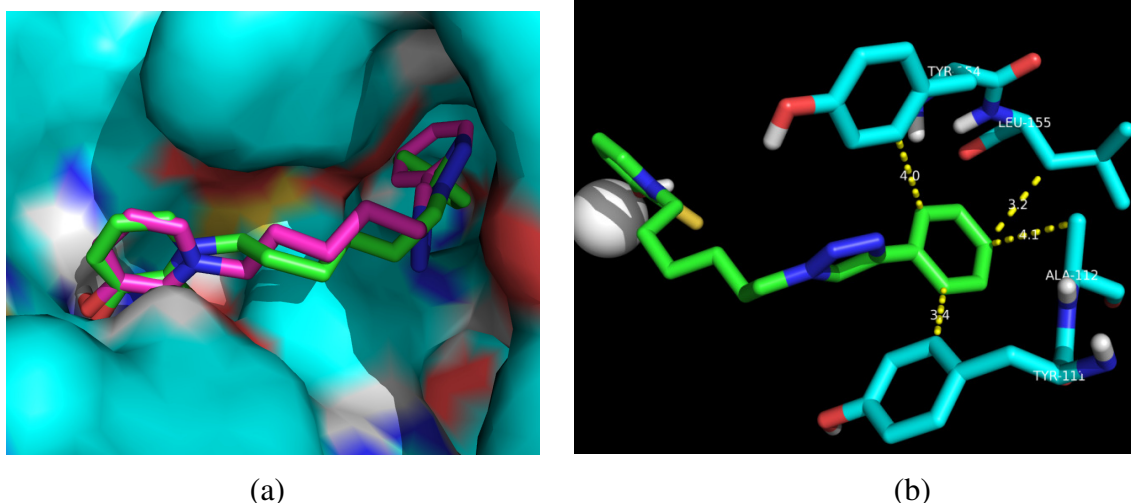


Figure 5-20. (a) Overlay of docked structures of **25d** and **25e**; (b) Docked structure of **25e** against HDAC8 showing key AA residues forming deep pocket around phenyl cap group.

Similarly, compound **30d** binds to same pocket as discussed earlier (Figure 5-21). However para-cyano substitution on cap group **30d** causes its phenyl ring to be pushed out of the binding pocket seen for compound **25d** (Figure 5-20). Though two tyrosine residues are not far away from the phenyl cap group (~ 3.2 Å), their orientation is not optimum for pi-stacking interaction with the phenyl group of **30d**. Moreover, hydrophobic interactions with Ala112 and Leu155 are completely lost. However, there is a compensatory pi-stacking interaction with Trp141 which may explain the better activity for compound **30d** relative to **25e**.

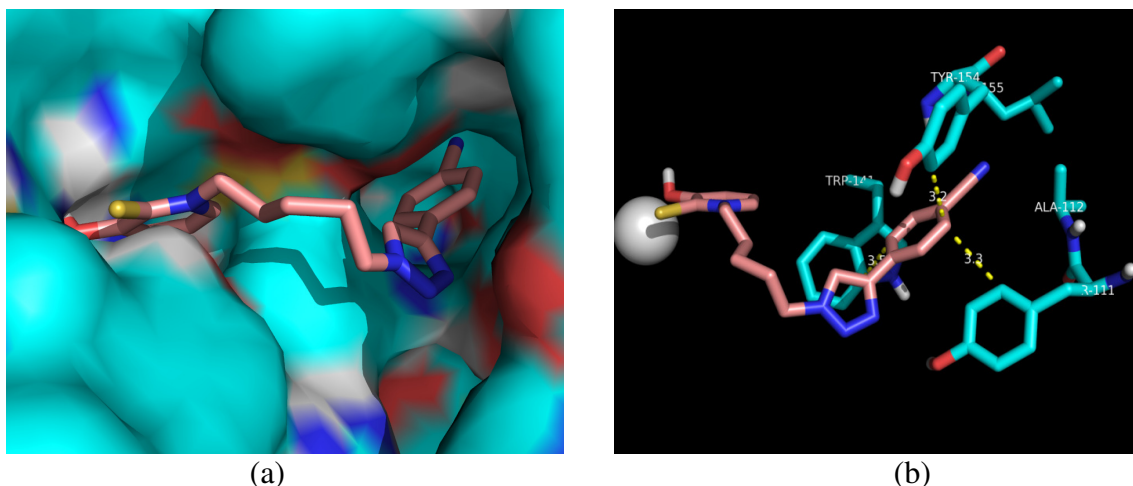


Figure 5-21. (a) Docked structure of **30d**; (b) Docked structure of **30d** against HDAC8 showing key AA residues forming deep pocket around phenyl cap group.

The preference for the HDAC8 isoform over HDAC1 was consistent for almost all of the compounds tested in this series. This is an important and interesting observation considering the fact that other aromatic ZBG such as benzamide showed HDAC1 selectivity (250 fold).⁵³ To obtain information on the structural basis of the observed disparity in the HDAC isoform selectivity for these compounds, we performed molecular docking analysis on lead compound **12d** as previously described on two HDAC isoforms

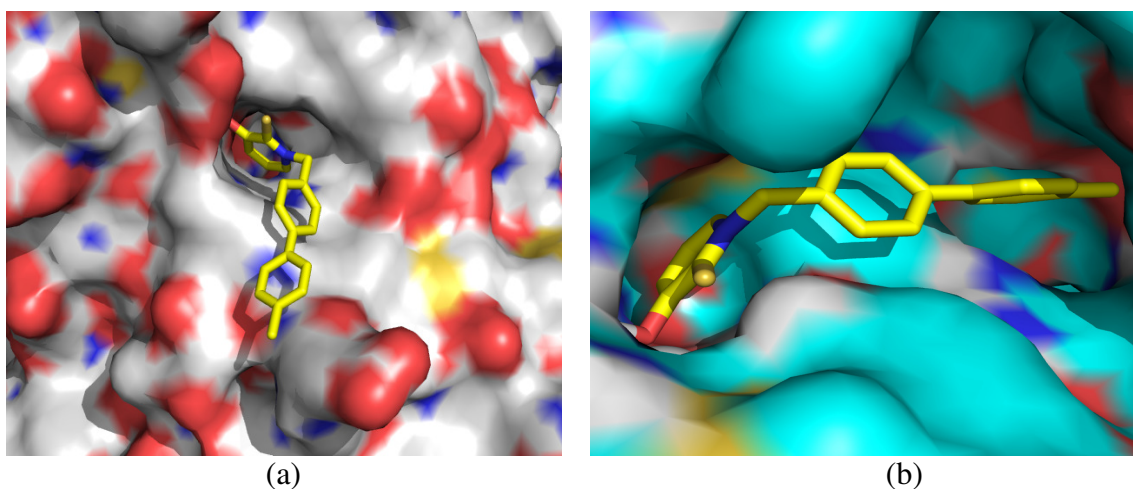


Figure 5-22. (a) Docked structure of **12d** against HDAC1. (b) Docked structure of **12d** against HDAC8

tested. HDAC8 docking revealed that **12d** orients optimally at the active site which tracks well with inhibition activity observed for **12d**. However, HDAC1 docking of **12d** reveal that there is no fruitful interaction of compound **12d** at HDAC1 enzyme active site. Moreover, ZBG of **12d** is far away from Zn^{2+} ion and that could be the reason that no HDAC1 inhibition was noticed. Repeated docking confirmed that the ZBG of **12d** was unable to deeply penetrate ($\sim 14 \text{ \AA}$) the Zn^{2+} active site of HDAC1.

5.14 Conclusion

We have used fragment based and structure based drug design approaches to successfully incorporate a novel nonhydroxamate ZBG into HDACi design. We have disclosed for the first time that heterocyclic aromatic 3-HPT based ZBG are compatible with HDAC inhibition. Preliminary biological studies on these compounds reveal isoform selectivity for HDAC8 enzyme as relative to HDAC1. Molecular docking studies performed on this novel ZBG furnished interesting information about HDAC8 active site and how this information could be used to generate more potent and selective analogs. Ongoing biological study on more HDAC isoforms should lead to better understanding of these 3-HPT based HDACi. In addition to 3-HPT; 3-hydroxypyridin-4-ones, pyrones, thiopyrones represent other good choices of ZBG that can be incorporated for more potent and selective HDAC inhibition.

5.15 General Procedures and Experimental

Bromoalkanoic acid, benzyl bromide, 4-bromobenzylbromide, 4-(bromomethyl)-1,1'-biphenyl, 3-methoxy-2(1H)-pyridone, propargyl bromide, phenylacetylene and representative boronic acids were purchased from either Sigma-Aldrich or Alfa-Aesar. Anhydrous solvents and other reagents were purchased and used without further purification. Analtech silica gel plates (60 F₂₅₄) were used for analytical TLC, and Analtech preparative TLC plates (UV 254, 2000 μ m) were used for purification. UV light was used to examine the spots. Silica gel (200–400 Mesh) was used in column chromatography. NMR spectra were recorded on a Varian-Gemini 400 magnetic resonance spectrometer. ¹H NMR spectra were recorded in parts per million (ppm) relative to the peak of CDCl₃, (7.24 ppm), CD₃OD (3.31 ppm), or DMSO-*d*₆ (2.49 ppm). ¹³C spectra were recorded relative to the central peak of the CDCl₃ triplet (77.0 ppm), CD₃OD (49.0 ppm), or the DMSO-*d*₆ septet (39.7 ppm), and were recorded with complete heterodecoupling. Multiplicities are described using the abbreviation s, singlet; d, doublet; t, triplet; q, quartet; m, multiplet; and app, apparent. High-resolution mass spectra were recorded at the Georgia Institute of Technology mass spectrometry facility in Atlanta. Synthesis of 1a was adapted from literature protocol.⁵⁴ Azidoalkanols (**1a-1f**) were prepared according to literature protocols⁵⁵ and was used without further purification. Synthesis of phenyl azide and 4-azido-*N,N*-dimethylaniline were adapted from literature protocols.⁵⁶

Synthesis of 1-methyl-3-methoxypyridin-2-one (**4a**)

To a stirring reaction mixture of 3-methoxypyridin-2-one (0.2 g, 1.6 mmol) and KOH (0.18 g, 3.2 mmol) in methanol was added MeI (0.68 g, 4.8 mmol) dropwise in condenser equipped round bottom flask. After overnight stirring at room temperature revealed quantitative formation of product. Reaction mixture was then diluted with water (35 mL) and CHCl₃ (40 mL). Organic layer was washed with water (1X35 mL), brine (1X30 mL) and dried over Na₂SO₄ and solvent was evaporated off under vacuo to yield pure **4a** (0.20 g, 89%) as a colorless oil. ¹H NMR (400 MHz, CDCl₃) δ 6.66 (m, 1H), 6.35 (d, *J* = 7.4 Hz, 1H), 5.83 (t, *J* = 7.1 Hz, 1H), 3.52 (s, 3H), 3.28 (s, 3H). ¹³C NMR (100 MHz, CDCl₃) δ 158.01, 149.56, 128.81, 111.91, 104.31, 55.44, 37.10.

1-Benzyl-3-methoxypyridin-2-one (**4b**)

To a stirring reaction mixture of 3-methoxypyridin-2-one (0.2 g, 1.6 mmol) and K₂CO₃ (0.66 g, 4.8 mmol) in DMF (8 mL) was added benzyl bromide (0.33 g, 1.92 mmol) dropwise in a condenser equipped round bottom flask. Reaction mixture was then heated to 100 °C. After overnight stirring, reaction mixture was cooled down and diluted with water (40 mL) and CHCl₃ (50 mL). Organic layer was washed with water (3X40 mL), brine (1X30 mL) and dried over Na₂SO₄ and solvent was evaporated off under vacuo to yield pure **4b** (0.26 g, 75%) as a colorless oil without any further purification needed. ¹H NMR (400 MHz, CDCl₃) δ 7.26 (m, 5H), 6.85 (dd, *J* = 6.9, 1.7 Hz, 1H), 6.54 (dd, *J* = 7.5, 1.6 Hz, 1H), 6.03 (m, 1H), 5.13 (s, 2H), 3.76 (s, 3H). ¹³C NMR (100 MHz, CDCl₃) δ 157.94, 150.05, 136.31, 128.56, 128.01, 127.74, 127.70, 111.82, 104.83, 104.81, 55.64, 51.64.

1-(1,1'-Biphenylmethyl)-3-methoxypyridin-2-one (4c)

Reaction of 3-methoxypyridin-2-one (0.2 g, 1.6 mmol), K₂CO₃ (0.66 g, 4.8 mmol), (4-bromomethyl)-1,1'-biphenyl (0.47 g, 1.92 mmol) in DMF (8 mL) according to method described for synthesis of **4b** followed by column chromatography with CH₂Cl₂, acetone (0-15% gradient), MeOH (0-5% gradient) afforded pure **4c** (0.35 g, 76%) as a colorless oil. ¹H NMR (400 MHz, CDCl₃) δ 7.48 (dd, *J* = 25.9, 20.6 Hz, 4H), 7.32 (m, 5H), 6.88 (m, 1H), 6.54 (d, *J* = 7.2 Hz, 1H), 6.04 (t, *J* = 7.1 Hz, 1H), 5.16 (s, 2H), 3.76 (s, 3H). ¹³C NMR (100 MHz, CDCl₃) δ 157.86, 149.97, 140.51, 140.24, 135.28, 128.51, 128.40, 127.71, 127.16, 127.13, 126.74, 111.82, 104.80, 55.56, 51.36.

1-Methyl-3-hydroxypyridin-2-one (5a)

To a solution of **4a** (0.1 g, 0.68 mmol) in dry CH₂Cl₂ (8 mL) was slowly added 1M BBr₃ (0.82 mL) at -30 °C under inert atmosphere. The reaction mixture was stirred for 48 h at room temperature. The mixture was again cooled to -30 °C & then MeOH (5 mL) was slowly added to the mixture. After evaporation of solvent, the residue was adjusted to pH 7 with 1M NaOH and then extracted with CHCl₃ (3 X 30mL). The combined organic layer dried over Na₂SO₄. After evaporation of solvent, the residue was purified by prep-TLC with CH₂Cl₂:Acetone:MeOH (10:1:0.2) to give 61 mg (72%) of pure off white solid **5a**. ¹H NMR (400 MHz, CDCl₃) δ 7.92 (s, 1H), 6.78 (dd, *J* = 11.1, 7.1 Hz, 2H), 6.10 (t, *J* = 7.0 Hz, 1H), 3.57 (s, 3H). ¹³C NMR (100 MHz, CDCl₃) δ 158.82, 146.67, 127.63, 114.36, 106.68, 37.28. HRMS (EI) calcd for C₆H₇NO₂ [M]⁺ 125.0477 found 125.0477.

1-Benzyl-3-hydroxypyridin-2-one (**5b**)

Reaction of **4b** (0.15 g, 0.55 mmol) with 1M BBr₃ (0.66 mL) in dry CH₂Cl₂ (5 mL) within 48 h according to procedure **5a** afforded pure **5b** (0.13 g, 90%) as slightly brownish solid. ¹H NMR (400 MHz, CDCl₃) δ 7.31 (m, 5H), 6.83 (m, 3H), 6.14 (t, *J* = 7.1 Hz, 1H), 5.19 (s, 2H). ¹³C NMR (100 MHz, CDCl₃) δ 158.62, 146.78, 135.82, 128.74, 127.97, 126.53, 113.94, 106.95, 52.18. HRMS (EI) calcd for C₁₂H₁₁NO₂ [M]⁺ 201.0792 found 201.0790.

1-(1,1'-Biphenylmethyl)-3-hydroxypyridin-2-one (**5c**)

Reaction of **4c** (0.13 g, 0.43 mmol) with 1M BBr₃ (0.51 mL) in dry CH₂Cl₂ (7 mL) within 48 h according to procedure **5a** afforded pure **5c** (0.1 g, 82%) as slightly brownish solid. ¹H NMR (400 MHz, DMSO-*d*₆) δ 9.06 (s, 1H), 7.61 (d, *J* = 7.5 Hz, 4H), 7.36 (m, 6H), 6.70 (d, *J* = 6.5 Hz, 1H), 6.12 (t, *J* = 6.9 Hz, 1H), 5.16 (s, 2H). ¹³C NMR (100 MHz, DMSO-*d*₆) δ 147.02, 139.77, 139.46, 136.58, 128.93, 128.35, 128.15, 127.49, 126.86, 126.66, 114.75, 105.64, 51.07. HRMS (EI) calcd for C₁₈H₁₅NO₂ [M]⁺ 277.1101 found 277.1103.

1-Benzyl-3-methoxypyridin-2-thione (**6b**)

A suspension of **4b** (0.060 g, 0.28 mmol) and Lawesson's reagent (0.067 g, 0.17 mmol) in toluene (10 mL) was heated to reflux overnight. Reaction mixture was then cooled to room temperature. Toluene was evaporated off under vacuo and resulting crude solid was directly loaded on prep-TLC. Elution with CH₂Cl₂: Acetone: MeOH (5:1:0.2) gave **6b** 53 mg (82%) of yellow solid. ¹H NMR (400 MHz, CDCl₃) δ 7.30 (m, 6H), 6.65 (d, *J* = 7.7

Hz, 1H), 6.54 (t, $J = 7.0$ Hz, 1H), 5.89 (s, 2H), 3.88 (s, 3H). ^{13}C NMR (100 MHz, CDCl_3) δ 173.18, 159.01, 135.18, 131.70, 128.72, 128.03, 127.98, 111.57, 109.63, 58.79, 56.61. HRMS (EI) calcd for $\text{C}_{13}\text{H}_{13}\text{NOS}$ $[\text{M}]^+$ 231.0718 found 231.0716.

1-(1,1'-Biphenylmethyl)-3-methoxypyridin-2-thione (6c)

Reaction of **4c** (0.13 g, 0.44 mmol) and Lawesson's reagent (0.11 g, 0.27 mmol) in toluene according to method described for synthesis of **6b** afforded 122 mg of **6c** (88%) of yellow solid. ^1H NMR (400 MHz, CDCl_3) δ 7.52 (m, 1H), 7.35 (m, 2H), 6.66 (dd, $J = 7.8, 1.3$ Hz, 1H), 6.55 (dd, $J = 7.8, 6.6$ Hz, 1H), 5.93 (s, 1H), 3.89 (s, 1H). ^{13}C NMR (100 MHz, CDCl_3) δ 173.08, 158.99, 140.81, 140.20, 134.14, 131.72, 128.61, 128.42, 127.35, 127.28, 126.83, 111.62, 109.67, 104.80, 58.52, 56.58. HRMS (EI) calcd for $\text{C}_{19}\text{H}_{17}\text{NOS}$ $[\text{M}]^+$ 307.1031 found 307.1029.

1-Benzyl-3-hydroxypyridin-2-thione (7b)

Reaction of **6b** (0.050 g, 0.21 mmol) with 1M BBr_3 (0.66 mL) in dry CH_2Cl_2 (5 mL) within 48 h according to procedure **5a** afforded pure **7b** (0.034 g, 72%) as olive green solid. ^1H NMR (400 MHz, CD_3OD) δ 7.34 (m, 3H), 6.84 (m, 1H), 5.83 (d, $J = 49.5$ Hz, 1H). ^{13}C NMR (100 MHz, CD_3OD) δ 128.12, 127.61, 127.27, 126.94, 113.77. HRMS (EI) calcd for $\text{C}_{12}\text{H}_{11}\text{NOS}$ $[\text{M}]^+$ 217.0561 found 217.0762.

1-(1,1'-Biphenylmethyl)-3-hydroxypyridin-2-thione (7c)

Reaction of **6c** (0.10 g, 0.32 mmol) with 1M BBr_3 (0.48 mL) in dry CH_2Cl_2 (5 mL) within 48 h according to procedure **5a** afforded pure **7c** (0.074 g, 90%) as olive green

solid. ^1H NMR (400 MHz, CD_3OD) δ 7.39 (m, 9H), 6.88 (m, 3H), 5.86 (s, 2H). ^{13}C NMR (100 MHz, CD_3OD) δ 141.33, 140.21, 128.71, 128.52, 127.49, 127.45, 126.89. HRMS (EI) calcd for $\text{C}_{18}\text{H}_{15}\text{NOS}$ $[\text{M}]^+$ 293.0874 found 293.0873.

1-(4-Bromobenzyl)-3-methoxypyridin-2(1H)-one (8)

To a stirring reaction mixture of 3-methoxypyridin-2-one (2.00 g, 16 mmol) and K_2CO_3 (4.42 g, 32 mmol) in THF was added 4-bromobenzyl bromide (5.20 g, 20.8 mmol) slowly. Reaction mixture was then heated to reflux and stirring continued overnight. Reaction mixture was then cooled down and separated into organic and aqueous layer by adding CH_2Cl_2 (120 mL) and water (60 mL). Organic layer was separated and subsequently washed with water (2 X 60 mL), brine (1 X 40 mL). Organic layer was dried on Na_2SO_4 and solvent was evaporated in vacuo. Crude yellowish solid was triturated with hexanes to give pure white solid **8** (3.49 g, 74%) without further purification. ^1H NMR (400 MHz, CDCl_3) δ 7.25 (m, 2H), 7.04 (m, 2H), 6.78 (dd, $J = 6.8, 1.2$ Hz, 1H), 6.45 (dd, $J = 7.2, 1.6$ Hz, 1H), 5.94 (t, $J = 7.2$ Hz, 1H), 4.95 (s, 2H), 3.64 (s, 3H). ^{13}C NMR (100 MHz, CDCl_3) δ 157.71, 149.91, 135.29, 131.49, 129.59, 127.53, 121.57, 111.82, 104.98, 55.54, 51.10. HRMS (EI) calcd for $\text{C}_{13}\text{H}_{12}\text{BrNO}_2$ $[\text{M}]^+$ 293.0051 found 293.0051.

Representative procedure for Suzuki coupling reactions for synthesis of 9 –

1-(4-Cyano-(1,1'-biphenylmethyl))-3-methoxyoxypyridin-2-one (9a)

8 (0.26 g, 0.86 mmol), (4-cyanophenyl)boronic acid (0.14 g, 0.95 mmol), 2M aq. K_2CO_3 (0.24 g, 1.73 mmol), toluene (8 mL), EtOH (4mL) and water (4mL) were added into

reaction flask equipped with magnetic stirrer and water condenser. The resulting suspension was degassed for 10 min by sparging with argon gas. $\text{Pd(PPh}_3)_4$ (2.5 mol%) was added and the reaction mixture was heated to reflux overnight under argon atmosphere. After cooling to room temperature, CH_2Cl_2 was added (50 mL) & washed with water (1 X 40 mL), brine (1 X 20 mL) and dried on Na_2SO_4 . Column chromatography using gradient CHCl_3 :Acetone:MeOH (with 5% - 20% of acetone and 1% - 8% MeOH gradual increase) gave pure off white solid **9a** (0.42 g, 78%). ^1H NMR (CDCl_3 , 400 MHz) δ 7.60 (m, 4H), 7.40 (m, 4H), 6.90 (dd, J = 6.8, 1.6 Hz, 1H), 6.55 (dd, J = 7.6, 1.6 Hz, 1H), 6.07 (t, J = 7.2 Hz, 1H), 5.16 (s, 2H), 3.75 (s, 3H). ^{13}C NMR (100 MHz, CDCl_3) δ 158.08, 150.28, 144.96, 138.62, 137.13, 132.56, 131.96, 128.85, 128.55, 128.43, 127.96, 127.60, 127.53, 118.88, 112.11, 110.88, 105.24, 56.20, 51.80. HRMS (EI) calcd for $\text{C}_{20}\text{H}_{16}\text{N}_2\text{O}_2$ $[\text{M}]^+$ 316.1212 found 316.1210.

1-(3-Cyano-(1,1'-biphenylmethyl))-3-methoxyoxypyridin-2-one (9b)

Reaction of **3** (0.25 g, 0.85 mmol), (3-cyanophenyl)boronic acid (0.14g, 0.93 mmol), 2M aq. K_2CO_3 (0.23 g, 1.69 mmol) and $\text{Pd(PPh}_3)_4$ (2.5 mol%) according to method described for synthesis of **9a** within 18 h afforded 175 mg of **9b** (66 %) of white solid. ^1H NMR (400 MHz, CDCl_3) δ 7.70 (m, 2H), 7.48 (m, 6H), 6.92 (dd, J = 6.9, 1.6 Hz, 1H), 6.57 (dd, J = 7.4, 1.4 Hz, 1H), 6.08 (t, J = 7.2 Hz, 1H), 5.16 (s, 2H), 3.76 (s, 3H). ^{13}C NMR (100 MHz, CDCl_3) δ 158.09, 150.24, 141.70, 138.33, 136.81, 131.38, 130.76, 130.45, 129.66, 128.87, 127.96, 127.36, 118.76, 112.82, 112.14, 105.26, 55.84, 51.66. HRMS (EI) calcd for $\text{C}_{20}\text{H}_{16}\text{N}_2\text{O}_2$ $[\text{M}]^+$ 316.1212 found 332.1216.

1-(2-Cyano-(1,1'-biphenylmethyl))-3-methoxyoxypyridin-2-one (9c)

Reaction of **3** (0.15 g, 0.50 mmol), (2-cyanophenyl)boronic acid (0.09 g, 0.60 mmol), 2M aq. K₂CO₃ (0.14 g, 1.69 mmol) and Pd(PPh₃)₄ (2.5 mol%) according to method described for synthesis of **9a** within 18 h afforded 118 mg of **9c** (75 %) of white solid. ¹H NMR (400 MHz, CDCl₃) δ 7.72 (m, 1H), 7.60 (m, 1H), 7.45 (m, 2H), 6.94 (dd, *J* = 6.9, 1.7 Hz, 1H), 6.60 (dd, *J* = 7.4, 1.6 Hz, 1H), 6.10 (t, *J* = 7.2 Hz, 1H), 5.21 (s, 1H), 3.80 (s, 1H). ¹³C NMR (100 MHz, CDCl₃) δ 158.01, 150.18, 144.70, 137.56, 136.94, 133.61, 132.78, 129.91, 129.01, 128.31, 127.92, 127.55, 118.54, 112.01, 110.94, 105.13, 55.74, 51.60. HRMS (EI) calcd for C₂₀H₁₆N₂O₂ [M]⁺ 316.1212 found 316.1201.

1-(4-Methyl-(1,1'-biphenylmethyl))-3-methoxyoxypyridin-2-one (9d)

Reaction of **8** (0.25g, 0.85 mmol), *p*-tolylboronic acid (0.14g, 1.02 mmol), 2M aq. K₂CO₃ (0.23g, 1.69 mmol), Pd(PPh₃)₄ (2.5 mol%) according to method described for synthesis of **9a** within 18 h afforded 259 mg of **9d** (quantitative) of white solid. ¹H NMR (400 MHz, CDCl₃) δ 7.49 (d, *J* = 8.1 Hz, 2H), 7.42 (d, *J* = 8.1 Hz, 2H), 7.33 (d, *J* = 8.1 Hz, 2H), 7.19 (d, *J* = 8.0 Hz, 2H), 6.88 (dd, *J* = 6.9, 1.6 Hz, 1H), 6.54 (dd, *J* = 7.4, 1.4 Hz, 1H), 6.03 (t, *J* = 7.2 Hz, 1H), 5.15 (s, 2H), 3.76 (s, 3H), 2.34 (s, 3H). ¹³C NMR (100 MHz, CDCl₃) δ 157.81, 149.88, 140.39, 137.29, 136.87, 134.93, 129.21, 128.35, 127.66, 126.91, 126.53, 111.75, 104.78, 55.51, 51.31, 20.80. HRMS (EI) calcd for C₂₀H₁₉NO₂ [M]⁺ 305.1416 found 305.1422.

1-(3-Methyl-(1,1'-biphenylmethyl))-3-methoxyoxypyridin-2-one (9e)

Reaction of **3** (0.20 g, 0.68 mmol), *m*-tolylboronic acid (0.11 g, 0.82 mmol), 2M aq. K_2CO_3 (0.19 g, 1.36 mmol) and $Pd(PPh_3)_4$ (2.5 mol%) according to method described for synthesis of **9a** within 18 h afforded 259 mg of **9e** (quantitative) of white solid. 1H NMR (400 MHz, $CDCl_3$) δ 7.49 (m, 1H), 7.29 (m, 2H), 7.11 (d, $J = 7.2$ Hz, 1H), 6.88 (dd, $J = 6.9, 1.7$ Hz, 1H), 6.53 (dd, $J = 7.4, 1.6$ Hz, 1H), 6.03 (t, $J = 7.2$ Hz, 1H), 5.15 (s, 1H), 3.75 (s, 1H), 2.35 (s, 1H). ^{13}C NMR (100 MHz, $CDCl_3$) δ 157.81, 149.86, 140.58, 140.16, 137.99, 135.11, 128.37, 128.29, 127.83, 127.66, 127.46, 127.10, 123.80, 111.81, 104.80, 55.48, 51.30, 21.19. HRMS (EI) calcd for $C_{20}H_{19}NO_2$ $[M]^+$ 305.1416 found 305.1415.

1-(2-Methyl-(1,1'-biphenylmethyl))-3-methoxyoxypyridin-2-one (9f)

Reaction of **3** (0.20 g, 0.68 mmol), *O*-tolylboronic acid (0.11 g, 0.82 mmol), 2M aq. K_2CO_3 (0.19 g, 1.36 mmol) and $Pd(PPh_3)_4$ (2.5 mol%) according to method described for synthesis of **9a** within 18 h afforded 243 mg of **9f** (98%) of white solid. 1H NMR (400 MHz, $CDCl_3$) δ 7.31 (d, $J = 7.9$ Hz, 1H), 7.17 (m, 2H), 6.93 (m, 1H), 6.56 (dd, $J = 7.4, 1.6$ Hz, 1H), 6.06 (t, $J = 7.2$ Hz, 1H), 5.18 (s, 1H), 3.76 (s, 1H), 2.20 (s, 1H). ^{13}C NMR (100 MHz, $CDCl_3$) δ 158.13, 150.23, 141.51, 141.26, 135.23, 135.00, 130.33, 129.68, 129.51, 128.13, 127.85, 127.34, 125.77, 112.13, 105.07, 55.82, 51.79, 20.45. HRMS (EI) calcd for $C_{20}H_{19}NO_2$ $[M]^+$ 305.1416 found 305.1419.

1-(4-Dimethylamino-(1,1'-biphenylmethyl))-3-methoxyoxypyridin-2-one (9g)

Reaction of **8** (0.25g, 0.85 mmol), (4-(dimethylamino)phenyl)boronic acid (0.17g, 1.02 mmol), 2M aq. K₂CO₃ (0.23g, 1.69 mmol), Pd(PPh₃)₄ (2.5 mol%) according to method described for synthesis of **9a** within 18 h afforded 230 mg of **9g** (81 %) as white solid. ¹H NMR (400 MHz, CDCl₃) δ 7.46 (m, 4H), 7.29 (m, 2H), 6.86 (dd, *J* = 7.2, 2.0 Hz, 1H), 7.73 (m, 2H), 6.52 (dd, *J* = 7.2, 1.6 Hz, 1H), 6.01 (t, *J* = 7.2 Hz, 1H), 5.13 (s, 2H), 3.76 (s, 3H), 2.93 (s, 6H). ¹³C NMR (100 MHz, CDCl₃) δ 157.86, 149.90, 149.73, 140.55, 133.81, 128.43, 128.04, 127.68, 127.28, 126.16, 112.40, 111.77, 104.69, 55.53, 51.31, 40.18. HRMS (EI) calcd for C₂₁H₂₂N₂O₂ [M]⁺ 334.1681 found 334.1684.

1-(4-(6-(Dimethylamino)pyridin-3-yl)benzyl)-3-methoxyoxypyridin-2-one (9h)

Reaction of **8** (0.43g, 1.44 mmol), (6-(dimethylamino)pyridine-3-yl)boronic acid (0.2 g, 1.20 mmol), 2M aq. K₂CO₃ (0.33g, 2.41 mmol), Pd(PPh₃)₄ (2.5 mol%) according to method described for synthesis of **9a** within 18 h afforded 335 mg of **9h** (83%) of white solid. ¹H NMR (400 MHz, CDCl₃) δ 8.28 (d, *J* = 2.3 Hz, 1H), 7.51 (dd, *J* = 8.8, 2.5 Hz, 1H), 7.33 (d, *J* = 8.2 Hz, 2H), 7.22 (d, *J* = 8.2 Hz, 2H), 6.80 (dd, *J* = 6.9, 1.6 Hz, 1H), 6.44 (m, 2H), 5.94 (t, *J* = 7.2 Hz, 1H), 5.04 (s, 2H), 3.66 (s, 3H), 2.97 (s, 6H). ¹³C NMR (100 MHz, CDCl₃) δ 158.12, 157.61, 149.68, 145.49, 137.75, 135.14, 134.20, 128.35, 127.54, 125.69, 123.15, 111.62, 105.23, 104.62, 55.36, 51.16, 37.66. HRMS (EI) calcd for C₂₀H₂₁N₃O₂ [M]⁺ 335.1634 found 335.1635.

1-(4-(Pyridin-4-yl)benzyl)-3-methoxy-pyridin-2-one (9i)

Reaction of **8** (0.25g, 0.85 mmol), pyridin-4-ylboronic acid (0.12g, 1.02 mmol), 2M aq. K₂CO₃ (0.23g, 1.69 mmol), Pd(PPh₃)₄ (2.5 mol%) according to method described for

synthesis of **9a** within 18 h afforded 203 mg of **9i** (82%) of white solid. ¹H NMR (400 MHz, CDCl₃) δ 8.54 (dd, *J* = 4.5, 1.6 Hz, 2H), 7.48 (m, 2H), 7.36 (m, 4H), 6.87 (dd, *J* = 6.9, 1.7 Hz, 1H), 6.53 (dd, *J* = 7.4, 1.6 Hz, 1H), 6.03 (t, *J* = 7.2 Hz, 1H), 5.13 (s, 2H), 3.72 (s, 3H). ¹³C NMR (100 MHz, CDCl₃) δ 157.82, 150.32, 150.01, 149.90, 147.40, 137.31, 137.28, 128.57, 127.68, 127.04, 121.22, 111.90, 104.98, 55.57, 51.42. HRMS (EI) calcd for C₁₈H₁₆N₂O₂ [M]⁺ 292.1212 found 292.1205.

Representative procedure for Thionation reactions for synthesis of 10 –

1-(4-Cyano-(1,1'-biphenylmethyl))-3-methoxyoxypyridin-2-thione (10a)

A suspension of **9a** (0.13 g, 0.42 mmol) and Lawesson's reagent (0.10 g, 0.25 mmol) in toluene (10 mL) was heated to reflux overnight. Reaction mixture was then cooled to room temperature. Toluene was evaporated off under vacuo and resulting crude solid was directly loaded on prep-TLC. Elution with CHCl₃: Acetone: EtOH (12:1:0.2) gave **10a** 123 mg (88%) of yellow solid. ¹H NMR (CDCl₃, 400 MHz) δ 7.60 (m, 4H), 7.40 (m, 4H), 6.90 (dd, *J* = 6.8, 1.6 Hz, 1H), 6.55 (dd, *J* = 7.6, 1.6 Hz, 1H), 6.07 (t, *J* = 7.2 Hz, 1H), 5.16 (s, 2H), 3.75 (s, 3H). ¹³C NMR (100 MHz, CDCl₃) δ 158.08, 150.28, 144.96, 138.62, 137.13, 132.56, 131.96, 128.85, 128.55, 128.43, 127.96, 127.60, 127.53, 118.88, 112.11, 110.88, 105.24, 56.20, 51.80 HRMS (EI) calcd for C₂₀H₁₆N₂OS [M]⁺ 332.0983 found 332.0987.

1-(3-Cyano-(1,1'-biphenylmethyl))-3-methoxypyridin-2-thione (10b)

Reaction of **9b** (0.11 g, 0.36 mmol) and Lawesson's reagent (0.09 g, 0.22 mmol) in toluene according to method described for synthesis of **10a** afforded 113 mg of **10b** (95%) of yellow solid. ¹H NMR (400 MHz, DMSO-*d*₆) δ 7.92 (m, 3H), 7.84 (m, 2H), 7.71 (d, *J* = 8.4 Hz, 2H), 7.36 (d, *J* = 8.8 Hz, 2H), 7.00 (m, 1H), 6.80 (m, 1H), 5.95 (s, 2H), 3.78 (s, 3H). ¹³C NMR (100 MHz, CDCl₃) δ 173.39, 159.26, 144.82, 138.81, 135.79, 132.55, 131.81, 128.65, 127.58, 127.50, 118.77, 111.80, 110.98, 109.69, 58.63, 56.74. HRMS (EI) calcd for C₂₀H₁₆N₂OS [M]⁺ 332.0983 found 332.0984.

1-(2-Cyano-(1,1'-biphenylmethyl))-3-methoxyoxypyridin-2-thione (10c)

Reaction of **9c** (0.09 g, 0.28 mmol) and Lawesson's reagent (0.07 g, 0.17 mmol) in toluene according to method described for synthesis of **10a** afforded 72 mg of **10c** (77%) of yellow solid. ¹H NMR (400 MHz, CDCl₃) δ 7.74 (m, 1H), 7.63 (td, *J* = 7.7, 1.4 Hz, 1H), 7.45 (m, 2H), 6.71 (dd, *J* = 7.8, 1.3 Hz, 1H), 6.62 (dd, *J* = 7.8, 6.6 Hz, 1H), 6.00 (s, 1H), 5.28 (s, 1H), 3.93 (s, 1H). ¹³C NMR (100 MHz, CDCl₃) δ 173.38, 159.22, 144.68, 137.79, 135.80, 133.67, 132.86, 131.95, 129.97, 129.17, 128.25, 127.66, 118.59, 111.84, 111.01, 109.76, 58.63, 56.74. HRMS (EI) calcd for C₂₀H₁₆N₂OS [M]⁺ 332.0983 found 332.0981.

1-(4-Methyl-(1,1'-biphenylmethyl))-3-methoxyoxypyridin-2-thione (10d)

Reaction of **9d** (0.12 g, 0.39 mmol) and Lawesson's reagent (0.09 g, 0.23 mmol) in toluene according to method described for synthesis of **10a** afforded 117 mg of **10d** (94%) as yellow solid. ¹H NMR (400 MHz, CDCl₃) δ 7.51 (m, 2H), 7.42 (m, 2H), 7.34 (m, 3H), 7.21 (dd, *J* = 8.4, 0.6 Hz, 2H), 6.66 (dd, *J* = 7.8, 1.2 Hz, 1H), 6.55 (dd, *J* = 7.8,

6.6 Hz, 1H), 5.92 (s, 2H), 3.89 (s, 3H), 2.36 (s, 3H). ^{13}C NMR (100 MHz, CDCl_3) δ 173.05, 158.97, 140.74, 137.30, 137.08, 133.81, 131.70, 129.33, 128.42, 127.12, 126.64, 111.59, 109.65, 58.52, 56.57, 20.91. HRMS (EI) calcd for $\text{C}_{20}\text{H}_{19}\text{NOS}$ $[\text{M}]^+$ 321.1187 found 321.1192.

1-(3-Methyl-(1,1'-biphenylmethyl))-3-methoxyoxypyridin-2-thione (10e)

Reaction of **9e** (0.12 g, 0.37 mmol) and Lawesson's reagent (0.09 g, 0.23 mmol) in toluene according to method described for synthesis of **10a** afforded 112 mg of **10e** (93%) as yellow solid. ^1H NMR (400 MHz, CDCl_3) δ 7.53 (m, 1H), 7.33 (m, 2H), 7.14 (dd, $J = 7.1, 0.6$ Hz, 1H), 6.67 (dd, $J = 7.8, 1.2$ Hz, 1H), 6.56 (m, 1H), 5.94 (s, 1H), 3.91 (s, 1H), 2.39 (s, 1H). ^{13}C NMR (100 MHz, CDCl_3) δ 173.21, 159.07, 141.06, 140.28, 138.24, 134.07, 131.72, 128.57, 128.48, 128.09, 127.69, 127.44, 124.01, 111.62, 109.66, 58.60, 56.63, 21.39. HRMS (EI) calcd for $\text{C}_{20}\text{H}_{19}\text{NOS}$ $[\text{M}]^+$ 305.1187 found 321.1188.

1-(2-Methyl-(1,1'-biphenylmethyl))-3-methoxyoxypyridin-2-thione (10f)

Reaction of **9f** (0.14 g, 0.45 mmol) and Lawesson's reagent (0.11 g, 0.27 mmol) in toluene according to method described for synthesis of **10a** afforded 118 mg of **10f** (86%) as yellow solid. ^1H NMR (400 MHz, CDCl_3) δ 7.42 (dd, $J = 6.6, 1.0$ Hz, 1H), 7.22 (m, 3H), 6.68 (d, $J = 7.3$ Hz, 1H), 6.59 (m, 1H), 5.96 (s, 1H), 3.90 (s, 1H), 2.22 (s, 1H). ^{13}C NMR (100 MHz, CDCl_3) δ 158.97, 141.54, 140.93, 135.02, 133.59, 131.79, 130.13, 129.46, 129.42, 127.65, 127.18, 125.57, 111.62, 109.67, 58.56, 56.57, 20.25. HRMS (EI) calcd for $\text{C}_{20}\text{H}_{19}\text{NOS}$ $[\text{M}]^+$ 305.1187 found 321.1189.

1-(4-Dimethylamino-(1,1'-biphenylmethyl))-3-methoxyoxypyridin-2-thione (10g)

Reaction of **9g** (0.22 g, 0.67 mmol) and Lawesson's reagent (0.16 g, 0.40 mmol) in toluene according to method described for synthesis of **10a** afforded 172 mg of **10g** (73%) as yellow solid. ^1H NMR (400 MHz, CDCl_3) δ 7.39 (m, 5H), 7.22 (m, 2H), 6.69 (m, 3H), 6.65 (m, 1H), 5.82 (s, 2H), 3.82 (s, 3H), 2.88 (s, 6H). ^{13}C NMR (100 MHz, CDCl_3) δ 172.36, 158.73, 149.92, 140.89, 132.48, 131.84, 128.44, 128.20, 127.29, 126.32, 112.69, 112.02, 110.17, 58.68, 56.31, 40.24. HRMS (EI) calcd for $\text{C}_{21}\text{H}_{22}\text{N}_2\text{OS}$ $[\text{M}]^+$ 350.1453 found 350.1451.

1-(4-(6-(Dimethylamino)pyridin-3-yl)benzyl))-3-methoxyoxypyridin-2-thione (10h)

Reaction of **9h** (0.14 g, 0.42 mmol) and Lawesson's reagent (0.10 g, 0.25 mmol) in toluene according to method described for synthesis of **10a** afforded 130 mg of **10h** (88%) of yellow solid. ^1H NMR (400 MHz, CDCl_3) δ 8.32 (d, $J = 2.3$ Hz, 1H), 7.56 (dd, $J = 8.6, 2.1$ Hz, 1H), 7.36 (dd, $J = 19.8, 7.3$ Hz, 3H), 7.26 (d, $J = 8.0$ Hz, 2H), 6.61 (d, $J = 7.8$ Hz, 1H), 6.50 (m, 2H), 5.85 (s, 2H), 3.83 (s, 3H), 3.03 (s, 6H). ^{13}C NMR (100 MHz, CDCl_3) δ 172.74, 158.80, 158.31, 145.65, 138.13, 135.32, 133.08, 131.66, 128.46, 125.95, 123.21, 111.57, 109.64, 105.42, 58.42, 56.47, 37.86. HRMS (EI) calcd for $\text{C}_{20}\text{H}_{21}\text{N}_3\text{OS}$ $[\text{M}]^+$ 351.1405 found 351.1405.

1-(4-(Pyridin-4-yl)benzyl)-3-methoxypyridin-2-thione (10i)

Reaction of **9i** (0.13 g, 0.45 mmol) and Lawesson's reagent (0.11 g, 0.27 mmol) in toluene according to method described for synthesis of **10a** afforded 104 mg of **10i** (76%) as yellow solid with greenish tinge. ^1H NMR (400 MHz, CDCl_3) δ 8.59 (d, $J = 5.9$ Hz,

2H), 7.55 (d, $J = 8.3$ Hz, 2H), 7.39 (m, 5H), 6.67 (dd, $J = 7.8, 1.1$ Hz, 1H), 6.58 (dd, $J = 7.7, 6.7$ Hz, 1H), 5.95 (s, 2H), 3.89 (s, 3H). ^{13}C NMR (100 MHz, CDCl_3) δ 173.29, 159.15, 150.11, 147.43, 137.67, 136.17, 131.78, 128.58, 127.28, 121.35, 111.72, 109.67, 58.54, 56.66. HRMS (EI) calcd for $\text{C}_{18}\text{H}_{16}\text{N}_2\text{OS}$ $[\text{M}]^+$ 308.0983 found 308.0975.

**Representative procedure for deprotection of *O*-methyl group for synthesis of 11 –
1-(4-Cyano-(1,1'-biphenylmethyl))-3-hydroxyoxypyridin-2-one (11a)**

To a solution of **9a** (0.1 g, 0.32 mmol) in dry CH_2Cl_2 (8 mL) was slowly added 1M BBr_3 (0.35 mL) at -30°C under argon atmosphere. The reaction mixture was stirred for 32 h at room temperature. The mixture was again cooled to -30°C & then MeOH (5 mL) was slowly added to the mixture. After evaporation of solvent, the residue was adjusted to pH 7 with 1M NaOH and then extracted with CHCl_3 (3 X 30mL). The combined organic layer dried over Na_2SO_4 . After evaporation of solvent, the residue was purified by prep-TLC with CHCl_3 : Acetone: EtOH (10:1:0.2) to give 89 mg of **11a** (94%) as pure slightly brownish solid. ^1H NMR (400 MHz, DMSO) δ 9.08 (s, 1H), 7.87 (dd, $J = 24.8, 7.9$ Hz, 4H), 7.71 (d, $J = 7.6$ Hz, 2H), 7.40 (d, $J = 7.7$ Hz, 2H), 7.29 (d, $J = 6.7$ Hz, 1H), 6.70 (d, $J = 6.7$ Hz, 1H), 6.13 (t, $J = 6.8$ Hz, 1H), 5.18 (s, 2H). ^{13}C NMR (100 MHz, CDCl_3) δ 147.11, 145.13, 139.24, 136.77, 132.87, 128.95, 127.97, 127.89, 127.06, 119.08, 114.15, 111.35, 107.55, 52.48, 29.93. HRMS (ESI) calcd for $\text{C}_{19}\text{H}_{15}\text{N}_2\text{O}_2$ $[\text{M}+\text{H}]^+$ 303.1128 found 303.1124.

1-(3-Cyano-(1,1'-biphenylmethyl))-3-hydroxyoxypyridin-2-one (11b)

Reaction of **9b** (0.05g, 0.15 mmol) with 1M BBr₃ (0.26 mL) in dry CH₂Cl₂ within 48 h according to procedure **11a** afforded pure **11b** (44 mg, quantitative) as slightly brownish solid. ¹H NMR (400 MHz, DMSO-*d*₆) δ 9.08 (s, 1H), 8.11 (s, 1H), 7.98 (d, *J* = 7.8 Hz, 1H), 7.70 (m, 4H), 7.40 (d, *J* = 7.7 Hz, 2H), 7.28 (d, *J* = 6.2 Hz, 1H), 6.70 (d, *J* = 6.8 Hz, 1H), 6.13 (t, *J* = 6.7 Hz, 1H), 5.17 (s, 2H). ¹³C NMR (100 MHz, CDCl₃) δ 146.78, 141.62, 138.62, 136.13, 131.31, 130.82, 130.51, 129.62, 128.71, 127.49, 126.66, 118.66, 113.90, 112.96, 107.26, 52.25. HRMS (EI) calcd for C₁₉H₁₄N₂O₂ [M+H]⁺ 302.1055 found 302.1055.

1-(2-Cyano-(1,1'-biphenylmethyl))-3-hydroxyoxypyridin-2-one (11c)

Reaction of **9c** (0.072g, 0.15 mmol) with 1M BBr₃ (0.34 mL) in dry CH₂Cl₂ within 48 h according to procedure **11a** afforded pure **11c** (61 mg, 90%) as slightly brownish solid. ¹H NMR (400 MHz, CDCl₃) δ 7.75 (d, *J* = 7.6 Hz, 1H), 7.63 (t, *J* = 7.7 Hz, 1H), 7.53 (d, *J* = 7.3 Hz, 1H), 7.43 (m, 2H), 7.12 (m, 1H), 6.86 (dd, *J* = 28.2, 6.6 Hz, 1H), 6.19 (t, *J* = 6.1 Hz, 1H), 5.25 (s, 1H). ¹³C NMR (100 MHz, CDCl₃) δ 144.67, 137.88, 136.42, 133.71, 132.85, 129.95, 129.23, 128.20, 127.69, 118.56, 111.08, 107.17, 52.13. HRMS (EI) calcd for C₁₉H₁₄N₂O₂ [M+H]⁺ 302.1055 found 302.1053.

1-(4-Methyl-(1,1'-biphenylmethyl))-3-hydroxyoxypyridin-2-one (11d)

Reaction of **9d** (0.06 g, 0.20 mmol) with 1M BBr₃ (0.30 mL) in dry CH₂Cl₂ (5 mL) within 48 h according to procedure **11a** afforded pure **11d** (57 mg, quantitative) as slightly brownish solid. ¹H NMR (400 MHz, DMSO-*d*₆) δ 9.07 (s, 1H), 7.57 (m, 2H), 7.50 (d, *J* = 8.1 Hz, 2H), 7.34 (d, *J* = 6.8 Hz, 2H), 7.25 (dd, *J* = 14.8, 7.1 Hz, 3H), 6.69 (d, *J* =

7.4 Hz, 1H), 6.11 (t, $J = 7.1$ Hz, 1H), 5.14 (s, 2H), 2.30 (s, 3H). ^{13}C NMR (100 MHz, DMSO- d_6) δ 139.81, 137.29, 137.22, 136.68, 129.94, 128.77, 127.00, 126.89, 51.69, 21.10. Even after repeated cycles, quaternary carbons couldn't be visualized. (No improvement with relaxation delay of 2 sec). HRMS (EI) calcd for $\text{C}_{19}\text{H}_{17}\text{NO}_2$ $[\text{M}]^+$ 291.1259 found 291.1250.

1-(3-Methyl-(1,1'-biphenylmethyl))-3-hydroxyoxypyridin-2-one (11e)

Reaction of **9e** (0.064 g, 0.20 mmol) with 1M BBr_3 (0.30 mL) in dry CH_2Cl_2 (5 mL) within 48 h according to procedure **11a** afforded pure **11e** (60 mg, quantitative) as slightly brownish solid. ^1H NMR (400 MHz, CDCl_3) δ 7.56 (d, $J = 7.5$ Hz, 1H), 7.33 (m, 2H), 7.17 (d, $J = 7.2$ Hz, 1H), 6.85 (dd, $J = 22.2, 6.4$ Hz, 1H), 6.16 (t, $J = 6.5$ Hz, 1H), 5.23 (s, 1H), 2.42 (s, 1H). ^{13}C NMR (100 MHz, CDCl_3) δ 146.71, 141.19, 140.38, 138.32, 134.70, 128.63, 128.41, 128.16, 127.79, 127.56, 126.60, 124.11, 113.66, 106.98, 52.10, 21.45. HRMS (EI) calcd for $\text{C}_{19}\text{H}_{17}\text{NO}_2$ $[\text{M}]^+$ 291.1259 found 291.1263.

1-(2-Methyl-(1,1'-biphenylmethyl))-3-hydroxyoxypyridin-2-one (11f)

Reaction of **9f** (0.077 g, 0.25 mmol) with 1M BBr_3 (0.38 mL) in dry CH_2Cl_2 (5 mL) within 48 h according to procedure **11a** afforded pure **11f** (65 mg, 90%) as slightly brownish solid. ^1H NMR (400 MHz, CDCl_3) δ 7.28 (m, 3H), 6.87 (dd, $J = 31.4, 6.8$ Hz, 1H), 6.18 (t, $J = 6.9$ Hz, 1H), 5.27 (d, $J = 16.7$ Hz, 1H), 2.26 (s, 1H). ^{13}C NMR (100 MHz, CDCl_3) δ 146.73, 141.81, 141.14, 135.24, 134.30, 130.31, 129.66, 127.68, 127.37, 126.73, 125.75, 113.59, 106.99, 52.21, 20.40. HRMS (EI) calcd for $\text{C}_{19}\text{H}_{17}\text{NO}_2$ $[\text{M}]^+$ 291.1259 found 291.1260.

1-(4-Dimethylamino-(1,1'-biphenylmethyl))-3-hydroxyoxypyridin-2-one (11g)

Reaction of **9g** (0.10 g, 0.30 mmol) with 1M BBr₃ (0.45 mL) in dry CH₂Cl₂ (8 mL) within 48 h according to procedure **11a** afforded pure **11g** (84 mg, 87%) as slightly brownish solid. ¹H NMR (400 MHz, DMSO-*d*₆) δ 9.06 (s, 1H), 7.52 (d, *J* = 8.0 Hz, 3H), 7.28 (m, 4H), 6.76 (m, 2H), 6.10 (t, *J* = 5.8 Hz, 1H), 5.12 (s, 2H), 2.90 (s, 6H). ¹³C NMR (100 MHz, CDCl₃) δ 158.71, 149.98, 146.62, 141.07, 135.81, 133.29, 128.83, 128.47, 128.21, 128.07, 127.98, 127.55, 126.57, 113.48, 112.60, 106.89, 52.11, 40.44. HRMS (EI) calcd for C₂₀H₂₀N₂O₂ [M]⁺ 320.1524 found 320.1512.

1-(4-(6-(Dimethylamino)pyridin-3-yl)benzyl))-3-hydroxyoxypyridin-2-one (11h)

Reaction of **9h** (0.10 g, 0.29 mmol) with 1M BBr₃ (0.45 mL) in dry CH₂Cl₂ (7 mL) within 48 h according to procedure **11a** afforded pure **11h** (67 mg, 83%) as slightly brownish solid. ¹H NMR (400 MHz, CDCl₃) δ 8.40 (s, 1H), 7.66 (d, *J* = 8.0 Hz, 1H), 7.49 (d, *J* = 7.7 Hz, 2H), 7.33 (d, *J* = 7.7 Hz, 2H), 6.84 (dd, *J* = 27.3, 6.8 Hz, 3H), 6.57 (d, *J* = 8.7 Hz, 1H), 6.15 (t, *J* = 7.0 Hz, 1H), 5.20 (s, 2H), 3.12 (s, 6H). ¹³C NMR (100 MHz, CDCl₃) δ 158.47, 146.67, 145.66, 138.31, 135.79, 133.89, 131.95, 128.49, 126.79, 126.28, 123.61, 114.16, 107.19, 105.94, 52.13, 38.15. HRMS (EI) calcd for C₁₉H₁₉N₃O₂ [M]⁺ 321.1477 found 321.1479.

1-(4-(Pyridin-4-yl)benzyl))-3-hydroxypyridin-2-one (11i)

Reaction of **9i** (0.10 g, 0.34 mmol) with 1M BBr₃ (0.51 mL) in dry CH₂Cl₂ within 48 h according to procedure **11a** afforded pure **11i** (79 mg, 83%) as slightly brownish solid. ¹H

NMR (400 MHz, CDCl₃) δ 8.65 (s, 2H), 7.46 (s, 2H), 7.39 (d, J = 7.9 Hz, 2H), 6.83 (dd, J = 22.5, 7.0 Hz, 2H), 6.16 (t, J = 7.0 Hz, 1H), 5.22 (s, 2H). ¹³C NMR (100 MHz, CDCl₃) δ 150.23, 147.62, 146.76, 137.98, 136.87, 128.66, 127.51, 126.64, 121.58, 113.66, 107.13, 52.19. HRMS (FAB) calcd for C₁₇H₁₅N₂O₂ [M+H]⁺ 279.1133 found 279.1147.

1-(4-Cyano-(1,1'-biphenylmethyl))-3-hydroxyoxypyridin-2-thione (12a)

Reaction of **10a** (0.10 g, 0.30 mmol) with 1M BBr₃ (0.33 mL) in dry CH₂Cl₂ (8 mL) within 48 h according to procedure **11a** afforded pure **12a** (84 mg, 88%) as olive green color solid. ¹H NMR (400 MHz, DMSO-d₆) δ 7.87 (m, 5H), 7.74 (d, J = 8.1 Hz, 2H), 7.37 (d, J = 8.1 Hz, 2H), 7.04 (m, 1H), 6.90 (d, J = 8.1 Hz, 1H), 5.87 (s, 2H). ¹³C NMR (100 MHz, CDCl₃) δ 164.47, 144.66, 139.24, 134.64, 132.60, 128.56, 127.74, 127.62, 118.75, 111.15, 61.79, 29.64. HRMS (EI) calcd for C₁₉H₁₅N₂OS [M]⁺ 318.0827 found 318.0828.

1-(3-Cyano-(1,1'-biphenylmethyl))-3-hydroxyoxypyridin-2-thione (12b)

Reaction of **10b** (0.07 g, 0.21 mmol) with 1M BBr₃ (0.32 mL) in dry CH₂Cl₂ (5 mL) within 48 h according to procedure **11a** afforded pure **12b** (53 mg, 79%) as olive green color solid. ¹H NMR (400 MHz, CD₃OD) δ 7.89 (m, 2H), 7.65 (m, 5H), 7.44 (d, J = 8.2 Hz, 2H), 7.02 (d, J = 7.7 Hz, 2H), 6.77 (m, 1H), 5.90 (s, 2H). ¹³C NMR (100 MHz, CD₃OD) δ 142.99, 140.04, 132.82, 132.18, 131.69, 131.12, 130.03, 129.97, 129.89,

128.69, 128.59, 119.83, 113.94, 106.40, 54.78. HRMS (EI) calcd for $C_{19}H_{14}N_2O_2$ $[M+H]^+$ 318.0827 found 318.0827

1-(2-Cyano-(1,1'-biphenylmethyl))-3-hydroxyoxypyridin-2-thione (12c)

Reaction of **10c** (0.042 g, 0.21 mmol) with 1M BBr_3 (0.19 mL) in dry CH_2Cl_2 (5 mL) within 48 h according to procedure **11a** afforded pure **12c** (31 mg, 78%) as olive green color solid. 1H NMR (400 MHz, CD_3OD) δ 7.77 (dd, $J = 7.7, 0.9$ Hz, 1H), 7.67 (m, 2H), 7.48 (m, 4H), 7.01 (d, $J = 13.1$ Hz, 1H), 6.70 (m, 1H), 5.90 (s, 1H). ^{13}C NMR (100 MHz, CD_3OD) δ 145.34, 138.90, 134.40, 133.88, 130.75, 129.88, 128.90, 128.62, 119.17, 115.12, 111.38. HRMS (EI) calcd for $C_{19}H_{14}N_2O_2$ $[M+H]^+$ 318.0821 found 318.0827

1-(4-Methyl-(1,1'-biphenylmethyl))-3-hydroxyoxypyridin-2-thione (12d)

Reaction of **10d** (0.06 g, 0.20 mmol) with 1M BBr_3 (0.30 mL) in dry CH_2Cl_2 (5 mL) within 48 h according to procedure **11a** afforded pure **12d** (45 mg, 73%) as olive green color solid. 1H NMR (400 MHz, CD_3OD) δ 7.70 (d, $J = 1.1$ Hz, 1H), 7.63 (d, $J = 6.3$ Hz, 1H), 7.55 (d, $J = 8.2$ Hz, 2H), 7.40 (m, 3H), 7.21 (d, $J = 8.1$ Hz, 2H), 7.03 (dd, $J = 14.9, 7.8$ Hz, 2H), 6.75 (t, $J = 7.0$ Hz, 1H), 5.87 (s, 2H), 2.35 (s, 3H). Even after repeated cycles, quaternary carbons couldn't be visualized. (No improvement with relaxation delay of 2 sec). HRMS (EI) calcd for $C_{19}H_{17}NOS$ $[M]^+$ 307.1031 found 307.1022.

1-(3-Methyl-(1,1'-biphenylmethyl))-3-hydroxyoxypyridin-2-thione (12e)

Reaction of **10e** (0.08 g, 0.20 mmol) with 1M BBr_3 (0.36 mL) in dry CH_2Cl_2 (5 mL) within 48 h according to procedure **11a** afforded pure **12e** (51 mg, 70%) as olive green

color solid. ^1H NMR (400 MHz, CD_3OD) δ 7.53 (m, 1H), 7.30 (m, 2H), 7.12 (d, $J = 7.2$ Hz, 1H), 6.97 (m, 1H), 6.68 (m, 1H), 5.81 (s, 1H), 2.36 (s, 1H). ^{13}C NMR (100 MHz, CD_3OD) δ 141.53, 140.21, 138.34, 128.62, 128.48, 128.21, 127.69, 127.54, 124.03, 21.19. HRMS (EI) calcd for $\text{C}_{19}\text{H}_{17}\text{NOS}$ $[\text{M}]^+$ 307.1031 found 307.1031.

1-(2-Methyl-(1,1'-biphenylmethyl))-3-hydroxyoxypyridin-2-thione (12f)

Reaction of **10f** (0.08 g, 0.20 mmol) with 1M BBr_3 (0.36 mL) in dry CH_2Cl_2 (5 mL) within 48 h according to procedure **11a** afforded pure **12f** (49 mg, 67%) as olive green color solid. ^1H NMR (400 MHz, CD_3OD) δ 7.54 (m, 1H), 7.19 (m, 3H), 6.98 (m, 1H), 6.70 (m, 1H), 5.83 (s, 1H), 2.19 (s, 1H). ^{13}C NMR (100 MHz, CD_3OD) δ 142.14, 140.99, 135.05, 130.21, 129.58, 129.48, 127.76, 127.33, 125.66, 20.02. HRMS (EI) calcd for $\text{C}_{19}\text{H}_{17}\text{NOS}$ $[\text{M}]^+$ 307.1031 found 307.1034.

1-(4-Dimethylamino-(1,1'-biphenylmethyl))-3-hydroxyoxypyridin-2-thione (12g)

Reaction of **10g** (0.11 g, 0.33 mmol) with 1M BBr_3 (0.39 mL) in dry CH_2Cl_2 (5 mL) within 48 h according to procedure **11a** afforded pure **12g** (68 mg, 62%) as olive green color solid. ^1H NMR (400 MHz, CDCl_3) δ 8.57 (d, $J = 8.5$ Hz, 1H), 7.53 (d, $J = 8.2$ Hz, 2H), 7.46 (m, 2H), 7.33 (d, $J = 8.0$ Hz, 3H), 6.97 (d, $J = 6.8$ Hz, 1H), 6.77 (d, $J = 8.8$ Hz, 2H), 6.62 (m, 1H), 5.79 (s, 2H), 2.98 (s, 6H). ^{13}C NMR (100 MHz, CDCl_3) δ 169.71, 155.14, 150.08, 141.51, 131.92, 130.80, 129.00, 128.83, 127.99, 127.58, 126.68, 113.58, 112.62, 111.90, 60.11, 40.45. HRMS (EI) calcd for $\text{C}_{20}\text{H}_{20}\text{N}_2\text{OS}$ $[\text{M}]^+$ 336.1296 found 336.1295.

1-(4-(6-(Dimethylamino)pyridin-3-yl)benzyl)-3-hydroxyoxypyridin-2-thione (12h)

Reaction of **10h** (0.064 g, 0.18 mmol) with 1M BBr₃ (0.27 mL) in dry CH₂Cl₂ (5 mL) within 48 h according to procedure **11a** afforded pure **12h** (48 mg, 79%) as olive green color solid. ¹H NMR (400 MHz, CDCl₃) δ 8.30 (s, 1H), 7.70 (d, *J* = 8.9 Hz, 1H), 7.46 (s, 2H), 7.31 (t, *J* = 7.6 Hz, 3H), 6.98 (d, *J* = 7.8 Hz, 1H), 6.67 (m, 2H), 5.75 (s, 2H), 3.11 (s, 8H). ¹³C NMR (100 MHz, CDCl₃) δ 157.02, 143.45, 142.18, 137.74, 136.98, 132.81, 128.75, 127.56, 126.37, 123.70, 114.43, 107.03, 38.48, 29.54. HRMS (EI) calcd for C₁₉H₁₉N₃OS [M]⁺ 337.1249 found 337.1251.

1-(4-(Pyridin-4-yl)benzyl)-3-hydroxypyridin-2-thione (12i)

Reaction of **10i** (0.08 g, 0.25 mmol) with 1M BBr₃ (0.38 mL) in dry CH₂Cl₂ (5 mL) within 48 h according to procedure **11a** afforded pure **12i** (65 mg, 88%) as olive green color solid. ¹H NMR (400 MHz, CDCl₃) δ 8.65 (d, *J* = 5.3 Hz, 2H), 8.55 (s, 1H), 7.62 (d, *J* = 8.0 Hz, 2H), 7.42 (m, 5H), 6.99 (d, *J* = 7.5 Hz, 1H), 6.67 (t, *J* = 7.0 Hz, 1H), 5.85 (s, 2H). ¹³C NMR (100 MHz, CDCl₃) δ 170.05, 155.32, 150.25, 147.44, 138.22, 135.48, 130.91, 128.80, 127.55, 121.48, 113.73, 111.94, 59.91. HRMS (EI) calcd for C₁₇H₁₄N₂OS [M]⁺ 294.0827 found 294.0823.

1-Propargyl-3-methoxypyridin-2-one (13)

To a stirring solution of 3-methoxy-2-pyridinone (1.00 g, 8.00 mmol) in DMF (25 mL), was added propargyl bromide (80 wt% solution in toluene, 1.5 equiv) and K₂CO₃ (3.313 g, 24 mmol). Reaction mixture was heated to 100 °C. After overnight reaction, reaction mixture was partitioned between EtOAc (120 mL) and water (100 mL). Organic layer

was separated and washed repeatedly with water (7 X 100 mL) and brine (1 X 60 mL). Organic layer was dried on Na₂SO₄ and evaporated under vacuo to yield dark brown crude product. Column chromatography using gradient CH₂Cl₂:Acetone (max 20%) gave pure **13** (0.79 g, 60%) as a slightly brownish solid. ¹H NMR (CDCl₃, 400 MHz) δ 2.36 (1H, t, *J* = 2.8), 3.67 (3H, m), 4.66 (1H, d, *J* = 2.8), 6.05 (1H, t, *J* = 7.2), 6.50 (1H, dd, *J* = 1.6, 7.2), 7.11 (1H, dd, *J* = 1.6, 6.8); ¹³C NMR (CDCl₃, 100 MHz) δ 37.2, 55.5, 74.6, 77.3, 104.8, 112.0, 126.3, 149.4, 157.1. HRMS (EI) calcd for C₉H₉NO₂ [M]⁺ 163.0633 found 163.0636

1-Phenyltriazolylmethyl-3-methoxypyridin-2-one (14a)

13 (0.32 g, 1.951 mmol) and phenylazide (0.348 g, 2.926 mmol) were dissolved in anhydrous THF (10 mL) and stirred under argon at room temperature. Copper (I) iodide (0.011 g, 0.07 mmol) and Hunig's base (0.1 mL) were then added to the reaction mixture, and stirring continued for 4 h. The reaction mixture was diluted with CH₂Cl₂ (40 mL) and washed with 1:4 NH₄OH/saturated NH₄Cl (3 x 30 mL) and saturated NH₄Cl (30 mL). The organic layer was dried over Na₂SO₄ and concentrated *in vacuo*. The crude product was triturated with hexanes to give 510 mg (92%) of white solid **14a**. ¹H NMR (CDCl₃, 400 MHz) δ 3.58 (3H, s), 5.11 (2H, s), 5.93 (1H, t, *J* = 7.6), 6.42 (1H, d, *J* = 7.2), 7.07 (1H, d, *J* = 6.4), 7.16-7.20 (1H, m), 7.26 (2H, t, *J* = 7.6), 7.49 (2H, d, *J* = 8.0); ¹³C NMR (CDCl₃, 100 MHz) δ 44.2, 55.2, 104.7, 112.0, 119.7, 121.8, 127.9, 128.1, 129.0, 136.2, 142.8, 149.3, 157.2. HRMS (EI) calcd for C₁₅H₁₄N₄O₂ [M]⁺ 282.1117 found 282.1115.

1-(4-Dimethylamino)phenyltriazolylmethyl-3-methoxypyridin-2-one (14b)

Reaction of 4-azido-*N,N*-dimethylaniline (0.09 g, 0.61 mmol) and **13** (0.10 g, 0.61 mmol) within 4 h as described for synthesis of **14a** gave compound **14b** (0.13 g, 68 %) as a white solid. ¹H NMR (400 MHz, CDCl₃) δ 8.04 (s, 1H), 7.41 (m, 2H), 7.15 (dd, *J* = 6.9, 1.7 Hz, 1H), 6.62 (m, 2H), 6.51 (dd, *J* = 7.5, 1.6 Hz, 1H), 6.03 (m, 1H), 5.19 (s, 2H), 3.70 (s, 3H), 2.89 (s, 6H). ¹³C NMR (100 MHz, CDCl₃) δ 157.54, 150.18, 149.65, 142.60, 128.17, 126.18, 121.90, 121.43, 112.20, 111.84, 104.93, 55.55, 44.54, 40.08. HRMS (EI) calcd for C₁₇H₁₉N₅O₂ [M]⁺ 325.1539 found 325.1544.

1-Phenyltriazolylmethyl-3-hydroxypyridin-2-one (**15a**)

Reaction of **14a** (0.212 g, 0.75 mmol) and 1M BBr₃ in CH₂Cl₂ (1.5 equiv) withing 48 h as described for the synthesis of **11a** gave compound **15a** (0.123 g, 61%) as light brown solid. ¹H NMR (DMSO-*d*₆, 400 MHz) δ 5.27 (2H, s), 6.13 (1H, t, *J* = 6.4), 6.67 (1H, d, *J* = 7.2), 7.30 (1H, d, *J* = 5.6), 7.45-7.49 (1H, m), 7.57 (2H, t, *J* = 7.6), 7.87 (2H, d, *J* = 8.0), 8.73 (1H, s), 9.08 (1H, s); ¹³C NMR (100 MHz, CDCl₃) δ 136.59, 129.60, 128.94, 122.29, 120.62, 107.99, 29.29. (quaternary cabons were not seen). HRMS (EI) calcd for C₁₄H₁₂N₄O₂ [M]⁺ 268.0960 found 268.0967.

1-(4-Dimethylamino)phenylltriazolylmethyl-3-hydroxypyridin-2-one (**15b**)

Reaction of **14b** (0.045 g, 0.14 mmol) and 1M BBr₃ in CH₂Cl₂ (0.22 mL, 1.5 equiv) withing 48 h as described for the synthesis of **11a** gave compound **15b** (0.033 g, 77%) as light brown solid. ¹H NMR (400 MHz, CDCl₃) δ 8.08 (s, 1H), 7.48 (dd, *J* = 19.9, 8.4 Hz, 2H), 7.18 (d, *J* = 6.7 Hz, 1H), 6.69 (ddd, *J* = 25.8, 24.8, 7.5 Hz, 4H), 6.16 (t, *J* = 6.9 Hz, 1H), 5.31 (s, 2H), 2.98 (m, 6H). ¹³C NMR (100 MHz, CDCl₃) δ 158.35, 150.52, 146.68,

142.48, 127.10, 126.44, 122.06, 121.88, 121.76, 112.12, 107.14, 44.66, 40.33. HRMS (EI) calcd for $C_{16}H_{17}N_5O_2 [M]^+$ 311.1382 found 311.1386.

1-Phenyltriazolylmethyl-3-methoxypyridin-2-thione (16a)

Reaction of **14a** (0.295 g, 1.04 mmol) and Lawesson's reagent (0.252 g, 0.624 mmol) in toluene (15 mL) within 12 h as described for the synthesis of **10a** gave compound **16a** (0.291 g, 94%) as yellow solid. 1H NMR ($CDCl_3$, 400 MHz) δ 3.90 (3H, s), 6.04 (2H, s), 6.62-6.68 (2H, m), 7.38-7.42 (1H, m), 7.48 (2H, t, $J = 7.2$), 7.68 (2H, d, $J = 8.0$), 7.82 (1H, d, $J = 4.8$), 8.53 (1H, s); ^{13}C NMR ($CDCl_3$, 100 MHz) δ 50.9, 56.4, 110.0, 112.0, 120.2, 122.4, 128.5, 129.3, 132.2, 136.4, 141.9, 158.7, 171.5 HRMS (EI) calcd for $C_{15}H_{14}N_4O_2 [M]^+$ 282.1117 found 282.1115. HRMS (EI) calcd for $C_{15}H_{14}N_4OS [M]^+$ 298.0888 found 298.0888.

1-(4-Dimethylamino)phenyltriazolylmethyl-3-methoxypyridin-2-thione (16b)

Reaction of **14b** (0.078 g, 0.248 mmol) and Lawesson's reagent (0.06 g, 0.15 mmol) in toluene (8 mL) within 12 h as described for the synthesis of **10a** gave compound **16b** (0.07 g, 84%) as yellow solid. 1H NMR (400 MHz, $CDCl_3$) δ 8.36 (s, 1H), 7.81 (dd, $J = 6.4, 1.5$ Hz, 1H), 7.46 (m, 2H), 6.66 (m, 4H), 6.01 (s, 2H), 3.87 (s, 3H), 2.97 (s, 6H). ^{13}C NMR (100 MHz, $CDCl_3$) δ 171.82, 158.93, 150.44, 141.54, 132.44, 126.29, 122.49, 121.77, 112.10, 112.03, 110.14, 56.65, 51.20, 40.29. HRMS (EI) calcd for $C_{17}H_{19}N_5OS [M]^+$ 314.1310 found 314.1304.

1-Phenyltriazolylmethyl-3-hydroxypyridin-2-thione (17a)

Reaction of **16a** (0.28 g, 0.93 mmol) and 1M BBr₃ in CH₂Cl₂ (1.5 equiv) within 48 h as described for the synthesis of **11a** gave compound **17a** (0.178 g, 67%) as olive green solid. ¹H NMR (400 MHz, CDCl₃) δ 8.43 (d, *J* = 16.6 Hz, 1H), 8.39 (s, 1H), 7.79 (dd, *J* = 6.6, 1.3 Hz, 1H), 7.69 (m, 2H), 7.46 (m, 3H), 6.97 (dd, *J* = 7.7, 1.2 Hz, 1H), 6.69 (dd, *J* = 7.6, 6.8 Hz, 1H), 5.94 (s, 2H). ¹³C NMR (100 MHz, CDCl₃) δ 168.59, 155.12, 141.60, 136.66, 131.65, 129.69, 128.99, 122.57, 120.60, 114.04, 112.47, 77.30, 76.99, 76.67, 52.08. HRMS (EI) calcd for C₁₄H₁₂N₄OS [M]⁺ 284.0730 found 284.0732.

1-(4-Dimethylamino)phenylltriazolylmethyl-3-hydroxypyridin-2-thione (17b)

Reaction of **16b** (0.07 g, 0.212 mmol) and 1M BBr₃ in CH₂Cl₂ (0.64 mL, 1.5 equiv) within 48 h as described for the synthesis of **11a** gave compound **17b** (0.032 g, 48%) as olive green solid. ¹H NMR (400 MHz, CDCl₃) δ 8.42 (s, 1H), 8.29 (d, *J* = 11.5 Hz, 1H), 7.79 (d, *J* = 6.4 Hz, 1H), 7.50 (m, 2H), 6.98 (dd, *J* = 36.5, 28.9 Hz, 2H), 6.72 (m, 3H), 5.94 (s, 2H), 3.01 (d, *J* = 2.7 Hz, 6H). ¹³C NMR (100 MHz, CDCl₃) δ 155.09, 150.66, 141.13, 131.72, 127.68, 126.27, 122.45, 121.97, 114.04, 112.52, 112.16, 52.21, 40.41. HRMS (EI) calcd for C₁₆H₁₇N₅OS [M]⁺ 327.1154 found 327.1154.

Representative Procedure for Conversion of Azidoalkanol to azidoalkyl methanesulfonate 19 –

2-Azidoethyl methanesulfonate (19a) –

To a solution of compound 2-azidoethanol (1.00 g, 11.49 mmol) in THF (25 mL) and triethylamine (Et₃N) (2.418 mL, 17.24 mmol) was added mesyl chloride (1.328 mL, 17.24 mmol) at 0 °C, and the mixture was allowed to warm to room temperature. Stirring

continued for 3 h, during which TLC revealed a quantitative conversion into a higher R_f product. CH_2Cl_2 (70 mL) and saturated sodium bicarbonate (50 mL) were added, and the two layers were separated. The organic layer was washed with sodium bicarbonate (2×50 mL), saturated brine (45 mL) and dried over Na_2SO_4 . Solvent was evaporated off to give crude compound **19a** (1.70 g) as a colorless oil, which was used for next step without further purification.

2-Azidopropyl methanesulfonate (19b) –

Reaction of 3-azidopropanol (1.00 g, 9.90 mmol) and mesyl chloride (1.14 mL, 14.85 mmol) within 3 h as described for synthesis of **19a** gave compound **19b** (1.18 g) as a crude colorless oil.

2-Azidobutyl methanesulfonate (19c) –

Reaction of 4-azidobutanol (0.80 g, 6.95 mmol) and mesyl chloride (1.48 mL, 10.43 mmol) within 3 h as described for synthesis of **19a** gave compound **19b** (1.33 g) as a crude colorless oil.

2-Azidopentyl methanesulfonate (19d) –

Reaction of 5-azidopentanol (1.1 g, 8.53 mmol) and mesyl chloride (0.98 mL, 12.79 mmol) within 3 h as described for synthesis of **19a** gave compound **19d** (1.54 g) as a crude colorless oil.

2-Azidoethyl methanesulfonate (19e) –

Reaction of 6-azidoethanol (0.74 g, 5.22 mmol) and mesyl chloride (0.61 mL, 7.83 mmol) within 3 h as described for synthesis of **19a** gave compound **19e** (0.87 g) as a crude colorless oil.

2-Azidoethyl methanesulfonate (19f) –

Reaction of 7-azidoheptanol (0.55 g, 3.49 mmol) and mesyl chloride (0.41 mL, 5.30 mmol) within 3 h as described for synthesis of **19a** gave compound **19f** (0.79 g) as a crude colorless oil.

Representative procedure for synthesis of 1-(2-azidoalkyl)-3-methoxypyridin-2-ones

1-(2-Azidoethyl)-3-methoxypyridin-2-one (20a)

3-methoxypyridin-2-one (0.40 g, 3.20 mmol), **19a** (0.79 g, 4.80 mmol), and K₂CO₃ (1.32 g, 9.60 mmol) stirred overnight in THF at reflux temperature. Reaction mixture was cooled down to room temperature. Reaction mixture was partitioned between CH₂Cl₂ (60 mL) and water (50 mL). Organic layer washed with water (2 x 35 mL), brine (1 x 30 mL). Organic layer dried on Na₂SO₄ and evaporated in vacuo. Crude product was purified by flash chromatography with stepwise gradient of CH₂Cl₂ and acetone (max 15%) to give 0.34 mg of **20a** (55%) as colorless oil. ¹H NMR (400 MHz, CDCl₃) δ 6.77 (dd, *J* = 6.9, 1.6 Hz, 1H), 6.48 (dd, *J* = 7.5, 1.6 Hz, 1H), 5.96 (m, 1H), 3.91 (m, 2H), 3.62 (s, 3H), 3.52 (m, 2H). ¹³C NMR (100 MHz, CDCl₃) δ 157.39, 149.41, 128.61, 112.16, 104.37, 55.36, 49.00, 48.91. HRMS (EI) calcd for C₈H₁₀N₄O₂ [M]⁺ 194.0804 found 194.0816.

1-(3-Azidopropyl)-3-benzyloxypyridin-2-one (20b)

Reaction of 3-benzyloxypyridin-2-one (0.40 g, 1.99 mmol) and **19b** (0.53 g, 2.98 mmol) within 16 h as described for synthesis of **20a** gave compound **20b** (0.30 g, 53%) as a colorless oil. ^1H NMR (300 MHz, CDCl_3) δ 7.28 (m, 5H), 6.84 (dd, $J = 6.9, 1.6$ Hz, 1H), 6.60 (dd, $J = 7.4, 1.5$ Hz, 1H), 5.98 (t, $J = 7.1$ Hz, 1H), 3.97 (t, $J = 6.8$ Hz, 2H), 3.28 (t, $J = 6.5$ Hz, 2H), 1.98 (p, $J = 6.7$ Hz, 2H). ^{13}C NMR (75 MHz, CDCl_3) δ 157.78, 148.65, 135.93, 128.85, 128.24, 127.69, 127.03, 115.16, 104.53, 70.39, 48.14, 47.06, 27.66. HRMS (EI) calcd for $\text{C}_{15}\text{H}_{16}\text{N}_4\text{O}_2$ $[\text{M}]^+$ 284.1273 found 284.1271.

1-(4-Azidobutyl)-3-benzyloxypyridin-2-one (20c)

Reaction of 3-benzyloxypyridin-2-one (0.40 g, 1.99 mmol) and **19c** (0.58 g, 2.98 mmol) within 16 h as described for synthesis of **20a** gave compound **20c** (0.36 g, 62%) as a colorless oil. ^1H NMR (400 MHz, CDCl_3) δ 7.22 (m, 5H), 6.78 (dd, $J = 6.9, 1.7$ Hz, 1H), 6.54 (dd, $J = 7.4, 1.7$ Hz, 1H), 5.91 (m, 1H), 4.96 (s, 2H), 3.85 (t, $J = 7.2$ Hz, 2H), 3.17 (t, $J = 6.8$ Hz, 2H), 1.71 (m, 2H), 1.48 (m, 2H). ^{13}C NMR (100 MHz, CDCl_3) δ 157.52, 148.27, 135.78, 128.37, 127.98, 127.42, 126.82, 114.92, 104.32, 70.09, 50.43, 48.46, 25.83, 25.42. HRMS (EI) calcd for $\text{C}_{16}\text{H}_{18}\text{N}_4\text{O}_2$ $[\text{M}]^+$ 298.1430 found 298.1446.

1-(5-Azidopentyl)-3-benzyloxypyridin-2-one (20d)

Reaction of 3-benzyloxypyridin-2-one (0.50 g, 2.49 mmol) and **19d** (0.62 g, 2.98 mmol) within 16 h as described for synthesis of **20a** gave compound **20d** (0.49 g, 63%) as a colorless oil. ^1H NMR (400 MHz, CDCl_3) δ 7.35 (d, $J = 8.0$ Hz, 2H), 7.23 (m, 3H), 6.81 (m, 1H), 6.56 (m, 1H), 5.94 (m, 1H), 5.01 (s, 2H), 3.85 (m, 2H), 3.18 (m, 2H), 1.71 (m,

2H), 1.54 (m, 2H), 1.32 (m, 2H). ^{13}C NMR (100 MHz, CDCl_3) δ 157.68, 148.47, 135.98, 128.60, 128.12, 127.53, 126.93, 115.09, 104.32, 70.27, 50.77, 49.21, 28.19, 28.06, 23.37. HRMS (EI) calcd for $\text{C}_{17}\text{H}_{20}\text{N}_4\text{O}_2$ $[\text{M}]^+$ 312.1586 found 312.1589.

1-(6-Azidohexyl)-3-benzyloxypyridin-2-one (20e)

Reaction of 3-benzyloxypyridin-2-one (0.50 g, 2.49 mmol) and **19d** (0.66 g, 2.98 mmol) within 16 h as described for synthesis of **20a** gave compound **20e** (0.48 g, 60%) as a colorless oil. ^1H NMR (400 MHz, CDCl_3) δ 7.15 (m, 5H), 6.65 (dd, $J = 7.4, 1.8$ Hz, 1H), 6.45 (dd, $J = 7.4, 1.8$ Hz, 1H), 5.81 (t, $J = 7.1$ Hz, 1H), 4.92 (s, 2H), 3.76 (t, $J = 6.8$ Hz, 2H), 3.05 (t, $J = 6.8$ Hz, 2H), 1.58 (m, 2H), 1.40 (m, 2H), 1.90 (m, 4H). ^{13}C NMR (100 MHz, CDCl_3) δ 157.55, 148.25, 135.95, 128.60, 128.10, 126.95, 126.50, 115.05, 104.90, 70.50, 51.05, 49.20, 28.65, 28.50, 26.20, 25.80. HRMS (FAB) calcd for $\text{C}_{18}\text{H}_{23}\text{N}_4\text{O}_2$ $[\text{M}+\text{H}]^+$ 327.1821 found 327.1848.

1-(7-Azidoheptyl)-3-benzyloxypyridin-2-one (20f)

Reaction of 3-benzyloxypyridin-2-one (0.79 g, 3.38 mmol) and **19f** (0.81 g, 4.05 mmol) within 16 h as described for synthesis of **20a** gave compound **20f** (0.55 g, 48%) as a colorless oil. ^1H NMR (400 MHz, CDCl_3) δ 7.42 (dd, $J = 7.8, 1.0$ Hz, 2H), 7.31 (m, 3H), 6.85 (dd, $J = 6.9, 1.7$ Hz, 1H), 6.61 (dd, $J = 7.4, 1.7$ Hz, 1H), 5.99 (m, 1H), 5.09 (s, 2H), 3.93 (m, 2H), 3.23 (t, $J = 6.9$ Hz, 2H), 1.74 (m, 2H), 1.55 (m, 2H), 1.34 (m, 6H). ^{13}C NMR (100 MHz, CDCl_3) δ 158.32, 149.19, 136.63, 129.15, 128.74, 128.13, 127.52, 115.66, 104.69, 94.66, 70.96, 51.62, 50.03, 29.22, 28.98, 26.77, 26.72.

Representative procedure for synthesis of **21**

1-Phenyltriazolyethyl-3-methoxypyridin-2-one (**21a**)

Phenylacetylene (0.167 g, 1.63 mmol) and **20a** (0.265 g, 1.36 mmol) were dissolved in anhydrous THF (10 mL) and stirred under argon at room temperature. Copper (I) iodide (0.011 g, 0.07 mmol) and Hunig's base (0.1 mL) were then added to the reaction mixture, and stirring continued for 4 h. The reaction mixture was diluted with CH₂Cl₂ (40 mL) and washed with 1:4 NH₄OH/saturated NH₄Cl (3 x 30 mL) and saturated NH₄Cl (30 mL). The organic layer was dried over Na₂SO₄ and concentrated *in vacuo*. The crude product was triturated with hexanes to give 366 mg (91%) of white solid **21a**. ¹H NMR (400 MHz, CDCl₃) δ 7.68 (s, 1H), 7.47 (d, *J* = 7.5 Hz, 2H), 7.11 (m, 3H), 6.43 (d, *J* = 7.4 Hz, 1H), 6.35 (dd, *J* = 6.8, 0.9 Hz, 1H), 5.78 (t, *J* = 7.2 Hz, 1H), 4.57 (t, *J* = 5.7 Hz, 2H), 4.25 (t, *J* = 5.6 Hz, 2H), 3.53 (s, 3H). ¹³C NMR (100 MHz, CDCl₃) δ 157.70, 149.08, 147.21, 129.40, 128.30, 128.08, 127.80, 125.00, 120.91, 113.02, 105.44, 55.15, 49.72, 47.44. HRMS (EI) calcd for C₁₆H₁₆N₄O₂ [M]⁺ 296.1273 found 296.1268.

1-Phenyltriazolylpropyl-3-benzyloxypyridin-2-one (**21b**)

Reaction of phenylacetylene (0.127 g, 1.25 mmol) and **20b** (0.295 g, 1.04 mmol) within 4 h as described for synthesis of **21a** gave compound **21b** (0.31 g, 77%) as a white solid. ¹H NMR (400 MHz, CDCl₃) δ 8.00 (s, 1H), 7.77 (d, *J* = 7.3 Hz, 2H), 7.27 (m, 8H), 6.88 (d, *J* = 5.7 Hz, 1H), 6.57 (d, *J* = 6.4 Hz, 1H), 5.95 (t, *J* = 7.1 Hz, 1H), 4.99 (s, 2H), 4.34 (t, *J* = 6.4 Hz, 2H), 3.94 (t, *J* = 6.4 Hz, 2H), 2.32 (m, 2H). ¹³C NMR (100 MHz, CDCl₃) δ 157.92, 148.47, 147.30, 135.73, 130.26, 128.81, 128.49, 128.22, 127.76, 127.71, 127.01,

125.33, 120.16, 114.95, 104.83, 70.33, 47.00, 46.48, 29.30. HRMS (EI) calcd for $C_{23}H_{22}N_4O_2 [M]^+$ 386.1743 found 386.1734.

1-Phenyltriazolylbutyl-3-benzyloxypyridin-2-one (21c)

Reaction of phenylacetylene (0.124 g, 1.21 mmol) and **20c** (0.30 g, 1.01 mmol) within 4 h as described for synthesis of **21a** gave compound **21c** (0.31 g, 77%) as a white solid. 1H NMR (400 MHz, $CDCl_3$) δ 7.83 (s, 1H), 7.76 (m, 2H), 7.26 (m, 8H), 6.76 (dd, $J = 6.9$, 1.5 Hz, 1H), 6.56 (dd, $J = 7.4$, 1.5 Hz, 1H), 5.91 (t, $J = 7.1$ Hz, 1H), 4.99 (s, 2H), 4.31 (m, 2H), 3.89 (t, $J = 7.1$ Hz, 2H), 1.85 (m, 2H), 1.67 (m, 2H). ^{13}C NMR (100 MHz, $CDCl_3$) δ 157.71, 148.38, 147.20, 135.83, 130.29, 128.45, 128.41, 128.16, 127.68, 127.63, 126.96, 125.25, 119.87, 114.99, 104.60, 70.26, 49.11, 48.02, 26.78, 25.65. HRMS (EI) calcd for $C_{24}H_{24}N_4O_2 [M]^+$ 400.1899 found 400.1888.

1-Phenyltriazolylpentyl-3-benzyloxypyridin-2-one (21d)

Reaction of phenylacetylene (0.04 g, 0.32 mmol) and **20d** (0.10 g, 0.32 mmol) within 4 h as described for synthesis of **21a** gave compound **21d** (0.092 g, 72%) as a white solid. 1H NMR (400 MHz, $CDCl_3$) δ 7.78 (m, 3H), 7.30 (m, 8H), 6.79 (d, $J = 6.8$ Hz, 1H), 6.57 (d, $J = 7.3$ Hz, 1H), 5.94 (t, $J = 7.1$ Hz, 1H), 5.02 (s, 2H), 4.31 (t, $J = 7.0$ Hz, 2H), 3.87 (t, $J = 7.2$ Hz, 2H), 1.91 (m, 2H), 1.74 (m, 2H), 1.30 (m, 2H). ^{13}C NMR (100 MHz, $CDCl_3$) δ 157.80, 148.57, 147.39, 136.02, 130.44, 128.64, 128.56, 128.27, 127.81, 127.71, 127.05, 125.40, 119.57, 115.12, 104.49, 70.40, 49.71, 49.06, 29.42, 28.03, 23.05.

1-Phenyltriazolylhexyl-3-benzyloxypyridin-2-one (21e)

Reaction of phenylacetylene (0.80 g, 0.78 mmol) and **20e** (0.21 g, 0.65 mmol) within 4 h as described for synthesis of **21a** gave compound **21e** (0.16 g, 56%) as a white solid. NMR (400 MHz, CDCl₃) δ 7.66 (m, 3H), 7.20 (m, 8H), 6.68 (dd, J = 6.9, 1.5 Hz, 1H), 6.46 (dd, J = 7.4, 1.5 Hz, 1H), 5.82 (t, J = 7.1 Hz, 1H), 4.92 (s, 2H), 4.18 (t, J = 6.8 Hz, 2H), 3.75 (t, J = 6.8 Hz, 2H), 1.76 (m, 2H), 1.56 (m, 2H), 1.19 (m, 4H). ¹³C NMR (100 MHz, CDCl₃) δ 157.64, 148.46, 147.27, 135.95, 130.36, 128.57, 128.48, 128.19, 127.72, 127.60, 126.96, 125.32, 119.37, 115.02, 104.37, 70.45, 50.03, 49.35, 29.90, 28.66, 25.87, 25.78. HRMS (FAB) calcd for C₂₆H₂₉N₄O₂ [M+H]⁺ 429.2290 found 429.2291.

1-Phenyltriazolylheptyl-3-benzyloxypyridin-2-one (21f)

Reaction of phenylacetylene (0.90 g, 0.88 mmol) and **20f** (0.25 g, 0.735 mmol) within 4 h as described for synthesis of **21a** gave compound **21f** (0.23 g, 63%) as a white solid. ¹H NMR (400 MHz, CDCl₃) δ 7.79 (m, 3H), 7.31 (m, 8H), 6.83 (dd, J = 6.9, 1.7 Hz, 1H), 6.60 (dd, J = 7.4, 1.7 Hz, 1H), 5.97 (t, J = 7.1 Hz, 1H), 5.07 (s, 2H), 4.35 (t, J = 7.1 Hz, 2H), 3.91 (m, 2H), 1.88 (m, 2H), 1.71 (m, 2H), 1.32 (d, J = 10.0 Hz, 6H). ¹³C NMR (100 MHz, CDCl₃) δ 158.31, 149.13, 147.92, 136.57, 130.93, 129.15, 129.04, 128.74, 128.28, 128.15, 127.51, 125.90, 125.86, 119.75, 115.60, 104.79, 70.92, 50.52, 49.90, 30.42, 29.13, 28.72, 26.53, 26.46. HRMS (FAB) calcd for C₂₇H₃₁N₄O₂ [M+H]⁺ 443.2447 found 443.2494.

1-Phenyltriazolylethyl-3-hydroxypyridin-2-one (22a)

To a solution of **21a** (0.10 g, 0.338 mmol) in dry CH₂Cl₂ (8 mL) was slowly added 1M BBr₃ (1.2 equiv) at -30 °C under argon atmosphere. The reaction mixture was stirred for

48 h at room temperature. The mixture was again cooled to -30 °C and the MeOH (5 mL) was slowly added to the mixture. After evaporation of solvent, the residue was adjusted to pH 7 with 1M NaOH and then extracted with CHCl₃ (30 mL X 3). The combined organic layer dried over Na₂SO₄ to give 79 mg (83%) of **22a** as slightly brownish solid without any further purification required. ¹H NMR (400 MHz, DMSO) δ 9.11 (s, 1H), 8.51 (s, 1H), 7.78 (d, *J* = 7.3 Hz, 2H), 7.43 (t, *J* = 7.6 Hz, 2H), 7.31 (t, *J* = 7.3 Hz, 1H), 6.75 (d, *J* = 5.9 Hz, 1H), 6.64 (d, *J* = 6.0 Hz, 1H), 5.95 (t, *J* = 7.0 Hz, 1H), 4.76 (t, *J* = 5.5 Hz, 2H), 4.42 (t, *J* = 5.6 Hz, 2H). ¹³C NMR (100 MHz, DMSO) δ 158.25, 147.17, 146.77, 131.11, 129.34, 128.41, 128.31, 125.54, 122.23, 115.38, 105.76, 49.42, 48.33. HRMS (EI) calcd for C₁₅H₁₄N₄O₂ [M]⁺ 282.1117 found 282.1120.

1-Phenyltriazolylpropyl-3-hydroxypyridin-2-one (**22b**)

To a solution of **21b** (0.29 g, 1.01 mmol) in CH₂Cl₂:EtOAc:MeOH (2:2:1, 10 mL) was added 10% Pd on carbon (15 mg). Reaction was stirred under balloon hydrogen pressure for 5 h. Reaction mixture was filtered and solvent was evaporated. Column chromatography using gradient CH₂Cl₂:Acetone (max 20%) gave pure **22b** (0.19 g, 64%) as a slightly brownish solid. ¹H NMR (400 MHz, DMSO) δ 9.03 (s, 1H), 8.62 (s, 1H), 7.82 (d, *J* = 7.6 Hz, 2H), 7.38 (m, 3H), 7.15 (d, *J* = 6.6 Hz, 1H), 6.68 (d, *J* = 6.4 Hz, 1H), 6.11 (t, *J* = 6.7 Hz, 1H), 4.43 (t, *J* = 6.4 Hz, 2H), 3.99 (m, 2H), 2.27 (m, 2H). ¹³C NMR (100 MHz, CDCl₃) δ 147.49, 129.71, 128.52, 127.99, 125.29, 120.42, 107.98, 66.61, 47.10, 29.27. (expected aromatic carbons = 11; quaternary carbons can't be seen even after repeated cycles) HRMS (EI) calcd for C₁₆H₁₆N₄O₂ [M]⁺ 296.1273 found 296.1274.

1-Phenyltriazolylbutyl-3-hydroxypyridin-2-one (22c)

Reaction of **21c** (0.25 g, 0.62 mmol) in anhydrous THF as described for synthesis of **22b** gave **22c** (0.12 g, 63%) of pure product. ^1H NMR (400 MHz, CDCl_3) δ 7.79 (m, 3H), 7.41 (t, $J = 7.6$ Hz, 2H), 7.32 (t, $J = 7.4$ Hz, 1H), 6.76 (m, 3H), 6.13 (t, $J = 7.2$ Hz, 1H), 4.45 (t, $J = 6.8$ Hz, 2H), 4.02 (t, $J = 7.1$ Hz, 2H), 1.99 (m, 2H), 1.82 (m, 2H). ^{13}C NMR (100 MHz, CDCl_3) δ 158.47, 147.63, 146.62, 130.41, 128.69, 127.99, 126.60, 125.53, 119.80, 114.15, 107.10, 49.38, 48.57, 27.02, 26.01. HRMS (EI) calcd for $\text{C}_{17}\text{H}_{18}\text{N}_4\text{O}_2$ $[\text{M}]^+$ 310.1430 found 310.1425.

1-Phenyltriazolylpentyl-3-hydroxypyridin-2-one (22d)

Reaction of **21d** (0.085 g, 0.20 mmol) in anhydrous THF as described for synthesis of **22b** gave **22d** (0.045 g, 68%) of pure product. ^1H NMR (400 MHz, DMSO) δ 8.56 (s, 1H), 7.82 (d, $J = 8.1$ Hz, 2H), 7.43 (t, $J = 7.7$ Hz, 2H), 7.32 (t, $J = 7.4$ Hz, 1H), 7.10 (dd, $J = 6.8, 1.6$ Hz, 1H), 6.65 (dd, $J = 7.2, 1.5$ Hz, 1H), 6.05 (t, $J = 7.0$ Hz, 1H), 4.38 (t, $J = 7.0$ Hz, 2H), 3.89 (t, $J = 7.2$ Hz, 2H), 1.89 (m, 2H), 1.67 (m, 2H), 1.25 (m, 2H). ^{13}C NMR (100 MHz, CDCl_3) δ 158.44, 147.67, 146.61, 130.51, 128.72, 128.01, 126.71, 125.57, 119.54, 113.81, 106.86, 49.86, 49.38, 29.58, 28.31, 23.19. HRMS (FAB) calcd for $\text{C}_{18}\text{H}_{21}\text{N}_4\text{O}_2$ $[\text{M}+\text{H}]^+$ 325.1664 found 325.1683.

1-Phenyltriazolylhexyl-3-hydroxypyridin-2-one (22e)

Reaction of **21e** (0.15 g, 0.35 mmol) in anhydrous THF as described for synthesis of **22b** gave **22e** (0.081 g, 69%) of pure product. ^1H NMR (400 MHz, CDCl_3) δ 7.81 (m, 3H), 7.42 (m, 2H), 7.32 (m, 1H), 6.77 (m, 2H), 6.12 (t, $J = 7.1$ Hz, 1H), 4.38 (t, $J = 7.1$ Hz,

2H), 3.95 (m, 2H), 1.95 (m, 2H), 1.76 (d, $J = 7.0$ Hz, 2H), 1.39 (m, 4H). ^{13}C NMR (100 MHz, CDCl_3) δ 158.20, 147.25, 146.40, 130.30, 128.60, 127.85, 126.65, 125.40, 119.65, 113.90, 106.80, 50.20, 49.60, 30.05, 28.95, 26.00, 25.90. HRMS (FAB) calcd for $\text{C}_{19}\text{H}_{23}\text{N}_4\text{O}_2$ $[\text{M}+\text{H}]^+$ 339.1821 found 339.1814.

1-Phenyltriazolylheptyl-3-hydroxypyridin-2-one (22f)

Reaction of **21f** (0.22 g, 0.50 mmol) in anhydrous THF as described for synthesis of **22b** gave **22f** (0.13 g, 74%) of pure product. ^1H NMR (400 MHz, DMSO) δ 8.91 (s, 1H), 8.57 (s, 1H), 7.82 (d, $J = 7.4$ Hz, 2H), 7.42 (t, $J = 7.6$ Hz, 2H), 7.31 (t, $J = 7.3$ Hz, 1H), 7.09 (d, $J = 6.6$ Hz, 1H), 6.64 (d, $J = 7.0$ Hz, 1H), 6.04 (t, $J = 6.9$ Hz, 1H), 4.36 (t, $J = 7.0$ Hz, 2H), 3.86 (t, $J = 7.2$ Hz, 2H), 1.83 (m, 2H), 1.61 (m, 2H), 1.26 (m, 6H). ^{13}C NMR (100 MHz, CDCl_3) δ 158.80, 147.89, 147.00, 130.88, 129.05, 128.30, 127.12, 125.87, 119.83, 114.13, 107.10, 50.48, 50.05, 30.37, 29.20, 28.67, 26.46, 26.42. HRMS (FAB) calcd for $\text{C}_{20}\text{H}_{25}\text{N}_4\text{O}_2$ $[\text{M}+\text{H}]^+$ 353.1977 found 353.1992.

1-Phenyltriazolylethyl-3-methoxypyridin-2-thione (23)

To a stirring solution of Lawesson's reagent (0.075 g, 0.185 mmol) in toluene (10 mL), was added starting material **21a** (0.10g, 0.33 mmol). Reaction mixture was heated to reflux temperature. After overnight reaction, solvent was evaporated under reduced pressure. Crude product was dissolved in small amount of CH_2Cl_2 to load onto preparative-TLC and eluted with CHCl_3 :Acetone:EtOH (10:1:0.2) to give pure yellow solid **23** (0.07 g, 68%). ^1H NMR (400 MHz, CDCl_3) δ 7.69 (d, $J = 7.4$ Hz, 2H), 7.56 (s, 1H), 7.35 (t, $J = 7.5$ Hz, 2H), 7.28 (m, 1H), 6.97 (d, $J = 6.6$ Hz, 1H), 6.62 (d, $J = 7.8$ Hz,

1H), 6.37 (m, 1H), 5.13 (t, $J = 5.6$ Hz, 2H), 5.03 (t, $J = 5.6$ Hz, 2H), 3.86 (s, 3H). ^{13}C NMR (100 MHz, CDCl_3) δ 171.92, 158.94, 147.52, 132.68, 129.92, 128.69, 128.14, 125.43, 120.96, 111.72, 110.22, 56.72, 56.63, 46.38. HRMS (EI) calcd for $\text{C}_{16}\text{H}_{16}\text{N}_4\text{OS}$ $[\text{M}]^+$ 312.1045 found 312.1039.

1-Phenyltriazolylethyl-3-hydroxypyridin-2-thione (**24**)

Reaction of **23** (0.062 g, 0.198 mmol) and 1M BBr_3 in CH_2Cl_2 (0.218 mmol) within 48 h as described for synthesis of **11a** gave compound **24** (0.055 g, 93%) as a dark violet solid. ^1H NMR (400 MHz, CDCl_3) δ 8.40 (s, 1H), 7.73 (d, $J = 7.3$ Hz, 2H), 7.51 (s, 1H), 7.40 (t, $J = 7.5$ Hz, 2H), 7.33 (t, $J = 7.3$ Hz, 1H), 6.95 (dd, $J = 9.2, 7.2$ Hz, 2H), 6.46 (m, 1H), 5.08 (m, 4H). ^{13}C NMR (100 MHz, CDCl_3) δ 168.47, 155.10, 147.75, 132.00, 129.82, 128.77, 128.30, 125.53, 120.90, 113.66, 112.61, 57.45, 46.41. HRMS (EI) calcd for $\text{C}_{15}\text{H}_{14}\text{N}_4\text{OS}$ $[\text{M}]^+$ 298.0888 found 298.0888.

1-Phenyltriazolylpropyl-3-hydroxypyridin-2-thione (**25b**)

22b (0.062 g, 0.21 mmol) was ground together with P_4S_{10} (0.047g, 0.105 mmol) in mortar and pestle to form grey powder. The powder was stirred under argon in a flask fitted with condenser and heated to 175°C for 2 h. The reaction flask was covered with aluminium foil during reaction. After 2h of reaction, flask was cooled down to room temperature. 25 mL of CH_2Cl_2 :MeOH (10%) mixtures was added and stirred for 15 min. This reaction mixture then washed with water (2 X 30 mL). Organic layer dried with Na_2SO_4 and evaporated to yield crude product which was purified by prep-TLC (Eluent - CH_2Cl_2 :MeOH (8%) to give **25b** (0.04 g, 60%) as olive green solid. ^1H NMR (400

MHz, CDCl₃) δ 8.47 (s, 1H), 7.82 (m, 3H), 7.50 (d, J = 6.5 Hz, 1H), 7.43 (t, J = 7.5 Hz, 2H), 7.34 (t, J = 7.4 Hz, 1H), 6.97 (m, 1H), 6.66 (m, 1H), 4.62 (t, J = 6.9 Hz, 2H), 4.48 (m, 2H). ¹³C NMR (100 MHz, CDCl₃) δ 168.59, 155.22, 148.03, 131.85, 130.17, 128.84, 128.29, 125.61, 119.84, 113.87, 112.28, 54.99, 46.95, 28.02. HRMS (EI) calcd for C₁₆H₁₆N₄OS [M]⁺ 312.1045 found 312.1060.

1-Phenyltriazolylbutyl-3-hydroxypyridin-2-thione (25c)

Reaction of **22c** (0.055 g, 0.18 mmol) and P₄S₁₀ (0.051 g, 0.115 mmol) under neat conditions as described for synthesis of **25b** gave compound **25c** (0.032 g, 55%) as a olive green solid. δ 8.50 (s, 1H), 7.81 (m, 3H), 7.36 (m, 4H), 6.94 (d, J = 7.6 Hz, 1H), 6.62 (t, J = 6.8 Hz, 1H), 4.54 (t, J = 7.6 Hz, 2H), 4.46 (t, J = 6.4 Hz, 2H), 2.03 (m, 4H). ¹³C NMR (100 MHz, CDCl₃) δ 168.51, 155.08, 147.73, 131.02, 130.36, 128.79, 128.13, 125.58, 119.91, 113.87, 112.10, 56.96, 49.41, 27.02, 25.08. HRMS (EI) calcd for C₁₇H₁₈N₄OS [M]⁺ 326.1201 found 326.1200.

1-Phenyltriazolylpentyl-3-hydroxypyridin-2-thione (25d)

Reaction of **22d** (0.025 g, 0.077 mmol) and P₄S₁₀ (0.020 g, 0.046 mmol) under neat conditions as described for synthesis of **25b** gave compound **25d** (0.019 g, 73%) as a olive green solid. ¹H NMR (400 MHz, DMSO) δ 8.55 (d, J = 2.9 Hz, 2H), 7.83 (t, J = 7.8 Hz, 3H), 7.43 (q, J = 7.4 Hz, 2H), 7.32 (t, J = 6.6 Hz, 1H), 7.08 (m, 1H), 6.92 (dd, J = 31.0, 6.8 Hz, 1H), 6.81 (m, 1H), 4.51 (m, 2H), 4.41 (t, J = 7.0 Hz, 2H), 1.89 (m, 4H), 1.32 (m, 2H). ¹³C NMR (100 MHz, CDCl₃) δ 168.37, 155.10, 147.66, 131.04, 130.46,

128.75, 128.05, 125.57, 119.68, 113.69, 111.96, 57.73, 49.73, 29.47, 27.12, 23.04.

HRMS (EI) calcd for $C_{18}H_{20}N_4OS$ $[M]^+$ 340.1358 found 326.1364.

1-Phenyltriazolylhexyl-3-hydroxypyridin-2-thione (25e)

Reaction of **22e** (0.18 g, 0.532 mmol) and P_4S_{10} (0.118 g, 0.266 mmol) under neat conditions as described for synthesis of **25b** gave compound **25e** (0.080 g, 42%) as a olive green semi-solid. 1H NMR (400 MHz, $CDCl_3$) δ 8.57 (s, 1H), 7.83 (d, J = 7.5 Hz, 2H), 7.76 (s, 1H), 7.41 (t, J = 7.5 Hz, 2H), 7.32 (m, 2H), 6.94 (m, 1H), 6.72 (m, 1H), 4.49 (m, 2H), 4.40 (t, J = 6.9 Hz, 2H), 1.97 (m, 4H), 1.36 (m, 4H). ^{13}C NMR (100 MHz, $CDCl_3$) δ 164.38, 162.90, 147.70, 130.54, 128.76, 128.03, 126.64, 125.61, 119.51, 118.75, 118.29, 59.74, 50.10, 29.91, 27.99, 25.82, 25.65. HRMS (ESI) calcd for $C_{19}H_{23}N_4OS$ $[M+H]^+$ 355.1587 found 355.1632.

1-Phenyltriazolylheptyl-3-hydroxypyridin-2-thione (25f)

Reaction of **22f** (0.12 g, 0.532 mmol) and P_4S_{10} (0.076 g, 0.17 mmol) under neat conditions as described for synthesis of **25b** gave compound **25f** (0.054 g, 43%) as a olive green semi-solid. 1H NMR (400 MHz, DMSO) δ 8.55 (m, 1H), 7.81 (d, J = 8.2 Hz, 2H), 7.65 (d, J = 6.2 Hz, 1H), 7.42 (m, 2H), 7.30 (m, 1H), 7.02 (m, 1H), 6.85 (m, 1H), 4.50 (m, 2H), 4.36 (t, J = 7.1 Hz, 2H), 1.85 (d, J = 7.0 Hz, 4H), 1.33 (s, 6H). ^{13}C NMR (100 MHz, $CDCl_3$) δ 147.76, 130.66, 128.76, 130.39, 128.98, 128.80, 128.06, 125.97, 125.67, 119.46, 60.10, 50.25, 30.11, 29.67, 28.33, 26.13, 26.10.

HRMS (FAB) calcd for $C_{20}H_{25}N_4OS$ $[M+H]^+$ 369.1749 found 369.1762.

1-(4-Tolyl)triazolypentyl-3-methoxypyridin-2-thione (28a)

Reaction of **27a** (0.235 g, 0.667 mmol) and Lawesson's reagent (0.162 g, 0.40 mmol) in toluene (12 mL) within 12h as described for the synthesis of **10a** gave compound **28a** (0.232 g, 95%) as yellow solid. ^1H NMR (400 MHz, CDCl_3) δ 7.77 (s, 1H), 7.73 (d, J = 8.2 Hz, 2H), 7.33 (m, 1H), 7.25 (dd, J = 11.4, 5.2 Hz, 2H), 6.66 (d, J = 7.8 Hz, 1H), 6.59 (dd, J = 7.8, 6.5 Hz, 1H), 4.60 (m, 2H), 4.43 (t, J = 6.9 Hz, 2H), 3.91 (s, 3H), 2.38 (s, 3H), 2.01 (m, 4H), 1.43 (m, 2H); ^{13}C NMR (75 MHz, CDCl_3) δ 171.03, 158.50, 147.11, 137.37, 131.77, 129.02, 127.33, 125.03, 119.32, 111.60, 109.78, 56.27, 49.28, 30.48, 29.05, 26.51, 22.57, 20.82. HRMS (EI) calcd for $\text{C}_{20}\text{H}_{24}\text{N}_4\text{OS}$ $[\text{M}]^+$ 368.1671 found 368.1667.

1-(3-Tolyl)triazolypentyl-3-methoxypyridin-2-thione (28b)

Reaction of **27b** (0.137 g, 0.389 mmol) and Lawesson's reagent (0.094 g, 0.223 mmol) in toluene (10 mL) within 12 h as described for the synthesis of **10a** gave compound **28b** (0.104 g, 73%) as yellow solid. ^1H NMR (400 MHz, CDCl_3) δ 7.78 (s, 1H), 7.62 (s, 1H), 7.54 (d, J = 7.7 Hz, 1H), 7.26 (m, 2H), 7.07 (d, J = 7.6 Hz, 1H), 6.59 (m, 1H), 6.52 (dd, J = 7.8, 6.5 Hz, 1H), 4.50 (m, 2H), 4.34 (t, J = 7.0 Hz, 2H), 3.81 (s, 3H), 2.32 (s, 3H), 1.90 (m, 4H), 1.33 (m, 2H); ^{13}C NMR (100 MHz, CDCl_3) δ 171.47, 158.81, 147.45, 138.19, 131.83, 130.21, 128.58, 128.46, 126.03, 122.48, 119.68, 111.72, 109.80, 56.55, 56.47, 49.50, 29.24, 26.70, 22.77, 21.18. HRMS (EI) calcd for $\text{C}_{20}\text{H}_{24}\text{N}_4\text{OS}$ $[\text{M}]^+$ 368.1671 found 368.1682.

1-(2-Tolyl)triazolypentyl-3-methoxypyridin-2-thione (28c)

Reaction of **27c** (0.124 g, 0.351 mmol) and Lawesson's reagent (0.085 g, 0.21 mmol) in toluene (10 mL) within 12 h as described for the synthesis of **10a** gave compound **28c** (0.093 g, 72%) as yellow solid. ^1H NMR (400 MHz, CDCl_3) δ 7.72 (m, 1H), 7.27 (m, 2H), 6.60 (m, 1H), 4.57 (m, 1H), 4.42 (t, $J = 7.0$ Hz, 1H), 3.86 (s, 1H), 2.44 (s, 1H), 1.99 (m, 2H), 1.41 (dt, $J = 15.2, 7.6$ Hz, 1H). ^{13}C NMR (100 MHz, CDCl_3) δ 171.81, 159.04, 146.84, 135.33, 131.86, 130.74, 129.81, 128.68, 127.94, 125.93, 121.86, 111.78, 109.79, 104.88, 56.75, 56.61, 49.60, 29.45, 26.85, 22.97, 21.36. HRMS (EI) calcd for $\text{C}_{20}\text{H}_{24}\text{N}_4\text{OS}$ $[\text{M}]^+$ 368.1671 found 368.1662.

1-(4-Benzonitrile)triazolypentyl-3-methoxypyridin-2-thione (28d)

Reaction of **27d** (0.210 g, 0.551 mmol) and Lawesson's reagent (0.133 g, 0.330 mmol) in toluene (12 mL) within 12 h as described for the synthesis of **10a** gave compound **28d** (0.146 g, 67%) as yellow solid. ^1H NMR (400 MHz, CDCl_3) δ 7.64 (m, 3H), 7.28 (m, 1H), 6.73 (d, $J = 8.3$ Hz, 2H), 6.61 (d, $J = 7.6$ Hz, 1H), 6.52 (t, $J = 7.1$ Hz, 1H), 4.50 (m, 2H), 4.31 (t, $J = 6.7$ Hz, 2H), 3.81 (s, 3H), 2.92 (s, 6H), 1.89 (m, 4H), 1.32 (m, 2H); ^{13}C NMR (100 MHz, CDCl_3) δ 171.44, 158.81, 149.78, 147.77, 131.91, 126.37, 119.05, 118.34, 112.52, 111.73, 109.84, 56.60, 56.49, 49.44, 40.45, 29.29, 26.74, 22.81. HRMS (EI) calcd for $\text{C}_{21}\text{H}_{27}\text{N}_5\text{OS}$ $[\text{M}]^+$ 397.1936 found 397.1928.

1-(3-Benzonitrile)triazolypentyl-3-methoxypyridin-2-thione (28e)

Reaction of **27e** (0.190 g, 0.523 mmol) and Lawesson's reagent (0.130 g, 0.314 mmol) in toluene (10 mL) within 12 h as described for the synthesis of **10a** gave compound **28e** (0.133 g, 67%) as yellow solid. ^1H NMR (400 MHz, CDCl_3) δ 7.98 (s, 1H), 7.84 (d, $J =$

8.4 Hz, 2H), 7.56 (d, J = 8.4 Hz, 2H), 7.30 (d, J = 6.5 Hz, 1H), 6.60 (d, J = 7.0 Hz, 1H), 6.52 (dd, J = 7.7, 6.6 Hz, 1H), 4.48 (m, 2H), 4.34 (t, J = 6.9 Hz, 2H), 3.76 (s, 3H), 1.88 (m, 4H), 1.31 (m, 2H). ^{13}C NMR (100 MHz, CDCl_3) δ 171.23, 158.70, 145.36, 134.76, 132.30, 131.78, 125.68, 121.20, 118.49, 111.83, 110.73, 109.92, 56.43, 49.50, 29.01, 26.56, 22.56. HRMS (EI) calcd for $\text{C}_{20}\text{H}_{21}\text{N}_5\text{OS} [\text{M}]^+$ 379.1467 found 379.1466.

1-(4-(*N,N*-dimethylaniline))triazolypentyl-3-methoxypyridin-2-thione (28f)

Reaction of **27f** (0.145 g, 0.40 mmol) and Lawesson's reagent (0.098 g, 0.241 mmol) in toluene (10 mL) within 12 h as described for the synthesis of **10a** gave compound **28f** (0.149 g, 98%) as yellow solid. ^1H NMR (400 MHz, CDCl_3) δ 8.12 (t, J = 1.4 Hz, 1H), 8.06 (m, 1H), 7.90 (s, 1H), 7.59 (dt, J = 7.7, 1.4 Hz, 1H), 7.52 (t, J = 7.8 Hz, 1H), 7.33 (dd, J = 6.5, 1.4 Hz, 1H), 6.67 (dd, J = 7.9, 1.3 Hz, 1H), 6.60 (dd, J = 7.8, 6.5 Hz, 1H), 4.59 (m, 2H), 4.46 (t, J = 6.9 Hz, 2H), 3.89 (s, 3H), 2.02 (m, 4H), 1.43 (m, 2H); ^{13}C NMR (100 MHz, CDCl_3) δ 171.30, 158.73, 145.13, 131.82, 131.71, 130.97, 129.52, 129.44, 128.64, 120.61, 118.28, 112.49, 111.81, 109.91, 56.44, 49.62, 29.11, 26.64, 22.68. HRMS (EI) calcd for $\text{C}_{20}\text{H}_{21}\text{N}_5\text{OS} [\text{M}]^+$ 379.1467 found 379.1469.

1-(4-(3-Trifluomethyl)-benzonitrile)triazolypentyl-3-methoxypyridin-2-thione (28g)

Reaction of **27g** (0.090 g, 0.2088 mmol) and Lawesson's reagent (0.051 g, 0.1252 mmol) in toluene (10 mL) within 12 h as described for the synthesis of **10a** gave compound **28g** (0.075 g, 81%) as yellow solid. ^1H NMR (400 MHz, CDCl_3) δ 8.28 (s, 1H), 8.12 (d, J = 6.7 Hz, 2H), 7.86 (d, J = 8.1 Hz, 1H), 7.36 (d, J = 6.5 Hz, 1H), 6.68 (d, J = 7.8 Hz, 1H), 6.61 (t, J = 7.2 Hz, 1H), 4.59 (m, 2H), 4.47 (m, 2H), 3.88 (s, 3H), 2.02 (m, 4H), 1.43 (m,

2H); ^{13}C NMR (100 MHz, CDCl_3) δ 171.84, 159.14, 144.54, 135.55, 135.22, 133.51, 133.18, 131.81, 128.59, 121.86, 120.86, 115.46, 112.00, 109.97, 108.47, 77.31, 76.99, 76.67, 56.69, 49.87, 29.19, 26.77, 22.77. HRMS (EI) calcd for $\text{C}_{21}\text{H}_{20}\text{N}_5\text{OSF}_3$ $[\text{M}]^+$ 447.1341 found 447.1341.

1-(4-Tolyl)triazolypentyl-3-hydroxypyridin-2-one (29a)

Reaction of **27a** (0.10 g, 0.284 mmol) and 1M BBr_3 (0.34 mL) in CH_2Cl_2 (8 mL) within 48 h as described for the synthesis of **11a** gave compound **29a** (0.049 g, 52%) as light brown solid. ^1H NMR (400 MHz, CDCl_3) δ 7.71 (m, 3H), 7.24 (m, 2H), 6.76 (t, $J = 6.4$ Hz, 2H), 6.12 (t, $J = 7.0$ Hz, 1H), 4.40 (t, $J = 6.9$ Hz, 2H), 3.96 (t, $J = 7.1$ Hz, 2H), 2.38 (s, 3H), 2.00 (m, 2H), 1.82 (m, 2H), 1.39 (m, 2H); ^{13}C NMR (100 MHz, DMSO) δ 171.80, 146.31, 137.02, 129.40, 128.08, 125.02, 120.79, 114.36, 105.20, 49.27, 48.22, 29.17, 28.01, 22.85, 20.82. HRMS (EI) calcd for $\text{C}_{19}\text{H}_{22}\text{N}_4\text{O}_2$ $[\text{M}]^+$ 338.1743 found 338.1750.

1-(3-Tolyl)triazolypentyl-3-hydroxypyridin-2-one (29b)

Reaction of **27b** (0.073 g, 0.207 mmol) and 1M BBr_3 (0.24 mL) in CH_2Cl_2 (8 mL) within 48 h as described for the synthesis of **11a** gave compound **29b** (52 mg, 74%) as light brown solid. ^1H NMR (400 MHz, CDCl_3) δ 7.74 (s, 1H), 7.67 (s, 1H), 7.59 (d, $J = 7.7$ Hz, 1H), 7.30 (t, $J = 7.6$ Hz, 1H), 7.14 (d, $J = 7.4$ Hz, 1H), 6.76 (t, $J = 6.2$ Hz, 2H), 6.12 (t, $J = 7.1$ Hz, 1H), 4.39 (t, $J = 6.9$ Hz, 2H), 3.96 (t, $J = 7.2$ Hz, 2H), 2.39 (s, 3H), 1.99 (m, 2H), 1.80 (m, 2H), 1.38 (m, 2H). ^{13}C NMR (100 MHz, CDCl_3) δ 158.58, 147.87, 146.52, 138.46, 130.38, 128.86, 128.67, 126.75, 126.31, 122.72, 119.48, 113.61, 106.85,

49.91, 49.45, 29.65, 28.38, 23.27, 21.38. HRMS (EI) calcd for $C_{19}H_{22}N_4O_2$ $[M]^+$ 338.1743 found 338.1741.

1-(2-Tolyl)triazolypentyl-3-hydroxypyridin-2-one (29c)

Reaction of **27c** (0.065 g, 0.18 mmol) and 1M BBr_3 (0.27 mL) in CH_2Cl_2 (8 mL) within 48 h as described for the synthesis of **11a** gave compound **29c** (54 mg, 87%) as light brown solid. 1H NMR (400 MHz, dmsO) δ 8.92 (s, 1H), 8.36 (s, 1H), 7.71 (m, 1H), 7.25 (m, 1H), 7.09 (d, J = 6.8 Hz, 1H), 6.64 (d, J = 6.9 Hz, 1H), 6.04 (t, J = 7.0 Hz, 1H), 4.39 (t, J = 6.9 Hz, 1H), 3.88 (t, J = 7.0 Hz, 1H), 2.41 (s, 1H), 1.90 (m, 1H), 1.67 (m, 1H), 1.25 (m, 1H). ^{13}C NMR (100 MHz, CD_3OD) δ 146.28, 135.00, 130.15, 128.96, 128.21, 127.72, 125.38, 122.09, 106.72, 49.43, 48.98, 29.05, 27.78, 22.69, 20.09. HRMS (EI) calcd for $C_{19}H_{22}N_4O_2$ $[M]^+$ 338.1743 found 338.1741.

1-(4-Benzonitrile)triazolypentyl-3-hydroxypyridin-2-one (29d)

Reaction of **27d** (0.075 g, 0.197 mmol) and 1M BBr_3 (0.24 mL) in CH_2Cl_2 (8 mL) within 48 h as described for the synthesis of **11a** gave compound **29d** (43 mg, 60%) as light brown solid. 1H NMR (400 MHz, $CDCl_3$) δ 7.69 (d, J = 8.8 Hz, 2H), 7.61 (s, 1H), 6.77 (m, 4H), 6.11 (t, J = 7.1 Hz, 1H), 4.37 (t, J = 6.9 Hz, 2H), 3.96 (t, J = 7.2 Hz, 2H), 2.99 (s, 6H), 1.99 (m, 2H), 1.81 (m, 2H), 1.39 (m, 2H). ^{13}C NMR (100 MHz, $CDCl_3$) δ 158.57, 150.35, 148.26, 146.61, 126.84, 126.61, 118.87, 118.11, 113.72, 112.49, 106.86, 49.83, 49.52, 40.46, 29.70, 28.41, 23.34. HRMS (EI) calcd for $C_{20}H_{25}N_5O_2$ $[M]^+$ 367.2008 found 367.2007.

1-(3-Benzonitrile)triazolypentyl-3-hydroxypyridin-2-one (29e)

Reaction of **27e** (0.09 g, 0.25 mmol) and 1M BBr₃ (0.30 mL) in CH₂Cl₂ (8 mL) within 48 h as described for the synthesis of **11a** gave compound **29e** (62 mg, 72%) as light brown solid. ¹H NMR (400 MHz, DMSO) δ 8.93 (s, 1H), 8.76 (s, 1H), 8.01 (d, *J* = 7.7 Hz, 2H), 7.90 (d, *J* = 8.0 Hz, 2H), 7.09 (d, *J* = 6.4 Hz, 1H), 6.64 (d, *J* = 7.1 Hz, 1H), 6.04 (t, *J* = 7.0 Hz, 1H), 4.41 (t, *J* = 6.5 Hz, 2H), 3.88 (t, *J* = 6.9 Hz, 2H), 1.89 (m, 2H), 1.67 (m, 2H), 1.24 (m, 2H). ¹³C NMR (100 MHz, CDCl₃) δ 146.62, 145.80, 134.92, 132.57, 126.69, 125.93, 120.88, 118.70, 114.06, 111.19, 107.06, 50.00, 49.29, 29.43, 28.28, 23.08. HRMS (EI) calcd for C₁₉H₁₉N₅O₂ [M]⁺ 349.1539 found 349.1544.

1-(4-(*N,N*-dimethylaniline))triazolypentyl-3-hydroxypyridin-2-one (29f)

Reaction of **27f** (0.078 g, 0.22 mmol) and 1M BBr₃ (0.26 mL) in CH₂Cl₂ (6 mL) within 48 h as described for the synthesis of **11a** gave compound **29f** (48 mg, 64%) as light brown solid. ¹H NMR (400 MHz, CD₃OD) δ 8.39 (s, 1H), 8.16 (s, 1H), 8.12 (d, *J* = 7.5 Hz, 1H), 7.68 (d, *J* = 7.5 Hz, 1H), 7.61 (t, *J* = 7.6 Hz, 1H), 7.04 (m, 1H), 6.76 (m, 1H), 6.21 (m, 1H), 4.45 (m, 2H), 3.99 (m, 2H), 2.01 (m, 2H), 1.78 (m, 2H), 1.33 (m, 2H). ¹³C NMR (100 MHz, CDCl₃) δ 145.61, 131.97, 131.31, 129.74, 129.65, 129.10, 120.30, 118.49, 112.99, 104.90, 50.07, 49.40, 29.52, 28.37, 23.17. HRMS (EI) calcd for C₁₉H₁₉N₅O₂ [M]⁺ 349.1539 found 349.1539.

1-(4-(3-Trifluoromethyl)-benzonitrile)triazolypentyl-3-hydroxypyridin-2-one (29g)

Reaction of **27g** (0.042 g, 0.097 mmol) and 1M BBr₃ (0.17 mL) in CH₂Cl₂ (6 mL) within 48 h as described for the synthesis of **11a** gave compound **29g** (35 mg, 85%) as light brown solid. ¹H NMR (400 MHz, CDCl₃) δ 8.24 (s, 1H), 8.12 (d, *J* = 7.9 Hz, 1H), 8.00

(s, 1H), 7.86 (d, $J = 7.9$ Hz, 1H), 6.75 (t, $J = 5.8$ Hz, 2H), 6.12 (t, $J = 7.0$ Hz, 1H), 4.44 (t, $J = 6.9$ Hz, 2H), 3.96 (t, $J = 7.1$ Hz, 2H), 2.02 (m, 2H), 1.81 (m, 2H), 1.37 (m, 2H). ^{13}C NMR (100 MHz, CDCl_3) δ 158.58, 146.54, 144.71, 135.49, 135.26, 128.57, 126.70, 123.59, 123.54, 121.46, 115.47, 113.82, 108.63, 107.02, 50.19, 49.31, 29.45, 28.30, 23.12. HRMS (EI) calcd for $\text{C}_{20}\text{H}_{18}\text{N}_5\text{O}_2\text{F}_3$ $[\text{M}]^+$ 417.1413 found 417.1425. HRMS (EI) calcd for $\text{C}_{20}\text{H}_{18}\text{N}_5\text{O}_2\text{F}_3$ $[\text{M}]^+$ 417.1413 found 417.1425.

1-(4-Tolyl)triazolypentyl-3-hydroxypyridin-2-thione (30a)

Reaction of **28a** (0.075 g, 0.203 mmol) and 1M BBr_3 (0.24 mL) in CH_2Cl_2 (8 mL) within 48 h as described for the synthesis of **11a** gave compound **30a** (0.042 g, 62%) as olive green solid. ^1H NMR (400 MHz, CD_3OD) δ 8.18 (s, 1H), 7.66 (d, $J = 8.0$ Hz, 2H), 7.55 (d, $J = 5.7$ Hz, 1H), 7.20 (d, $J = 7.7$ Hz, 2H), 6.97 (d, $J = 6.7$ Hz, 1H), 4.55 (m, 2H), 4.43 (t, $J = 6.7$ Hz, 2H), 2.34 (s, 3H), 2.01 (m, 4H), 1.39 (t, $J = 22.5$ Hz, 2H). ^{13}C NMR (100 MHz, CD_3OD) δ 149.25, 139.68, 130.93, 129.13, 127.01, 122.27, 51.41, 30.95, 24.51, 21.83. HRMS (EI) calcd for $\text{C}_{19}\text{H}_{22}\text{N}_4\text{OS}$ $[\text{M}]^+$ 354.1514 found 354.1512.

1-(3-Tolyl)triazolypentyl-3-hydroxypyridin-2-thione (30b)

Reaction of **28b** (0.10 g, 0.271 mmol) and 1M BBr_3 (0.33 mL) in CH_2Cl_2 (8 mL) within 48 h as described for the synthesis of **11a** gave compound **30b** (0.053 g, 56%) as olive green solid. ^1H NMR (400 MHz, CD_3OD) δ 8.20 (s, 1H), 7.61 (s, 1H), 7.55 (m, 2H), 7.26 (t, $J = 7.6$ Hz, 1H), 7.12 (d, $J = 7.5$ Hz, 1H), 6.92 (m, 2H), 4.55 (m, 2H), 4.44 (t, $J = 6.7$ Hz, 2H), 2.36 (s, 3H), 2.01 (m, 4H), 1.41 (m, 2H). ^{13}C NMR (100 MHz, CD_3OD) δ 149.29, 140.05, 131.87, 131.78, 130.38, 130.20, 127.90, 127.63, 124.13, 122.51, 51.40,

31.07, 30.93, 28.97, 24.49, 22.02. HRMS (EI) calcd for C₁₉H₂₂N₄OS [M]⁺ 354.1514 found 354.1523.

1-(2-Tolyl)triazolypentyl-3-hydroxypyridin-2-thione (30c)

Reaction of **28c** (0.072 g, 0.195 mmol) and 1M BBr₃ (0.30 mL) in CH₂Cl₂ (8 mL) within 48 h as described for the synthesis of **11a** gave compound **30c** (0.046 g, 67%) as olive green solid. ¹H NMR (400 MHz, CD₃OD) δ 7.94 (s, 1H), 7.61 (m, 1H), 7.47 (s, 1H), 7.21 (m, 1H), 6.97 (m, 1H), 6.76 (m, 1H), 4.52 (m, 1H), 4.45 (t, *J* = 6.8 Hz, 1H), 2.38 (s, 1H), 2.01 (m, 2H), 1.43 (m, 1H). ¹³C NMR (100 MHz, CD₃OD) δ 146.74, 135.53, 130.65, 129.46, 128.69, 128.21, 125.88, 122.79, 53.41, 49.83, 29.42, 27.32, 22.98, 20.55. HRMS (EI) calcd for C₁₉H₂₂N₄OS [M]⁺ 354.1514 found 354.1509.

1-(4-Benzonitrile)triazolypentyl-3-hydroxypyridin-2-thione (30d)

Reaction of **28d** (0.10 g, 0.271 mmol) and 1M BBr₃ (0.33 mL) in CH₂Cl₂ (8 mL) within 48 h as described for the synthesis of **11a** gave compound **30d** (0.053 g, 56%) as olive green solid. ¹H NMR (400 MHz, DMSO-*d*₆) δ 8.53 (s, 1H), 8.27 (s, 1H), 7.82 (d, *J* = 7.1 Hz, 1H), 7.62 (d, *J* = 8.8 Hz, 2H), 7.06 (d, *J* = 7.5 Hz, 1H), 6.93 (m, 1H), 6.77 (m, 2H), 4.52 (d, *J* = 6.9 Hz, 2H), 4.36 (t, *J* = 7.0 Hz, 2H), 3.21 (s, 6H), 1.88 (m, 4H), 1.34 (m, 2H). HRMS (EI) calcd for C₂₀H₂₅N₅OS [M]⁺ 383.1780 found 383.1776.

1-(3-Benzonitrile)triazolypentyl-3-hydroxypyridin-2-thione (30e)

Reaction of **28e** (0.095 g, 0.25 mmol) and 1M BBr₃ (0.30 mL) in CH₂Cl₂ (8 mL) within 48 h as described for the synthesis of **11a** gave compound **30e** (0.055 g, 60%) as olive green solid. ¹H NMR (400 MHz, DMSO) δ 8.76 (s, 1H), 8.01 (d, *J* = 8.1 Hz, 2H), 7.87

(m, 2H), 7.65 (d, $J = 6.4$ Hz, 1H), 7.00 (m, 1H), 6.87 (d, $J = 8.2$ Hz, 1H), 6.70 (m, 1H), 4.44 (m, 4H), 1.89 (m, 4H), 1.31 (m, 2H). ^{13}C NMR (100 MHz, CDCl_3) δ 168.23, 155.01, 145.75, 134.86, 132.56, 131.00, 125.91, 121.05, 118.68, 113.76, 112.04, 111.17, 57.64, 49.81, 29.31, 27.06, 22.91. HRMS (EI) calcd for $\text{C}_{19}\text{H}_{19}\text{N}_5\text{OS}$ $[\text{M}]^+$ 365.1310 found 365.1313.

1-(4-(*N,N*-dimethylaniline)triazolypentyl-3-hydroxypyridin-2-thione (30f)

Reaction of **28f** (0.105 g, 0.25 mmol) and 1M BBr_3 (0.33 mL) in CH_2Cl_2 (8 mL) within 48 h as described for the synthesis of **11a** gave compound **30f** (0.072 g, 66%) as olive green solid. ^1H NMR (400 MHz, CD_3OD) δ 8.38 (s, 1H), 8.15 (s, 1H), 8.10 (d, $J = 7.9$ Hz, 1H), 7.63 (m, 3H), 6.95 (d, $J = 7.5$ Hz, 1H), 6.67 (m, 1H), 4.57 (m, 2H), 4.48 (t, $J = 7.0$ Hz, 2H), 2.03 (m, 4H), 1.43 (m, 2H). ^{13}C NMR (100 MHz, CD_3OD) δ 145.34, 132.04, 131.14, 129.72, 129.58, 128.63, 121.75, 112.74, 104.99, 49.79, 29.08, 27.04, 22.73. HRMS (EI) calcd for $\text{C}_{19}\text{H}_{19}\text{N}_5\text{OS}$ $[\text{M}]^+$ 365.1310 found 365.1310.

1-(4-(3-Trifluoromethyl)-benzonitrile)triazolypentyl-3-hydroxypyridin-2-thione (30g)

Reaction of **28g** (0.105 g, 0.25 mmol) and 1M BBr_3 (0.33 mL) in CH_2Cl_2 (8 mL) within 48 h as described for the synthesis of **11a** gave compound **30g** (0.072 g, 66%) as olive green solid. ^1H NMR (400 MHz, CD_3OD) δ 8.59 (s, 1H), 8.35 (s, 1H), 8.21 (d, $J = 7.8$ Hz, 1H), 8.00 (t, $J = 9.5$ Hz, 1H), 7.58 (d, $J = 6.2$ Hz, 1H), 6.96 (d, $J = 7.5$ Hz, 1H), 6.72 (m, 1H), 4.57 (m, 4H), 2.04 (m, 4H), 1.42 (m, 2H). ^{13}C NMR (100 MHz, CD_3OD) δ 146.09, 137.48, 137.24, 134.79, 130.46, 125.55, 124.87, 123.60, 122.77, 116.84, 109.75,

55.10, 51.63, 30.84, 28.90, 24.47. HRMS (EI) calcd for C₁₉H₁₉N₅OS [M]⁺ 365.1310 found 365.1310. HRMS (EI) calcd for C₂₀H₁₈N₅OS [M]⁺ 433.1184 found 433.1189.

5.16 References:

1. Jenuwein, T.; Allis, C. D. *Science* **2001**, 293 (5532), 1074.
2. Johnstone, R. W. *Nat. Rev. Drug Discovery* **2002**, 1 (4), 287.
3. Bolden, J. E.; Peart, M. J.; Johnstone, R. W. *Nat. Rev. Drug Discovery* **2006**, 5 (9), 755.
4. Somech, R.; Izraeli, S.; Simon, A. J. *Cancer Treat. Rev.* **2004**, 30 (5), 461.
5. Boyes, J.; Byfield, P.; Nakatani, Y.; Ogryzko, V. *Nature* **1998**, 396 (6711), 594.
6. Gu, W.; Roeder, R. G. *Cell* **1997**, 90 (4), 595.
7. Jin, S.; Scotto, K. W. *Mol. Cell. Biol.* **1998**, 18 (7), 4377.
8. Vigushin, D. M.; Coombes, R. C. *Curr. Cancer Drug Targets* **2004**, 4 (2), 205.
9. Yang, X. J.; Seto, E. *Nat. Rev. Mol. Cell Biol.* **2008**, 9 (3), 206.
10. Choudhary, C.; Kumar, C.; Gnad, F.; Nielsen, M. L.; Rehman, M.; Walther, T. C.; Olsen, J. V.; Mann, M. *Science* **2009**, 325 (5942), 834.
11. (a) Cardinale, J. P.; Sriramula, S.; Pariaut, R.; Guggilam, A.; Mariappan, N.; Elks, C. M.; Francis, J. *Hypertension* **2010**, 56, 437. (b) Dietz, K. C.; Casaccia, P. *Pharmacol. Res.* **2010**, 62, 11. (c) Patil, V.; Guerrant, W.; Chen, P. C.; Gryder, B.; Benicewicz, D. B.; Khan, S. I.; Tekwani, B. L.; Oyelere, A. K. *Bioorg. Med. Chem.* **2010**, 18, 415. (d) Wang, L.; de Zoeten, E. F.; Greene, M. I.; Hancock, W. W. *Nat. Rev. Drug Discovery* **2009**, 8, 969. (e) Welberg, L.; *Nature Rev. Drug Discovery* **2009**, 8, 538. (f) Kazantsev, A. G.; Thompson, L. M. *Nature Rev. Drug Discovery* **2008**, 7, 854. (g) Marks, P. A.; Dokmanovic, M. *Expert Opin. Invest. Drugs* **2005**, 14, 1497. (h) Bolden, J. E.; Peart, M. J.; Johnstone, R. W. *Nat. Rev. Drug Disc.* **2006**, 5, 769 (i) Butler, K. V.; Kozikowski, A. P. *Curr. Pharm. Des.* **2008**, 14, 505 (j) Paris, M.; Porcelloni, M.; Binaschi, M.; Fattori, D. *J. Med. Chem.* **2008**, 51, 1505 (k) Rotili, D.; Simonetti, G.; Savarino, A.; Palamara, A. T.; Migliaccio, A. R.; Mai, A. *Curr. Top. Med. Chem.* **2009**, 9, 272.
12. Khabele, D.; Son, D. S.; Parl, A. K.; Goldberg, G. L.; Augenlicht, L. H.; Mariadason, J. M. and Rice, V. M. *Cancer Biol. Ther.* **2007**, 6, 795.

13. Song, J.; Noh, J. H.; Lee, J. H. ; Eun, J. W.; Ahn, Y. M.; Kim, S. Y.; Lee, S. H.; Park, W. S.; Yoo, N. J. ; Lee, J. Y. and Nam, S. W. *APMIS* **2005**, 113, 264.
14. Bartling, B.; Hofmann, H. S.; Boettger, T.; Hansen, G.; Burdach, S.; Silber, R. E. and Simm, A. *Lung Cancer* **2005**, 49, 145.
15. KrennHrubec, K.; Marshall, B. L.; Hedglin, M.; Verdin, E. and Ulrich, S. M., *Bioorg. Med. Chem. Lett.* **2007**, 17, 2874.
16. Saji, S.; Kawakami, M.; Hayashi, S.; Yoshida, N.; Hirose, M. ; Horiguchi, S. I.; Itoh, A.; Funata, N.; Schreiber, S. L.; Yoshida, M. and Toi, M. *Oncogene* **2005**, 24, 4531.
17. Miller, T. A.; Witter, D. J.; Belvedere, S. J., *Med. Chem.* **2003**, 46, 5097.
18. Finnin, M. S.; Donigian, J. R.; Cohen, A.; Richon, V. M.; Rifkind, R. A.; Marks, P. A.; Breslow, R.; Pavletich, N. P. *Nature* **1999**, 401, 188.
19. Skiles, J. W.; Gonnella, N. C.; Jeng, A. Y. *Curr. Med. Chem.* **2004**, 11, 2911.
20. Whittaker, M.; Floyd, C. D.; Brown, P.; Gearing, A. J. H. *Chem. Rev.* **1999**, 99, 2735.
21. (a) Jones, P.; Altamura, S.; Chakravarty, P. K.; Cecchetti, O.; De Francesco, R.; Gallinari, P.; Ingenito, R.; Meinke, P. T.; Petrocchi, A.; Rowley, M.; Scarpelli, R.; Serafini, S.; Steinkuehler, C. *Bioorg. Med. Chem. Lett.* **2006**, 16, 5948. (b) Suzuki, T.; Miyata, N. *Curr. Med. Chem.* **2006**, 13, 935. (c) Dehmelt, F.; Ciossek, T.; Maier, T.; Weinbrenner, S.; Schmidt, B.; Zoche, M.; Beckers, T. *Bioorg. Med. Chem. Lett.* **2007**, 17, 4746. (d) Chen, B.; Petukhov, P. A.; Jung, M.; Velena, A.; Eliseeva, E.; Dritschilo, A.; Kozikowski, A. P. *Med. Chem. Lett.* **2005**, 15, 1389. (e) Suzuki, T.; Matsuura, A.; Kouketsu, A.; Hisakawa, S.; Nakagawa, H.; Miyata, N. *Bioorg. Med. Chem.* **2005**, 13, 4332. (f) Vasudevan, A.; Ji, Z.; Frey, R. R.; Wada, C. K.; Steinman, D.; Heyman, H. R.; Guo, Y.; Curtin, M. L.; Guo, J.; Li, J.; Pease, L.; Glaser, K. B.; Marcotte, P. A.; Bouska, J. J.; Davidsen, S. K.; Michaelides, M. R. *Bioorg. Med. Chem. Lett.* **2003**, 13, 3909. (g) Moradei, O.; Maroun, C. R.; Paquin, I.; Vaisburg, A. *Curr. Med. Chem. Anti-Cancer Agents* **2005**, 5, 529. (h) Hanessian, S.; Vinci, V.; Auzzas, L.; Marzi, M.; Giannini, G. *Bioorg. Med. Chem. Lett.* **2006**, 16, 4784.
22. (a) Farkas, E.; Katz, Y.; Bhusare, S.; Reich, R.; Ręschenthaler, G. V., Kęnigsmann, M.; Breuer, E. *J. Biol. Inorg. Chem.* **2004**, 9, 307. (b) O'Brien, E. C.; Farkas, E.; Gil, M. J.; Fitzgerald, D.; Castineras, A.; Nolan, K. B. *J. Inorg. Biochem.* **2000**, 79, 47.
23. (a) Wong, J.; Hong, R.; Schreiber, S. *J. Am. Chem. Soc.* **2003**, 125, 5586. (b) Haggarty, S. J.; Koeller, K. M.; Wong, J. C.; Grozinger, C. M.; Schreiber, S.; *Proc. Natl. Acad. Sci. U.S.A.* **2003**, 100, 4389.

24. (a) Meutermans, W. D.; Bourne, G. T.; Golding, S. W.; Horton, D. A.; Campitelli, M. R.; Craik, D.; Scanlon, M.; Smythe, M. L. *Org. Lett.* **2003**, 5, 2711. (b) Glenn, M. P.; Kelso, M. J.; Tyndall, J. D.; Fairlie, D. P. *J. Am. Chem. Soc.* **2003**, 125, 640. (c) Shivashimpi, G. M.; Amagai, S.; Kato, T.; Nishino, N.; Maeda, S.; Nishino, T. G.; Yoshida, M. *Bioorg. Med. Chem.* **2007**, 15, 7830. (d) Oyelere, A. K.; Chen, P. C.; Guerrant, W.; Mwakwari, S. C.; Hood, R.; Zhang, Y.; Fan, Y. *J. Med. Chem.* **2009**, 52(2), 456. (e) Deshmukh, P. H.; Schulz-Fademrecht, C.; Procopiou, P. A.; Vigushin, D. A.; Coombes, R. C.; Barrett, A. G. M. *Adv. Synth. Catal.* **2007**, 349, 175.
25. Monneret, C. *Eur. J. Med. Chem.* **2005**, 40, 1.
26. Khan, N.; Jeffers, M.; Kumar, S.; Hackett, C.; Boldog, F.; Khramtsov, N.; Qian, X.; Mills, E.; Berghs, S. C.; Carey, N.; Finn, P. W.; Collins, L. S.; Tumber, A.; Ritchie, J. W.; Jensen, P. B.; Lichenstein, H. S. and Sehested, M. *Biochem. J.* **2008**, 409, 581.
27. Wong, J. C.; Hong, R. and Schreiber, S. L. *J. Am. Chem. Soc.* **2003**, 125, 5586.
28. Beckers, T.; Burkhardt, C.; Wieland, H.; Gimmnich, P.; Ciossek, T.; Maier, T. and Sanders, K. *Int. J. Cancer* **2007**, 121, 1138.
29. (a) Faith E. Jacobsen; Jana A. Lewis and Seth M. Cohen *ChemMedChem* **2007**, 2, 152. (b) Jennifer A. Jacobsen; Jessica L. Fullagar; Melissa T. Miller and Seth M. Cohen *J. Med. Chem.* **2011**, 54, 591. (c) David T. Puerta; Michael O. Griffin; Jana A. Lewis; Diego Romero-Perez; Ricardo Garcia; Francisco J. Villarreal; Seth M. Cohen *J. Biol. Inorg. Chem.* **2006**, 11: 131.
30. (a) Puerta, D. T.; Lewis, J. A.; Cohen, S. M. *J. Am. Chem. Soc.* **2004**, 126, 8388. (b) Puerta, D. T.; Griffin, M. O.; Lewis, J. A.; Romero-Perez, D.; Garcia, R.; Villarreal, F. J.; Cohen, S. M. *J. Biol. Inorg. Chem.* **2006**, 11, 131.
31. Sigel, H; McCormick *DB Acct Chem Res* **1970**; 3(6), 201.
32. Congreve, M.; Chessari, G.; Tisi, D.; Woodhead, A. J. *J. Med. Chem.* **2008**, 51, 3661.
33. Leach, A. R.; Hann, M. M.; Burrows, J. N.; Griffen, E. J. *Mol. Biosyst.* **2006**, 2, 429.
34. (a) Erlanson, D. A.; McDowell, R. S.; O'Brien, T. *J. Med. Chem.* **2004**, 47, 3463. (b) David, C. R.; Miles, C.; Christopher, W. M.; Robin, C. *Nature Reviews Drug Discovery* **2004**, 3, 660.
35. Hopkins, A. L.; Groom, C. R.; Alex, A. *Drug Discovery Today* **2004**, 9, 430–431.
36. (a) Agrawal, A.; Johnson, S. L.; Jacobsen, J. A.; Miller, M. T.; Chen, L.H.; Pellecchia, M.; Cohen, S. M. *ChemMedChem*, **2010**, 5, 195. (b) Puerta, D. T.;

- Cohen, S. M. *Inorg. Chem.* **2002**, 41, 5075. (c) Puerta, D. T.; Cohen, S. M. *Inorg. Chem.* **2003**, 42, 3423. (d) Puerta, D. T.; Schames, J. R.; Henchman, R. H.; McCammon, J. A.; Cohen, S. M. *Angew. Chem., Int. Ed.* **2003**, 42, 3772.
37. Li, H; Liu, A; Zhao, Z; Xu, Y; Lin, J; Jou, D; Li, C. *J. Med. Chem.* **2011**, 54(15), 5592.
38. (a) Cohen, S. M.; Xu, J.; Radkov, E.; Raymond, K. N.; Botta, M.; Barge, A.; Aime S. *Inorg. Chem.* **2000**, 39, 5747. (b) Cohen, S. M.; O'Sullivan, B.; Raymond, K. N. *Inorg. Chem.* **2000**, 39, 4339-4346. (c) Lewis, J.; Tran, B. L.; Puerta, D.; Rumberger, E. M.; Hendrickson, D. N.; Cohen, S. M.. *Dalton Trans.* **2005**, 2588.
39. Mwakwari, S.C.; Guerrant, W.; Patil, V.; Khan, S.I.; Tekwani, B.L.; Gurard-Levin, Z.A.; Mrksich, M.; Oyelere, A.K. *J. Med. Chem.* **2010**, 53, 6100.
40. Estiu, G.; Wiest, O. HDAC1 homology model. Personal communication.
41. Somoza, J. R.; Skene, R. J.; Katz, B. A.; Mol, C.; Ho, J. D.; Jennings, A. J.; Luong, C.; Arvai, A.; Buggy, J. J.; Chi, E.; Tang, J.; Sang, B.C.; Verner, E.; Wynands, R.; Leahy, E. M.; Dougan, D. R.; Snell, G.; Navre, M.; Knuth, M. W.; Swanson, R. V.; McRee, D. E.; Tari, L. W. *Structure* **2004**, 12(7):1325.
42. Chen, P.C.; Patil, V.; Guerrant, W.; Green, P.; Oyelere, A.K. *Bioorg. Med. Chem.* **2008**, 16, 4839.
43. Pacholec, M.; Bleasdale, J. E.; Chrunk, B.; Cunningham, D.; Flynn, D.; Garofalo, R. S.; Griffith, D.; Griffor, M.; Loulakis, P.; Pabst, B.; Qiu, X.; Stockman, B.; Thanabal, V.; Varghese, A.; Ward, J.; Withka, J.; Ahn, K. J. *Biol. Chem.* **2010**, 285 (11), 8340.
44. Beher, D.; Wu, J.; Cumine, S.; Kim, K. W.; Lu, S. C.; Atangan, L.; Wang, M. *Chem. Biol. Drug Des.* **2009**, 74 (6), 619.
45. Gurard-Levin, Z. A.; Kim, J.; Mrksich, M. *Chem. Bio. Chem.* **2009**, 10 (13), 2159.
46. Mrksich, M. *ACS, Nano* **2008**, 2 (1), 7.
47. Gurard-Levin, Z. A.; Mrksich, M. *Biochemistry* **2008**, 47 (23), 6242.
48. Min, D. H.; Yeo, W. S.; Mrksich, M. *Anal. Chem.* **2004**, 76 (14), 3923.
49. Cava, M. P.; Levinson, M. I. *Tetrahedron* **1985**, 41 (22): 5061.
50. Miyaura; Norio; Suzuki; Akira *Chemical reviews* **1979**, 95 (7): 2457.

51. (a) Rostovtsev, V. V.; Green, L. G.; Fokin, V. V.; Sharpless, K. B. A. *Angew Chem., Int. Ed.* **2002**, 41, 2596. (b) Tornøe, C. W.; Christensen, C.; Meldal, M. *J. Org. Chem.* **2002**, 67, 3057.
52. Lecher, H. Z.; Greenwood, R. A.; Whitehouse, K. C.; Chao, T. H. *J. Am. Chem. Soc.*, **1956**, 78 (19): 5018.
53. Beckers, T.; Burkhardt, C.; Wieland, H.; Gimmnich, P.; Ciossek, T.; Maier, T.; Sanders, K. *Int. J. Cancer* **2007**, 121, 1138.
54. Katoh, A.; Harada, K.; Saito, R. *Hemoglobin* **2006**, 30(1), 81.
55. (a) Lu, X.; R. Bittman *J. Org. Chem.*, **2005**, 70(12), 4746. (b) Aucagne, V.; Hanni, K., D.; Leigh, D. A.; Lusby, P. J.; Walker, D. B. *J. Am. Chem. Soc.* **2006**, 128(7), 2186. (b) Doerfler, M.; Tschammer, N.; Hamperl, K.; Huebner, H.; Gmeiner, P. *J. Med. Chem.* **2008**, 51(21), 6829. (c) Keisuke, A.; Matsubara, S. *Org. Lett.* **2010**, 12(21), 4988. (d) Wu, X.; Ling, C.; Bundle D. R. *Org. Lett.* **2004**, 6(24), 4407, (e) Nielson, A.; England, P. M. *J. Am. Chem. Soc.* **2007**, 129(16), 4902.
56. (a) Chakraborty, A.; Dey, S.; Sawoo, S.; Adarsh, N. N.; Sarkara, A. *Organometallics*, **2010**, 29 (23), 6619. (b) Jacob, A.; Simon, B.; Xifu, L. *Synlett* **2005**, (19), 2941.

CHAPTER 6

LEISHMANOLYSIS (GP63) AS AN ANTI-LEISHMANIAL TARGET

6.1 Leishmaniasis

Leishmaniasis is a tropical/sub-tropical parasitic disease caused by protozoan parasites of the genus *Leishmania*.¹ It is transmitted to humans by more than 20 leishmanial species and is transmitted by the bite of ~ 30 different phlebotomine sand fly species.^{1,5} The parasite exists in two different forms, promastigotes, the motile flagellated form found in the gut of the sandfly vector and amastigotes, the non-flagellated, non-motile form found in the mammalian host.² The *leishmania* parasites live in the macrophages as amastigotes. The macrophages are ingested by the fly during the blood-meal and the amastigotes are released into the stomach of insect. Almost immediately the amastigotes transform into the flagellate promastigote form. The promastigotes multiply by the binary fission and transfer to sandfly's proboscis. When the sandfly next feeds on a mammalian host, the *leishmania* promastigotes are transferred to the host. Once in the host the promastigotes are taken up by the macrophages where they rapidly revert back to the amastigote form. The released amastigotes are taken up by additional macrophages and thus complete leishmania life cycle.³

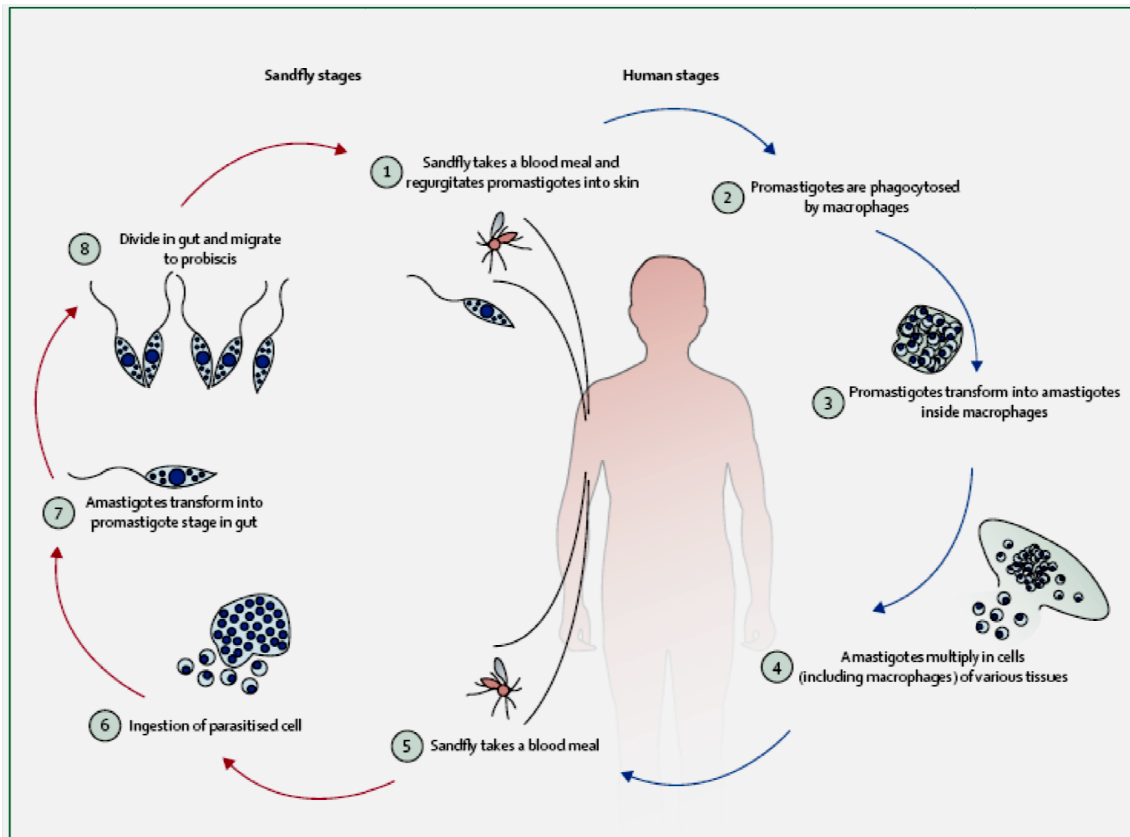


Figure 6-1. *Leishmania* life cycle³

Leishmaniasis consists of four main clinical forms: visceral leishmaniasis (VL; also known as kala azar), cutaneous leishmaniasis (CL), mucocutaneous leishmaniasis (MCL; also known as espundia), and post-kala-azar dermal leishmaniasis (PKDL). Among all of these, visceral leishmaniasis (VL) which is caused by parasite *Leishmania donovani* is fatal if left untreated.⁴

Leishmaniasis is contributing to significant morbidity and mortality worldwide. It has an estimated incidence of 500,000 new cases and 60,000 deaths each year, a death toll that is highest among all the parasitic diseases except malaria.⁵ Human leishmaniasis is distributed worldwide, but mainly concentrated in tropics and sub-tropics. The majority

of death toll occurs in developing countries such as Bangladesh, Brazil, Ethiopia, India, Nepal and Sudan sharing large percentage of death tolls.⁶



Red shades – visceral leishmaniasis affected area.

Figure 6-2. Leishmania worldwide endemics.⁶

Due to lack of effective vaccines and vector control measures, chemotherapy is used as front line defense against the disease. Leishmaniasis is an emerging serious threat to public health due to the increasing occurrence of opportunistic infection in human immunodeficiency virus-infected patients and the emergence of multi-drug resistant strains.⁷ Also, many drugs are too expensive to treat in developing countries where most of the infection occurs. The limited chemotherapeutic approach for the treatment of leishmanial infections is based on amphotericin B, miltefosine, paromomycin, and antimony agents like sodium stibogluconate and meglumine antimoniate.^{6,8} These are unsatisfactory agents because their toxicity causes serious side effects that often result in patients deserting the treatment. Moreover, these anti-leishmanial agents are high-priced and their modes of activity are poorly understood. According to the World Health Organization (WHO) report, infections caused by *Leishmania* are among the most

hazardous infectious diseases.^{4a} Therefore, there is an urgent need for affordable alternative agents to curtail leishmaniasis. To thrive in human hosts, *Leishmania* digest key host proteins, primarily to obtain nutrients and also to evade the host's immune system. It is well established that gp63, a zinc metalloprotease, is essential for the degradation of host proteins and it is an attractive target for the development of new chemotherapeutics against this deadly parasitic disease.⁹

6.2 Leishmanolysin (gp63)

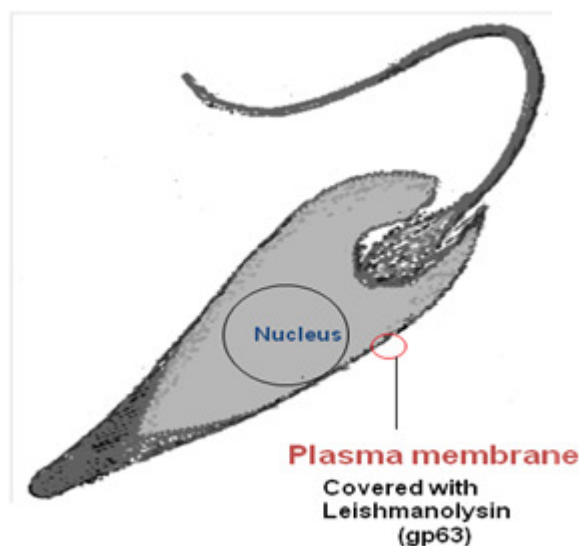


Figure 6-3. The Surface of the Promastigote Form of *Leishmania* is covered with Leishmanolysin (gp63).

The major surface glycoprotein gp63 (leishmanolysin; promastigote surface protease) is a zinc-metalloenzyme which is expressed in high density on the surface of the promastigote form of *Leishmania*, where it is enzymatically active against polypeptide surface.⁹ It has been established that gp63 is a virulence factor implicated in infection of leishmaniasis.¹⁰ With the aid of other major cell surface components such as the lipophosphoglycans (LPGs) and glycoinositolphospholipid (GIPL), gp63 enables

promastigotes to reach and infect sufficient macrophages to establish an infection. Despite the attractiveness of gp63 as anti-leishmanial target, there are currently no efficient, non-toxic inhibitors of gp63.⁹

6.3 Comparison of HDAC8 and gp63 enzyme active site

In previous chapter, I discussed the structural basis for HDAC8 selectivity by 3-HPT based HDACi (chapter 5, section 5.14). One of the finding is that the shallow nature of HDAC8 active site is conducive for 3-HPT chelation to the catalytic Zn^{2+} . In contrast, the 3-HPT analogs were not able to penetrate the deep active site of HDAC1. Intrigued by the selectivity of these 3-HPT based compounds, we decided to explore other zinc metalloenzyme which share structural attributes to HDAC8. A literature survey on zinc metalloenzymes revealed that gp63 (discussed in chapter 5) has also very shallow active site with catalytic zinc located at the surface and near the entrance of deep subpocket. (Figure 6-4) We hypothesized that the 3-HPT based HDAC8 selective inhibitors could also be potential hits for gp63. The lack of effective, non-toxic inhibitor of gp63 further instigated our efforts for developing inhibitors of gp63.

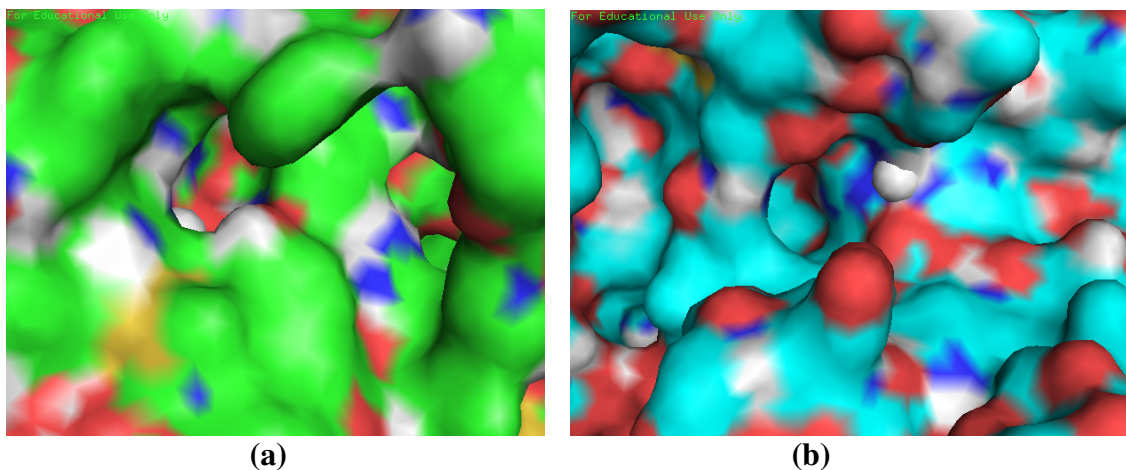


Figure 6-4. (a) Enzyme active site of HDAC8 (b) Enzyme active site of gp63

6.4 Design of 1st Generation GP63 Inhibitors by Molecular Docking Analysis

The crystal structure of gp63 from *Leishmania major* is available in the public domain (PDB code: 1LMLa) (Figure 6-5).¹¹ The structure revealed that gp63 contained an active site structural motif found in other zinc proteases such as HDAC enzymes.¹¹ We inferred that gp63 active site could be amenable to the design of specific inhibitors in similar manner to other zinc proteases. Our first specific goal in this study is to use molecular docking and the tools of Organic Chemistry to exemplify gp63 active site as a target for small molecules with anti-leishmanial activities. We anticipate gaining greater molecular insights on the functionalities at the active site of gp63 that could facilitate specific small molecule binding interactions. This development will guide a longer term structural optimization studies on lead inhibitors.

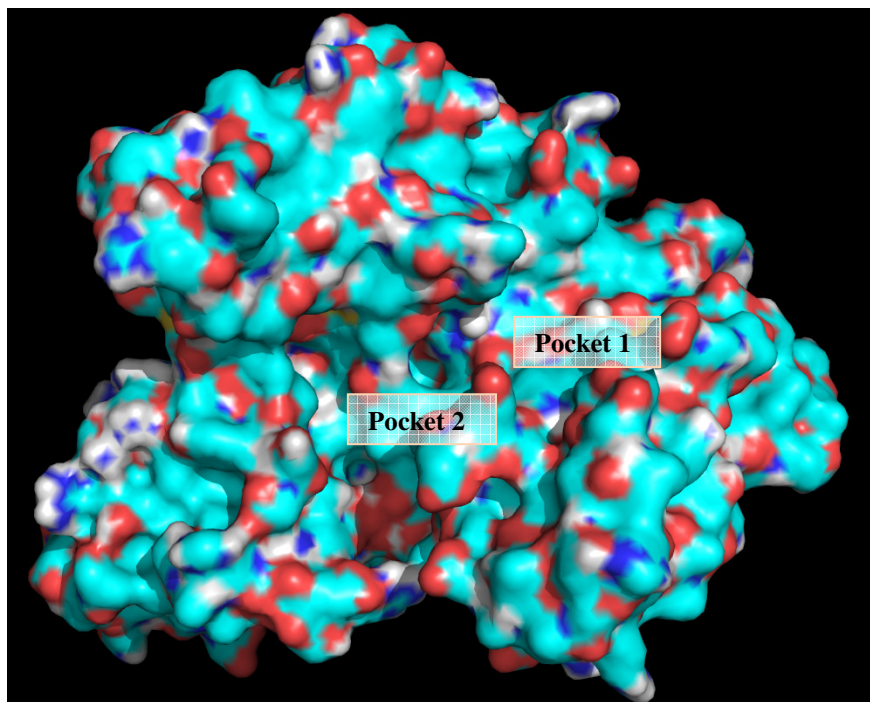
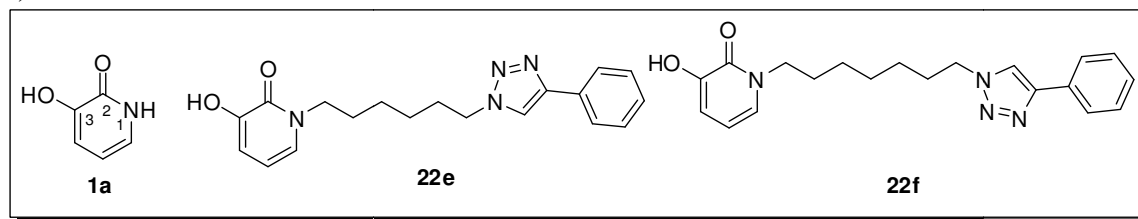


Figure 6-5. GP63 crystal structure¹¹ (Zinc is show in white color sphere for visualization purpose. Pocket 1 & pocket 2 indicate possible binding sites for inhibitor design)

We used molecular dock program (AutoDock) to probe the binding interactions between our proposed compounds and gp63 as described in chapter 5.¹² We began our studies by docking fragment 3-hydroxy-2-pyridinone against gp63. From a population of 100, the docked complexes for each inhibitor were selected according to the criteria of interaction energy in combination with geometrical matching quality.¹² In preliminary docking studies we observed that 3-hydroxypyridin-2(1H)-one **1a** bound within the vicinity of the active site Zn^{2+} ion (Fig. 3b), albeit with low binding energy. A close analysis of the docked structure revealed that the *N*-1 group of compound **1a** is pointing into a deep pocket, designated pocket-2, which constitutes one of the two binding pockets in gp63 active site.

Based on this observation, we designed compound **22e** and **22f** that linked the crucial 3-hydroxypyridin-2-ones moiety of **1a** to a triazolyl-phenyl ring through 6-C and 7-C methylene groups respectively. The 6-C and 7-C methylene groups were estimated to be ideal spacer for connecting the two groups based on the distance between the active site Zn^{2+} ion and the center of pocket-1. We anticipated that these compounds will present their 3-hydroxypyridin-2-one moiety closer to the Zn^{2+} ion, thereby result in stronger interaction. As anticipated, compounds **22e** and **22f** adopted docked orientations whereby the 3-hydroxypyridin-2-one moiety is much closer to the active site Zn^{2+} ion (Figure 6-6a). However, **22e** and **22f** each adopt two different docked orientations at two gp63 binding pockets (Figure 6-6b, 6-6c). Either docked conformation has stronger affinity relative to that of **1a**. Pocket 2 conformations of compounds **22e** and **22f** exhibit stronger binding affinities than pocket 1 conformations of **1a**.

a)



b)

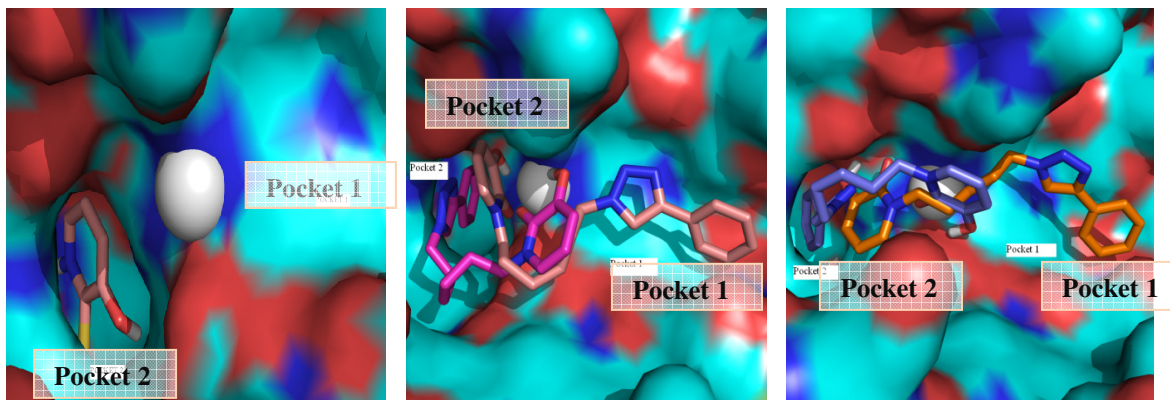


Figure 6-6. (a) Structures of first generation molecules based on 3-hydroxypyridin-2(1H)-one skeleton. (b) Docked structures of 3-hydroxypyridin-2(1H)-one **1a** and triazole-linked 3-hydroxypyridin-2-ones **22e** and **22f** at the active site of gp63.

The methylene linker of compound **22e** and **22f**, though make favorable hydrophobic contact in pocket-1, adopts energetically costly conformations with sharply twisted kinks in spacer region. We hypothesized that having rigid system, such as in biphenyl compound **5c**, could solve this problem. Unfortunately, docked structure **5c** made no productive interaction with enzyme active site. However, para-cyano substituted compound **11a** bind exclusively to pocket-1, with specific H-bonding interaction between pocket-1 Thr 229 and hydrophobic interaction with Pro347. Surprisingly, p-dimethylamino substituted compound **11g** has two nearly energetically equivalent conformations in pocket 1 and 2 with p-dimethylamino moiety making close contact with amino acid Gly 352 at the base of pocket-2 (Figure 6-6b)

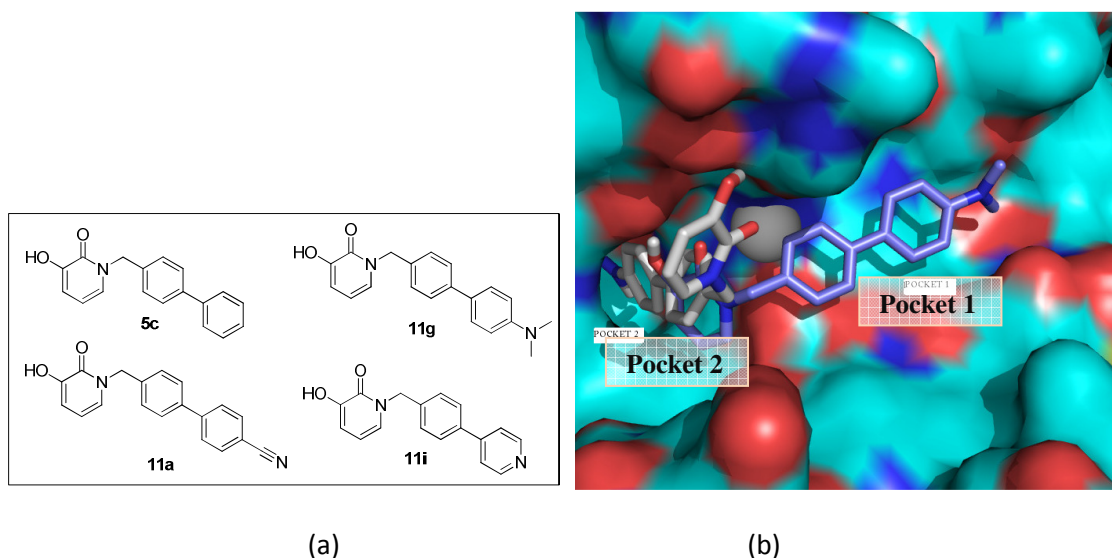


Figure 6-7. (a) Representative structures of gp63-binding small molecules used in molecular docking analysis. Docked structures of (b) p-dimethylamino substituted biphenyl compound **11g**

This led us to postulate that having p-pyridinyl ring as in compound **11i** instead of p-dimethylaminophenyl ring of compound **11g** should further enhance affinity for pocket-2. And to our delight, it indeed resulted in exclusively pocket-2 binding compound **11i** with very low binding energy. It makes near optimal interactions with key amino acid side-chain residues within pocket 2 (Figure 6-7).

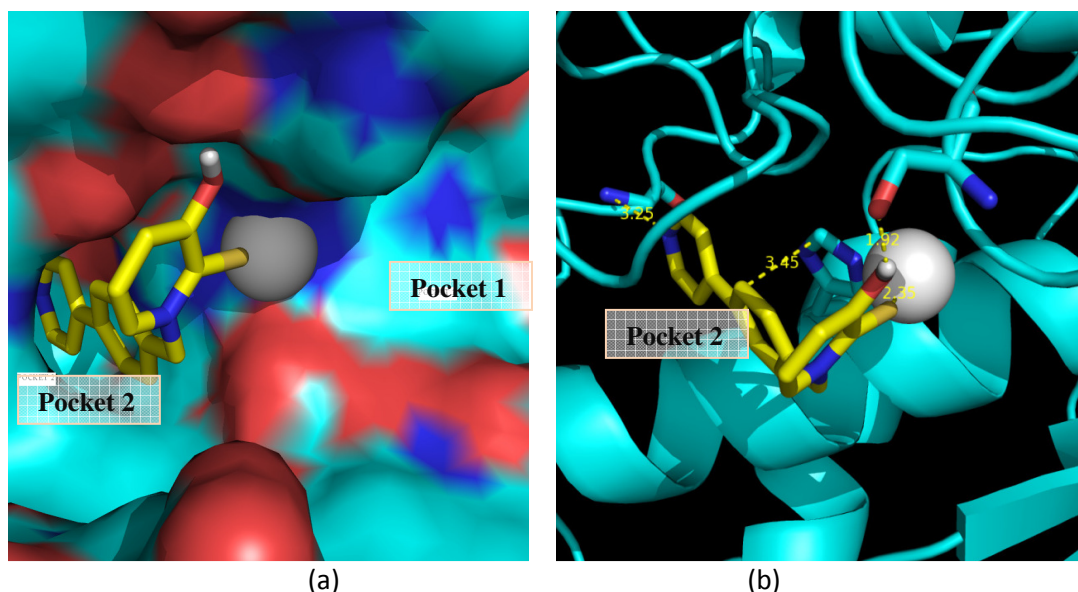


Figure 6-8. Docked structure of p-pyridinylbenzyl compound **11i** a) space filling model b) Cartoon model with compound **11i** making key interactions at active site.

To experimentally validate these *in silico* results, these compounds were synthesized as depicted in chapter 5 (Figure 5-13, 5-15, 5-16, 5-18). To obtain any evidence for the beneficial effect (or lack thereof) of incorporation of sulfur group¹⁴ into the ZBG of the 3-hydroxypyridin-2-one compounds described herein, we synthesized thione analogs as well and tested them for promastigote and the amastigote forms of the *L. donovani*.

6.5 Whole Cell Activities of 1st Generation Antileishmanials

Due to lack of standard *in vitro* assay for determining activity against gp63 enzyme, in collaboration with Dr. Tekwani's lab at University of Mississippi, we investigated the *in vitro* whole cell anti-leishmanial activity of 1st generation compounds against the promastigote and amastigote stage of *Leishmania donovani*. Interestingly, compounds **22e**, **22f**, **11a**, **11g** (pocket 1 binders) were all active, while compound **11i**

(exclusive pocket 2 binder) was found to be inactive. (Table 6-1) Therefore we surmised that pocket 1 is only drugable site at the active site of gp63.

Many of these compounds inhibit the viability of either stage of *L. donovani* with IC₅₀ values that tracked reasonably well with our molecular docking outputs (Figure 6-6, 6-7). The triazole-linked 3-hydroxypyridin-2-ones compounds **22e** and **22f** have modest anti-leishmanial activity. (Table 6-1) This is not unexpected as the presumably energetically costly conformations adopted by these compounds may prevent them from efficiently binding to gp63 active site (Figure 6-5). Conformationally rigid compounds **11a** and **11g** have IC₅₀ values that are about 3-4.5 fold more potent than the flexible compounds **22e** and **22f**. This result indicates that a rigid system is better suited to bind to the enzyme active. Interestingly for most of these compounds, incorporation of sulfur into the ZBG of the 3-hydroxypyridin-2-one compounds generally showed five to seven-fold better IC₅₀ relative to the corresponding non-thiolated compounds. An exciting exception is **12g** which shows almost 34-fold enhancement in anti-leishmanial activity relative to the corresponding carbonyl compound **11g** (Table 6-1).

To obtain evidence for compound selective toxicity, we investigated their effect on non-transformed vero cells. None of these compounds is cytotoxic to Vero cells at maximum tested conc. 5 µg/ml. Finally, cytotoxicity activity of some of these compounds against tumor derived macrophage cell line RAW 264.7 indicate ability of these compounds to obliterate transformed cells, possibly through HDAC8 inhibition.

The clear trend in activity exhibited by these 1st generation antileishmanial tracked well with their HDAC8 inhibition activities. Most of the compounds which showed good inhibition of HDAC8 were also active against *Leishmania* parasite. This

further supported our initial submission that the structural attributes of HDAC8 enzyme active site are shared by gp63 metalloenzyme as well. In light of this observation, we further pursued SAR study by subjecting additional HDAC8 selective compounds which we reported in previous chapter to screening against *L. donovani*.

Table 6-1. Preliminary Whole cell activity against the promastigote and amastigote form of *L. donovani*^a

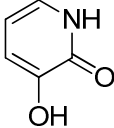
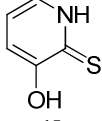
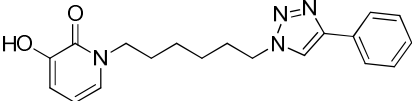
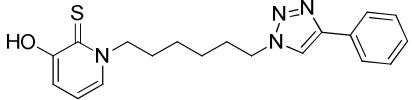
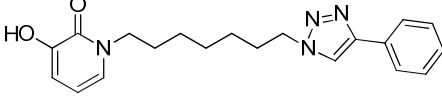
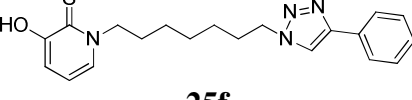
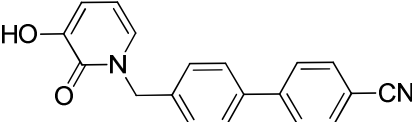
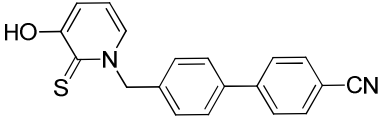
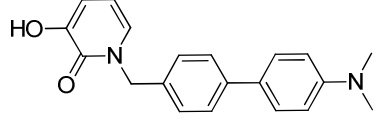
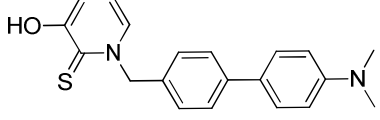
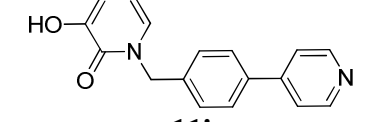
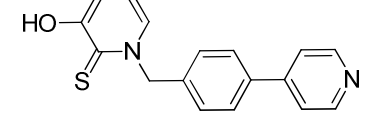
Compound	Promastigote		Amastigote		Cytotoxicity (VERO) ^c	Cytotoxicity (RAW 264.7) ^c
	IC ₅₀ (µg/ml)	IC ₉₀ (µg/ml)	IC ₅₀ (µg/ml)	IC ₉₀ (µg/ml)	IC ₅₀ (ng/ml)	IC ₅₀ (µg/ml)
 1a	NA	NA	18	35	NC	<1.6
 1b	6	27	NT	NT	NC	NT
 22e	21	> 40	6	30	NC	3.1
 25e	3.7	40	<1.6	5	NC	15
 22f	20.5	40	6.2	28	NC	3.2
 25f	3.6	12	<1.6	<1.6	NC	2.8
 11a	4.6	40	5	22	NC	1.8

Table 6-1 continued.

 12a	0.7	1.5	NT	NT	NC	NT
 11g	7.5	> 40	4	7.5	NC	23
 12g	0.22	1	NT	NT	NC	NT
 11i	NA	NA	21	>40	NC	13
 12i	NT	NT	NT	NT	NT	NT
Pentamidine	1.0	2.0	NT	NT	NT	NT
Amphotericine B	0.2	0.4	NT	NT	NT	NT
Miltefosine	5.1 ^b	NT	NT	NT	NT	NT

NC = Not cytotoxicity; NT = Not tested; ND = Not determined; NA = Inactive

^aWhole cell activities data were generated by Tekwani lab at University of Mississippi.

^bData from Saugar J. M. *et al.* J. Med. Chem. 2007, 50, 5994-6003 (converted from μM to $\mu\text{g/ml}$)

^cMaximum tested concentration = 5 $\mu\text{g/mL}$

6.6 Structure-Activity Relationship (SAR) of antileishmanial activity of HDAC8 Selective HDACi (2nd Generation Antileishmanials)

In order to pursue SAR studies of these antileishmanials, we screened additional HDAC8 selective compounds reported in earlier chapter (chapter 5, Table 5-1, 5-2, 5-3, 5-5). Activities of representative HDAC8 selective inhibitors are reported in Table 6-2. Against promastigote form, rigid systems such as compounds **11** and **12** fared much better than flexible systems such as more than 2-C methylene linker (Table 6-2). As expected, thione analogs showed several fold superior activity than carbonyl analogs. Changing position of cyano group from para- position (compound **12a**) to meta- position (compound **12b**) only slightly altered the activity in favor of meta-cyano substitution. Replacement of *N,N*-dimethylamino group of compound **12g** to other electron donating group such as methyl group (compound **12d**) was found to be tolerable. Among all triazole based linker compounds, compound **17a** with single methylene spacer showed best activity. There was steady decrease in potency as number of methylene spacer kept on increasing. However, for five methylene spacer there was increase in potency. Additional SAR on five methylene linker compounds did not improve IC₅₀ significantly with all of the activities ranged from 3 to 6 µg/ml (Table 6-2). However, six and seven-methylene compounds (**25e** and **25f**) again showed improvement in activity (Table 6-2). However they still couldn't surpass the IC₅₀ values of one-methylene linker compounds (compound **17a**). Activities for amastigote form were not available for all of the compounds by the time I write this report, however they seem to track well with their promastigote activities.

Table 6-2. Whole cell activity against the promastigote and amastigote form of *L. donovani*^a

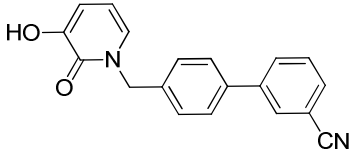
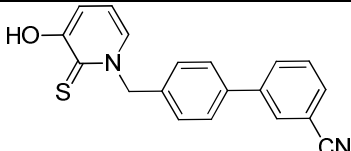
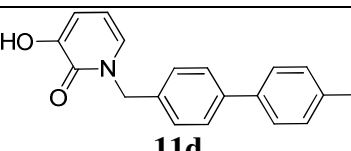
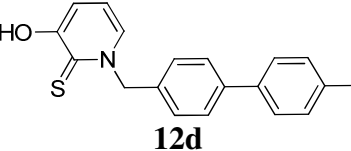
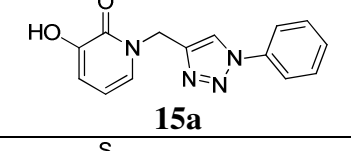
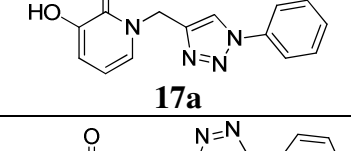
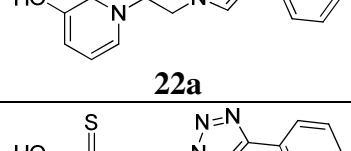
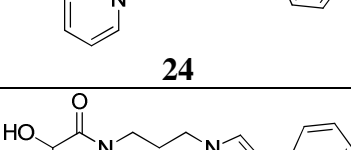
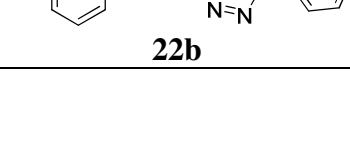
Compound	Promastigotes		Amastigotes		Cytotoxicity (VERO)	Cytotoxicity (RAW 264.7)
	IC ₅₀ (μg/ml)	IC ₉₀ (μg/ml)	IC ₅₀ (μg/ml)	IC ₉₀ (μg/ml)	IC ₅₀ (ng/ml)	IC ₅₀ (μg/ml)
 11b	9	>40	NT	NT	NC	NT
 12b	0.4	1.3	NT	NT	NC	NT
 11d	6	33	NT	NT	NC	NT
 12d	0.3	1.2	NT	NT	NC	NT
 15a	NA	NA	18	>40	NC	2.5
 17a	1.6	7.5	<1.6	<1.6	NC	2.8
 22a	NA	NA	19	>40	NC	10
 24	3.9	18	18	40	NC	2.3
 22b	NA	NA	20	>40	NC	14

Table 6-2 continued.

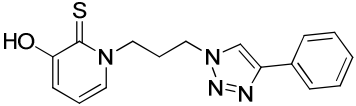
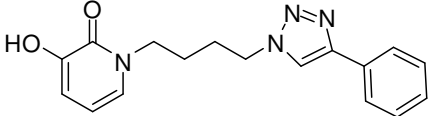
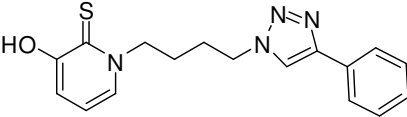
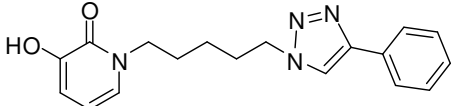
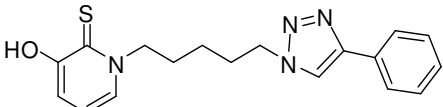
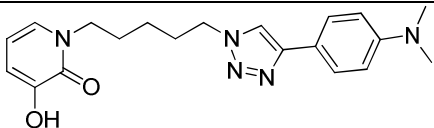
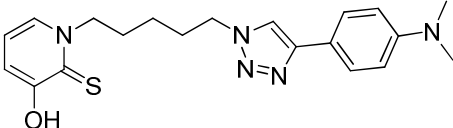
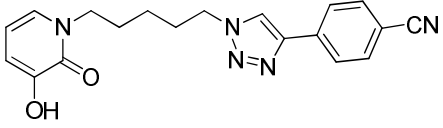
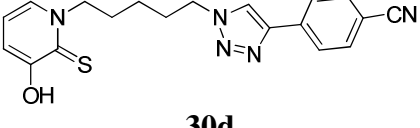
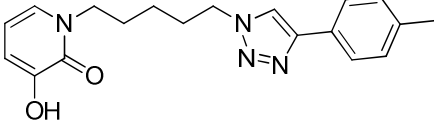
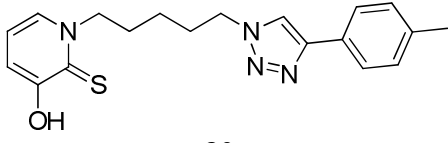
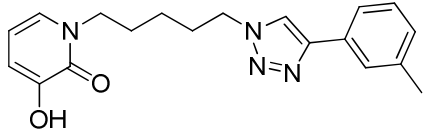
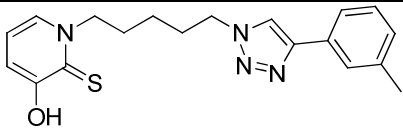
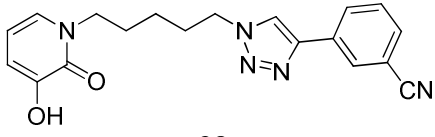
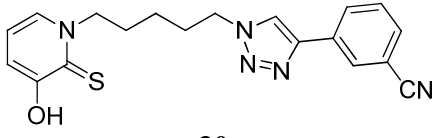
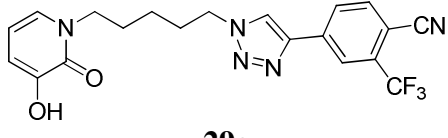
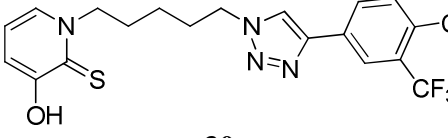
 <p>25b</p>	3.6	30	<1.6	4.1	NC	<1.6
 <p>22c</p>	NA	NA	9	33	NC	3
 <p>25c</p>	16	>40	4	7	NC	3.4
 <p>22d</p>	11	> 40	7	29	NC	2.6
 <p>25d</p>	4.2	18	4.1	13	NC	6.5
 <p>29f</p>	28	>40	NT	NT	NC	NT
 <p>30f</p>	3	>40	NT	NT	NC	NT
 <p>29d</p>	39	>40	NT	NT	NC	NT
 <p>30d</p>	3.9	40	NT	NT	NC	NT
 <p>29a</p>	26	>40	NT	NT	NC	NT

Table 6-2 continued.

 <p>30a</p>	2.9	7.9	NT	NT	NC	NT
 <p>29b</p>	24	>40	NT	NT	NC	NT
 <p>30b</p>	3.6	40	NT	NT	NC	NT
 <p>29e</p>	NA	NA	NT	NT	NC	NT
 <p>30e</p>	4	8	NT	NT	NC	NT
 <p>29g</p>	21	>40	NT	NT	NC	NT
 <p>30g</p>	4.7	20	NT	NT	NC	NT
Pentamidine	1.0	2.0	NT	NT	NT	NT
Amphotericin B	0.2	0.4	NT	NT	NT	NT
Miltefosine	5.1 ^b	NT	NT	NT	NT	NT

NC = Not cytotoxicity; NT = Not tested; ND = Not determined; NA = Inactive

^aWhole cell activities data were generated by Tekwani lab at University of Mississippi.

^bData from Saugar J. M. *et al.* J. Med. Chem. 2007, 50, 5994-6003 (converted from μM to $\mu\text{g/ml}$)

6.7 Conclusion

The lack of affordable effective agents for the treatment and management of Leishmaniasis is emerging as a serious threat to public health. Multidrug resistance has exacerbated the available treatment modalities for this parasitic infection. Using a combination of molecular docking and whole cell assays, we have identified a subset of lead compounds that inhibit the viability of the promastigote stage of *Leishmania donovani* with IC₅₀ comparable to Miltefosine, the only clinically approved oral drug against visceral leishmaniasis. Several compounds show high potency with limited cytotoxicity to normal mammalian cells. Future efforts will be directed to establish molecular mechanism of these compounds. Even though molecular dockings performed on gp63 enzyme helped us to corroborate our whole cell activities, there is possibility that these compounds might be hitting a putative HDAC8 homolog in *L. donovani* parasite. Nonetheless, this study introduces novel synthetic skeleton that can pave way for future drug discovery efforts in antileishmanial research.

6.8 References

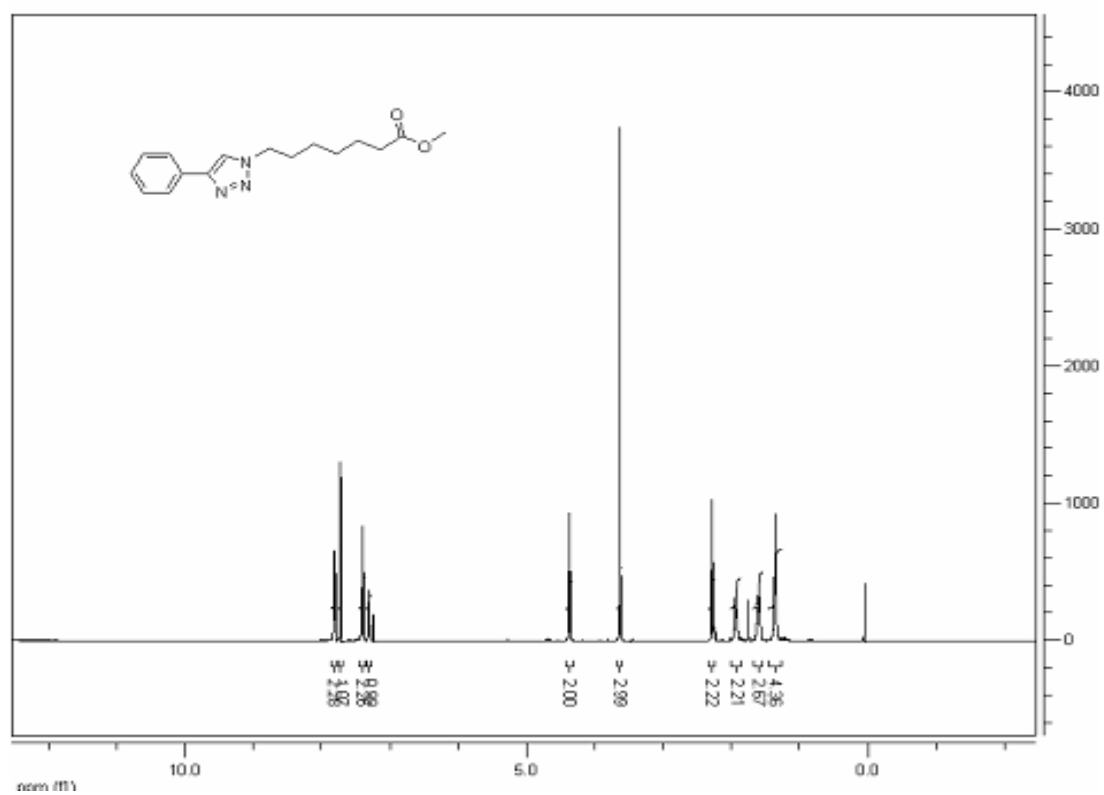
- 47 Akopyants, N. S.; Kimblin, N.; Secundino, N.; Patrick, R.; Peters, N.; Lawyer, P.; Dobson, D. E.; Beverley, S. M.; Sacks, D. L. *Science* **2009**, 324, 265.
- 48 Rogers, M.; Kropf, P.; Choi, B. S.; Dillon, R.; Podinovskaia, M.; Bates, P.; Muller, I. *PLoS Pathog.* **2009**, 5, e1000555.
- 49 Reithinger, R.; Dujardin, J. C.; Louzir, H.; Pirmez, C.; Alexander, B.; Brooker, S. *Cutaneous leishmaniasis, Lancet Infect Dis.* **2007**, 7(9), 581-96
- 50 (a) <http://www.who.int/tdr/diseases/leish/diseaseinfo.htm>.; (b) Sharma, U.; Singh, S. *Indian J. Exp. Biol.* **2009**, 47, 412.
- 51 WHO Report, Available at: <http://www.who.int/leishmaniasis/burden/en>.
- 52 Chappuis, F; Sundar, S; Hailu, A; Ghalib, H; Rijal, S; Peeling, R. W.; Alvar, J.; Boelaert, M. *Nat. Rev. Microbiol.* **2007**, 11, 873.

- 53 Mueller, M.; Ritmeijer, K.; Balasegaram, M.; Koummuki, Y.; Santana, M. R.; Davidson R. *Trans. R. Soc. Trop. Med. Hyg.* **2007** 101(1), 19.
- 54 (a) Sundar, S.; Chakravarty, J.; Rai, V. K.; *et al.* *Clin. Infect. Dis.* **2007** 45(5), 556.
(b) van Thiel P.P.A.M. *et al.* *Clinical Infectious Diseases* **2010**, 50 (1), 80.
- 55 a) Russell, D. *Eur. J. Biochem.* **1987**, 164, 213. b) Puentes, S. *et al J Immunol*, **1989**, 143, 3743.
- 56 Pandey, S; Chakraborti, P; Sharma, R.; Bandyopadhyay, S.; Sarkar, D.; Adhya, S. *J Biosci.* **2004**, 29(1), 15.
- 57 Schlagenhauf, E.; Etges, R.; Metcalf, P. *Structure* **1998**, 6, 1035.
- 58 Chen, P.C.; Patil, V.; Guerrant, W., Green, P.; Oyelere, A. K. *Bioorg. Med. Chem.* **2008**, 16, 4839.
- 59 Lu, Q.; Wang, D. S.; Chen, C. S. *et al. J. Med. Chem.* **2005**, 48, 5530.
- 60 Sigel, H; McCormick, D. B. *Acct. Chem. Res.* **1970**, 3(6), 201.

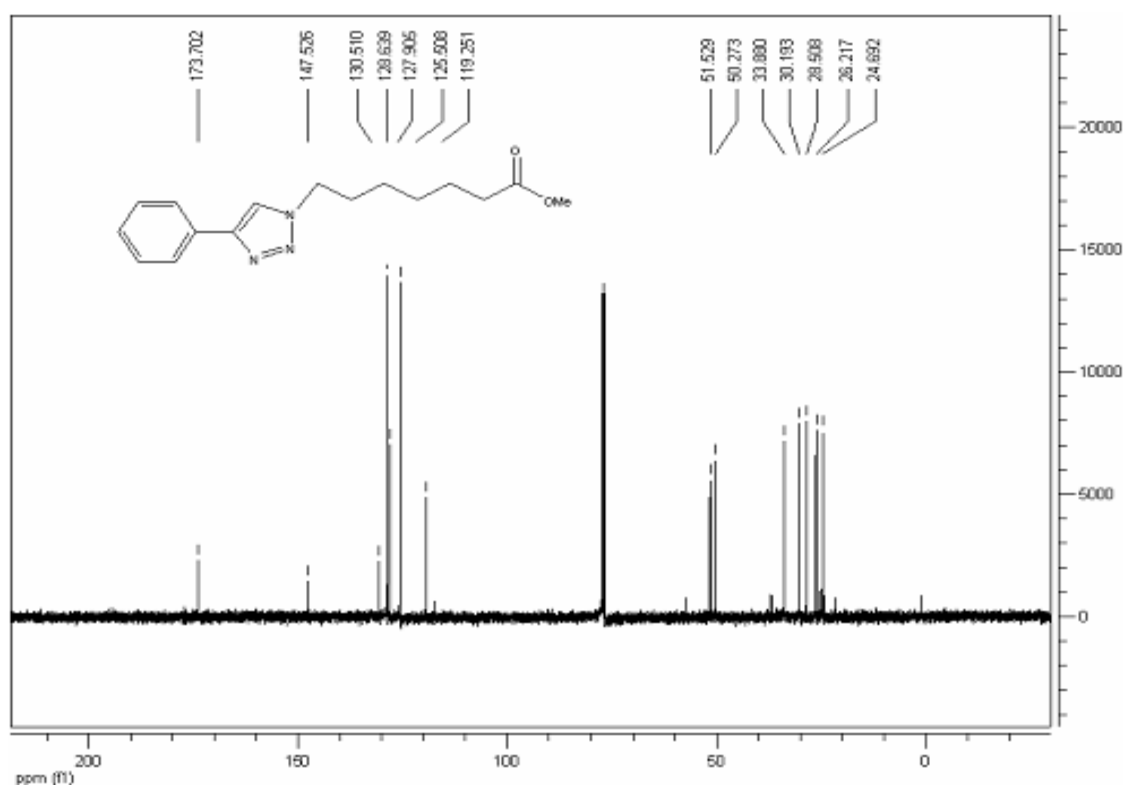
APPENDIX A

^1H and ^{13}C NMR characterization for SAHA-like Aryltriazolylhydroxamates HDACi
(Chapter 2)

^1H NMR of **3d**:



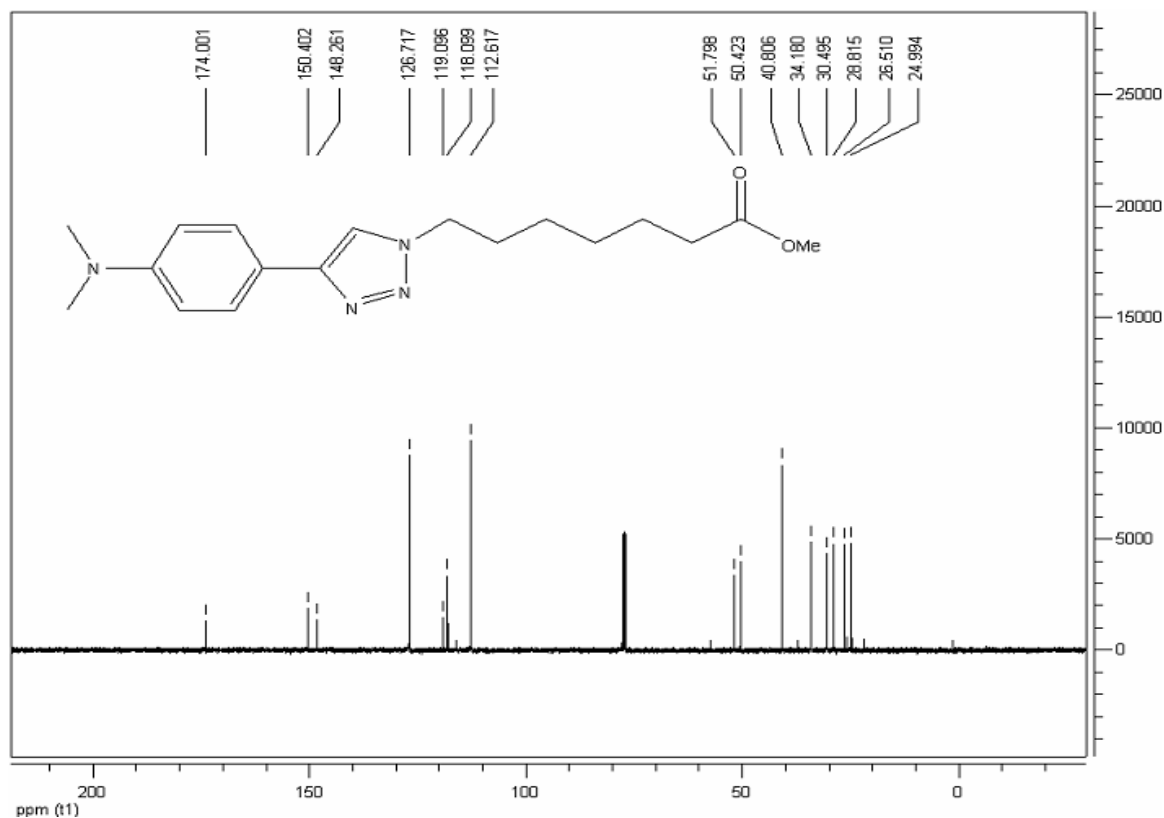
^{13}C NMR of **3d**:



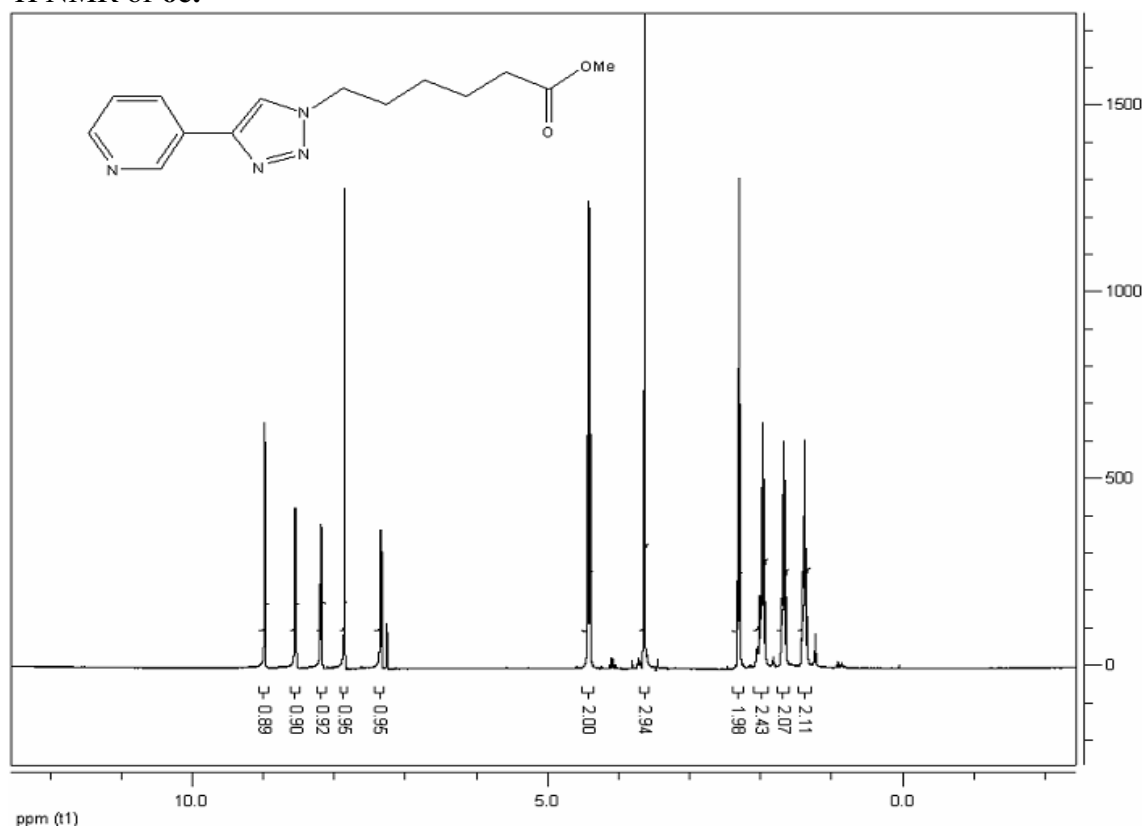
^1H NMR of **6b**:



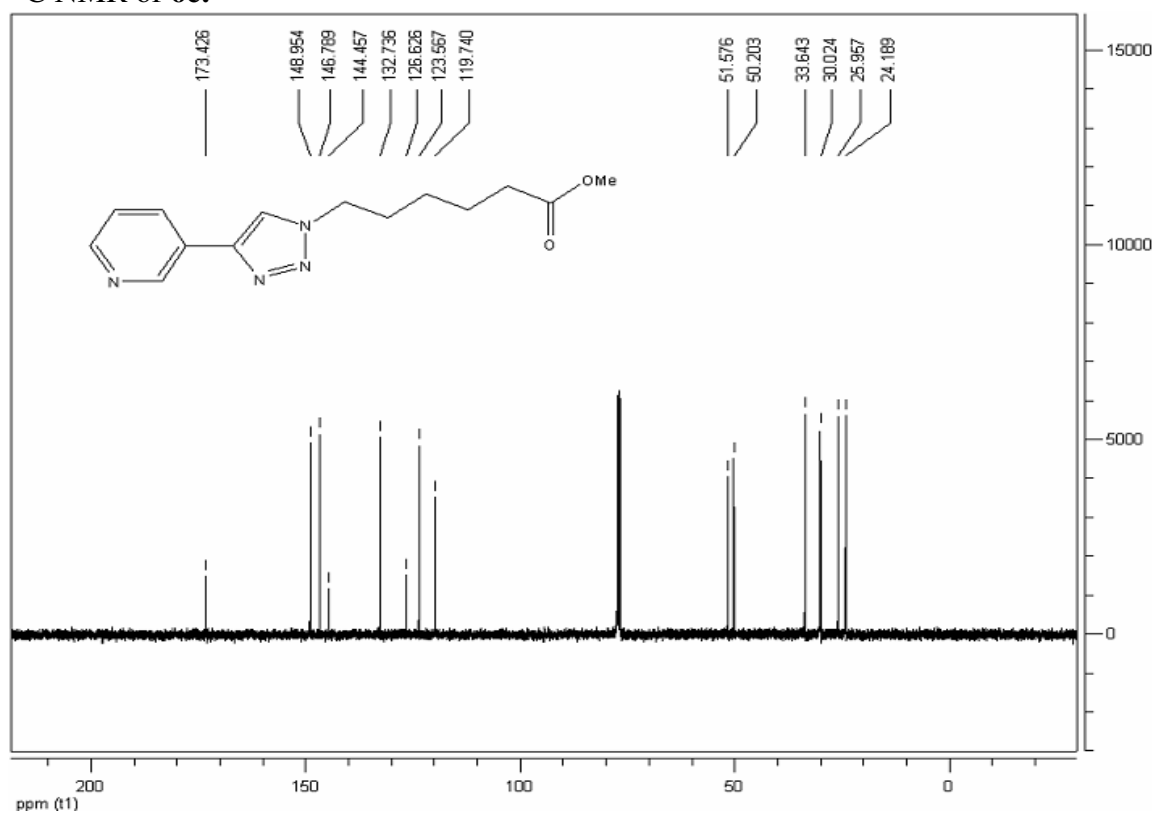
^{13}C NMR of **6b**:



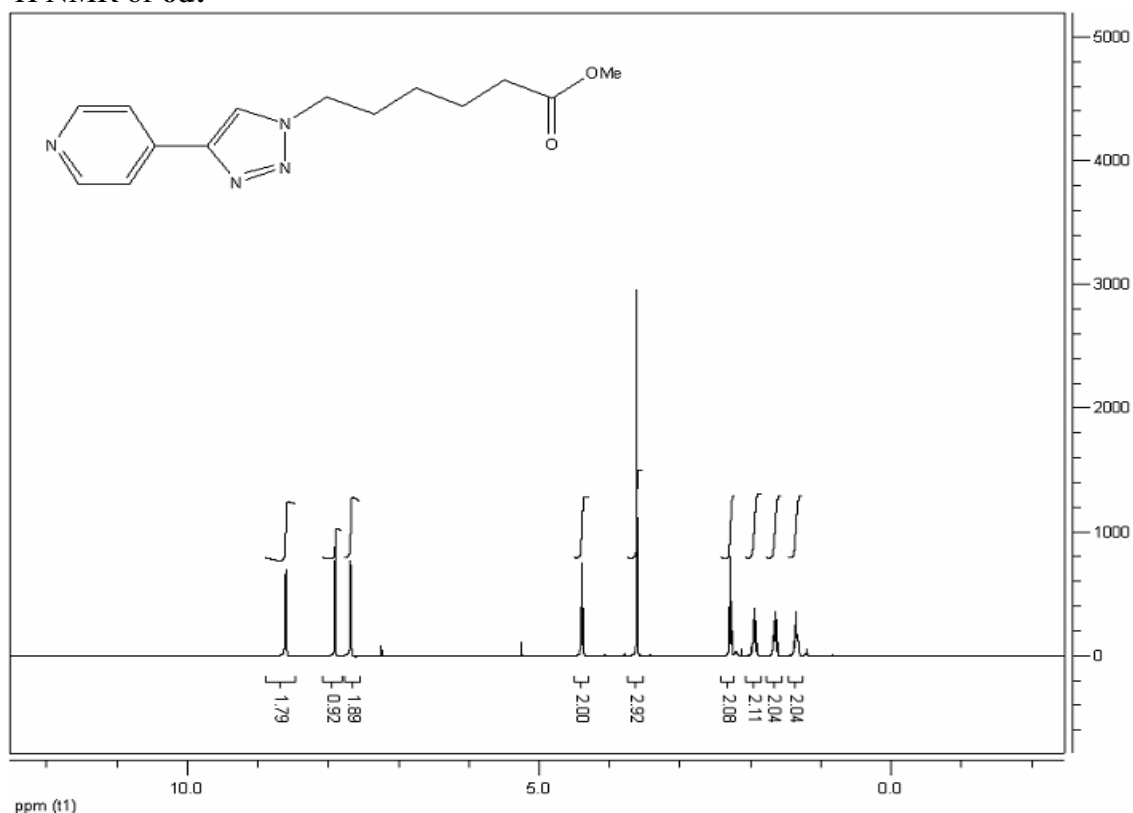
¹H NMR of **6c**:



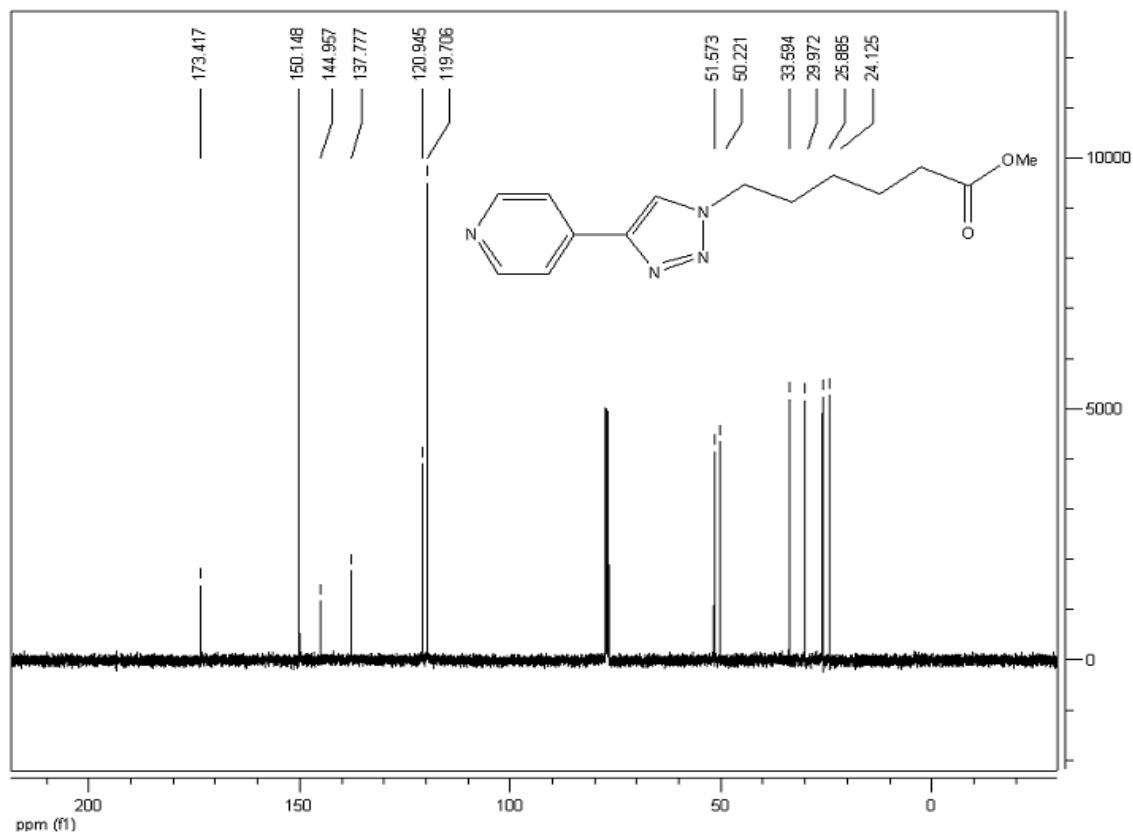
¹³C NMR of **6c**:



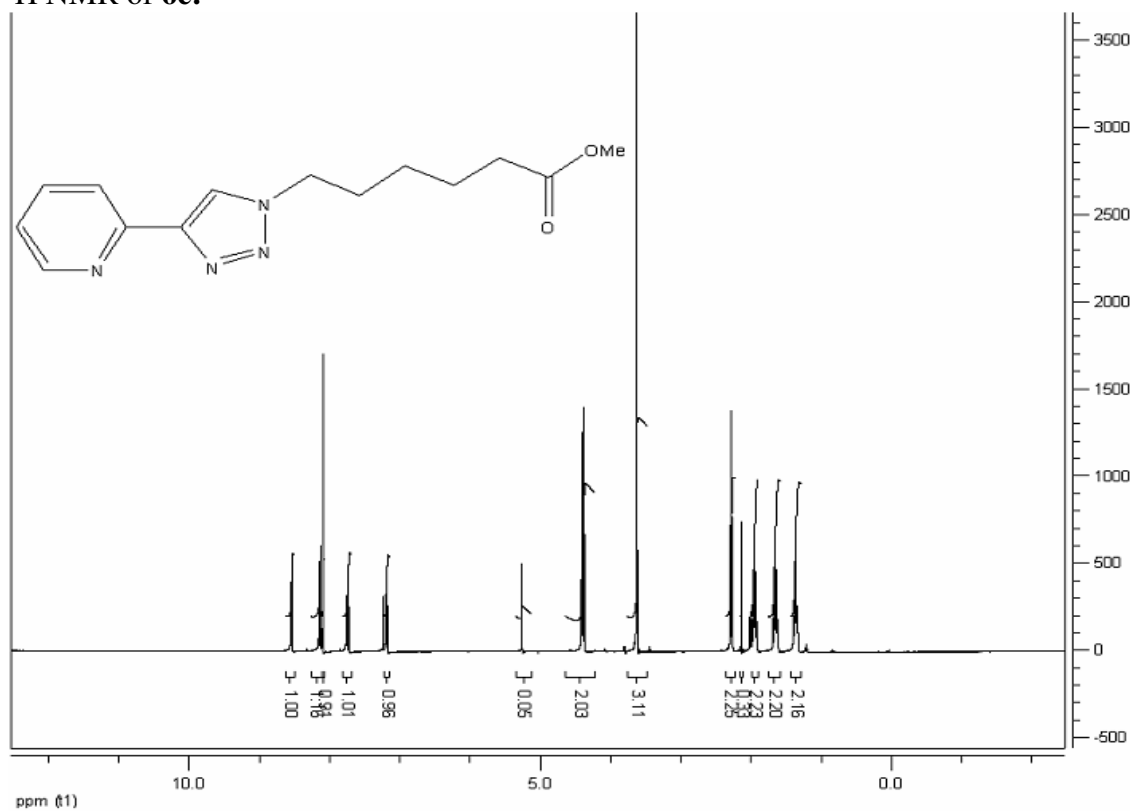
¹H NMR of **6d**:



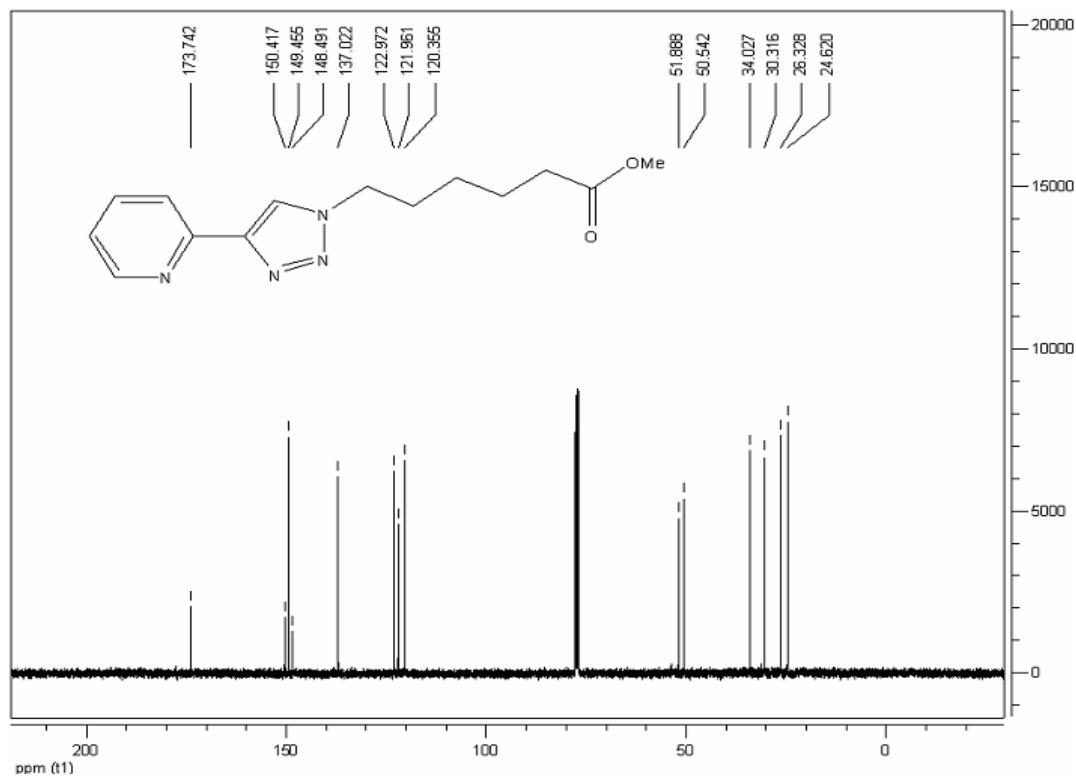
¹³C NMR of **6d**:



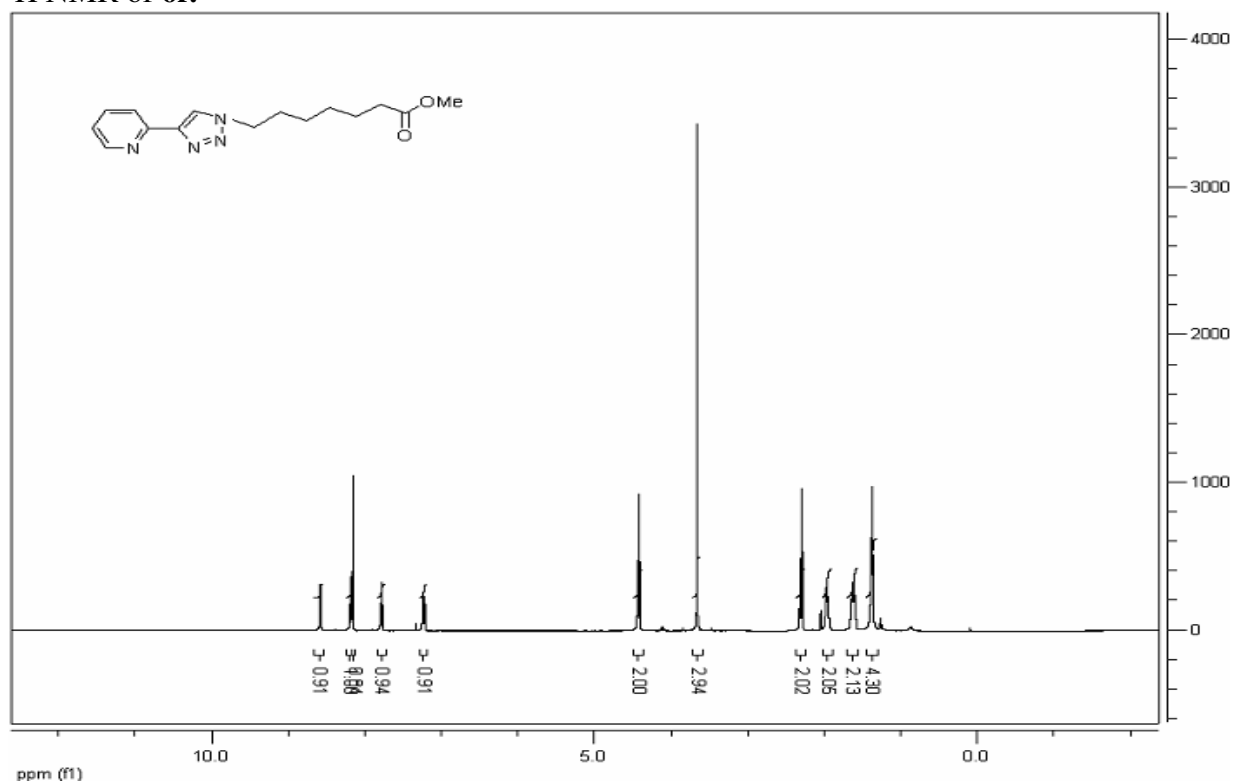
¹H NMR of **6e**:



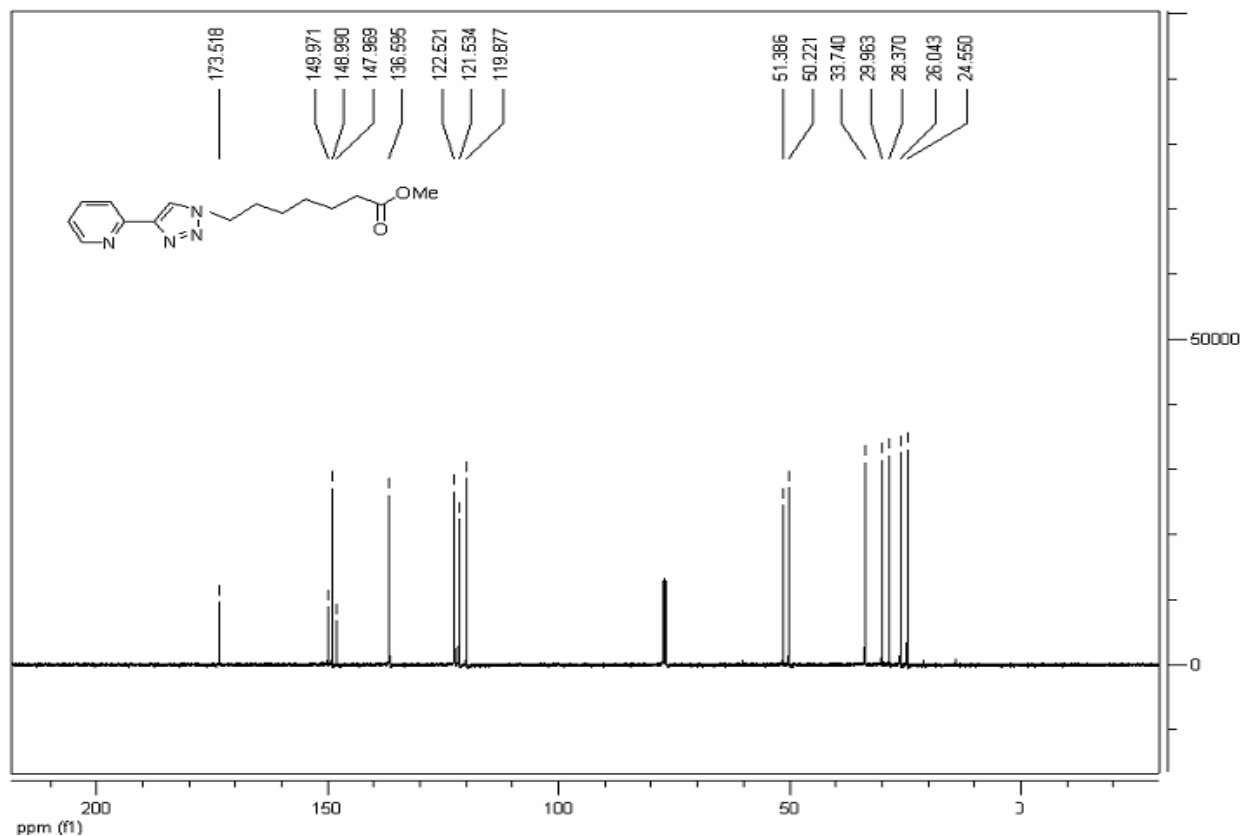
¹³C NMR of **6e**:



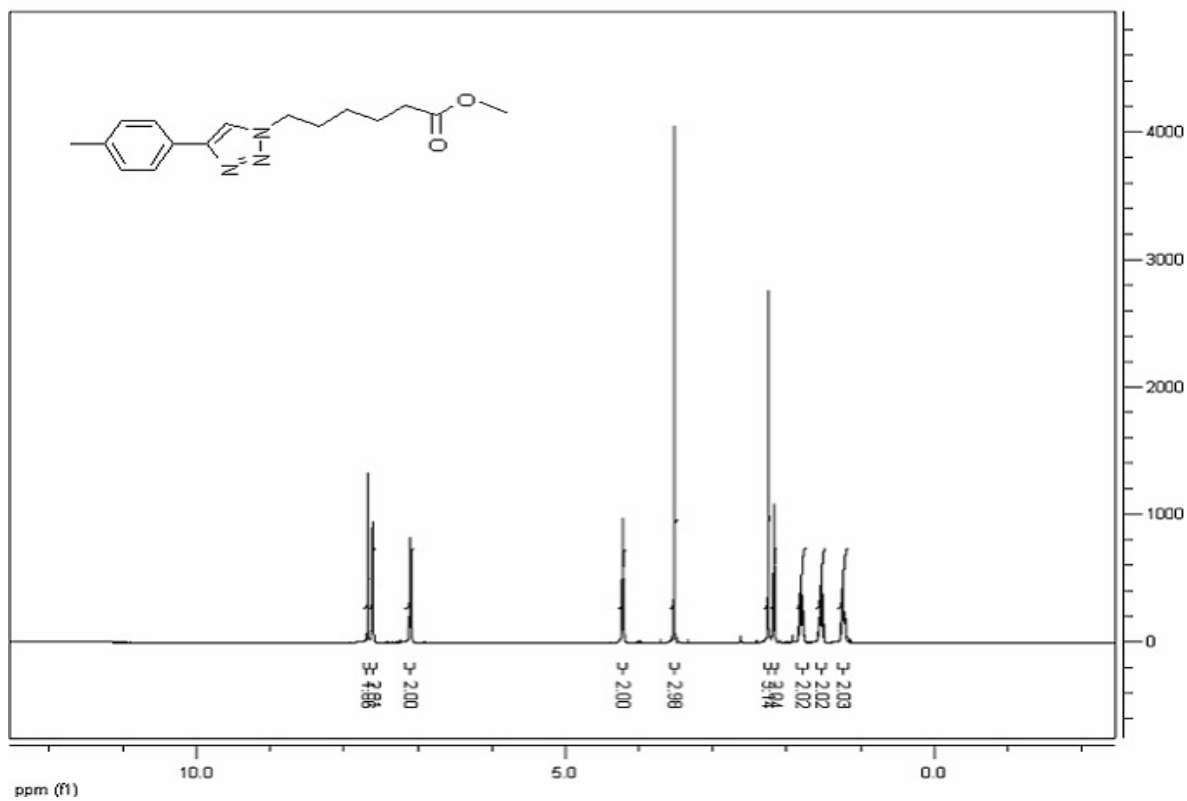
^1H NMR of **6f**:



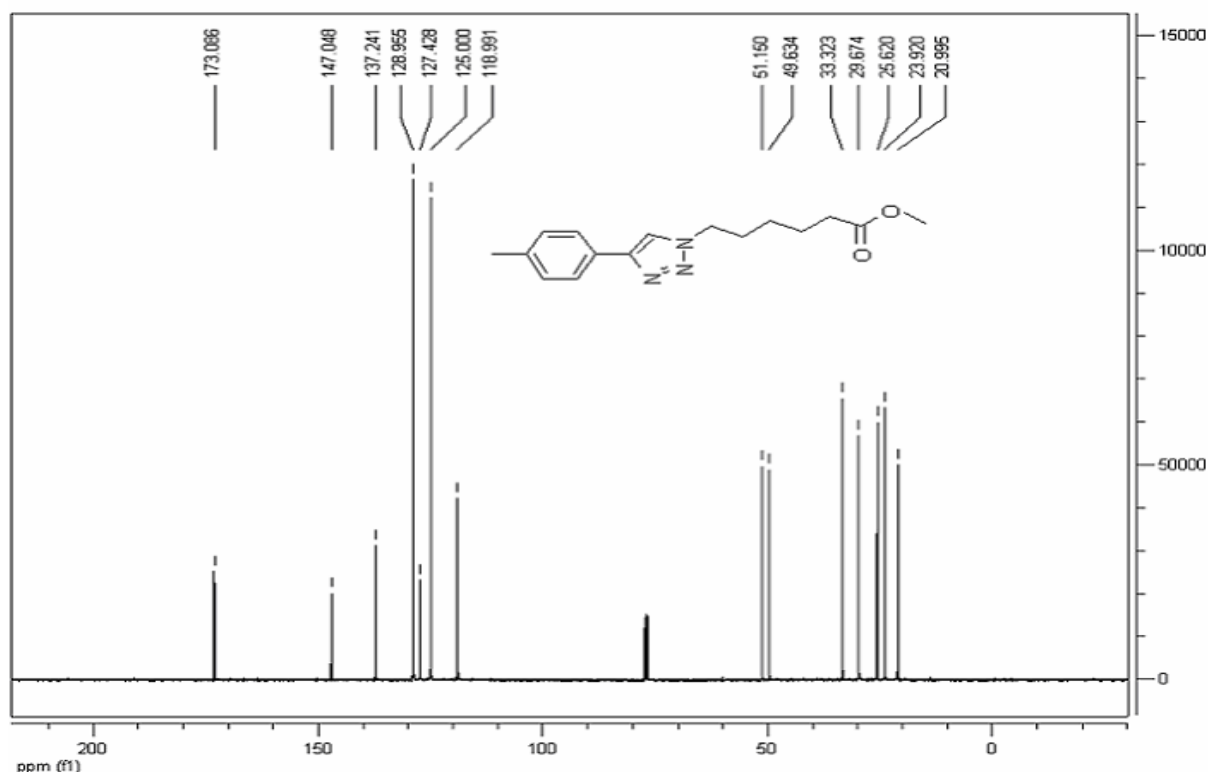
^{13}C NMR of **6f**:



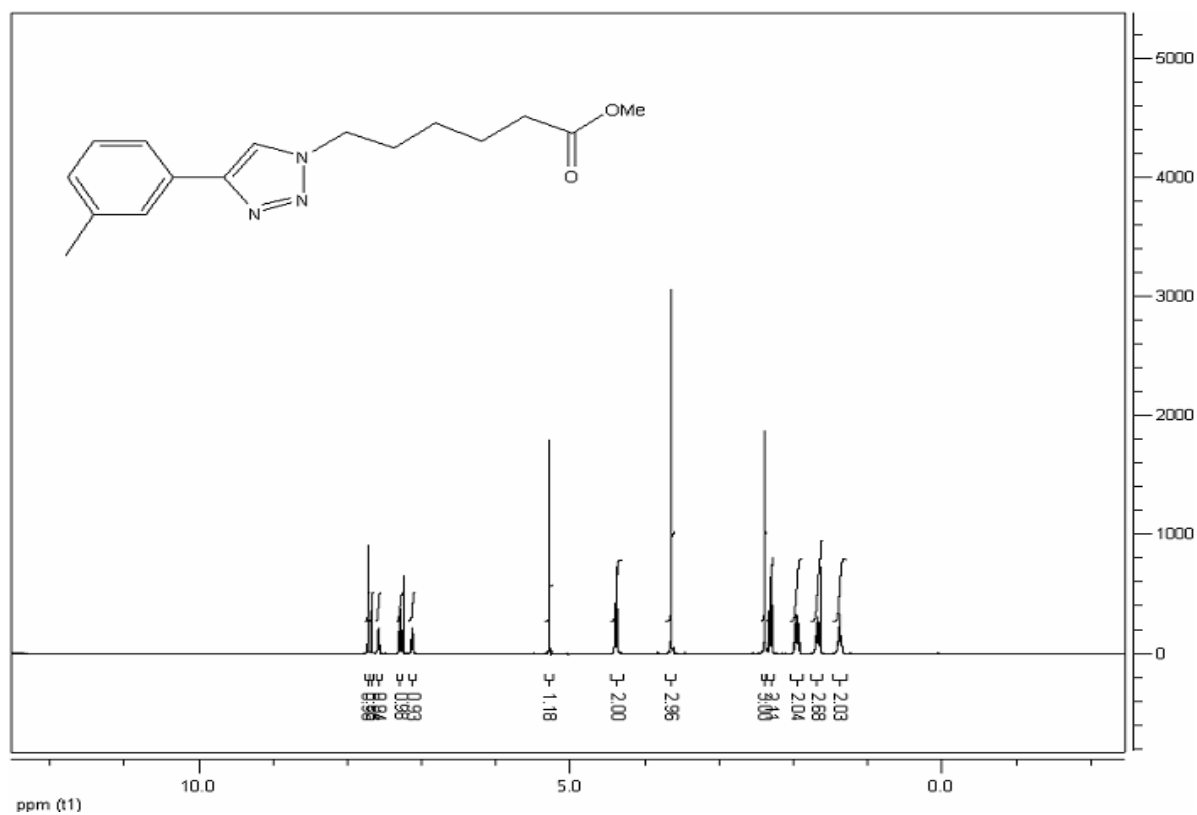
^1H NMR of **6g**:



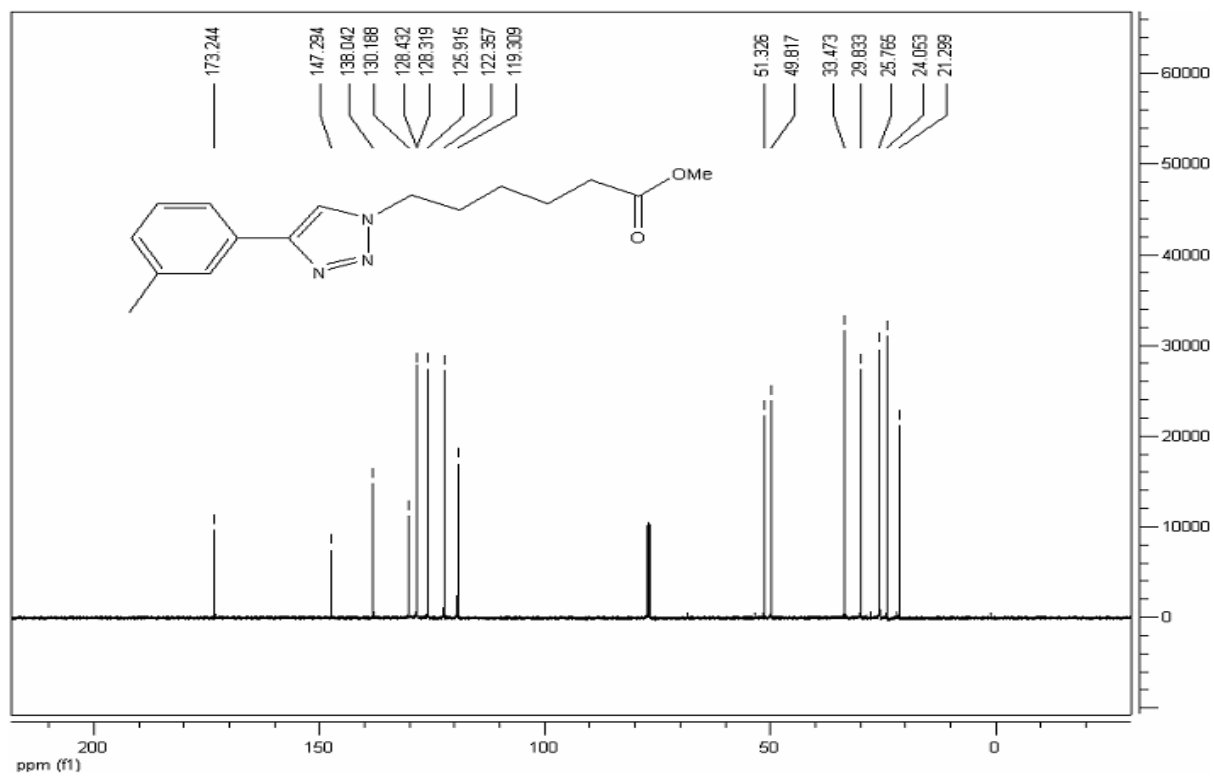
^{13}C NMR of **6g**:



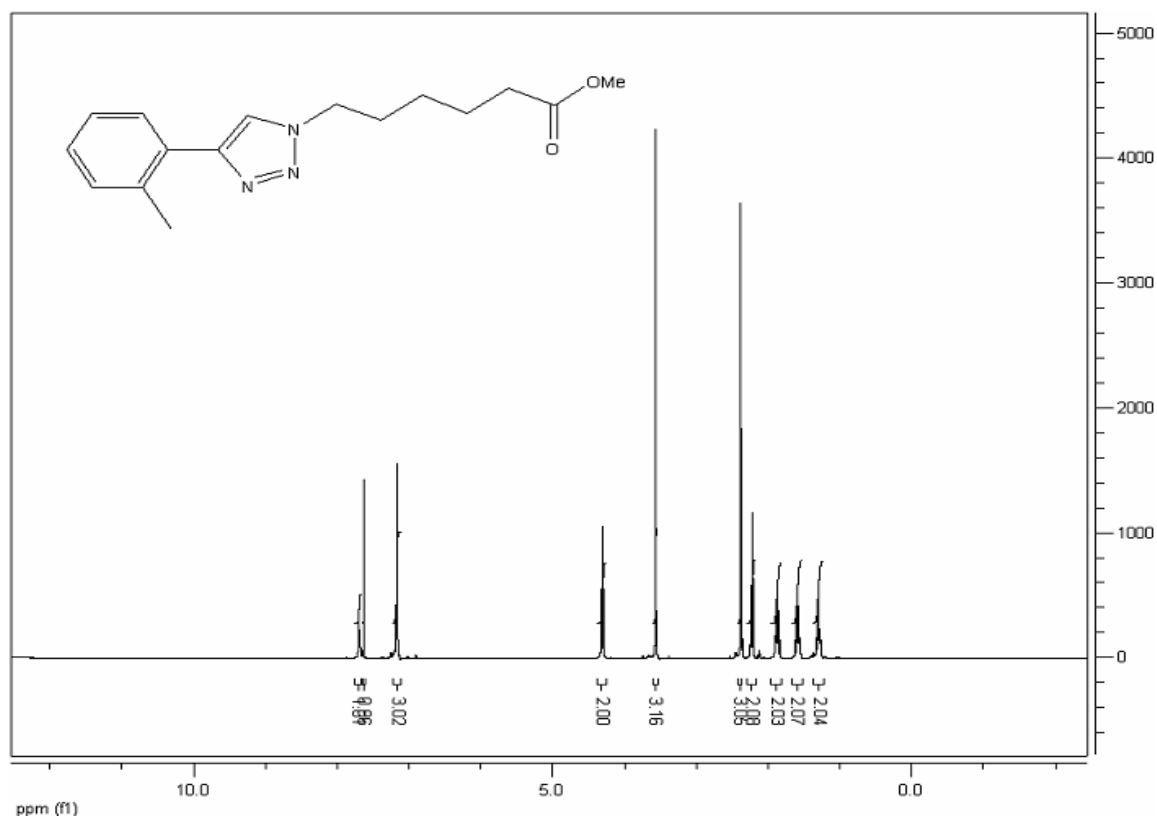
^1H NMR of **6h**:



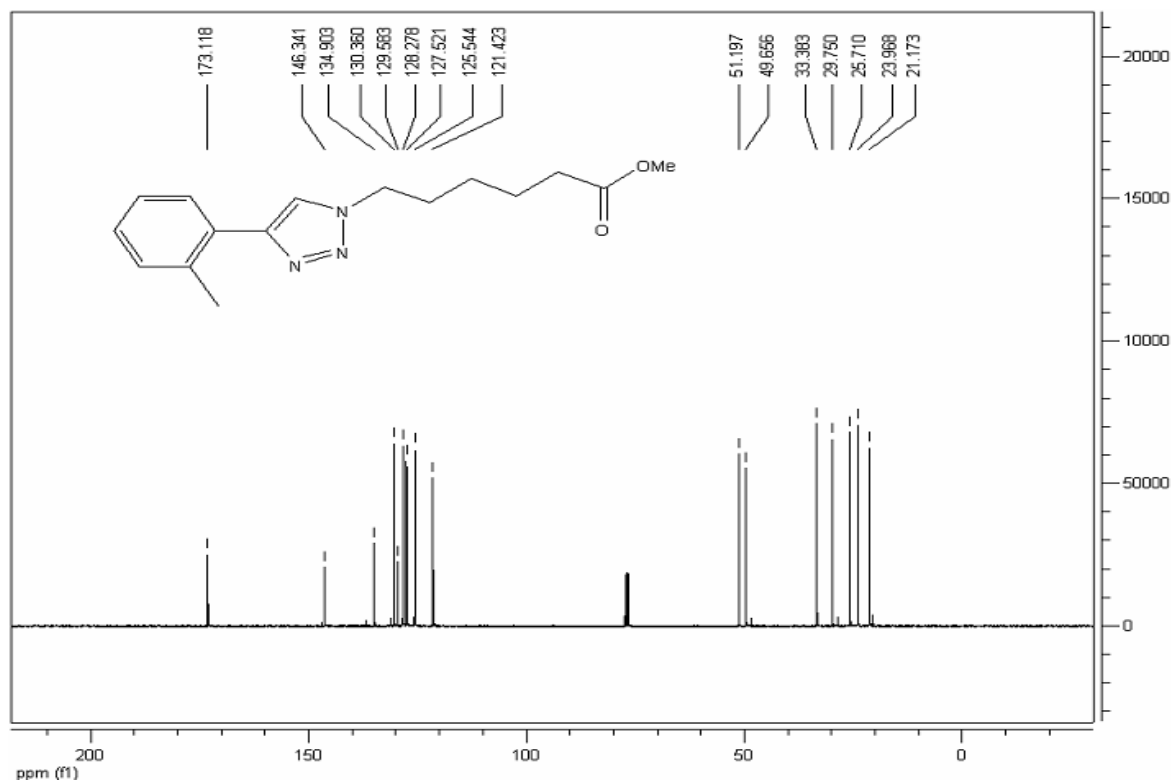
^{13}C NMR of **6h**:



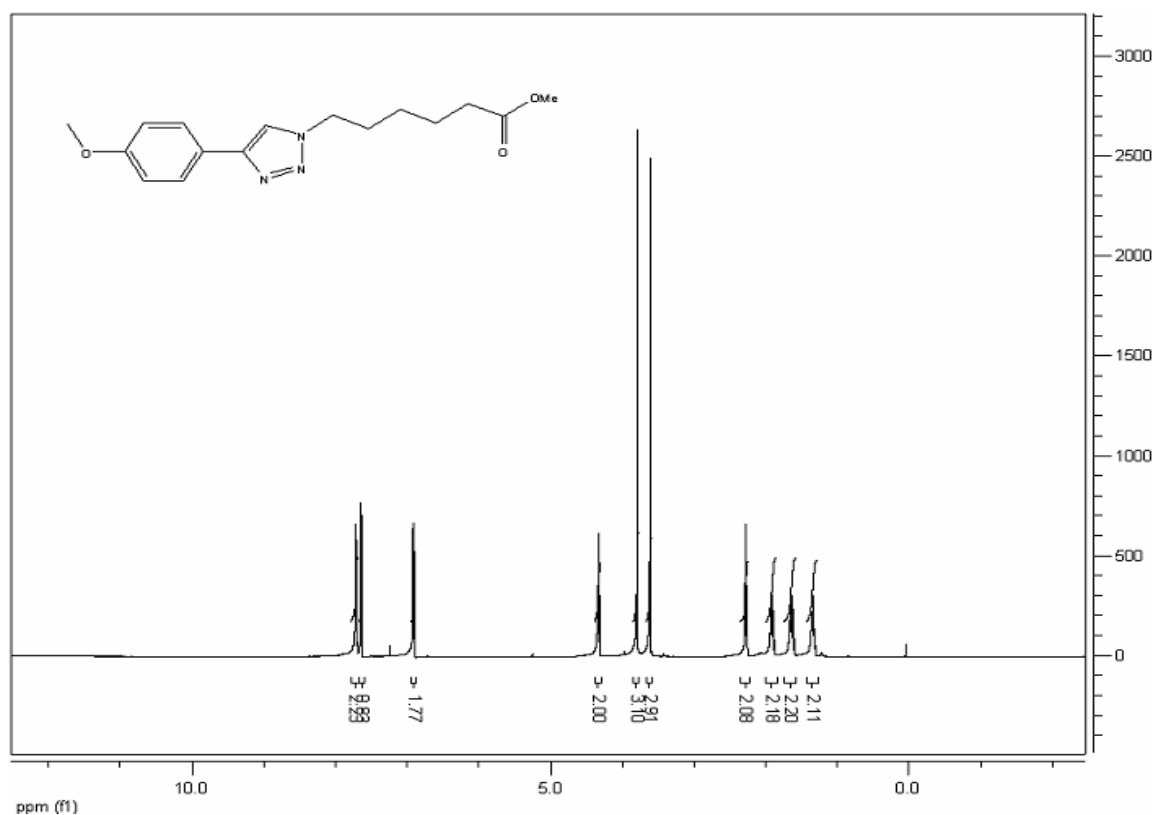
¹H NMR of **6i**:



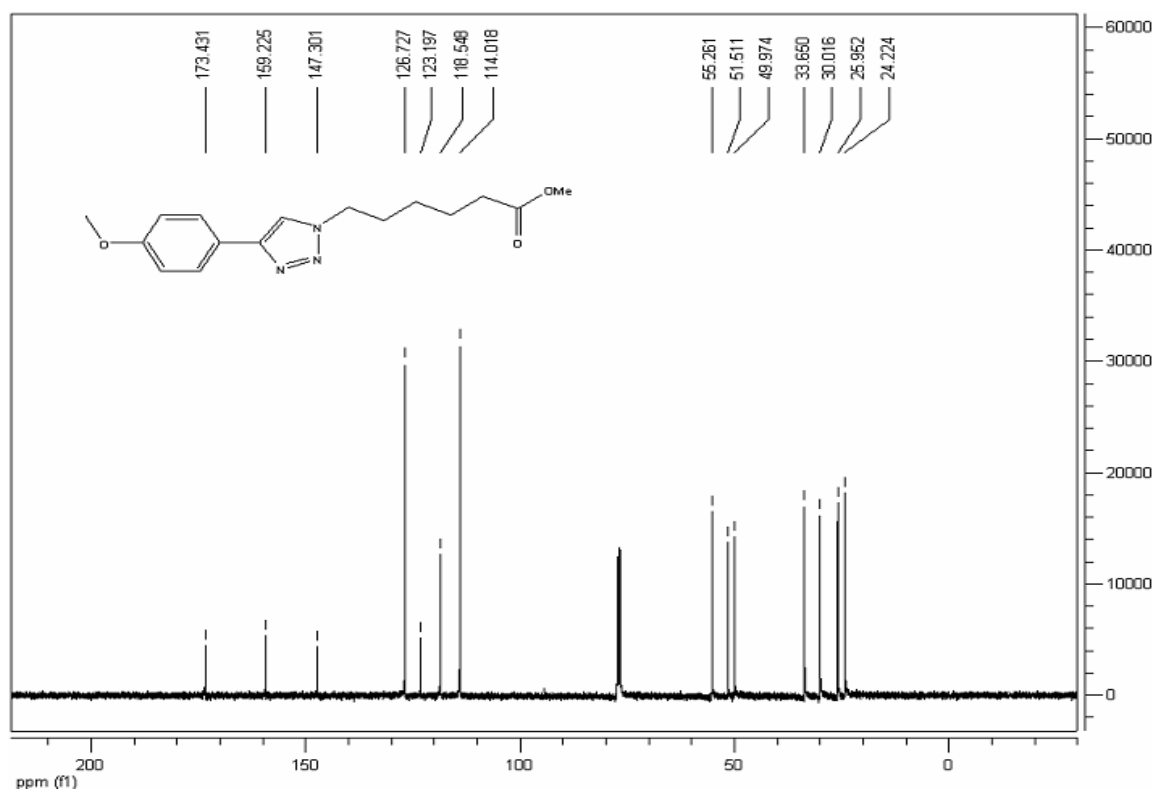
¹³C NMR of **6i**:



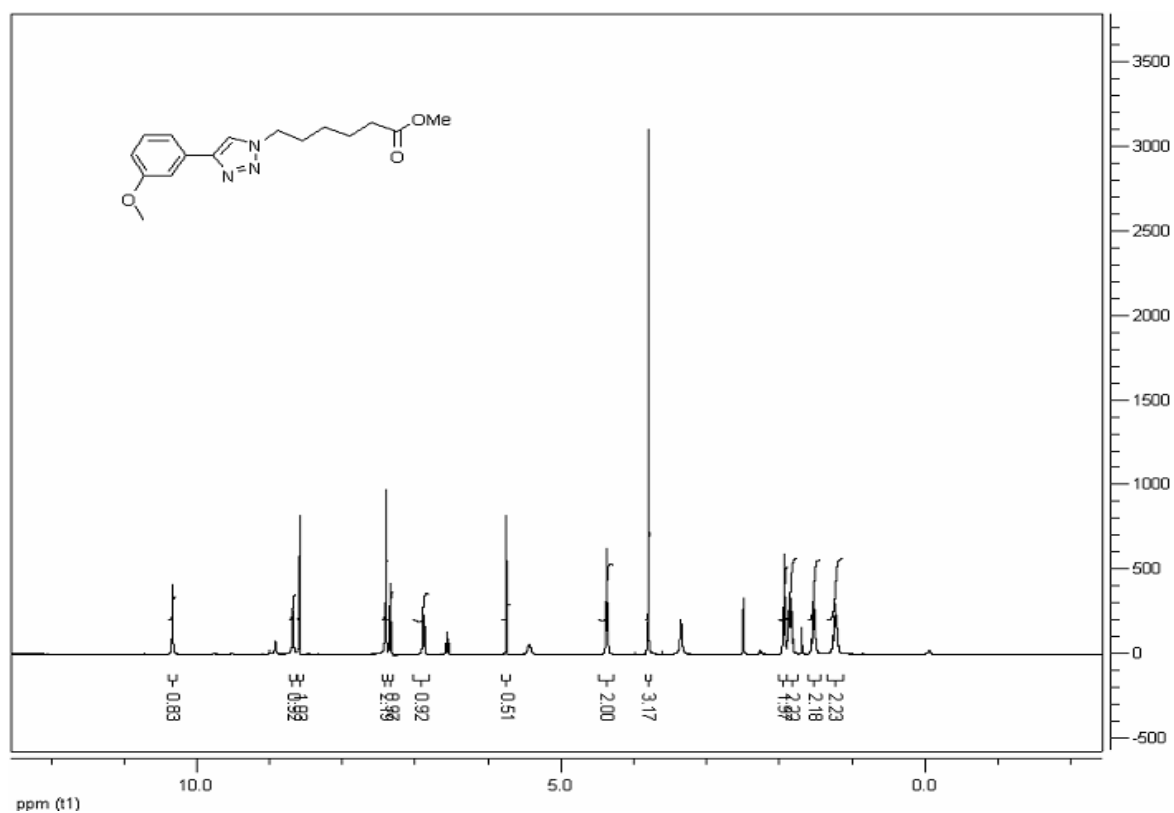
^1H NMR of **6j**:



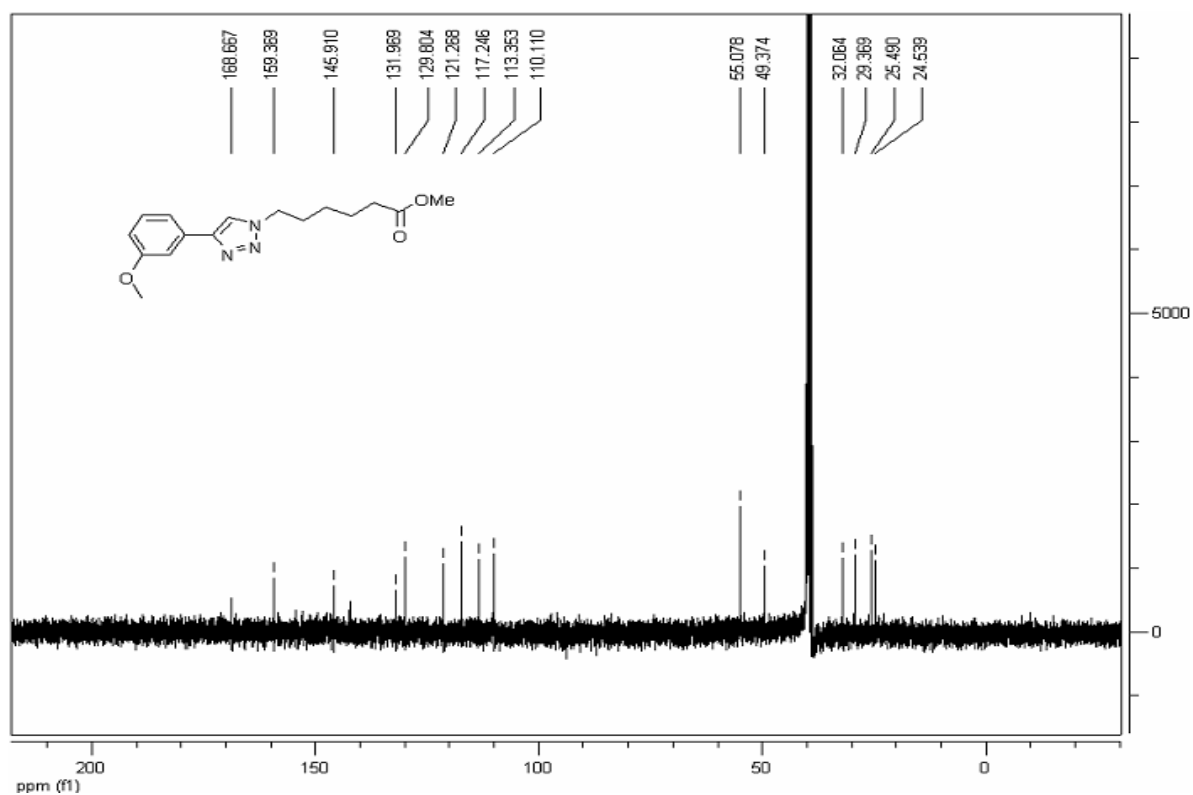
^{13}C NMR of **6j**:



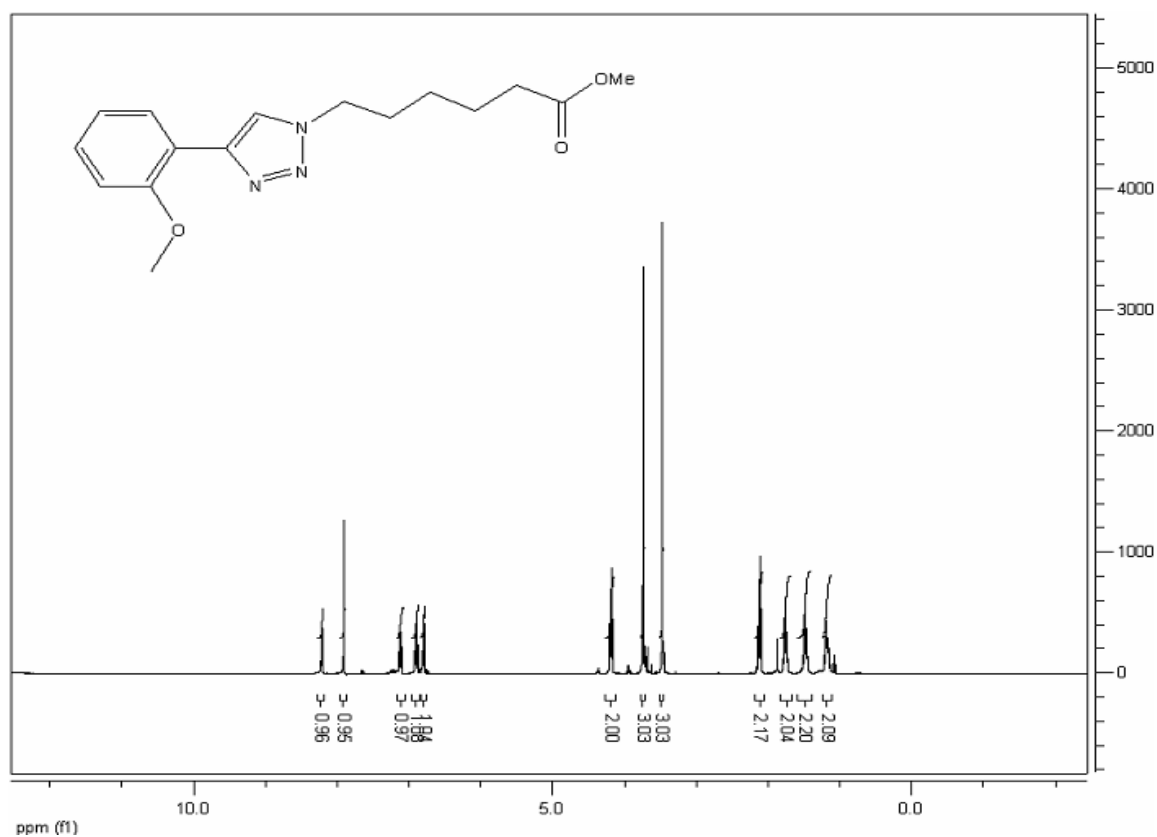
¹H NMR of **6k**:



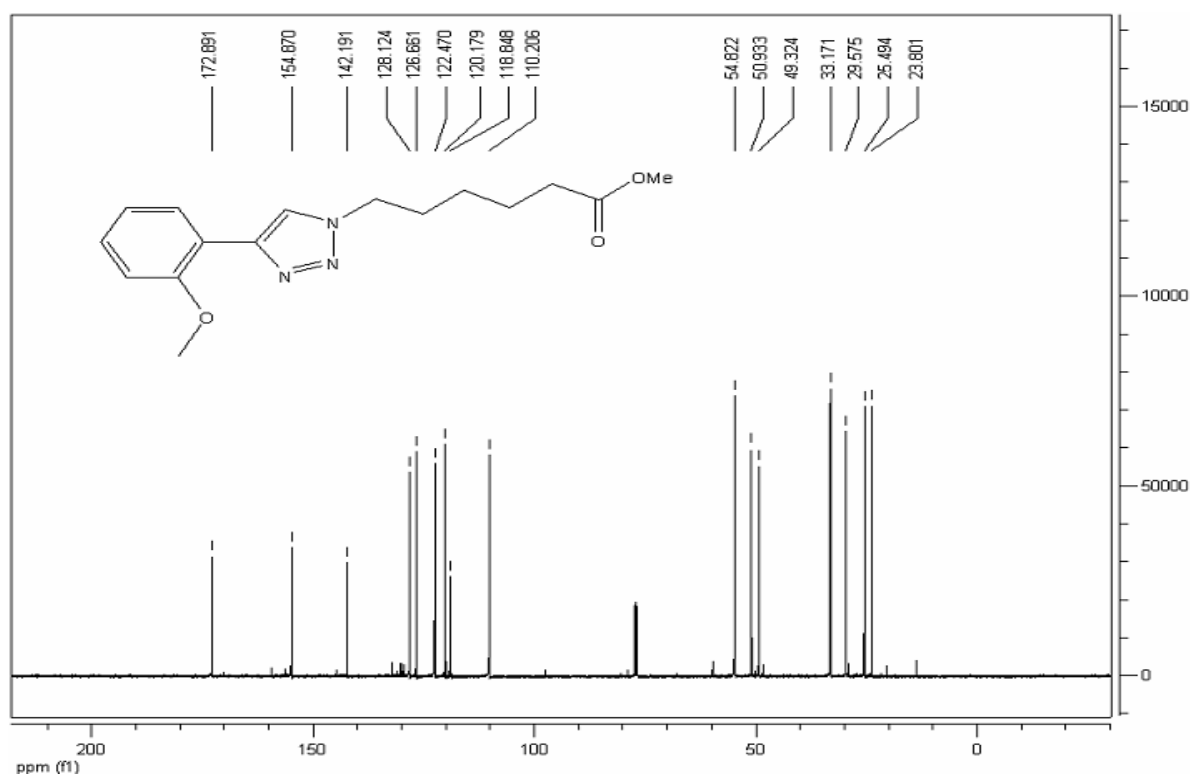
¹³C NMR of **6k**:



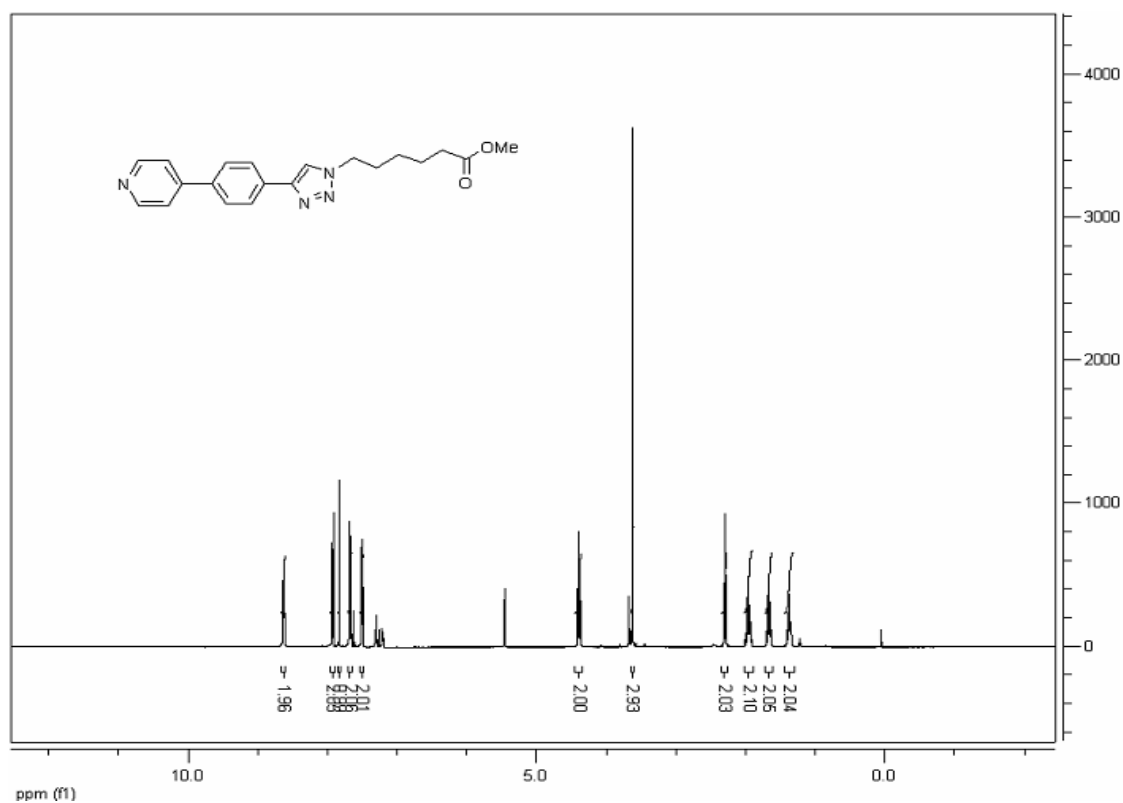
^1H NMR of **6l**:



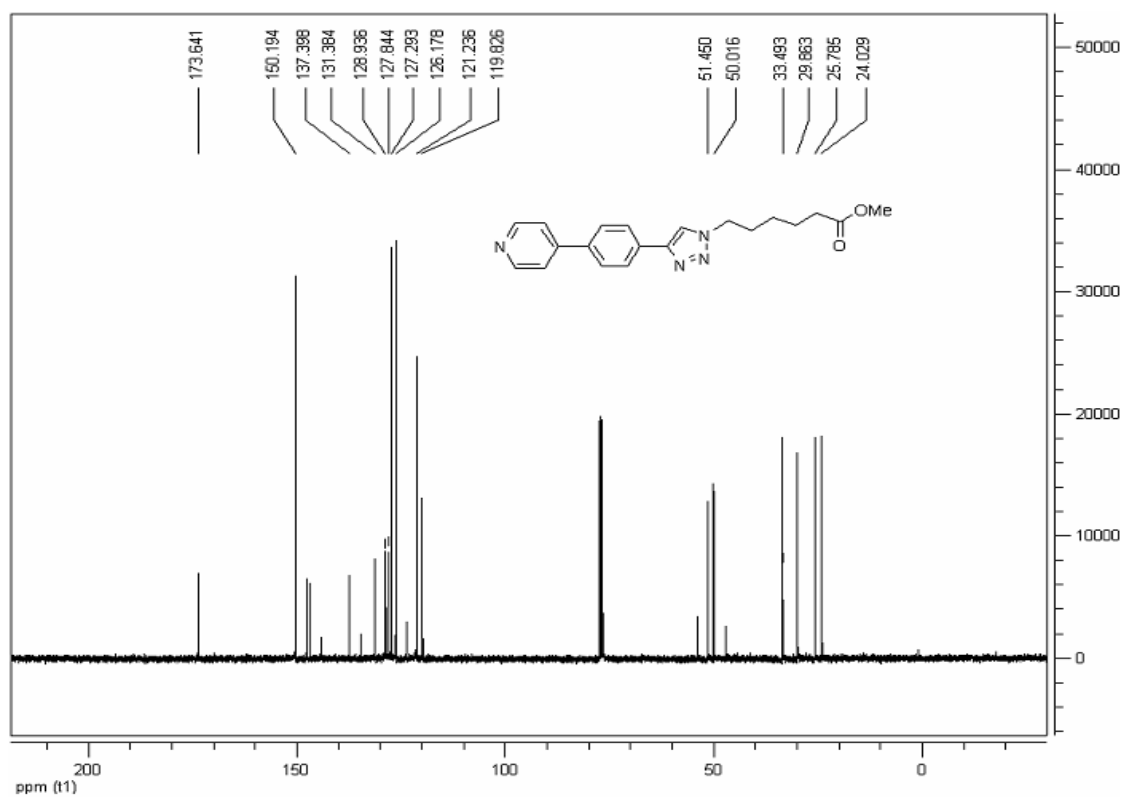
^{13}C NMR of **6l**:



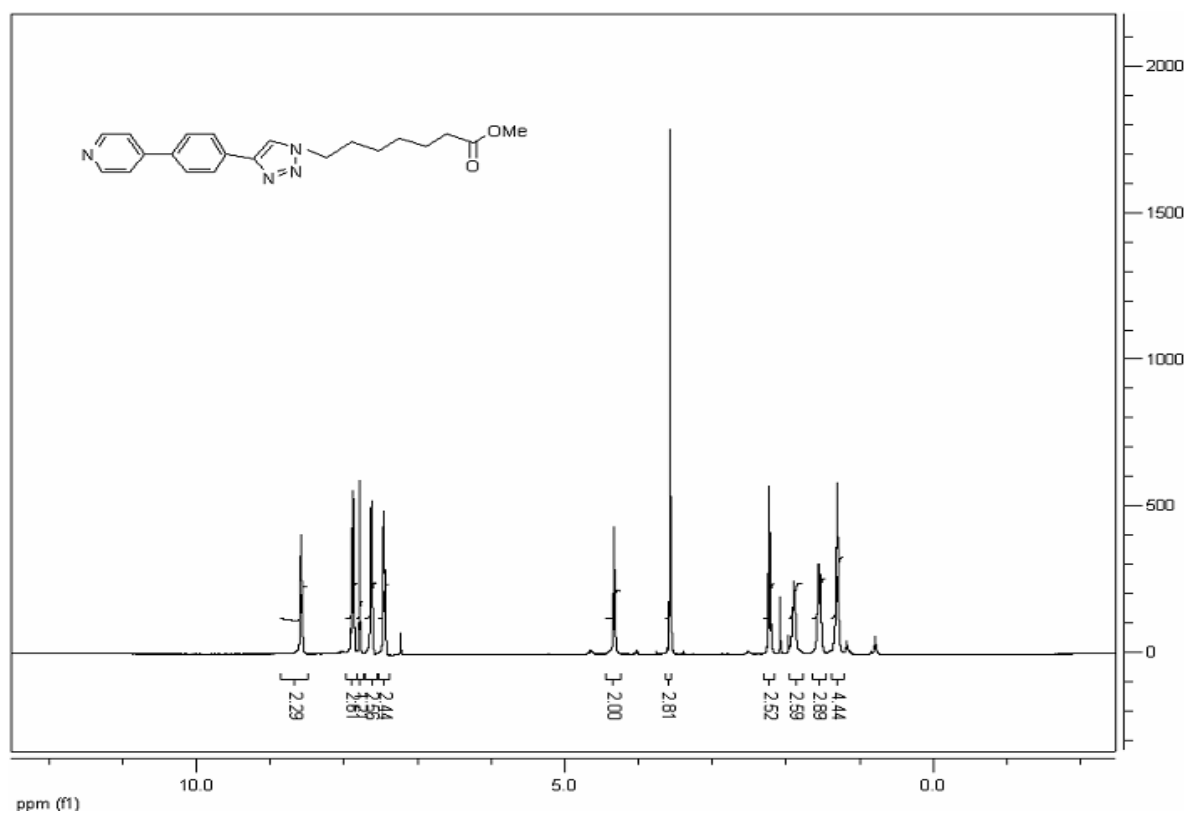
^1H NMR of **6s**:



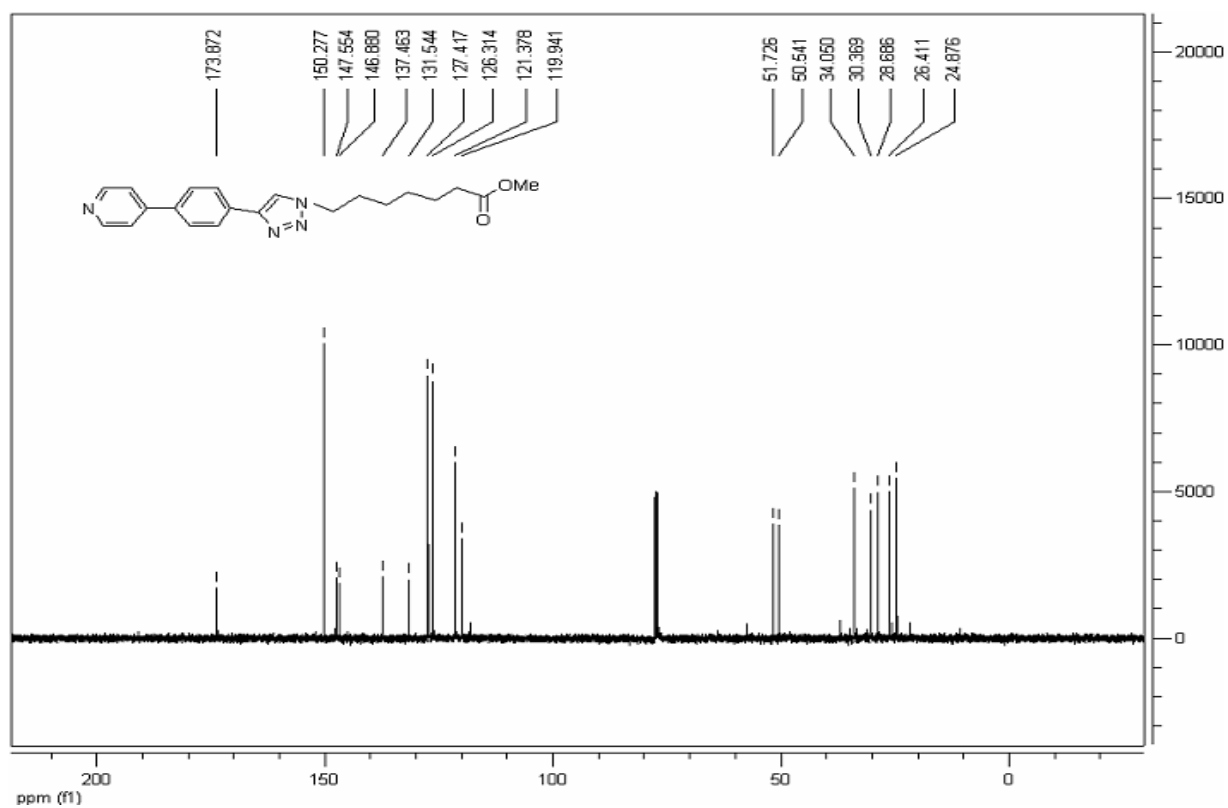
^{13}C NMR of **6s**:



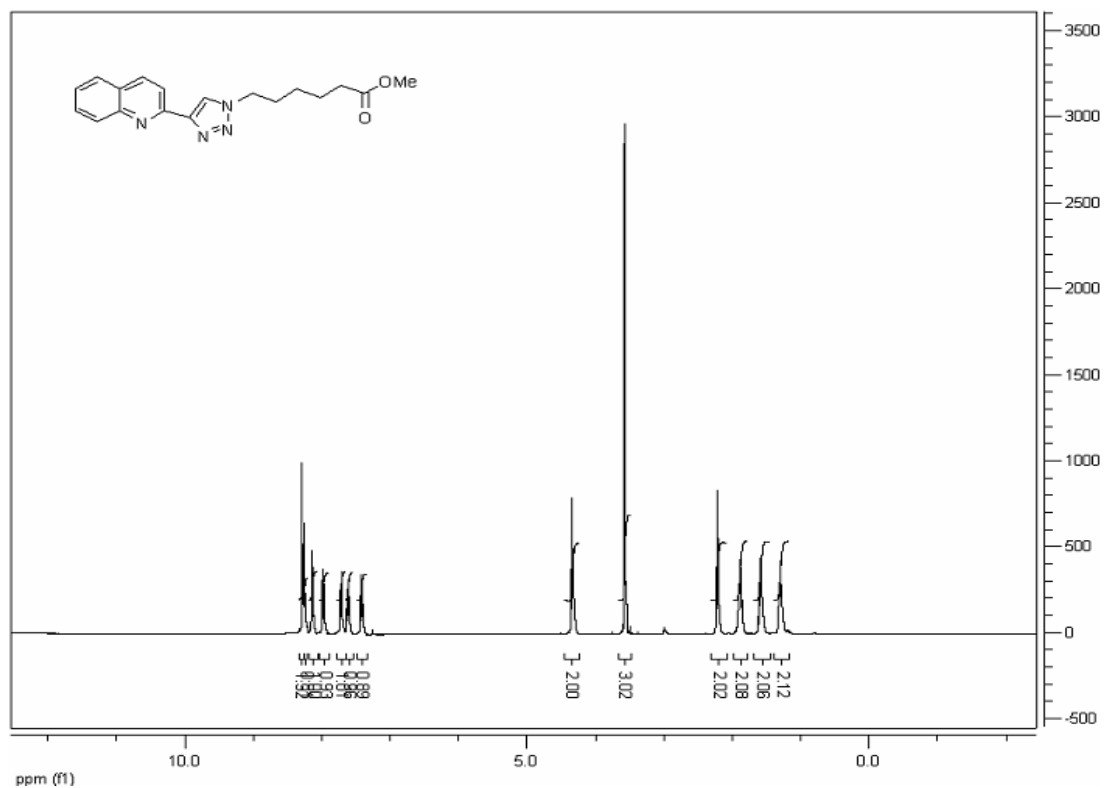
^1H NMR of **6t**:



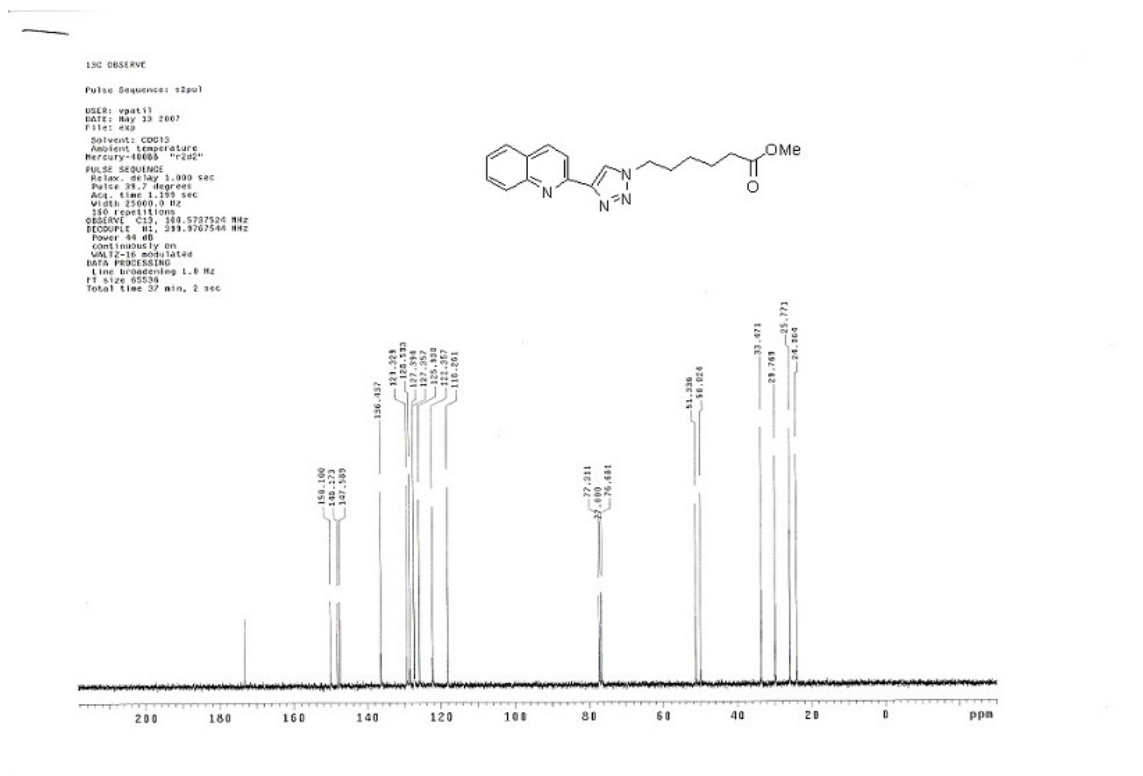
^{13}C NMR of **6t**:



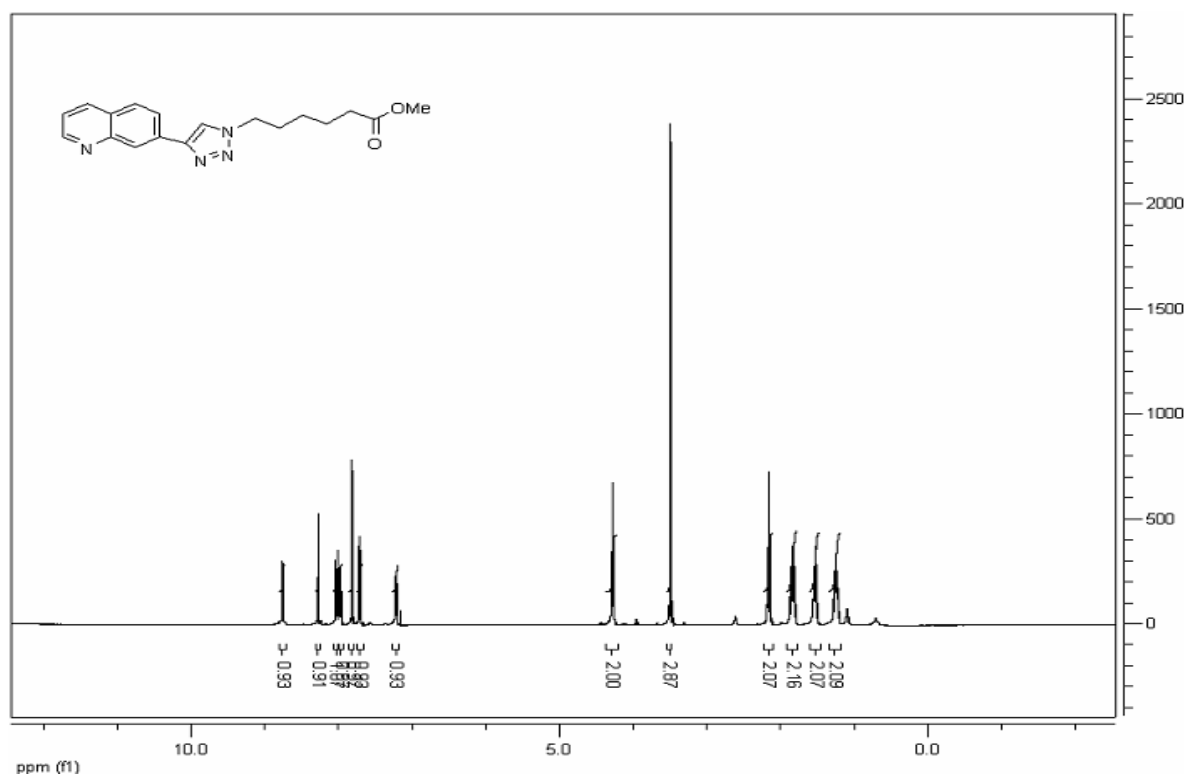
¹H NMR of **6w**:



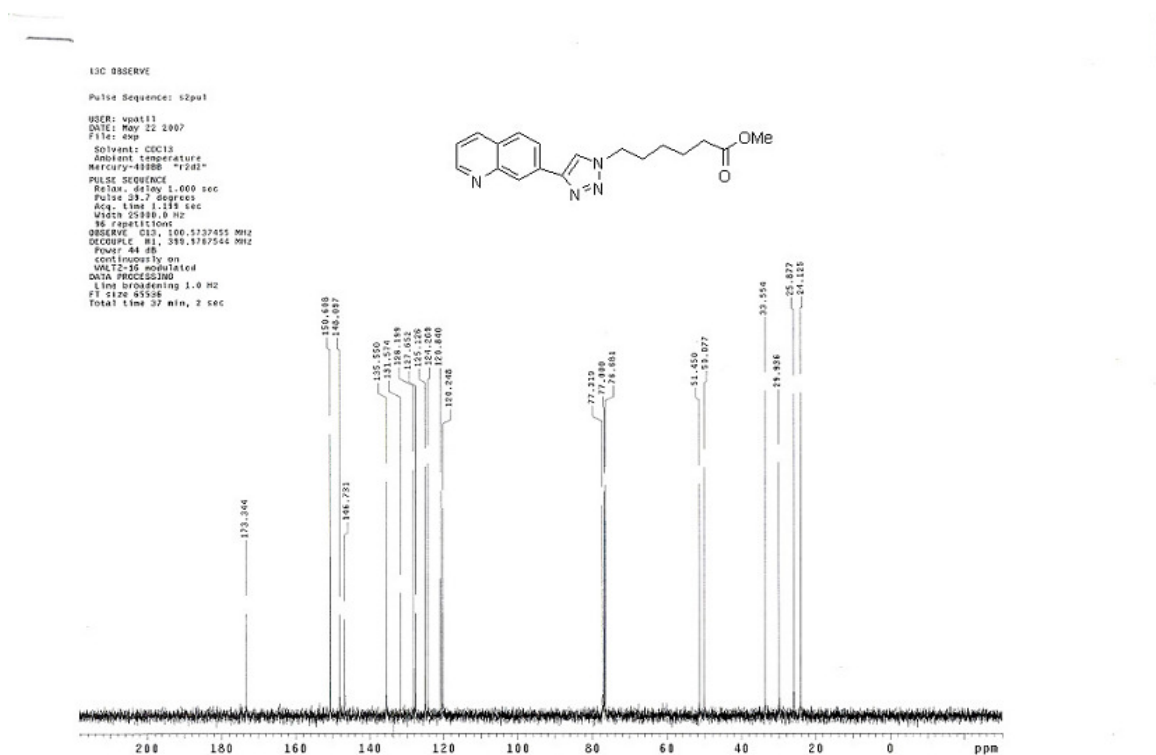
¹³C NMR of **6w**:



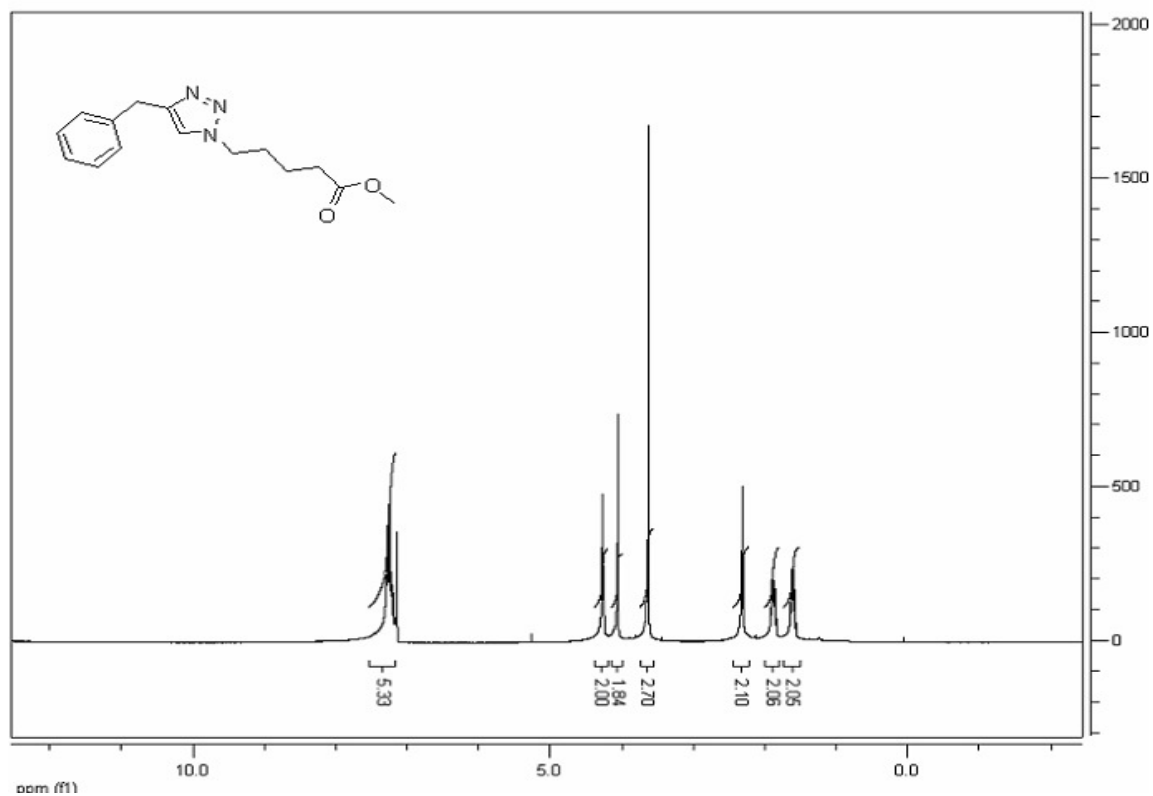
¹H NMR of **6x**:



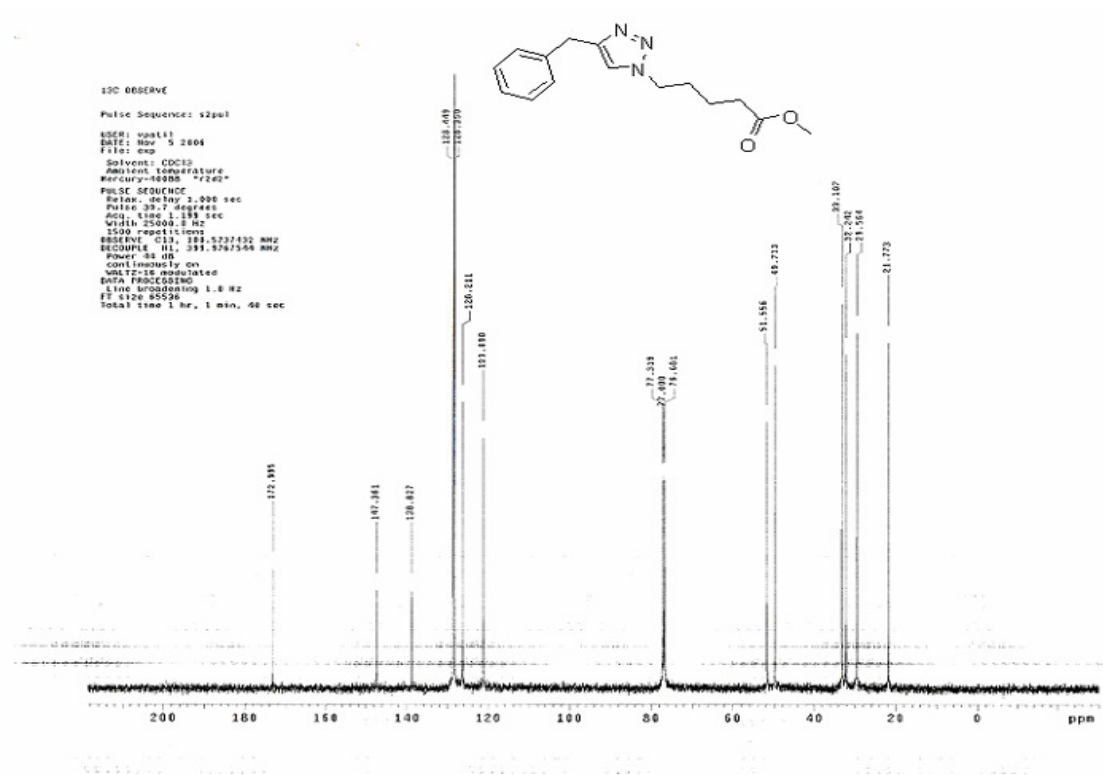
¹³C NMR of **6x**:



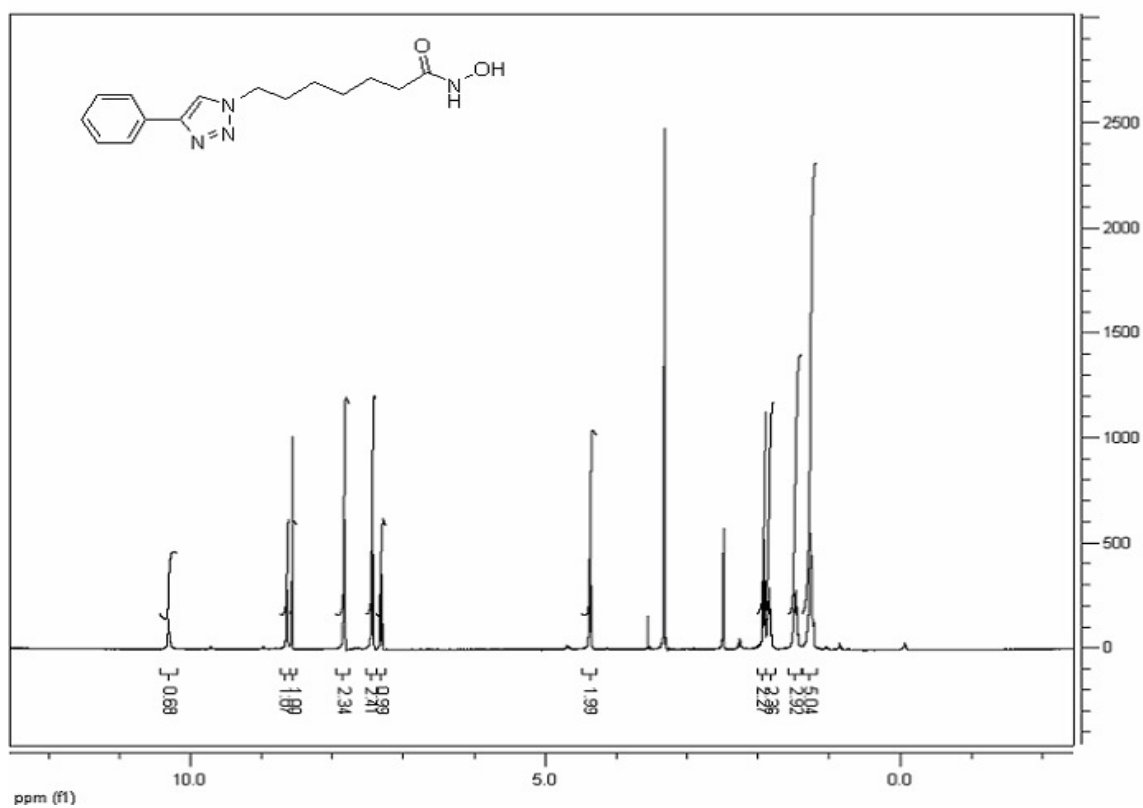
^1H NMR of **6y**:



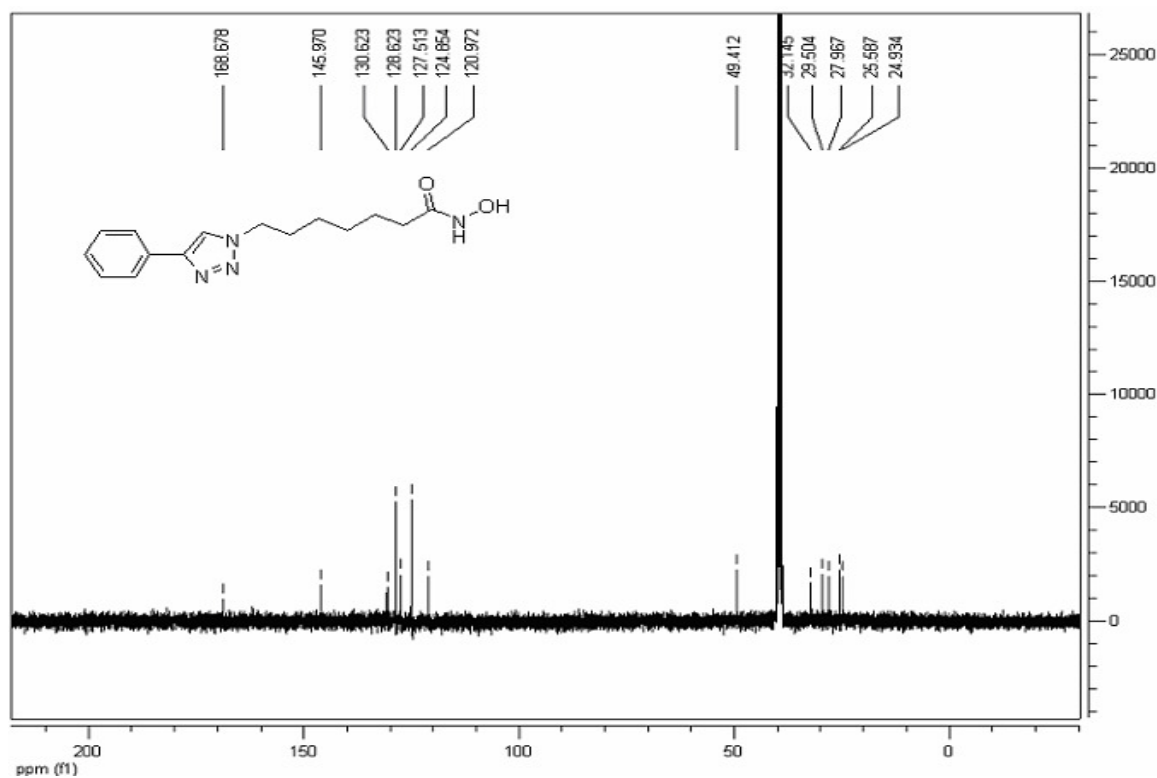
^{13}C NMR of **6y**:



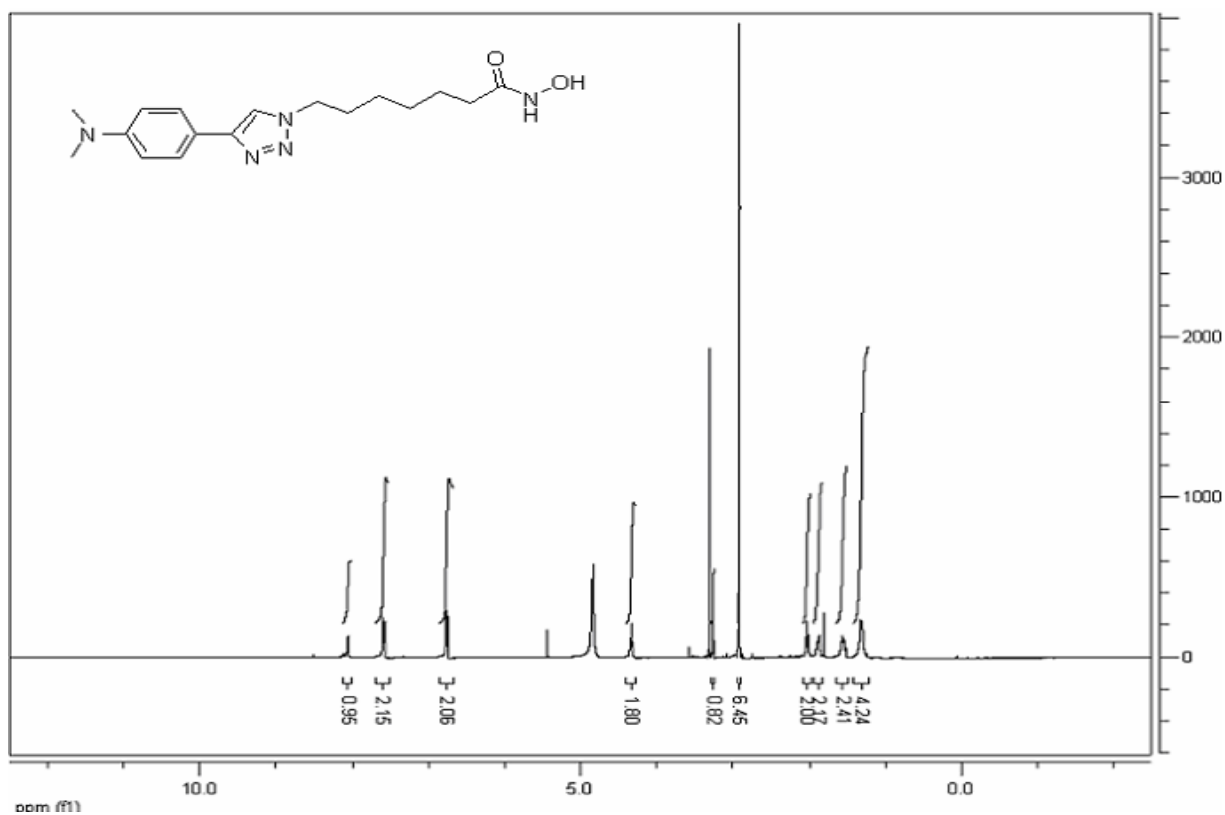
^1H NMR of **4d**:



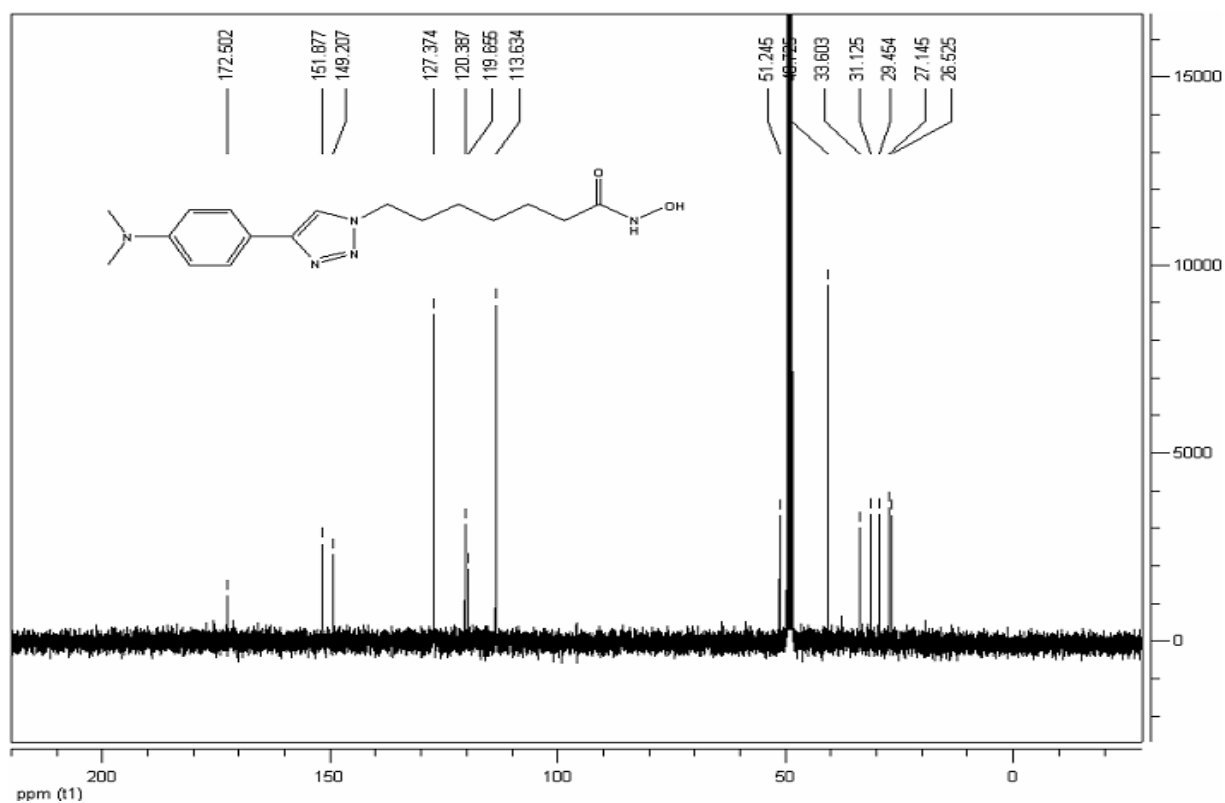
^{13}C NMR of **4d**:



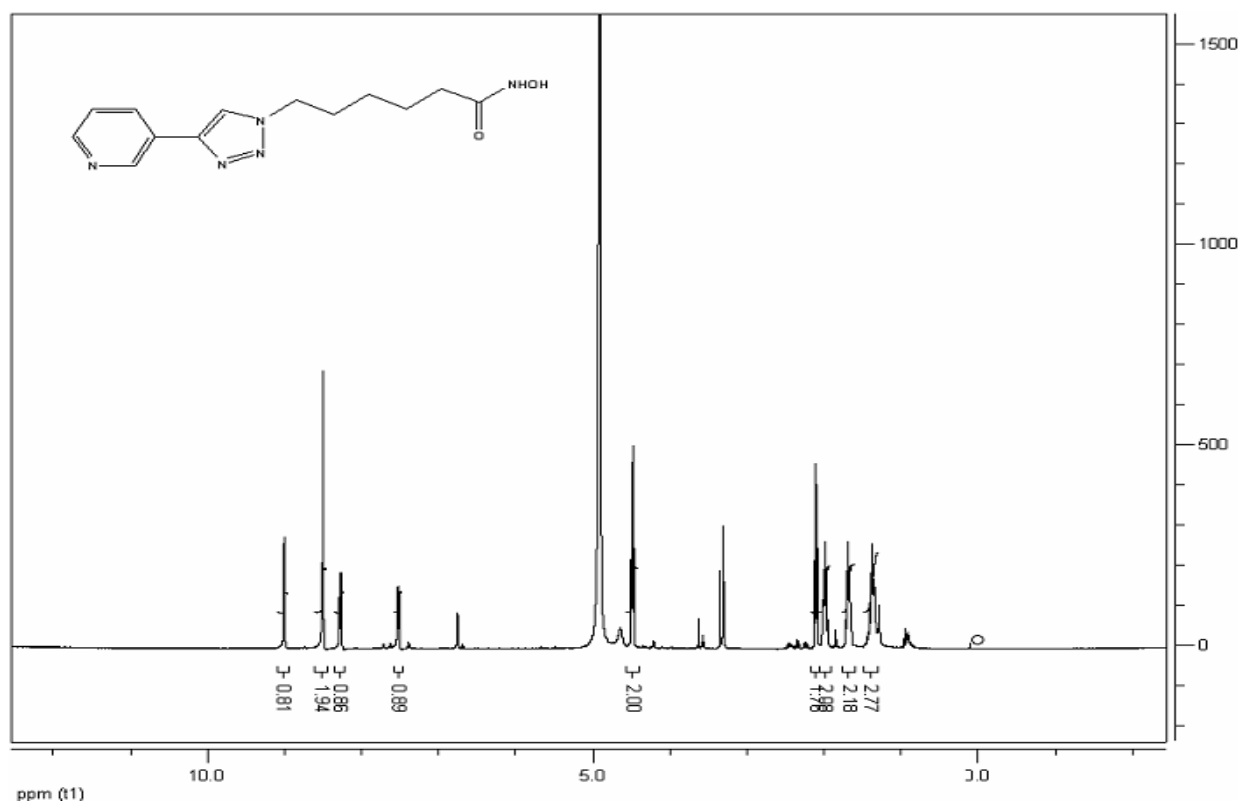
^1H NMR of **7b**:



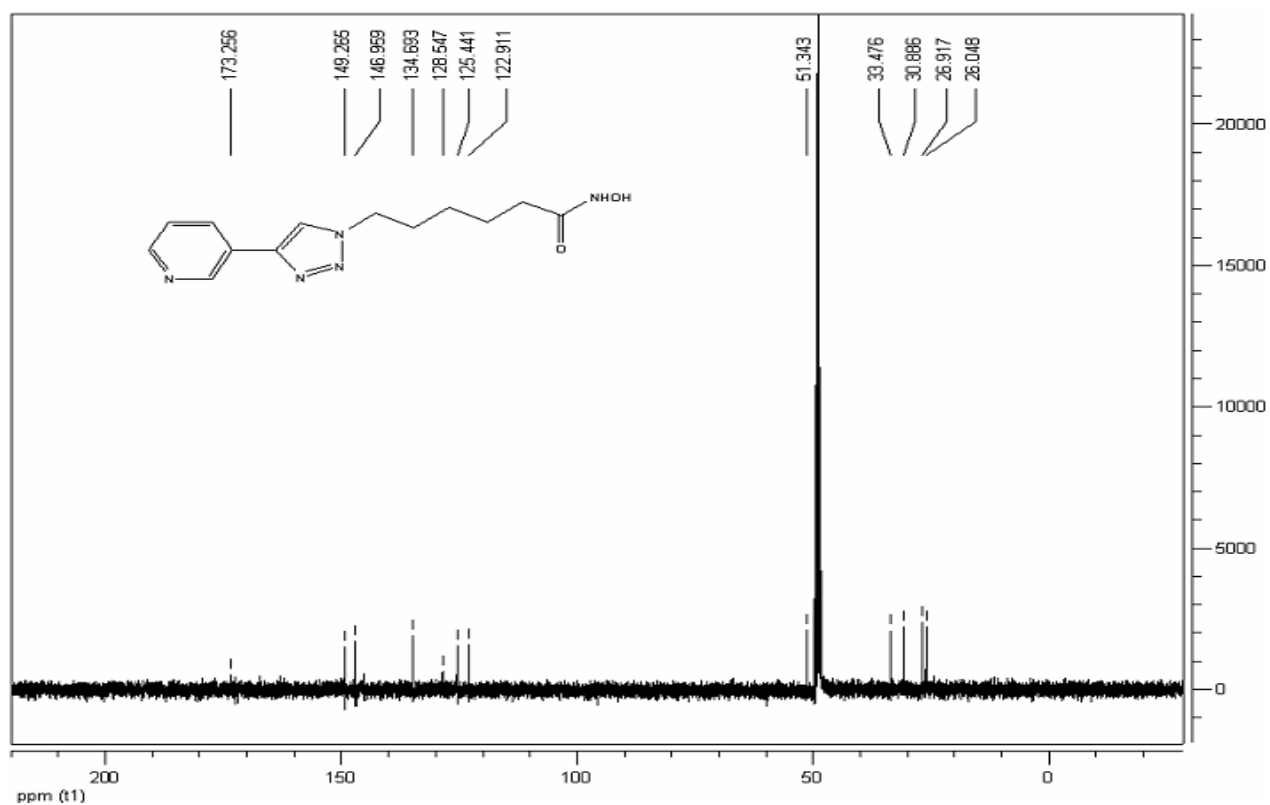
^{13}C NMR of **7b**:



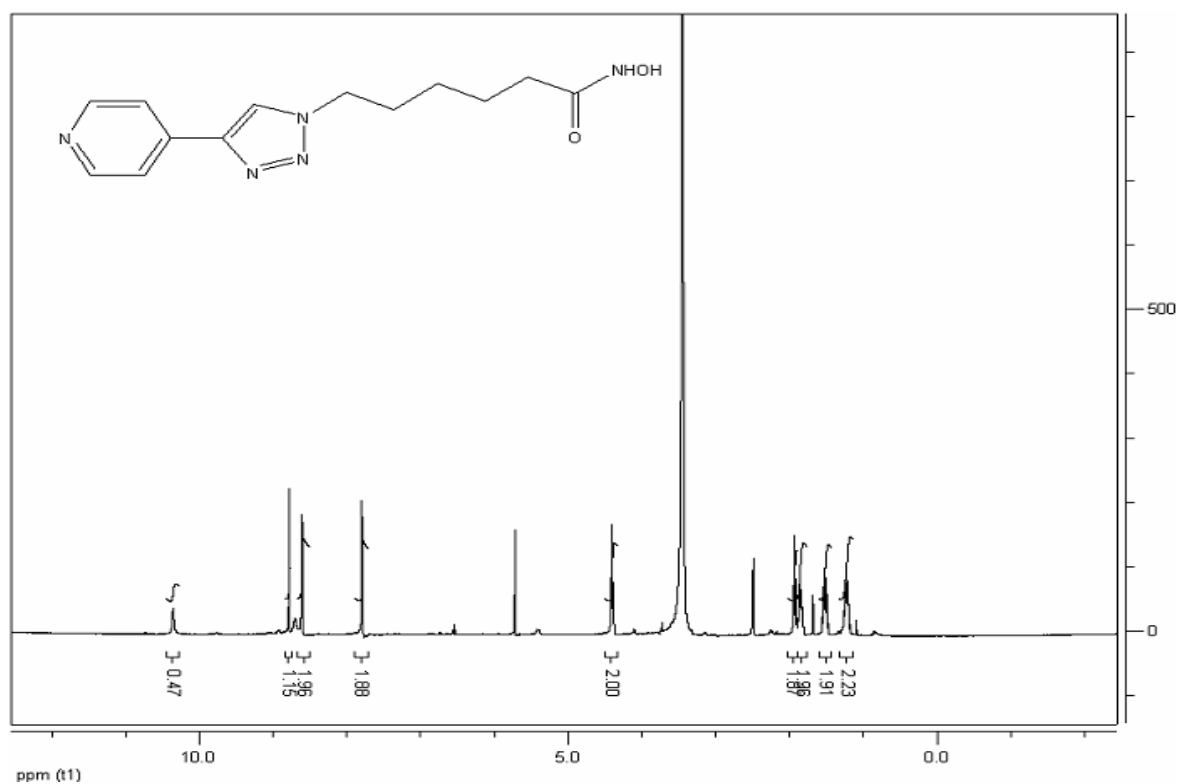
^1H NMR of **7c**:



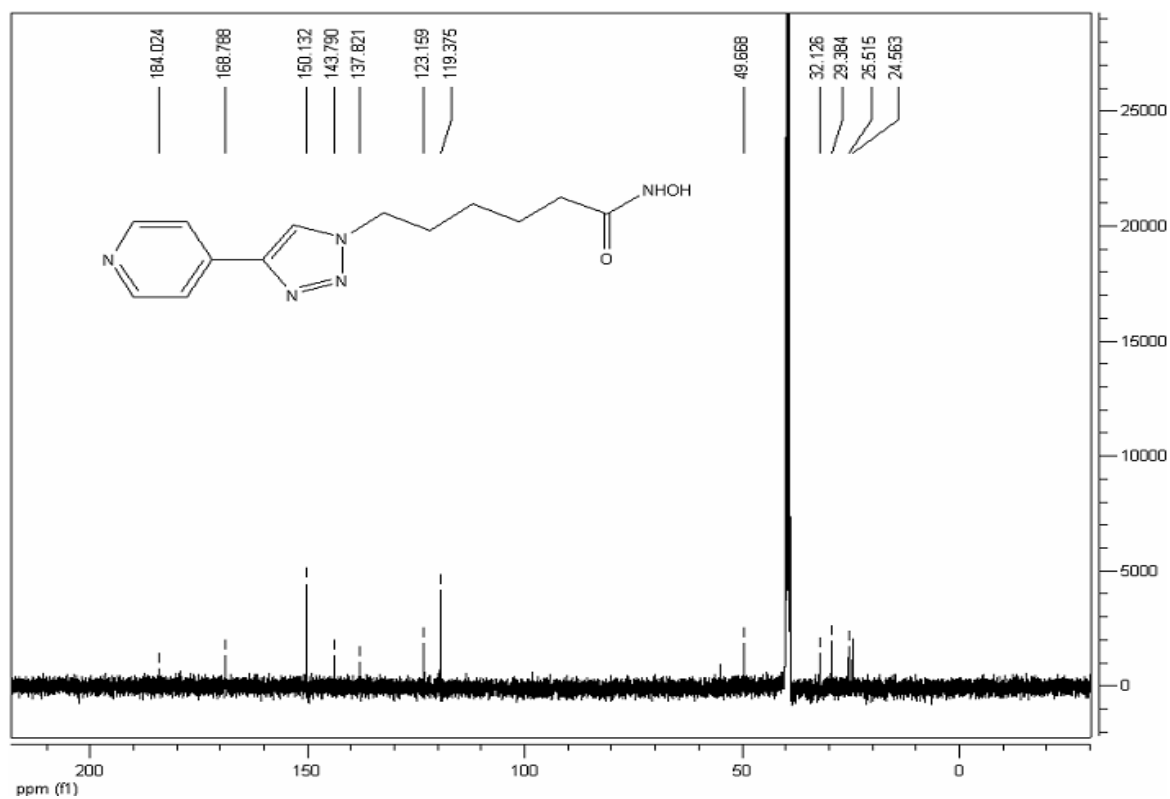
^{13}C NMR of **7c**:



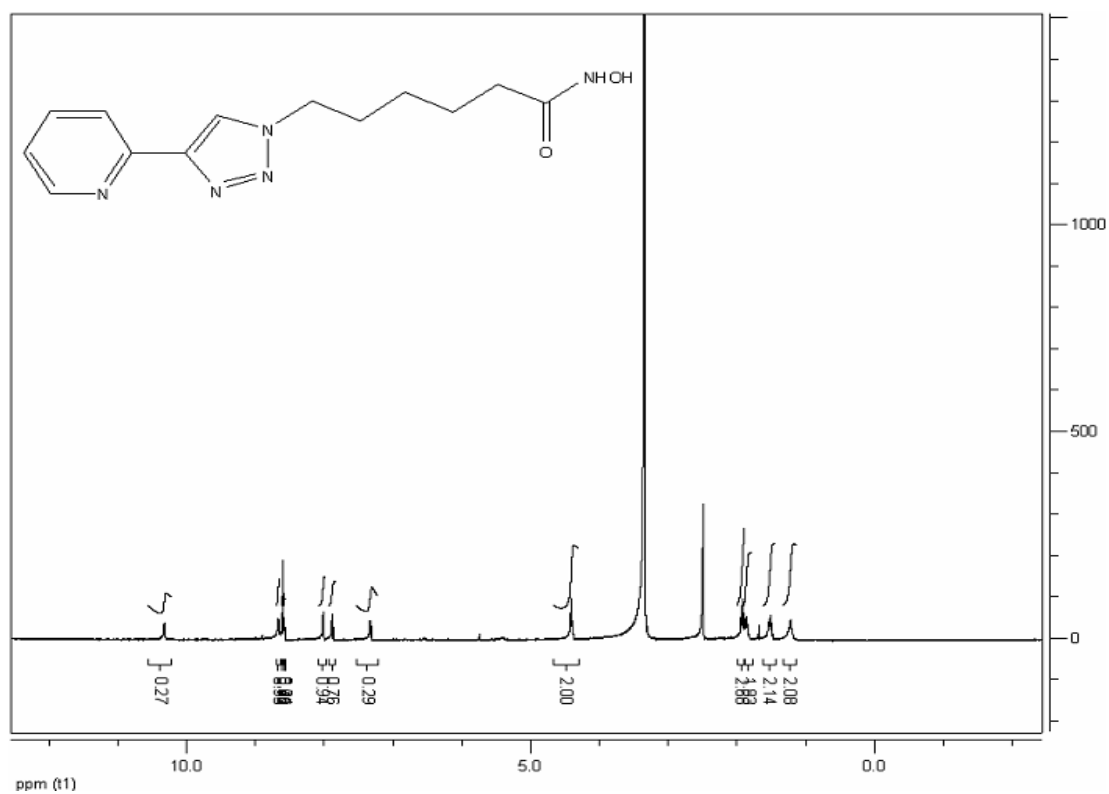
^1H NMR of **7d**:



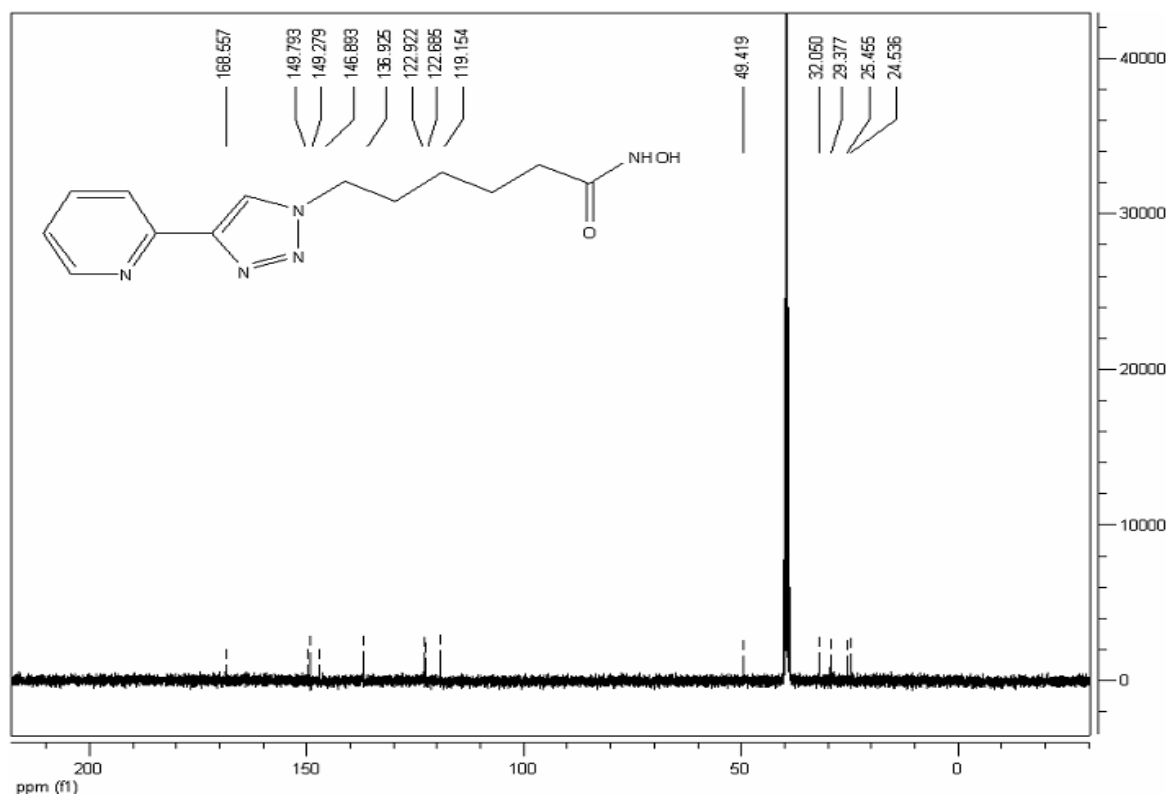
^{13}C NMR of **7d**:



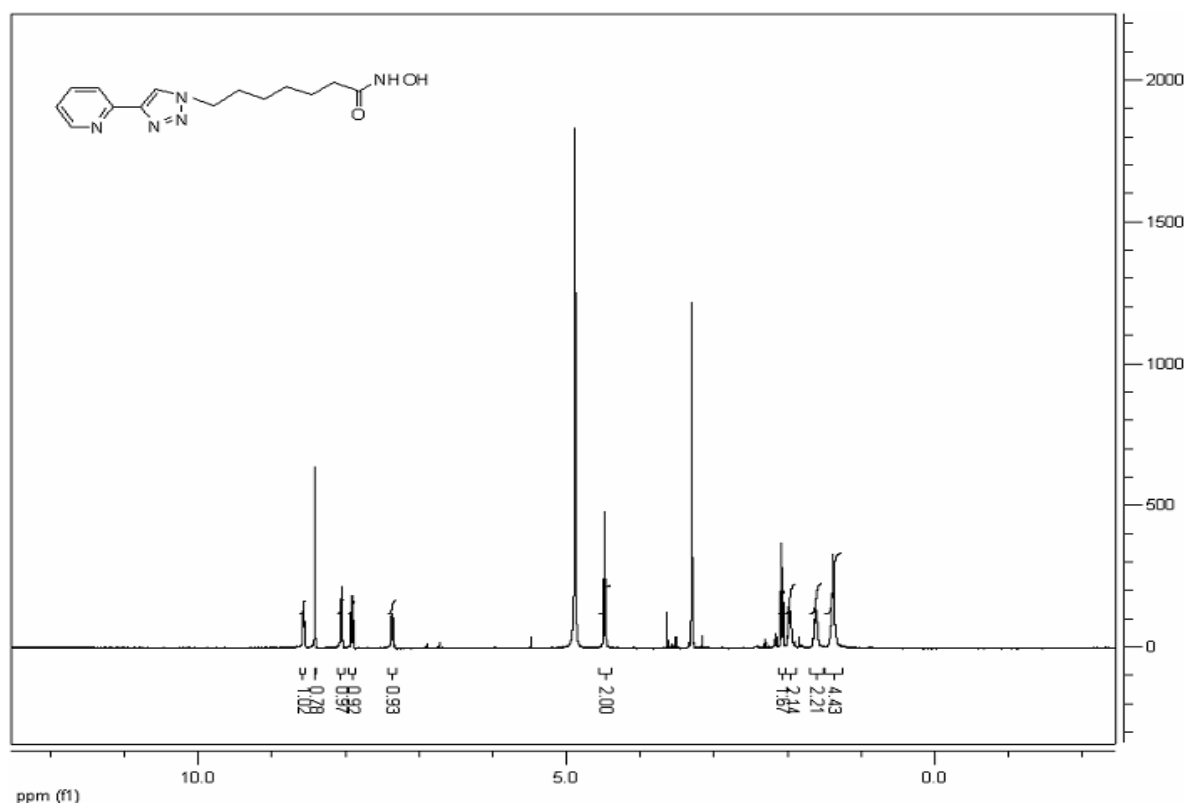
^1H NMR of **7e**:



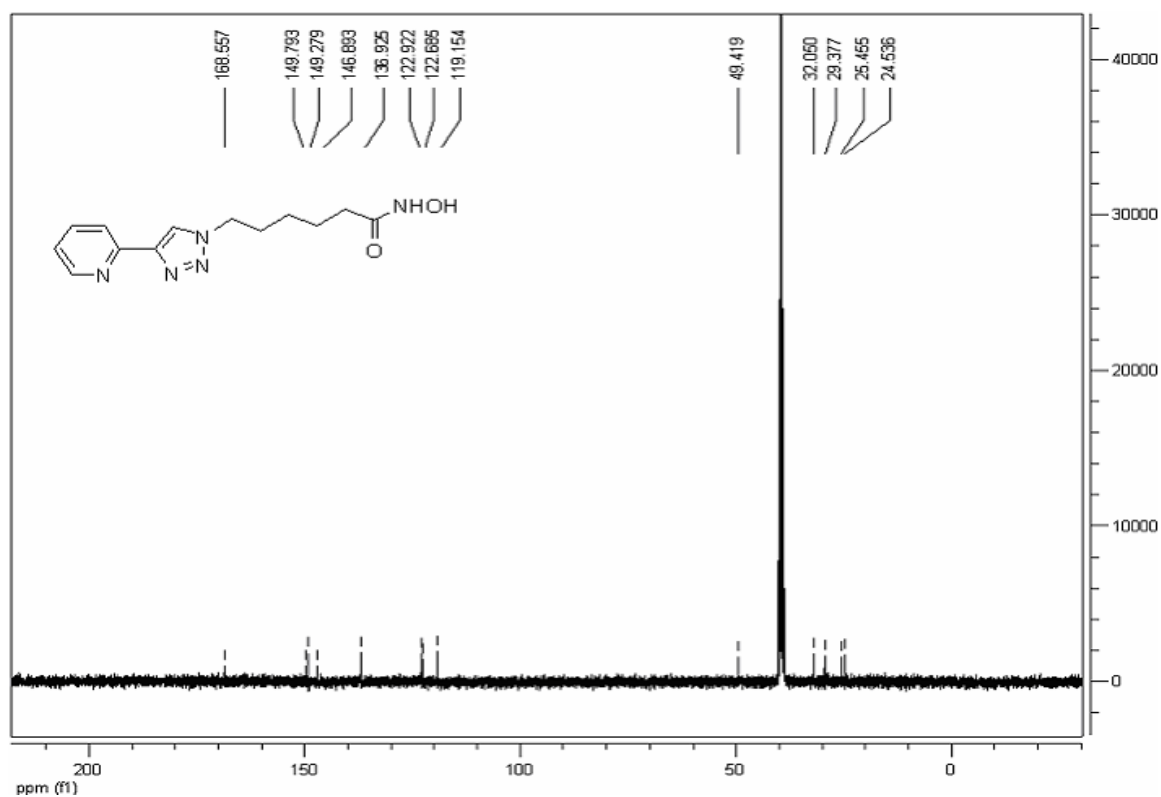
^{13}C NMR of **7e**:



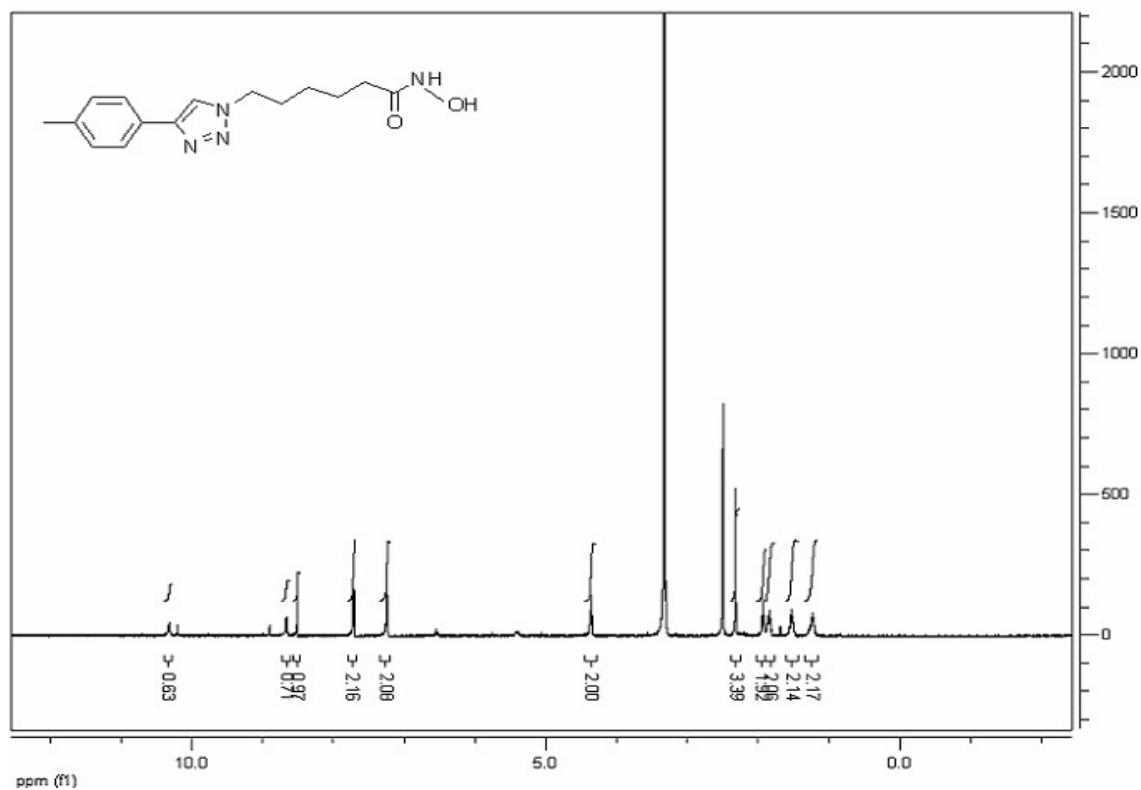
¹H NMR of **7f**:



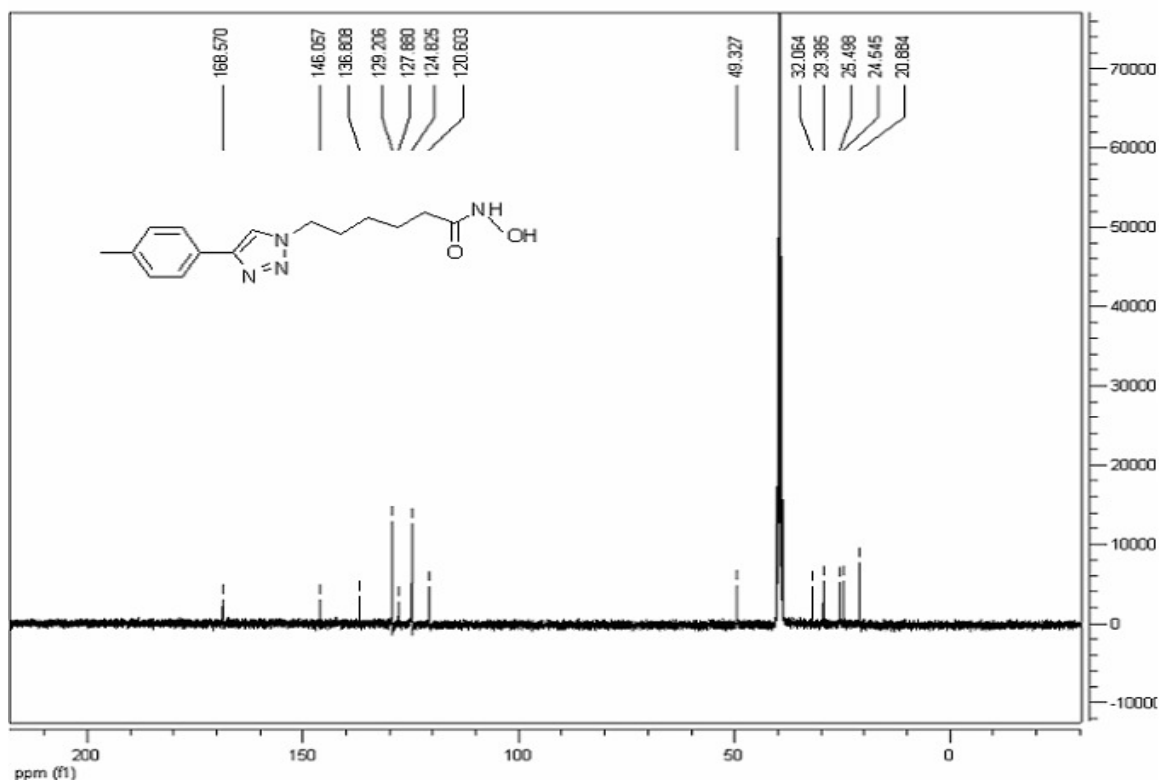
¹³C NMR of **7f**:



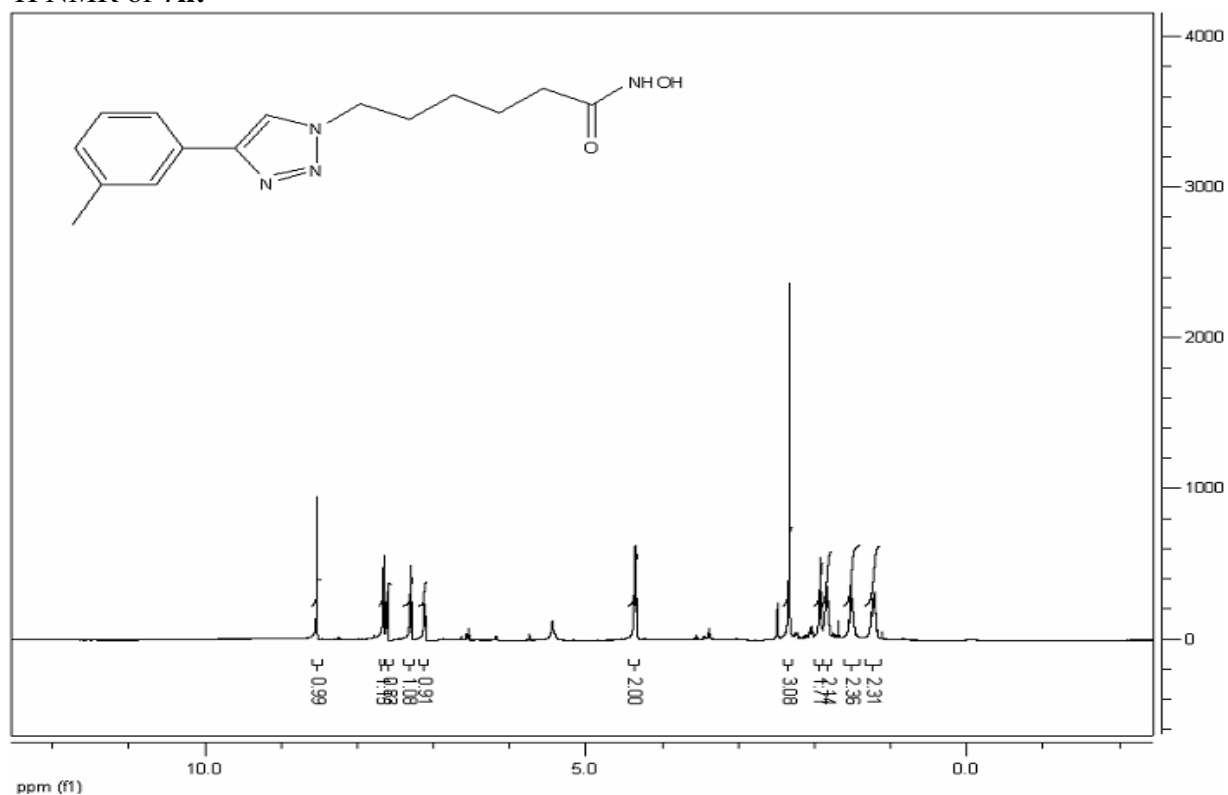
^1H NMR of **7g**:



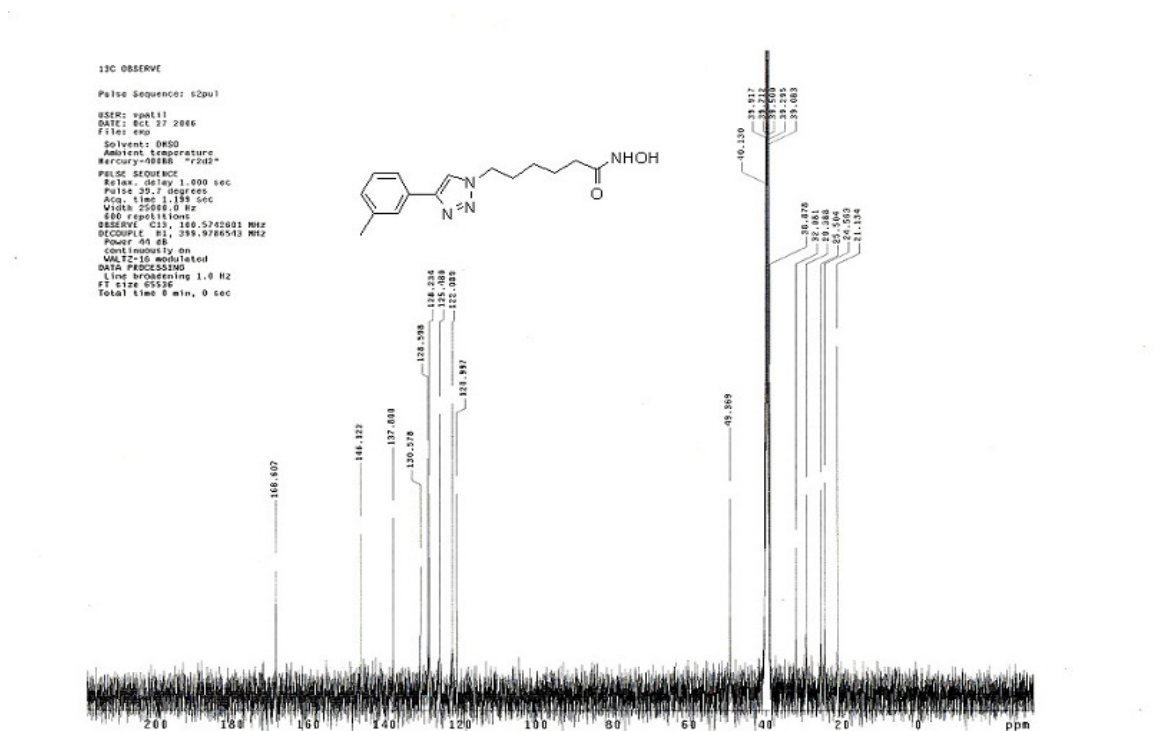
^{13}C NMR of **7g**:



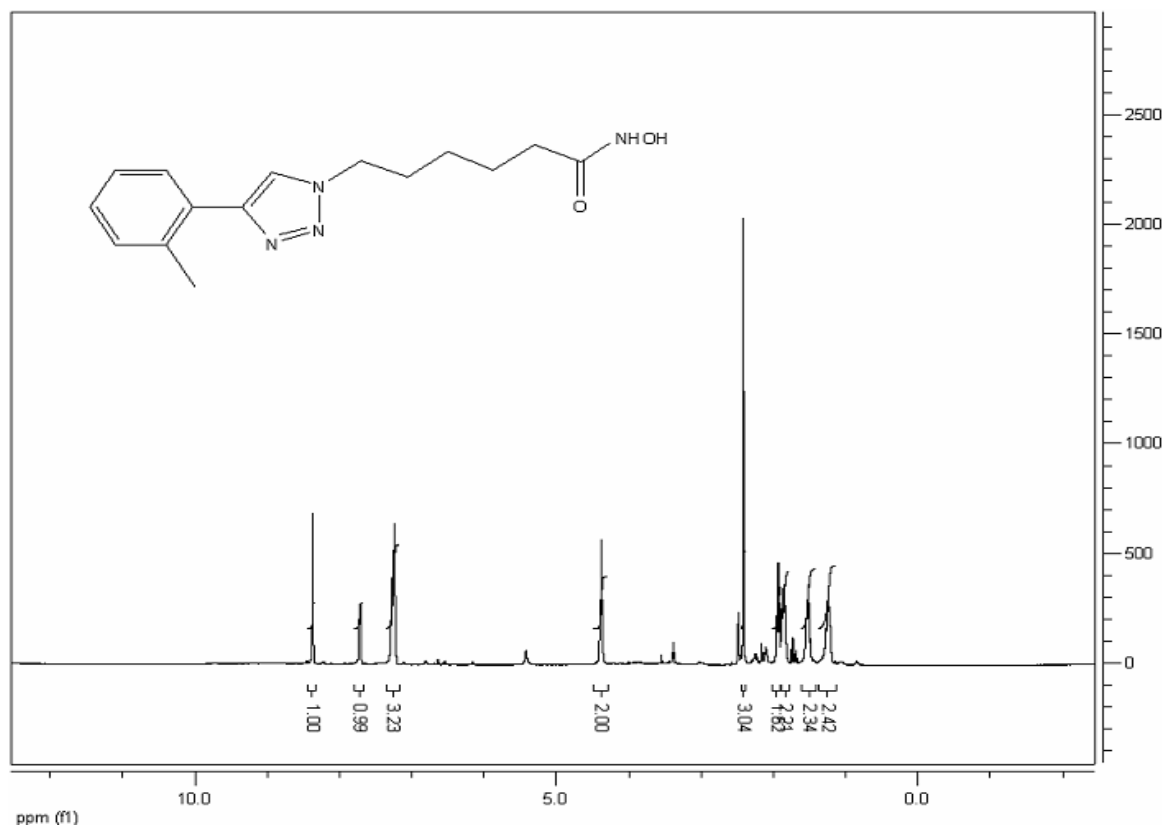
¹H NMR of **7h**:



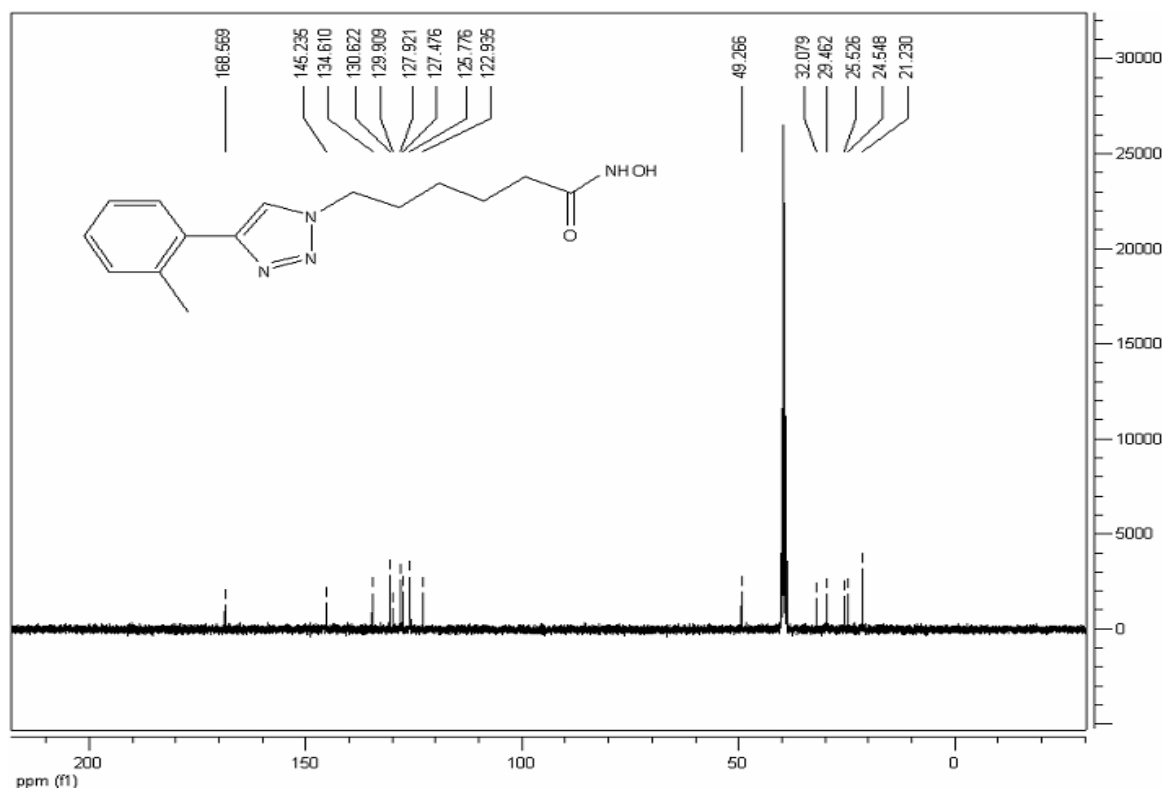
¹³C NMR of **7h**:



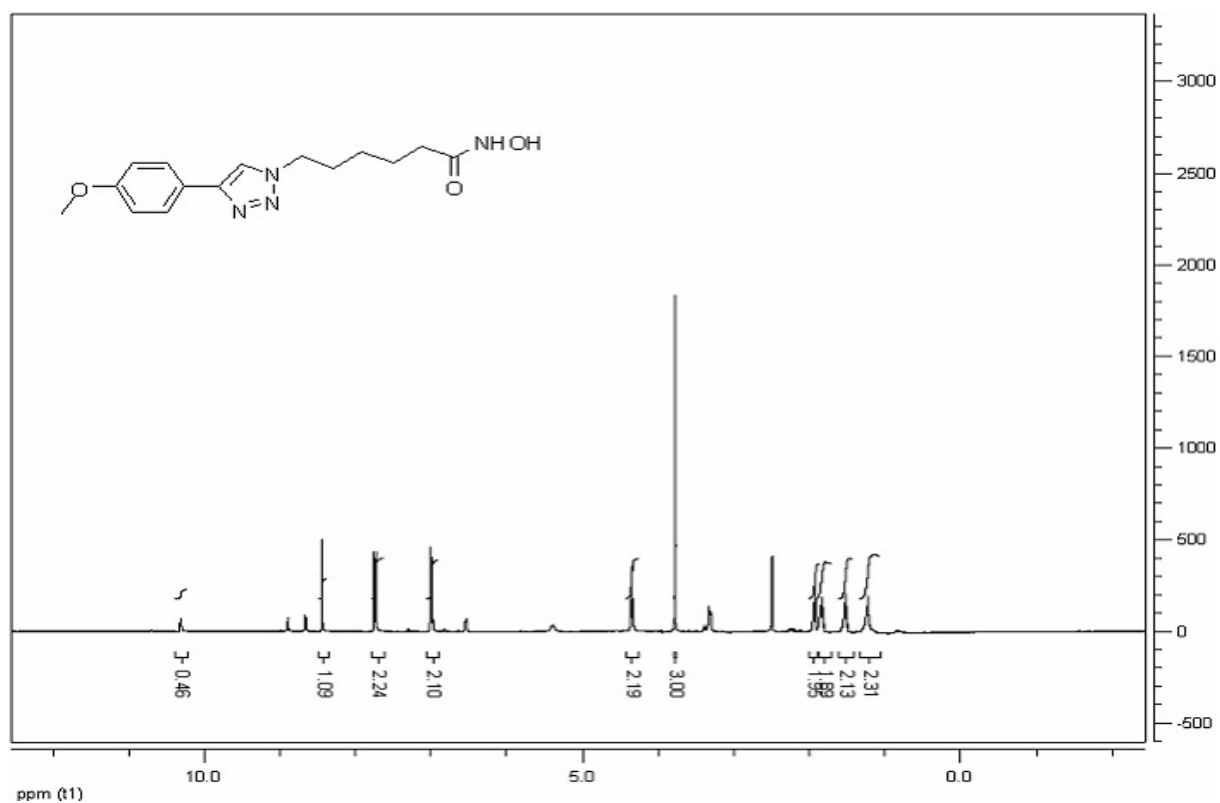
^1H NMR of **7i**:



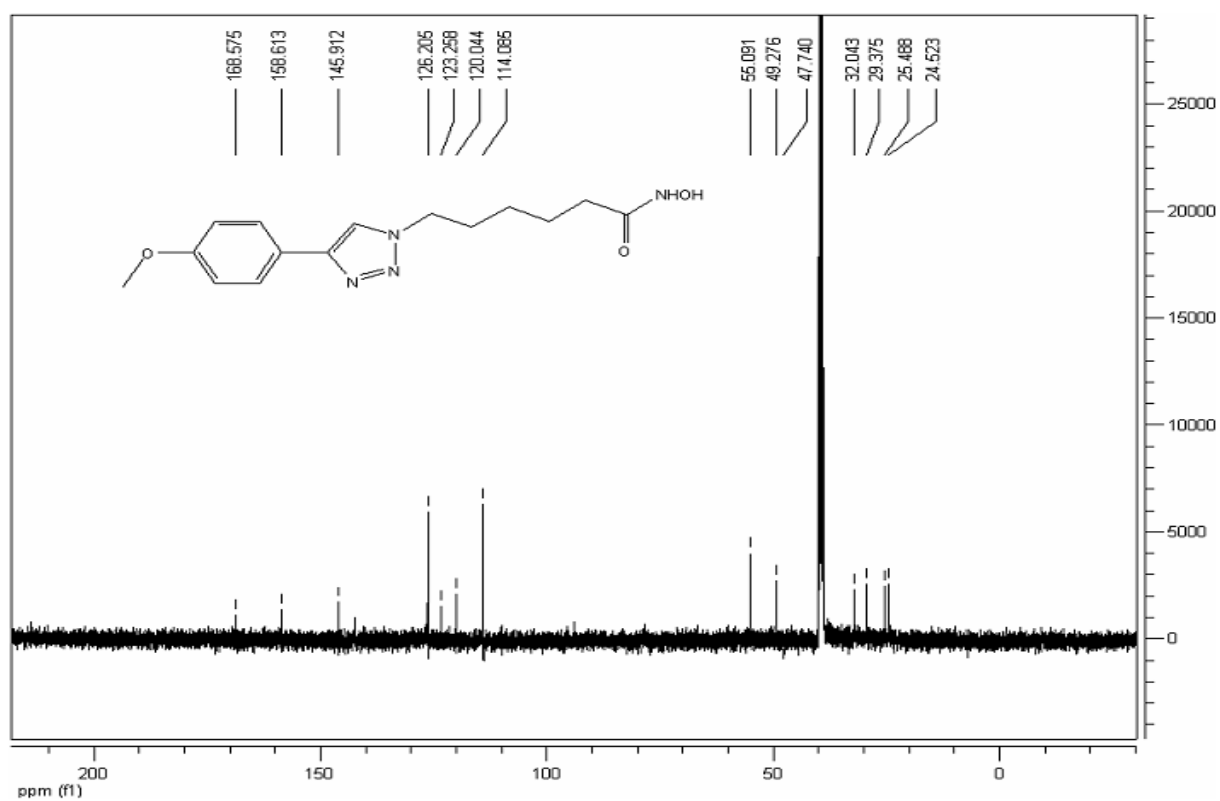
^{13}C NMR of **7i**:



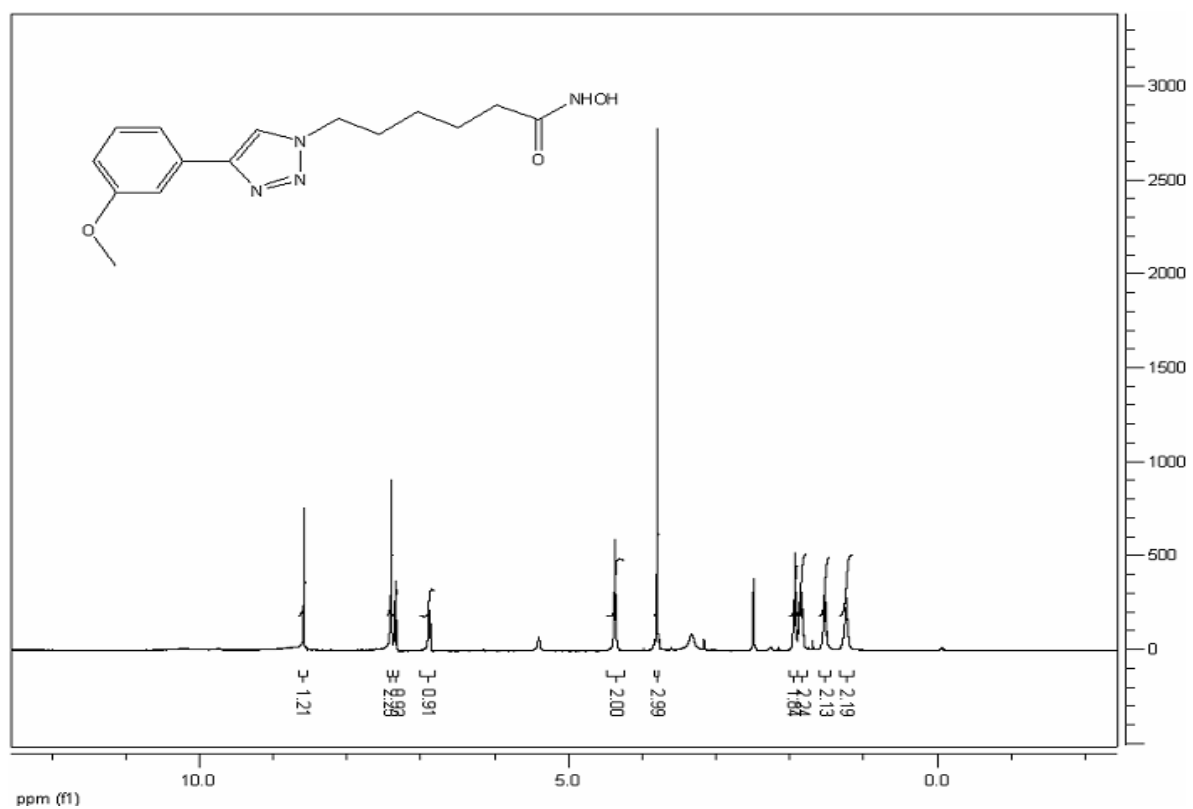
¹H NMR of **7j**:



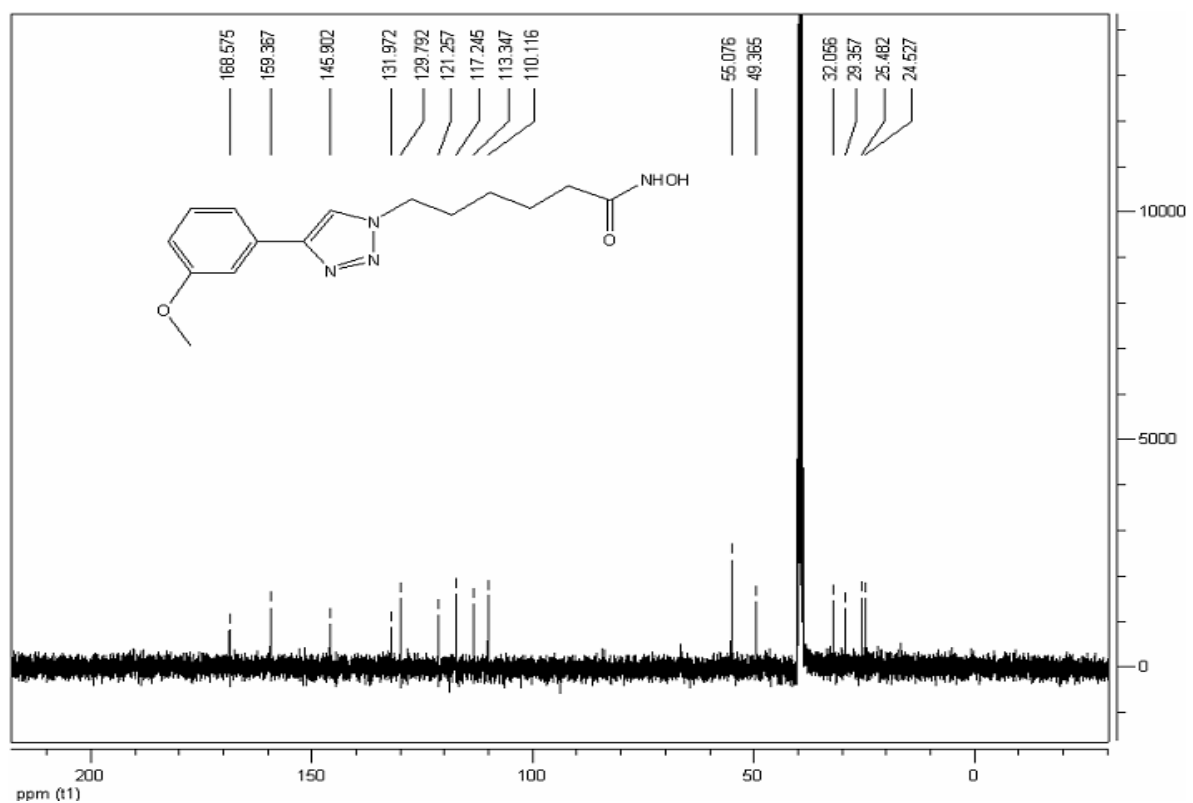
¹³C NMR of **7j**:



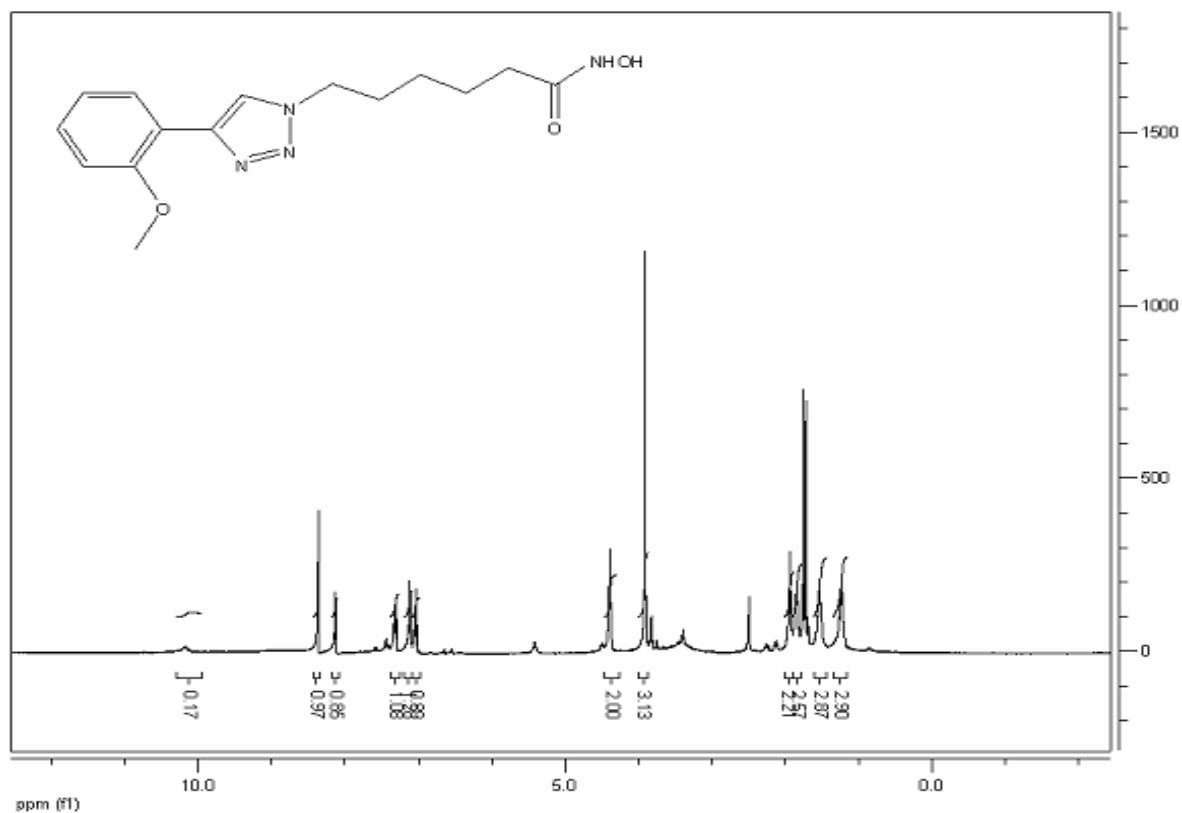
¹H NMR of **7k**:



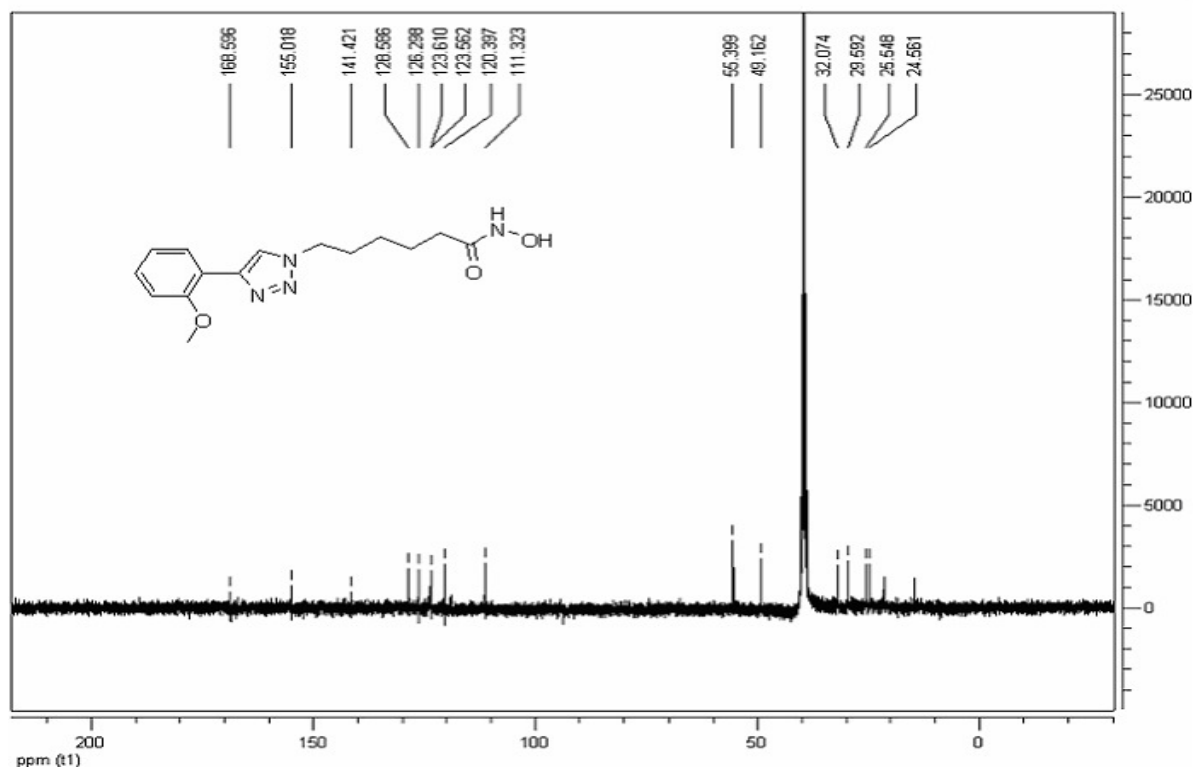
¹³C NMR of **7k**:



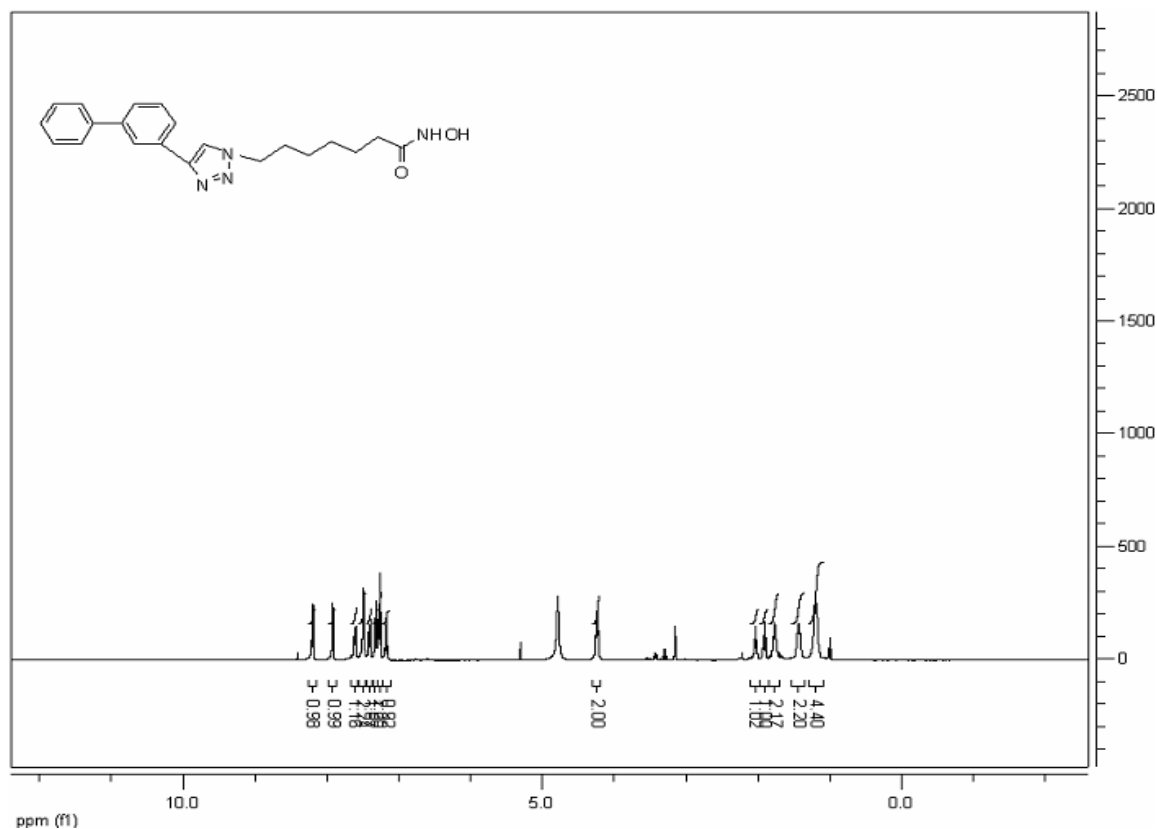
¹H NMR of **7l**:



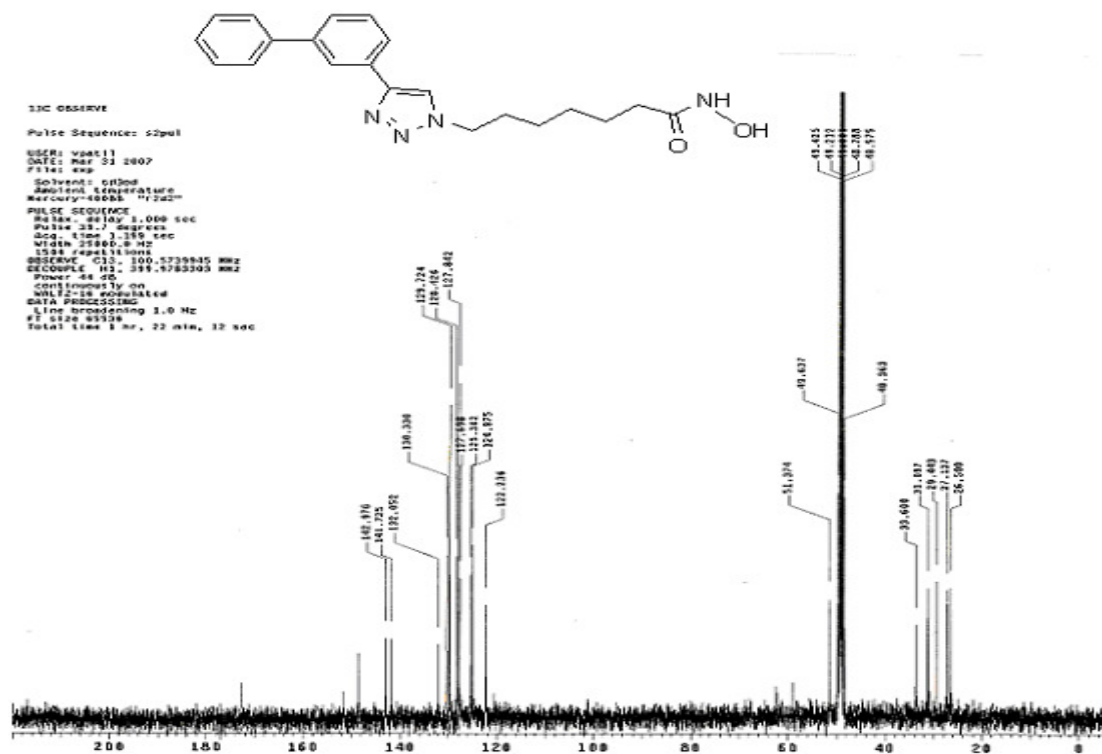
¹³C NMR of **7l**:



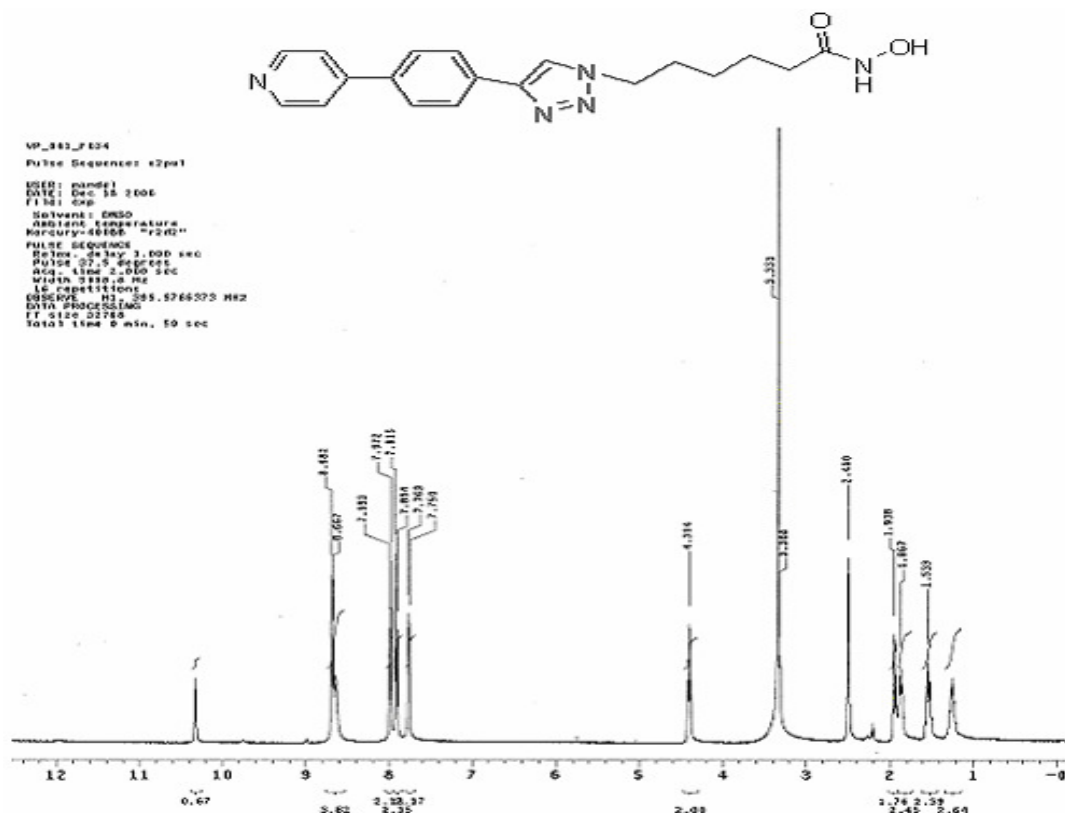
¹H NMR of **7q**:



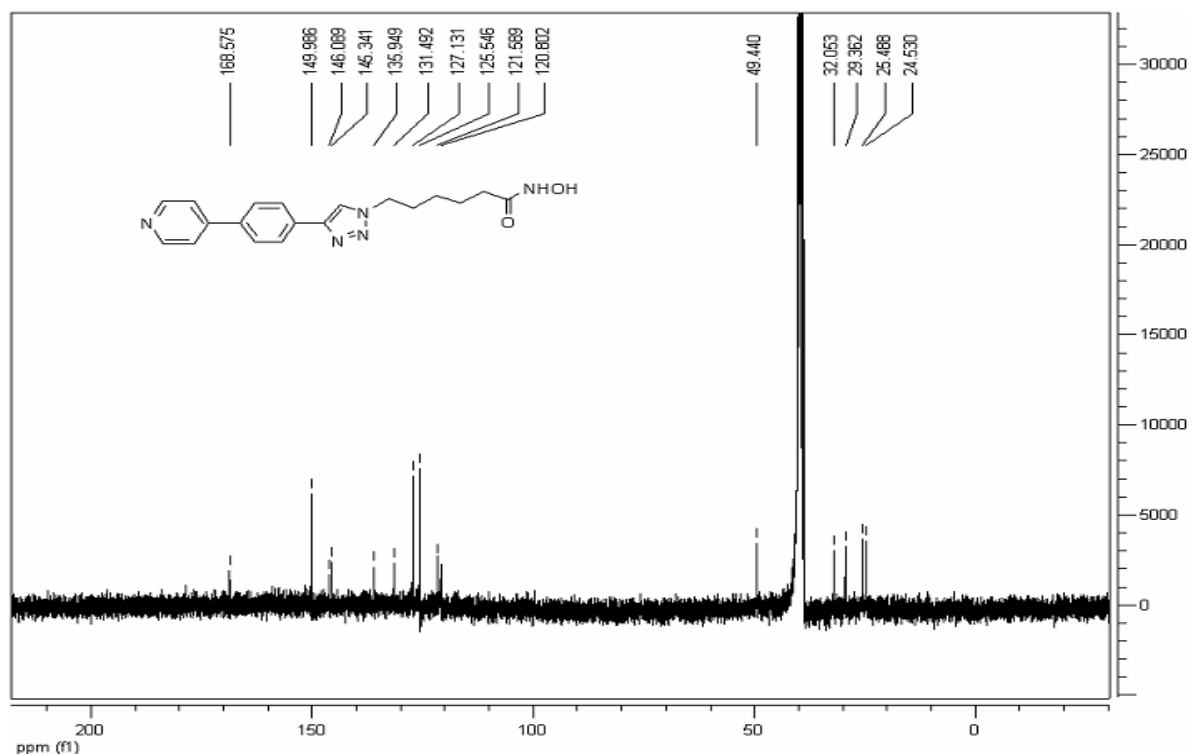
¹³C NMR of **7q**:



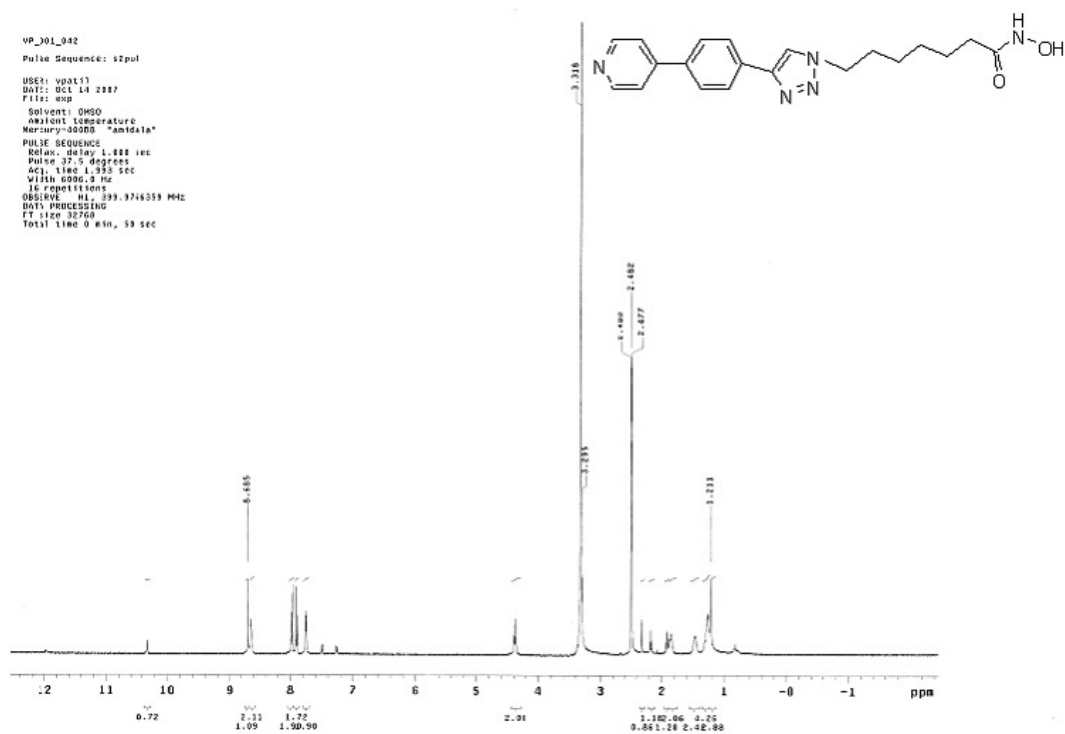
¹H NMR of **7s**:



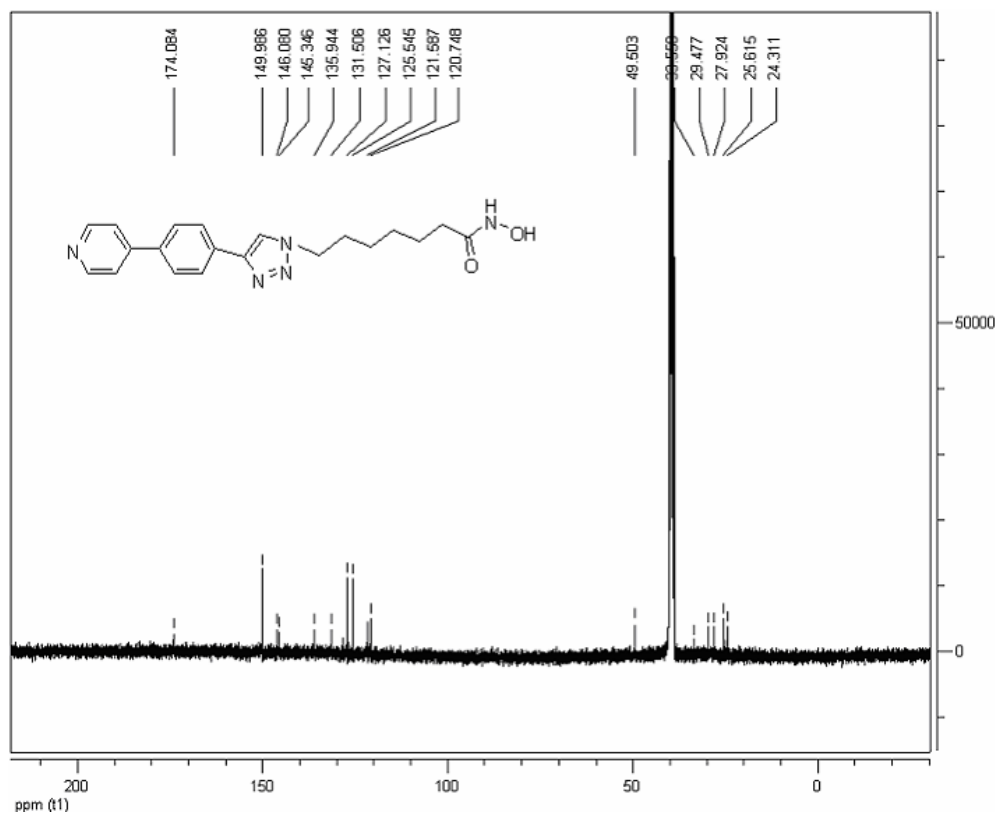
¹³C NMR of **7s**:



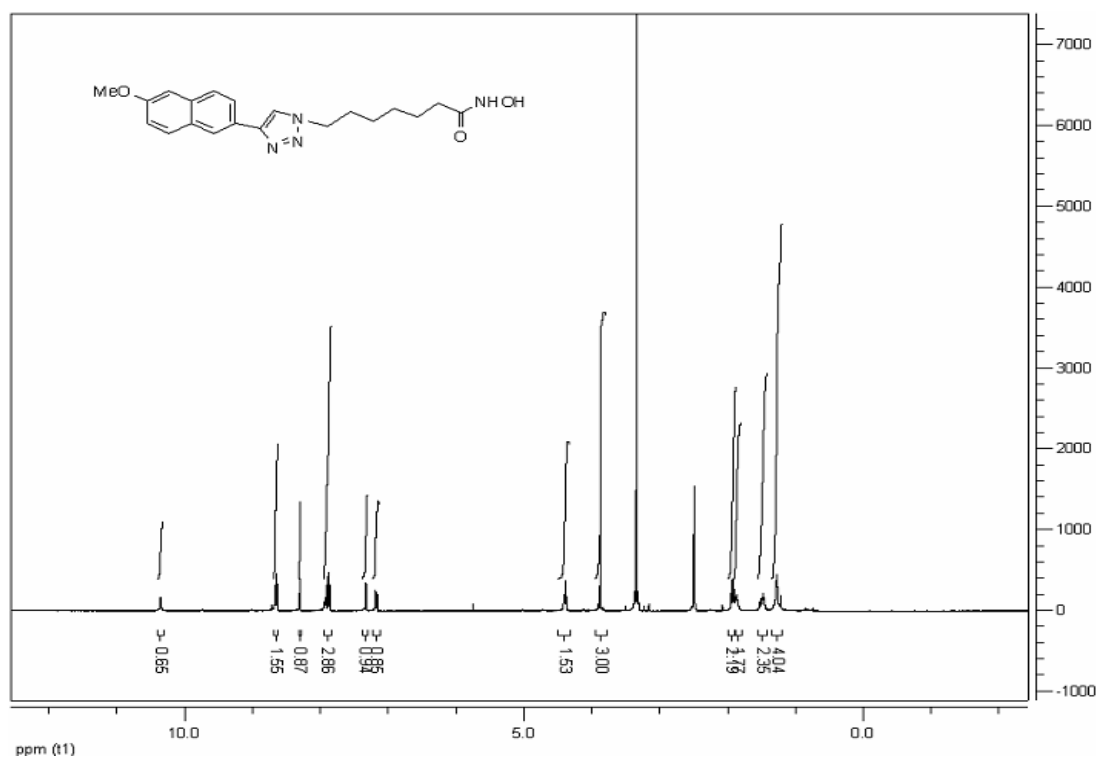
¹H NMR of **7t**:



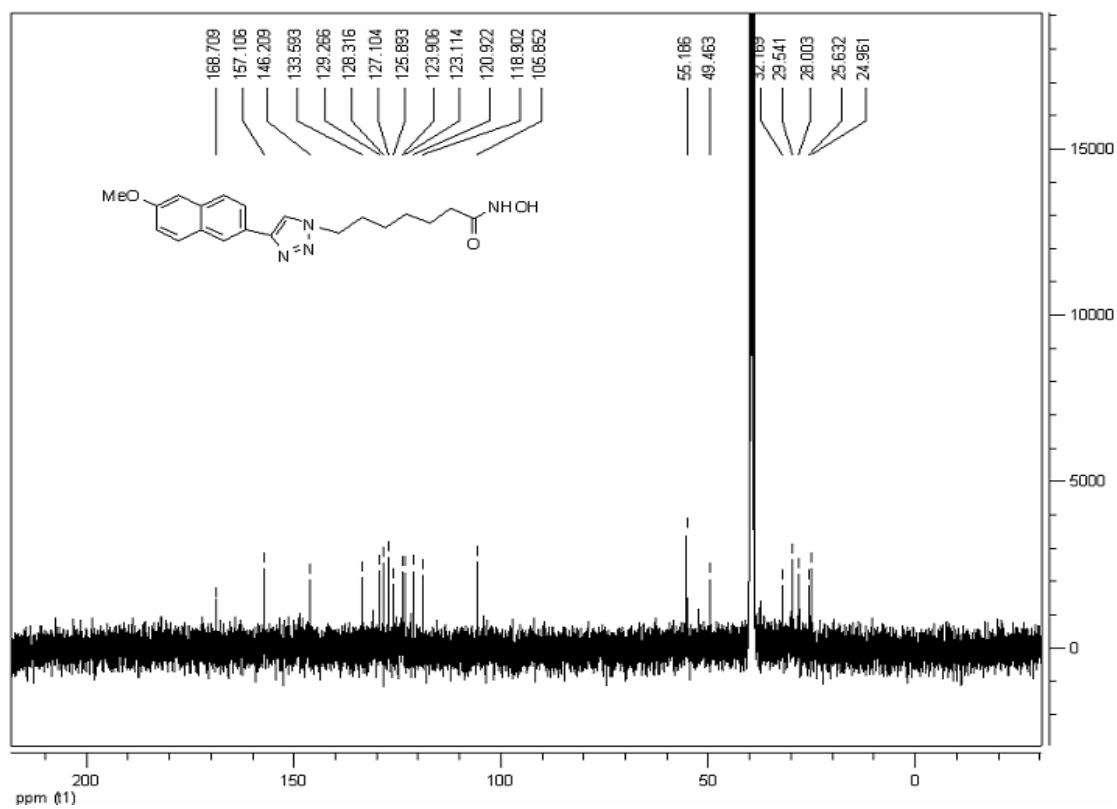
¹³C NMR of **7t**:



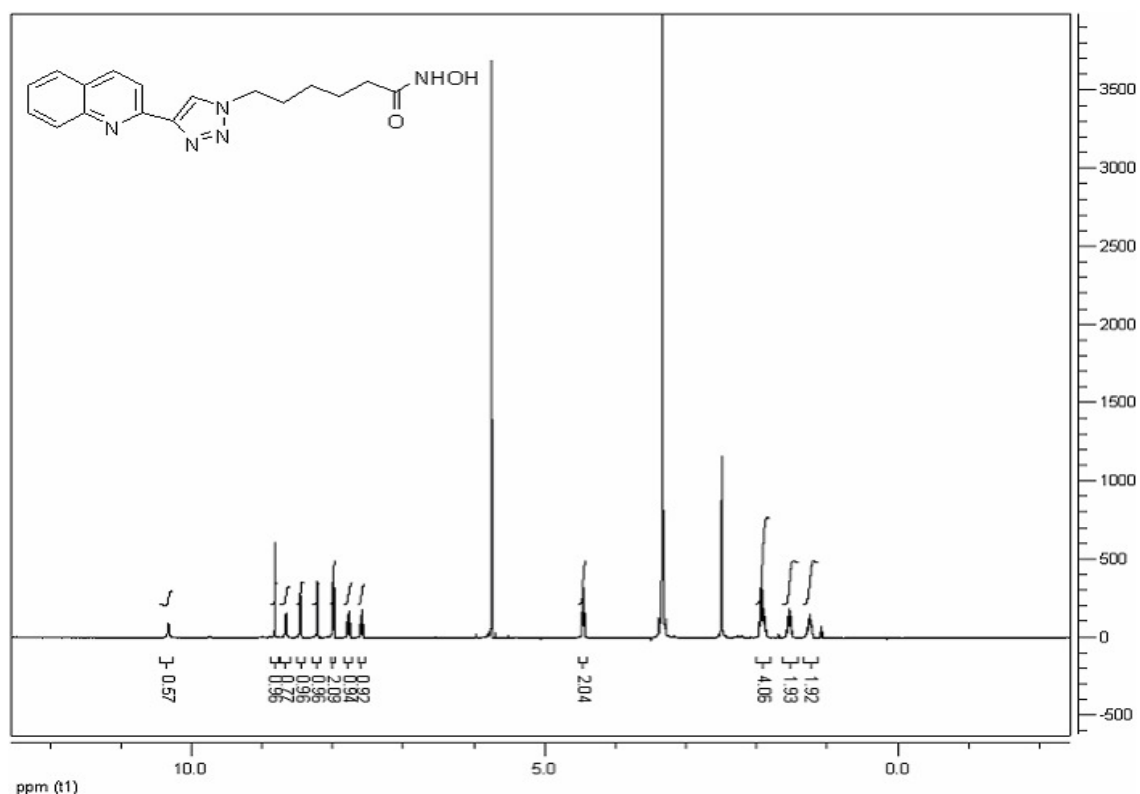
^1H NMR of **7v**:



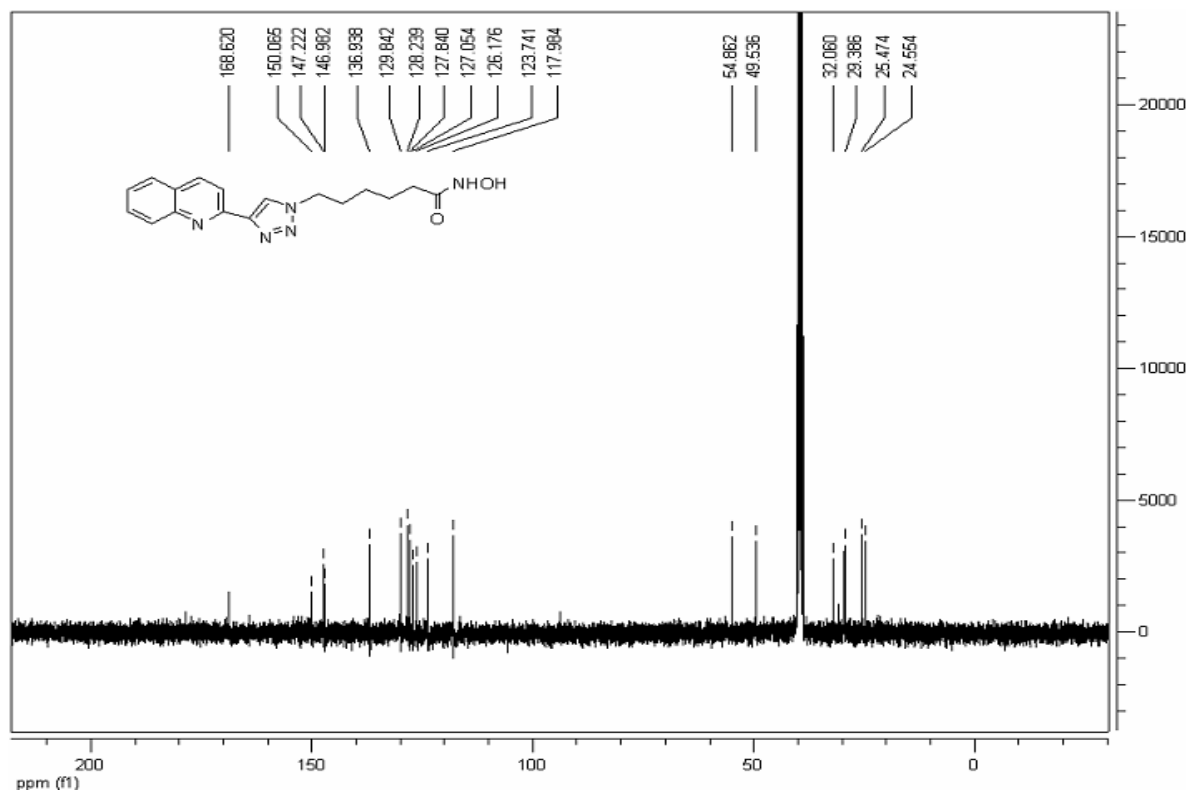
^{13}C NMR of **7v**:



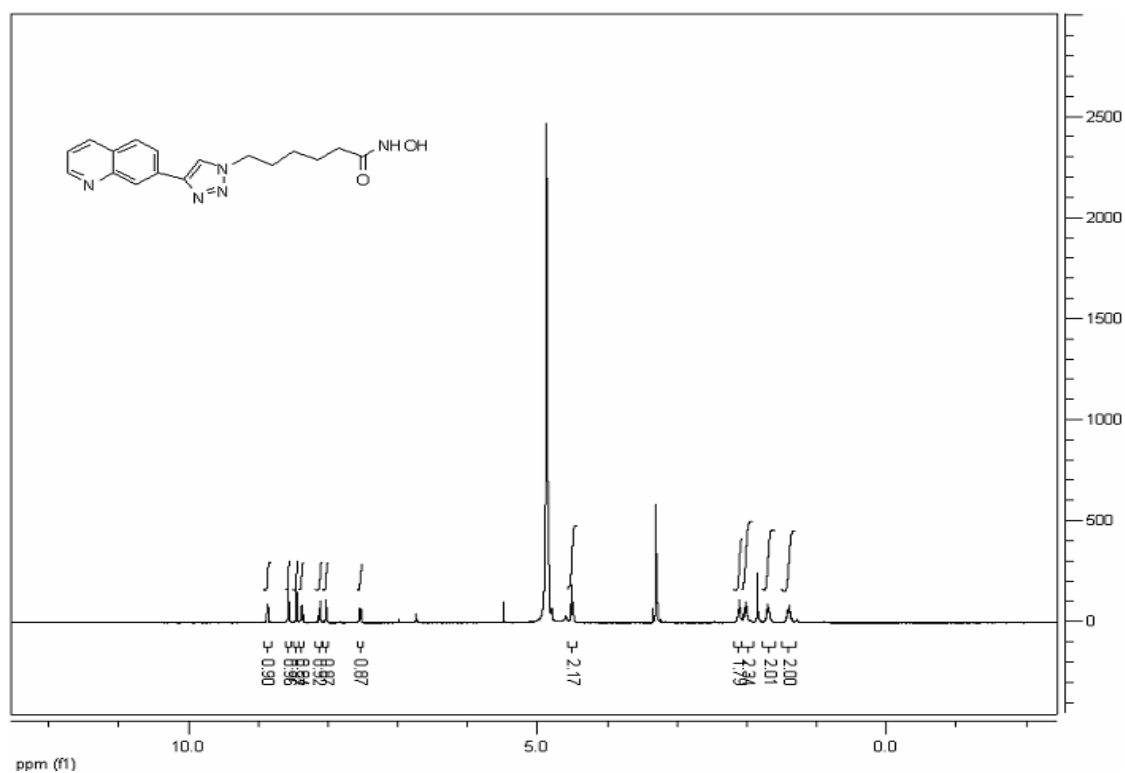
^1H NMR of **7w**:



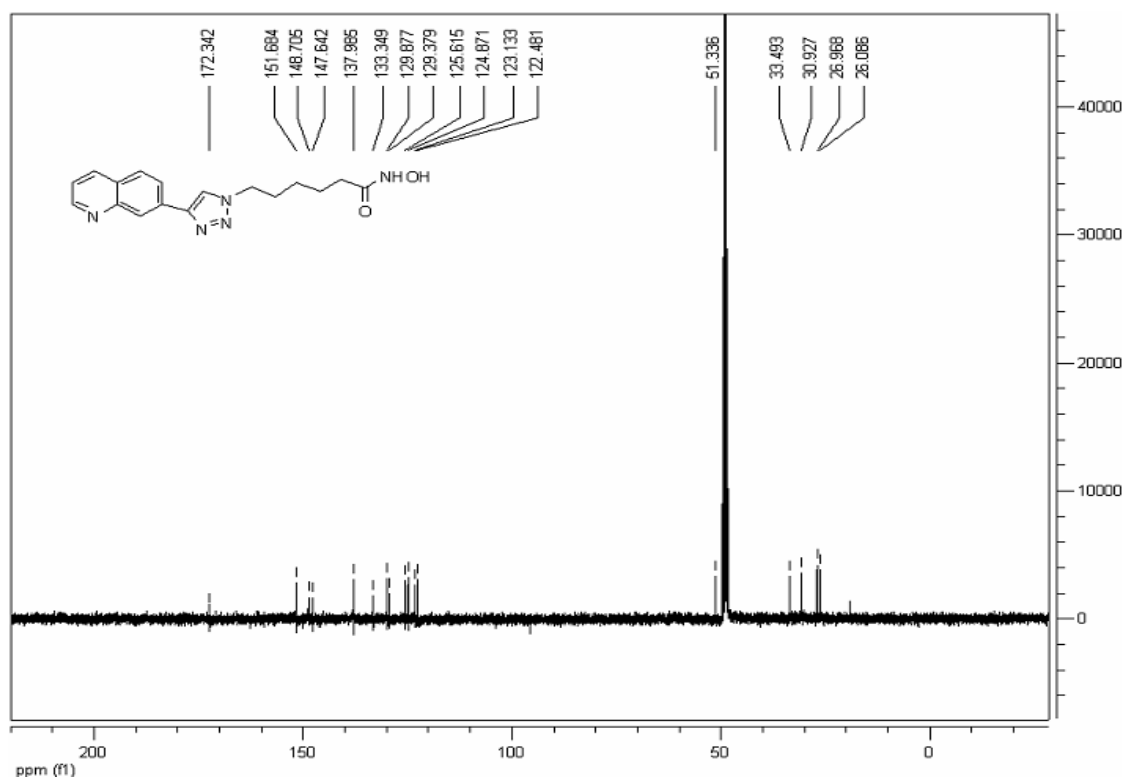
^{13}C NMR of **7w**:



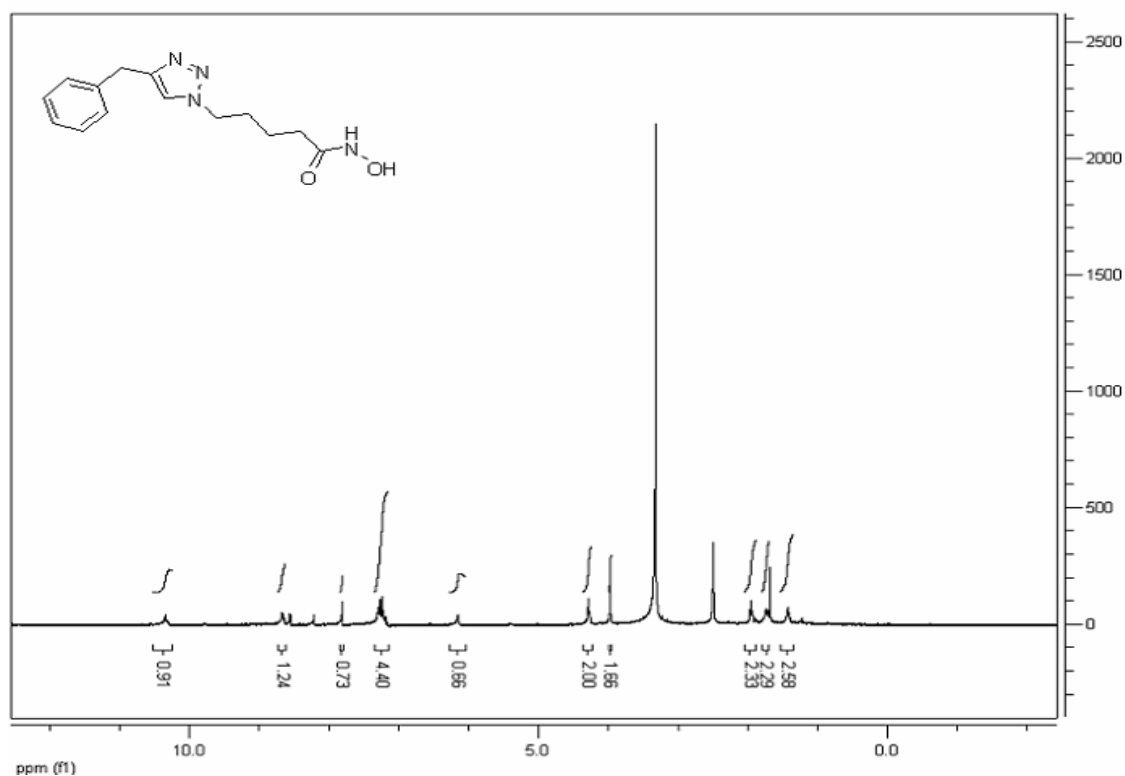
¹H NMR of **7x**:



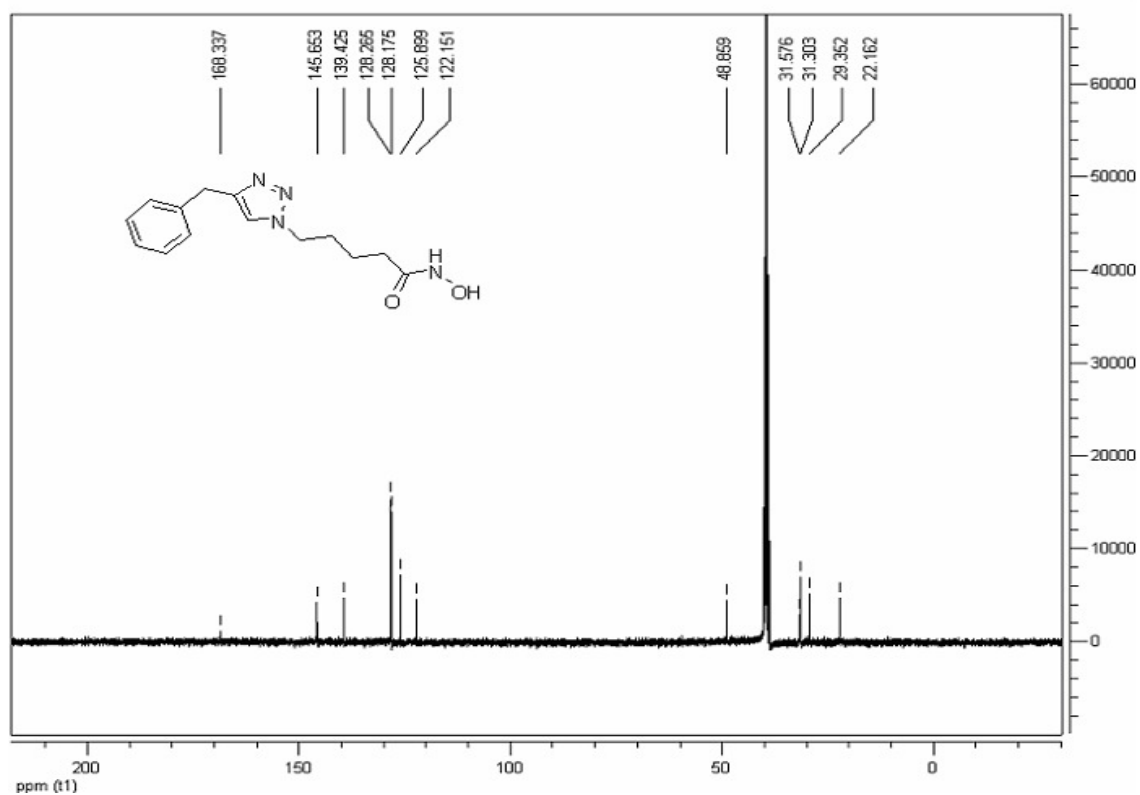
¹³C NMR of **7x**:



^1H NMR of **7y**:



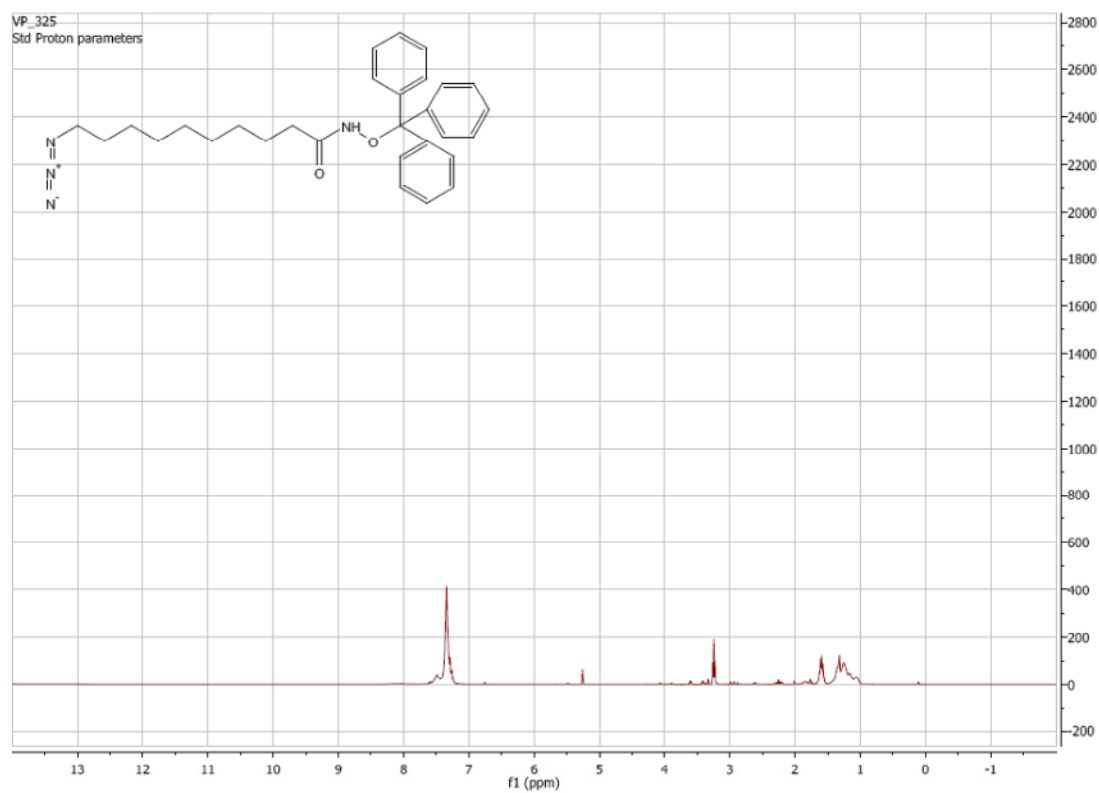
^{13}C NMR of **7y**:



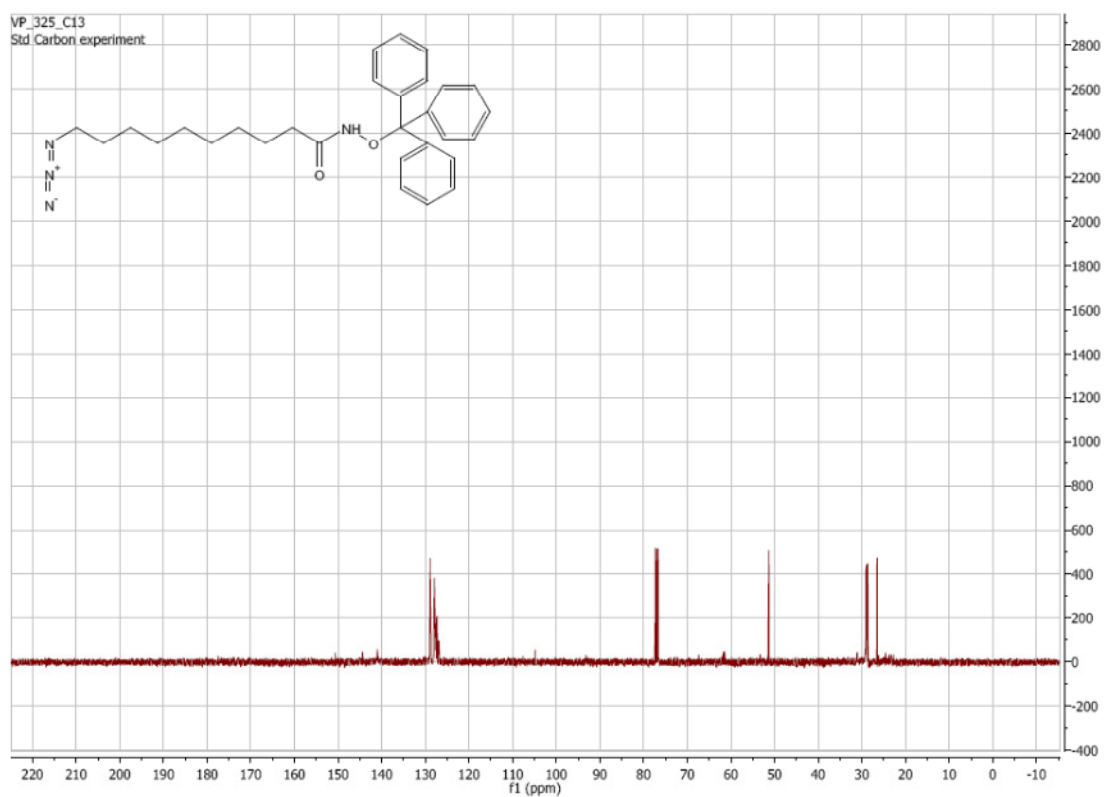
APPENDIX B

^1H and ^{13}C NMR characterization Zinc Chelating Spliceosome Assembly Inhibitors
(Chapter 3)

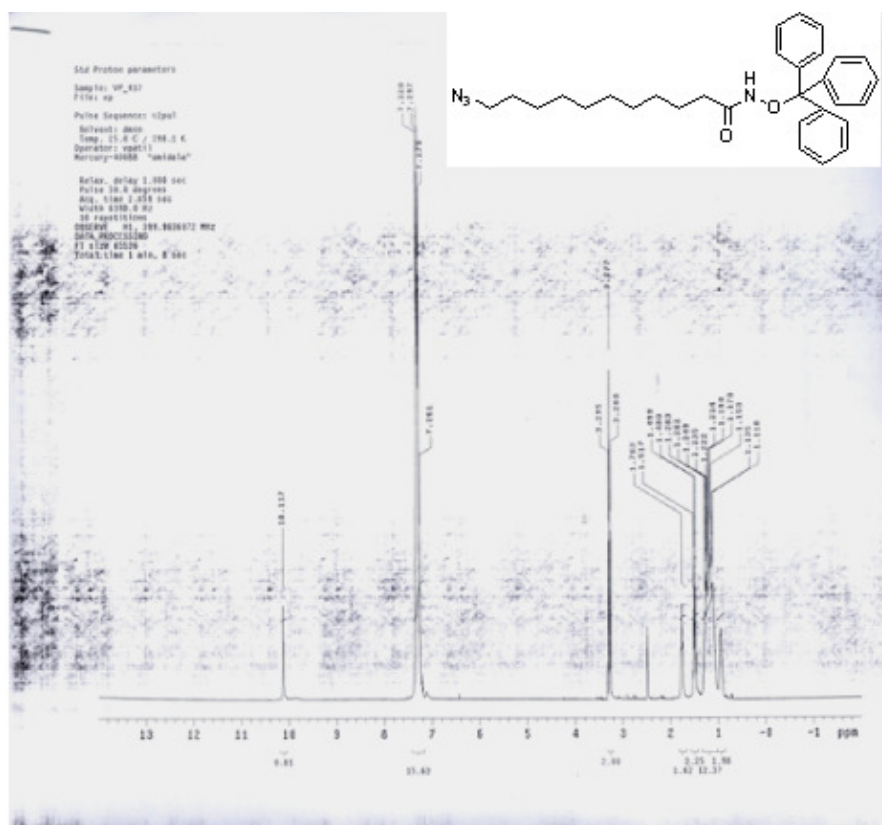
¹H NMR of **65b**:



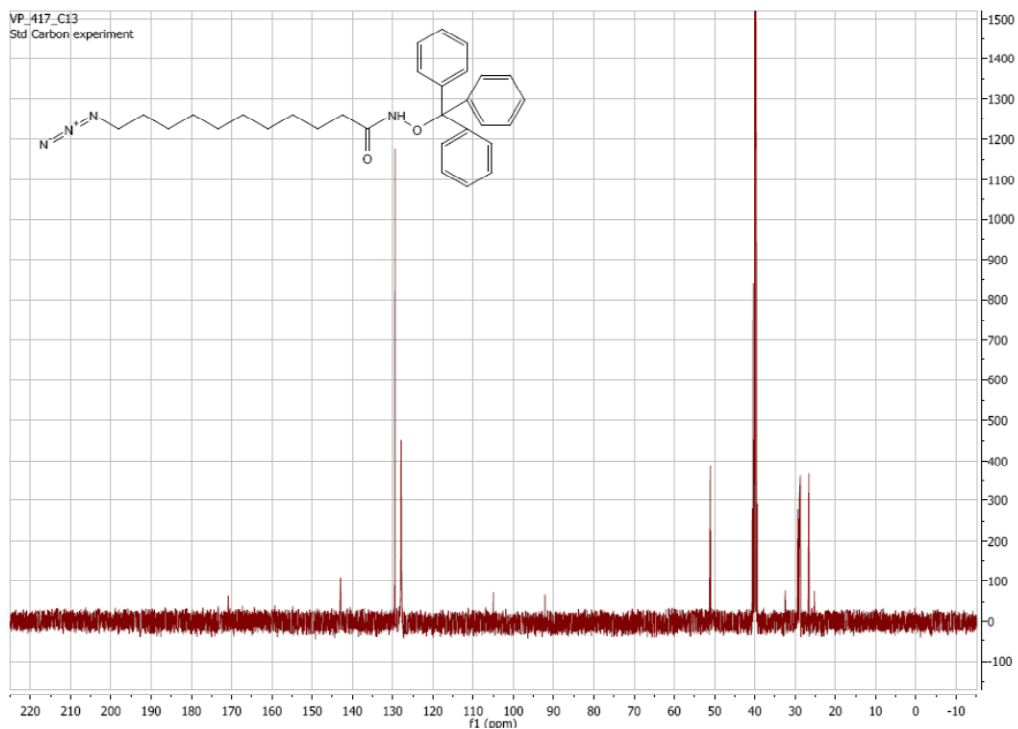
¹³C NMR of **65b**:



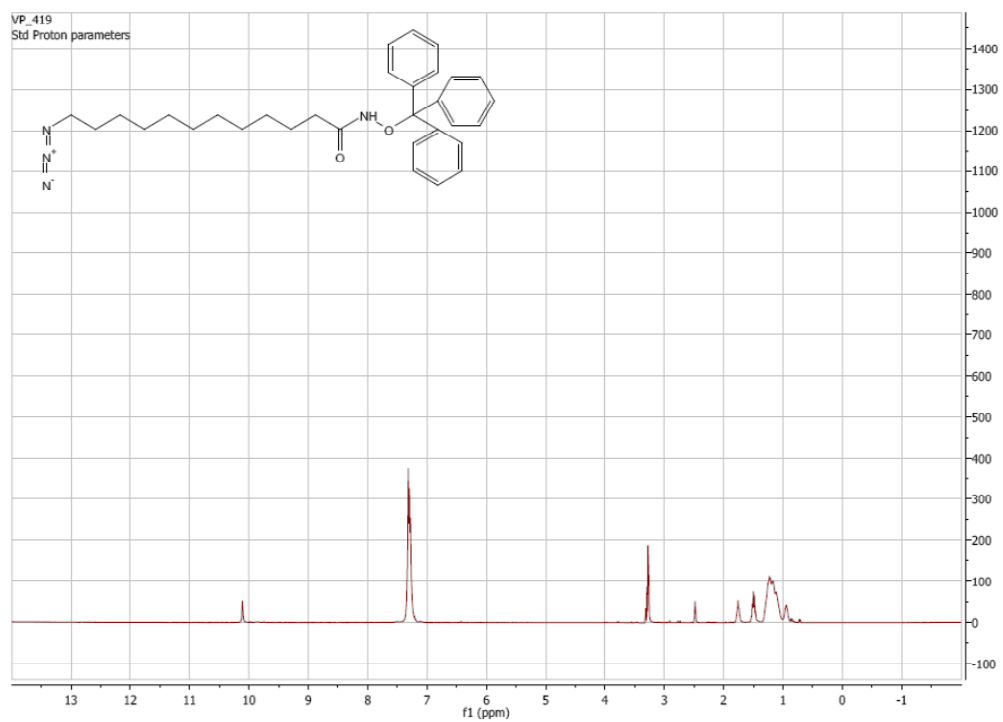
¹H NMR of **65c**:



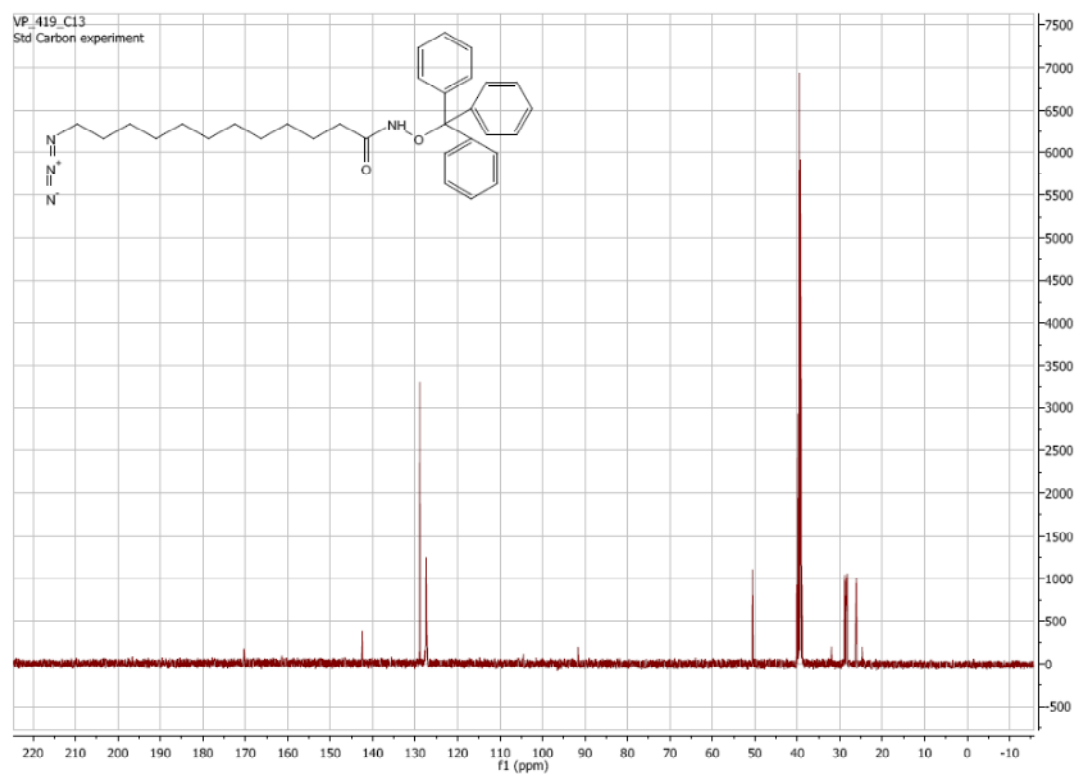
¹³C NMR of **65c**:



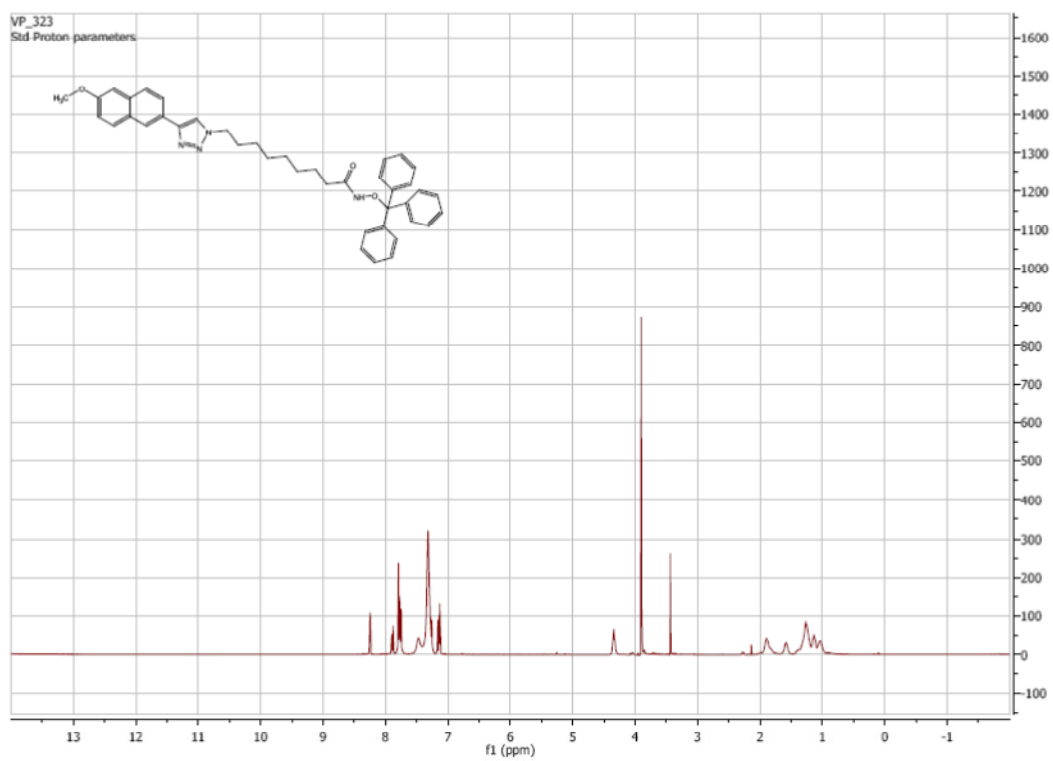
^1H NMR of **65d**:



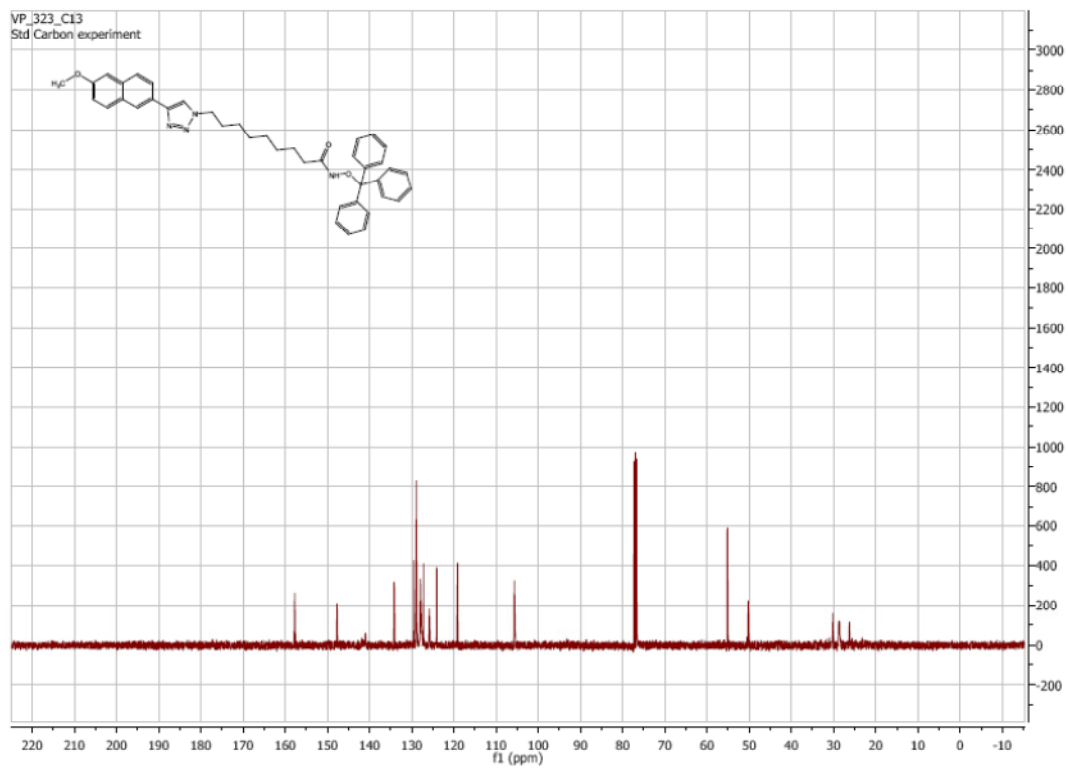
^{13}C NMR of **65d**:



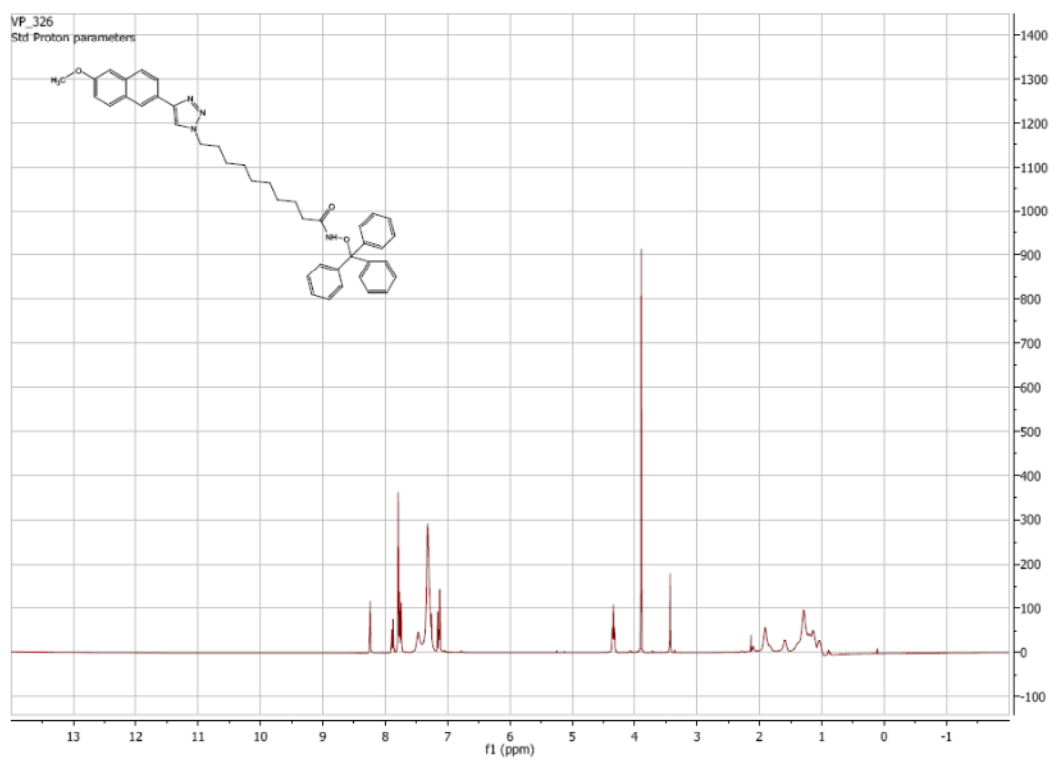
¹H NMR of **66a**:



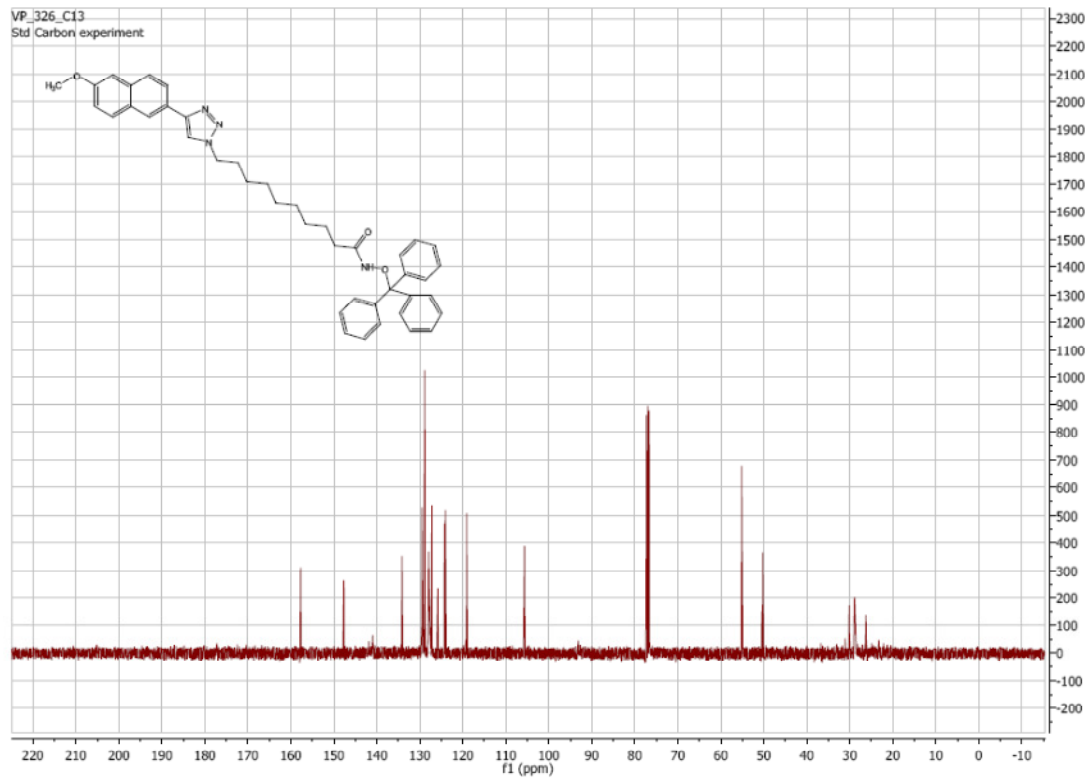
¹³C NMR of **66a**:



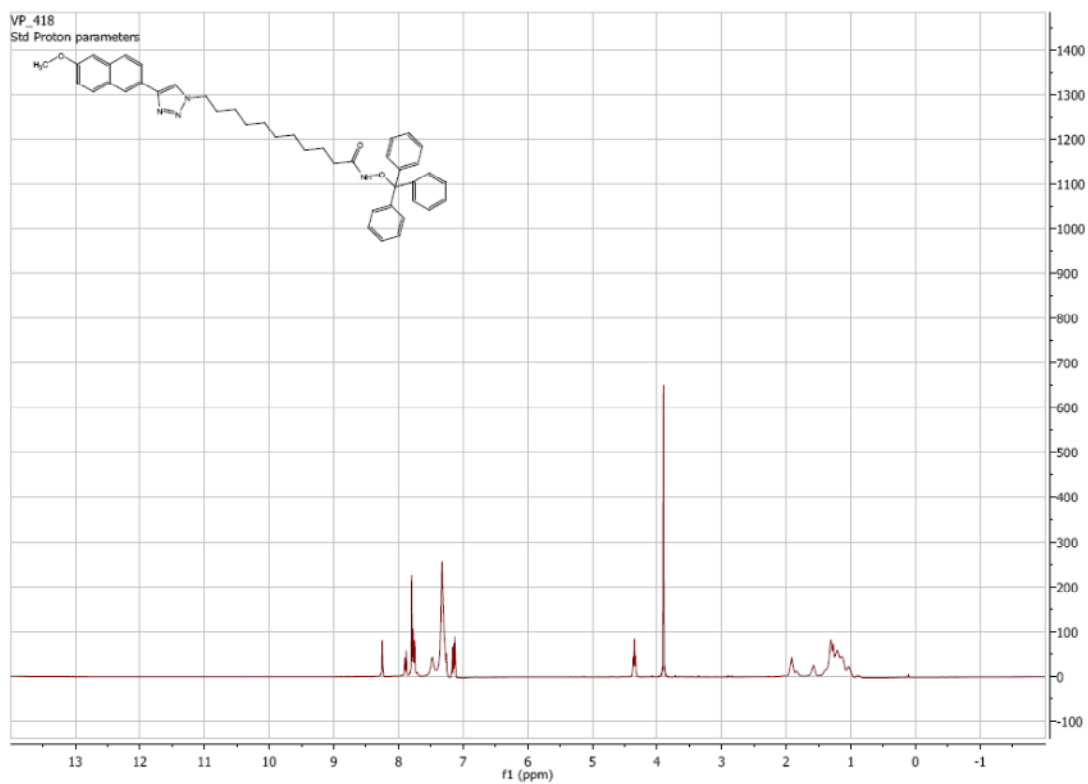
¹H NMR of **66b**:



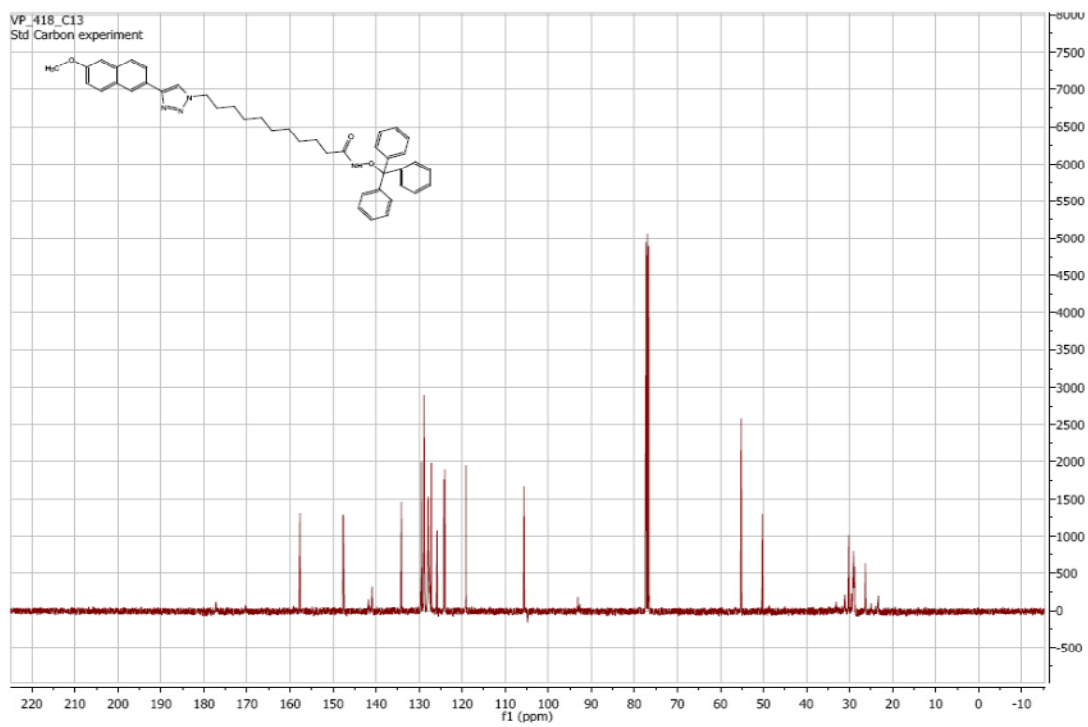
¹³C NMR of **66b**:



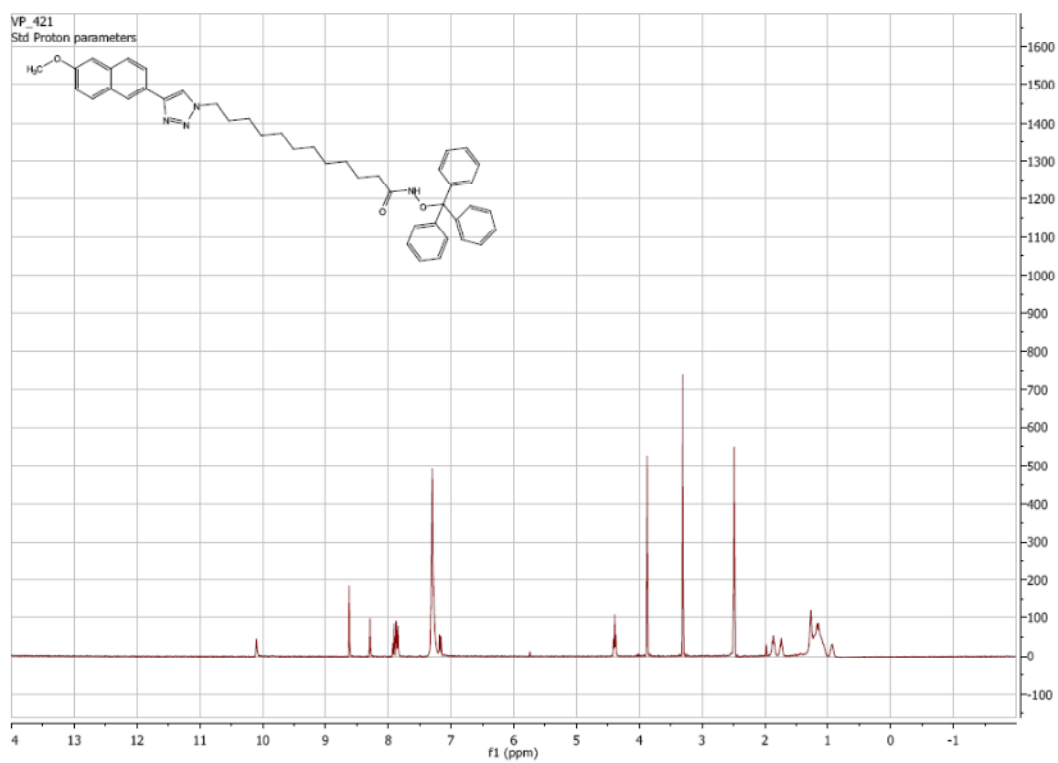
¹H NMR of **66c**:



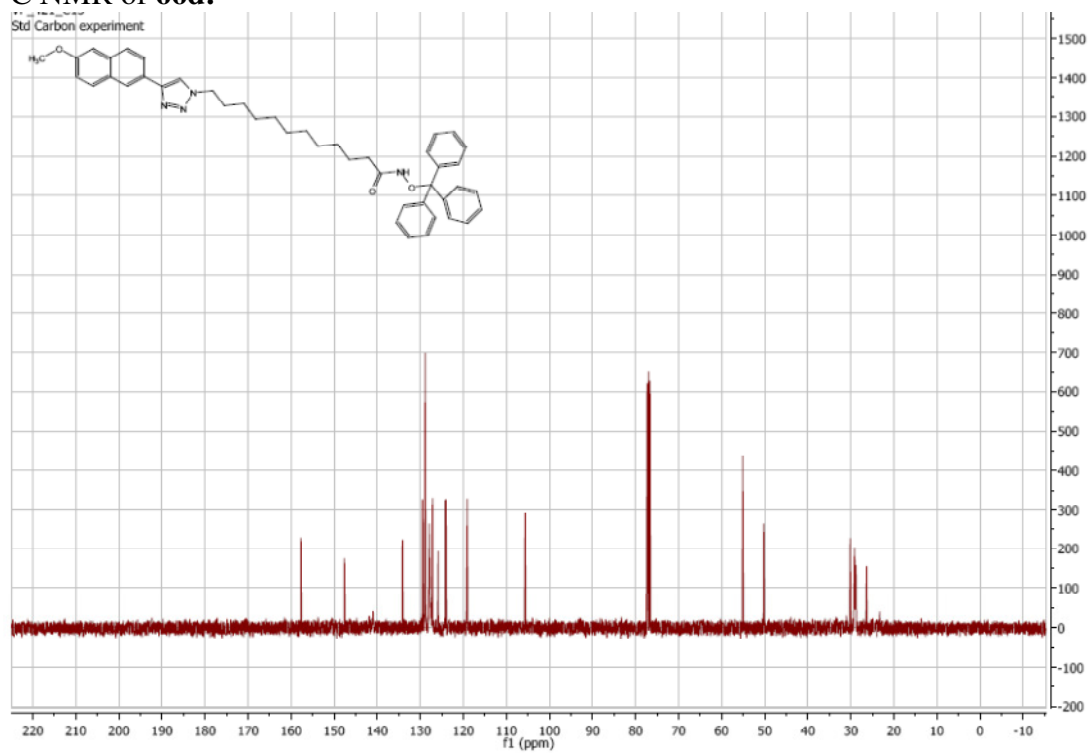
¹³C NMR of **66c**:



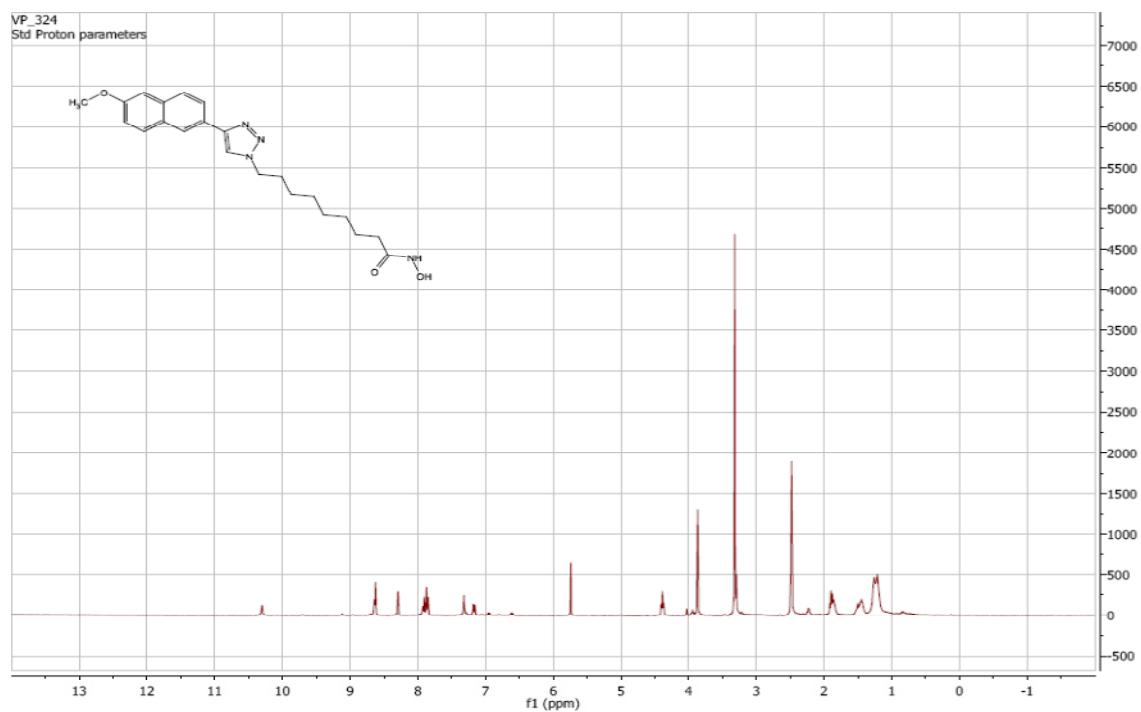
¹H NMR of **66d**:



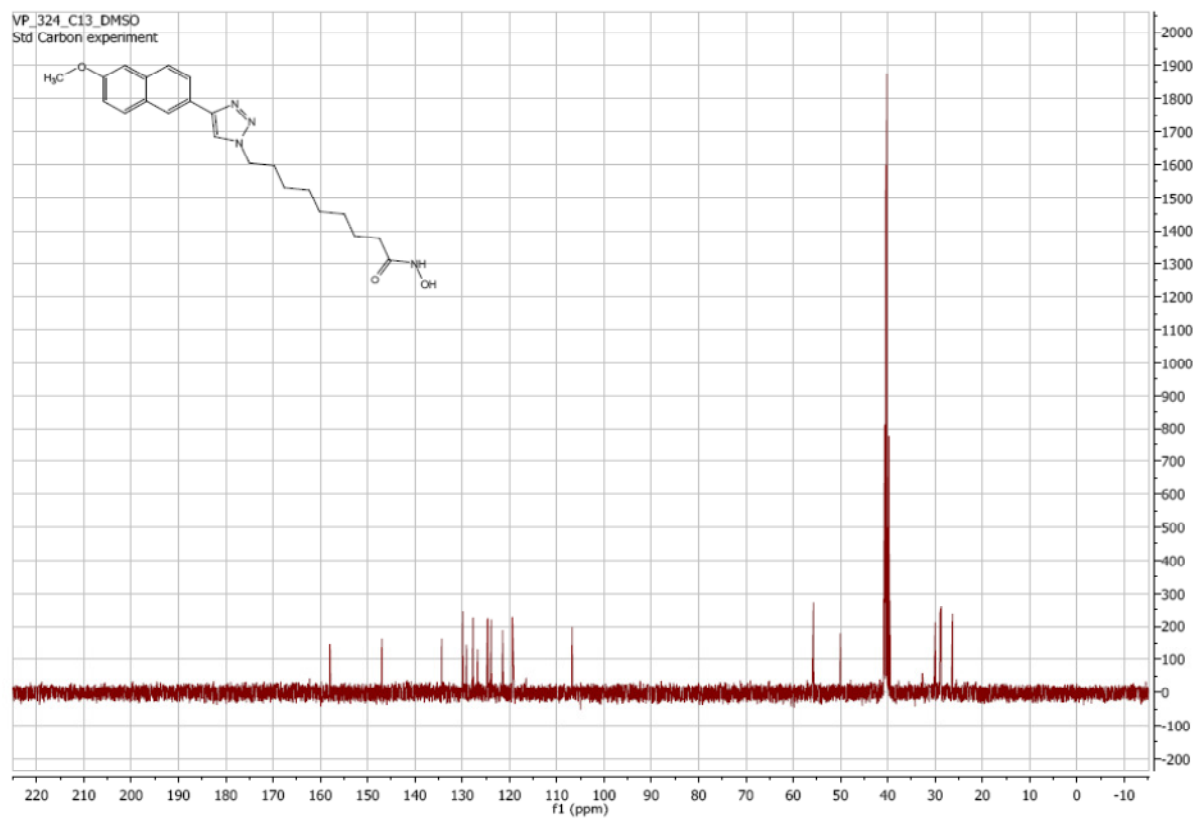
¹³C NMR of **66d**:



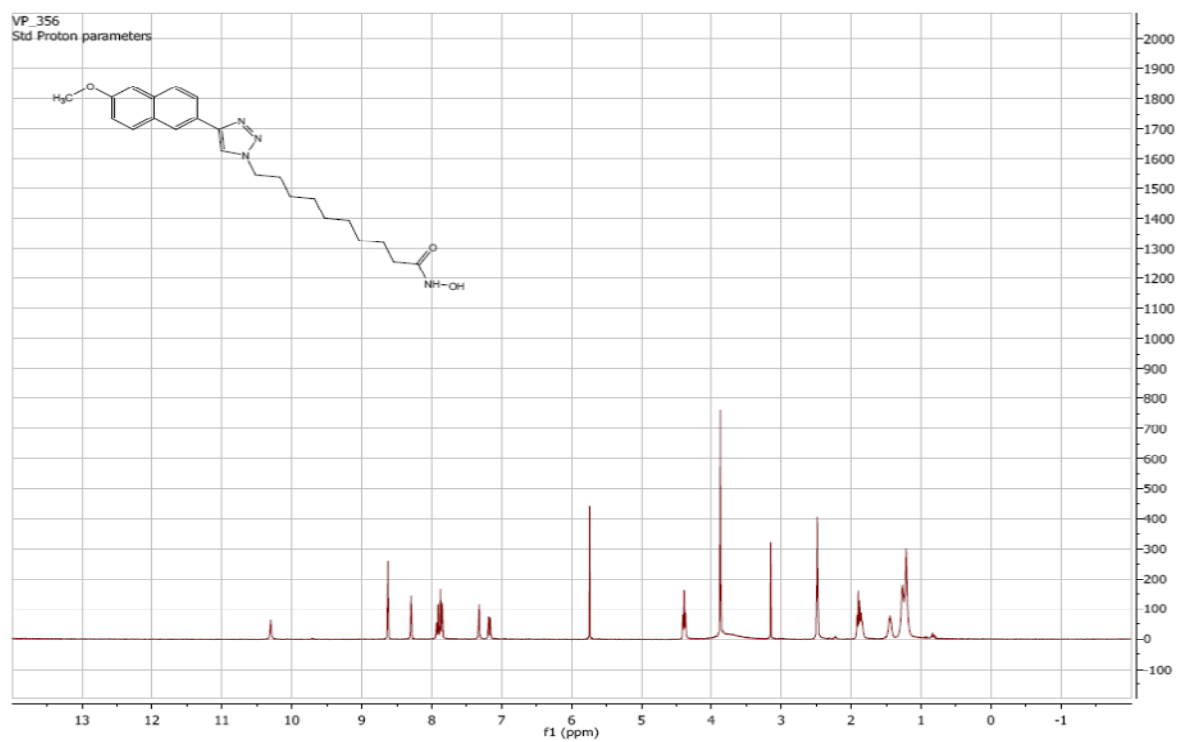
¹H NMR of **67a**:



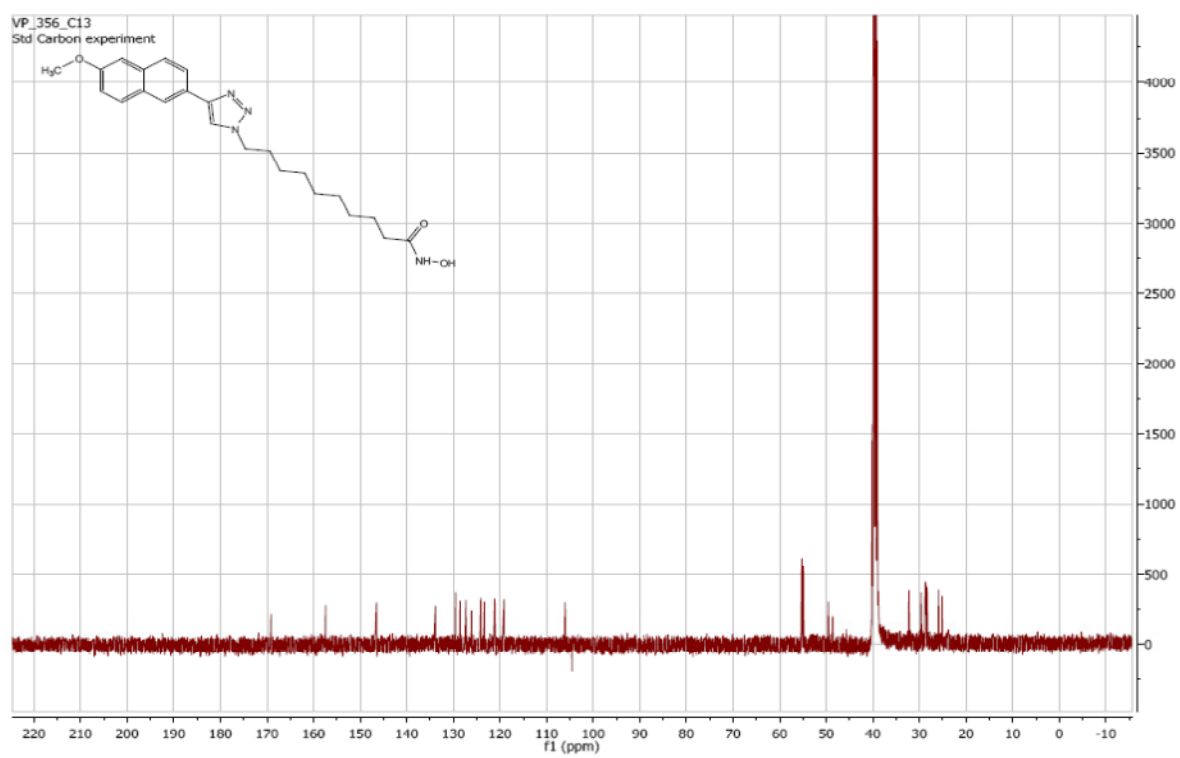
¹³C NMR of **67a**:



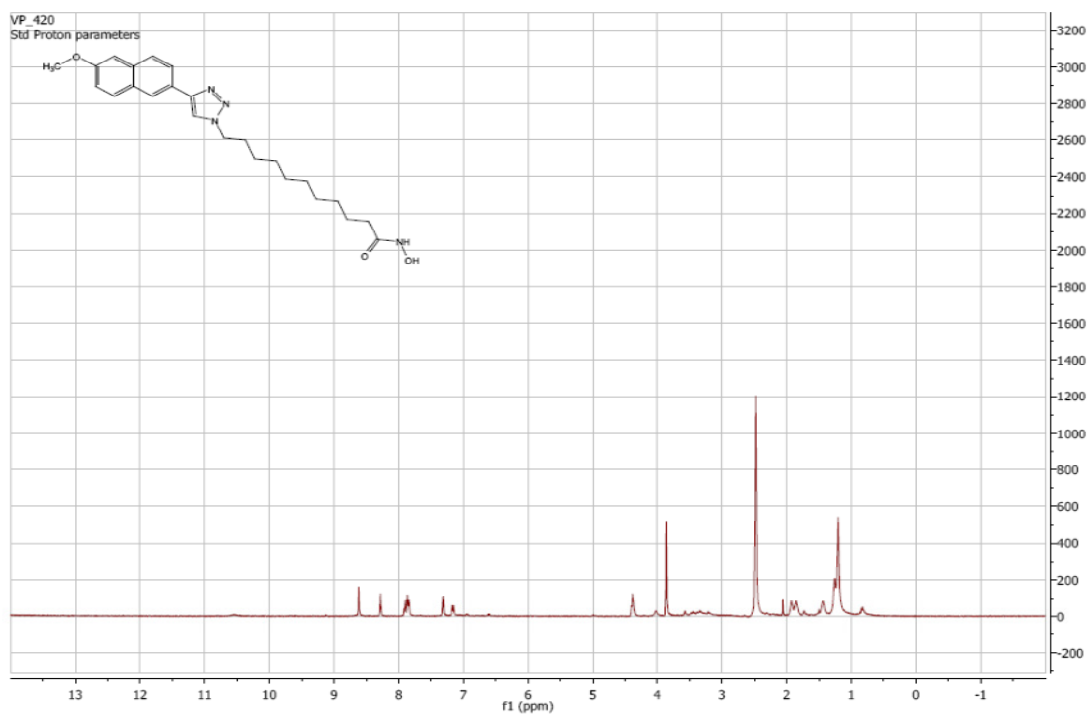
¹H NMR of **67b**:



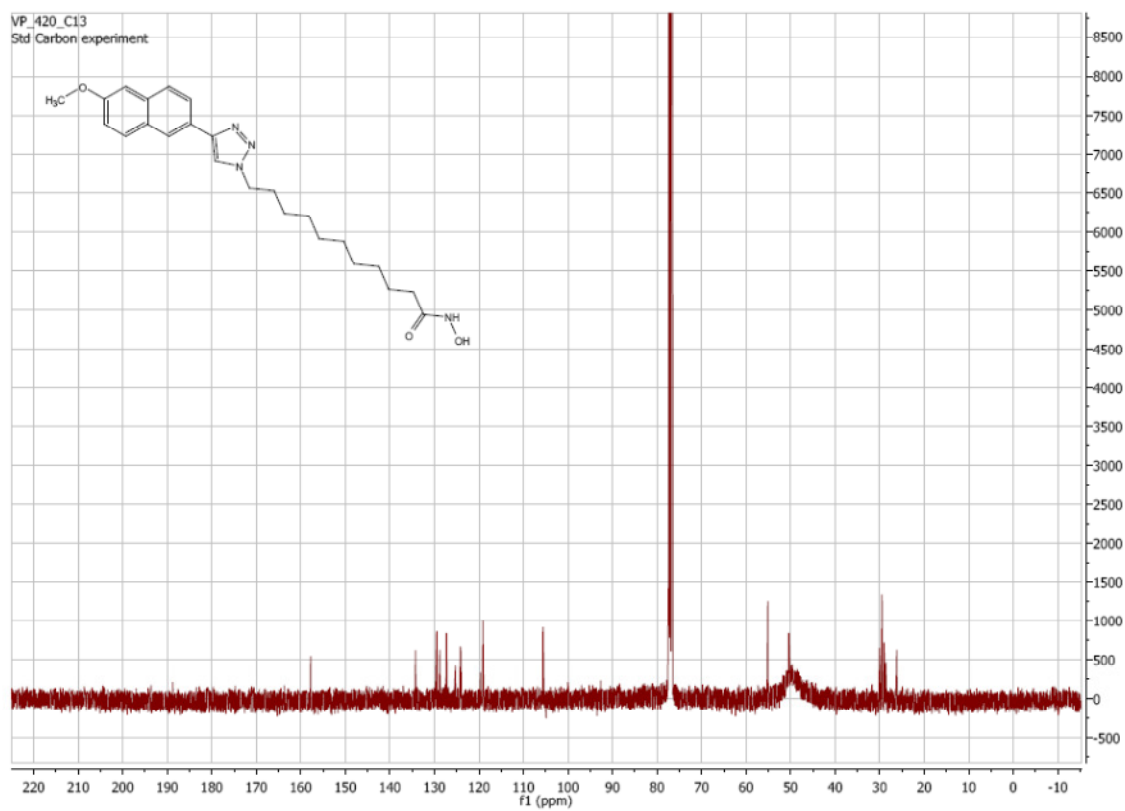
¹³C NMR of **67b**:



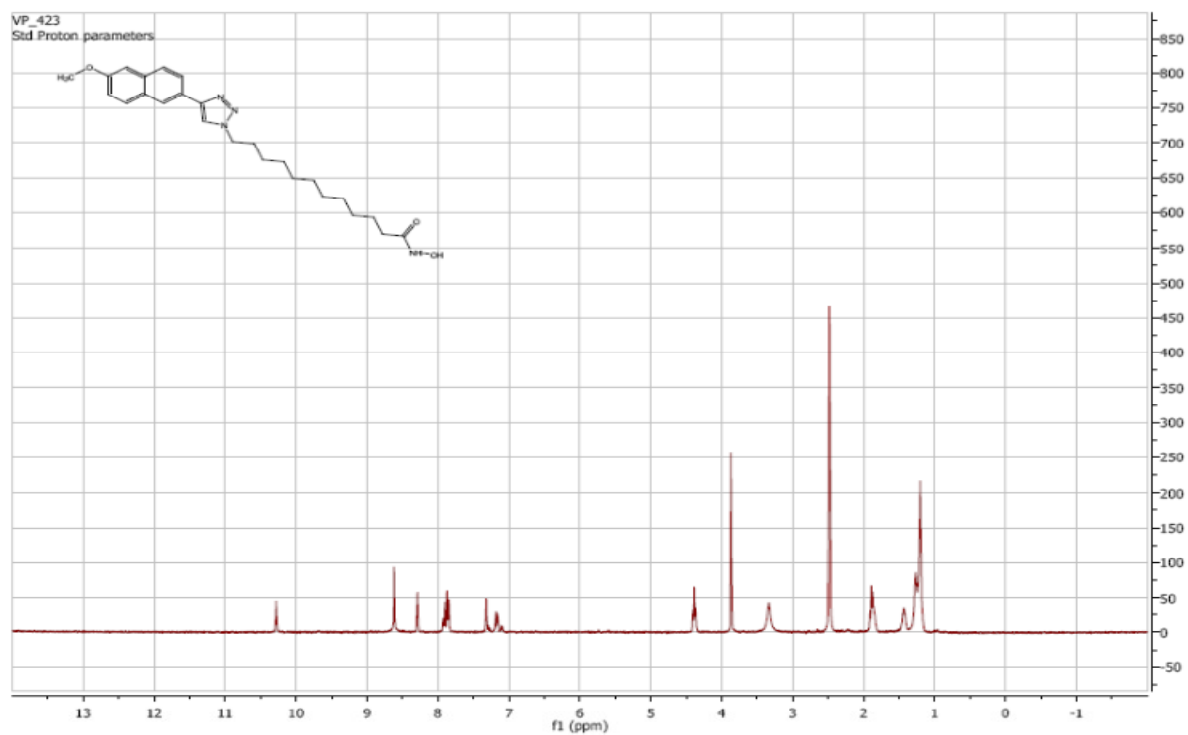
¹H NMR of **67c**:



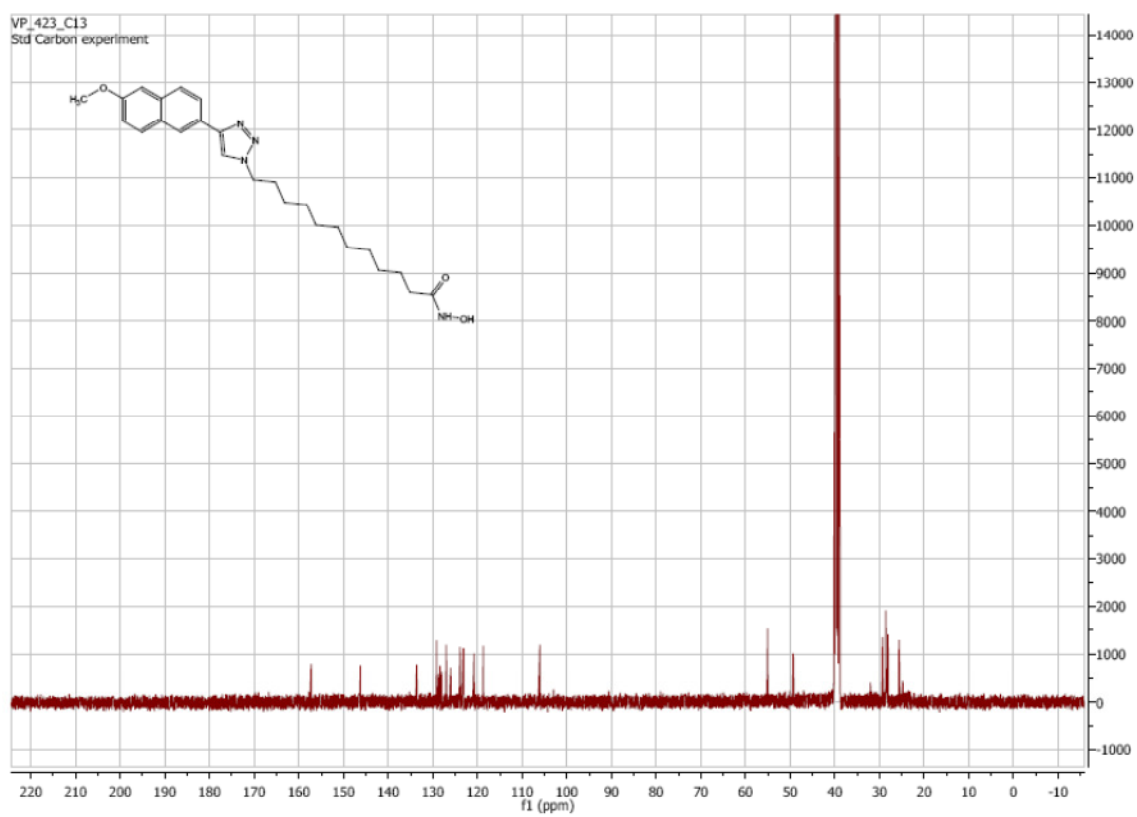
¹³C NMR of **67c**:



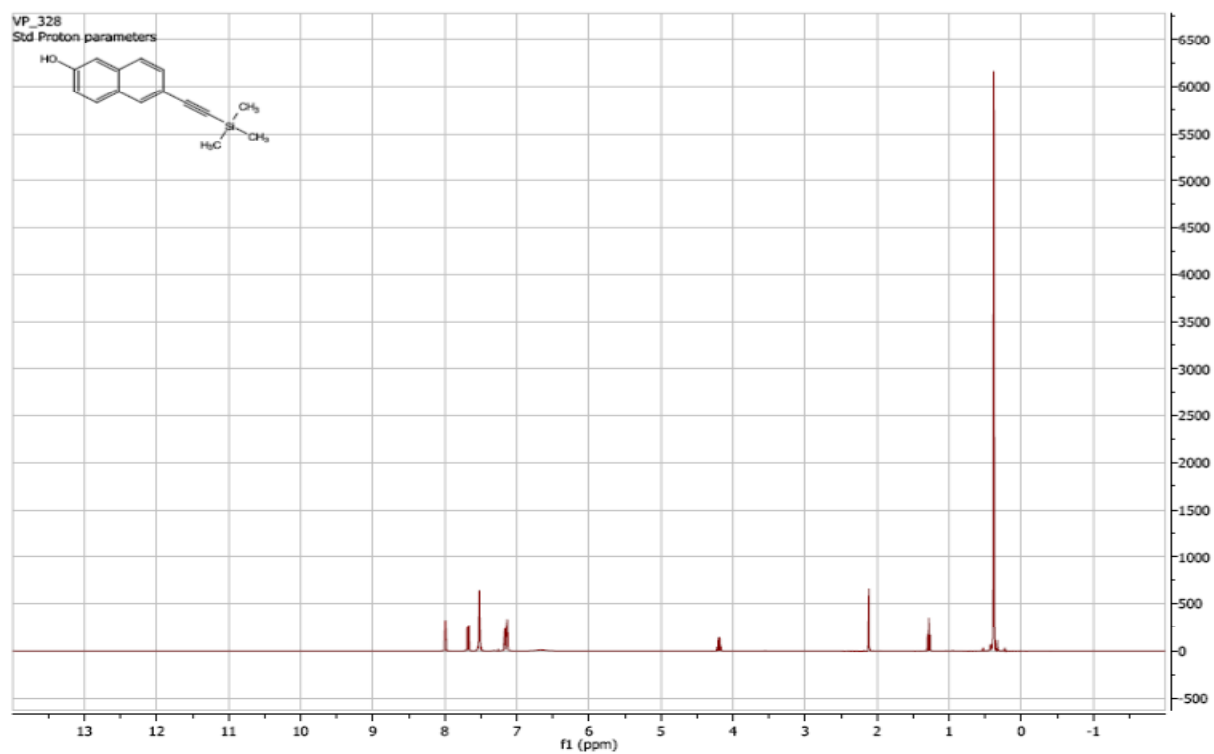
^1H NMR of **67d**:



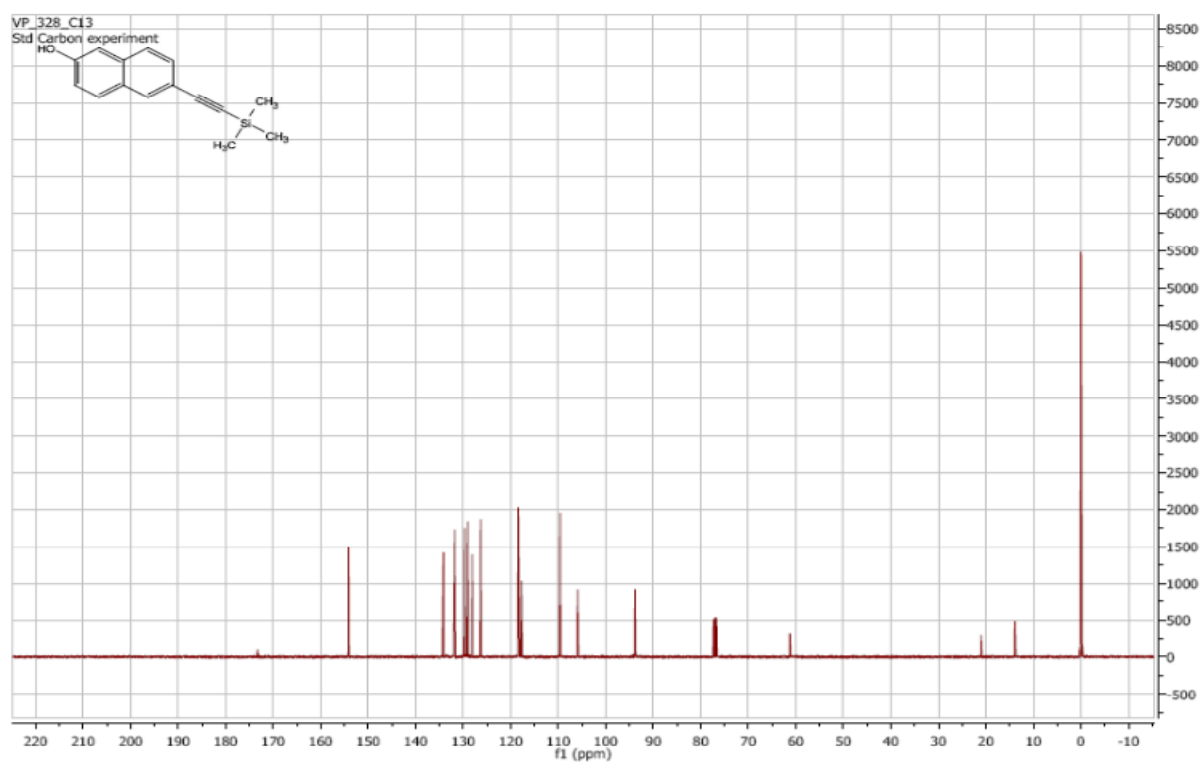
^{13}C NMR of **67d**:



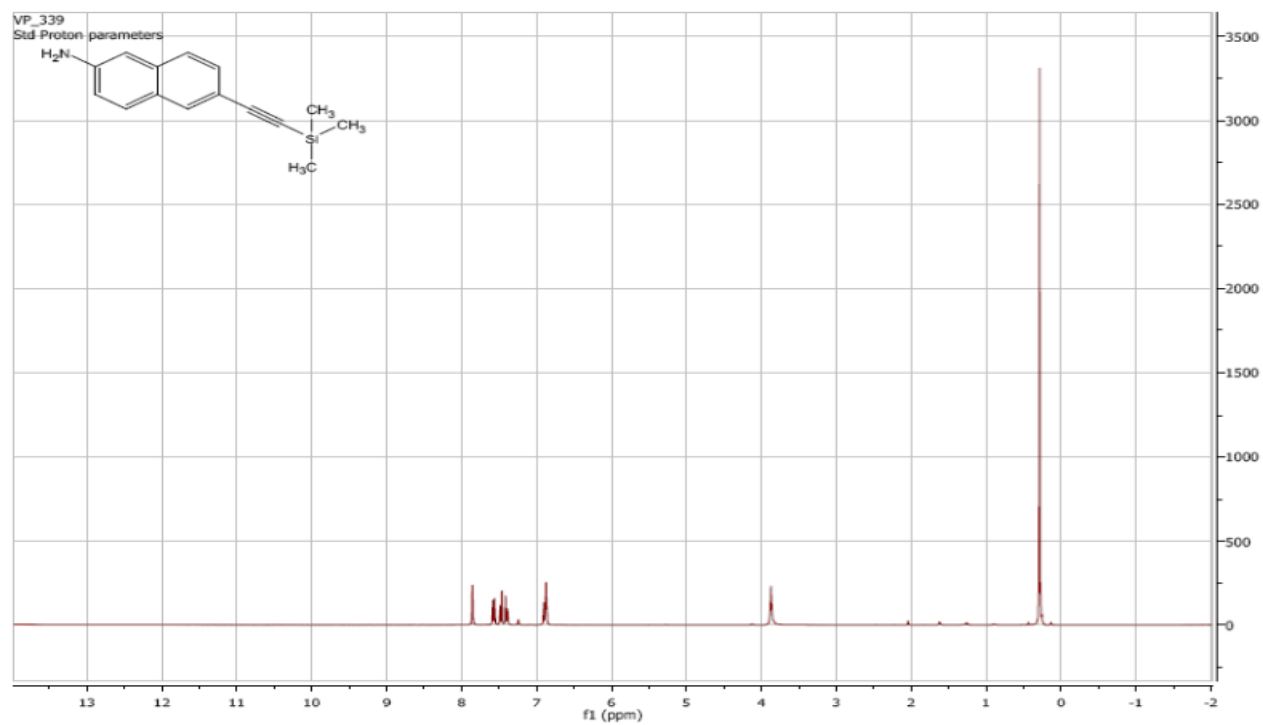
¹H NMR of **68a**:



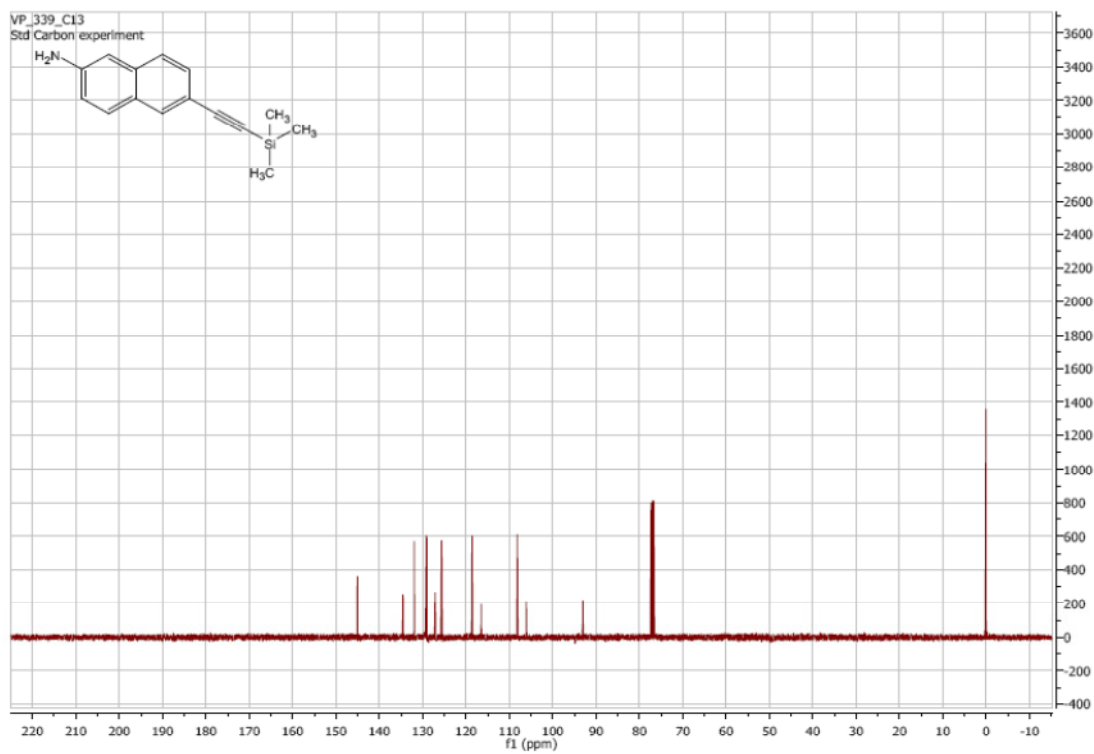
¹³C NMR of **68a**:



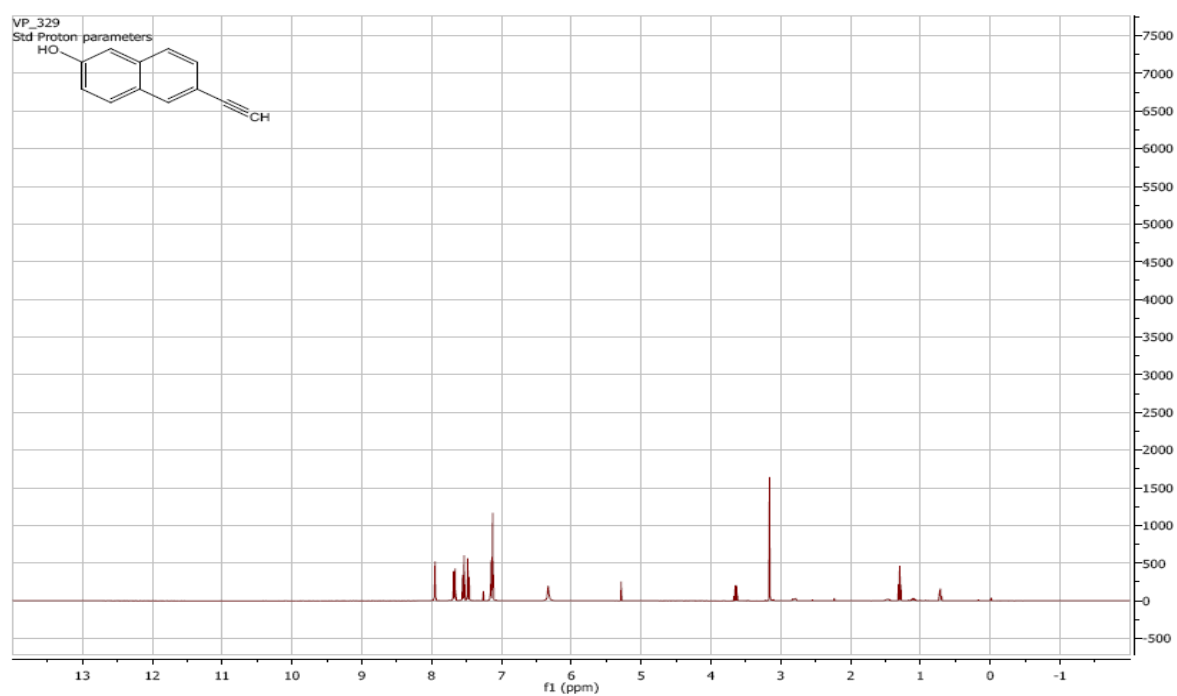
^1H NMR of **68b**:



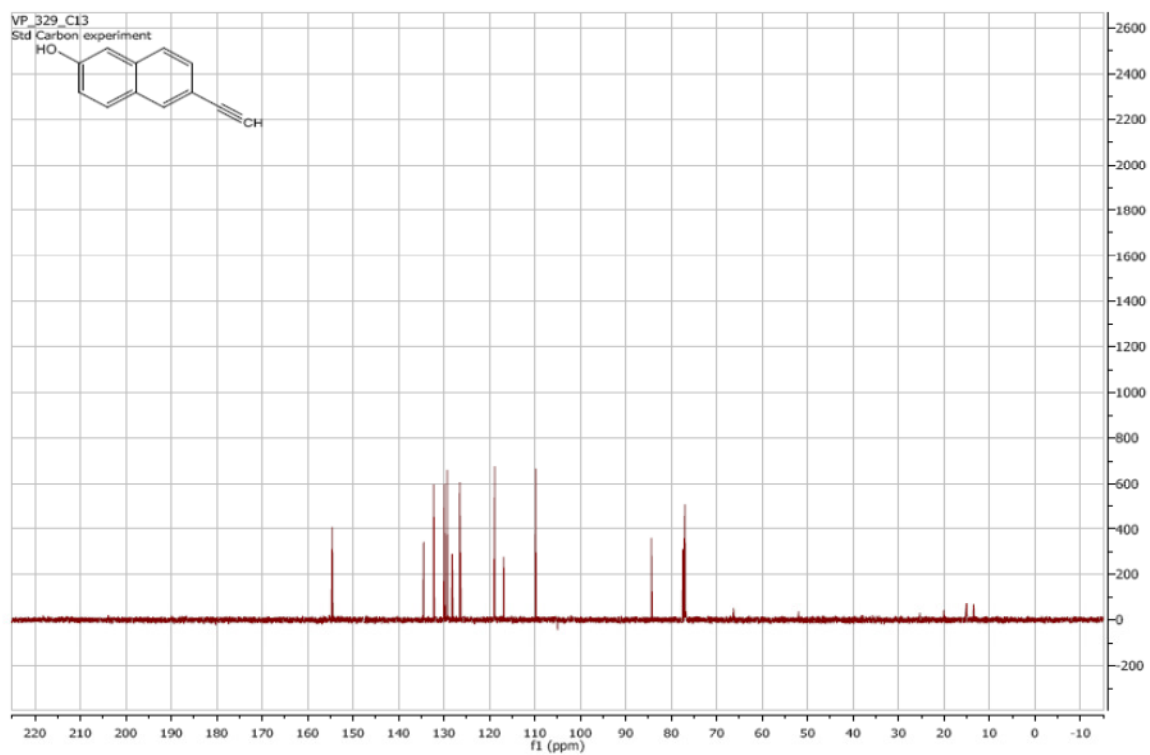
^{13}C NMR of **68b**:



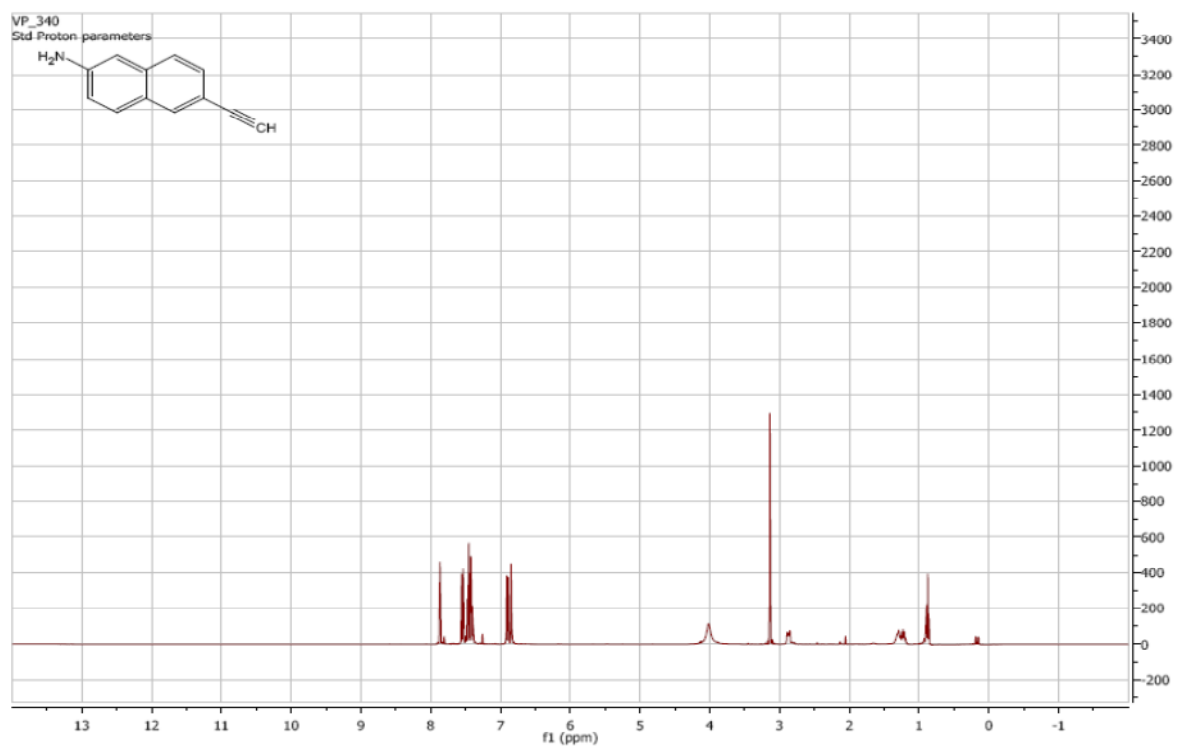
¹H NMR of **69a**:



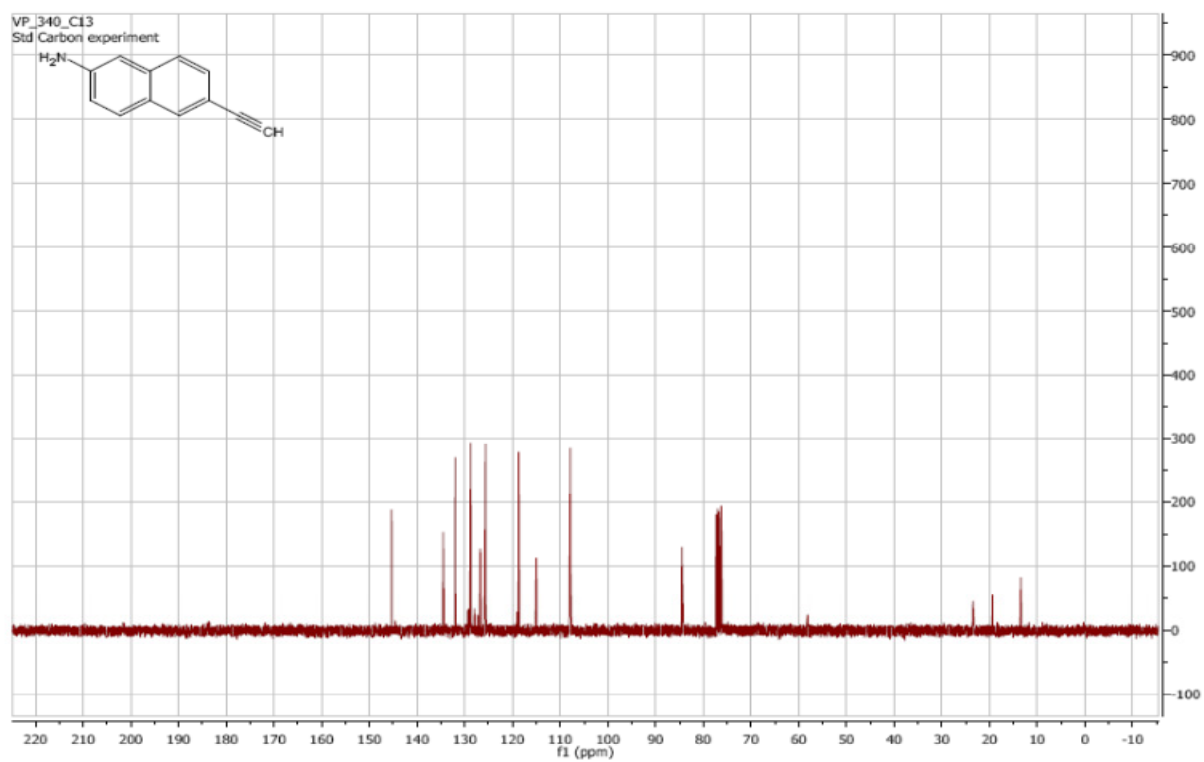
¹³C NMR of **69a**:

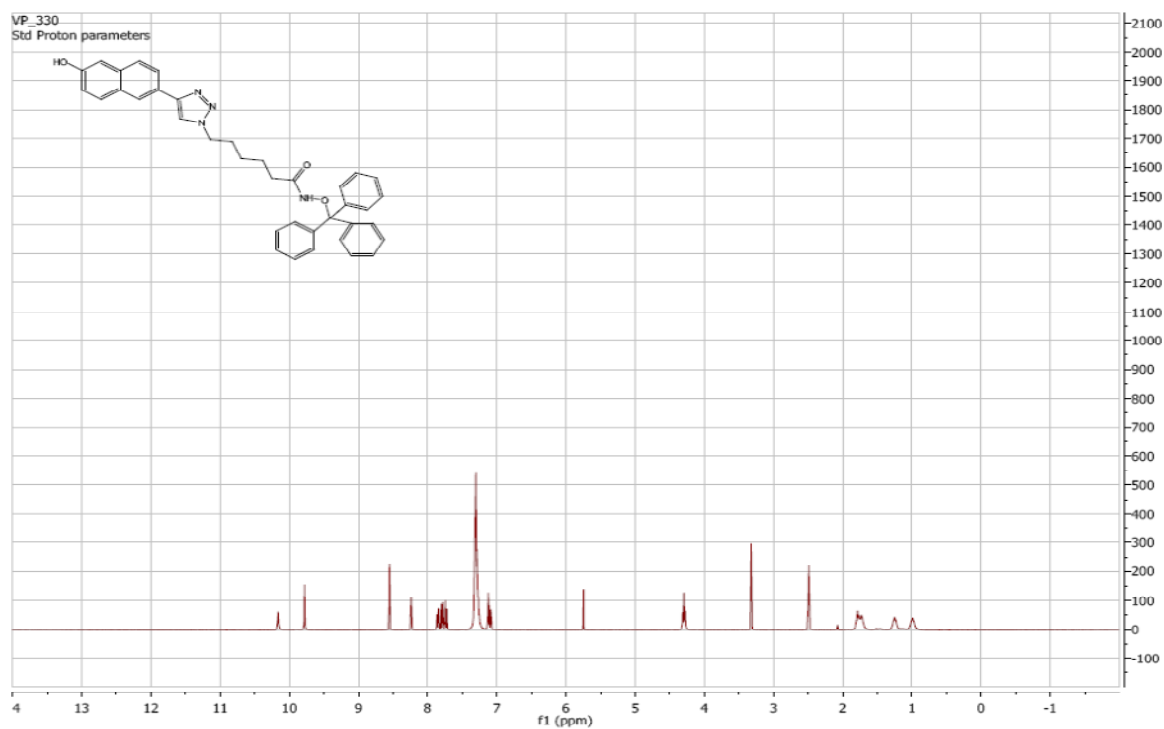
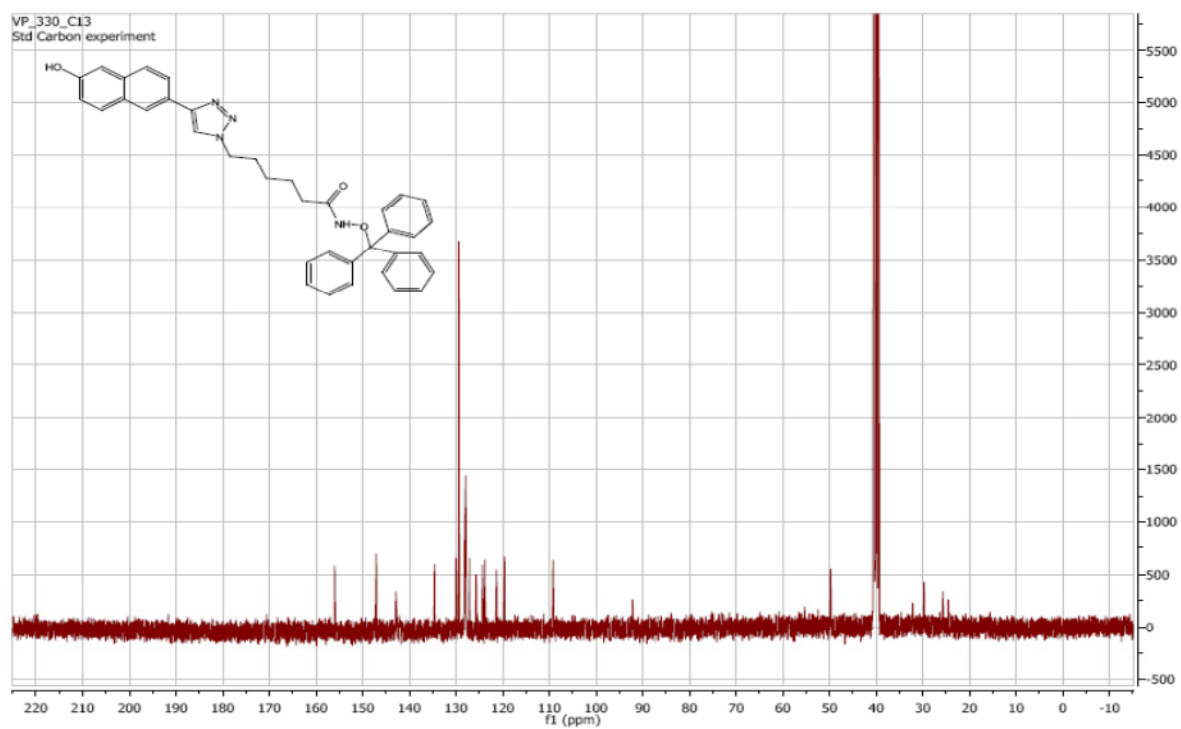


^1H NMR of **69b**:

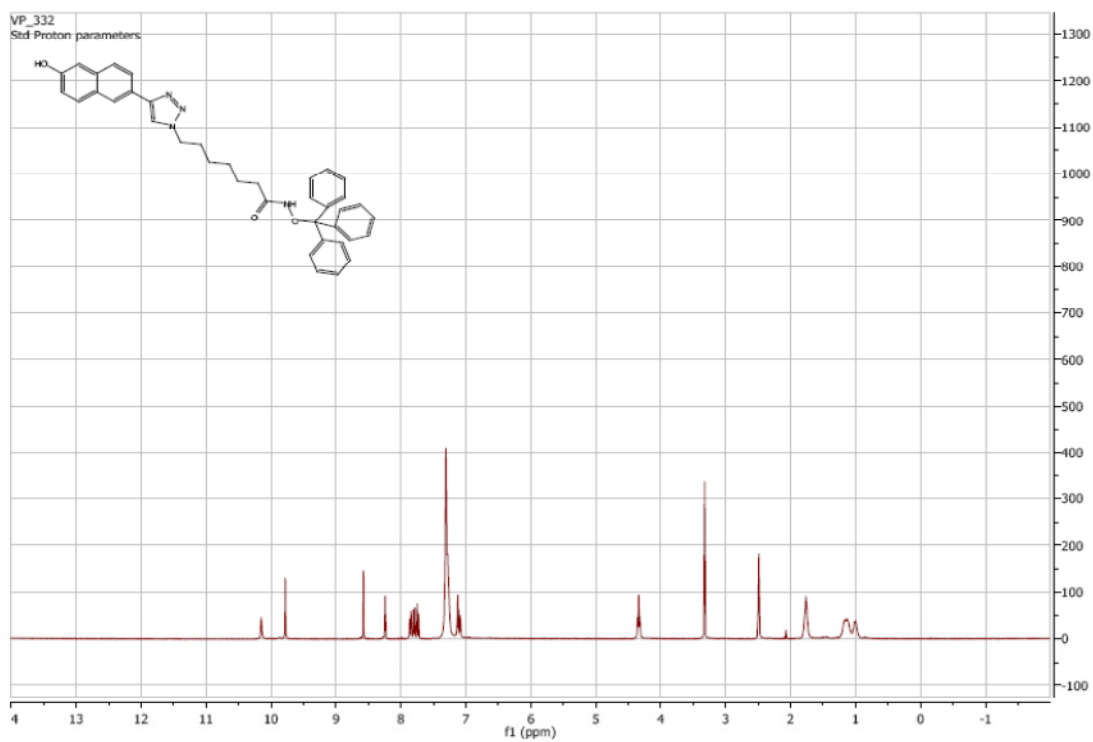


^{13}C NMR of **69b**:

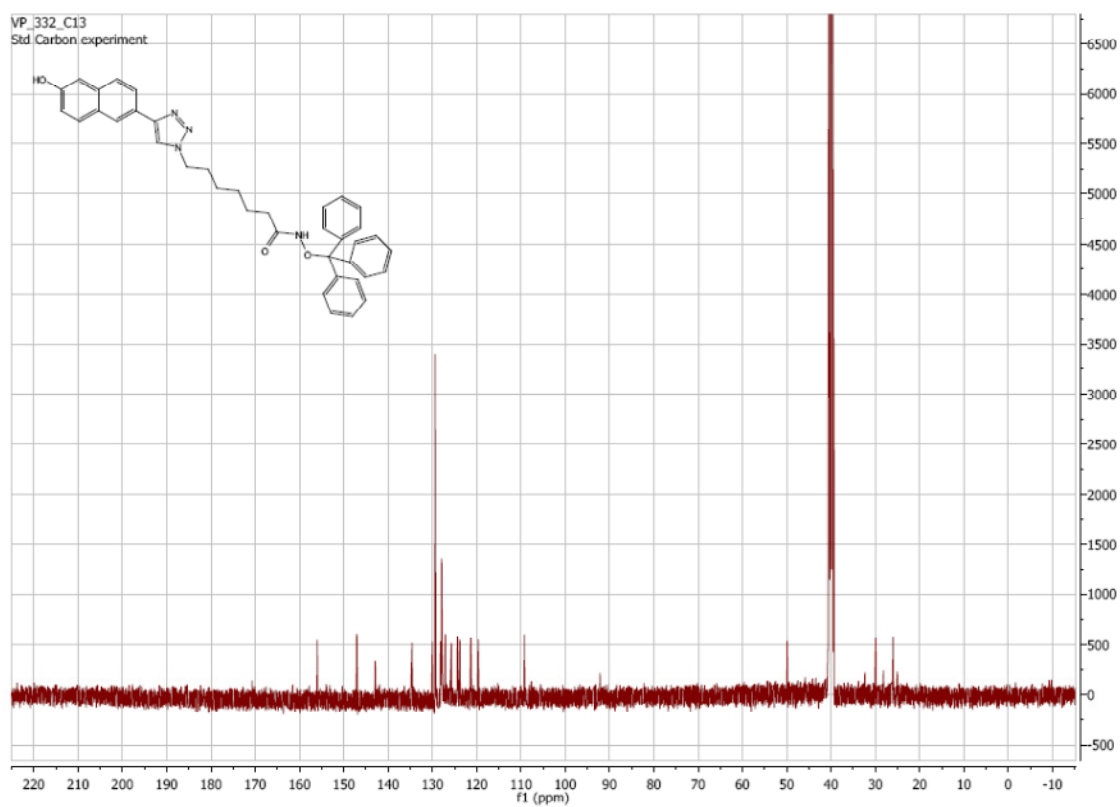


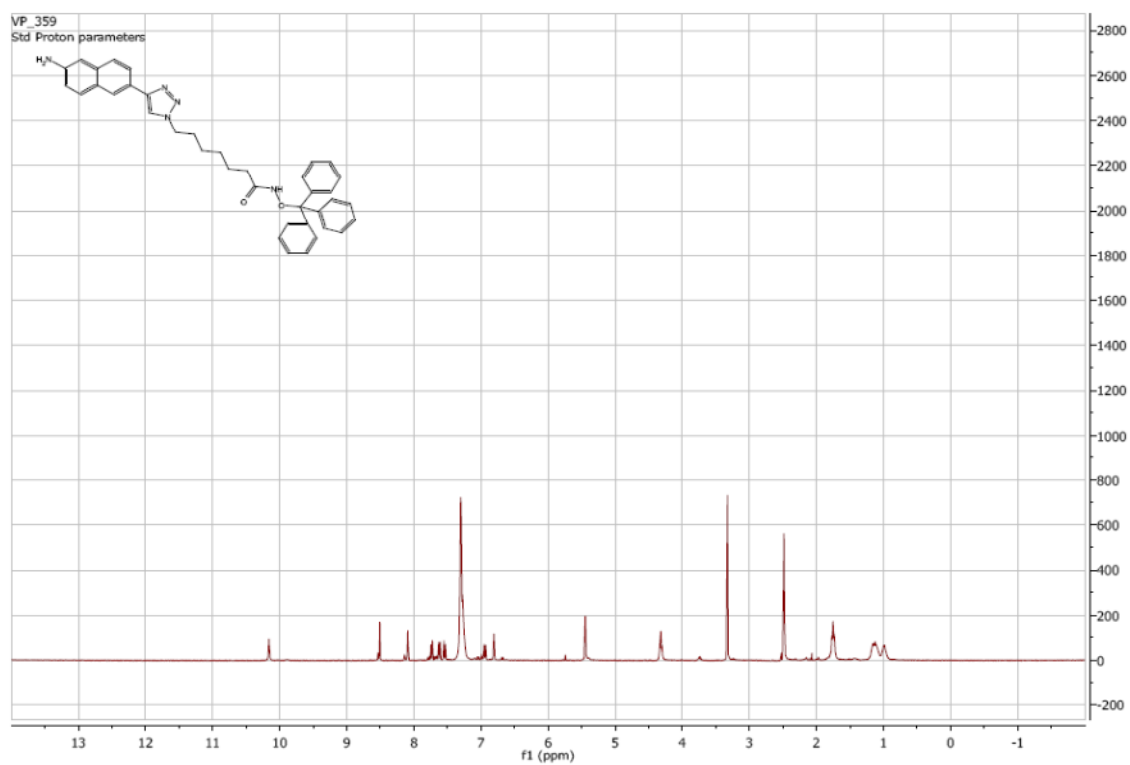
¹H NMR of **70a**: ^{13}C NMR of **70a**:

¹H NMR of **70b**:

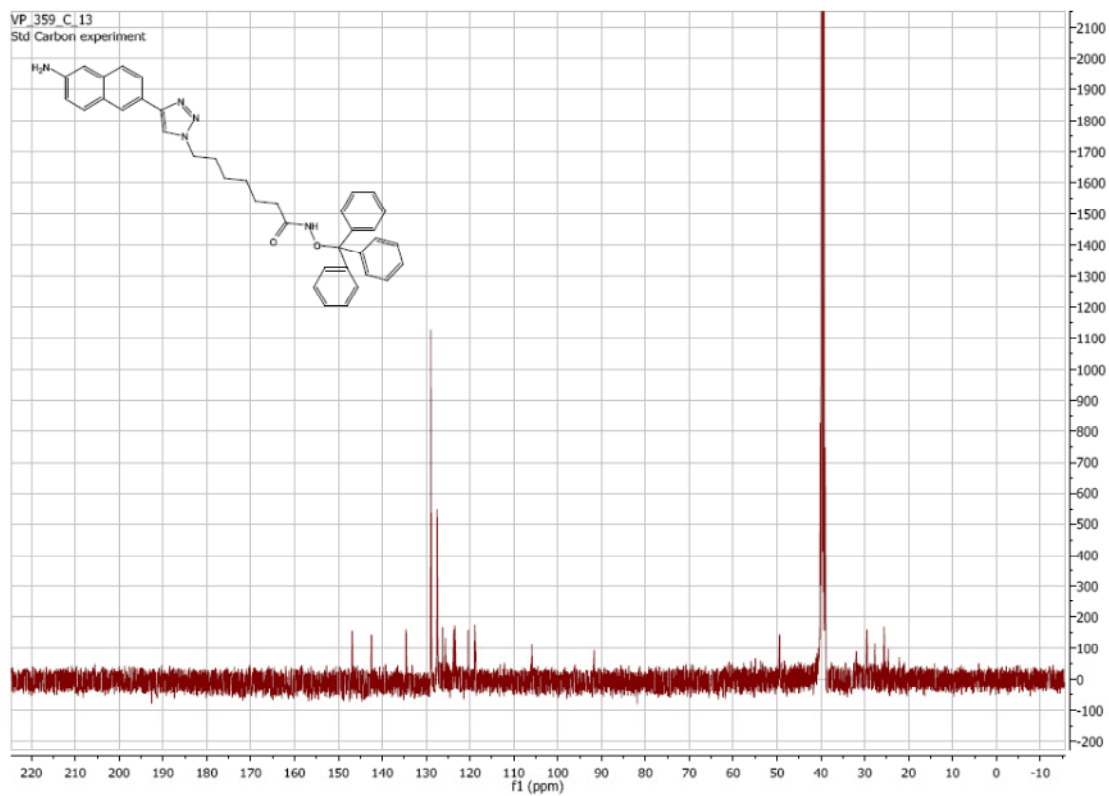


¹³C NMR of **70b**:

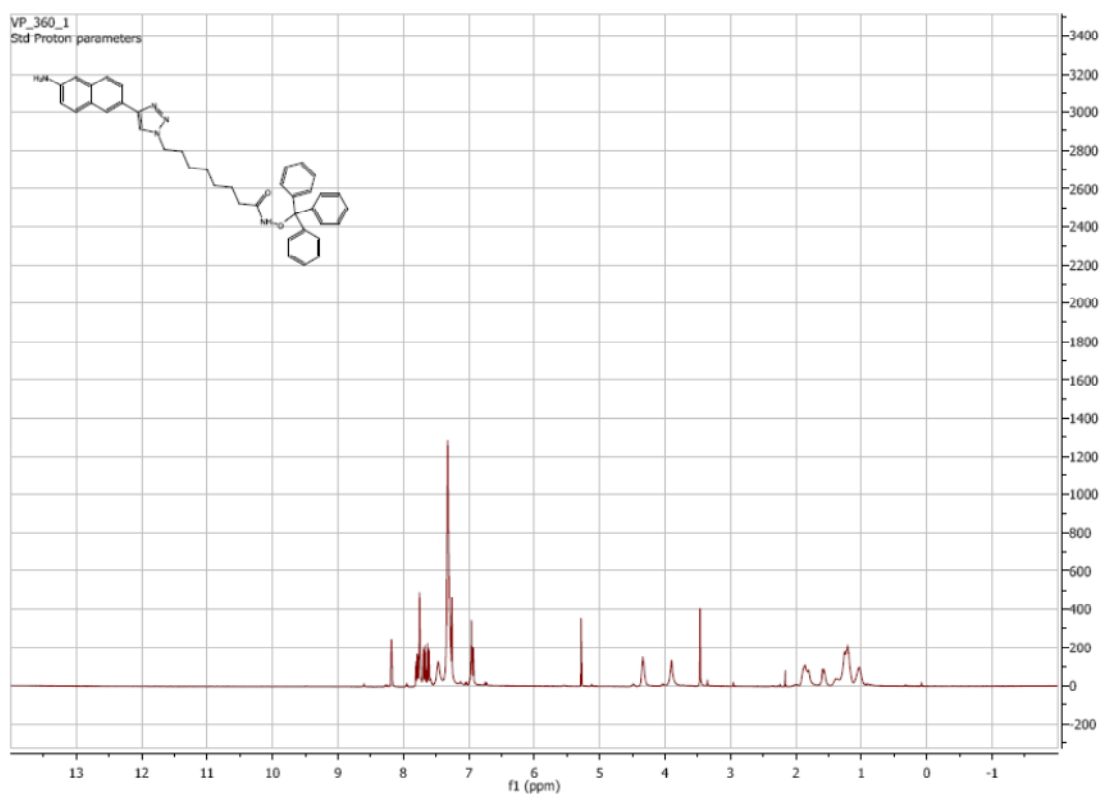


¹H NMR of **70c**:

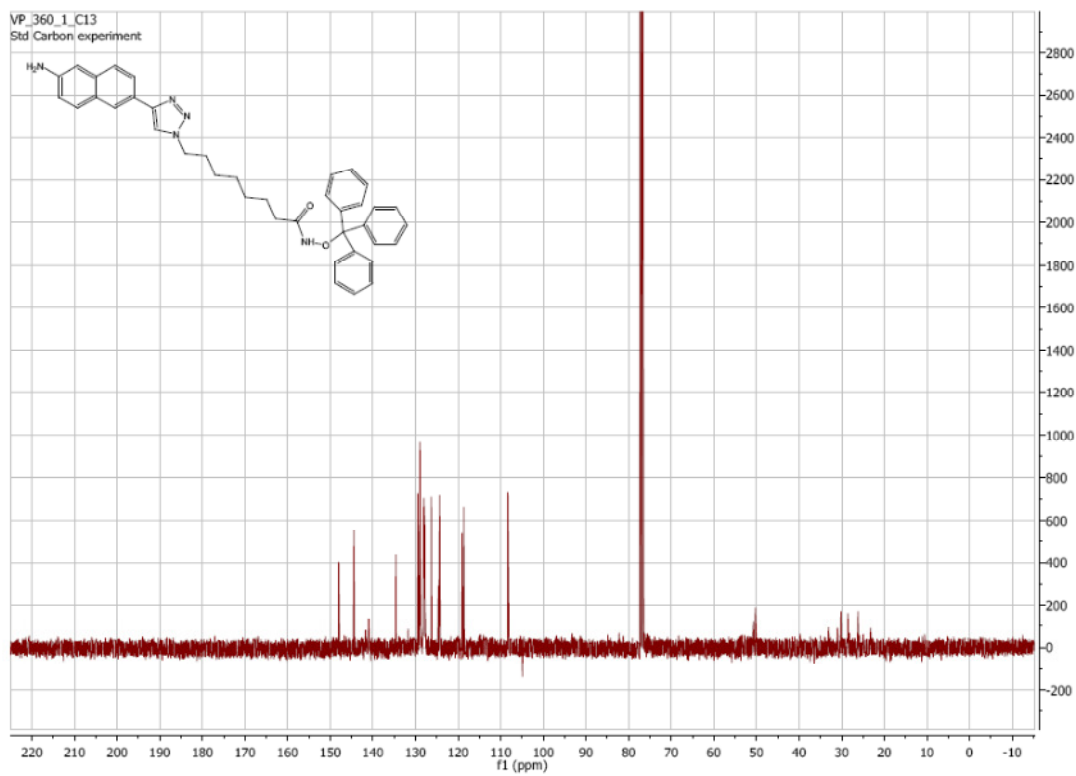
¹³C NMR of **70c**:



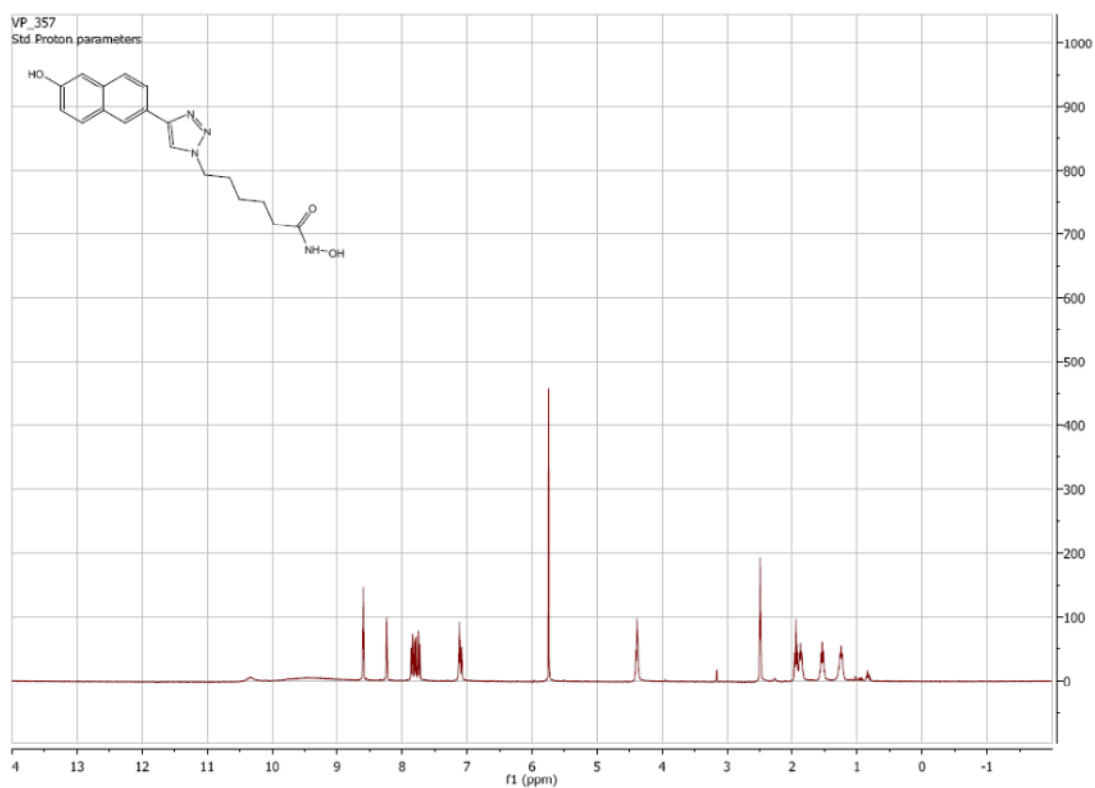
^1H NMR of **70d**:



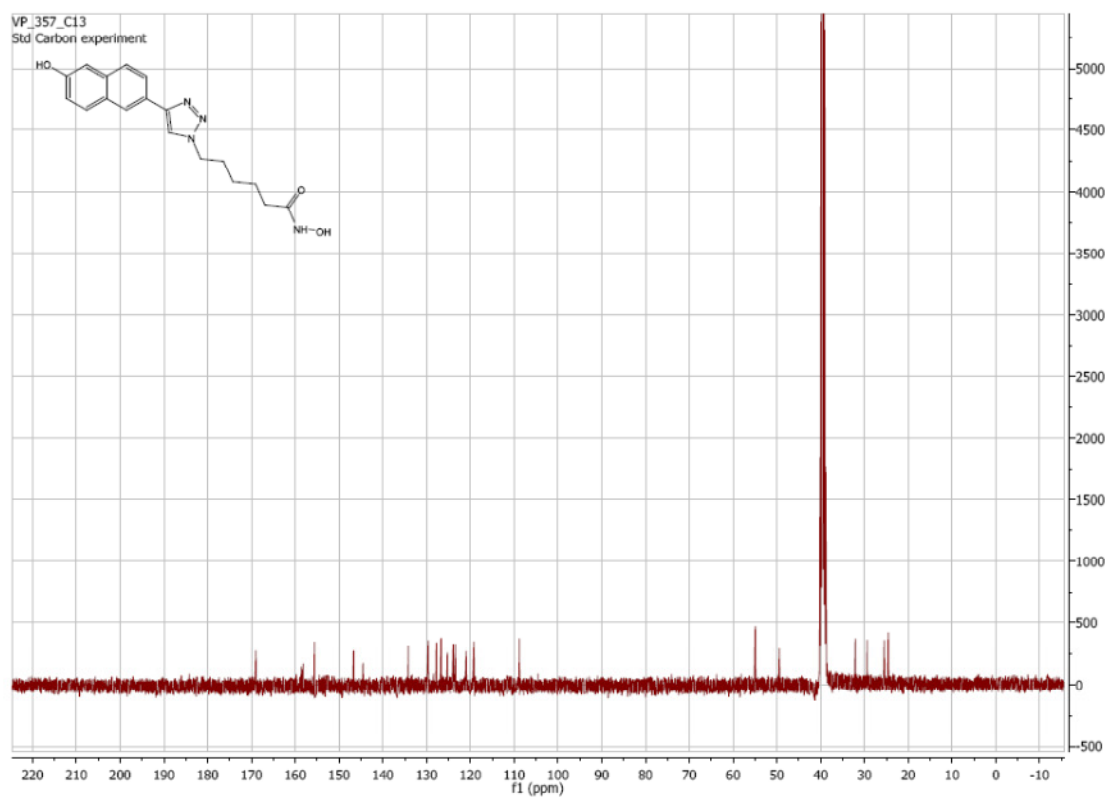
^{13}C NMR of **70d**:



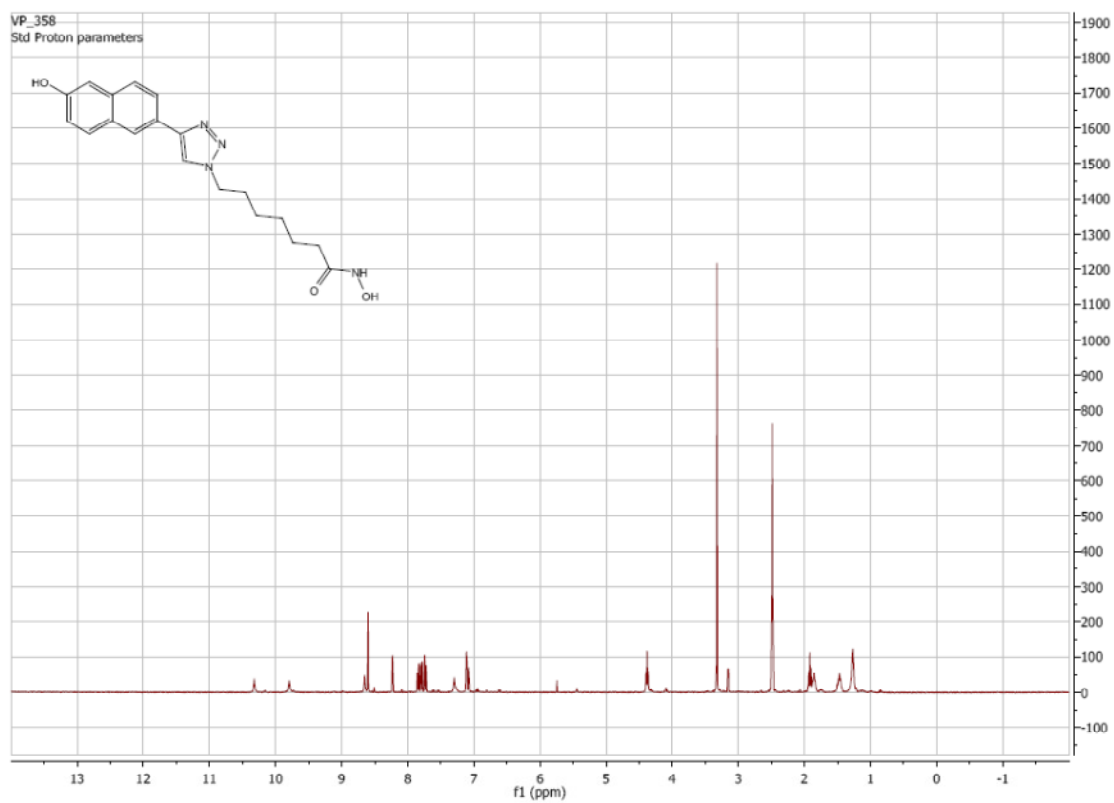
¹H NMR of **71a**:



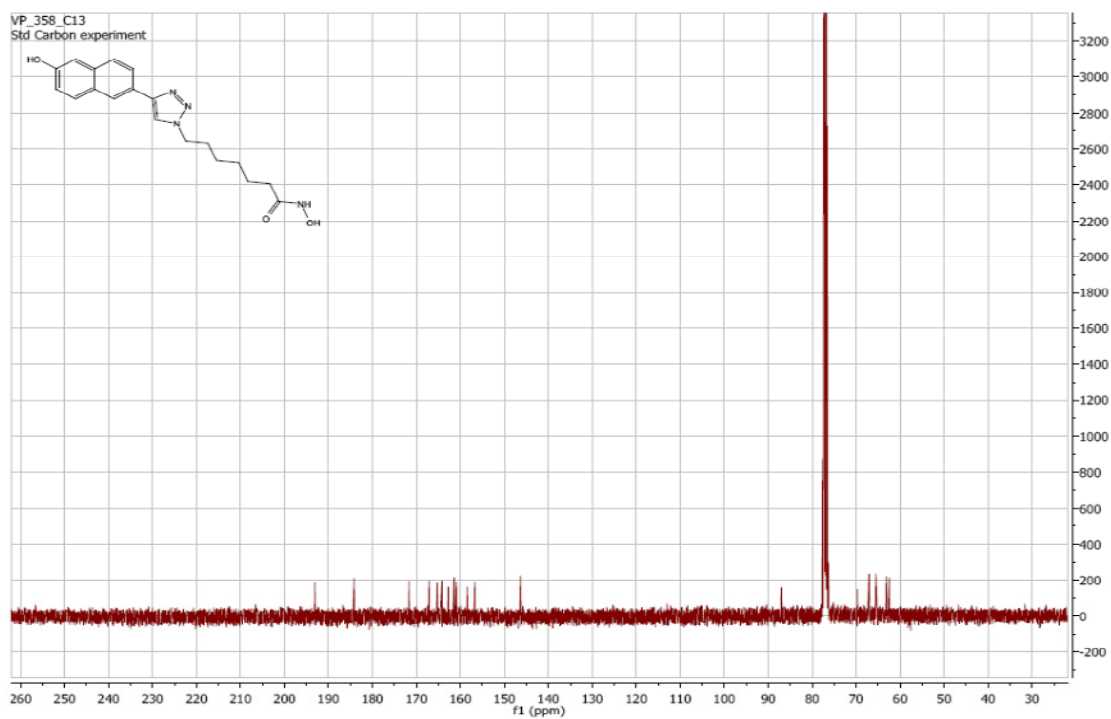
¹³C NMR of **71a**:



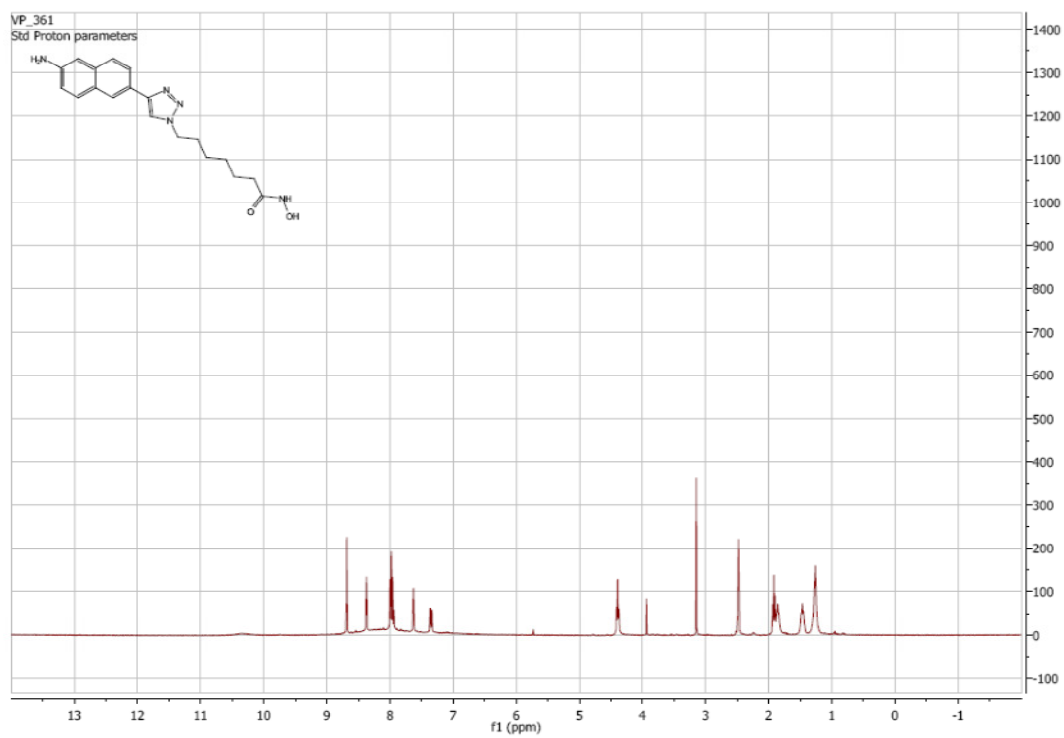
¹H NMR of **71b**:



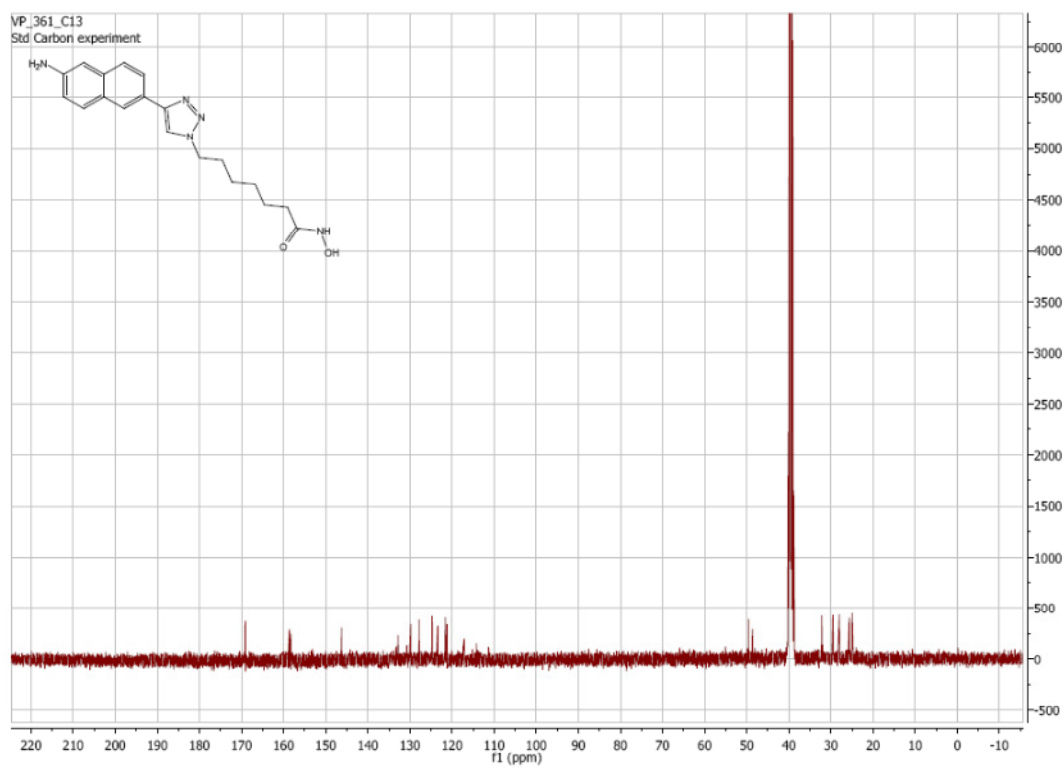
¹³C NMR of **71b**:



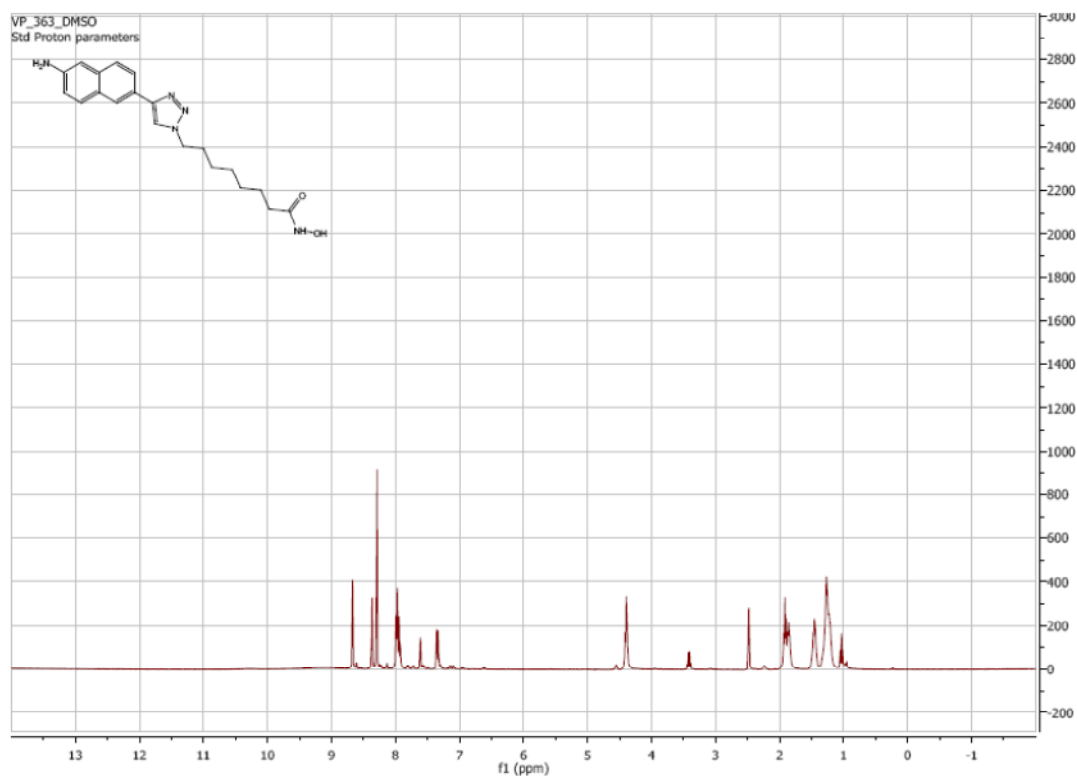
¹H NMR of **71c**:



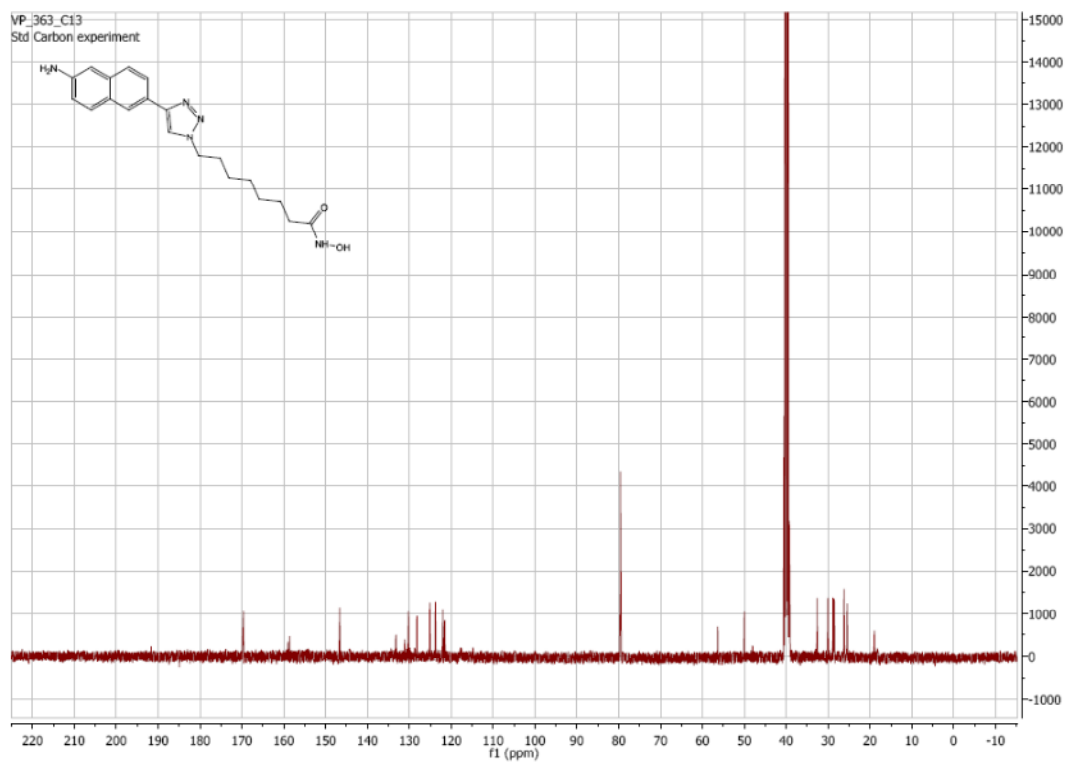
¹³C NMR of **71c**:



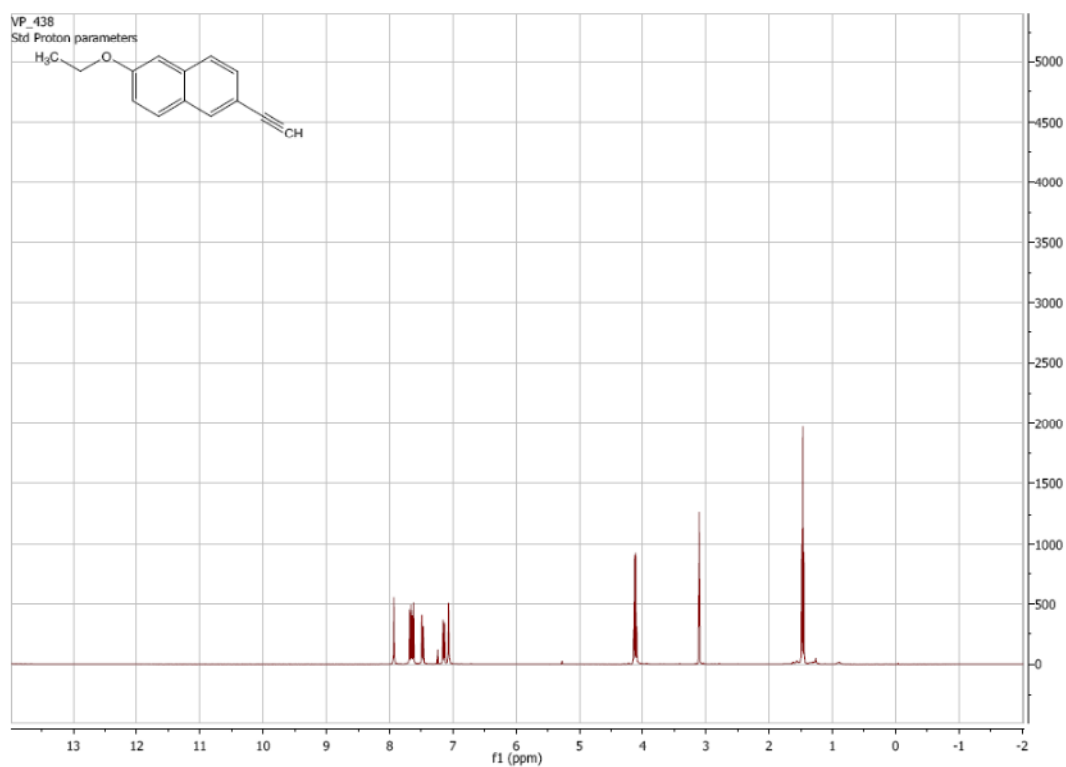
¹H NMR of **71d**:



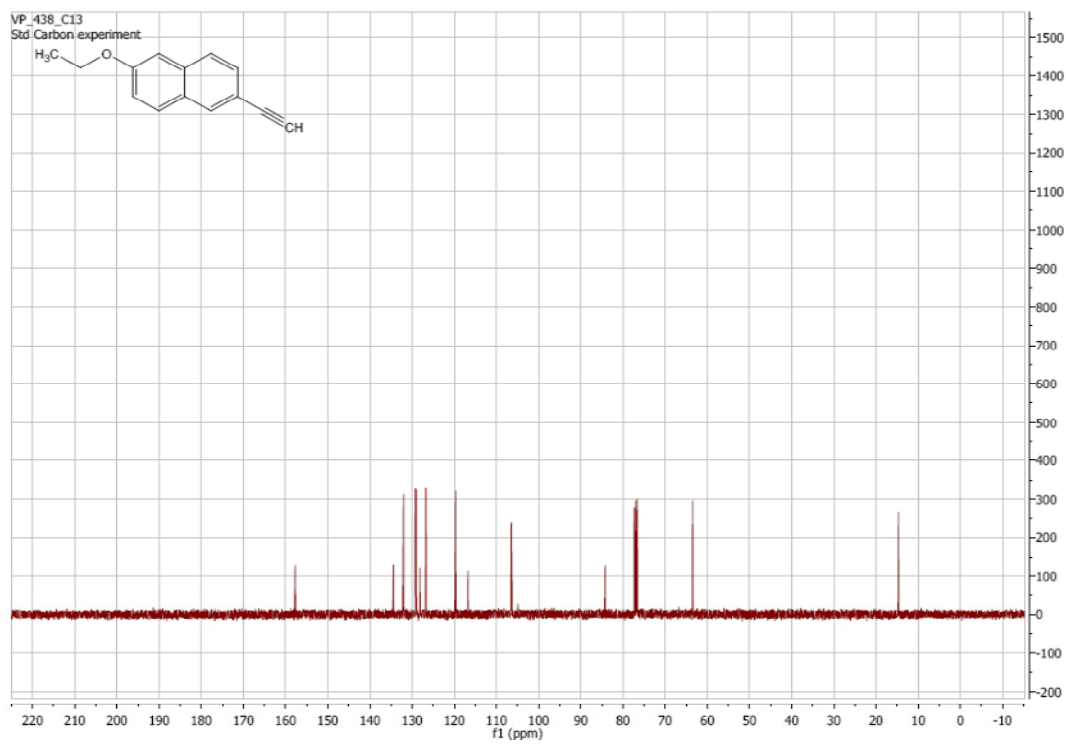
¹³C NMR of **71d**:



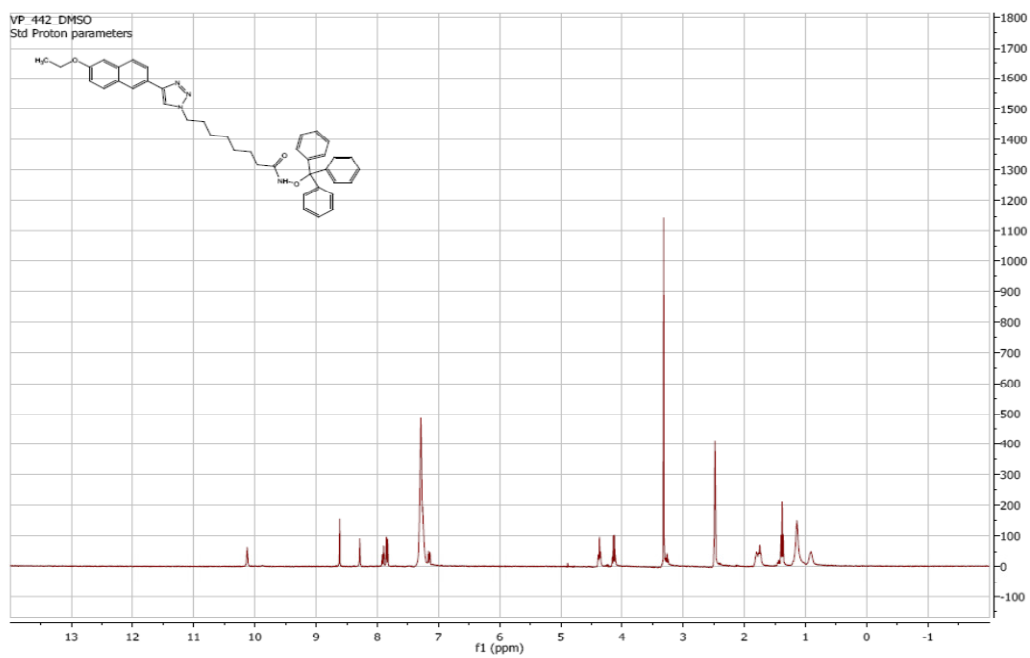
^1H NMR of **72**:



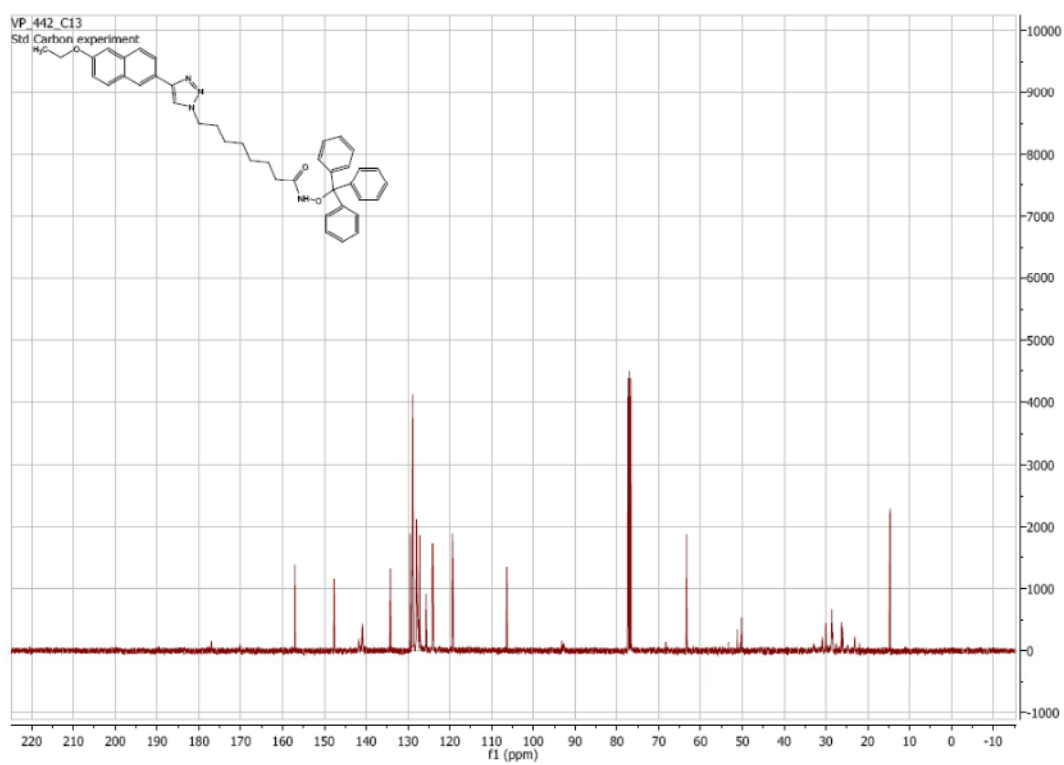
^{13}C NMR of **72**:



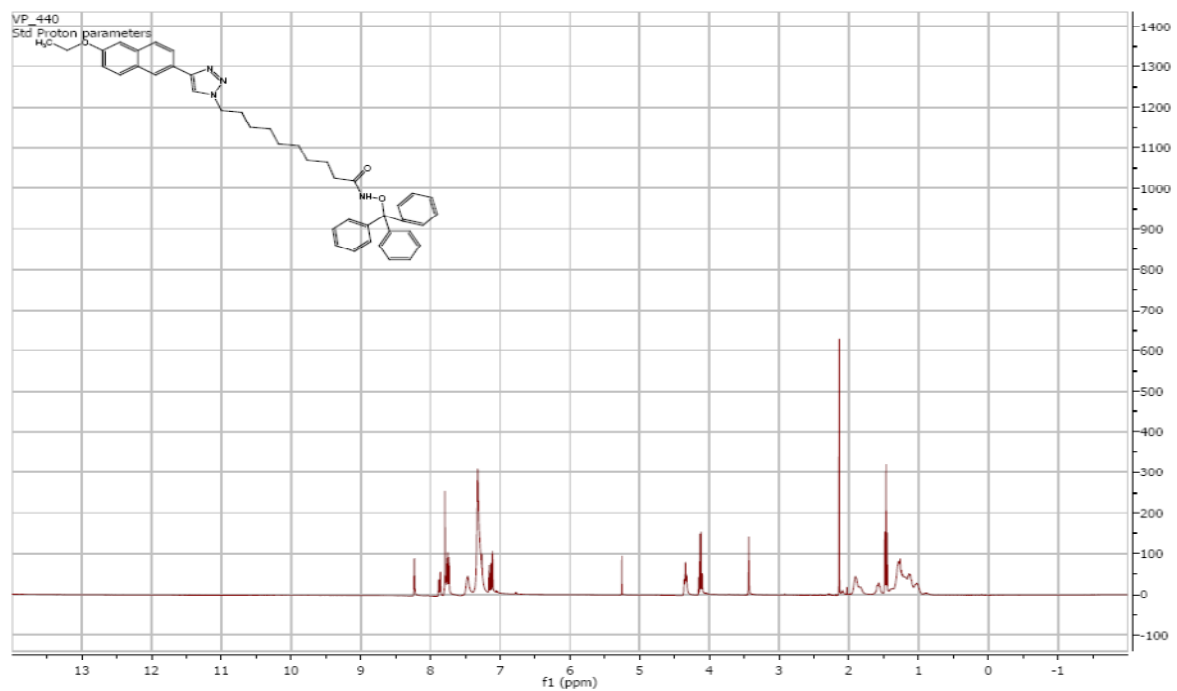
¹H NMR of **73a**:



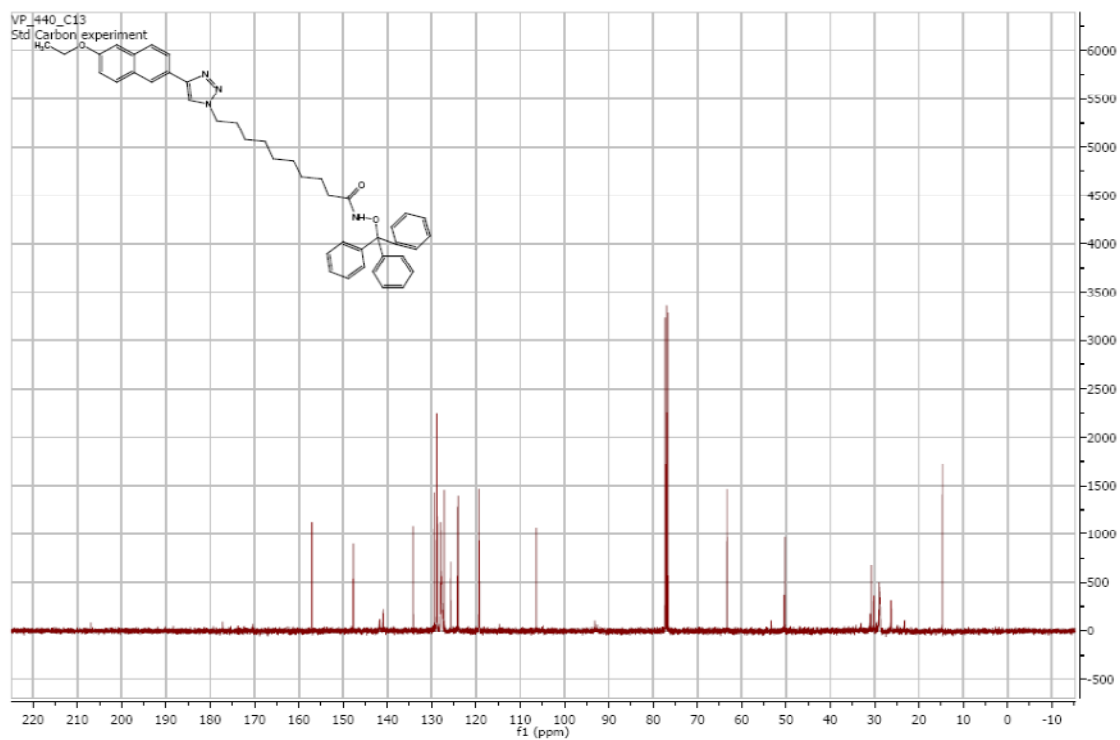
¹³C NMR of **73a**:



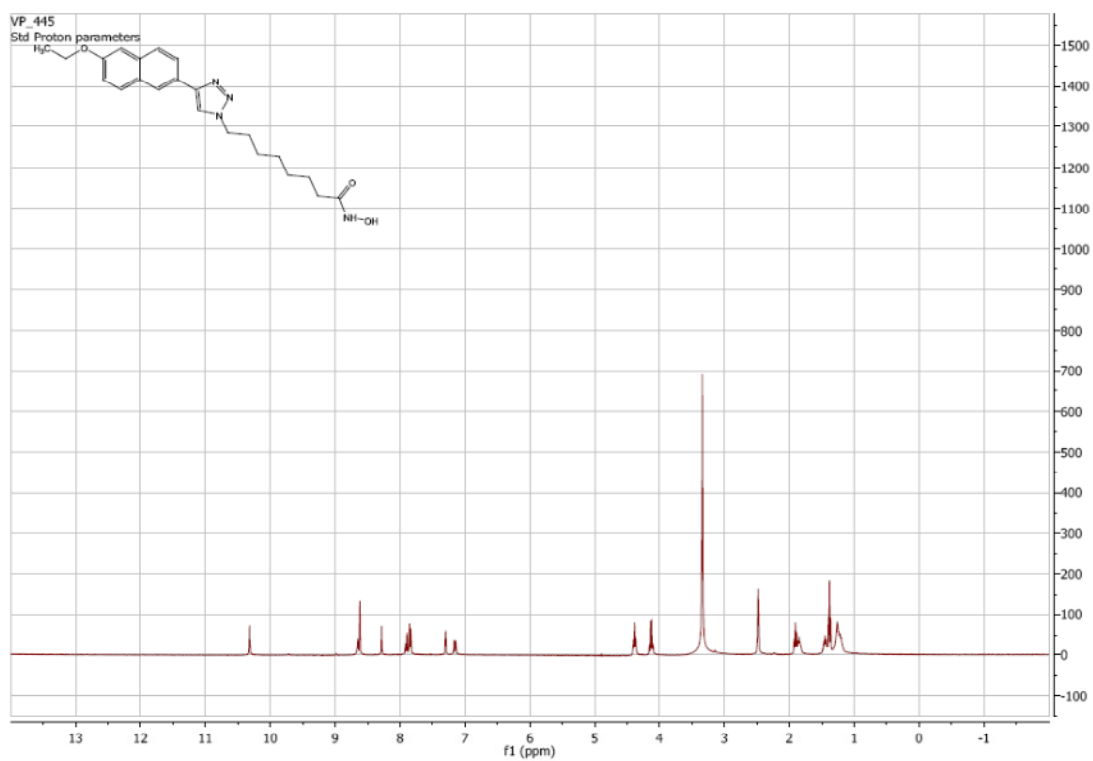
^1H NMR of 73b:



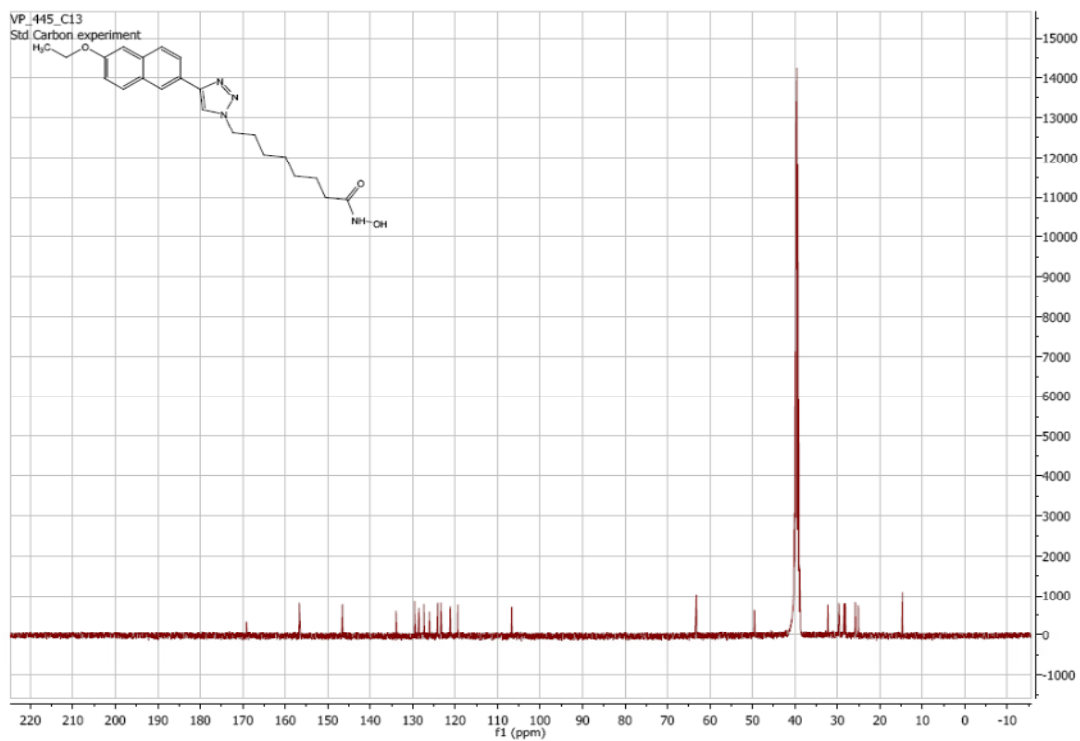
^{13}C NMR of 73b:



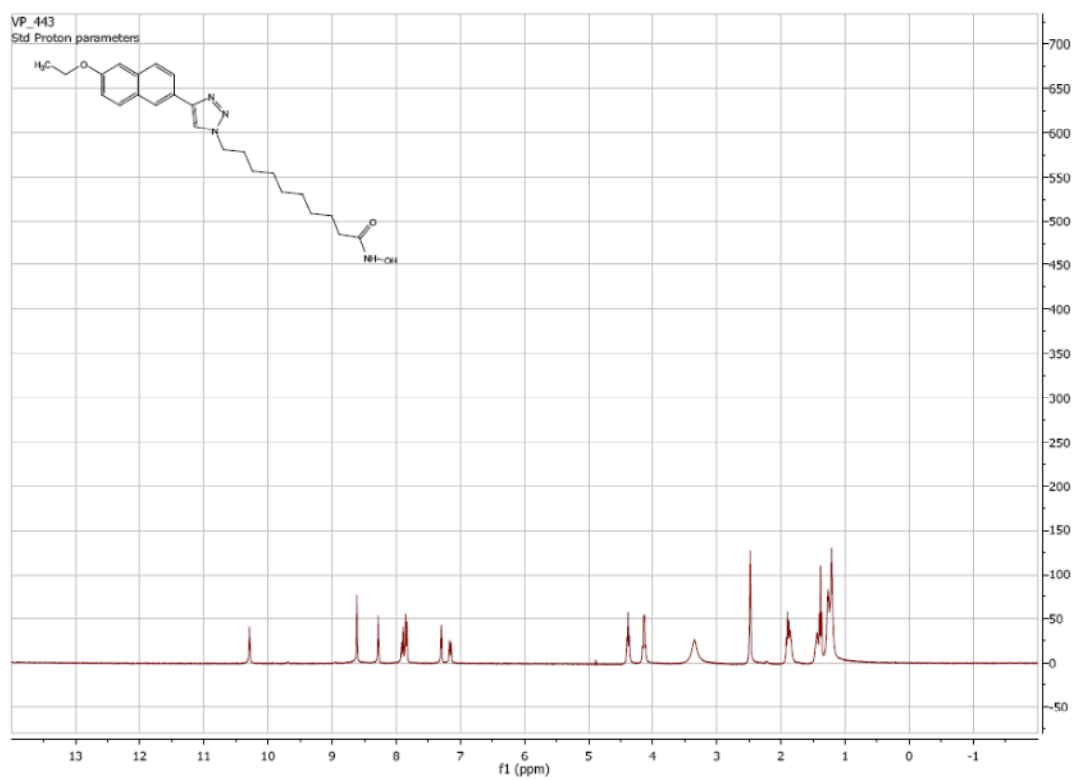
¹H NMR of **74a**:



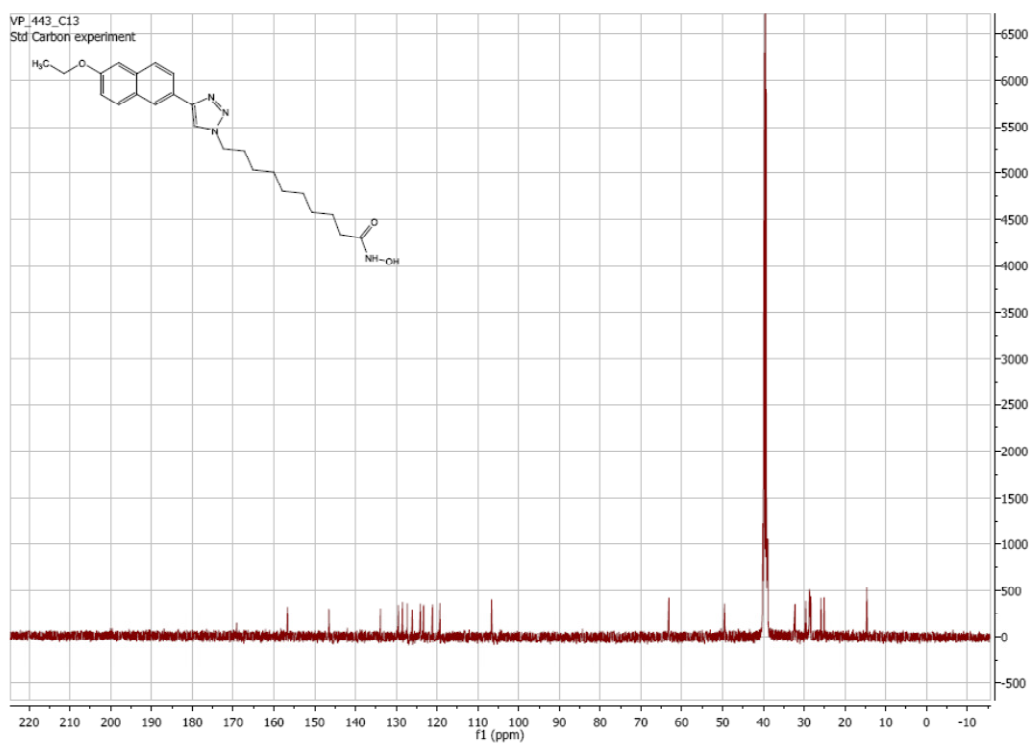
¹³C NMR of **74a**:



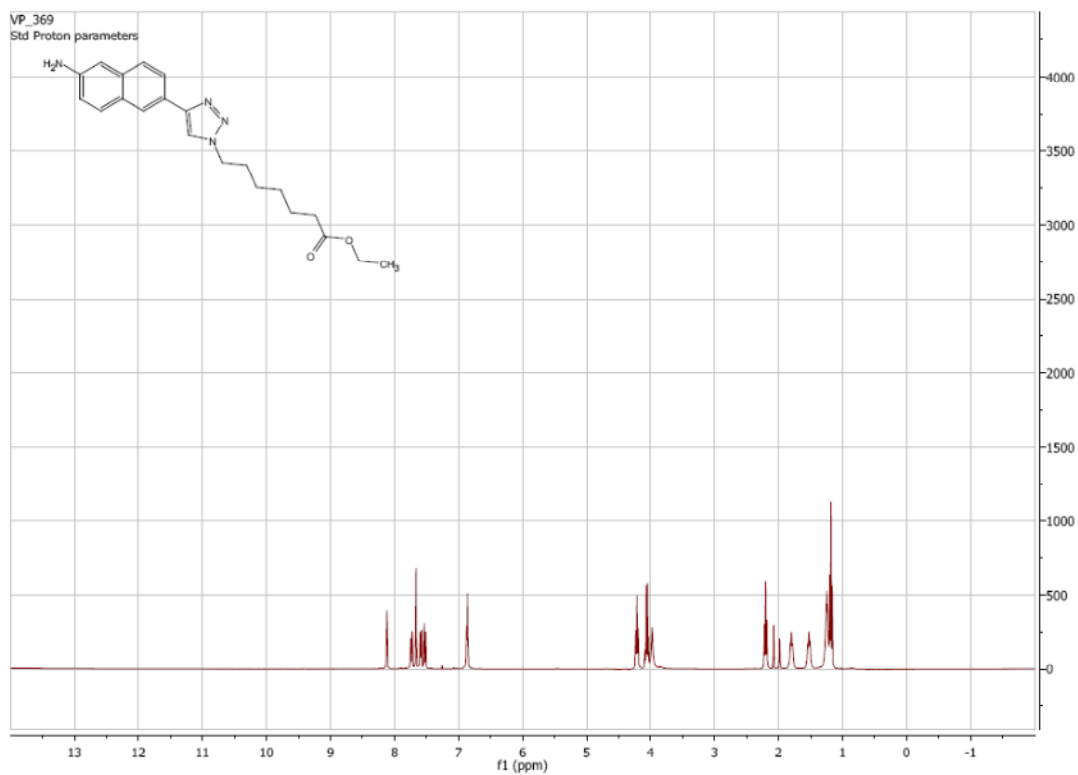
¹H NMR of **74b**:



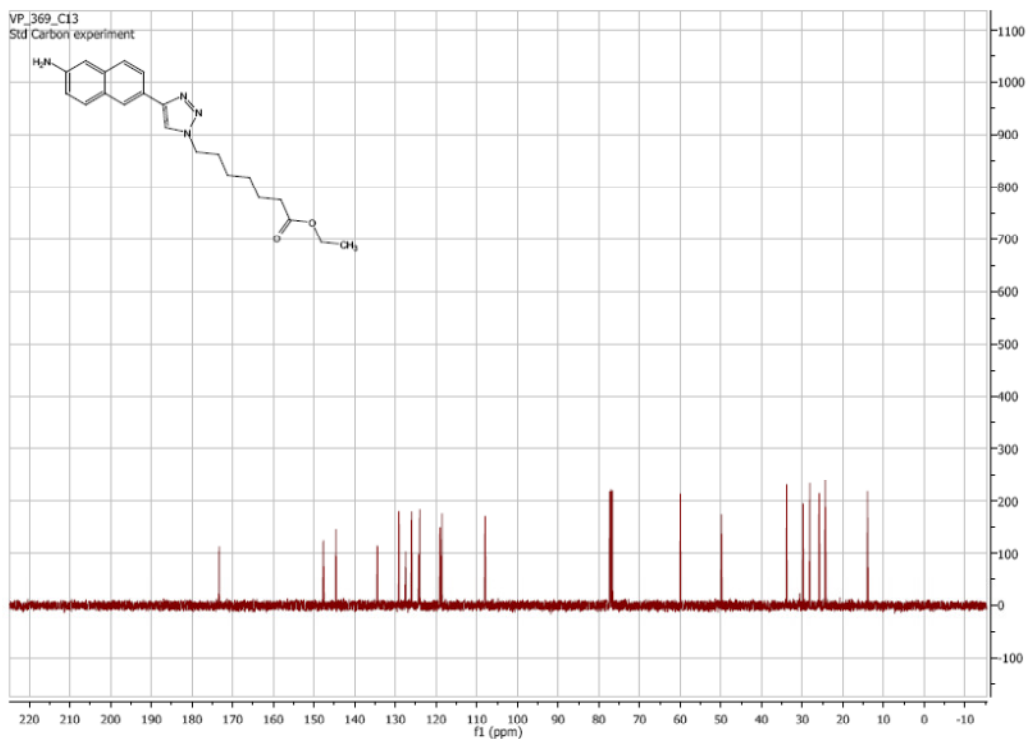
¹³C NMR of **74b**:



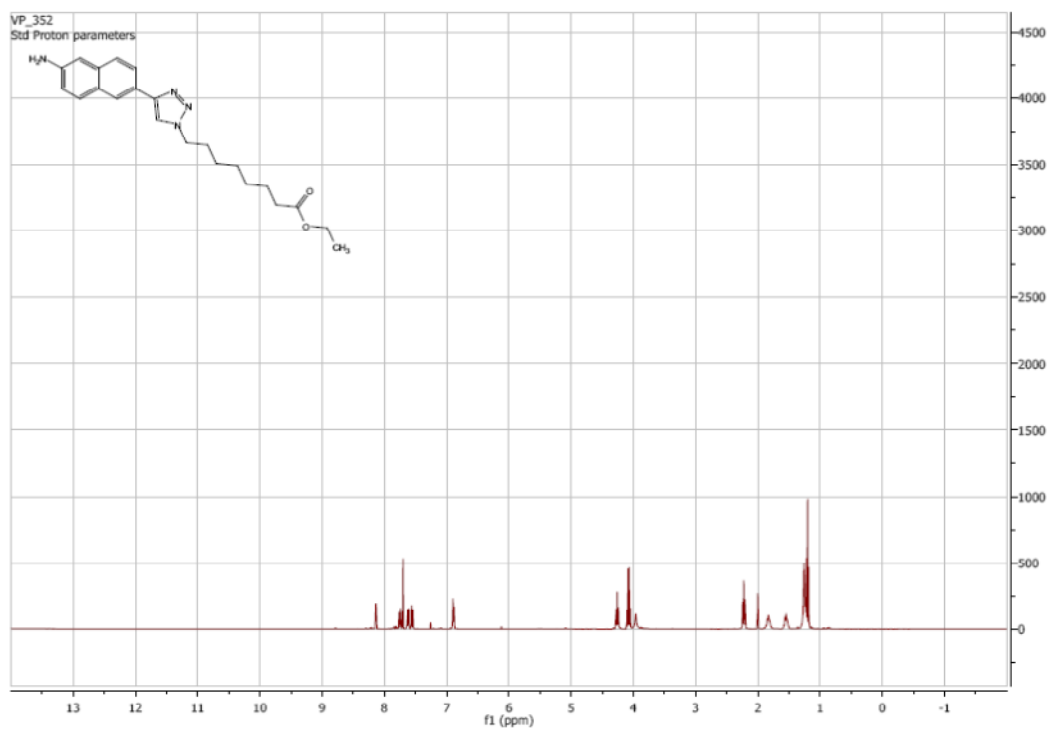
¹H NMR of **75a**:



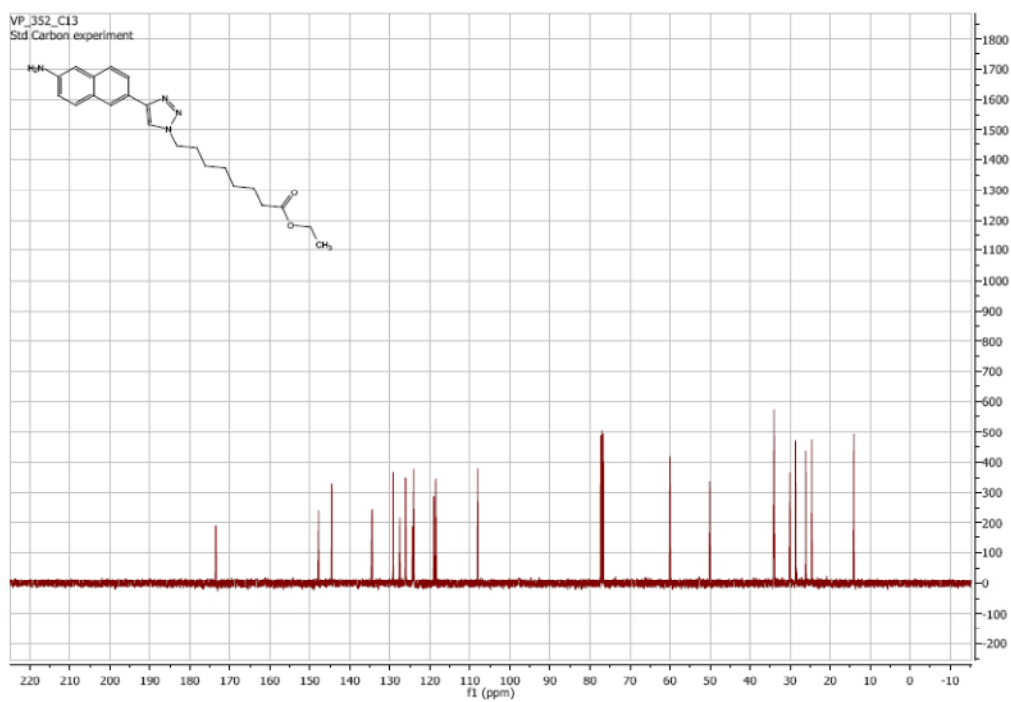
¹³C NMR of **75a**:



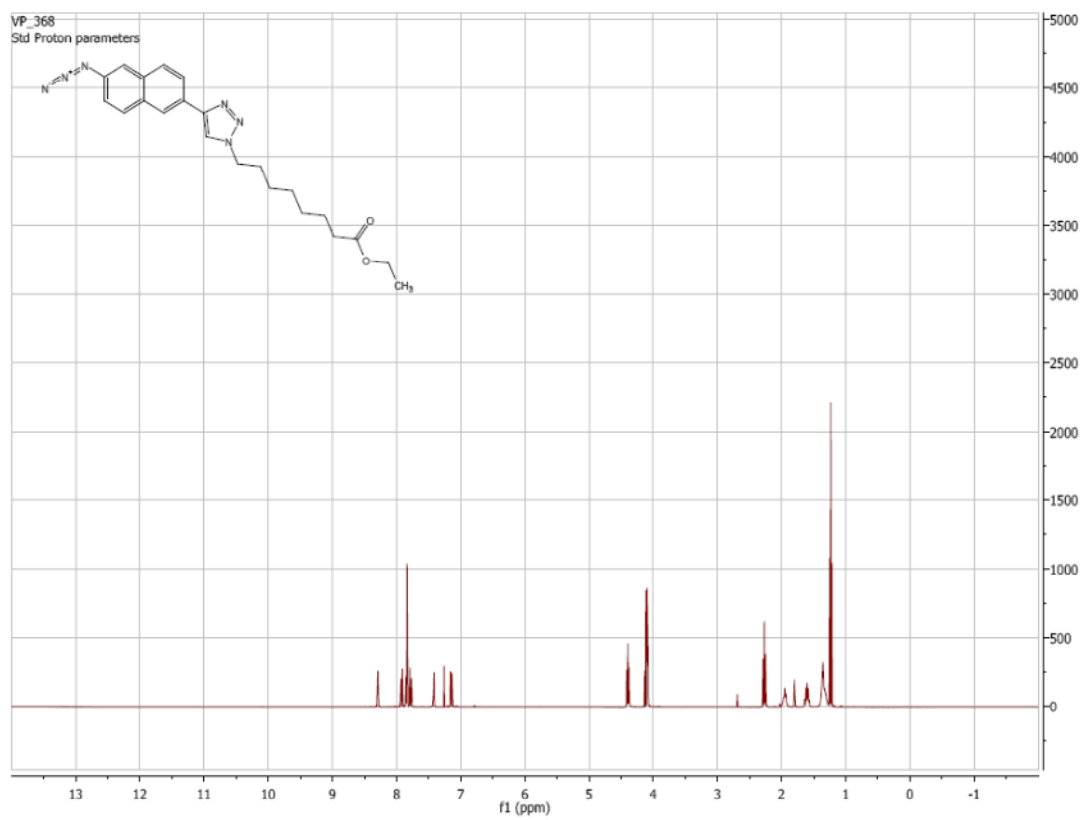
¹H NMR of **75b**:



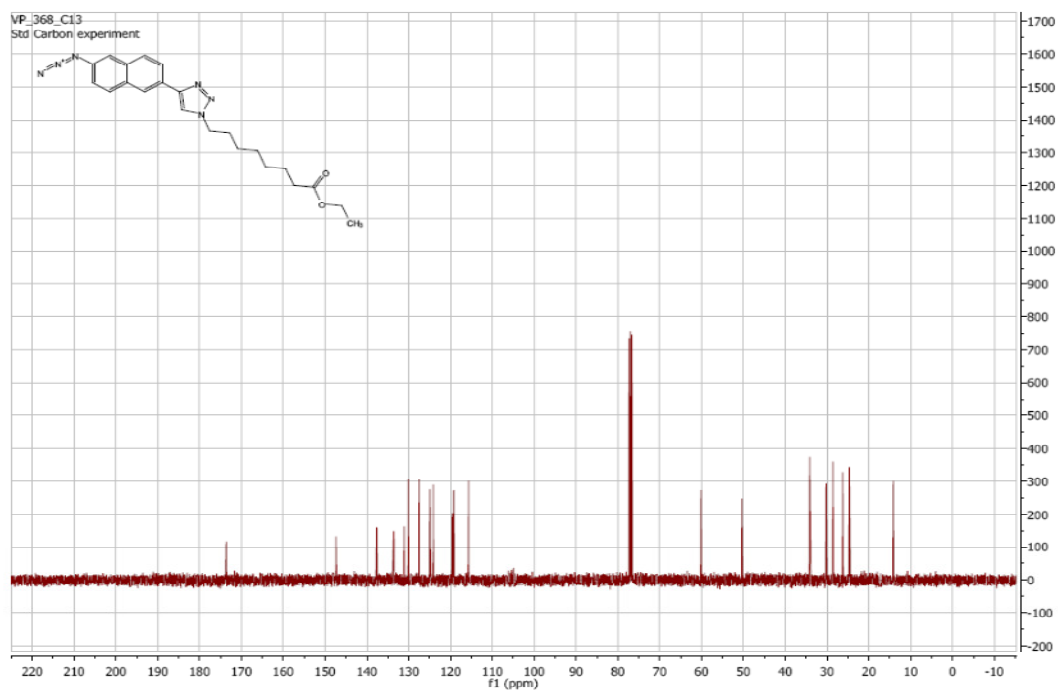
¹³C NMR of **75b**:



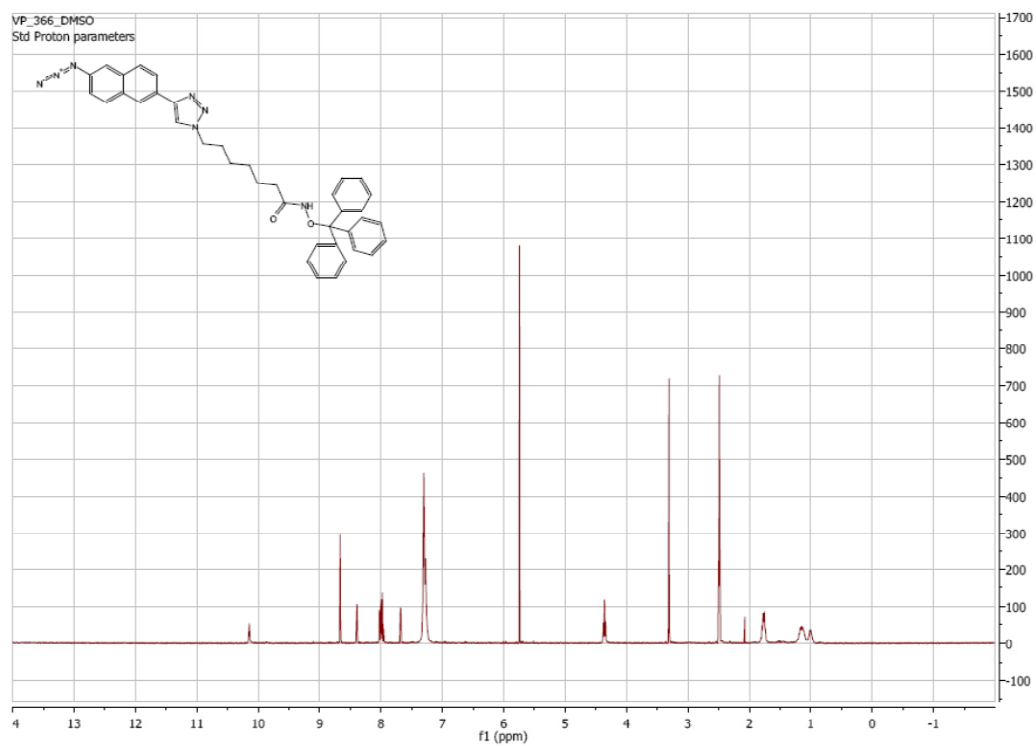
¹H NMR of **76b**:



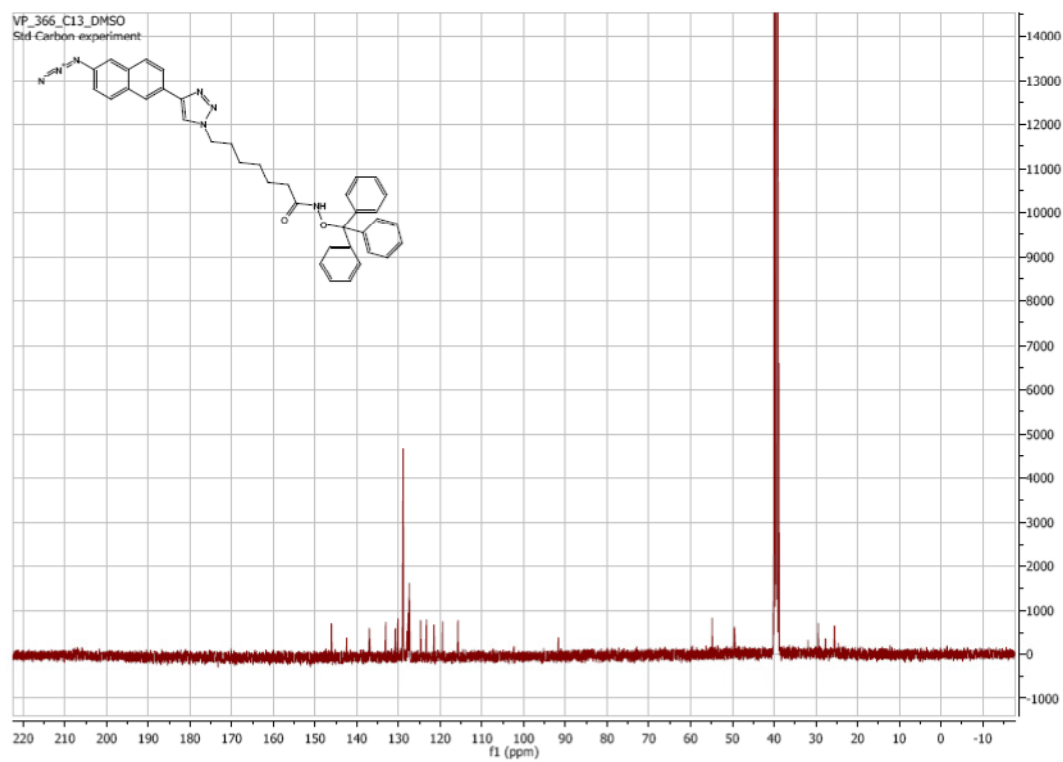
¹³C NMR of **76b**:



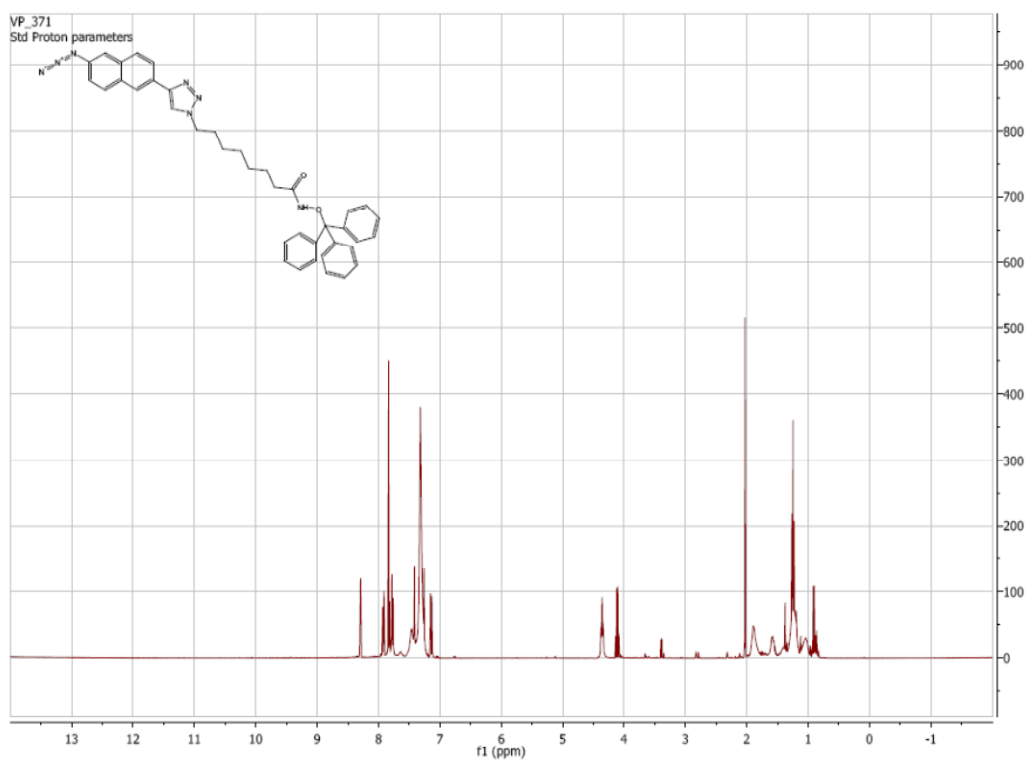
¹H NMR of **78a**:



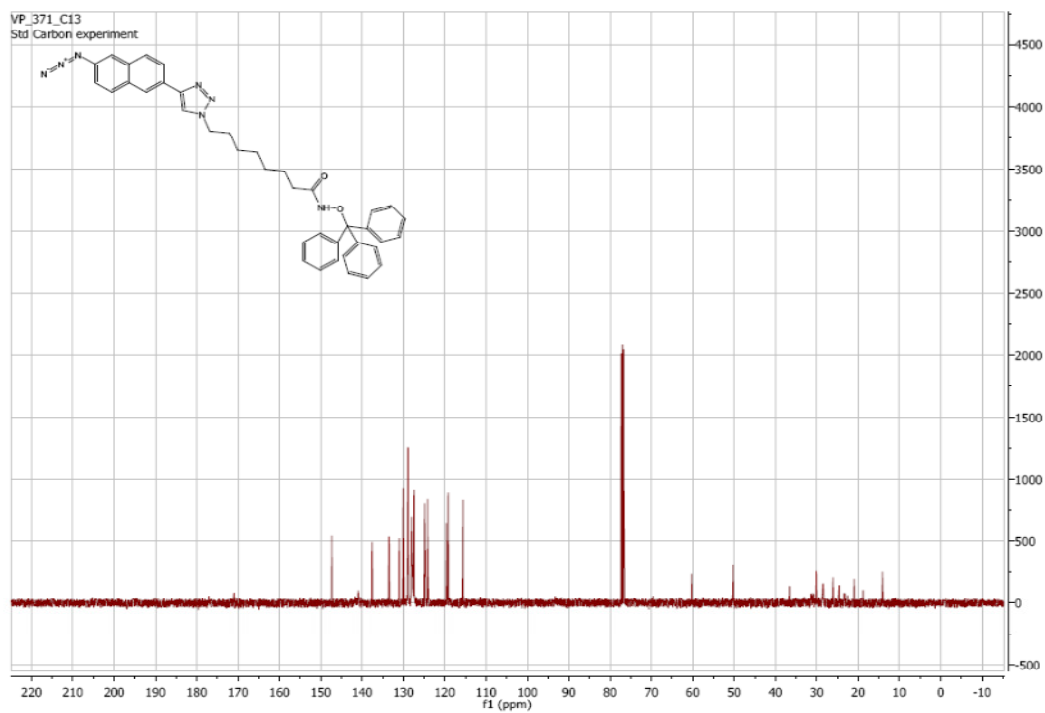
¹³C NMR of **78a**:



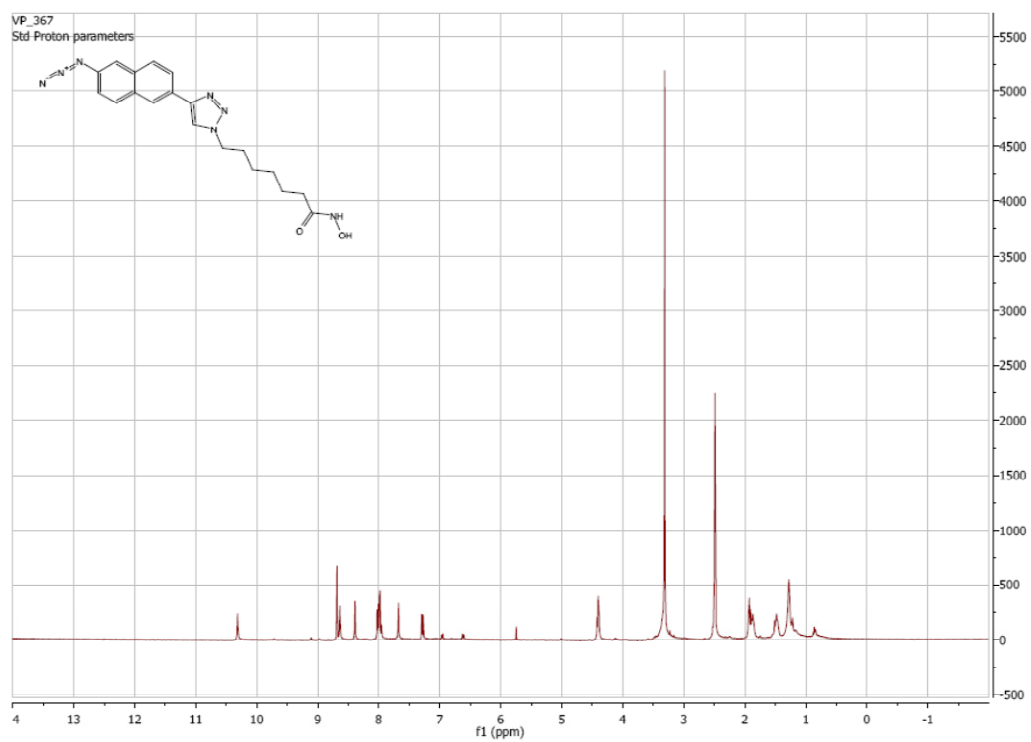
¹H NMR of **78b**:



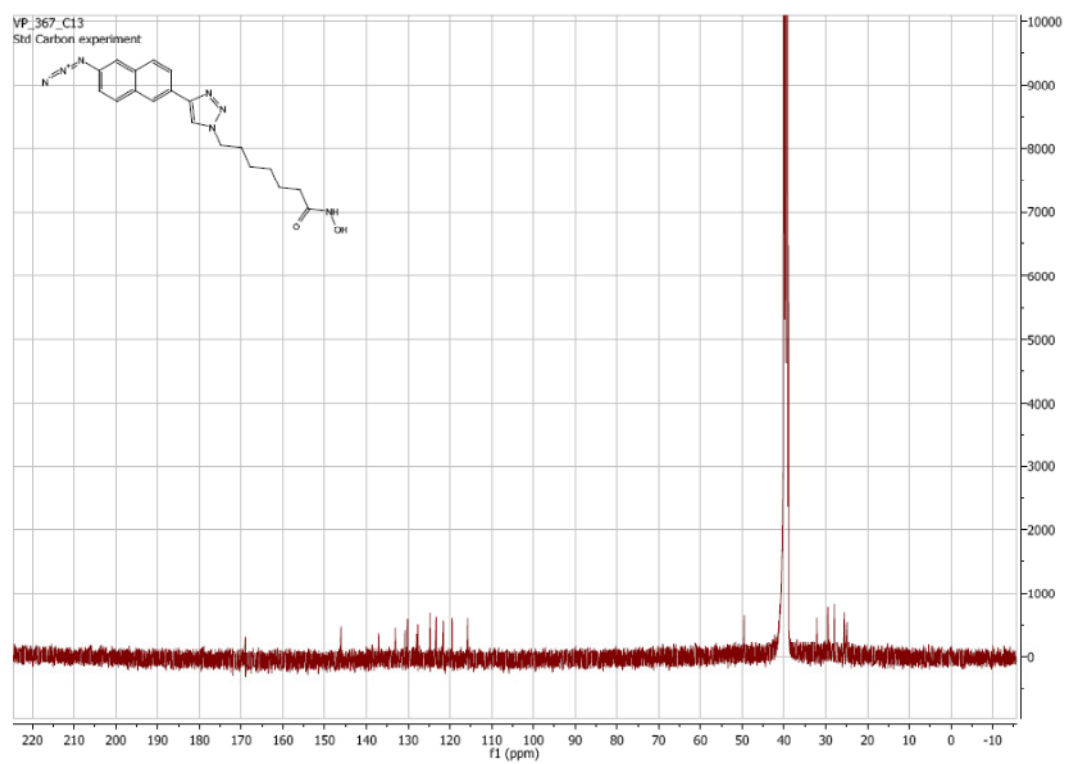
¹³C NMR of **78b**:



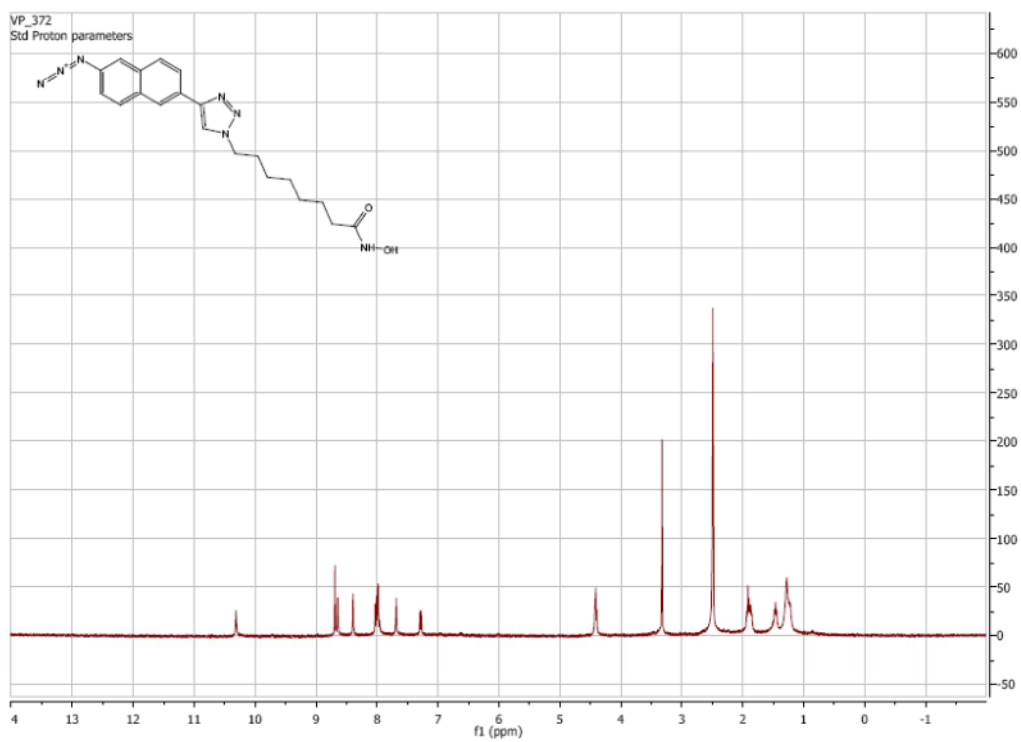
¹H NMR of **79a**:



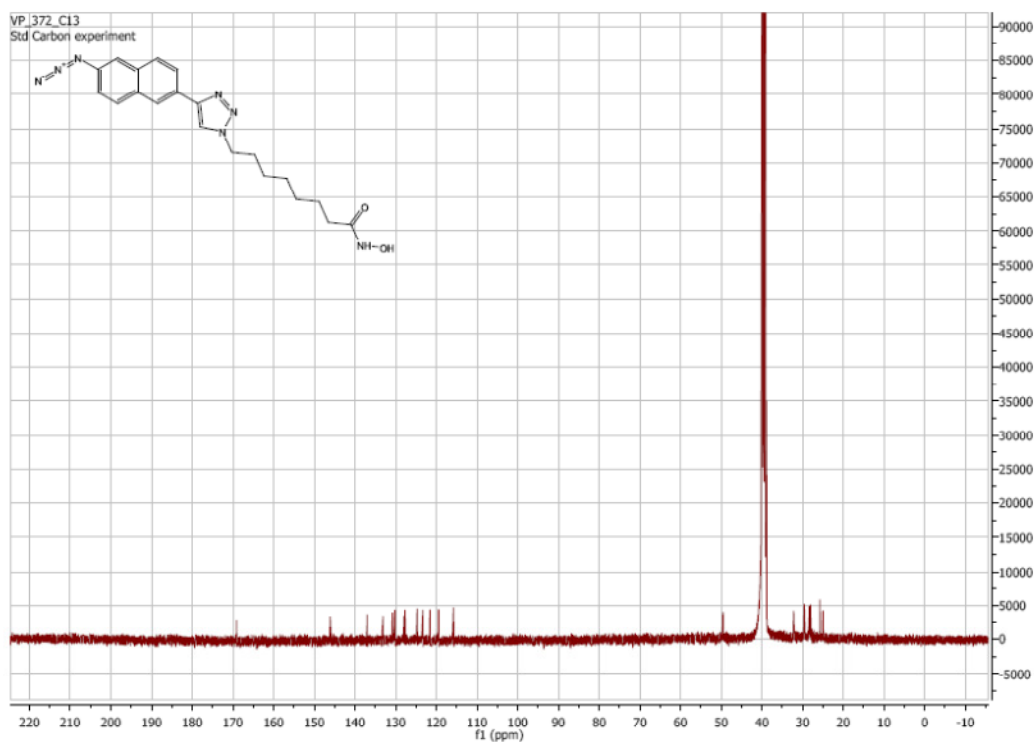
¹³C NMR of **79a**:



¹H NMR of **79a**:

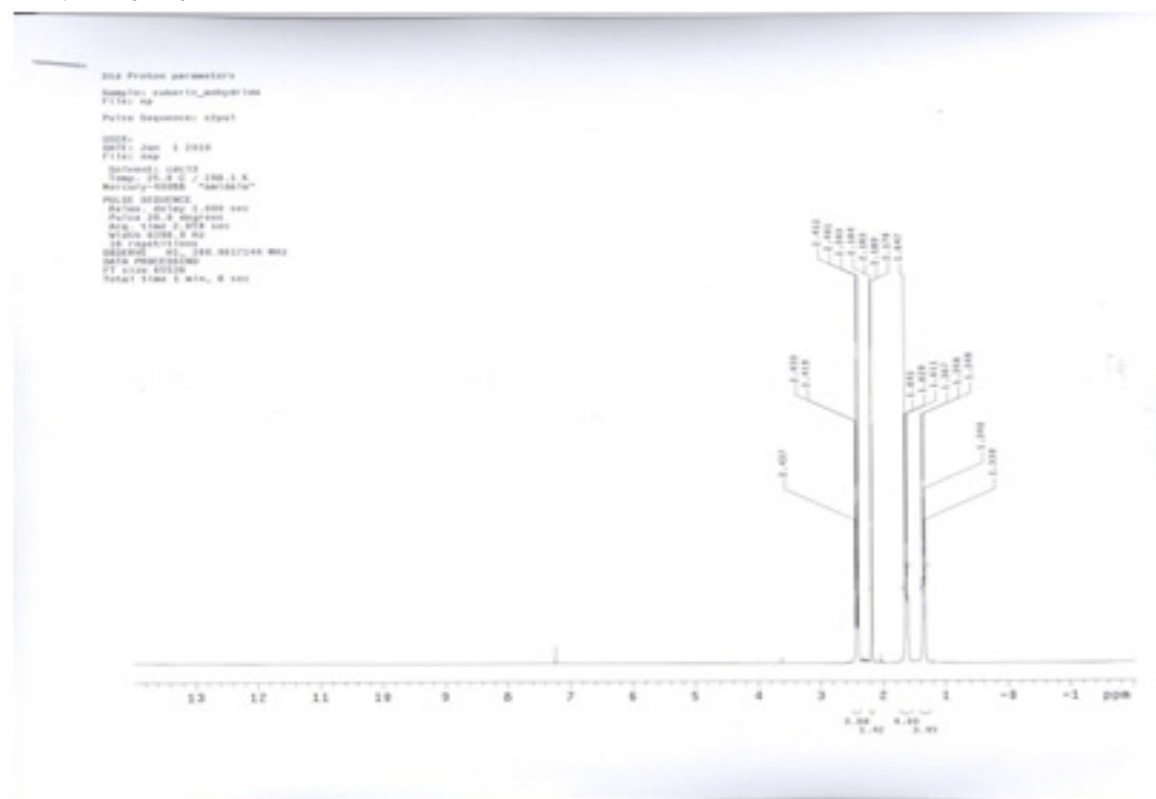
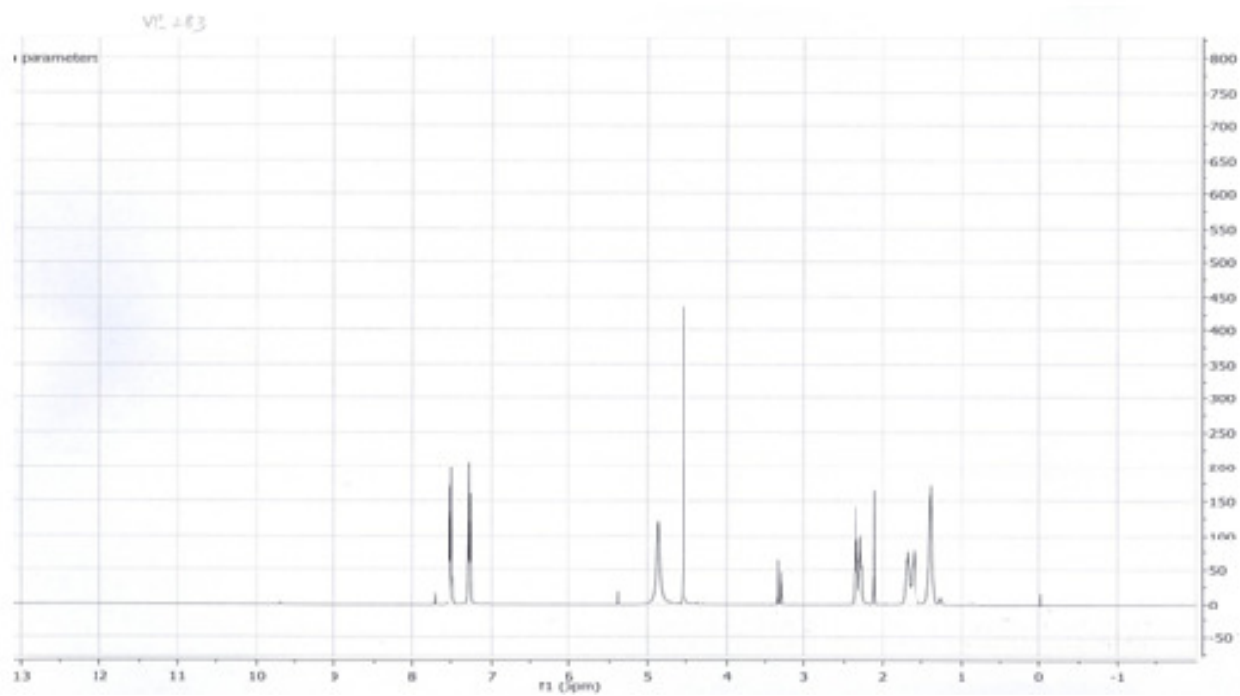


¹³C NMR of **79a**:

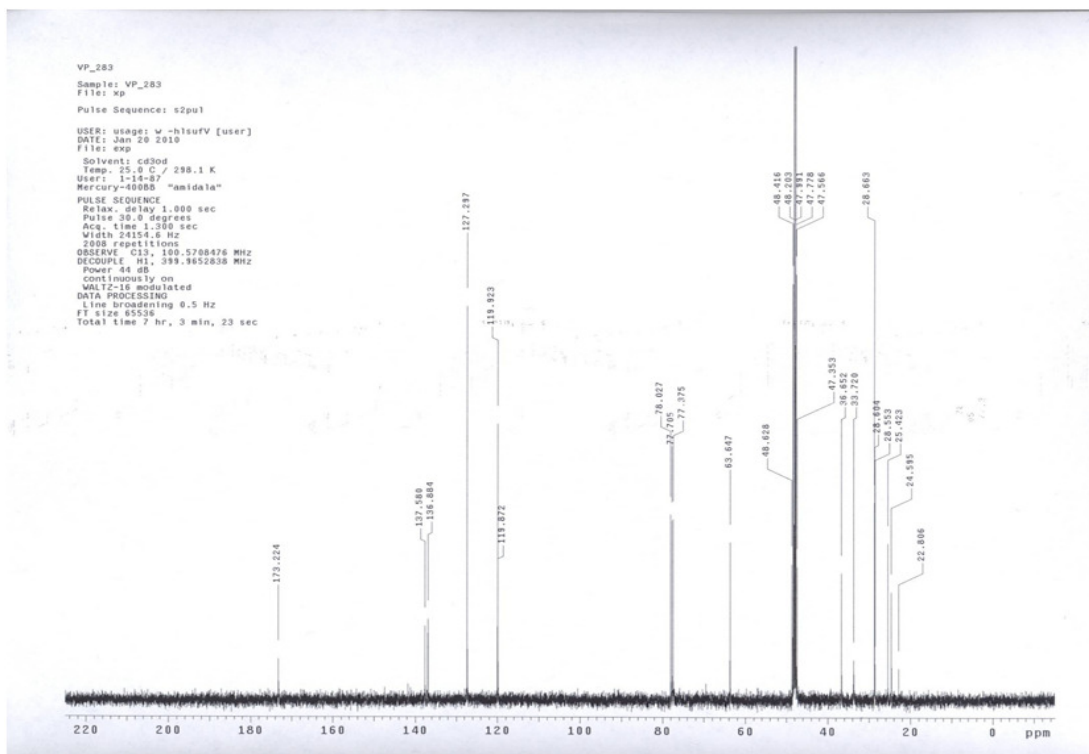


APPENDIX C

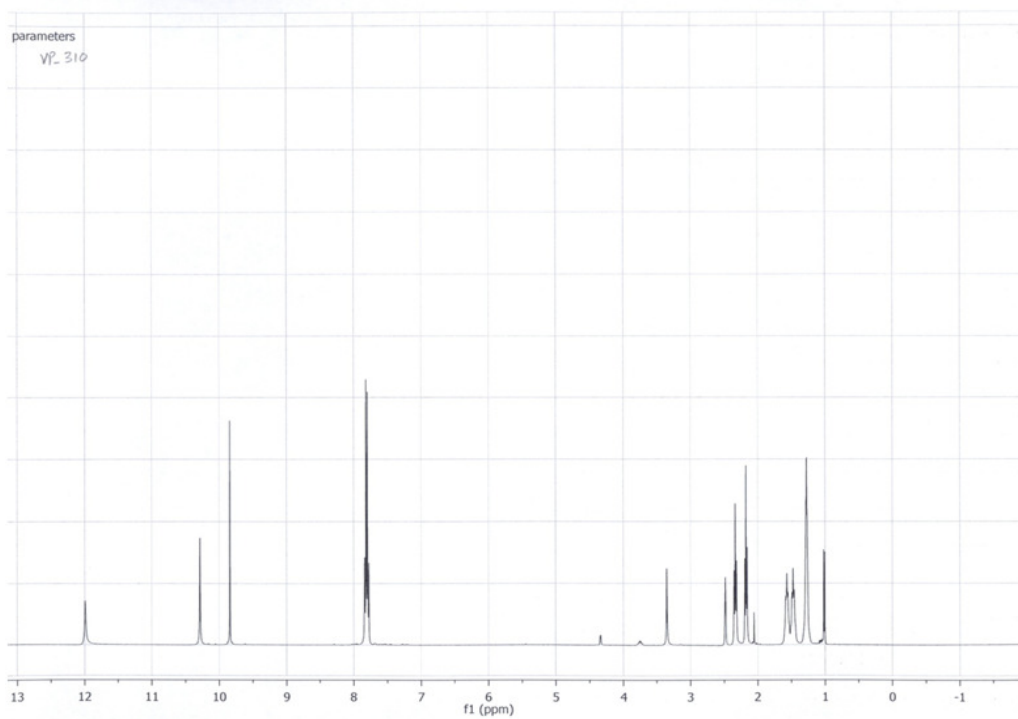
¹H and ¹³C NMR characterization for Dual Acting HDAC – Topoisomerase (Topo) inhibitors (Chapter 4)

¹H NMR of **2**:¹H NMR of **3**:

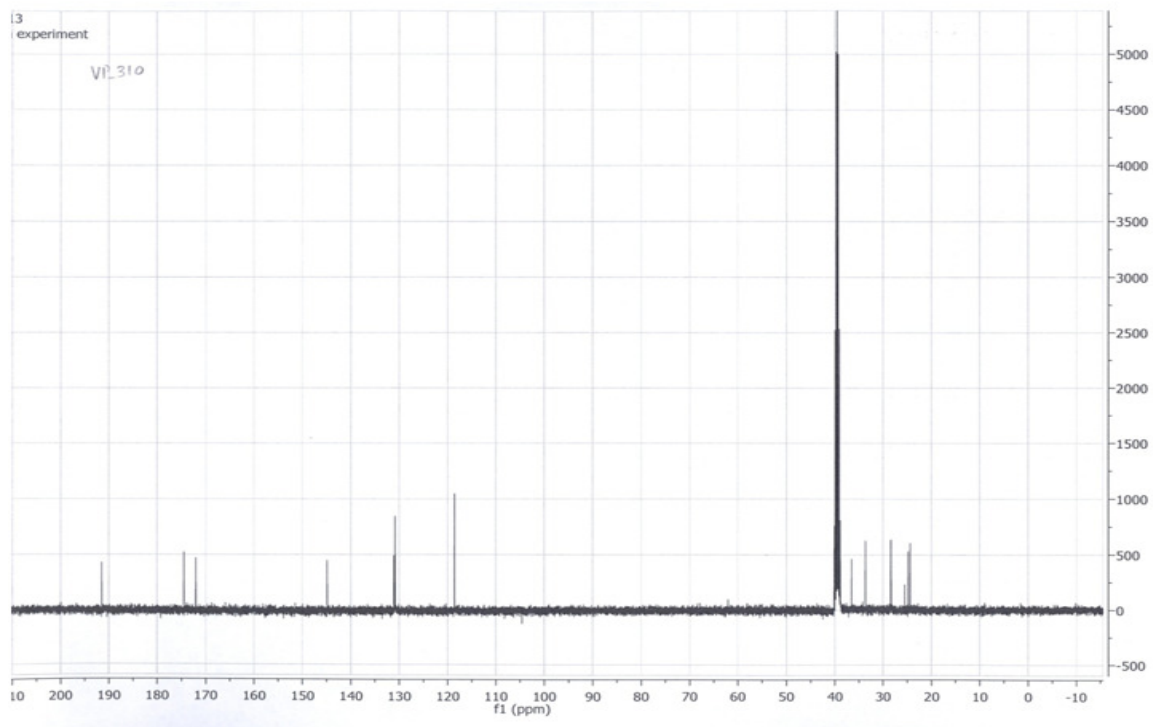
^{13}C NMR of **3**:



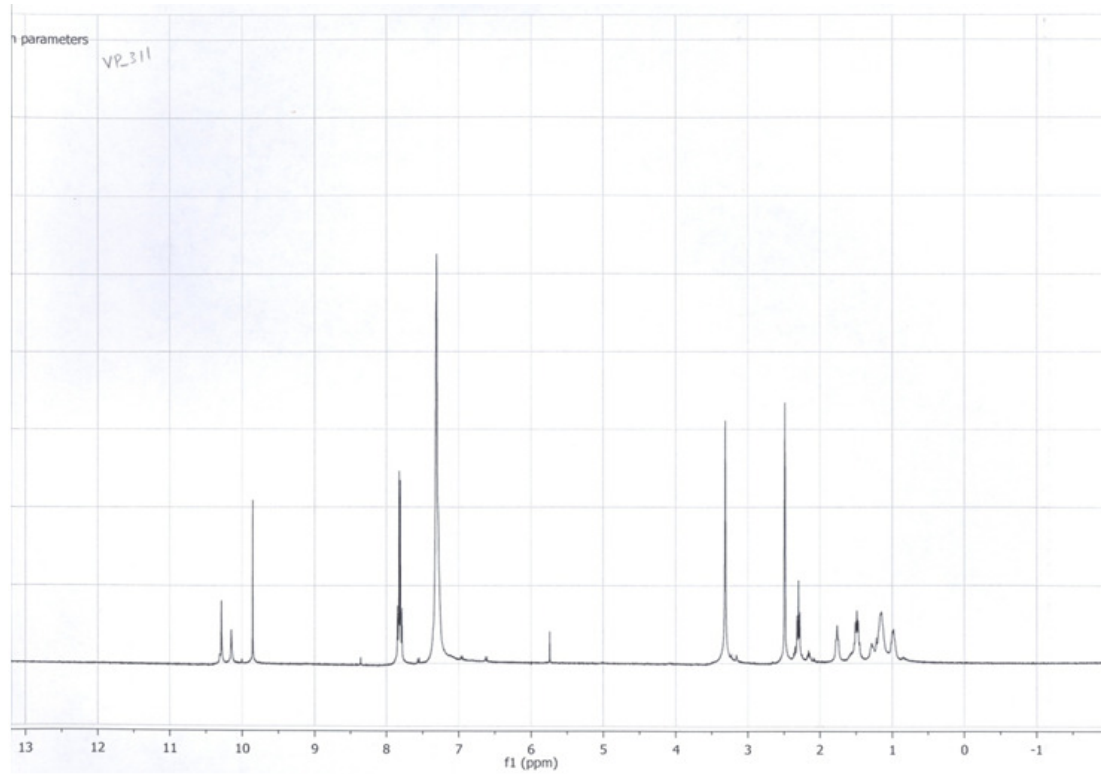
^1H NMR of **4**:



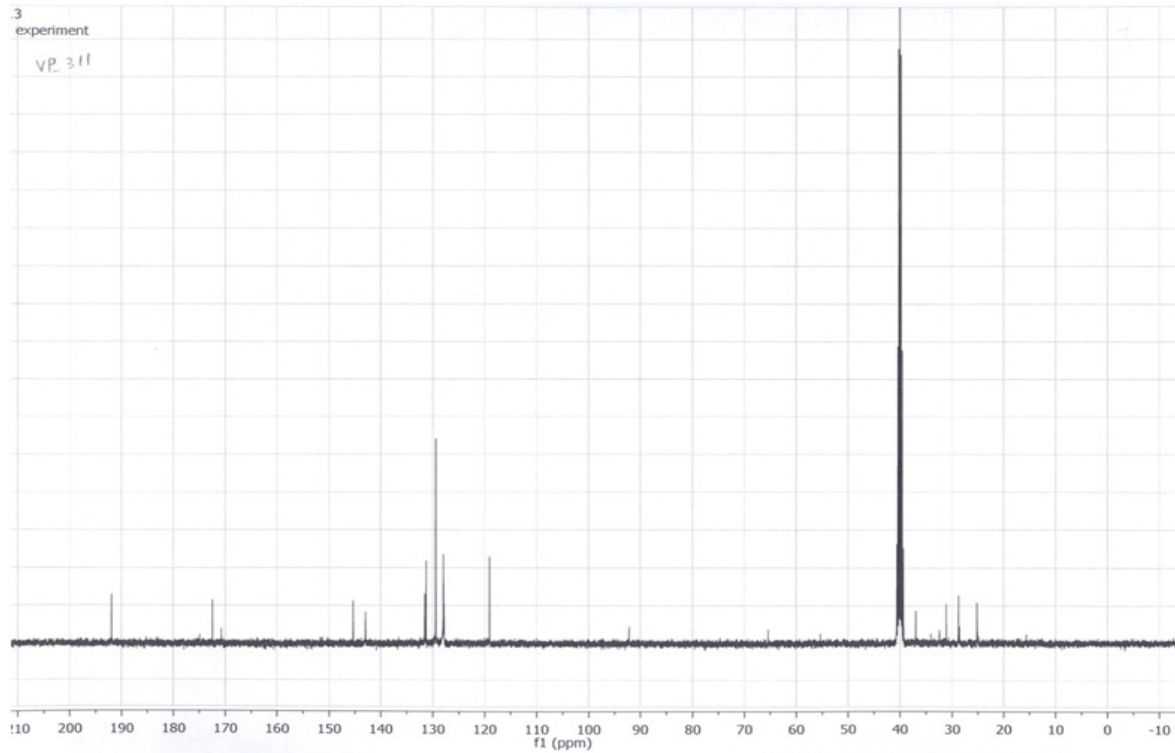
¹³C NMR of 4:



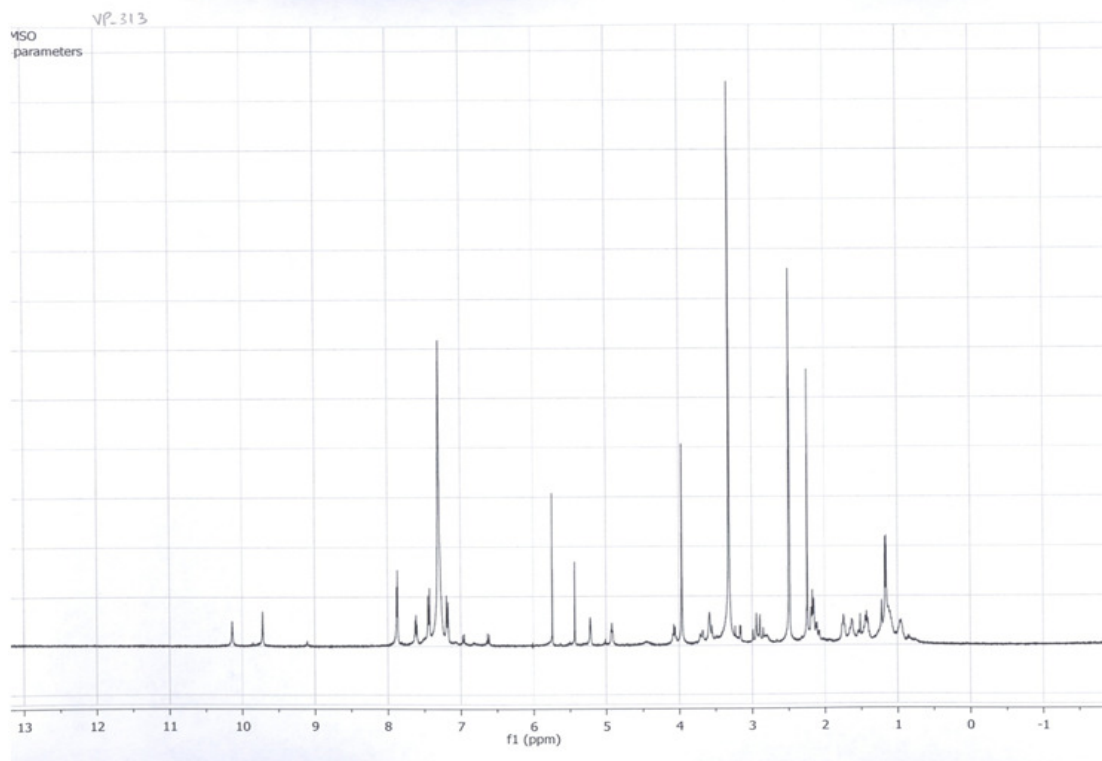
¹H NMR of 5:



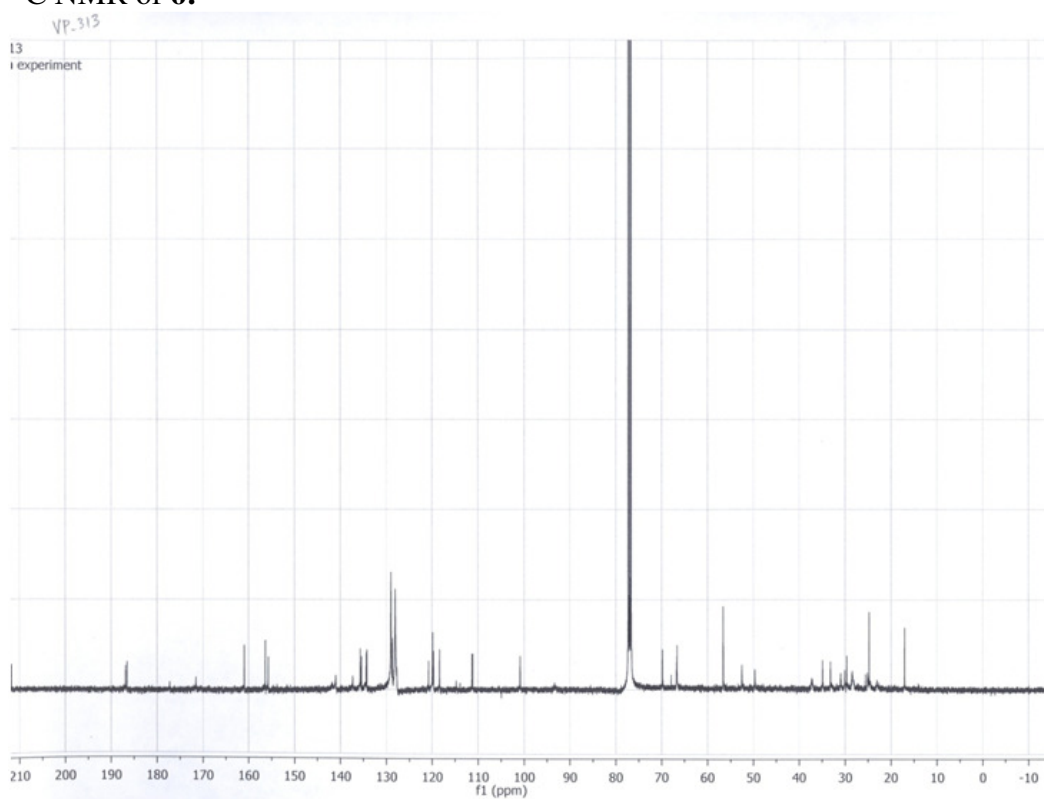
^{13}C NMR of 5:



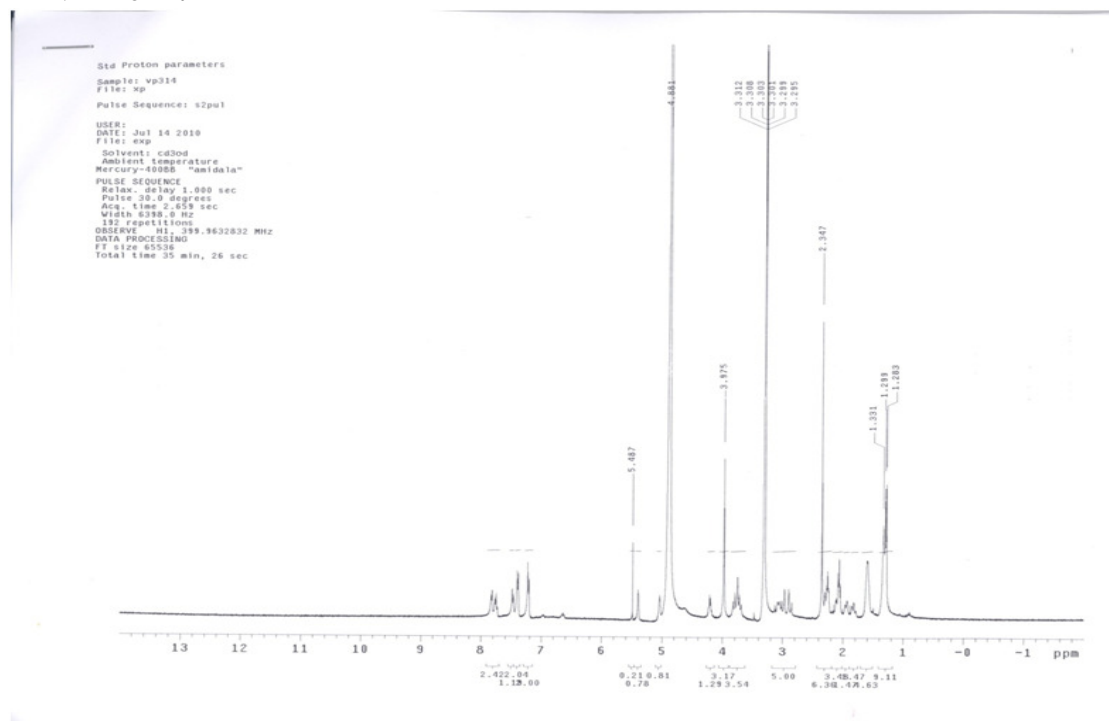
^1H NMR of 6:



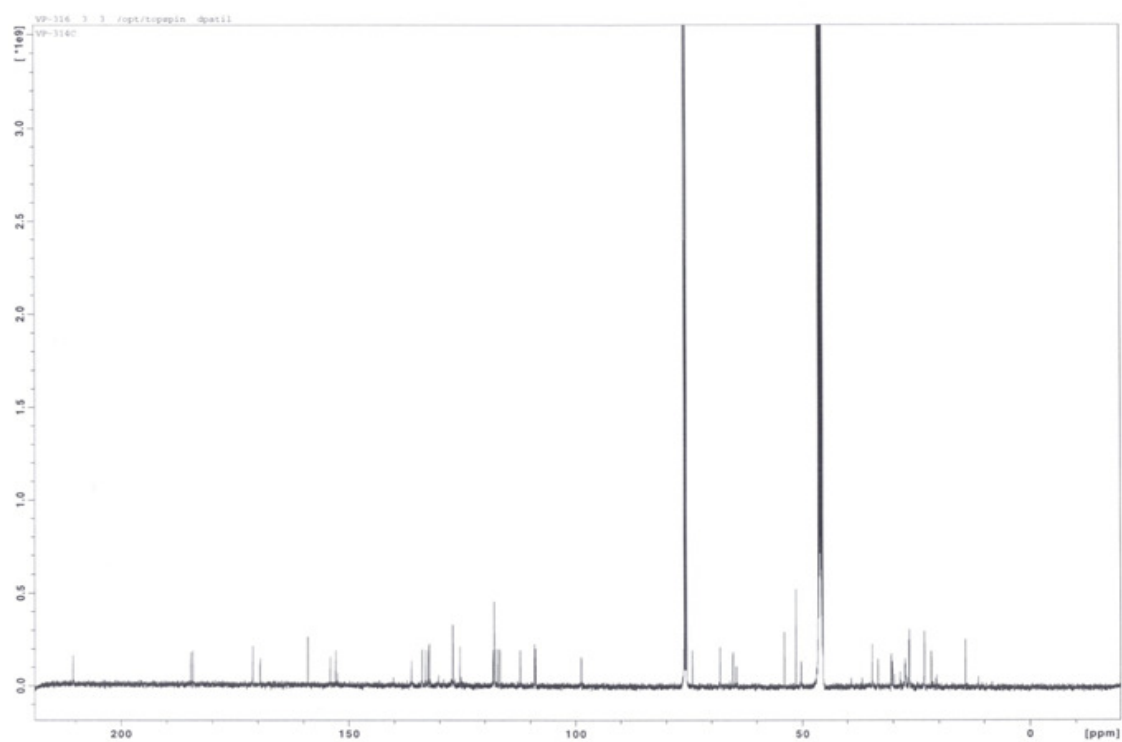
^{13}C NMR of **6**:



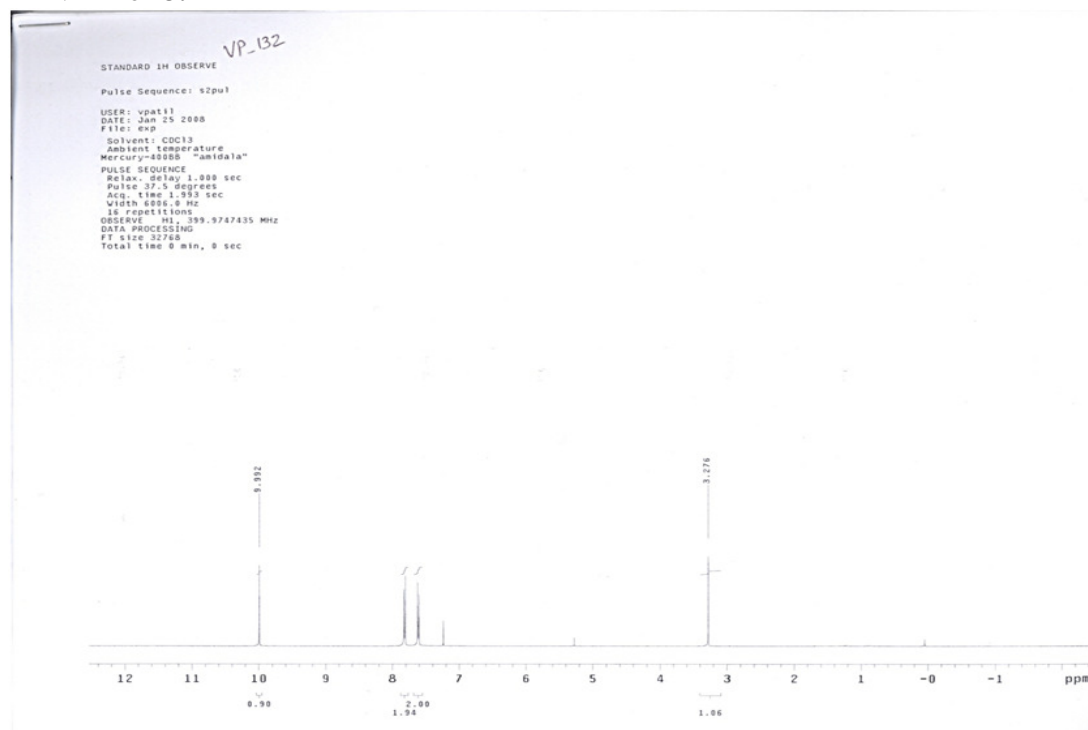
^1H NMR of **7**:



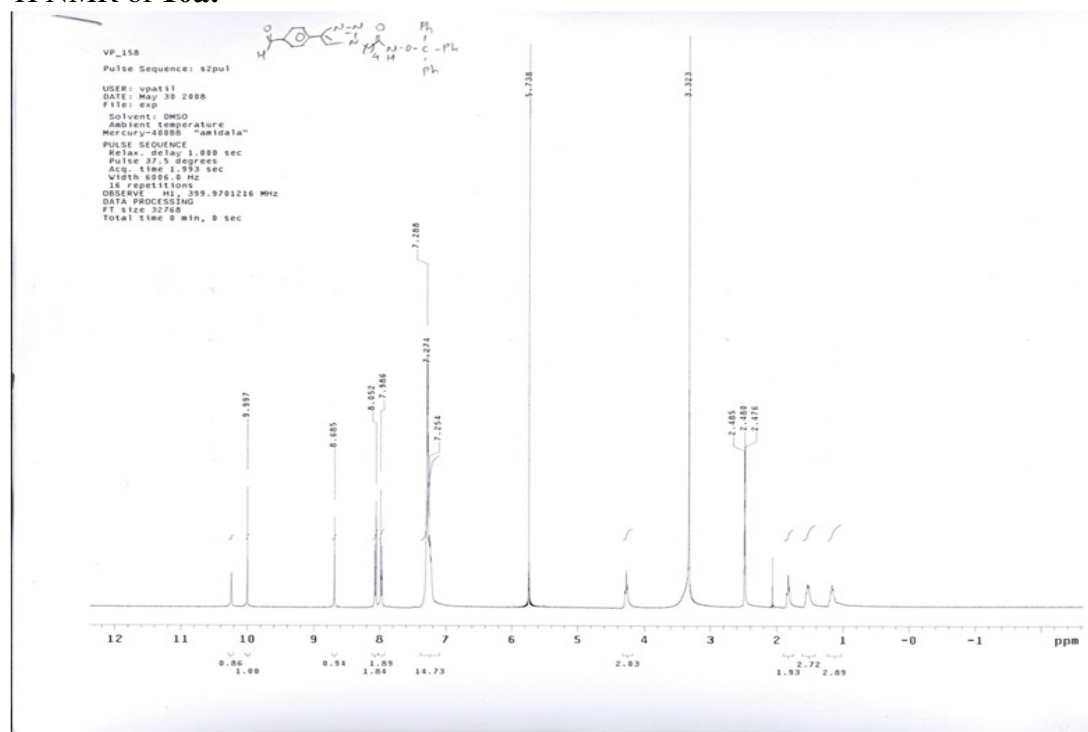
¹³C NMR of 7:



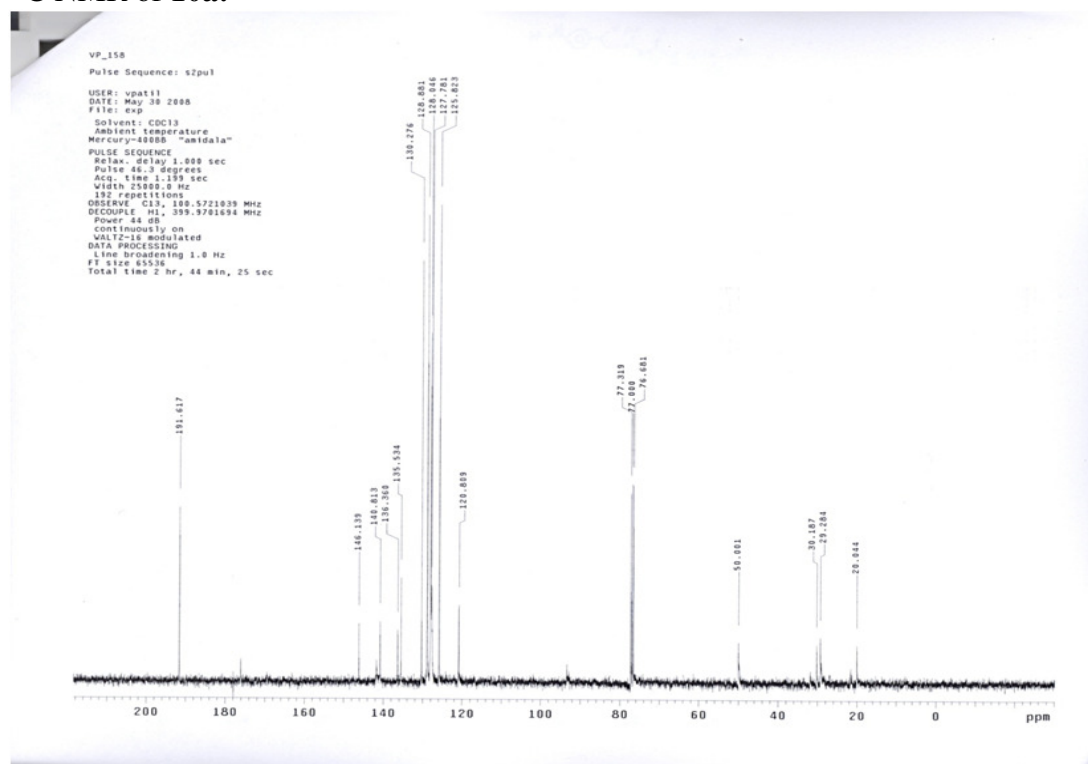
¹H NMR of 8:



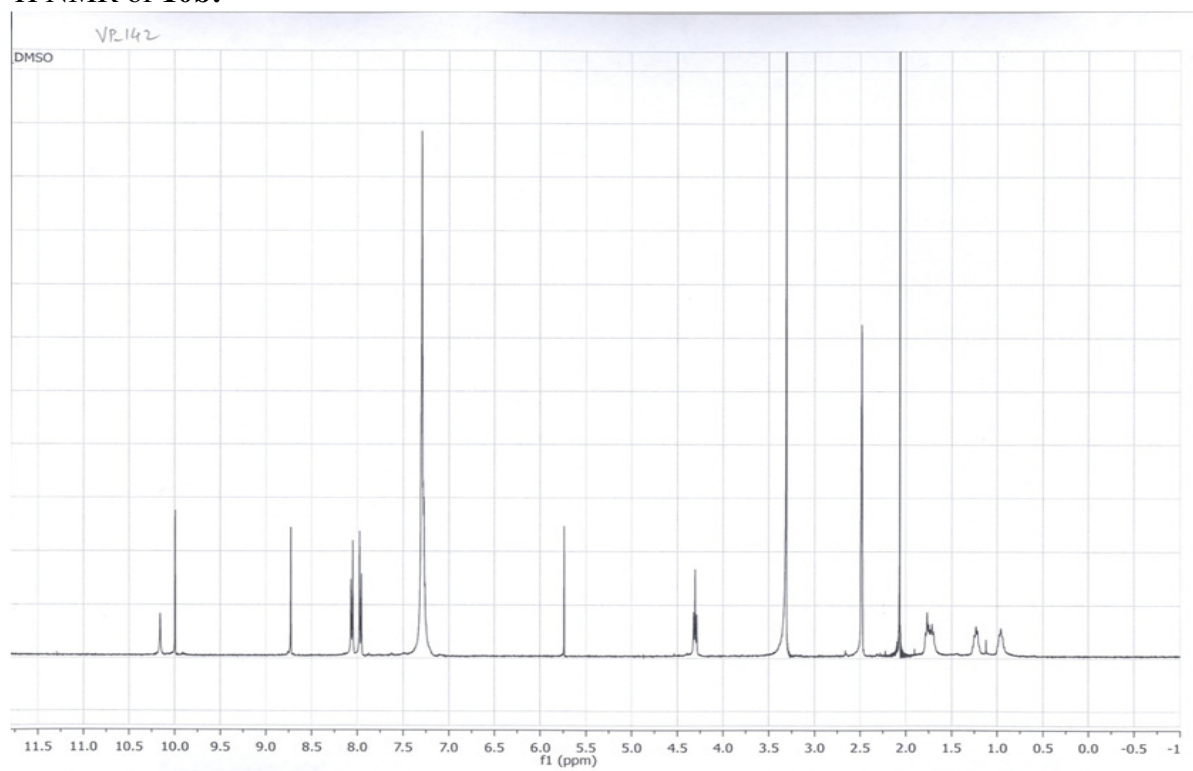
¹H NMR of 10a:



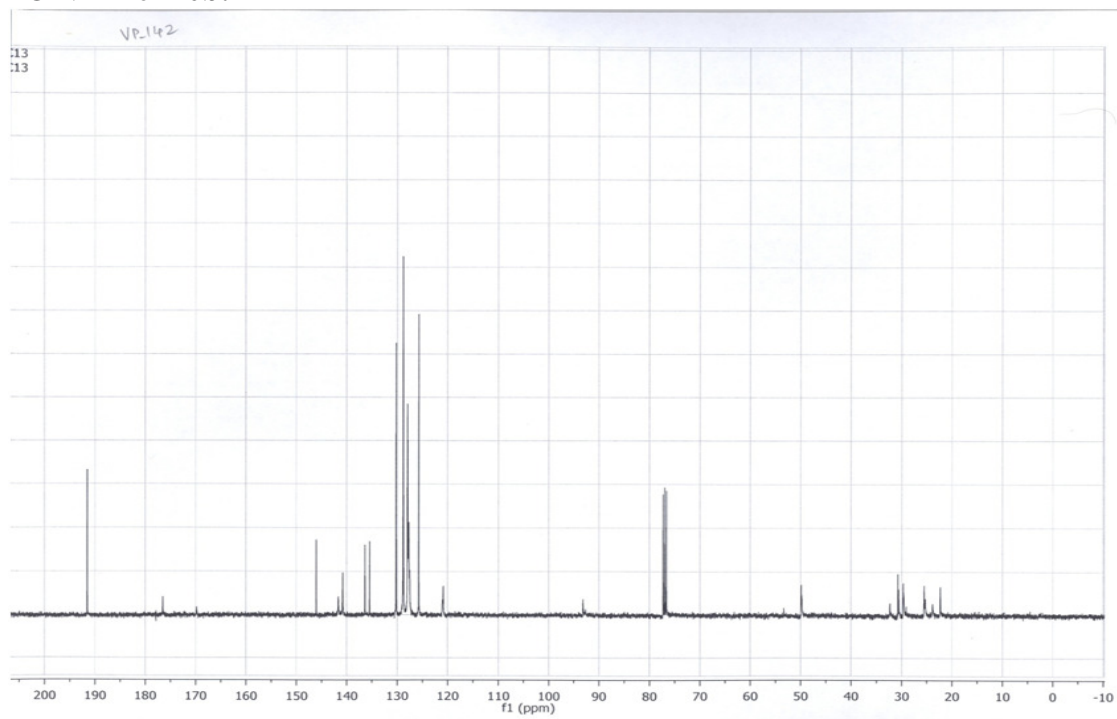
¹³C NMR of 10a:



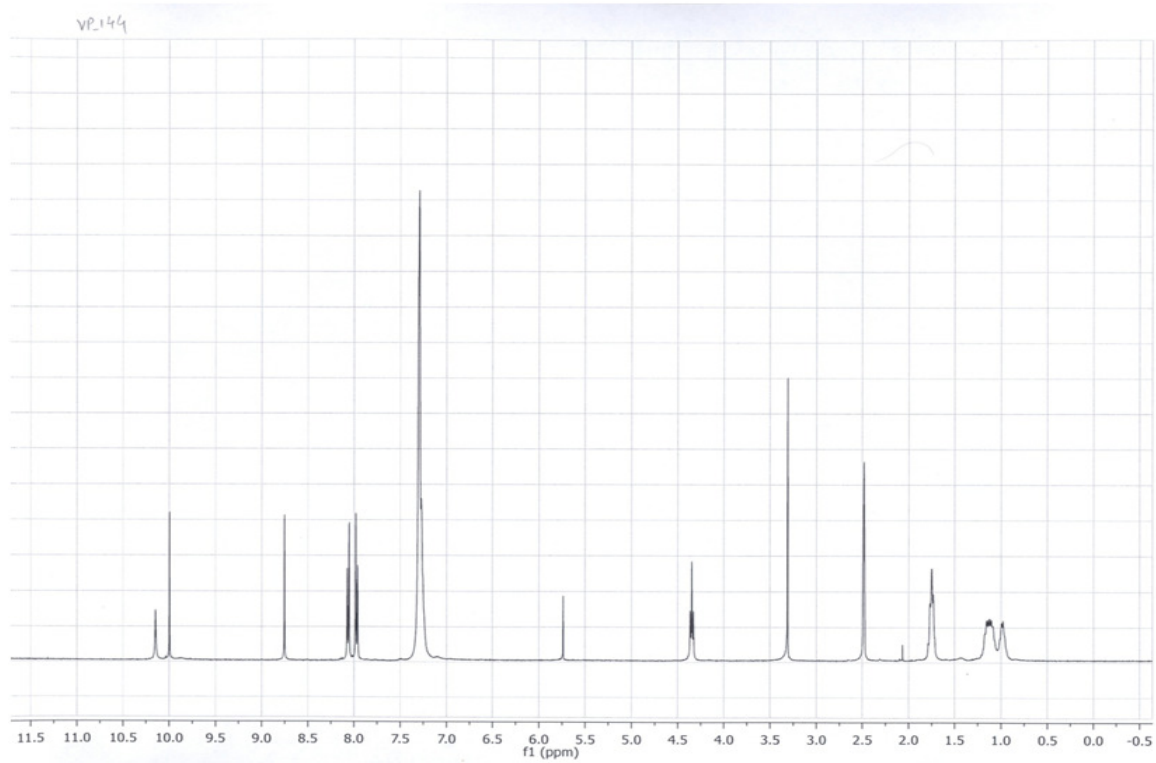
¹H NMR of **10b**:



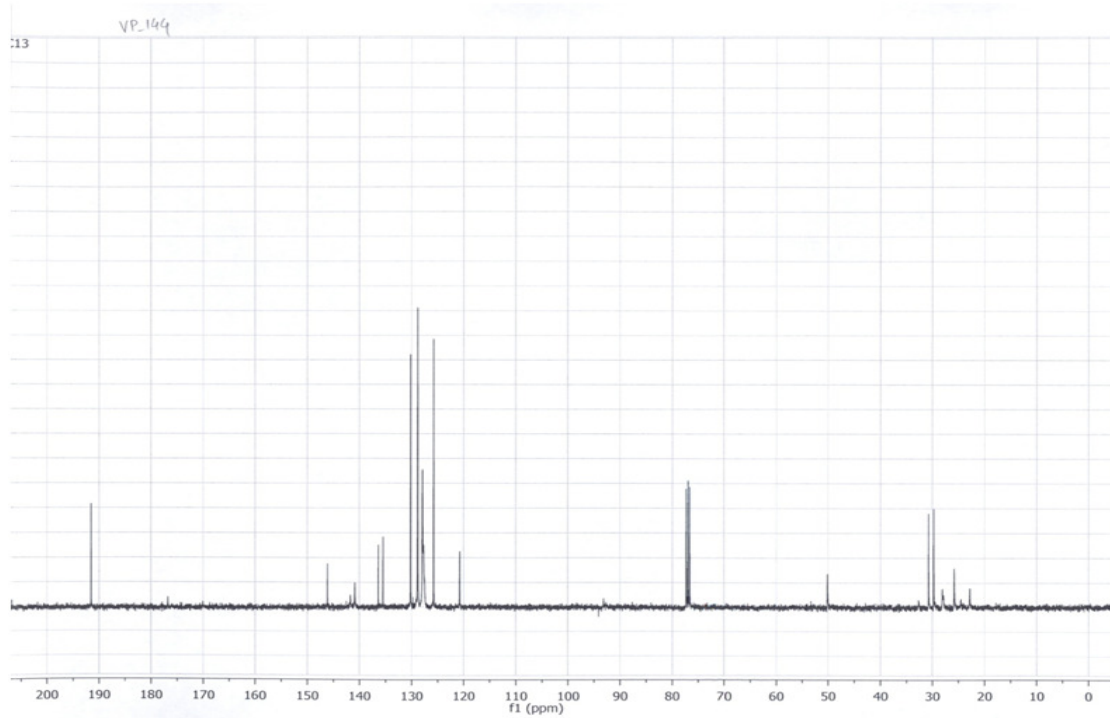
¹³C NMR of **10b**:



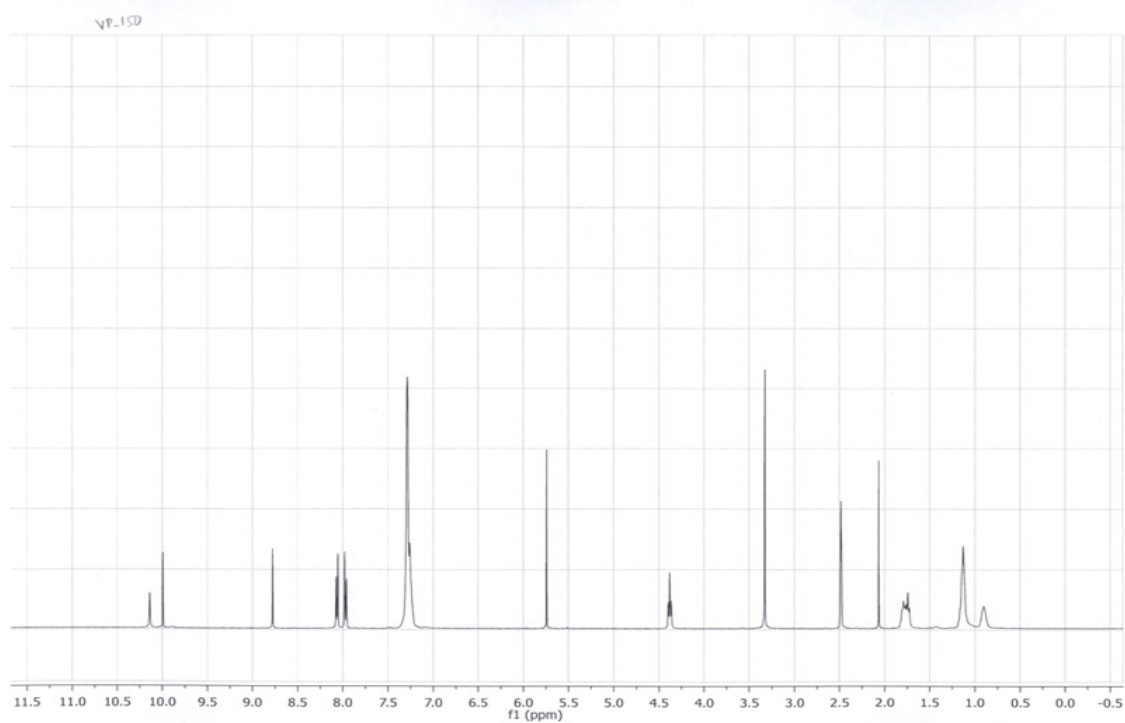
^1H NMR of 10c:



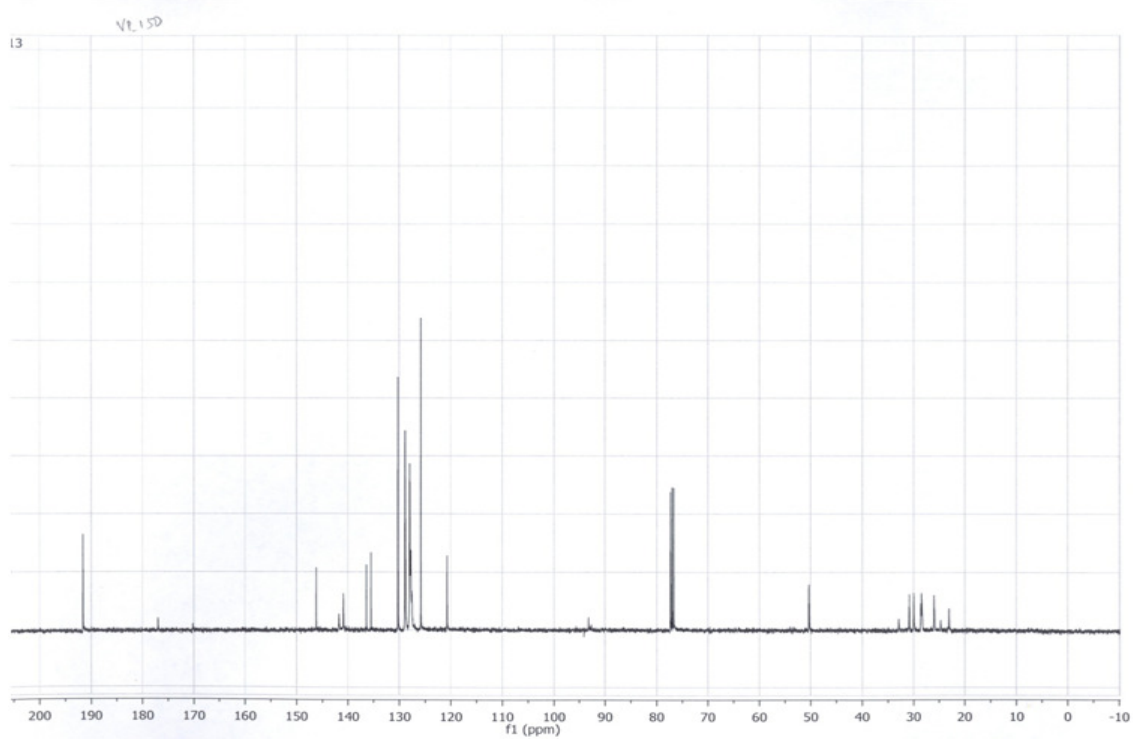
^{13}C NMR of 10c:



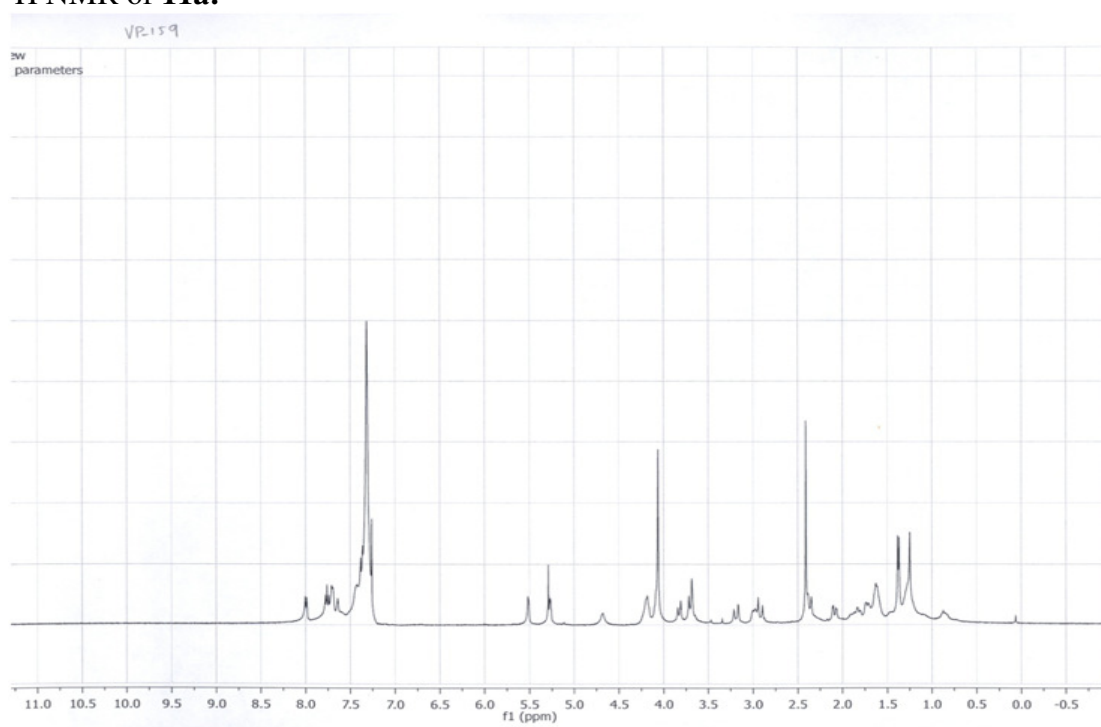
^1H NMR of 10d:



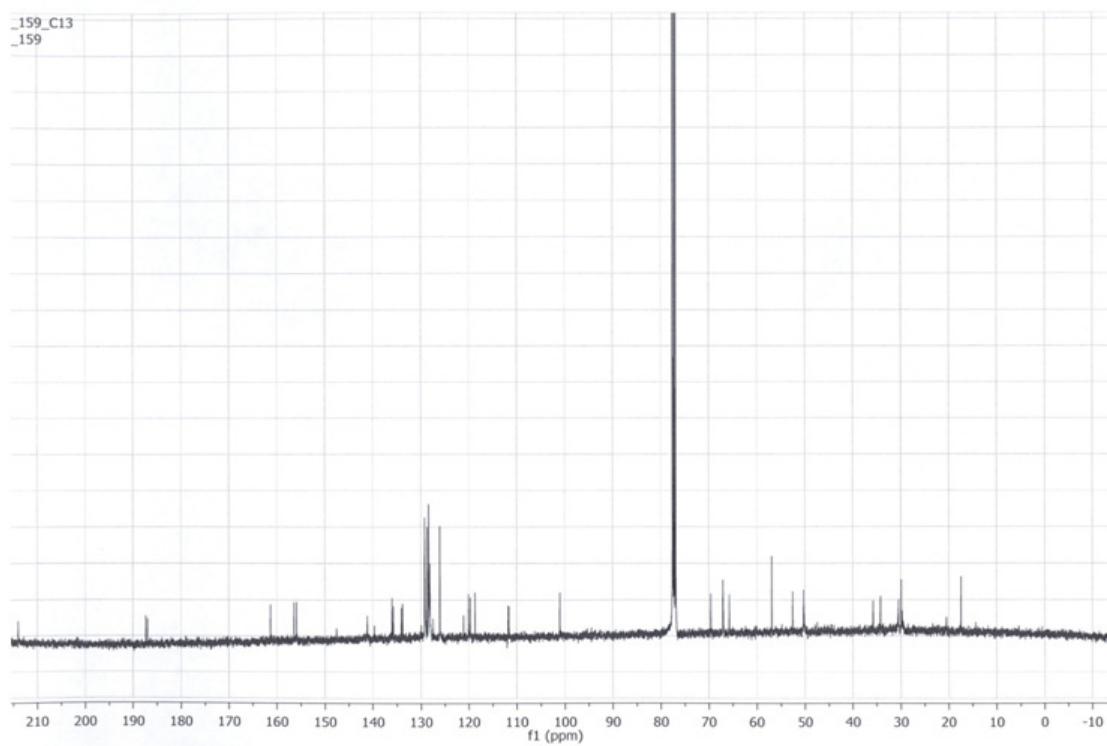
^{13}C NMR of 10d:



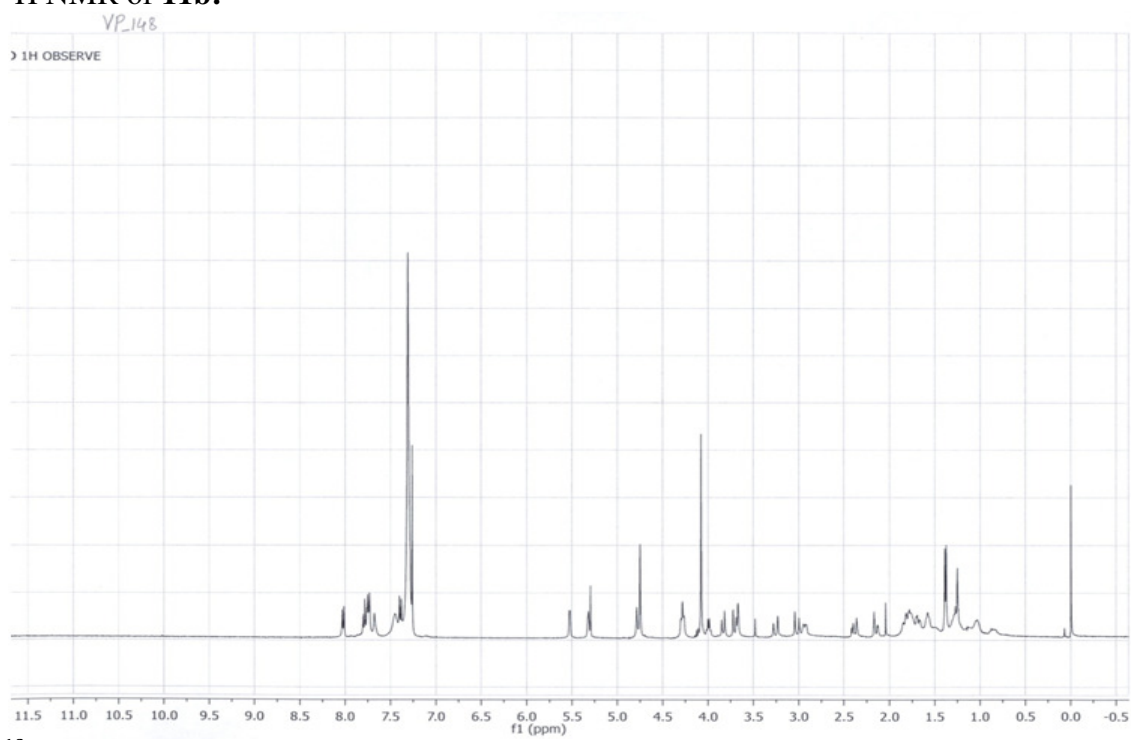
^1H NMR of 11a:



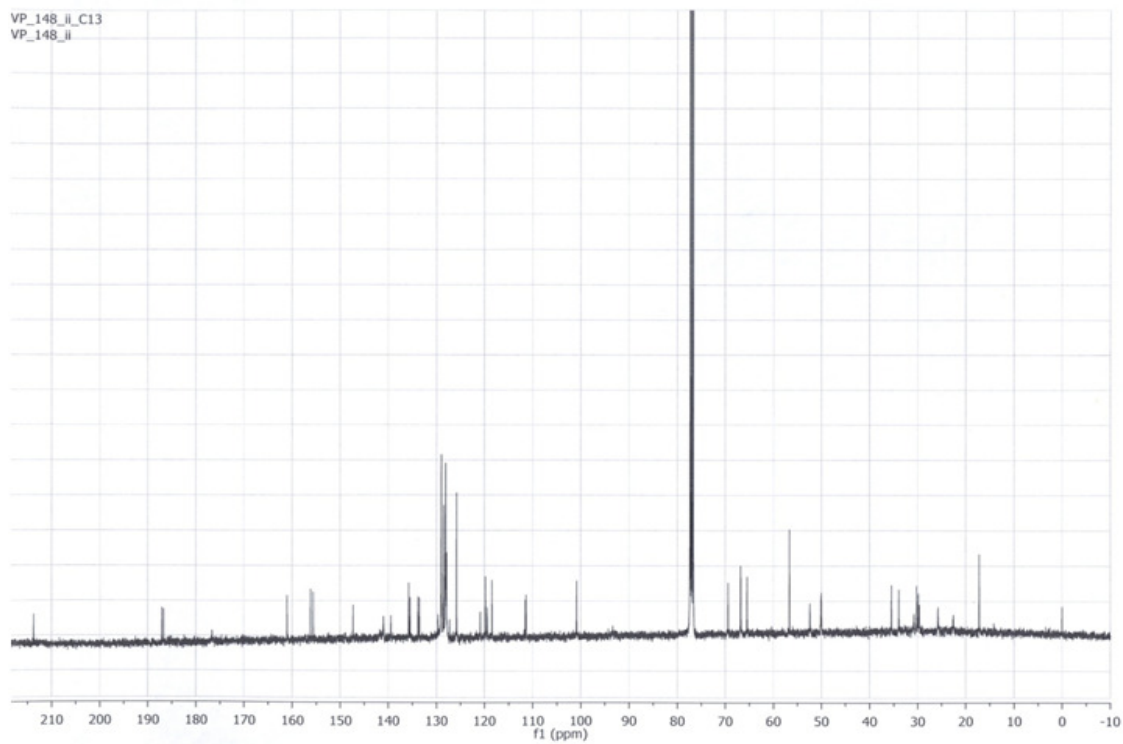
^{13}C NMR of 11a:



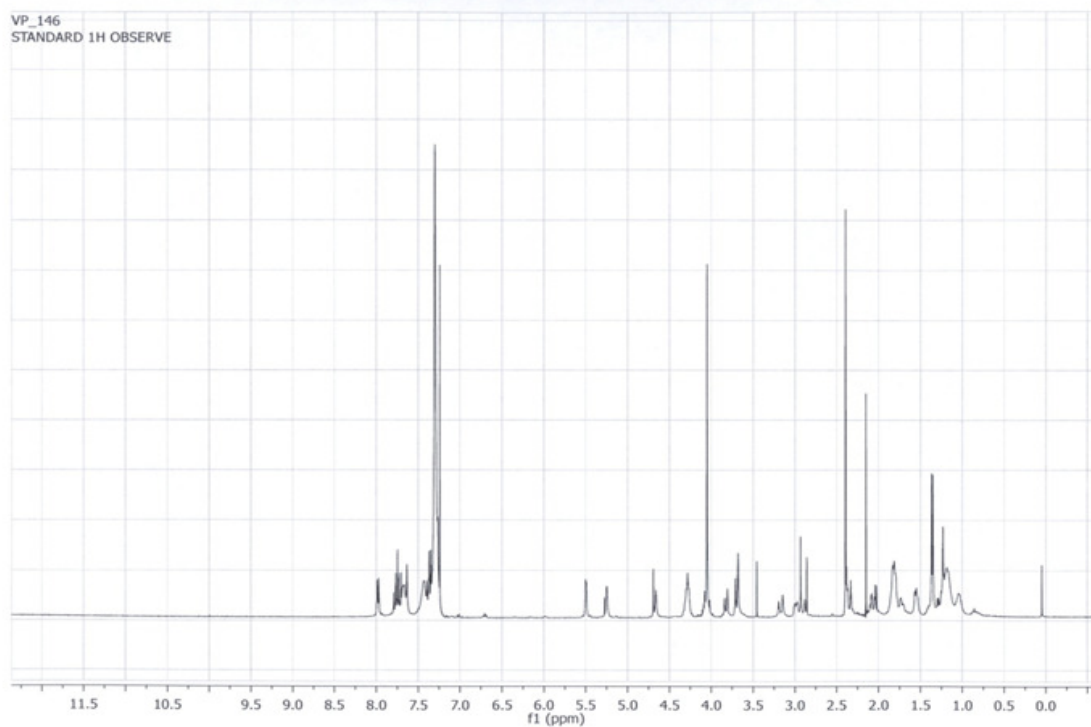
^1H NMR of 11b:



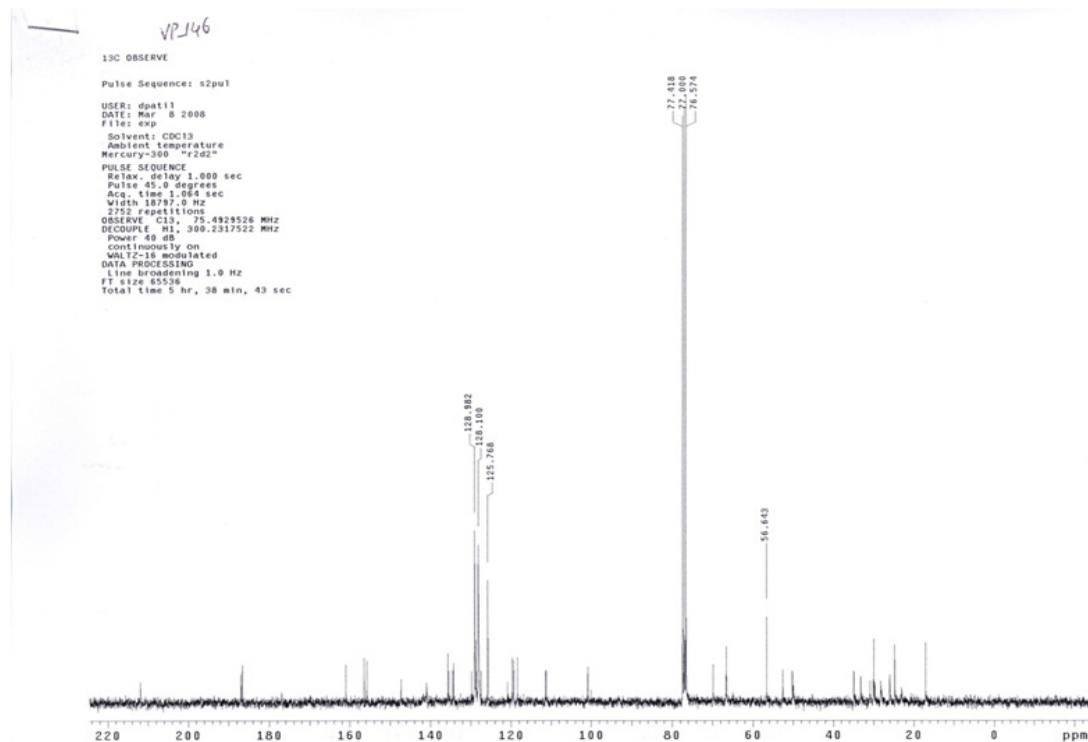
^{13}C NMR of 11b:



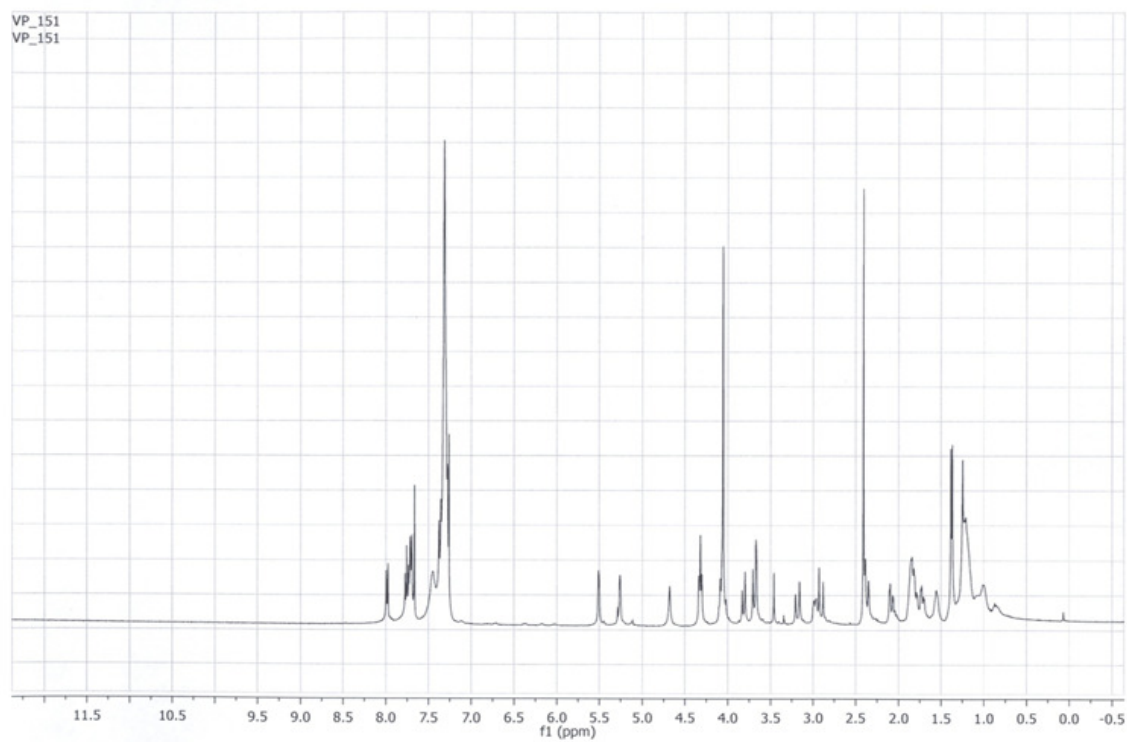
¹H NMR of **11c**:



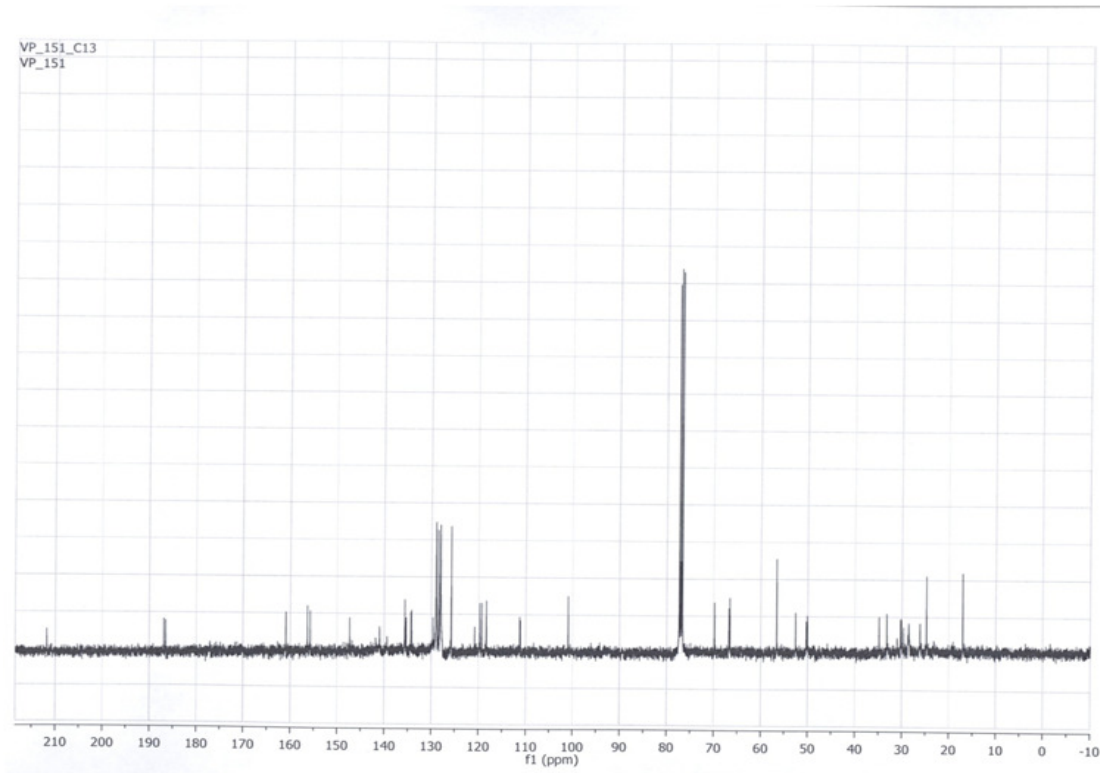
¹³C NMR of **11c**:



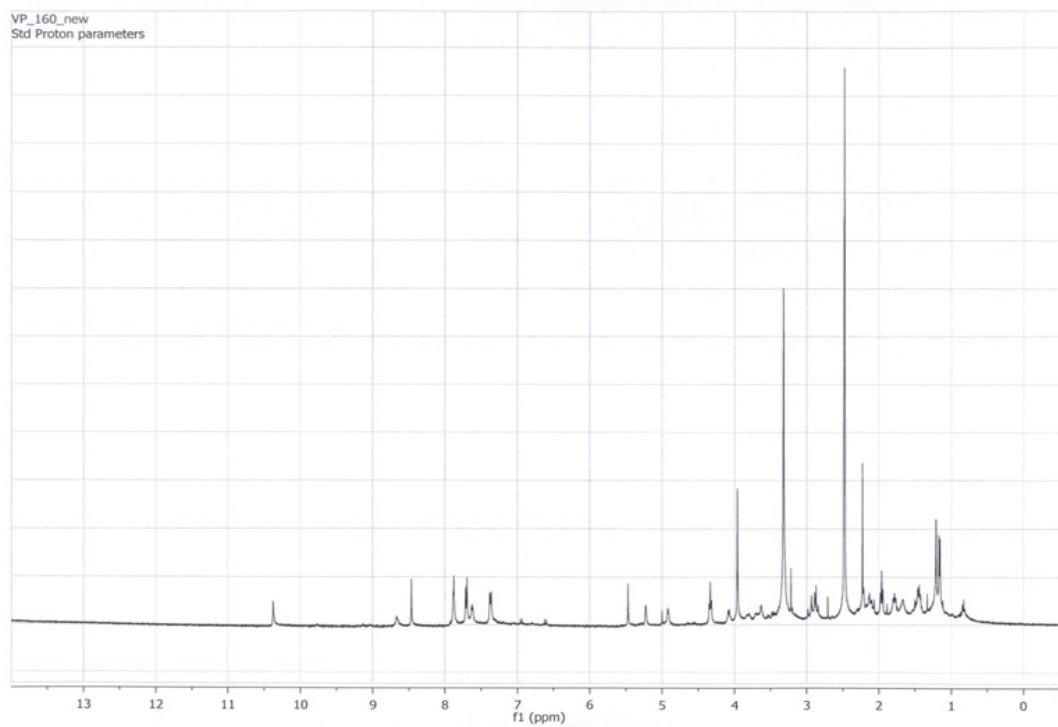
¹H NMR of **11d**:



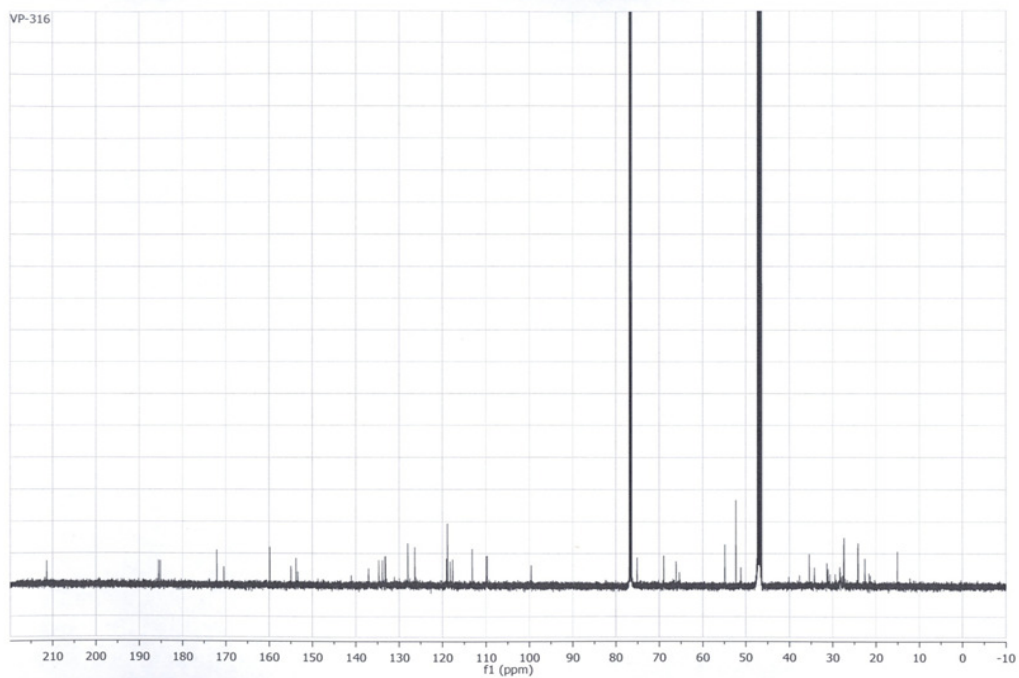
¹³C NMR of **11d**:



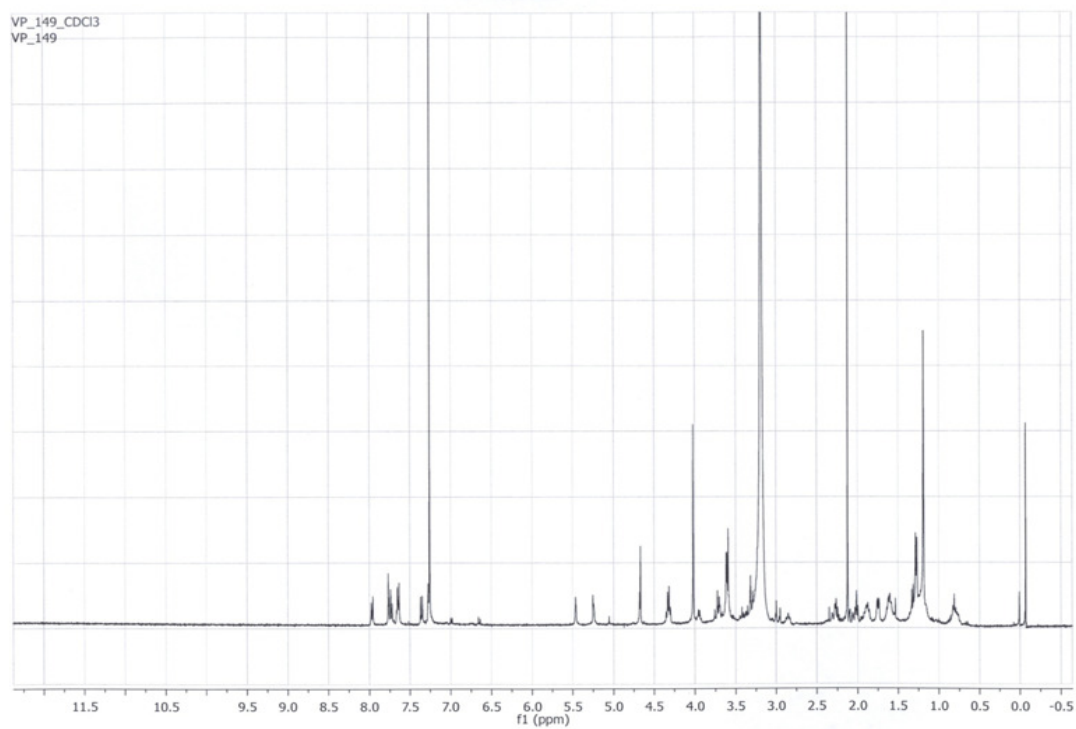
¹H NMR of **12a**



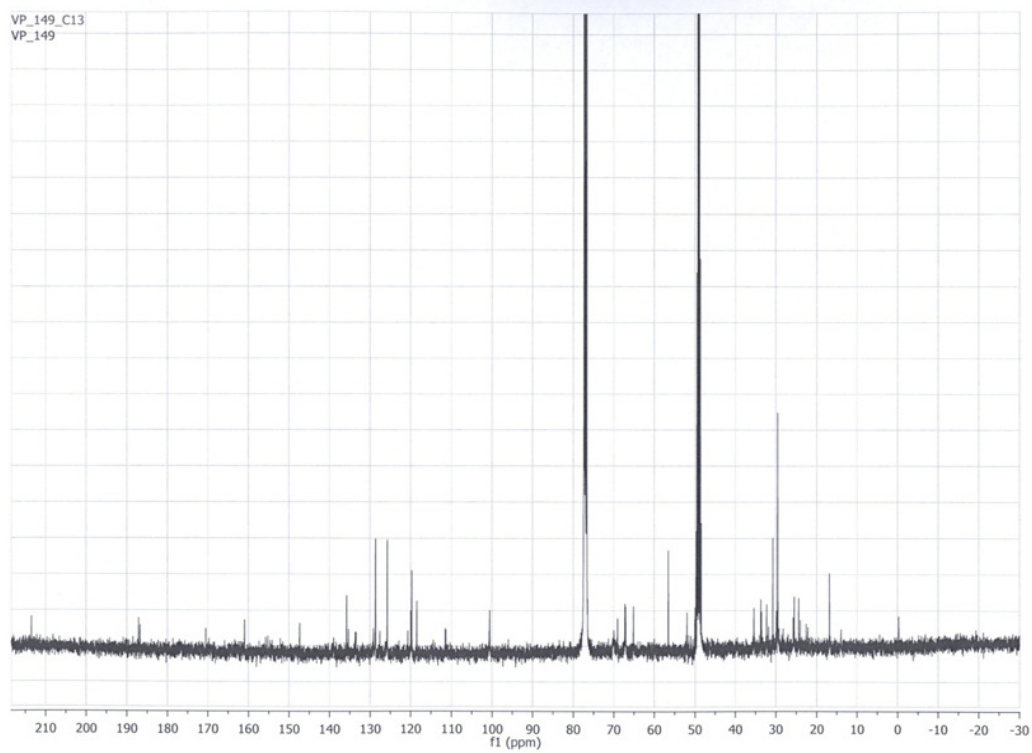
¹³C NMR of **12a**



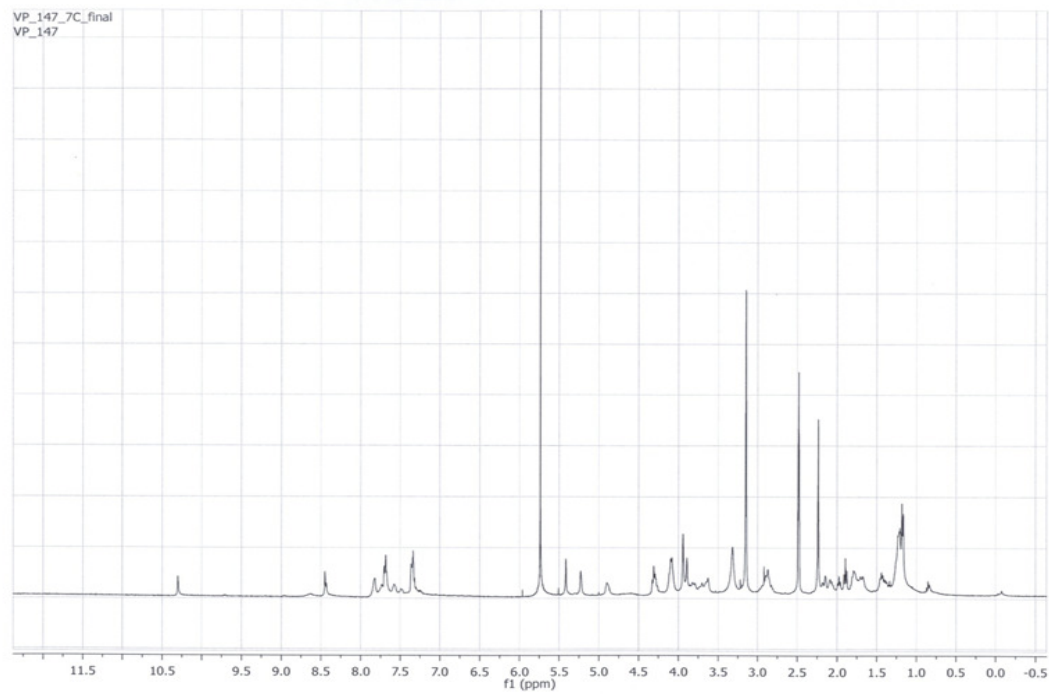
^1H NMR of **12b**



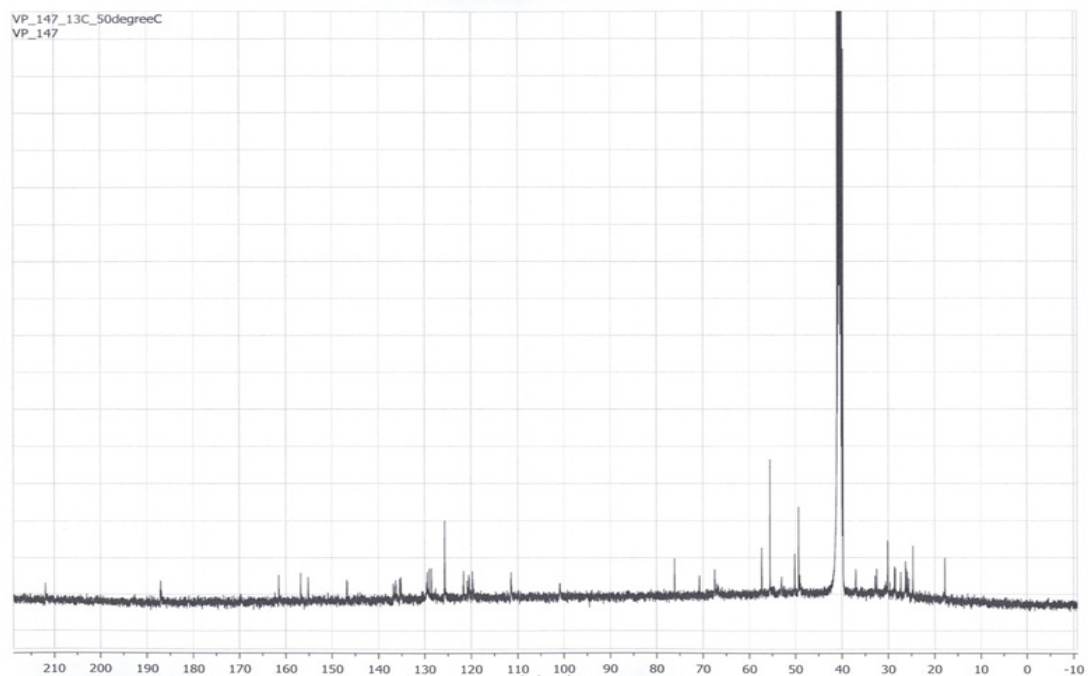
^{13}C NMR of **12b**



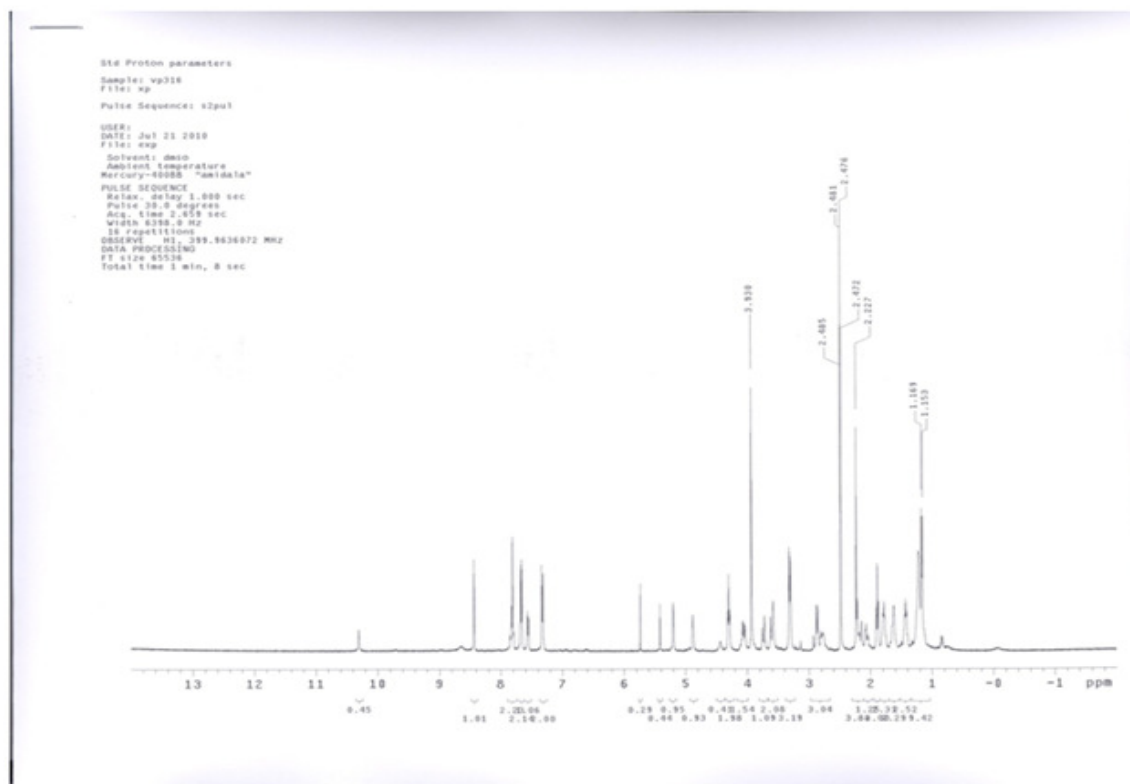
^1H NMR of **12c**



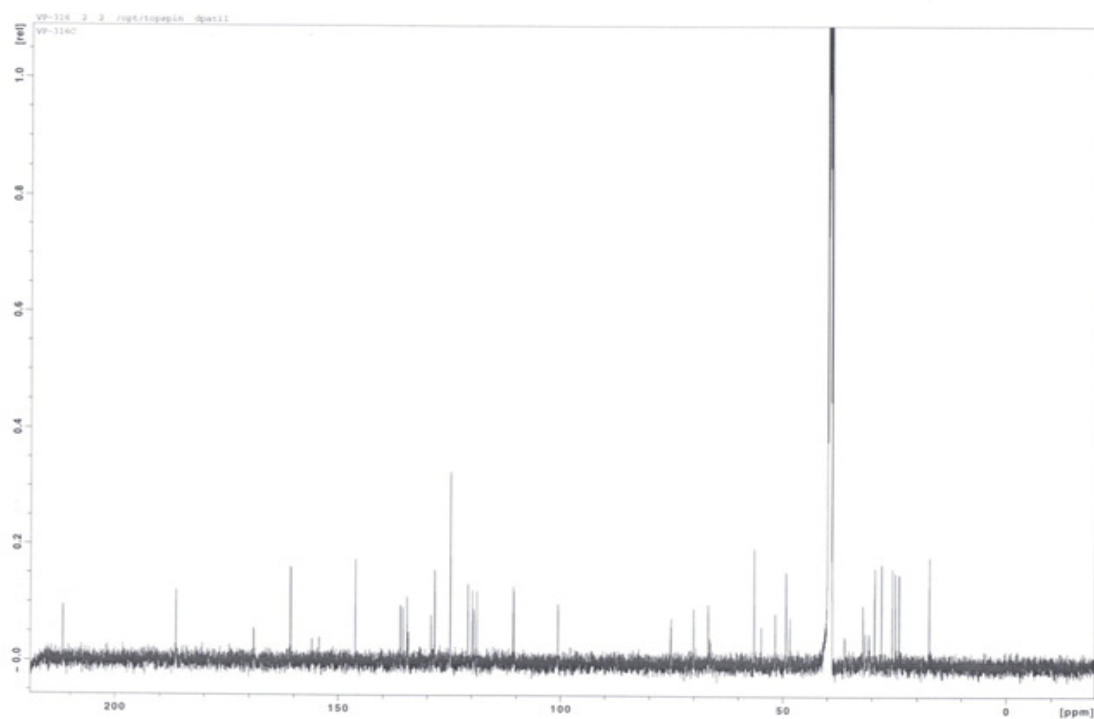
^{13}C NMR of **12c**



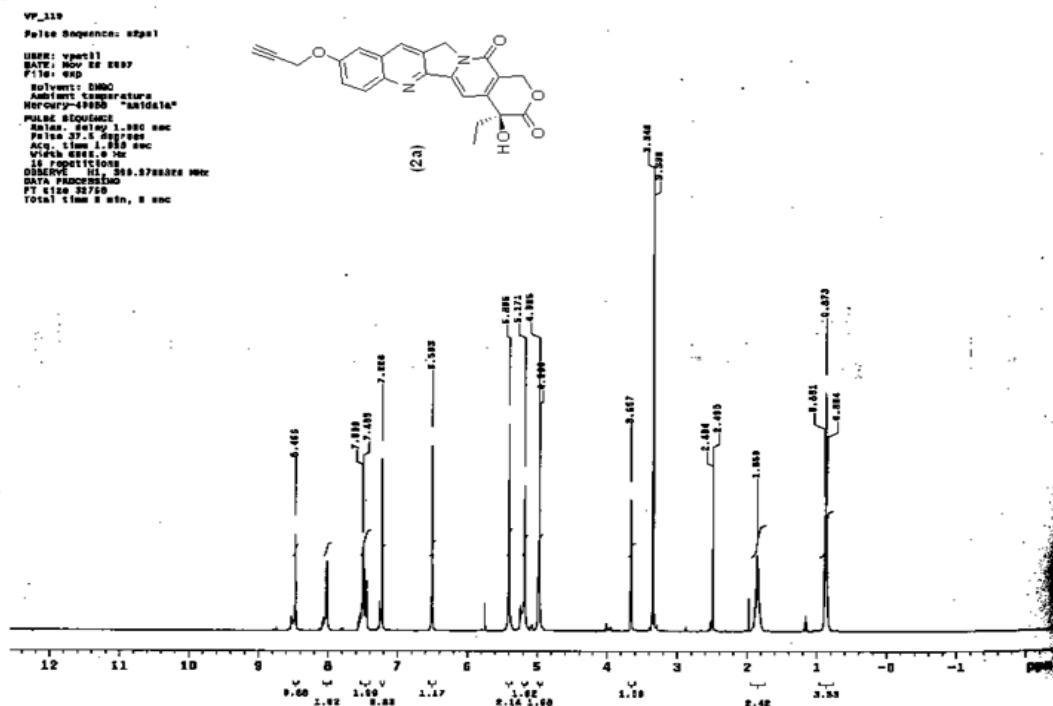
^1H NMR of 12d



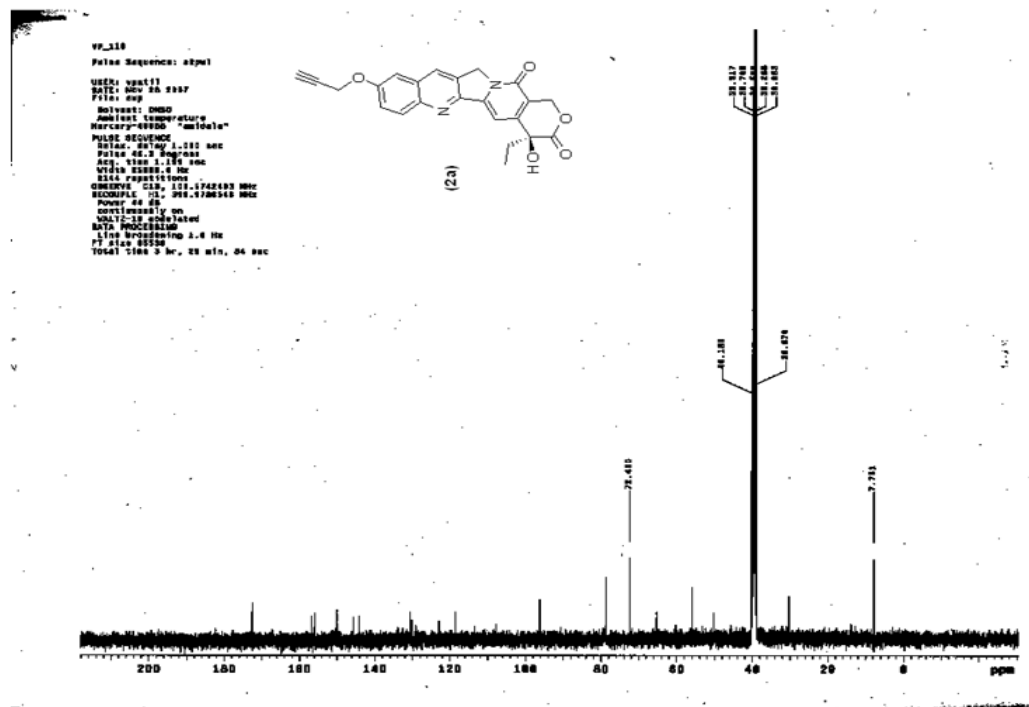
^{13}C NMR of 12d



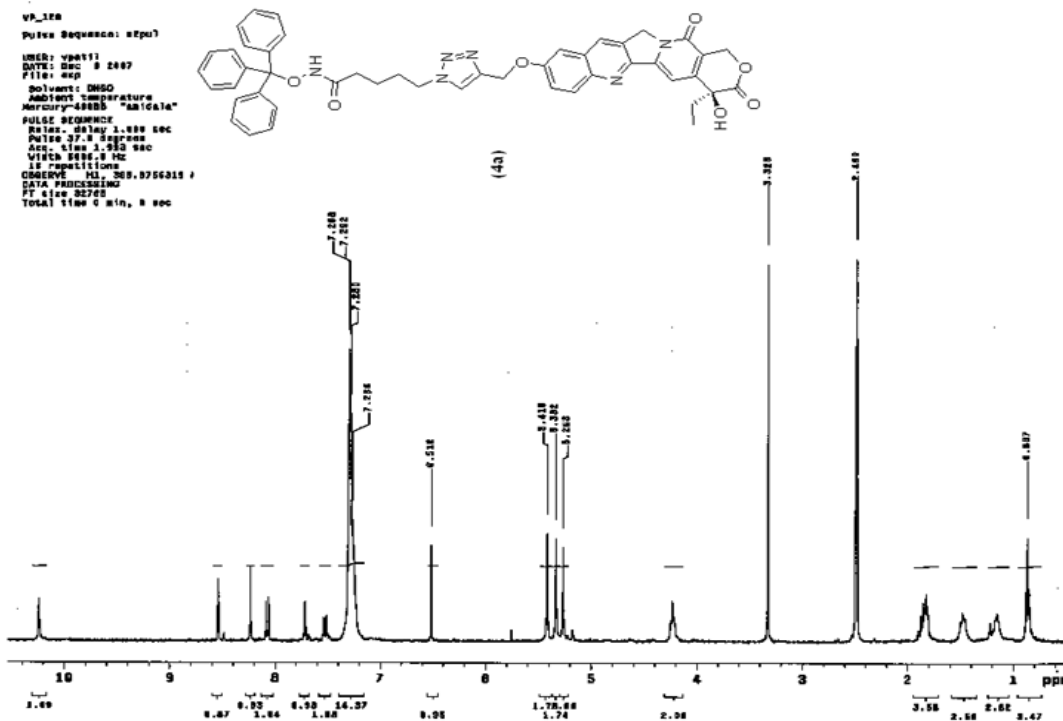
¹H NMR of 14a



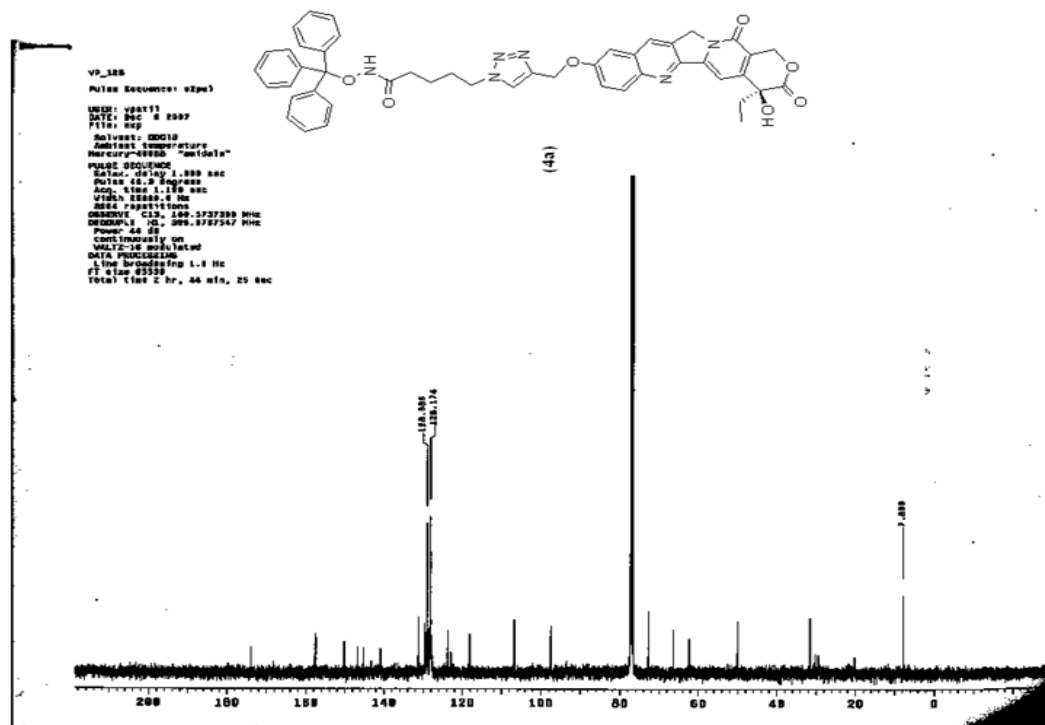
¹³C NMR of 14a



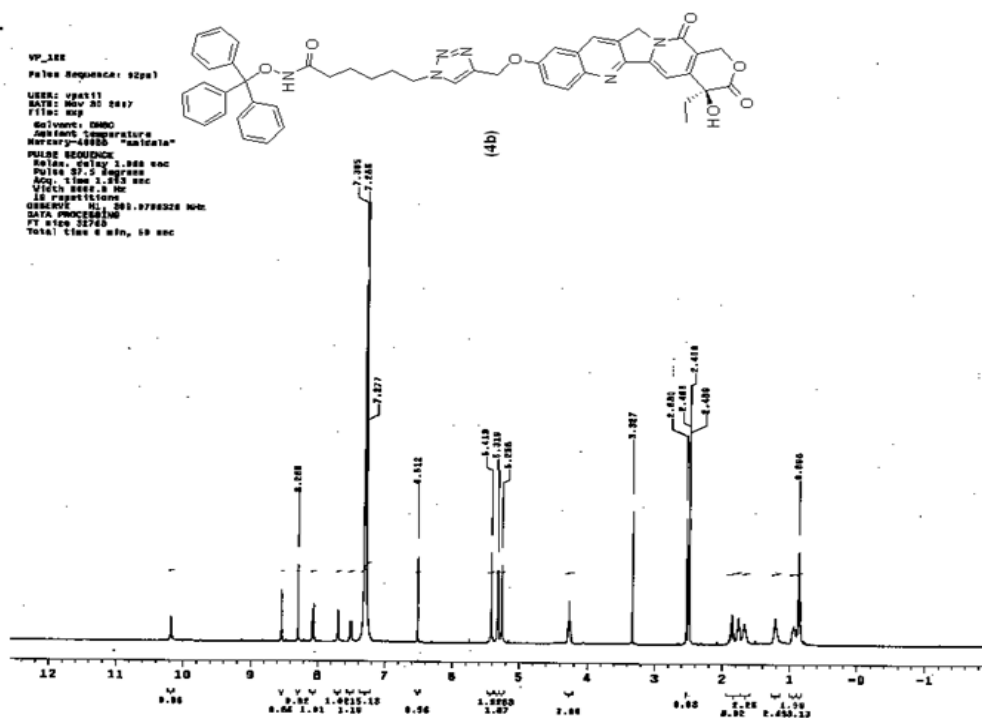
¹H NMR of 16a



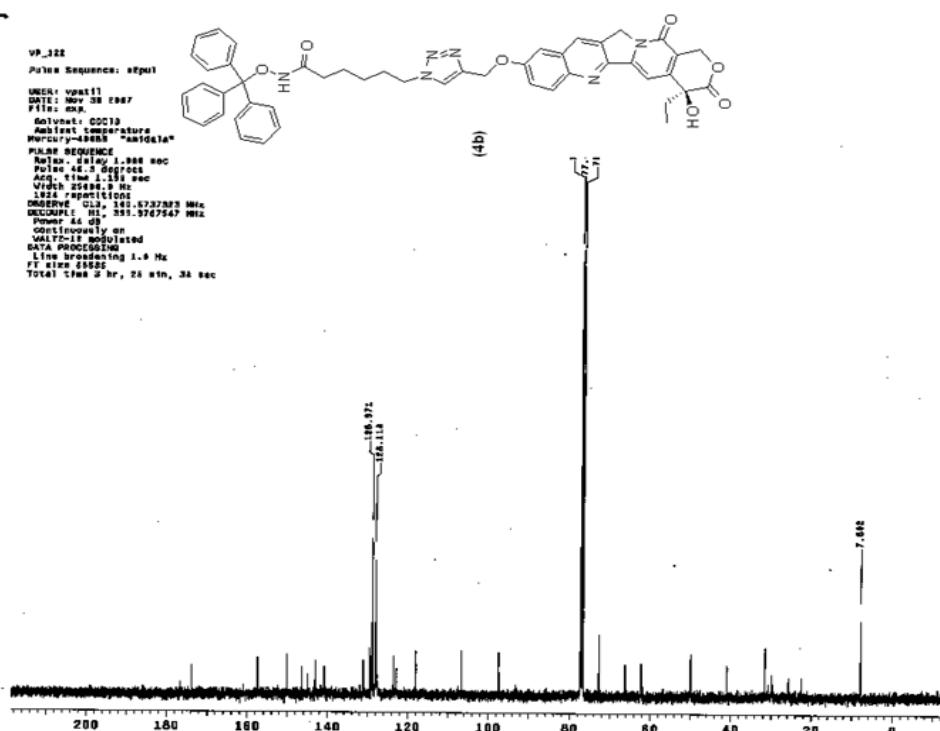
¹³C NMR of 16a



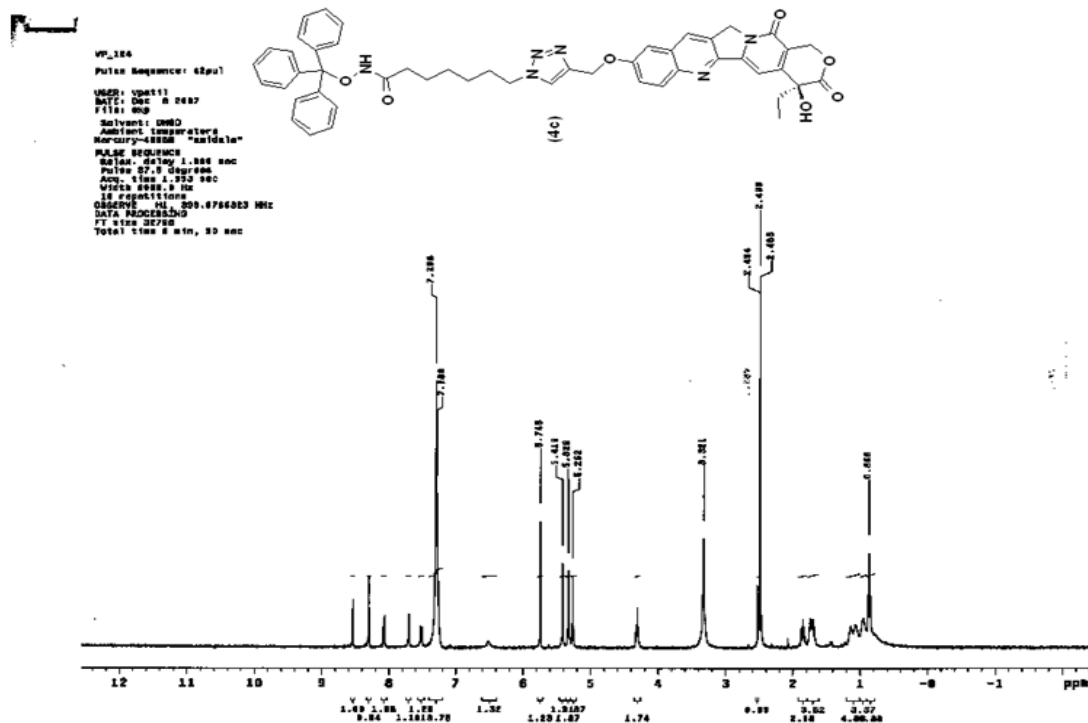
¹H NMR of 16b



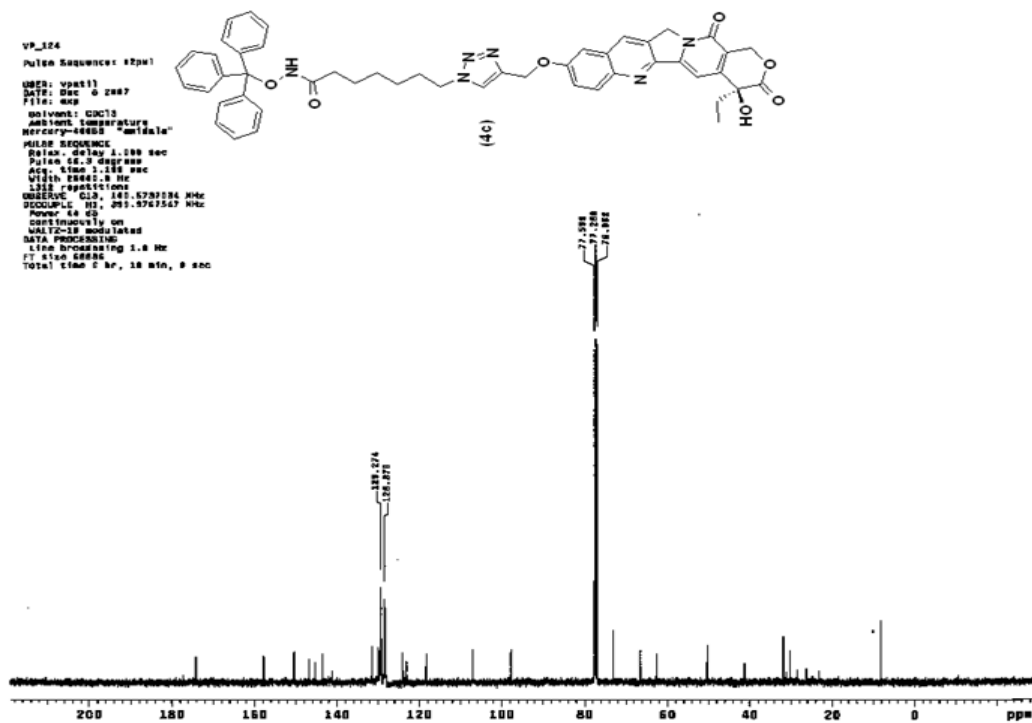
¹³C NMR of 16b



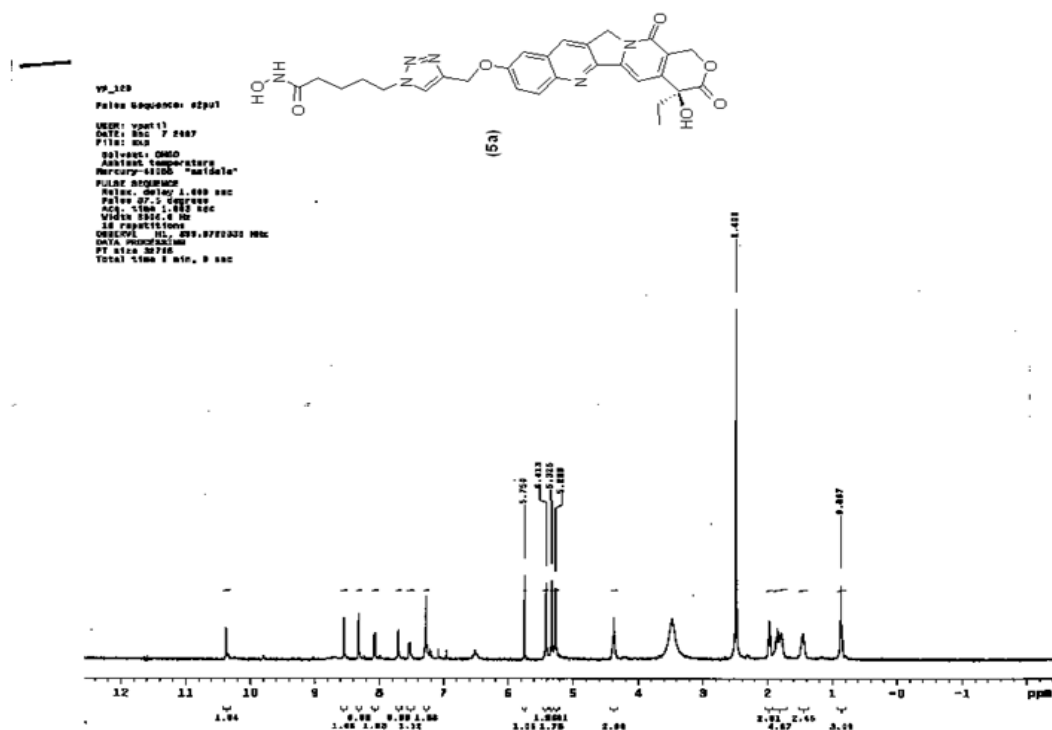
¹H NMR of 16c



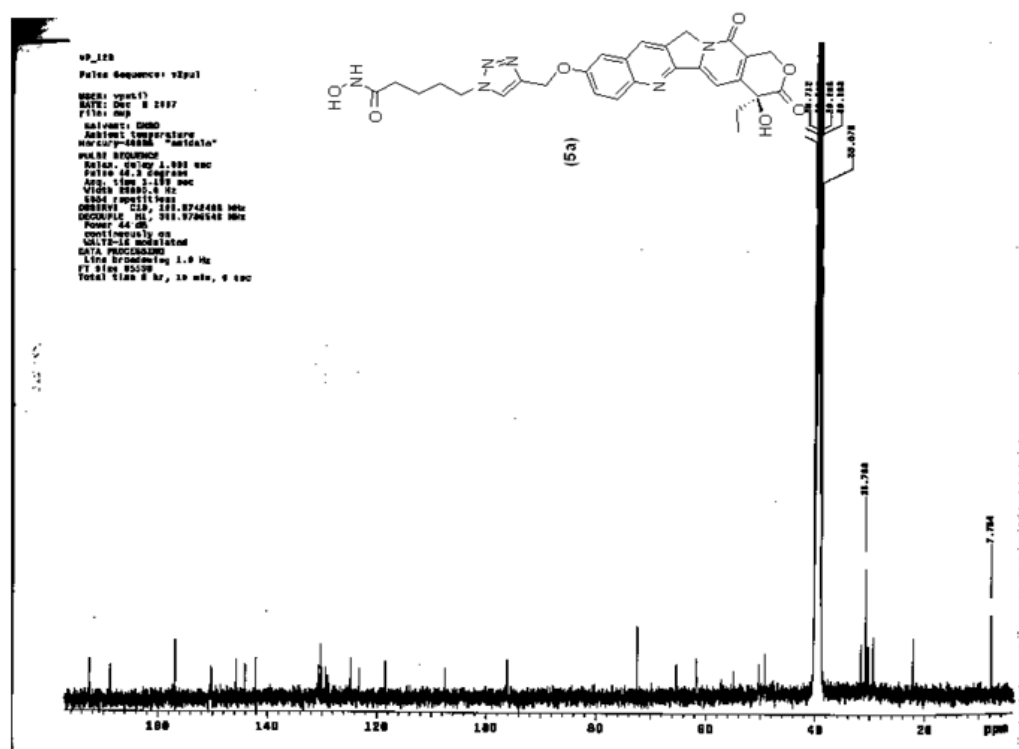
¹³C NMR of 16c

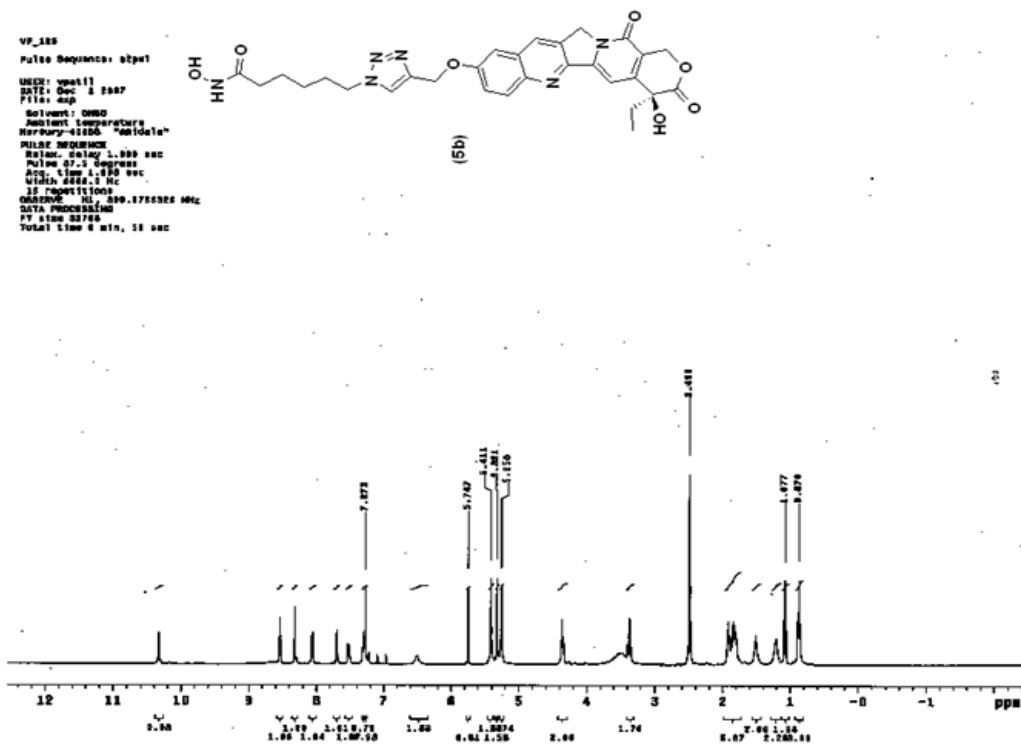
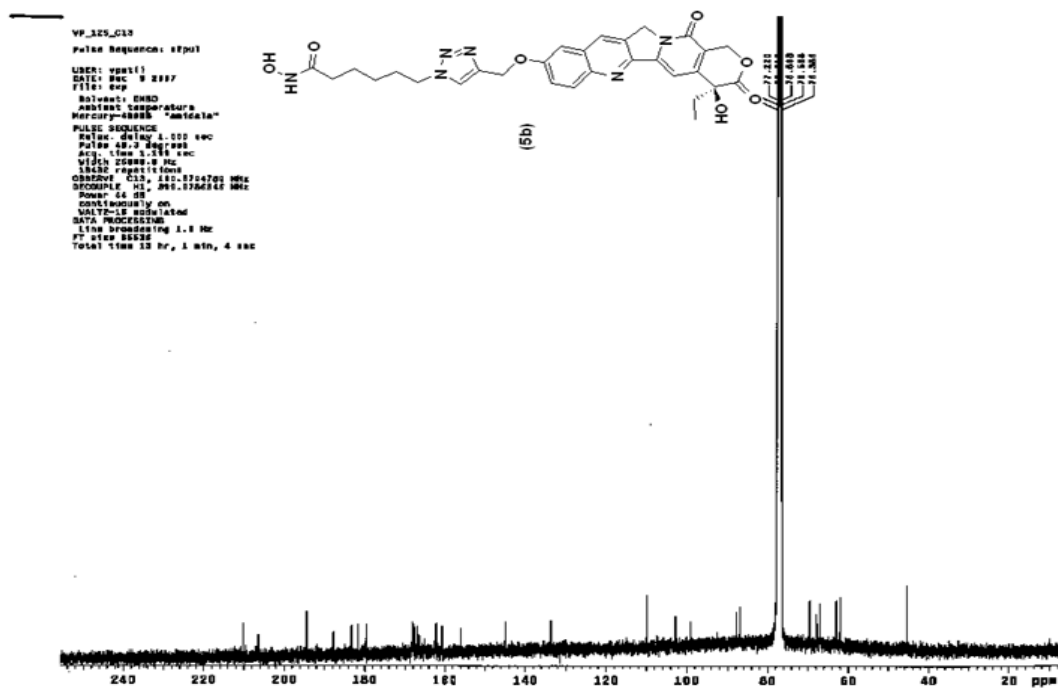


¹H NMR of 16a



¹³C NMR of 16a



¹H NMR of **16b** ^{13}C NMR of **16b**

APPENDIX D

HPLC Analysis of HDAC – Topo II Dual Inhibitors (Chapter 4)

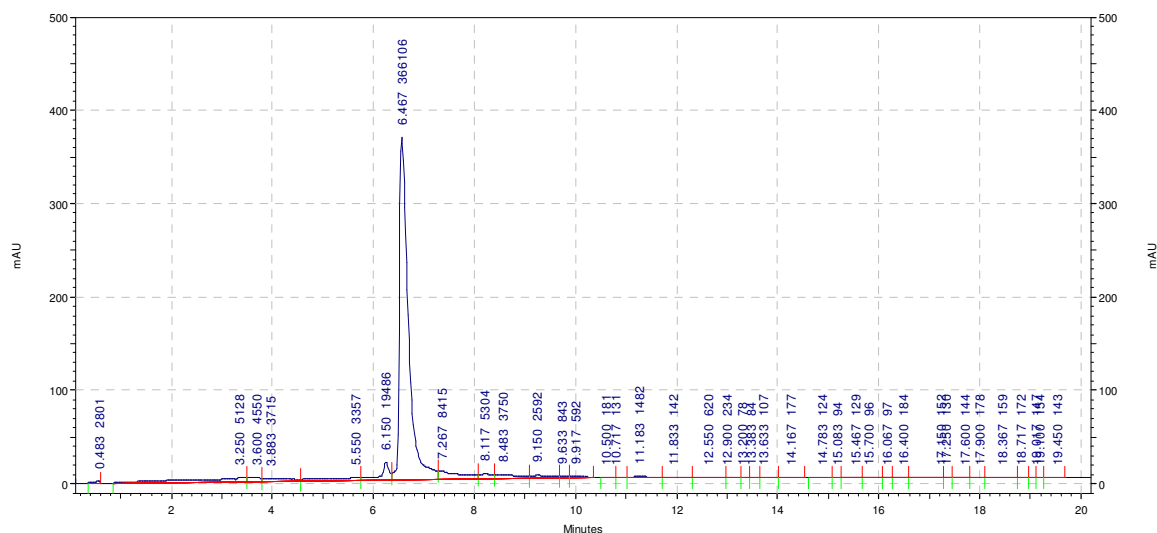
HPLC characterization of compounds 7 and 12a-d

Solvent A = 0.1% formic acid in water

Solvent B = 0.1 % formic acid in acetonitrile

Compound 7 –

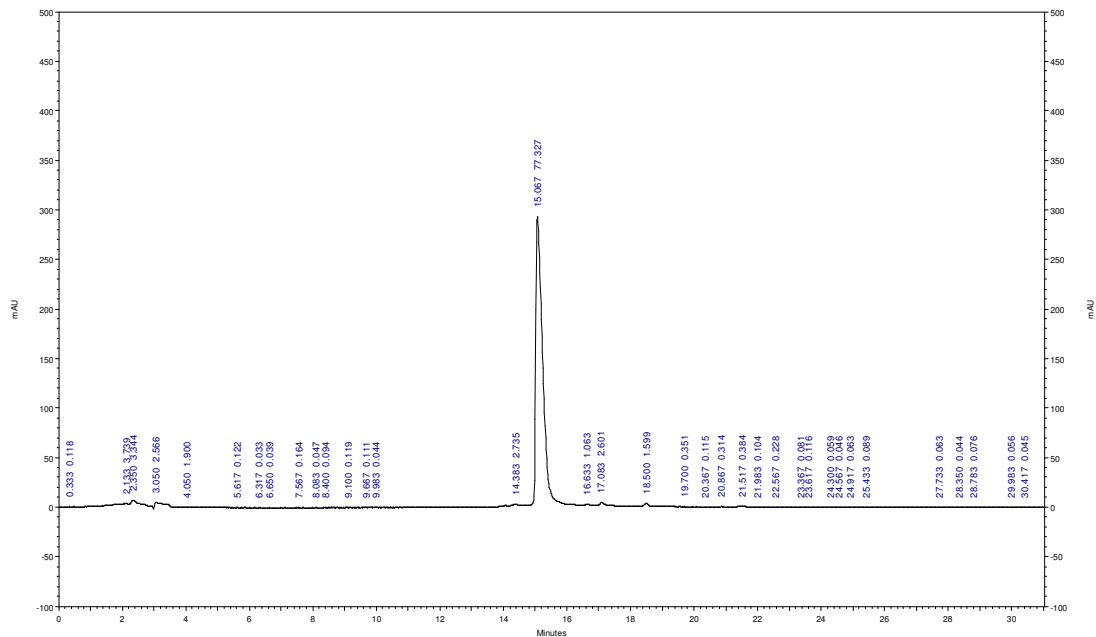
Retention time – 6.46 min; Solvent – Gradient 5% - 60% solvent B over 20 min



Compound 12a –

Retention time – 15.06 min

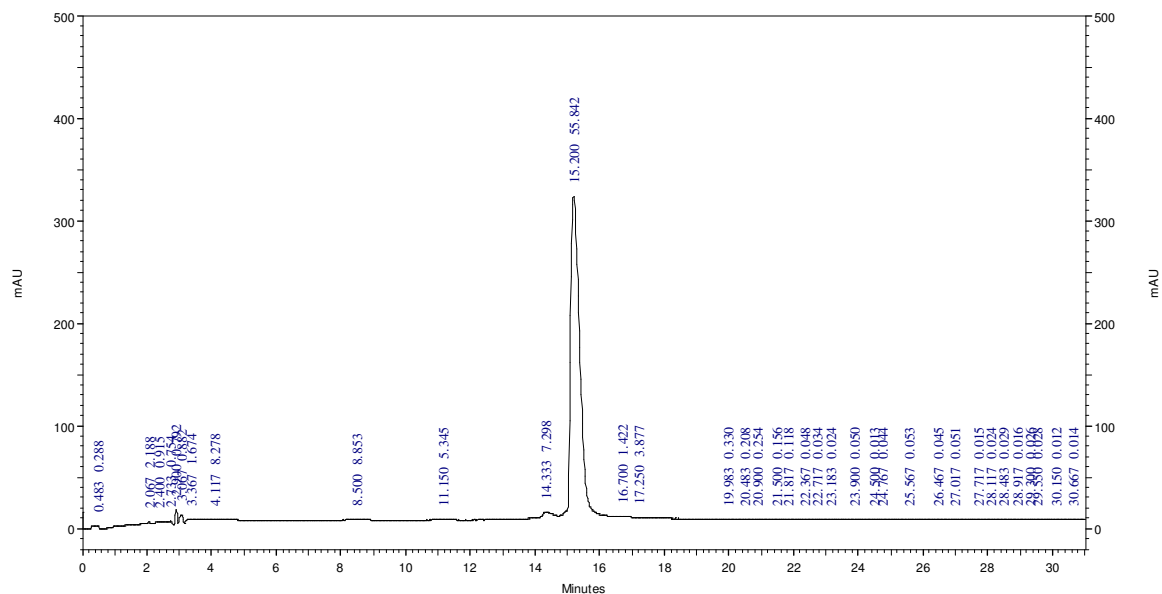
Solvent – Gradient 0% - 100% solvent B over 30 min



Compound **12b** –

Retention time – 15.20 min

Solvent – Gradient 0% - 100% solvent B over 30 min



Compound **12c** –

Retention time – 16.98 min

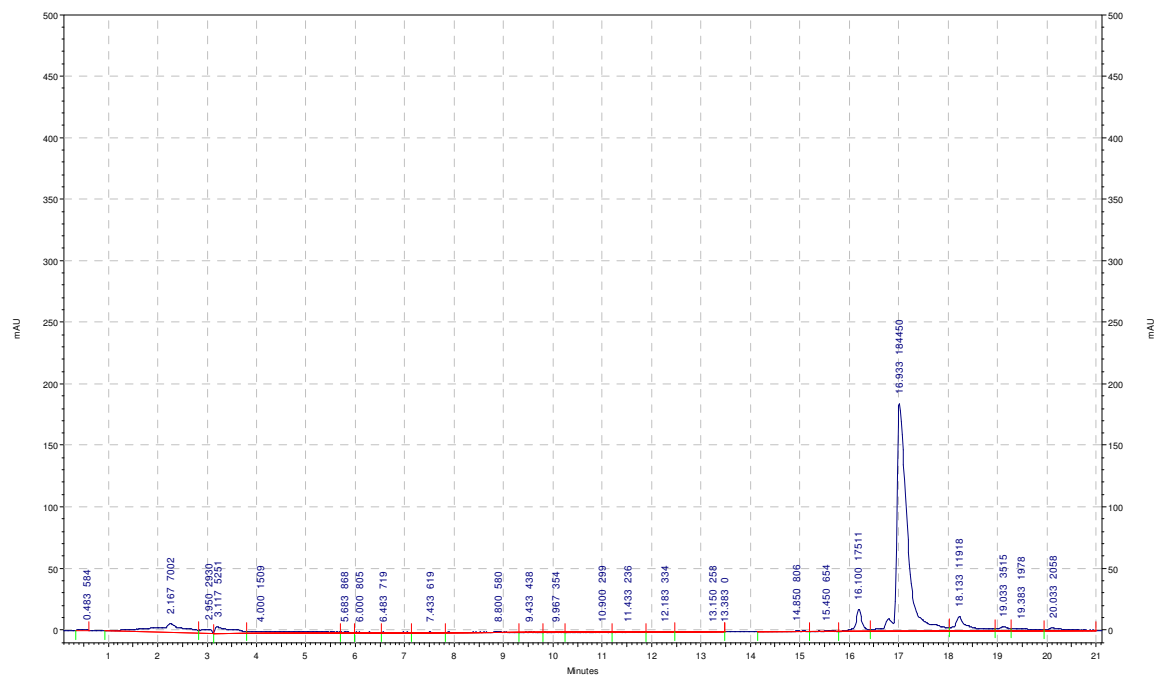
Solvent – Gradient 5% - 60% solvent B over 20 min



Compound **12d** –

Retention time – 16.93 min

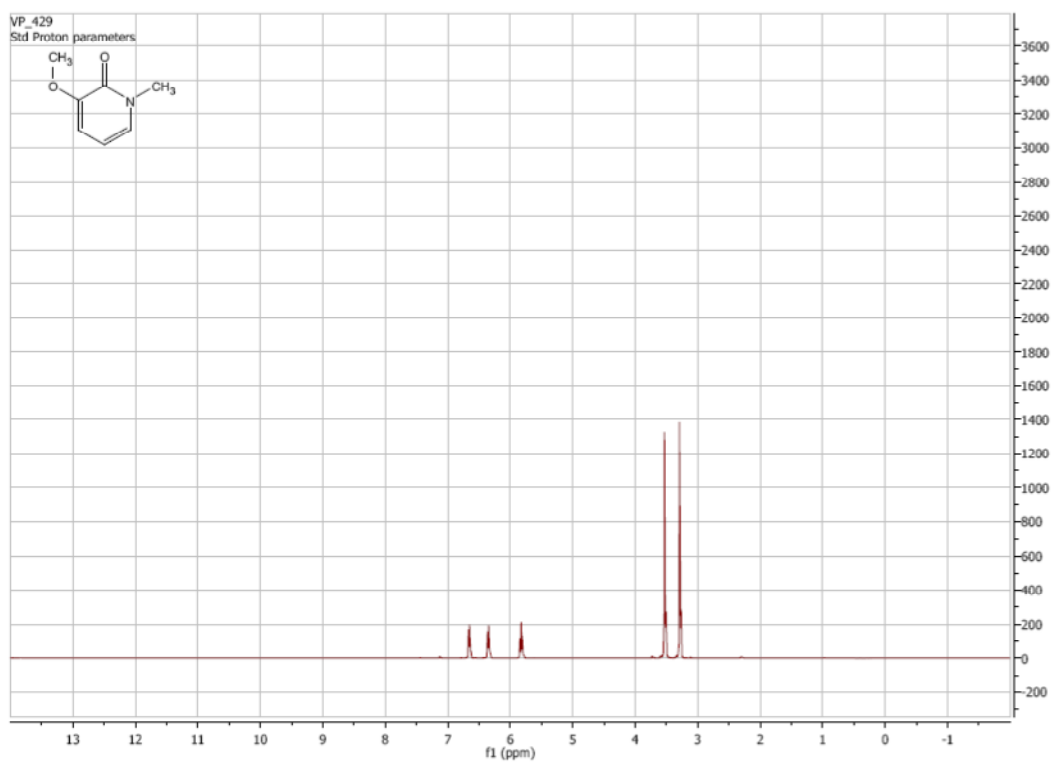
Solvent – Gradient 5% - 60% solvent B over 20 min



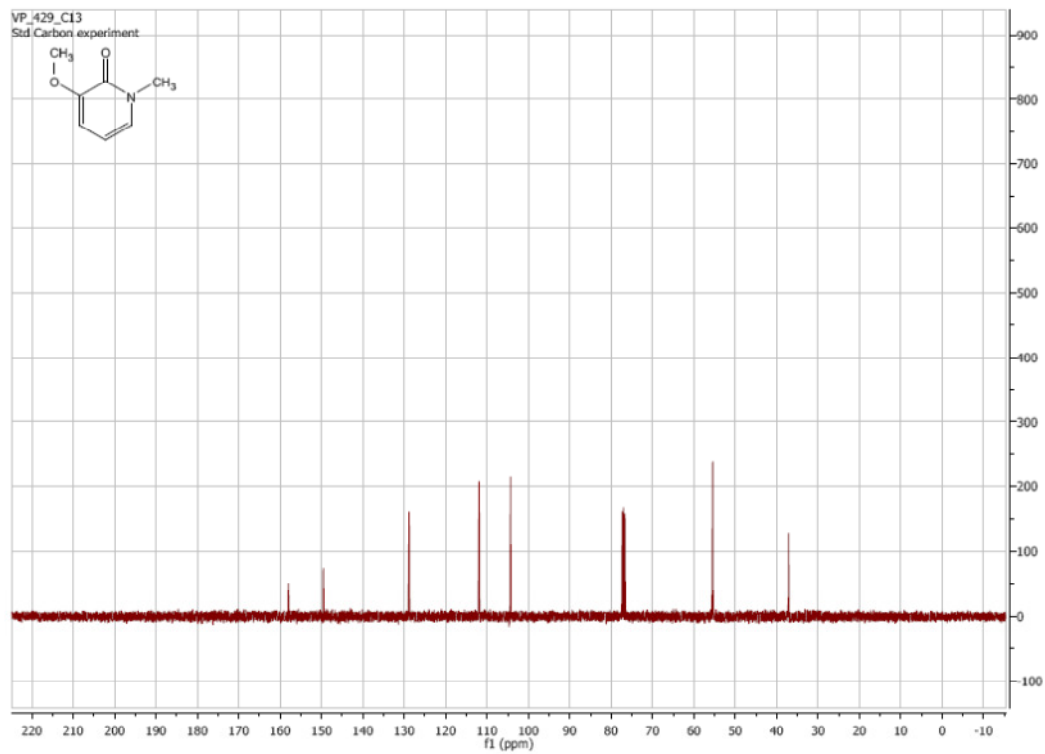
APPENDIX E

^1H and ^{13}C NMR characterization for Novel ZBG HDACi (Chapter 5)

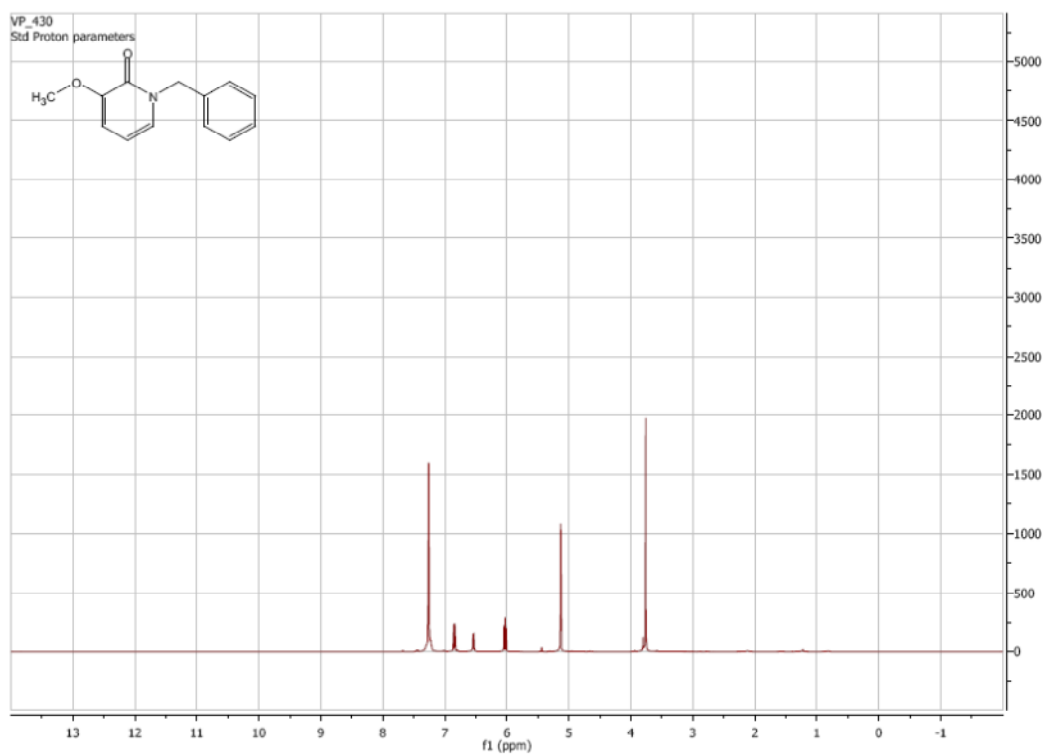
¹H NMR of **4a**:



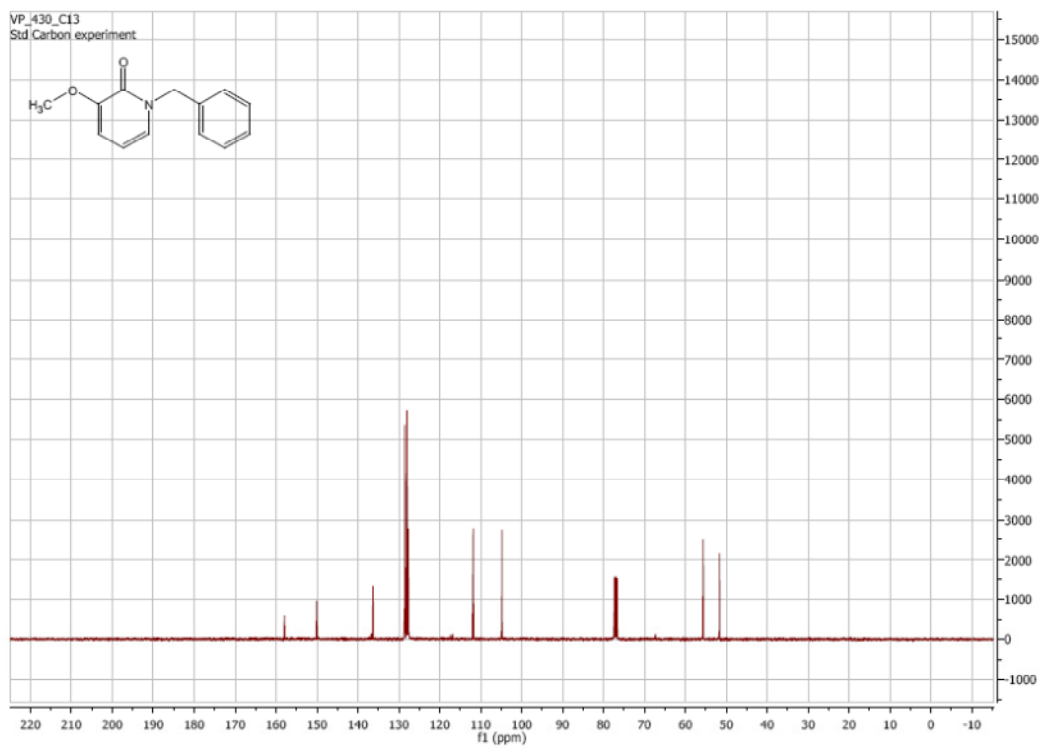
¹³C NMR of **4a**:



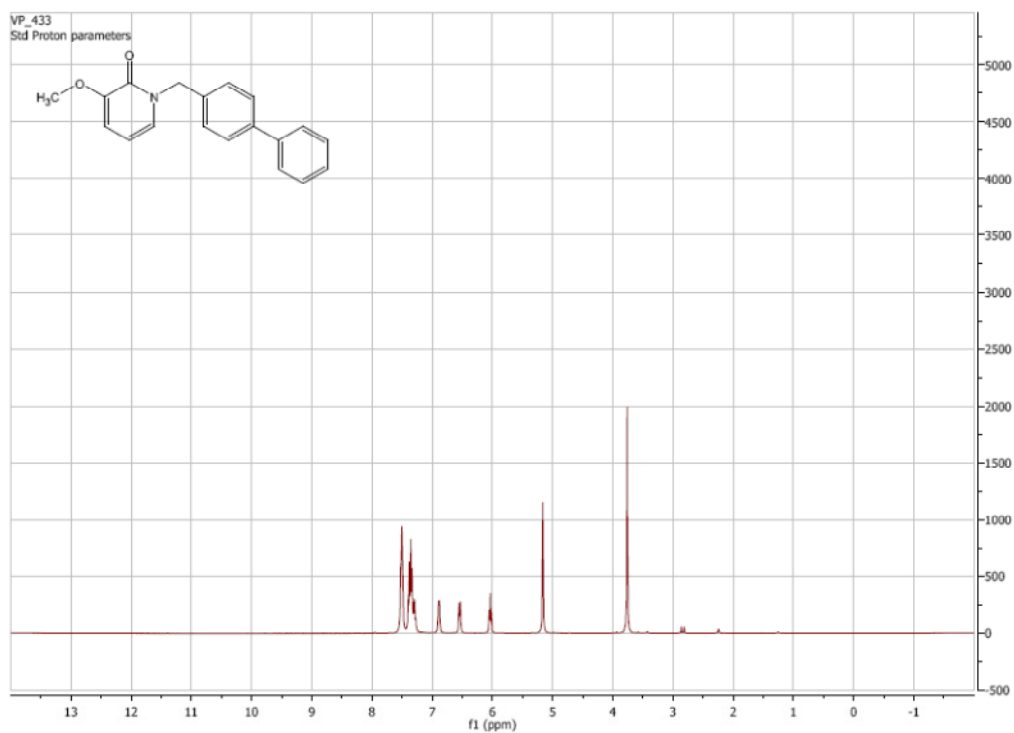
¹H NMR of **4b**:



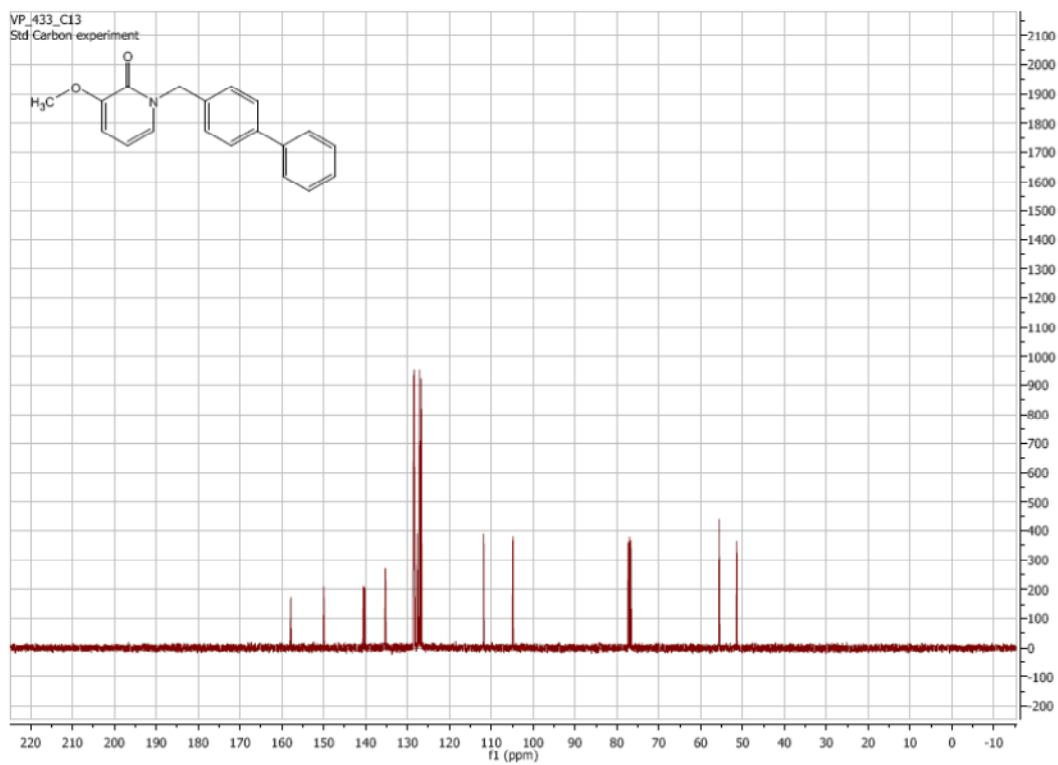
¹³C NMR of **4b**:



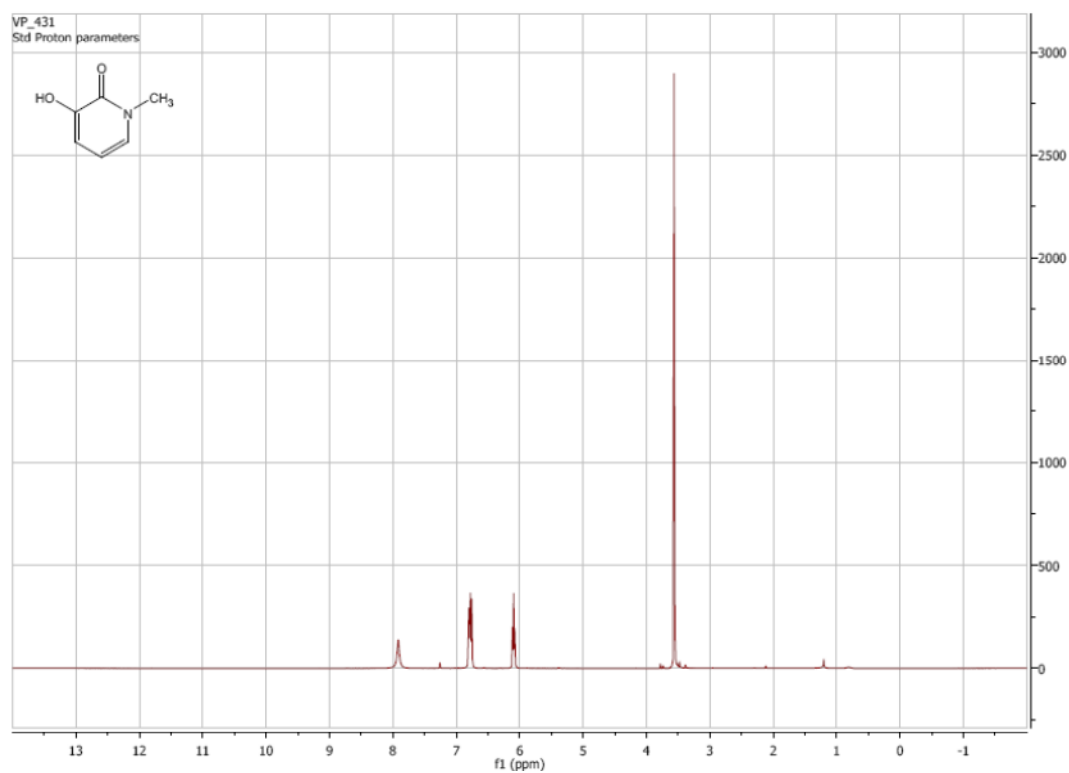
^1H NMR of **4c**:



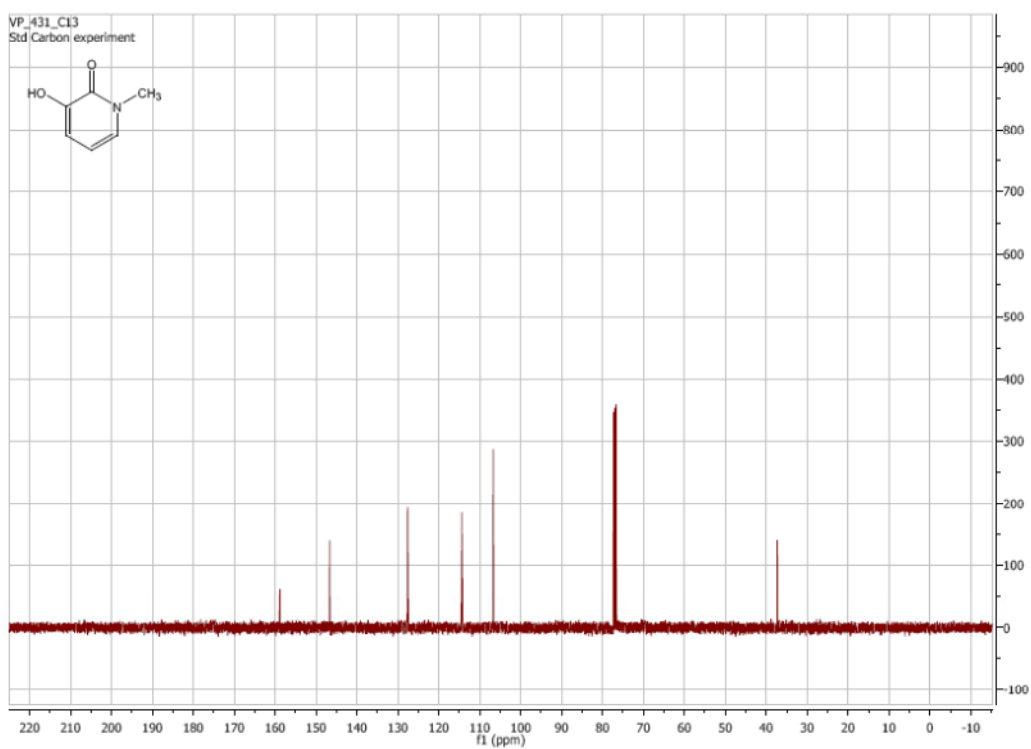
^{13}C NMR of **4c**:



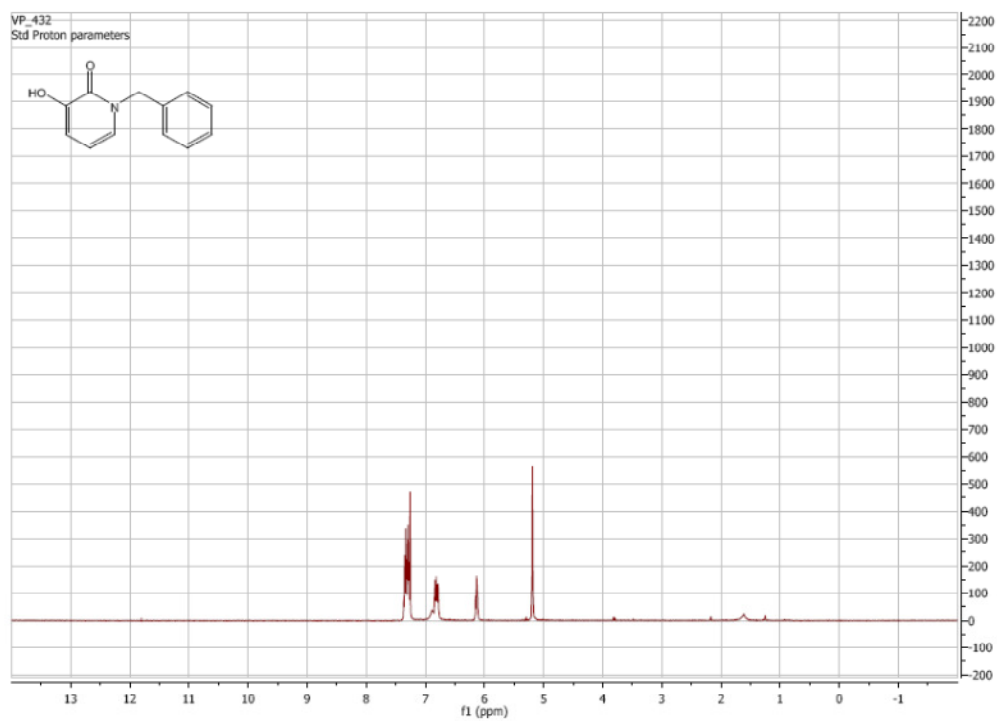
¹H NMR of **5a**:



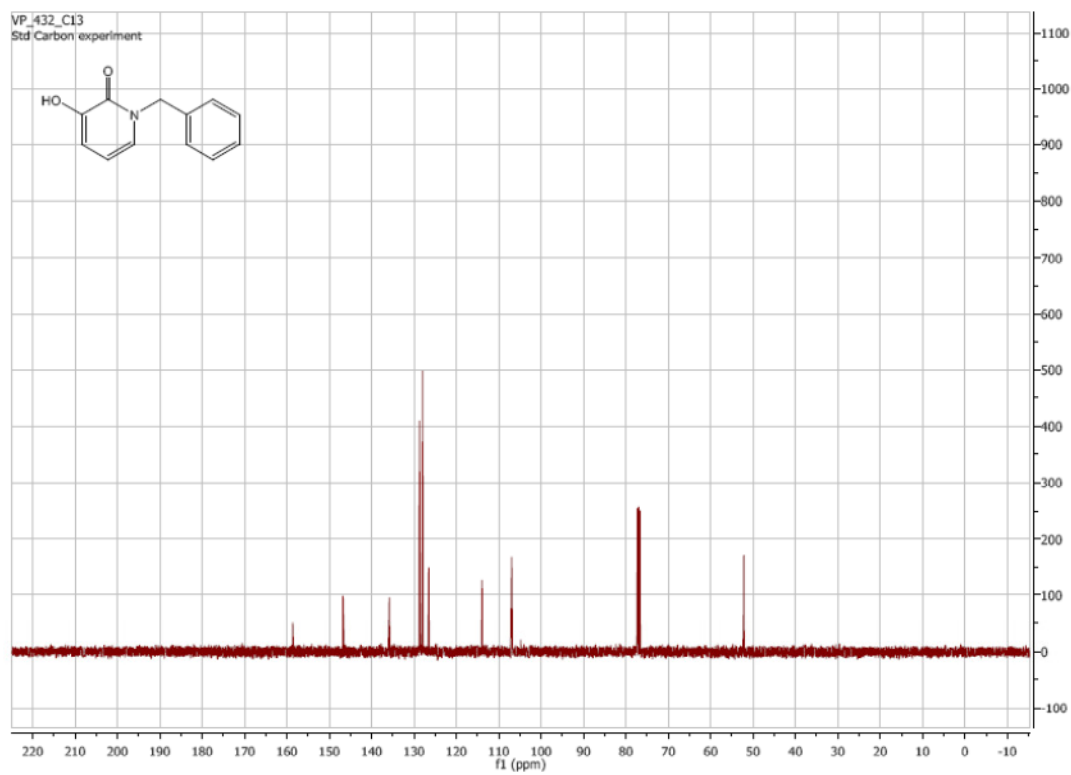
¹³C NMR of **5a**:



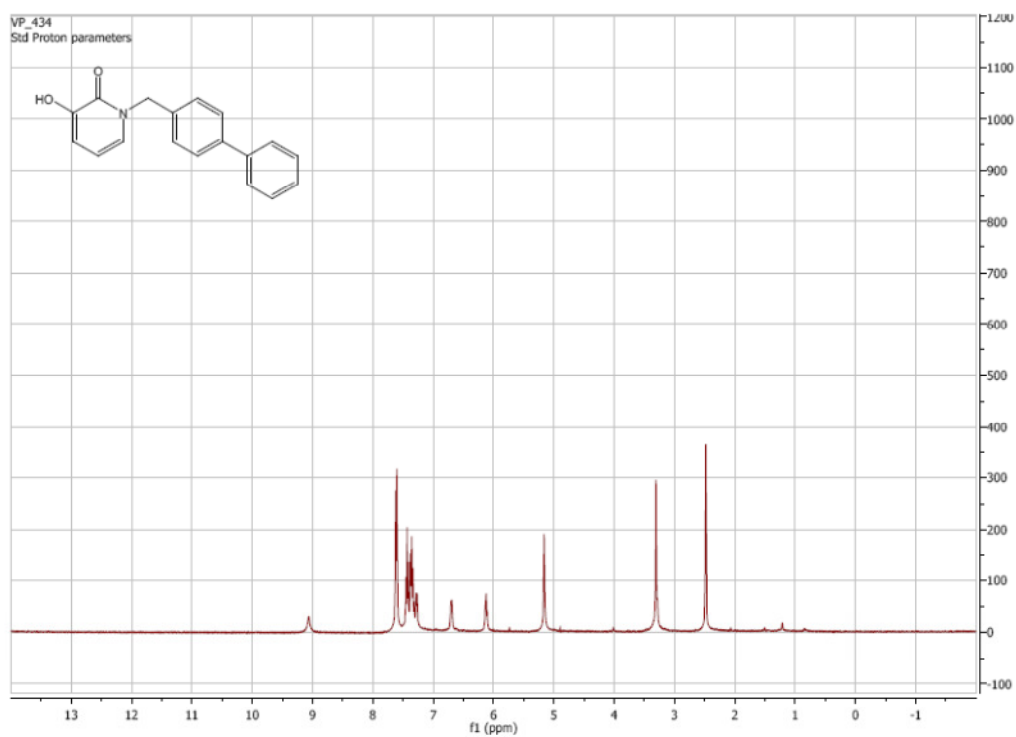
^1H NMR of **5b**:



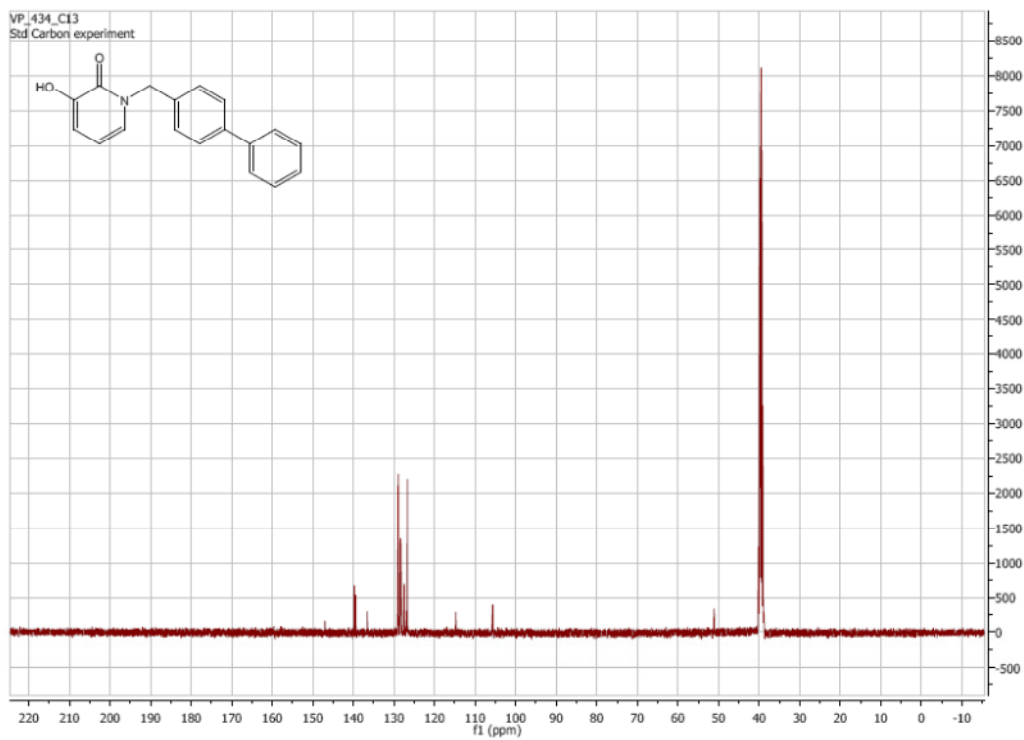
^{13}C NMR of **5b**:



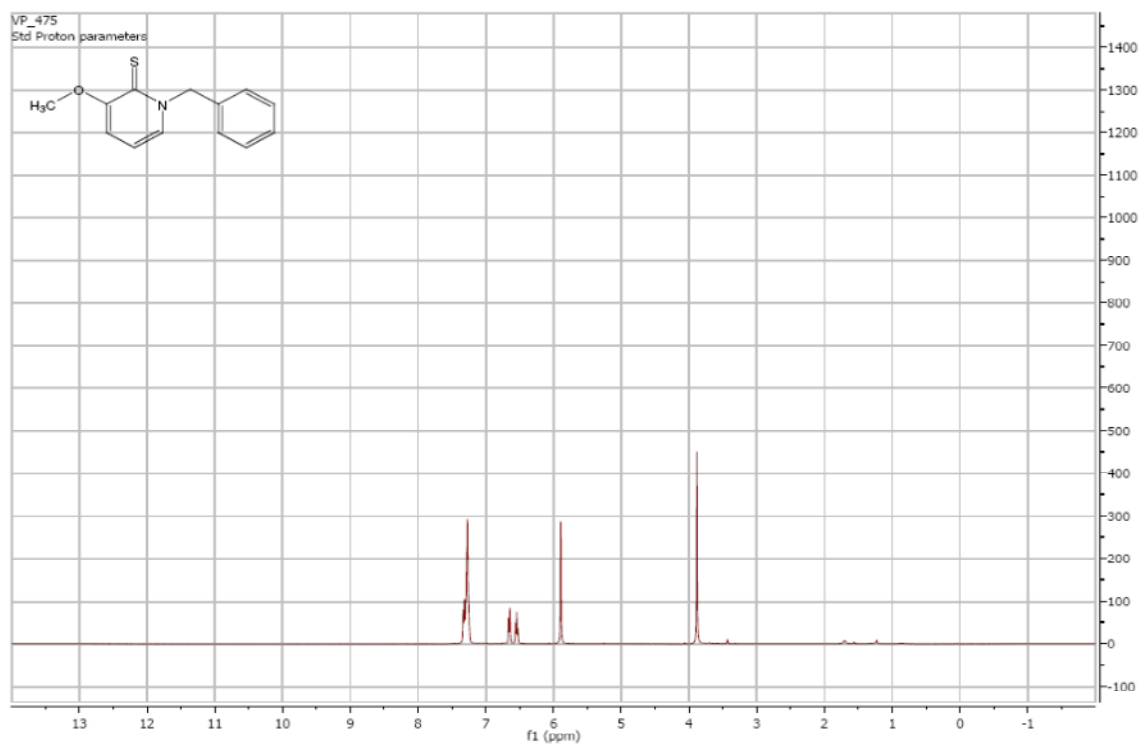
^1H NMR of **5c**:



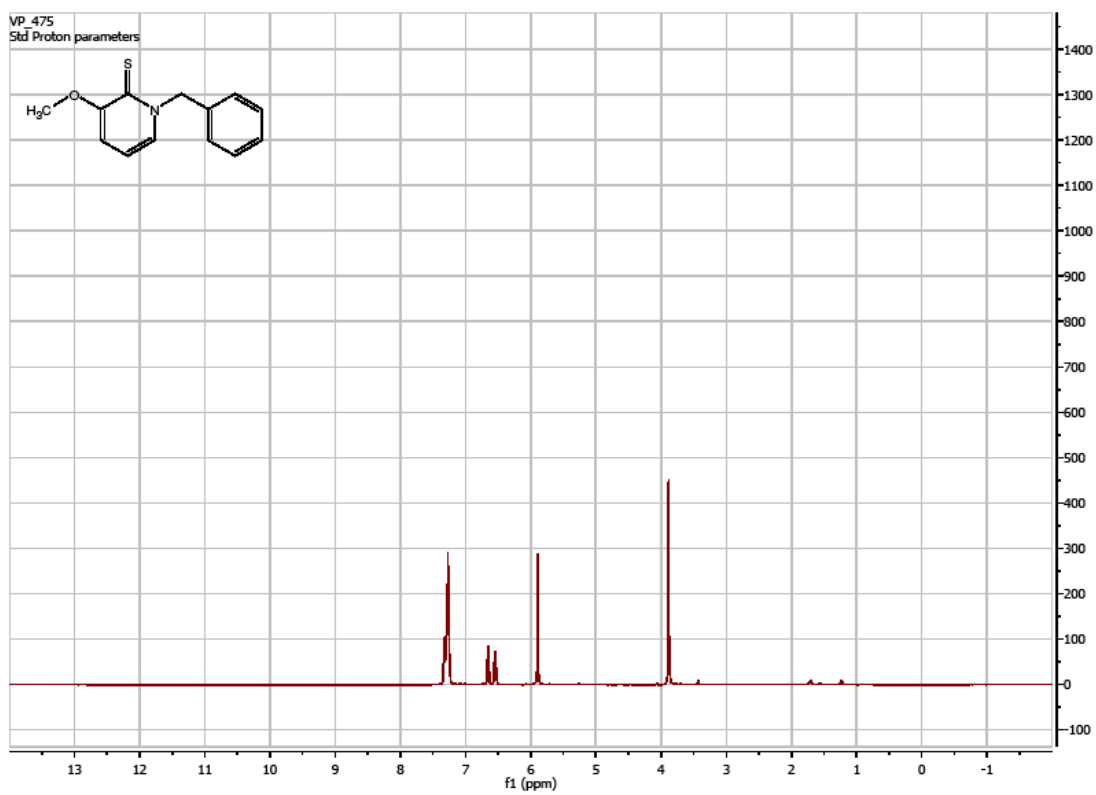
^{13}C NMR of **5c**:



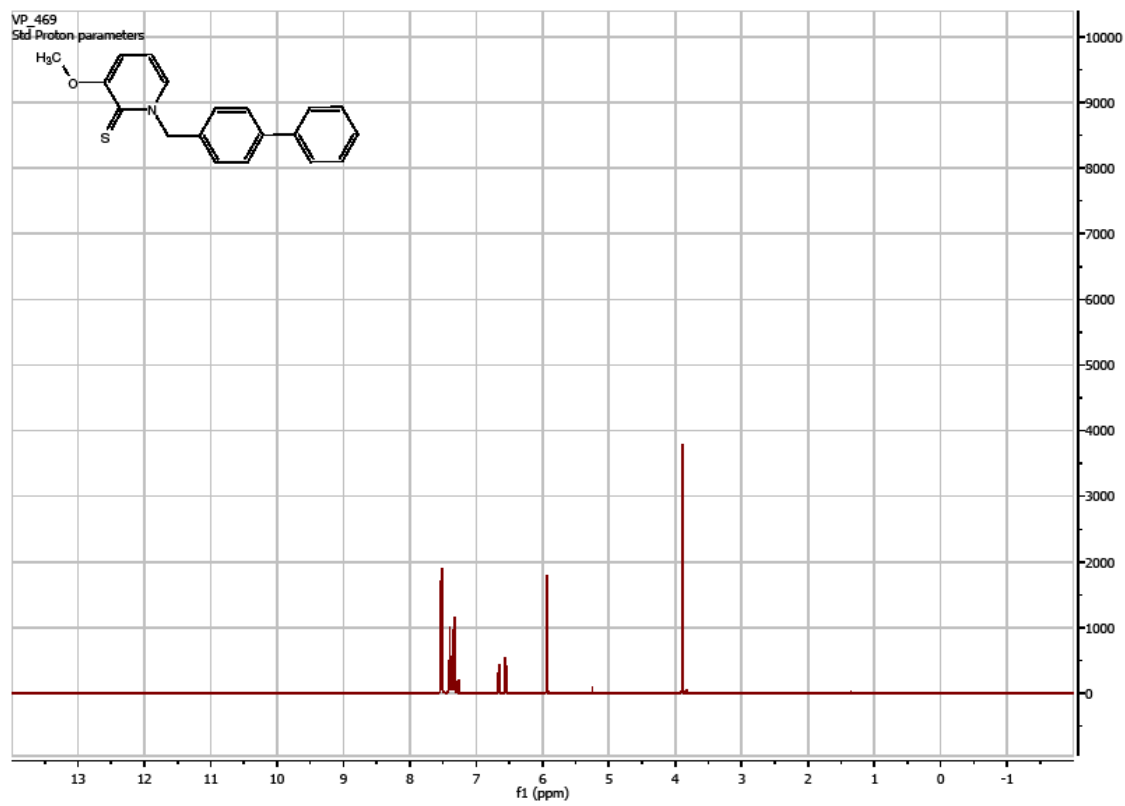
^1H NMR of **6b**:



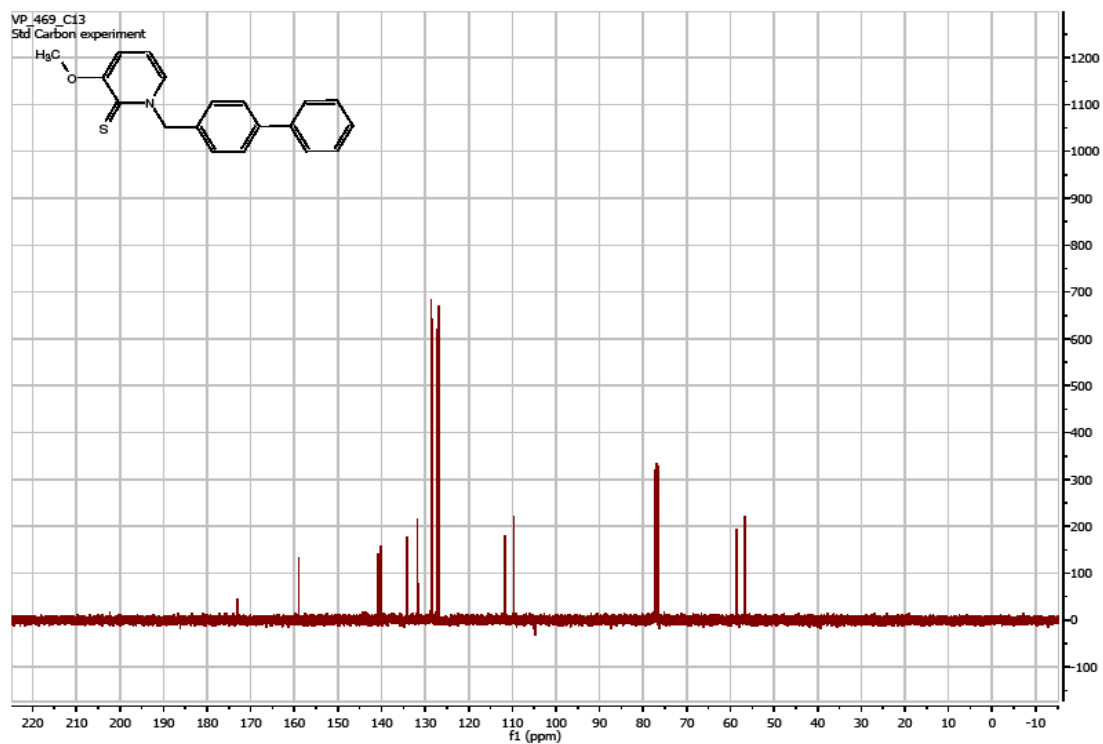
^{13}C NMR of **6b**:



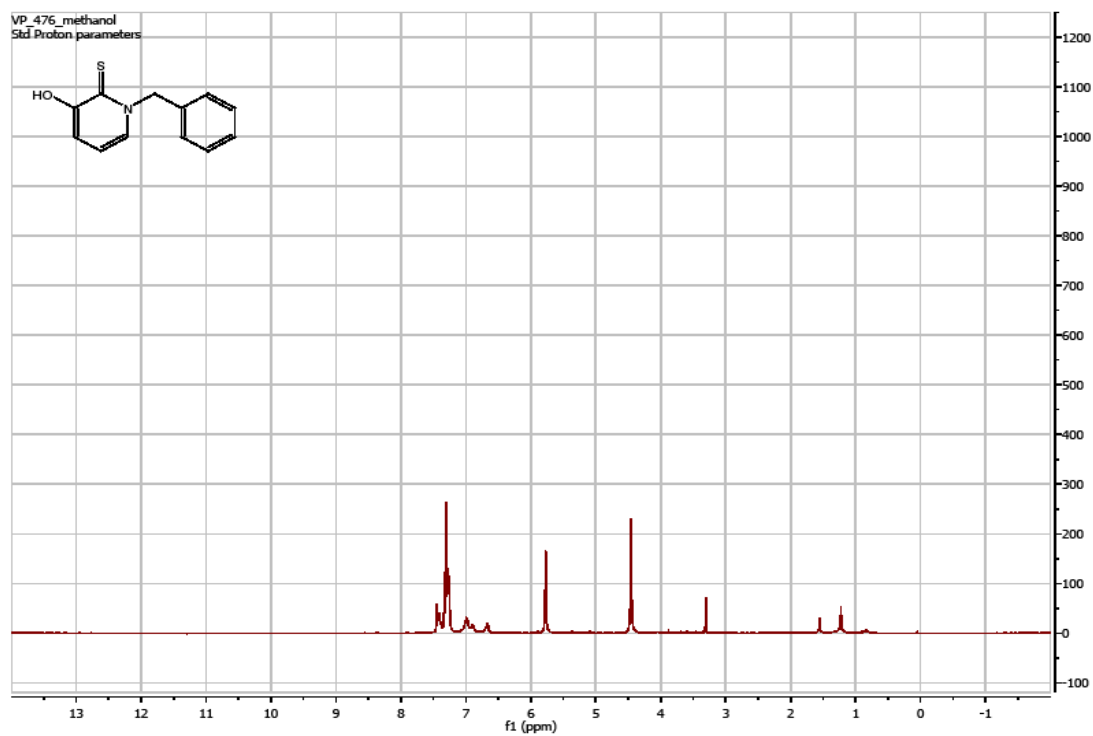
¹H NMR of **6c**:



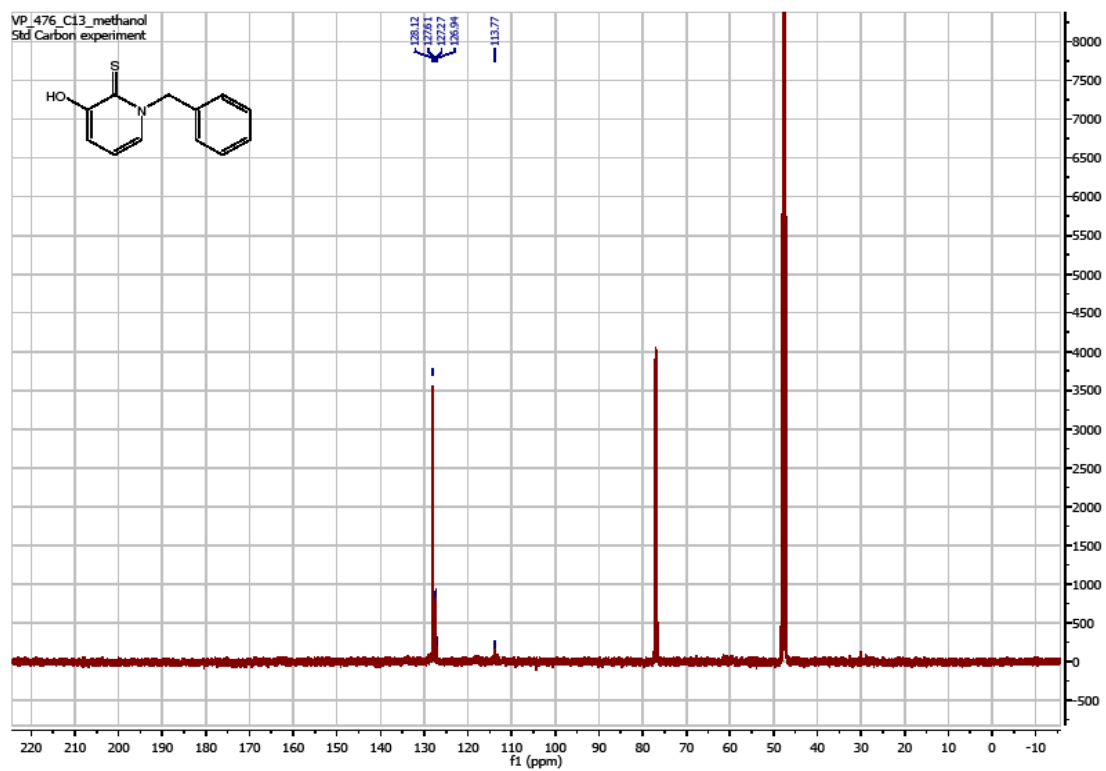
¹³C NMR of **6c**:



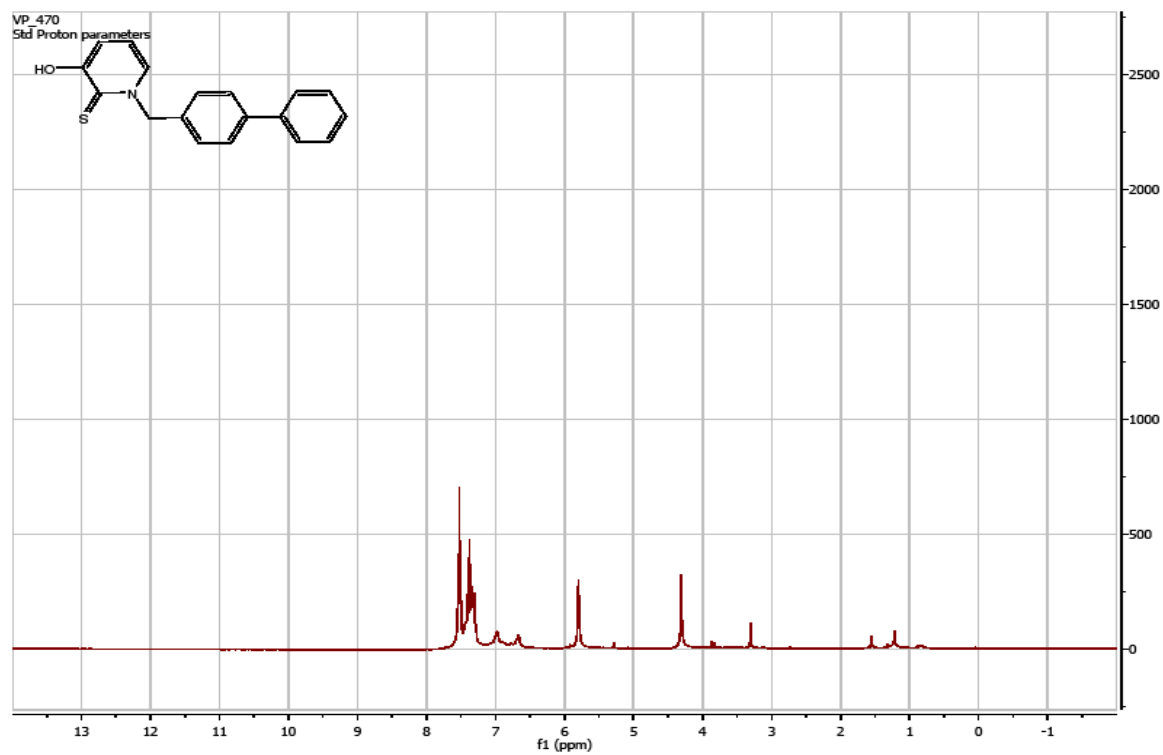
¹H NMR of **7b**:



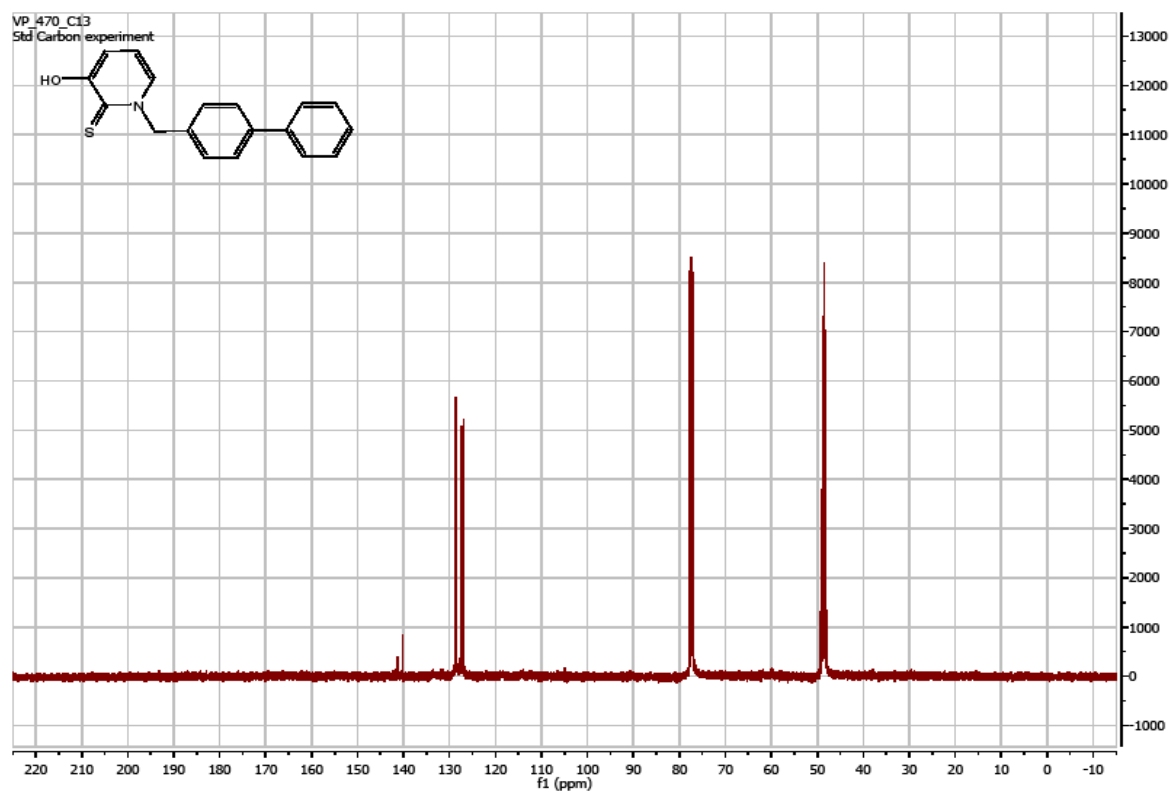
¹³C NMR of **7b**:



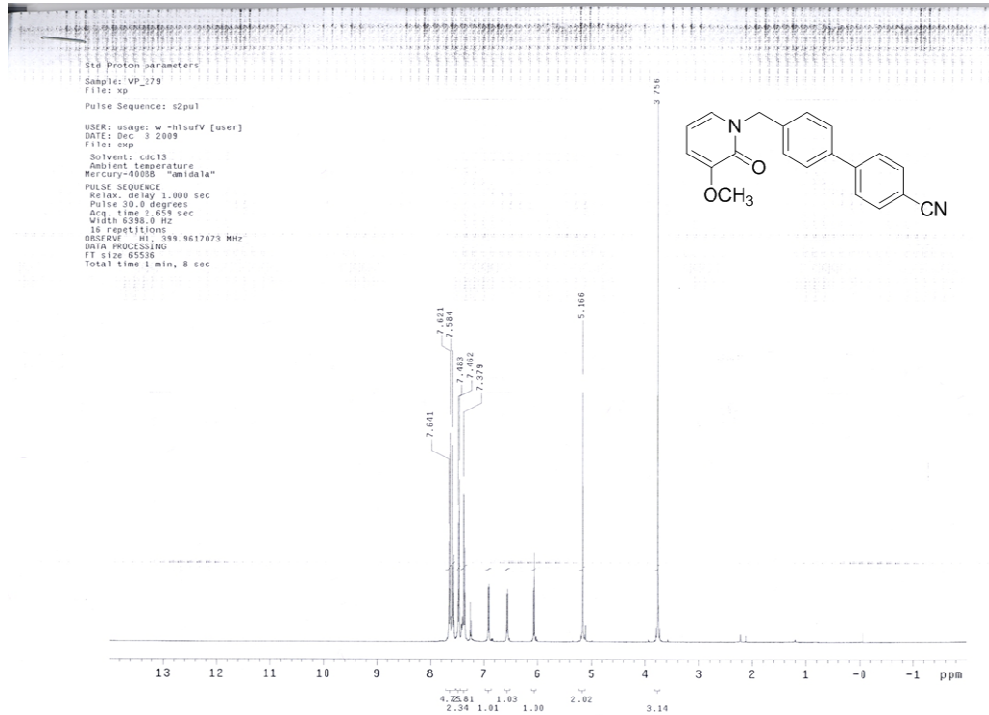
^1H NMR of **7c**:



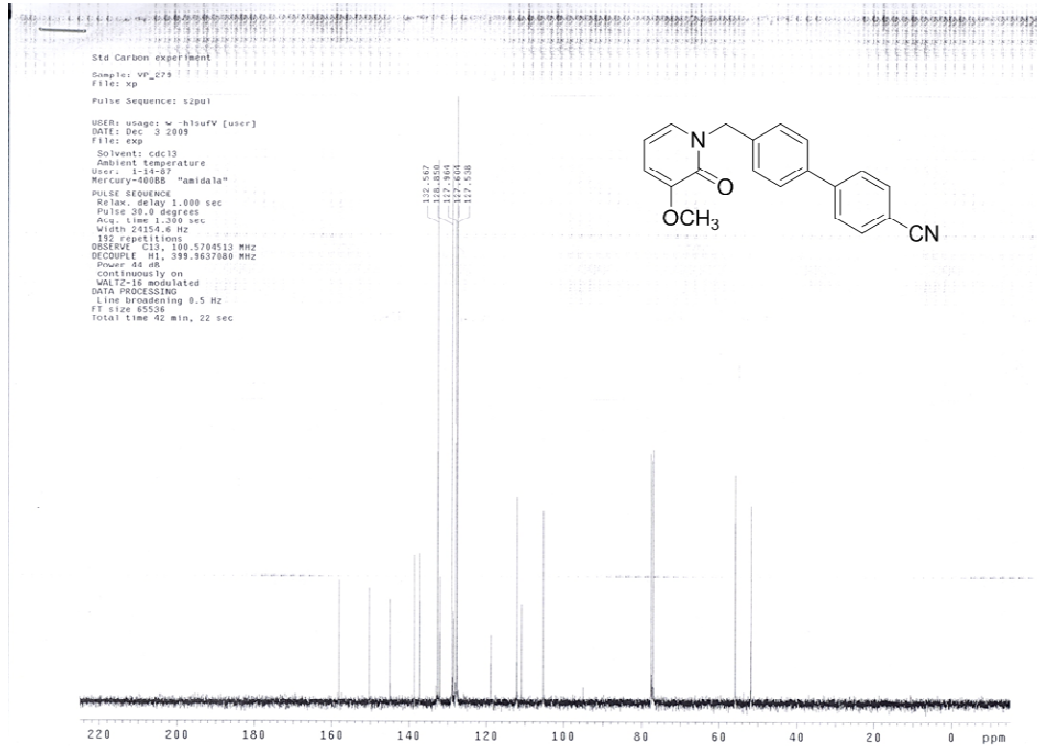
¹³C NMR of 7c:

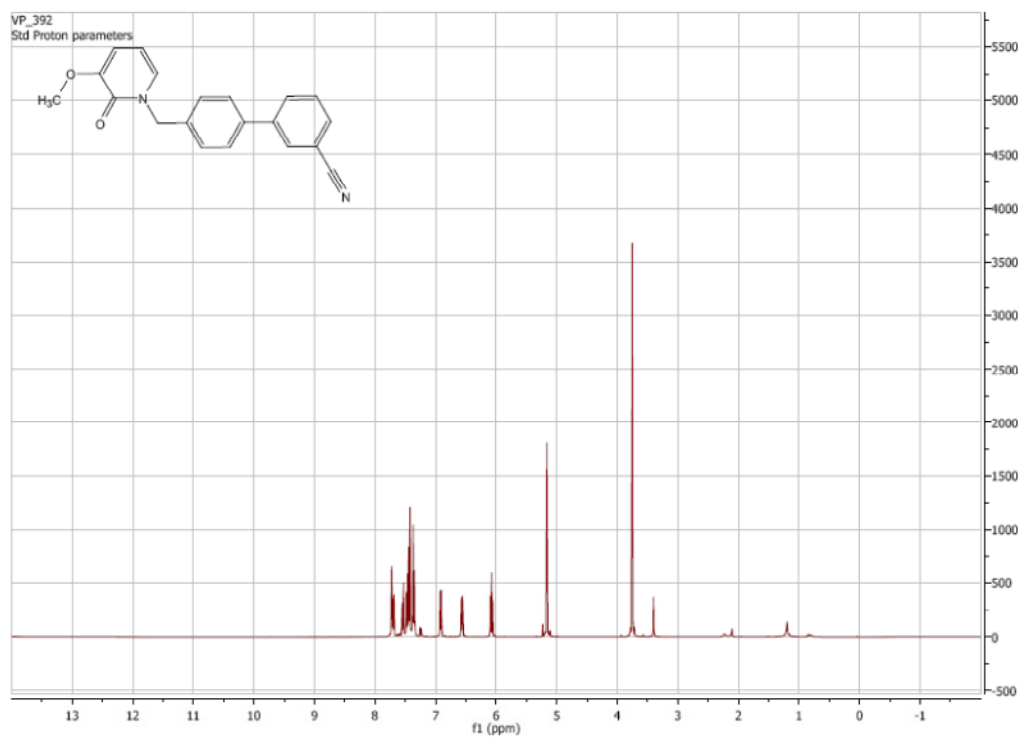
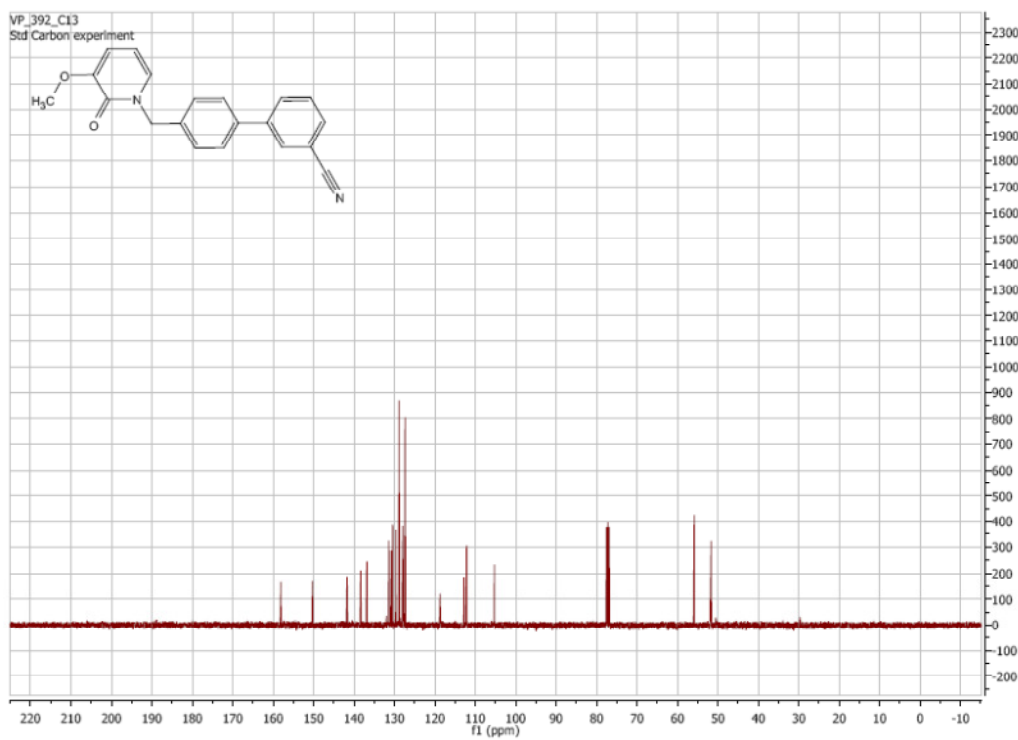


¹H NMR of 9a:

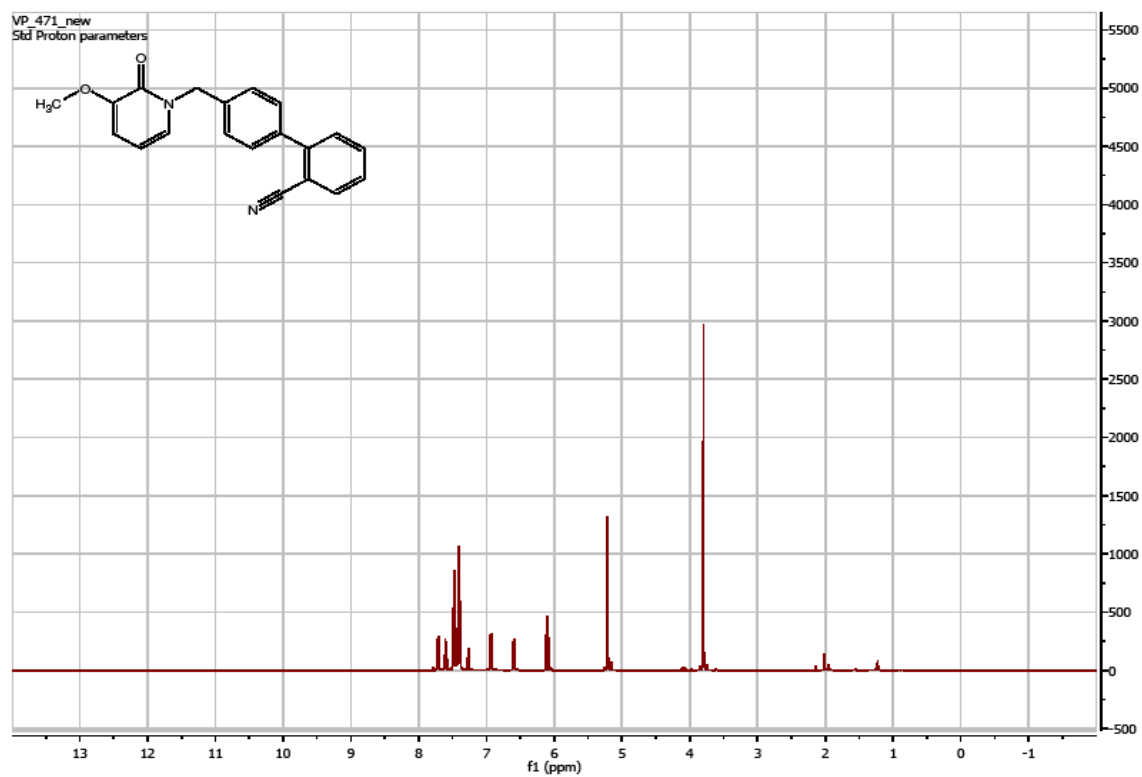


¹³C NMR of 9a:

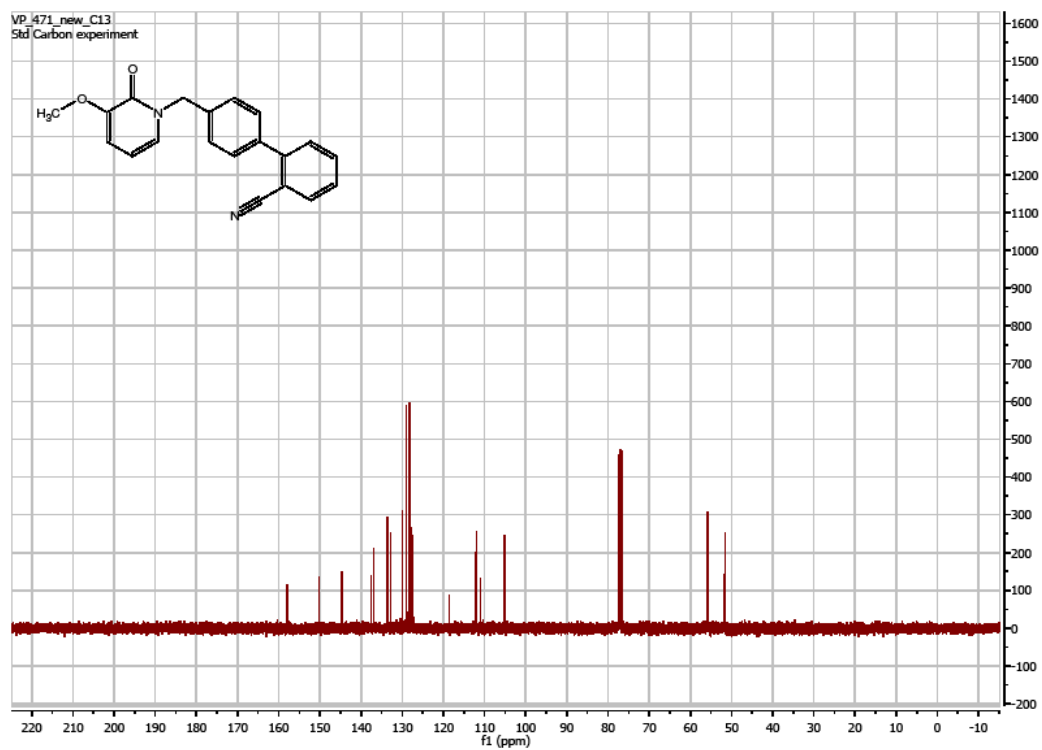


¹H NMR of **9b**: ^{13}C NMR of **9b**

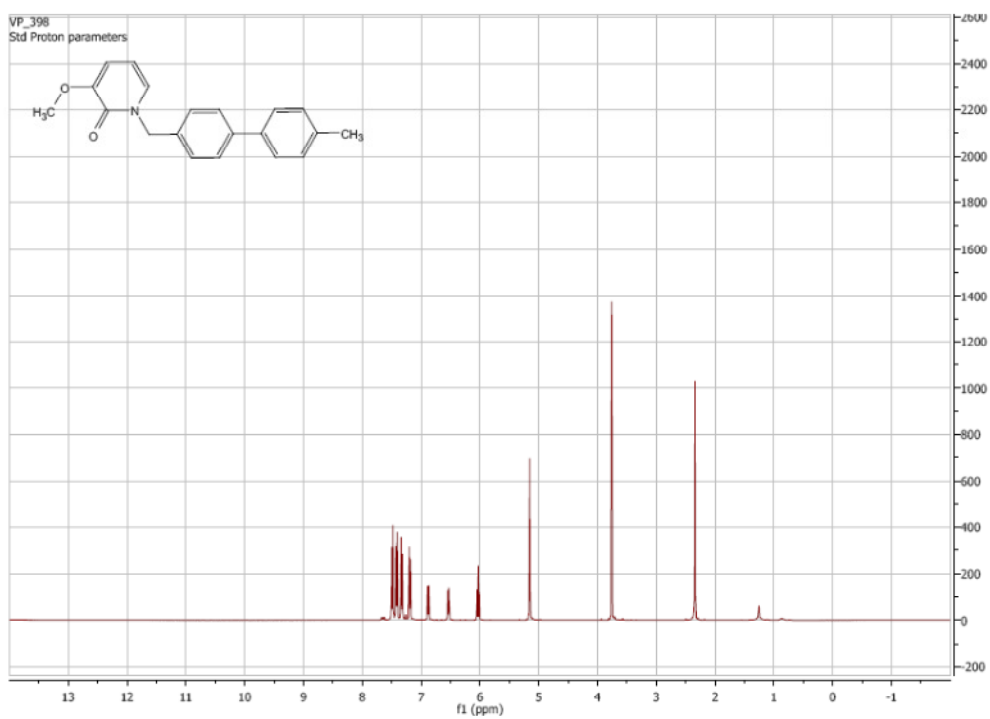
^1H NMR of **9c**:



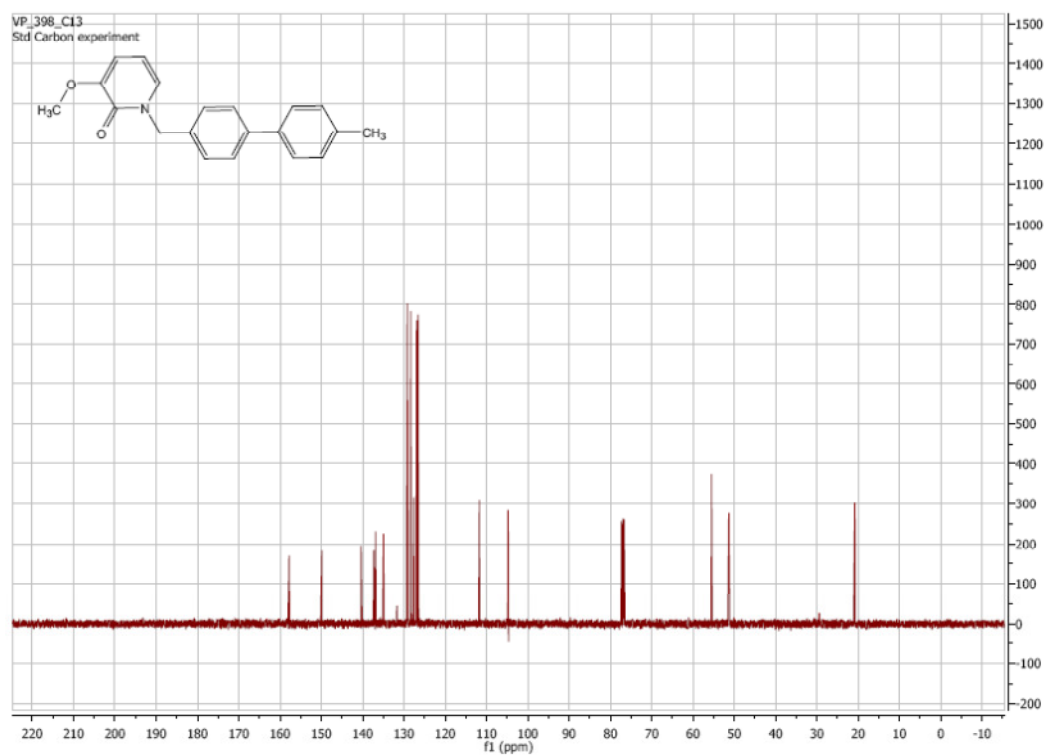
^{13}C NMR of **9c**:



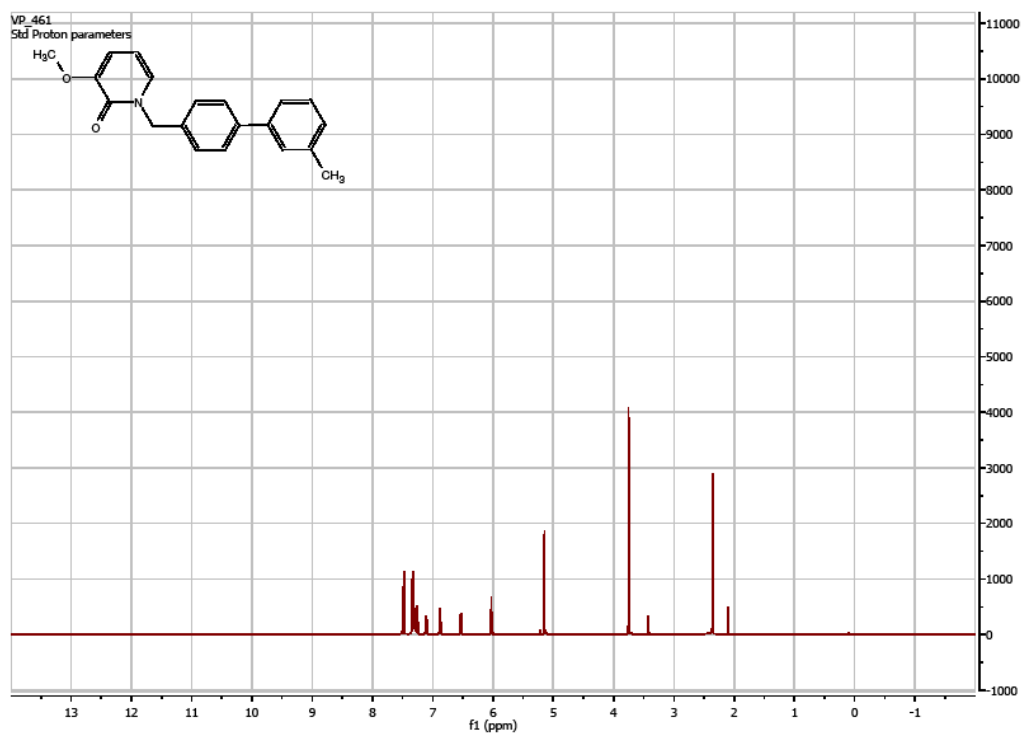
¹H NMR of **9d**:



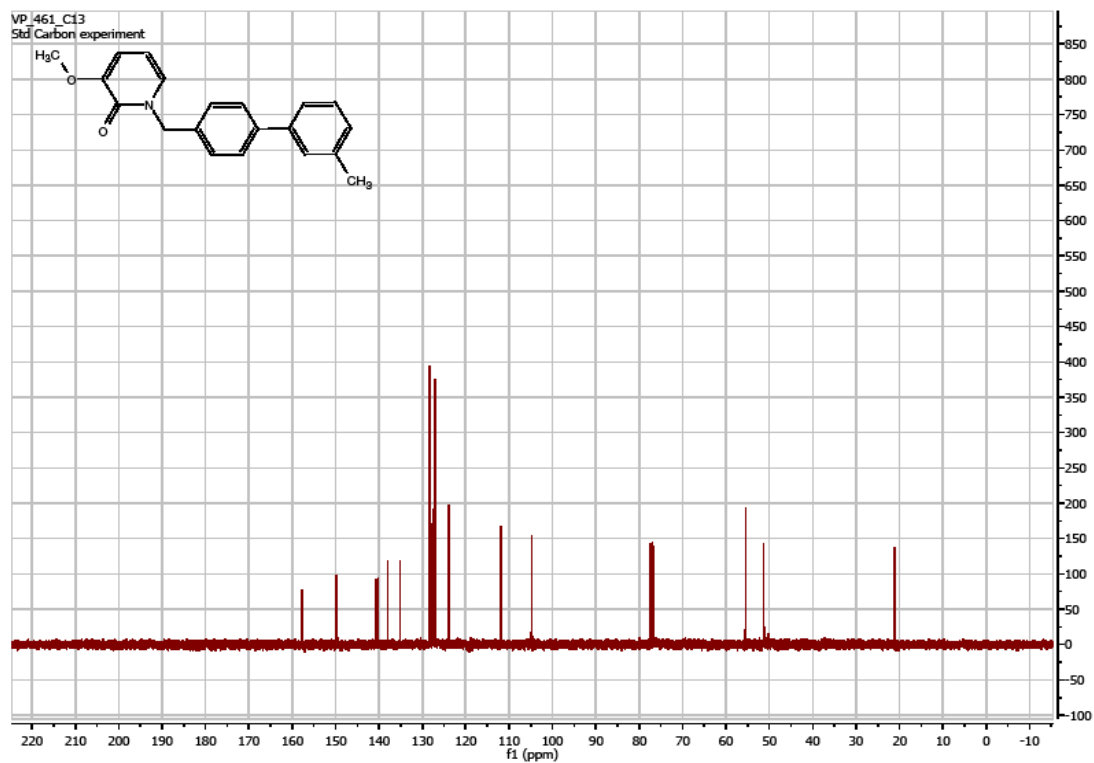
¹H NMR of **9d**:



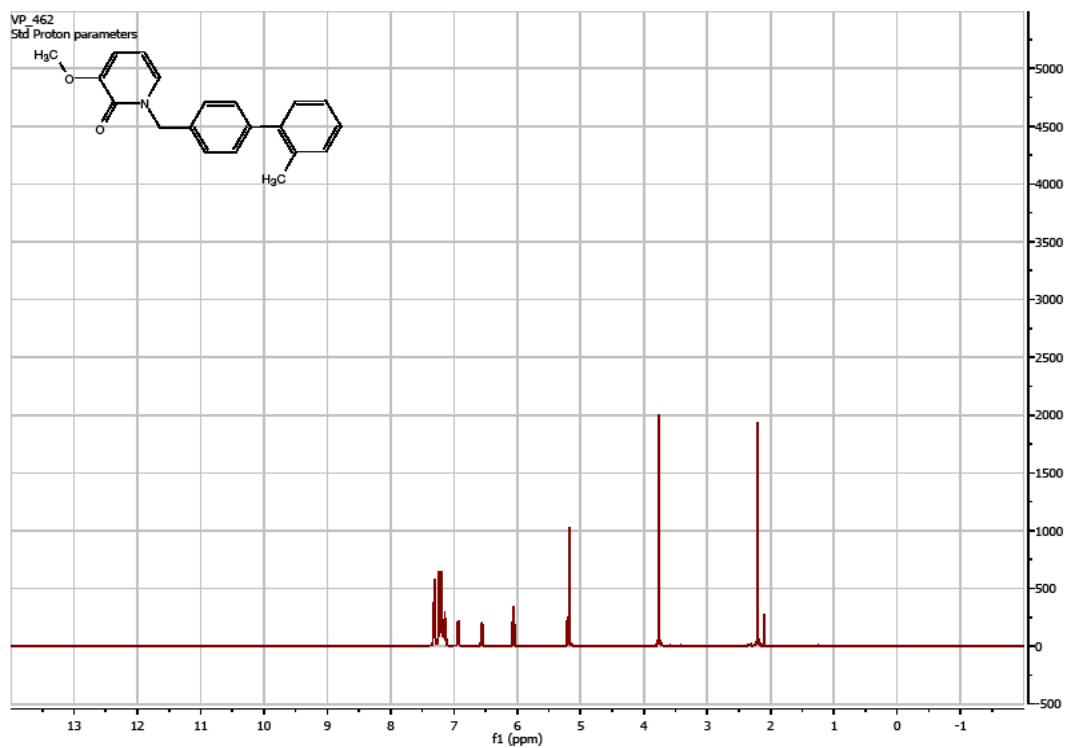
¹H NMR of 9e:



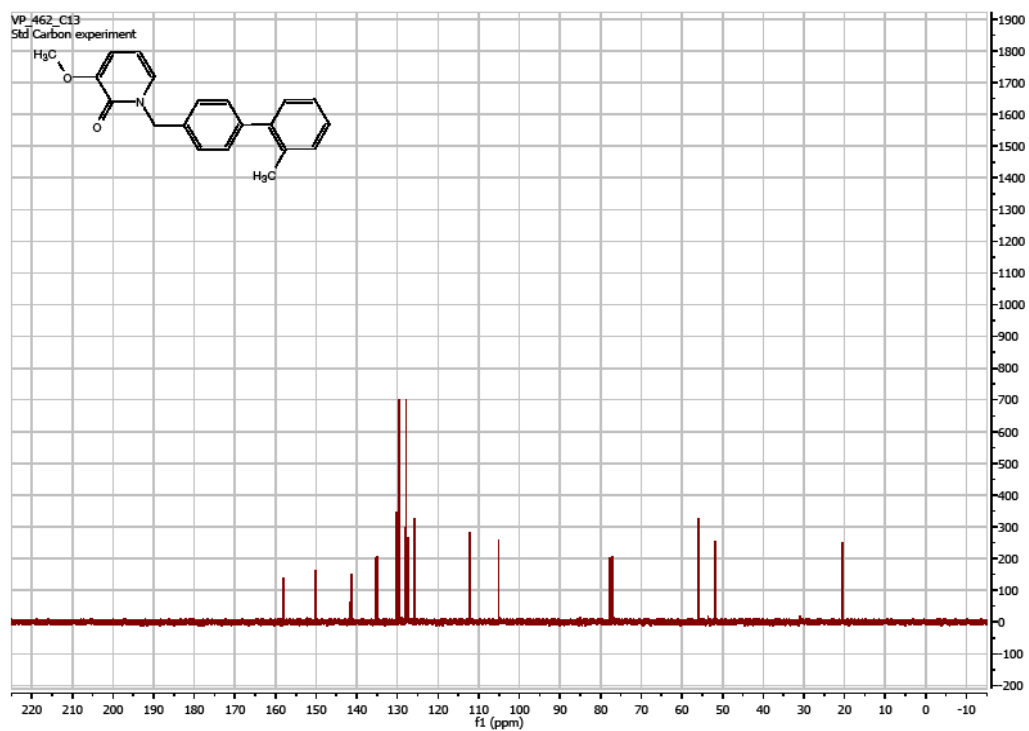
¹³C NMR of 9e:



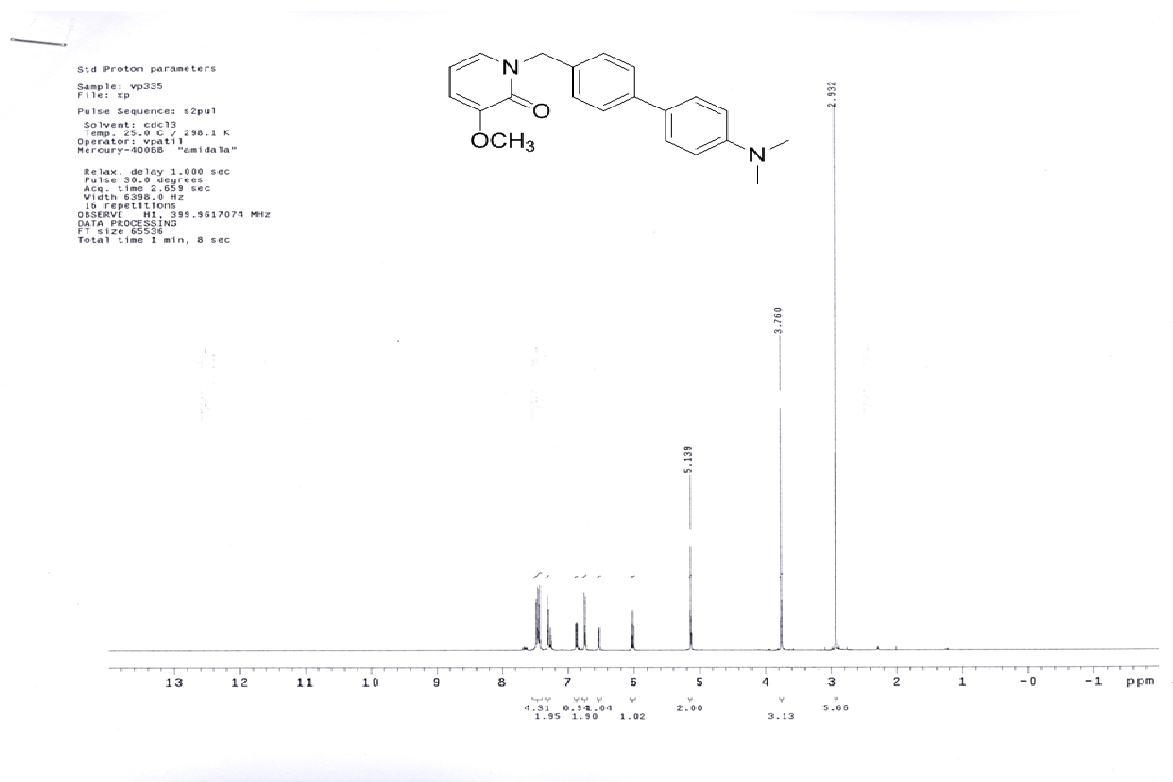
¹H NMR of **9f**:



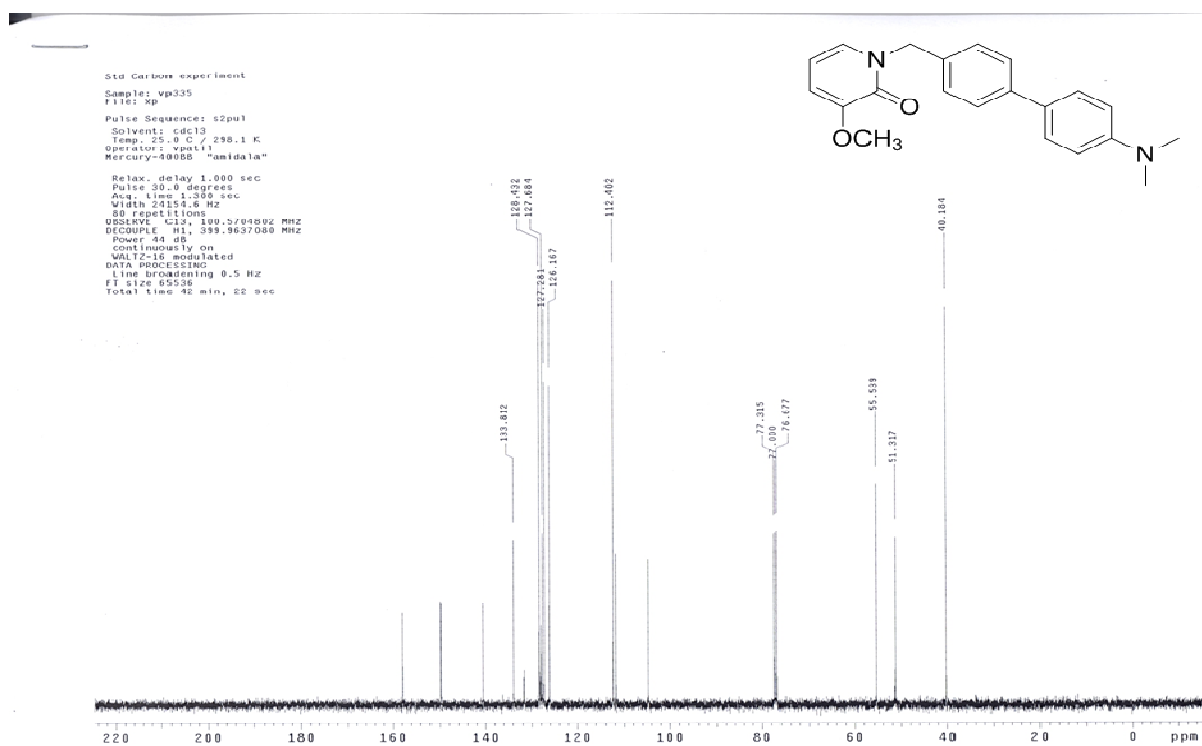
^{13}C NMR of **9f**:



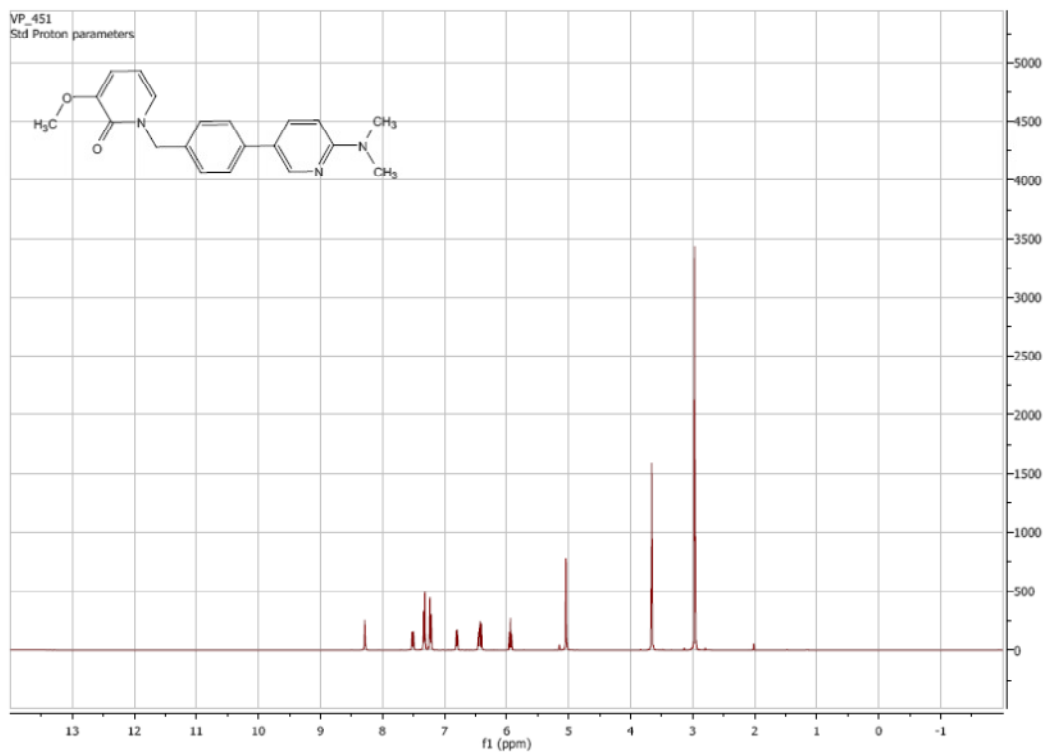
^1H NMR of **9g**:



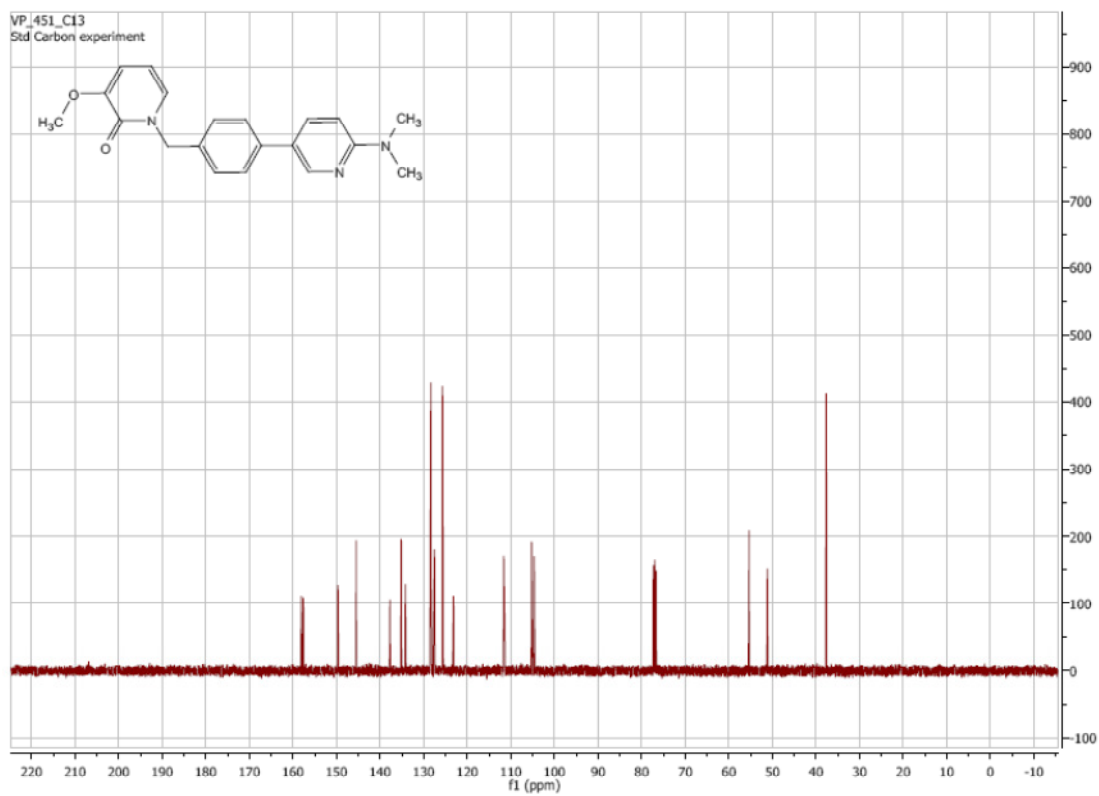
¹³C NMR of 9g:



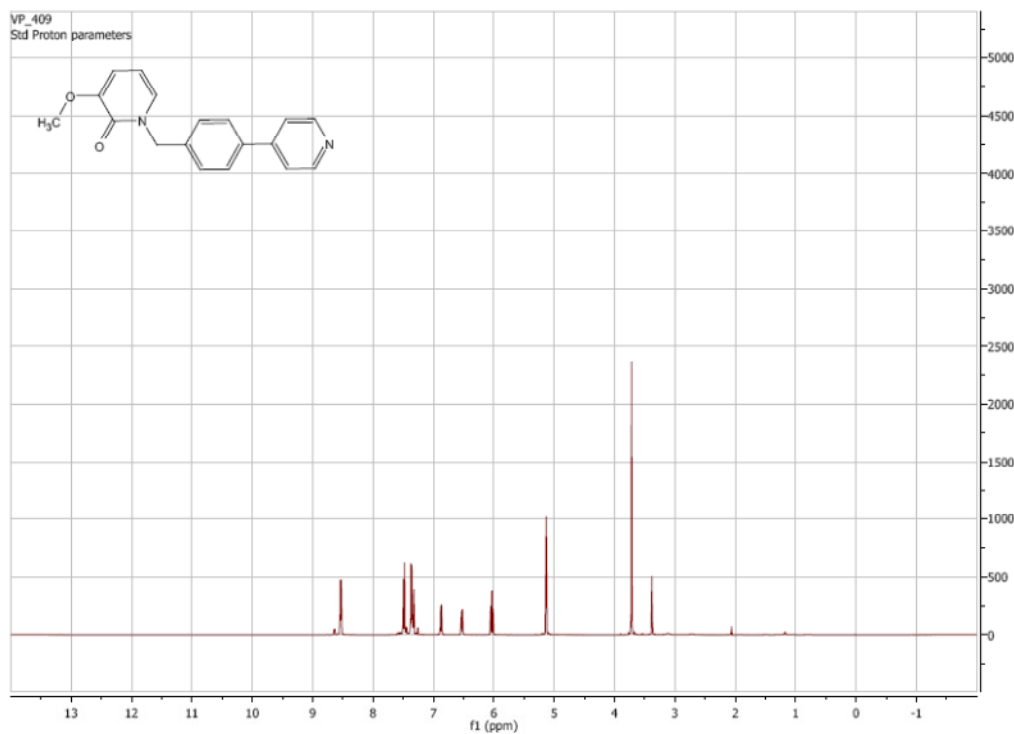
¹H NMR of 9h:



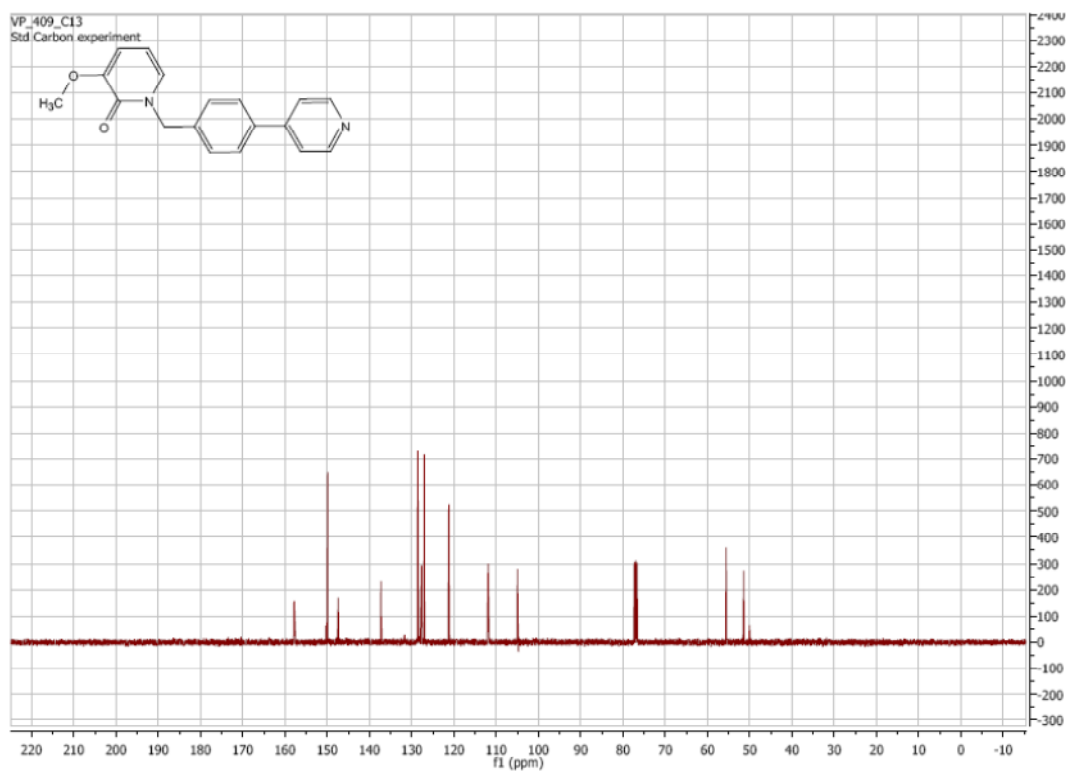
¹³C NMR of **9h**:



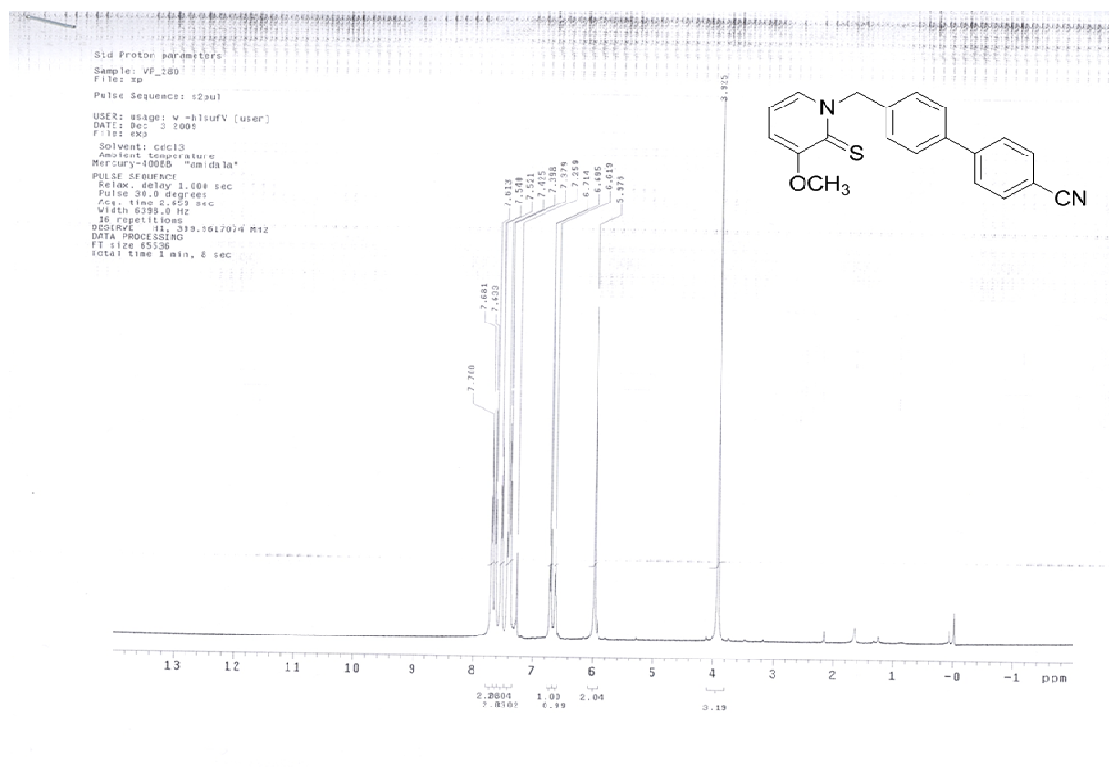
¹H NMR of **9i**:



¹³C NMR of **9i**:



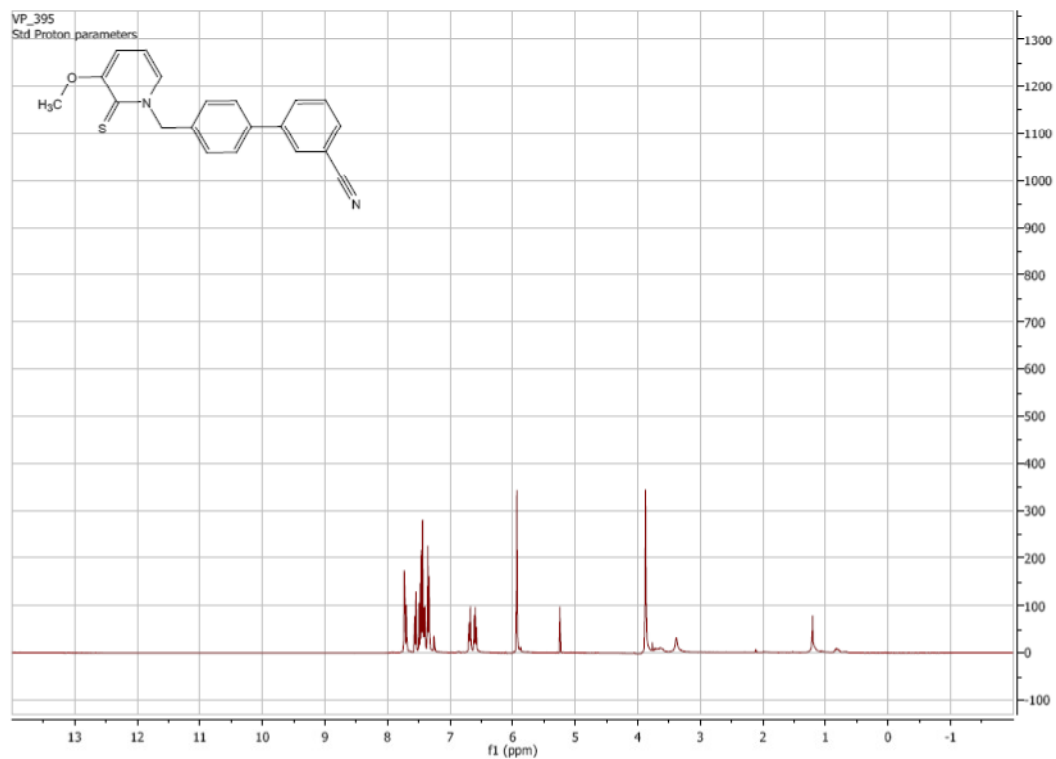
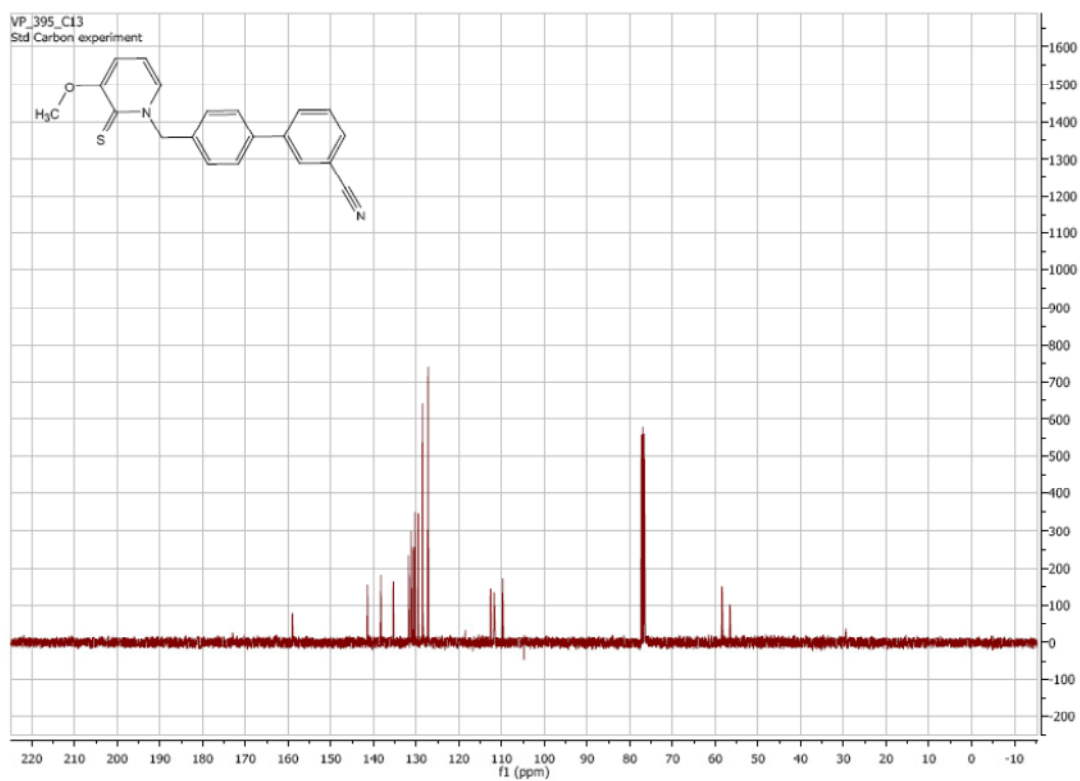
¹H NMR of **10a**:



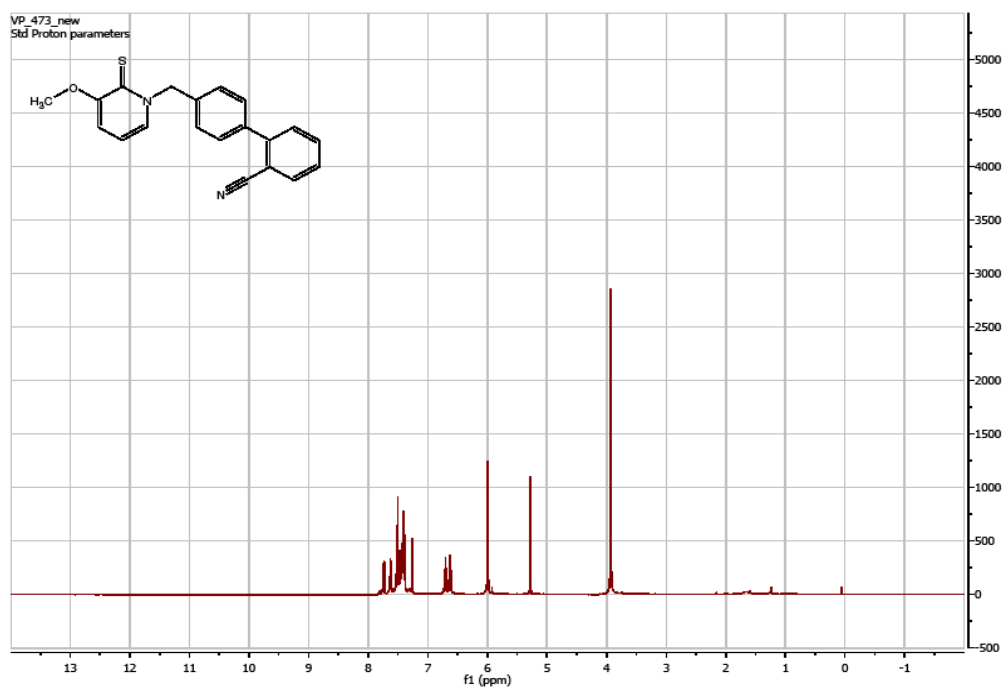
¹³C NMR of 10a:



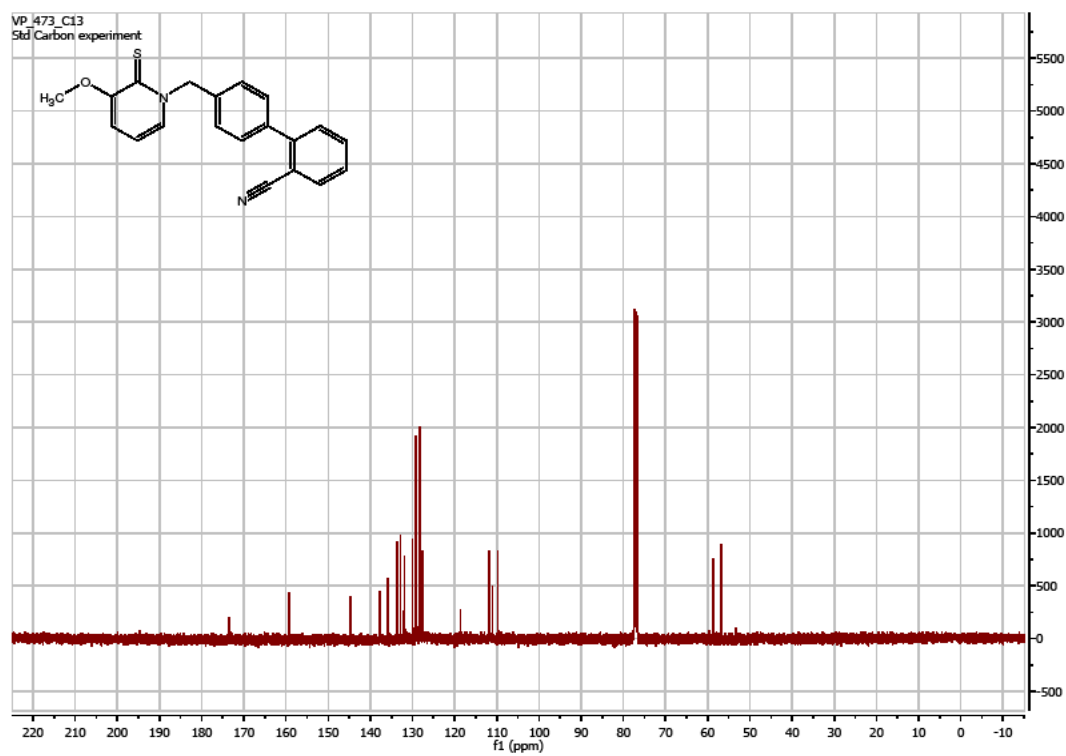
¹H NMR of 10b:

¹H NMR of **10b**:

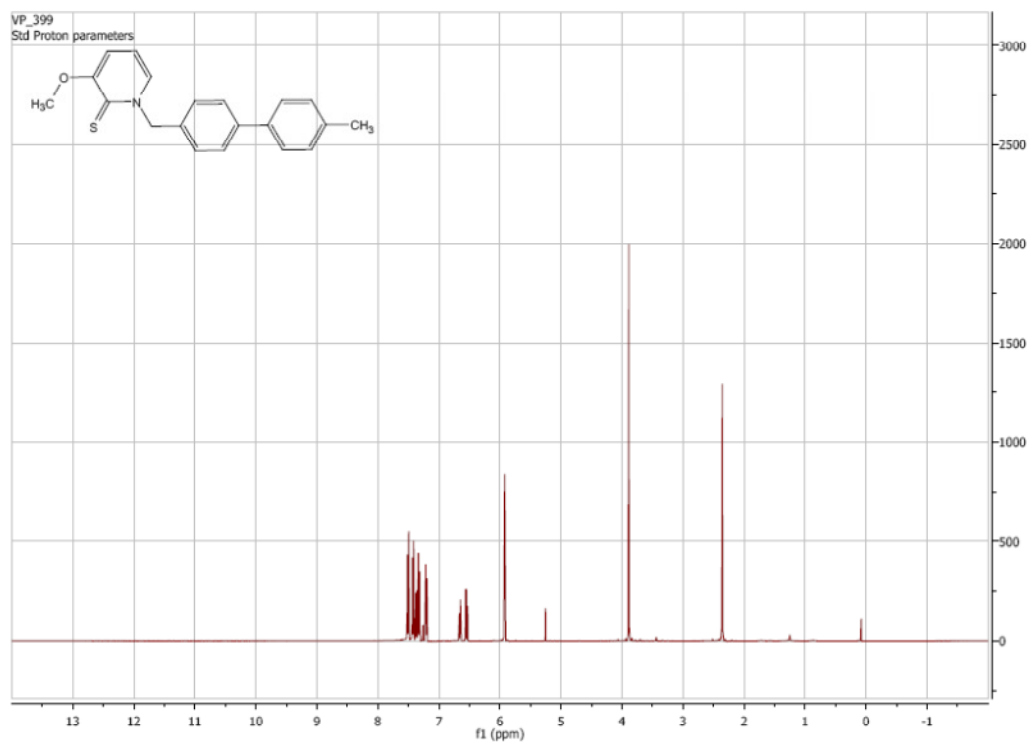
¹H NMR of **10c**:



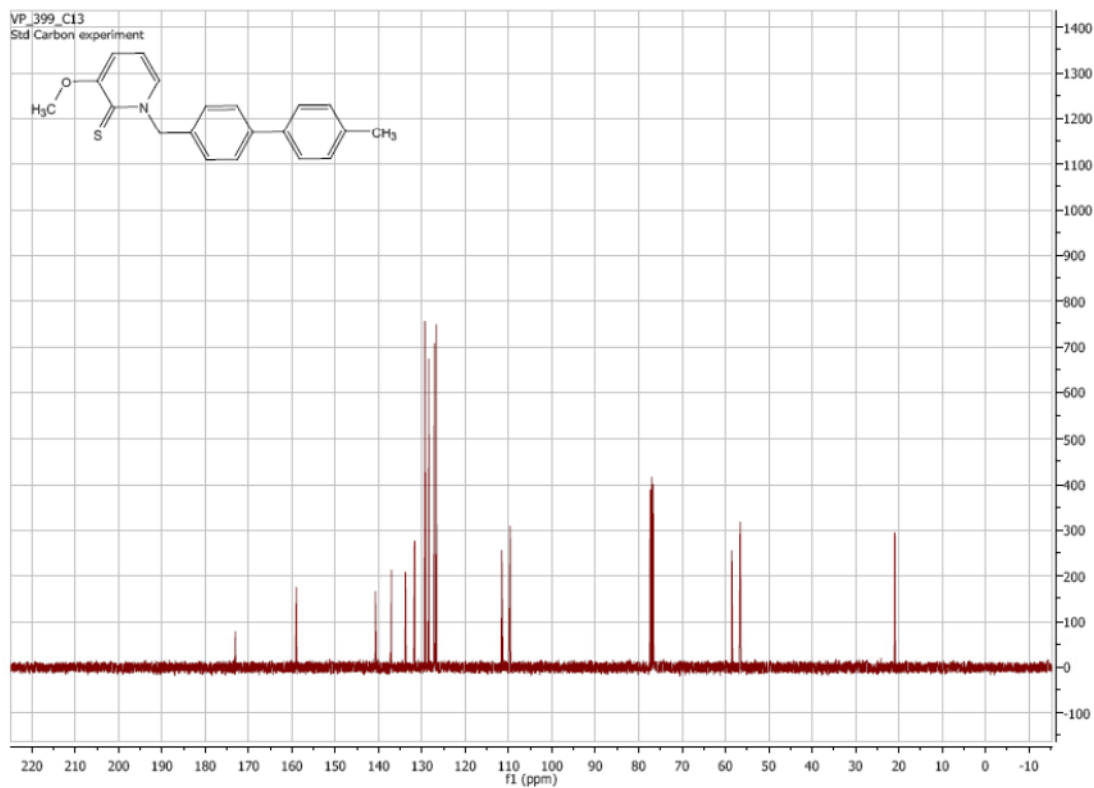
¹³C NMR **10c**:

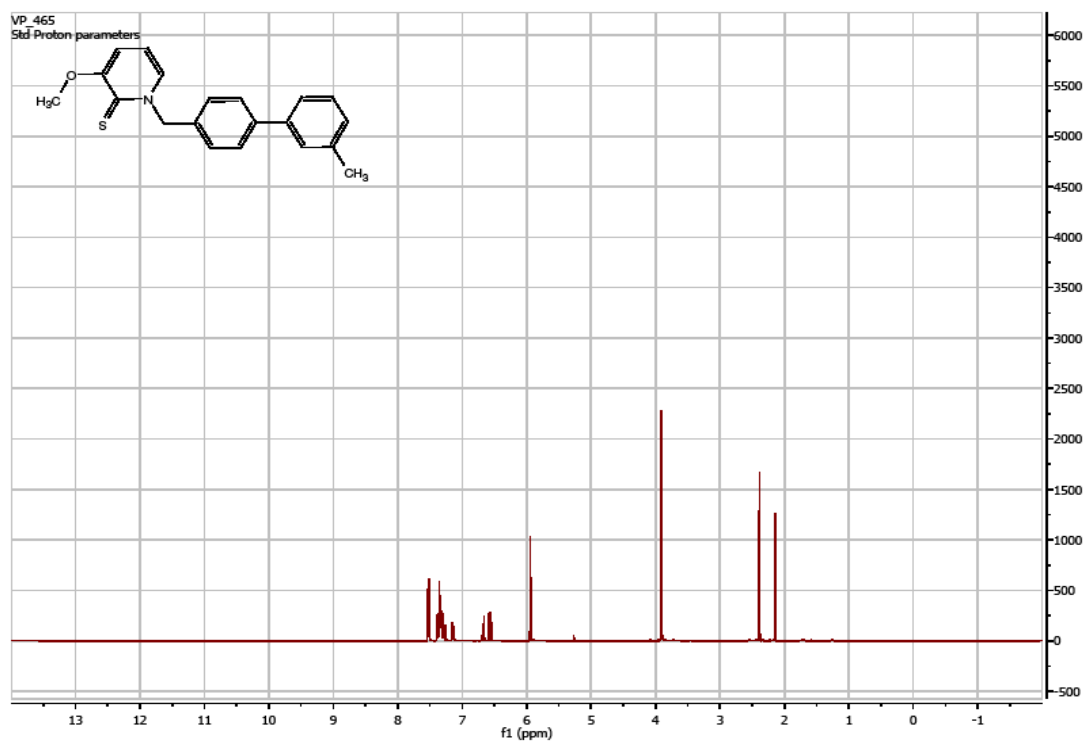
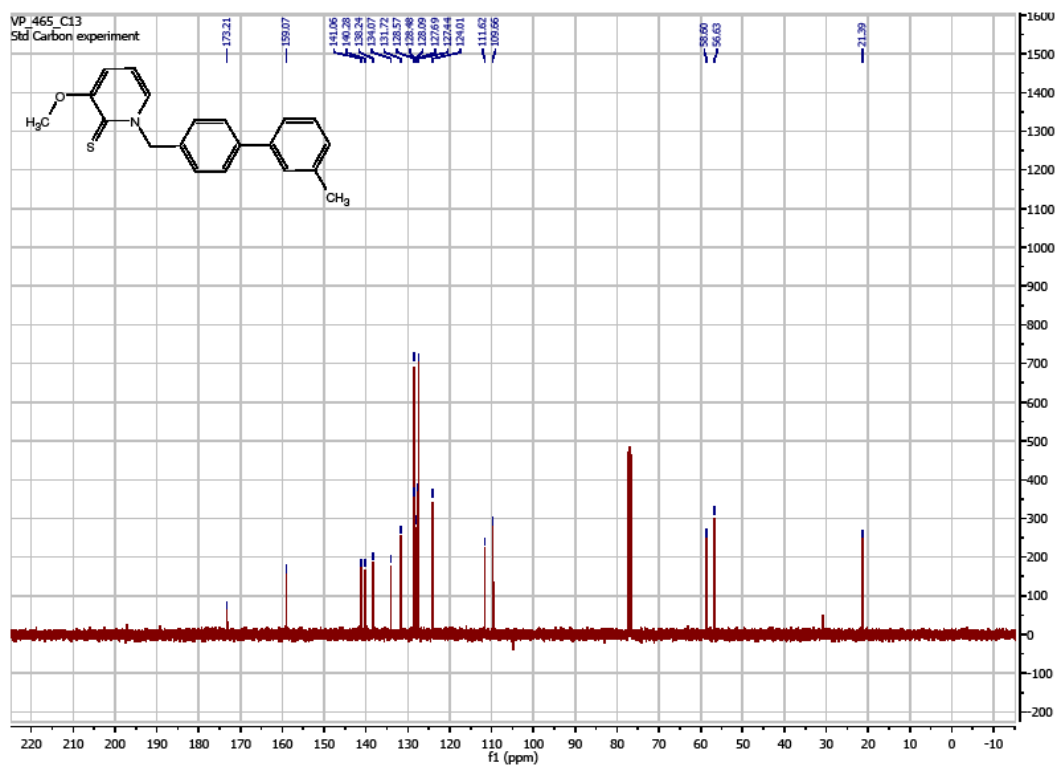


^1H NMR of **10d**:

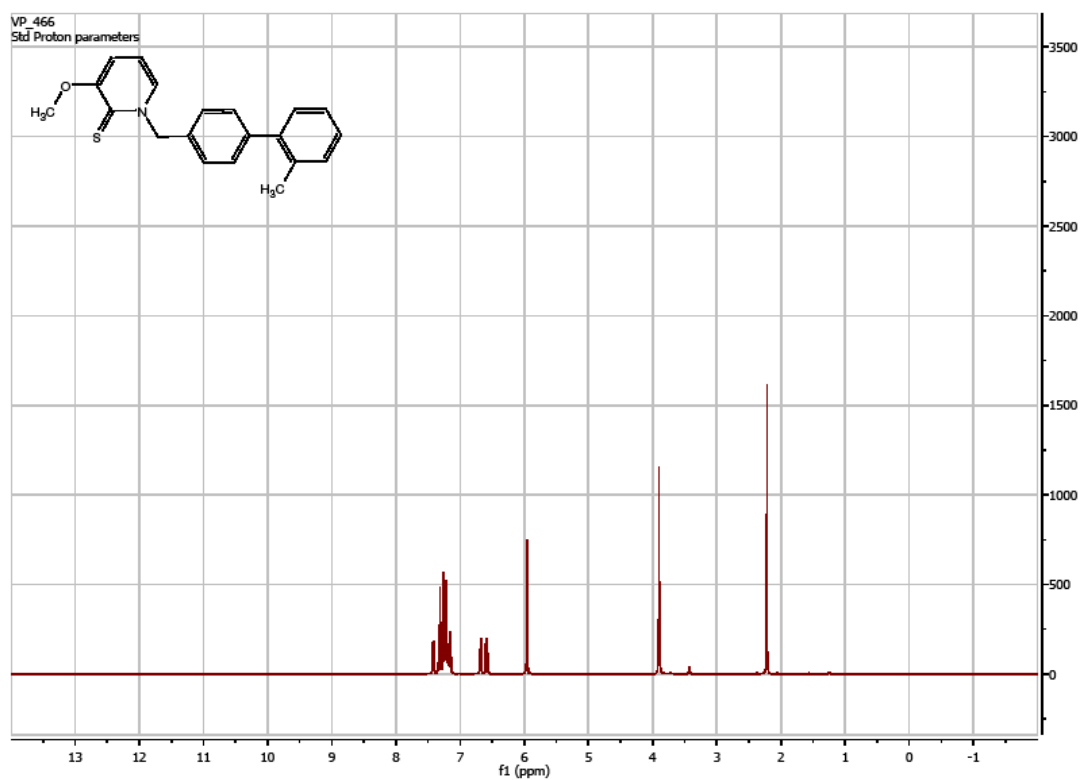


^{13}C NMR of **10d**:

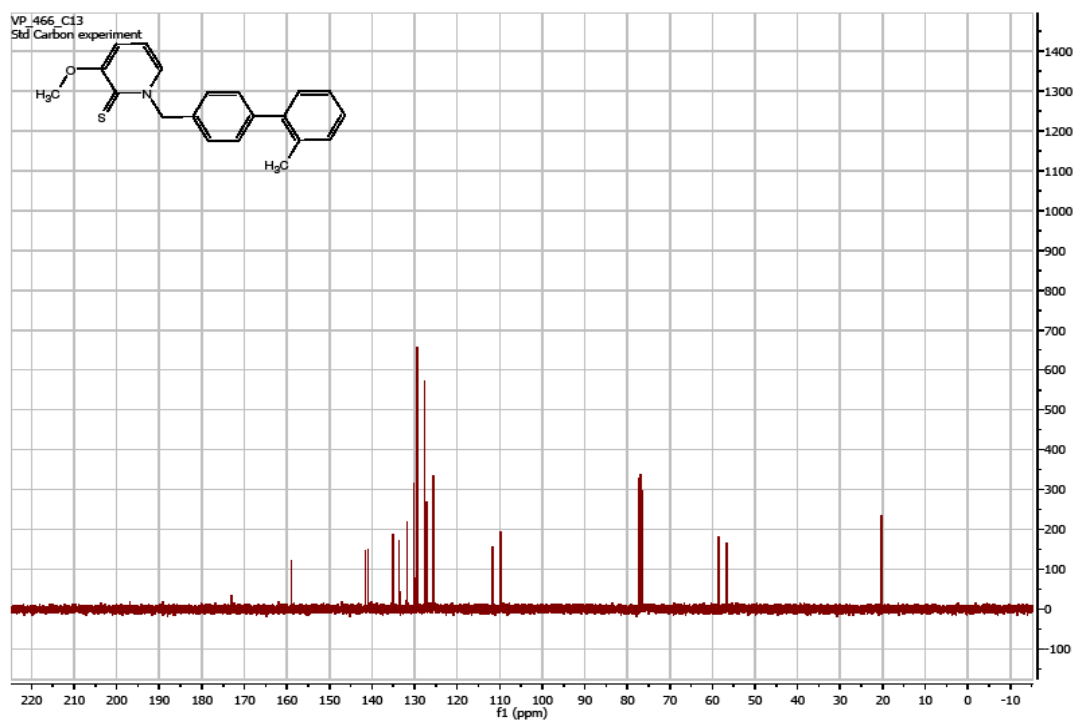


¹H NMR of **10e**: ^{13}C NMR of **10e**:

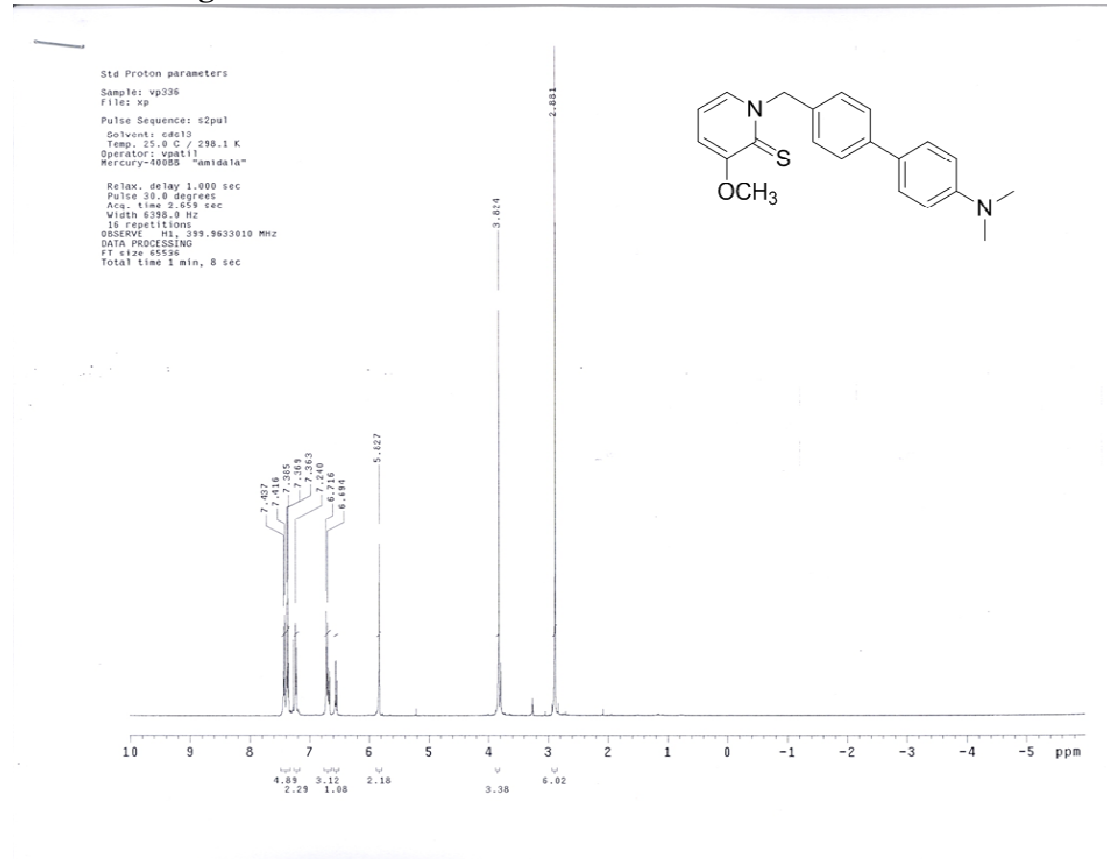
^1H NMR of **10f**:



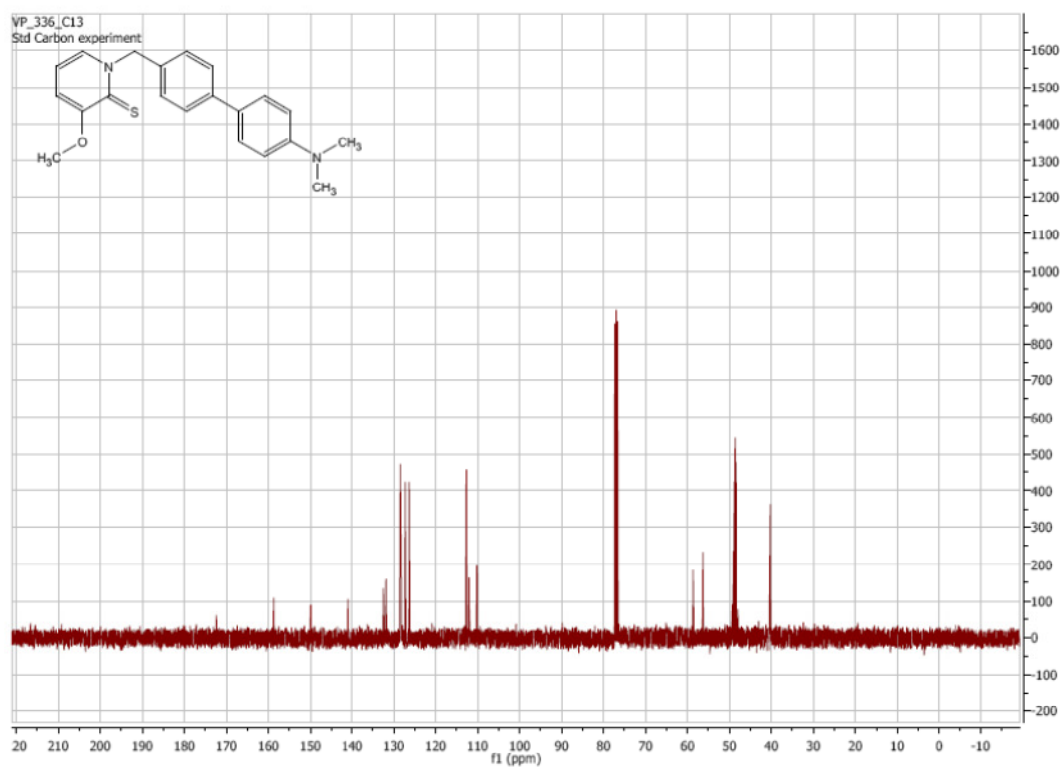
^{13}C NMR of **10f**:



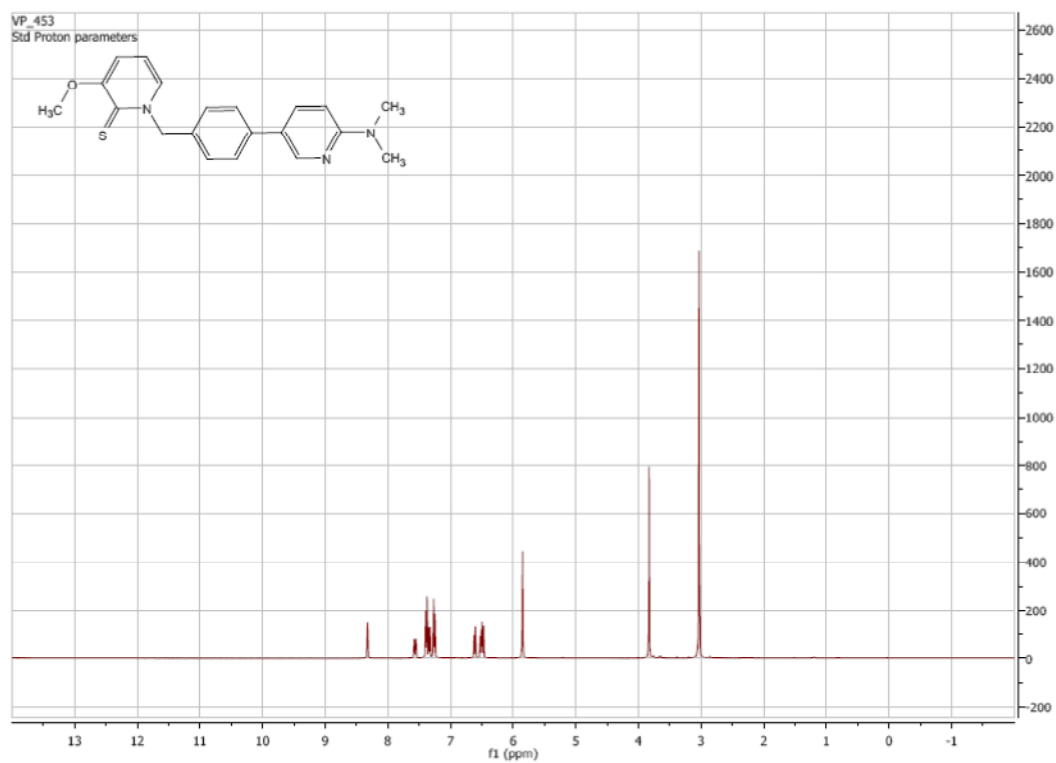
¹H NMR of 10g:



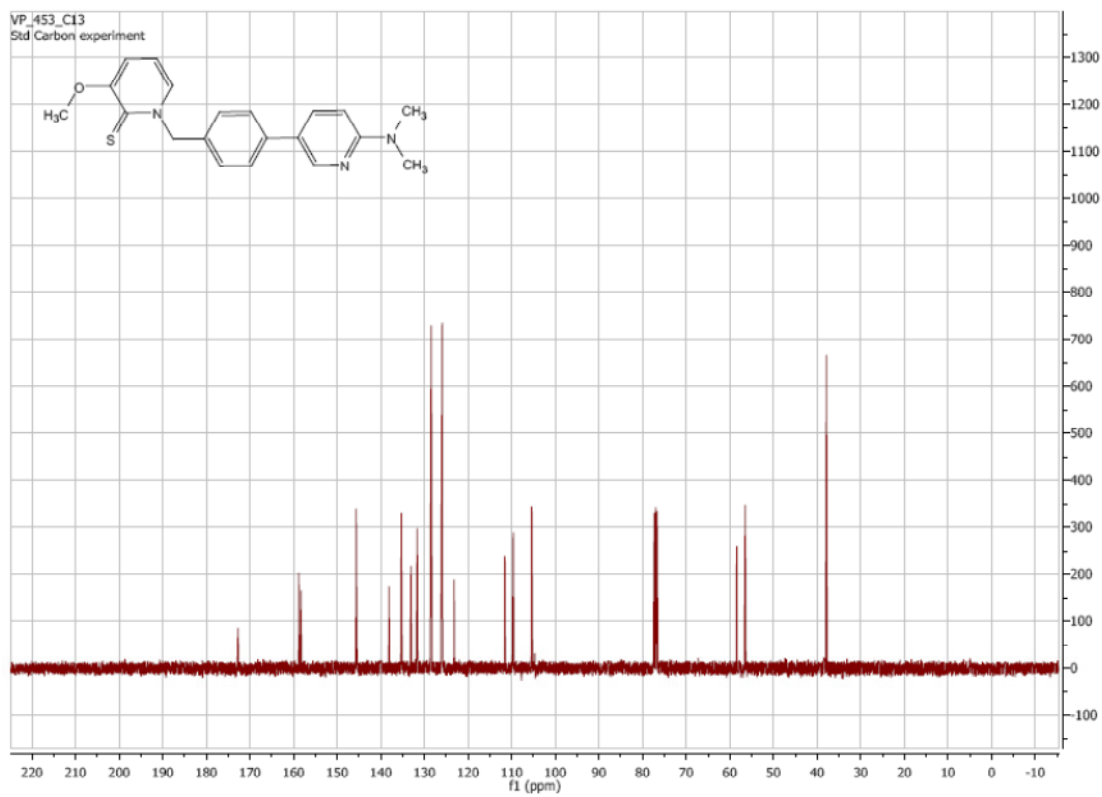
¹³C NMR of 10g



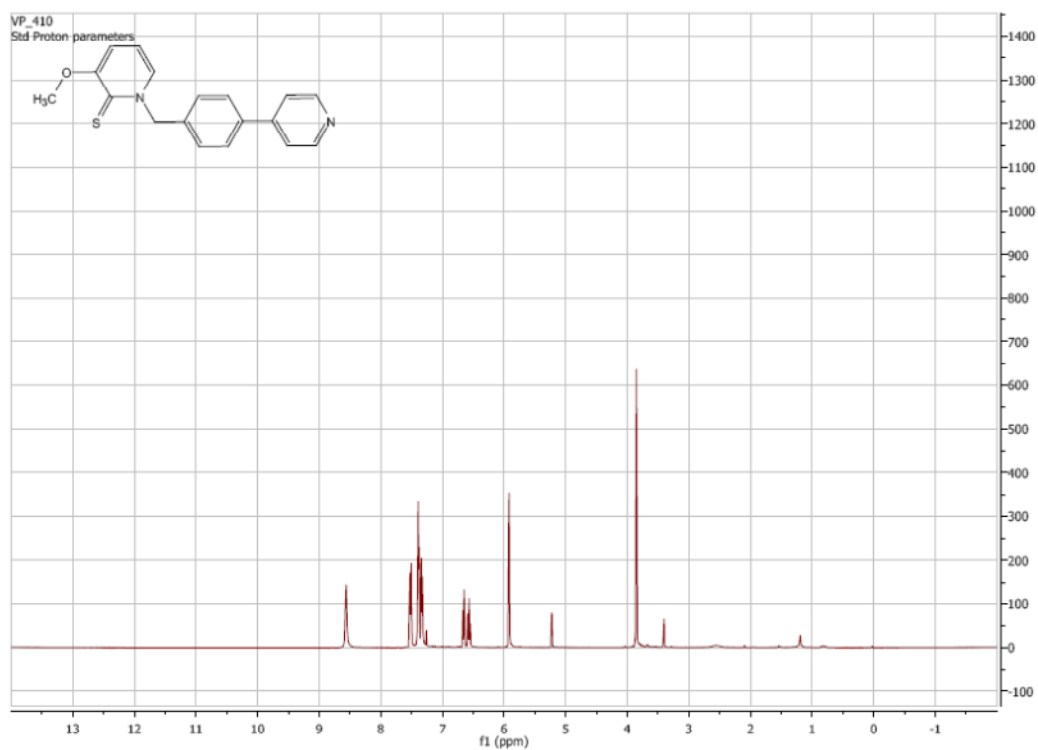
^1H NMR of **10h**:



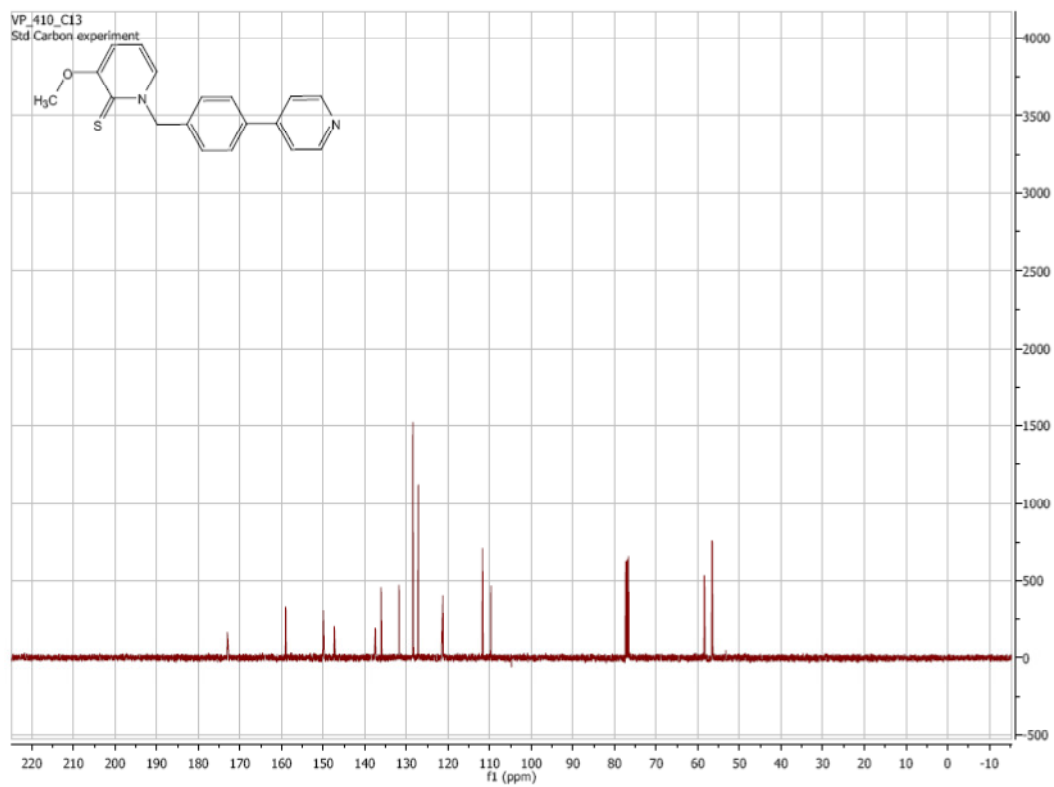
^{13}C NMR of **10h**:



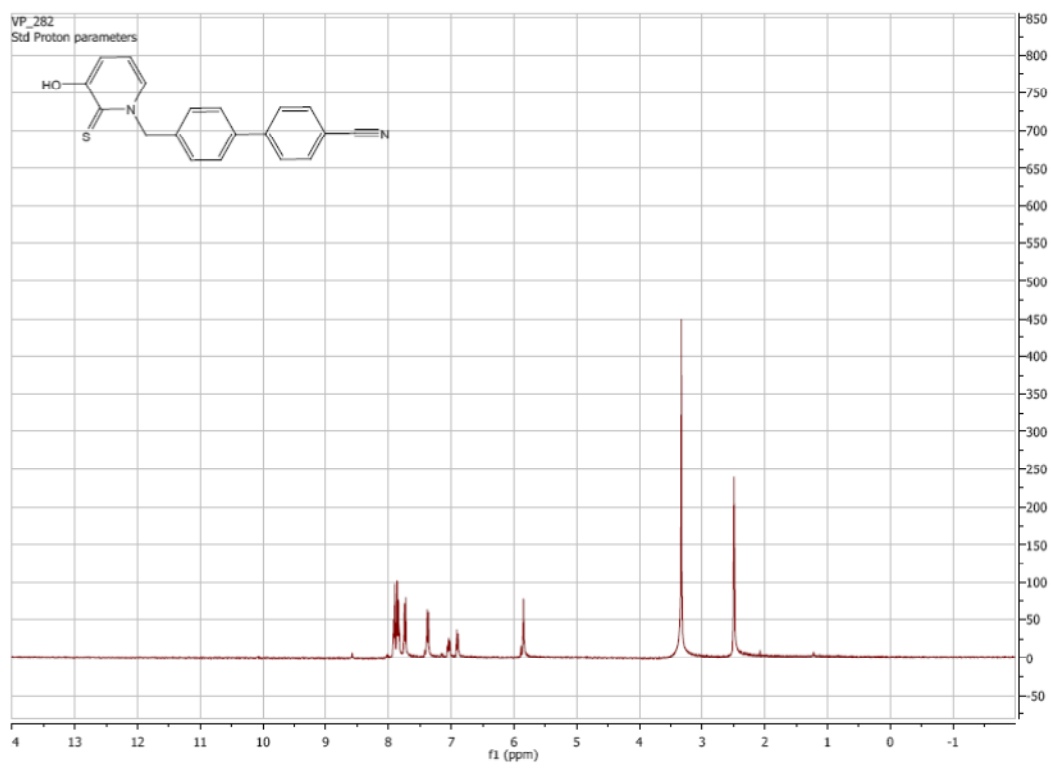
^1H NMR of **10i**:



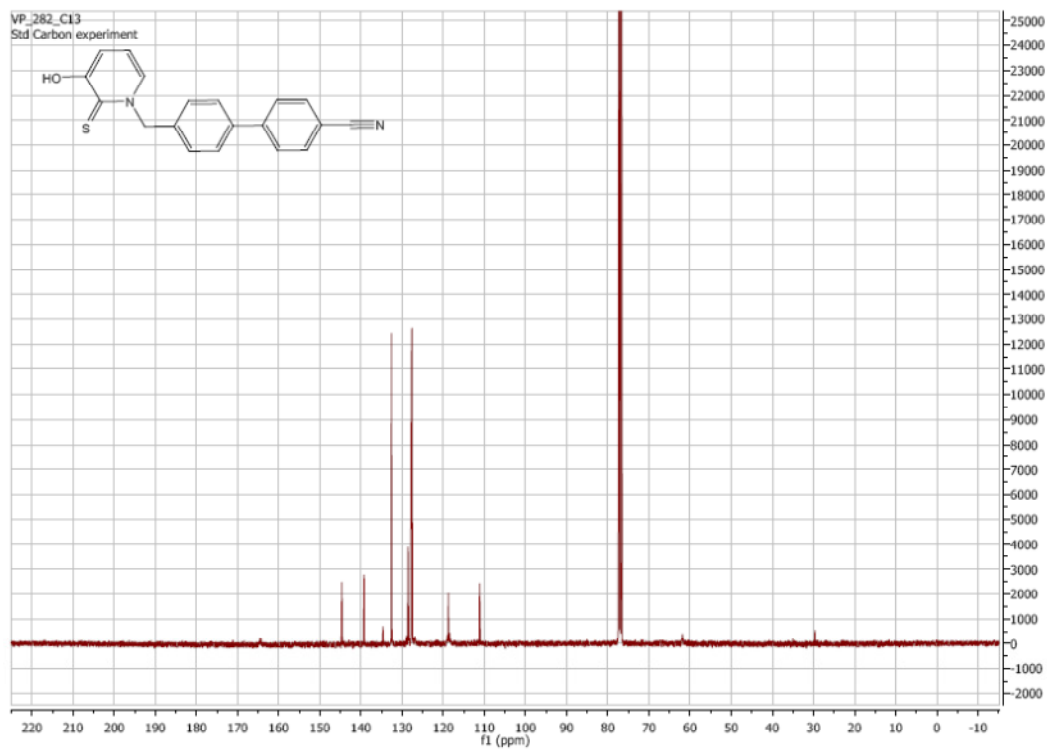
^{13}C NMR of **10i**:



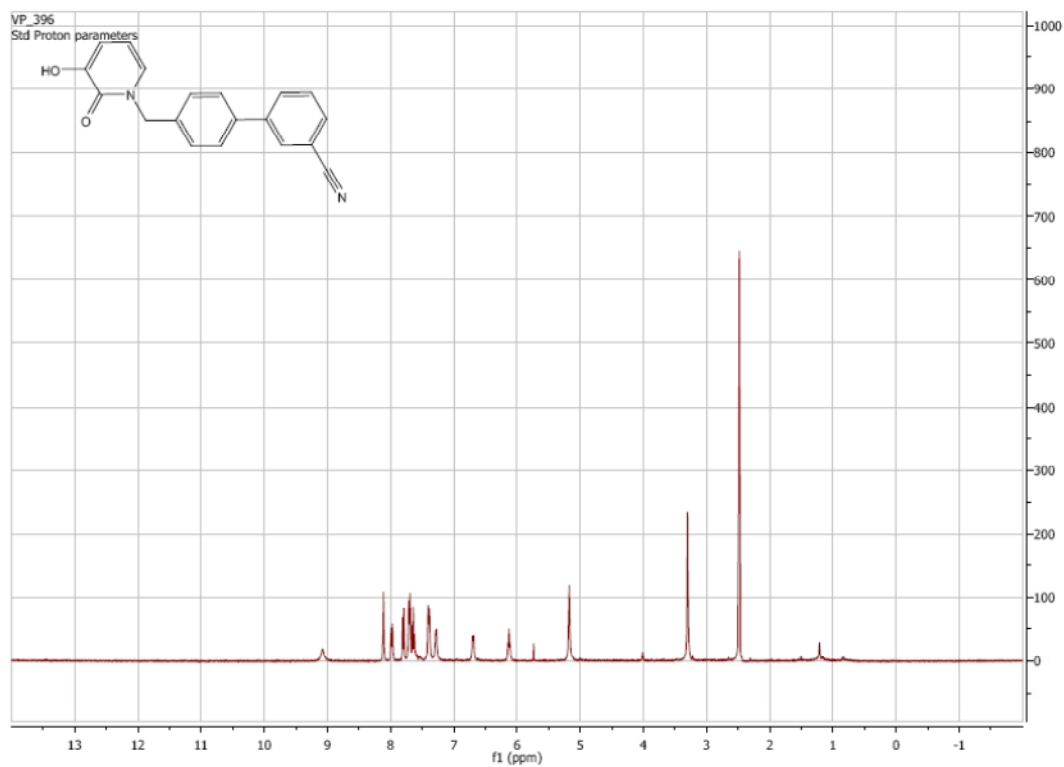
^1H NMR of **11a**:



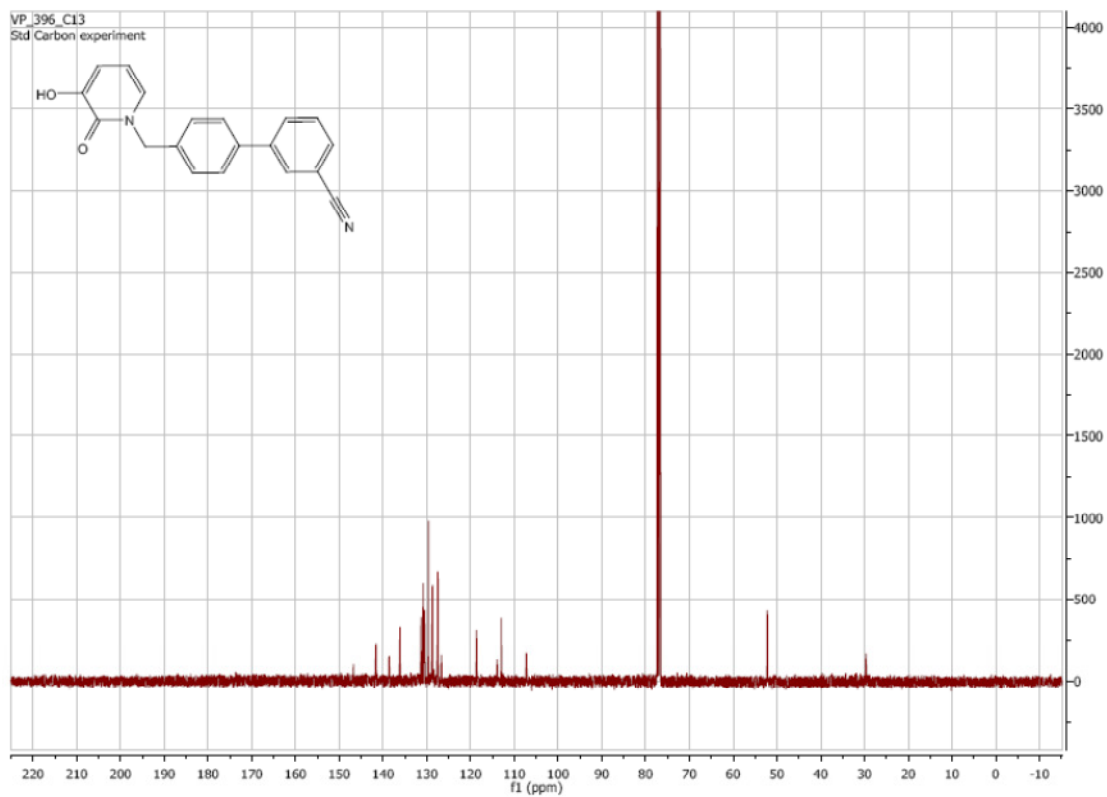
^{13}C NMR of **11a**:



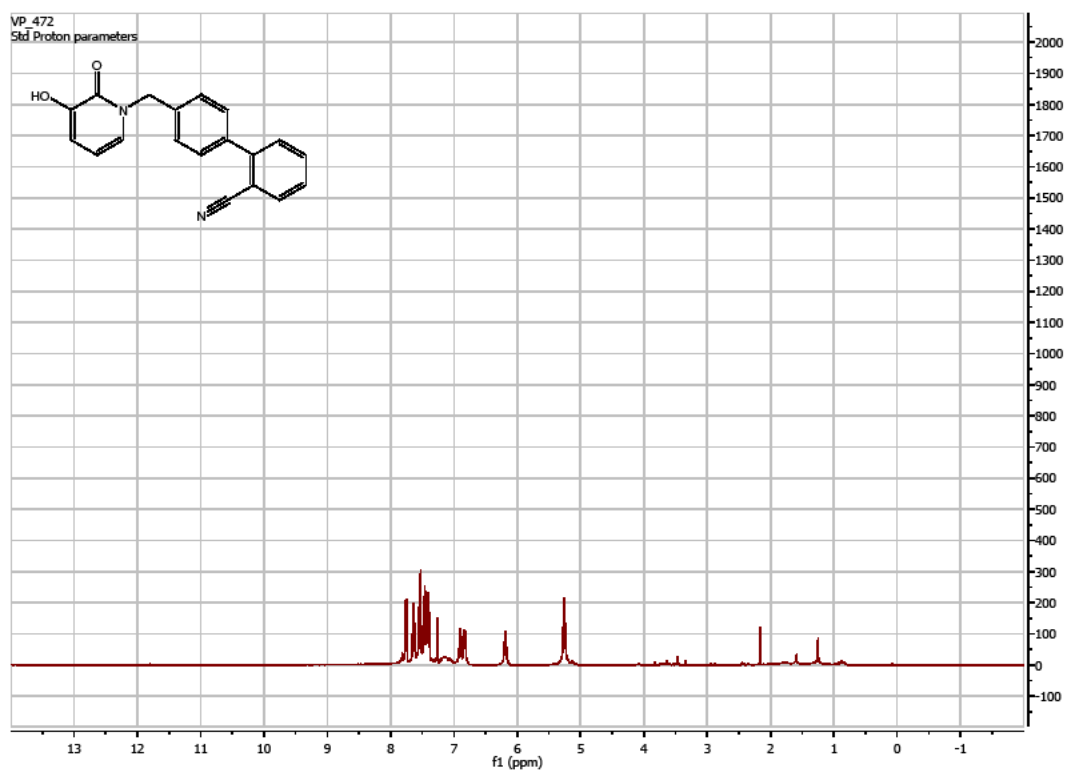
¹H NMR of **11b**:



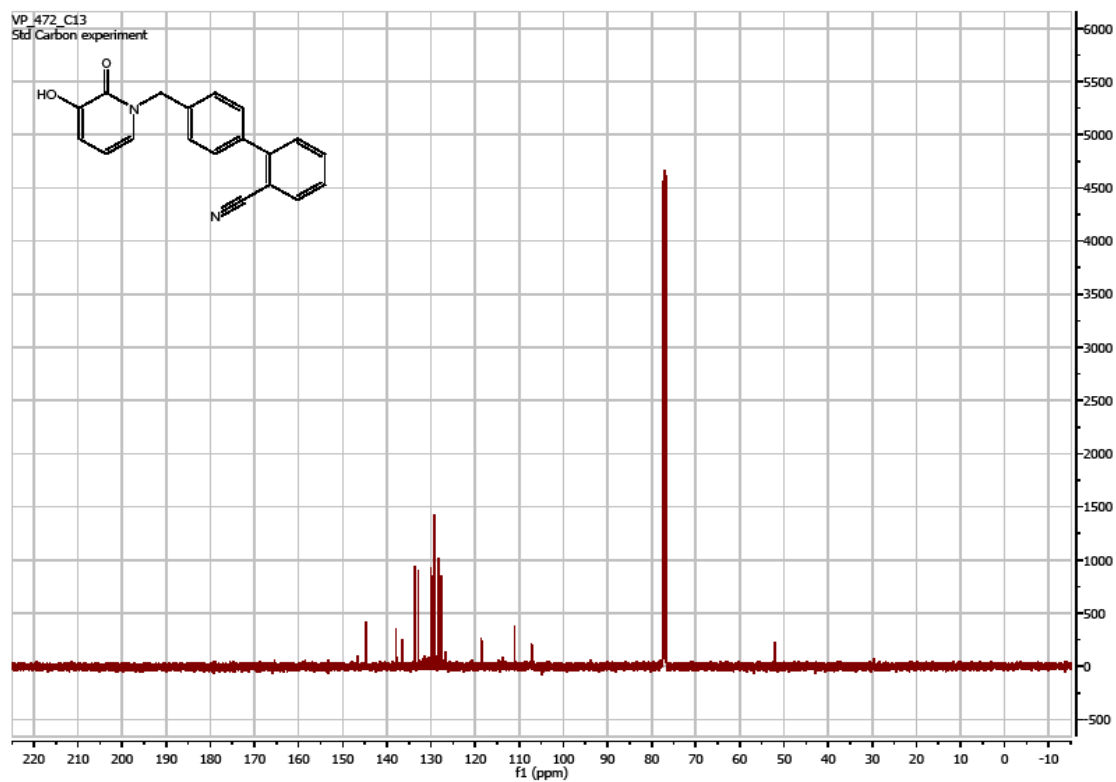
¹³C NMR of **11b**:



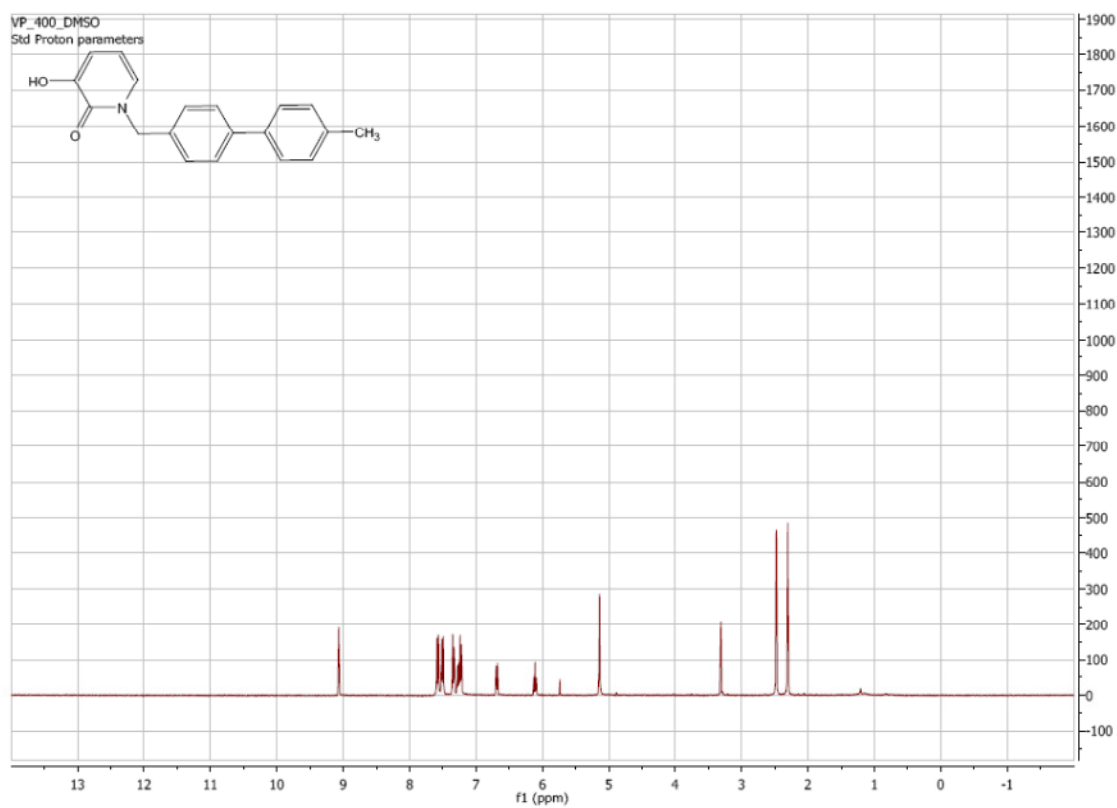
¹H NMR of **11c**:



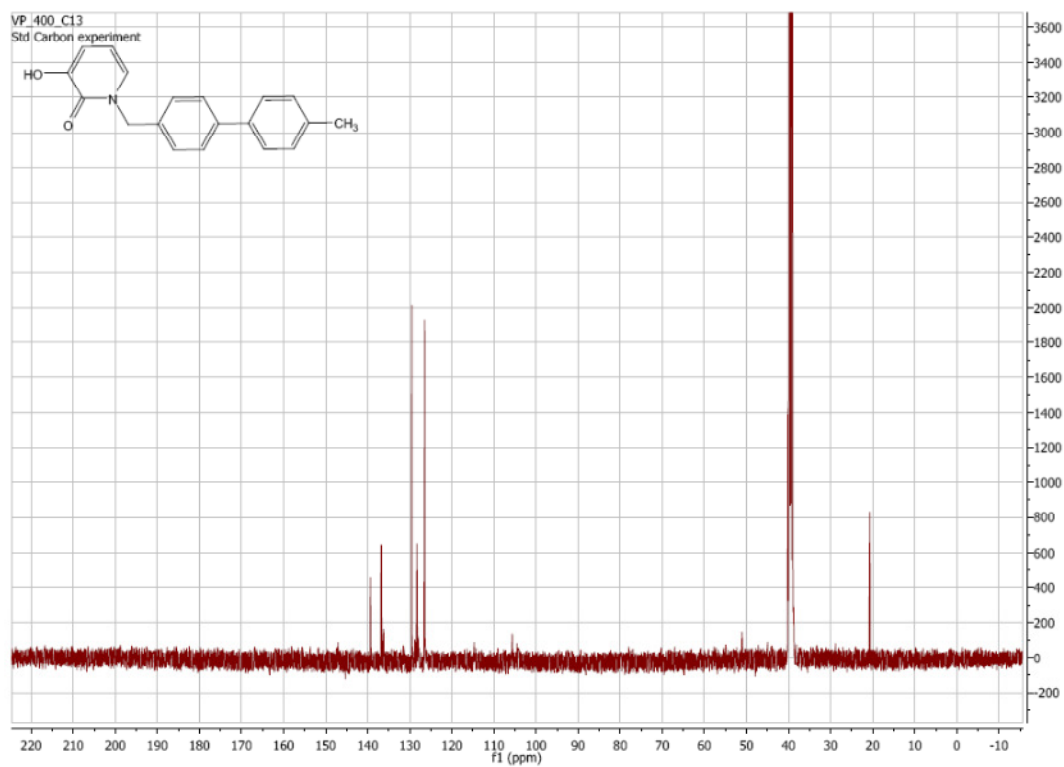
¹³C NMR of **11c**:



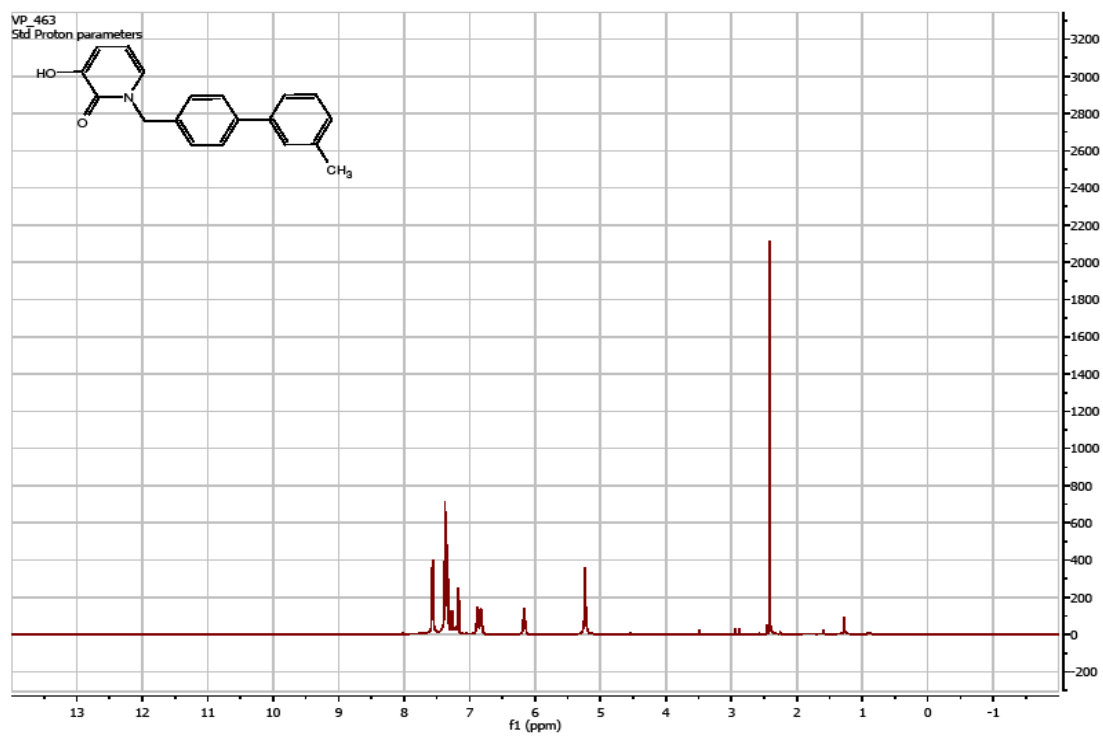
¹H NMR of **11d**:



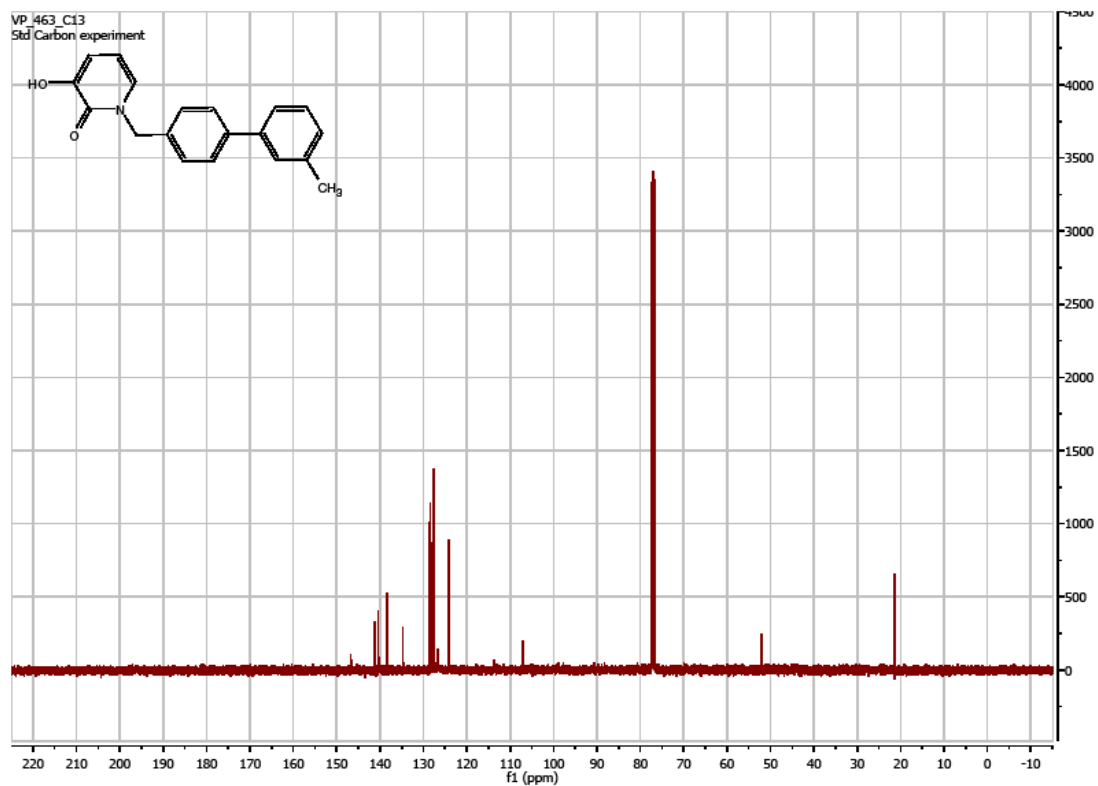
¹³C NMR of **11d**:



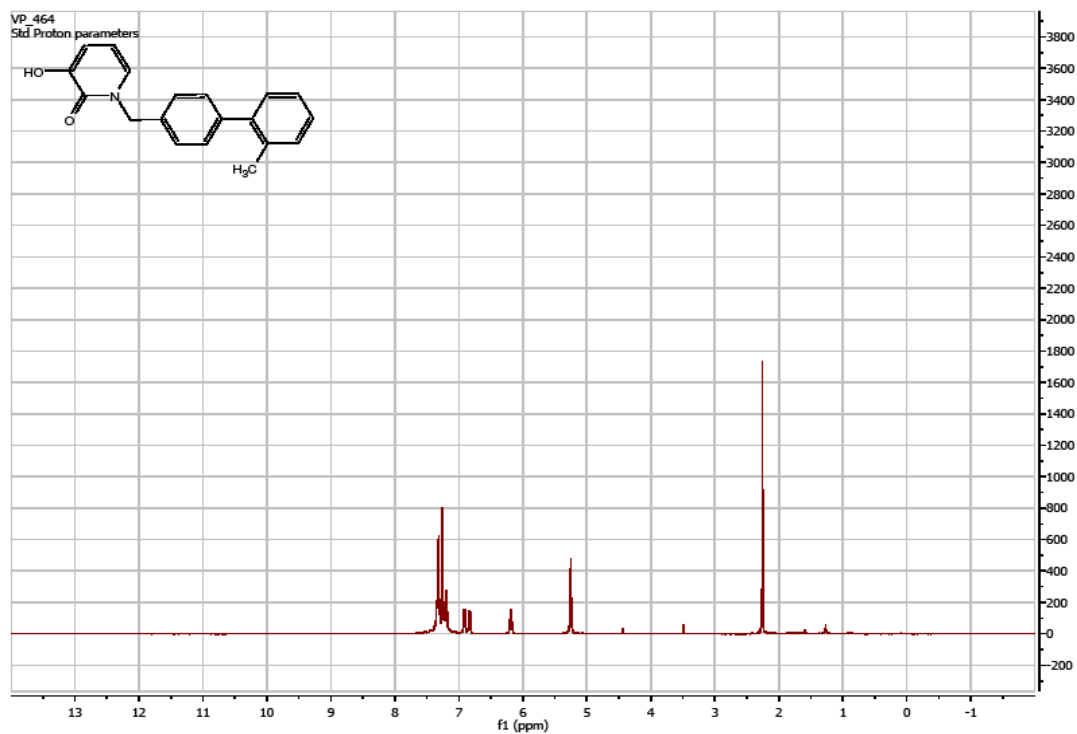
¹H NMR of **11e**:



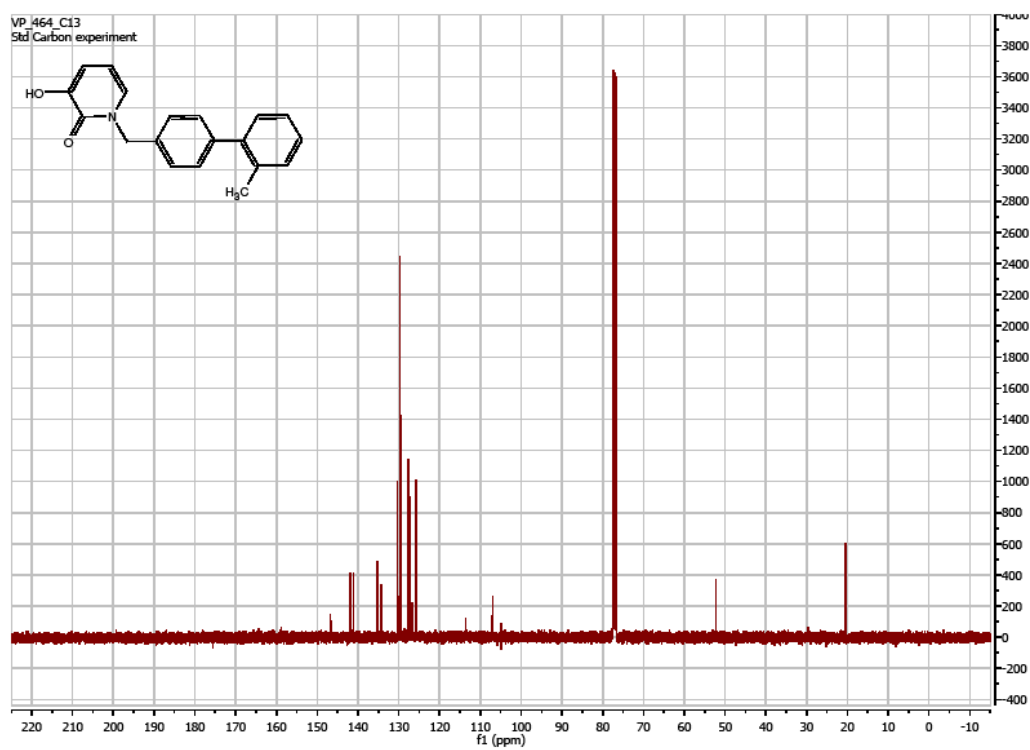
¹³C NMR of **11e**:



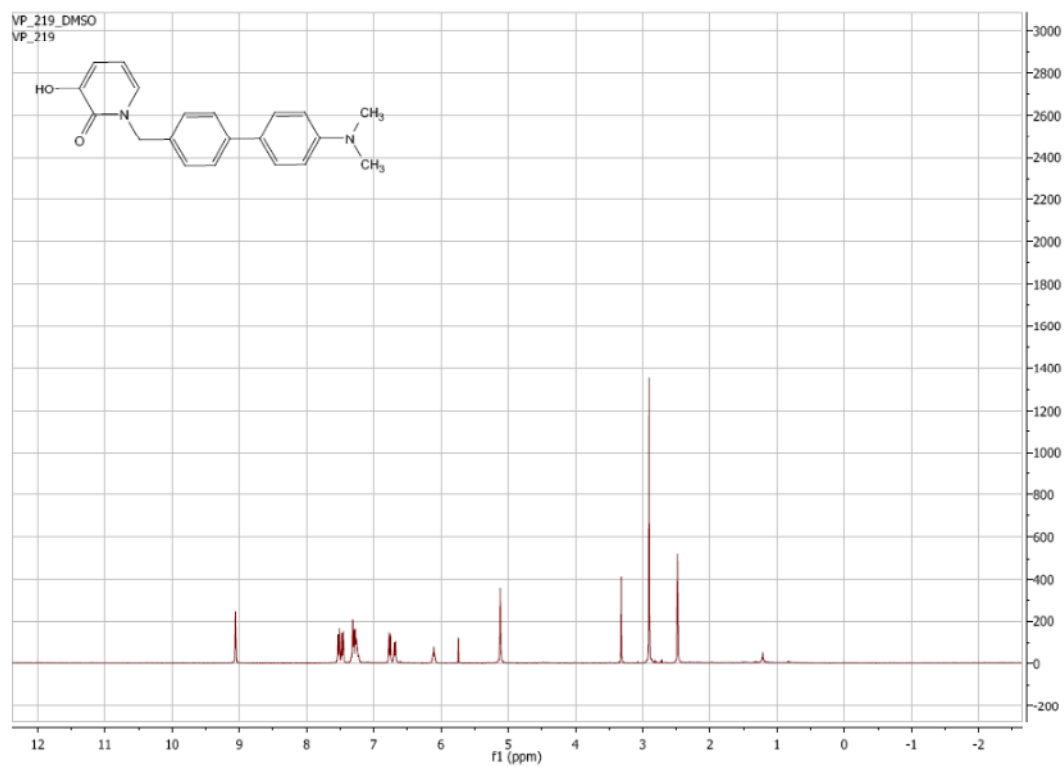
¹H NMR of **11f**:



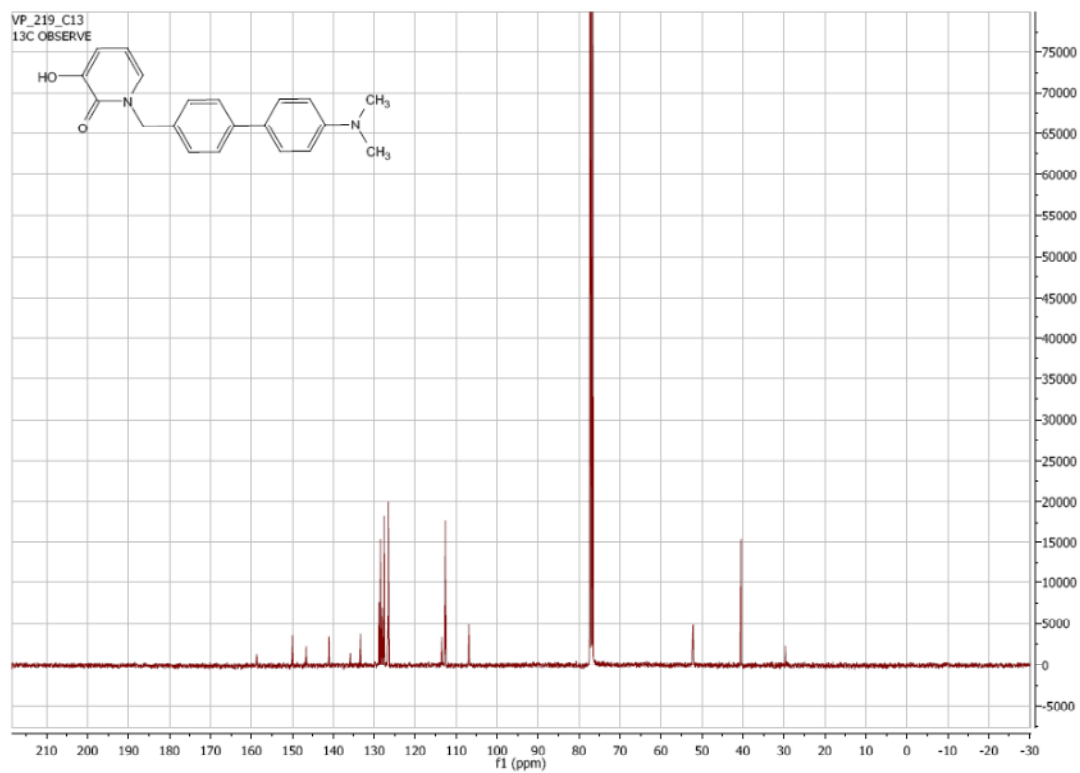
¹³C NMR of **11f**:



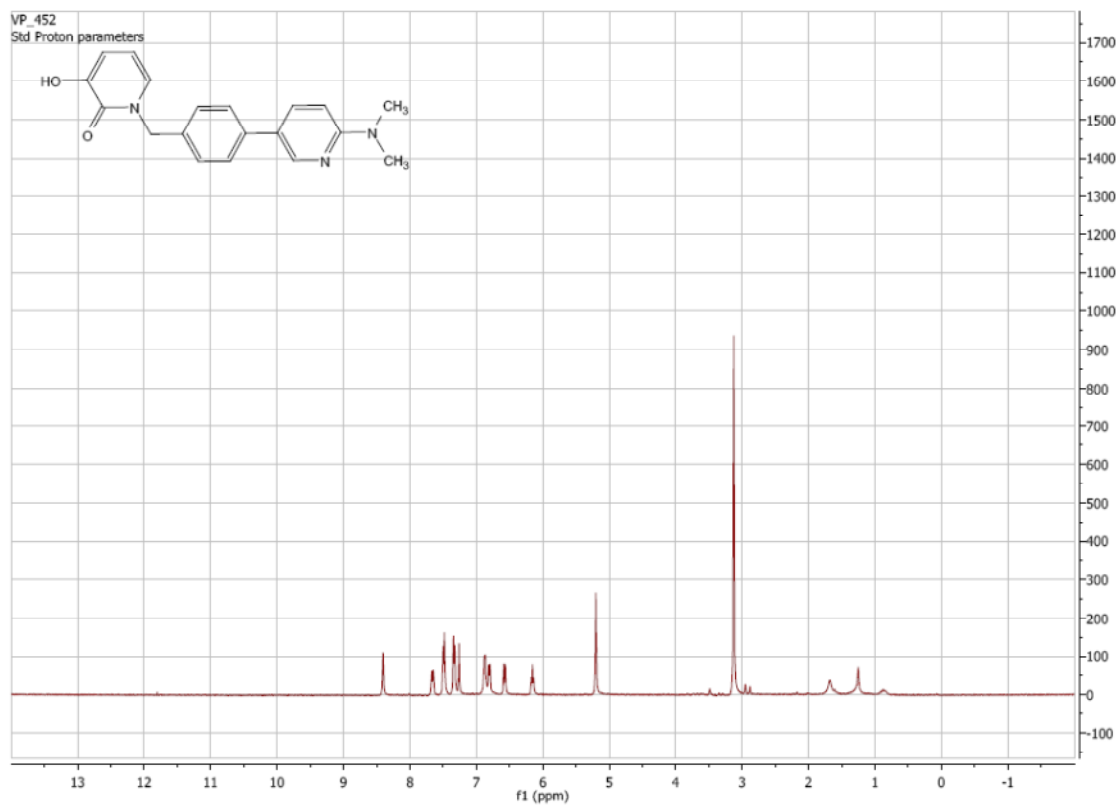
¹H NMR of **11g**:



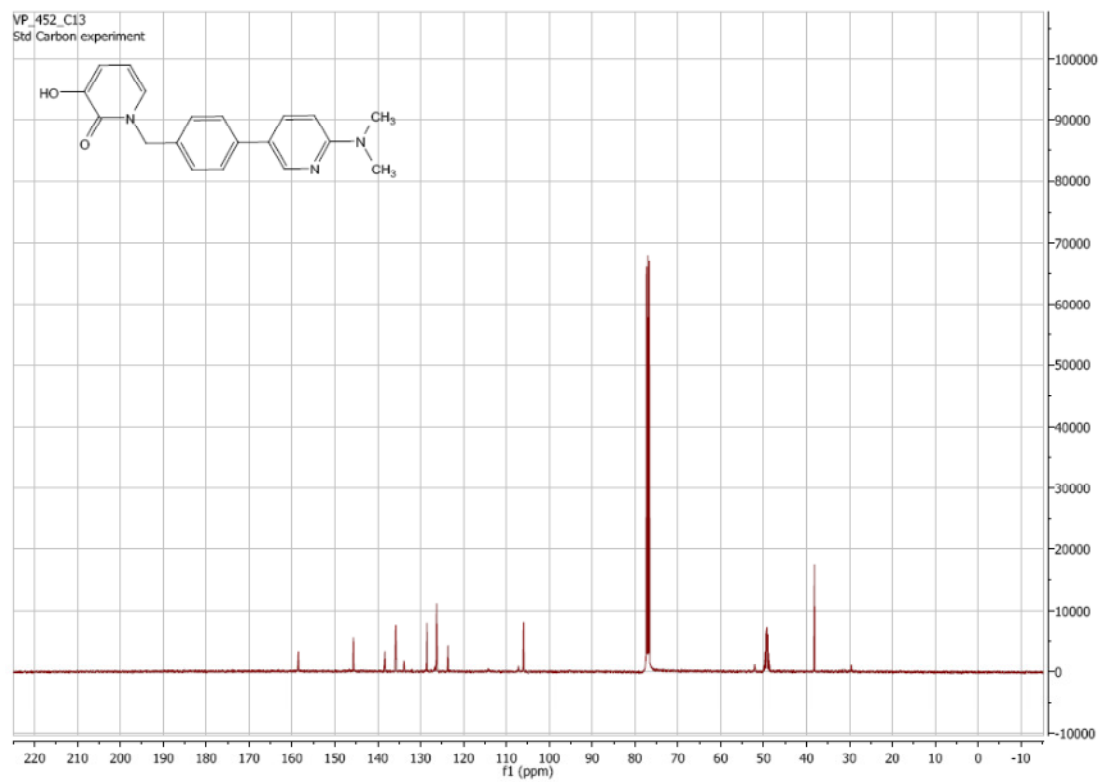
^{13}C NMR of **11g**:



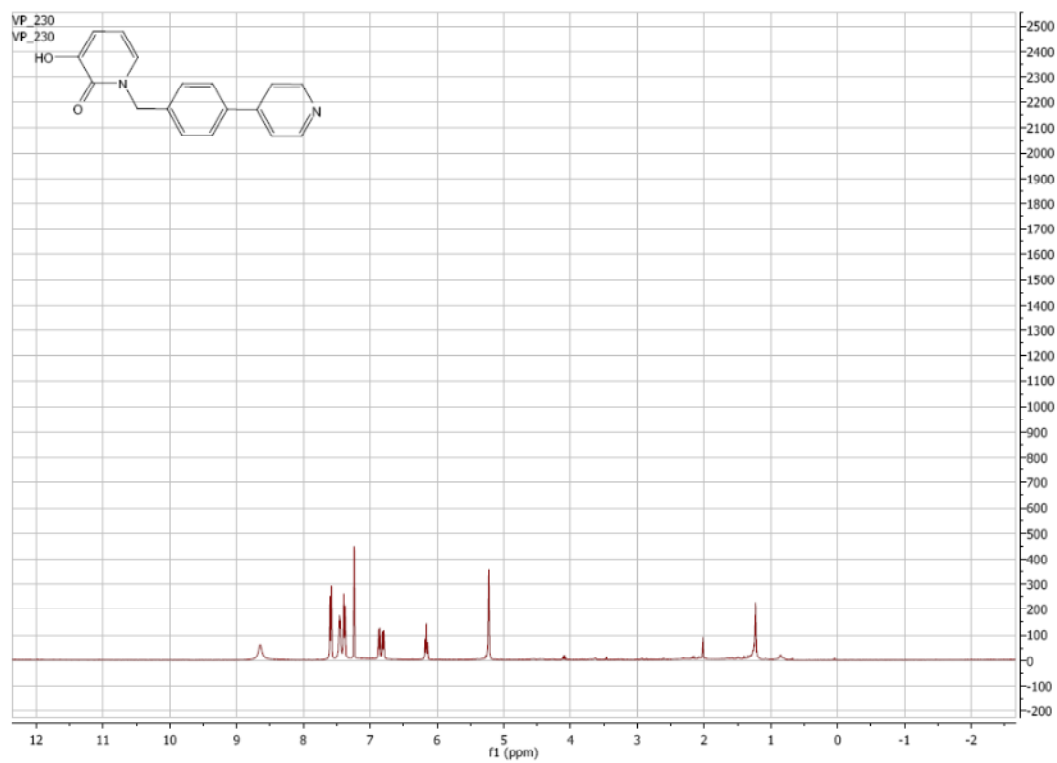
^{13}C NMR of **11h**:



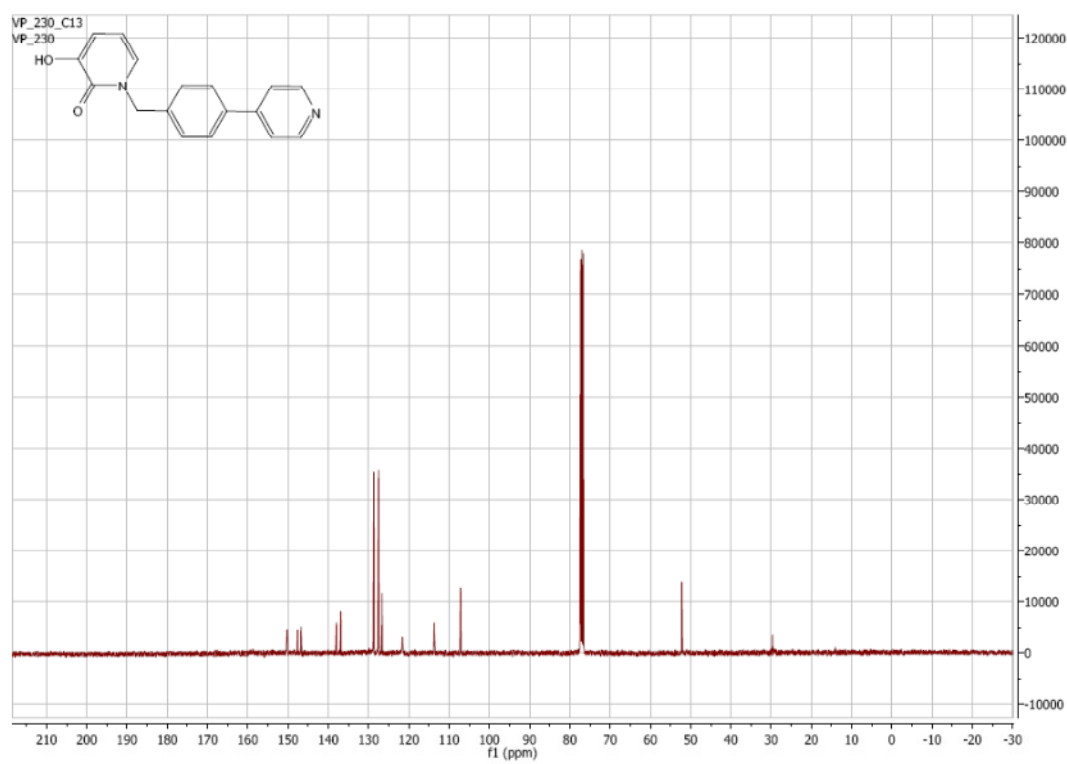
¹³C NMR of **11h**:



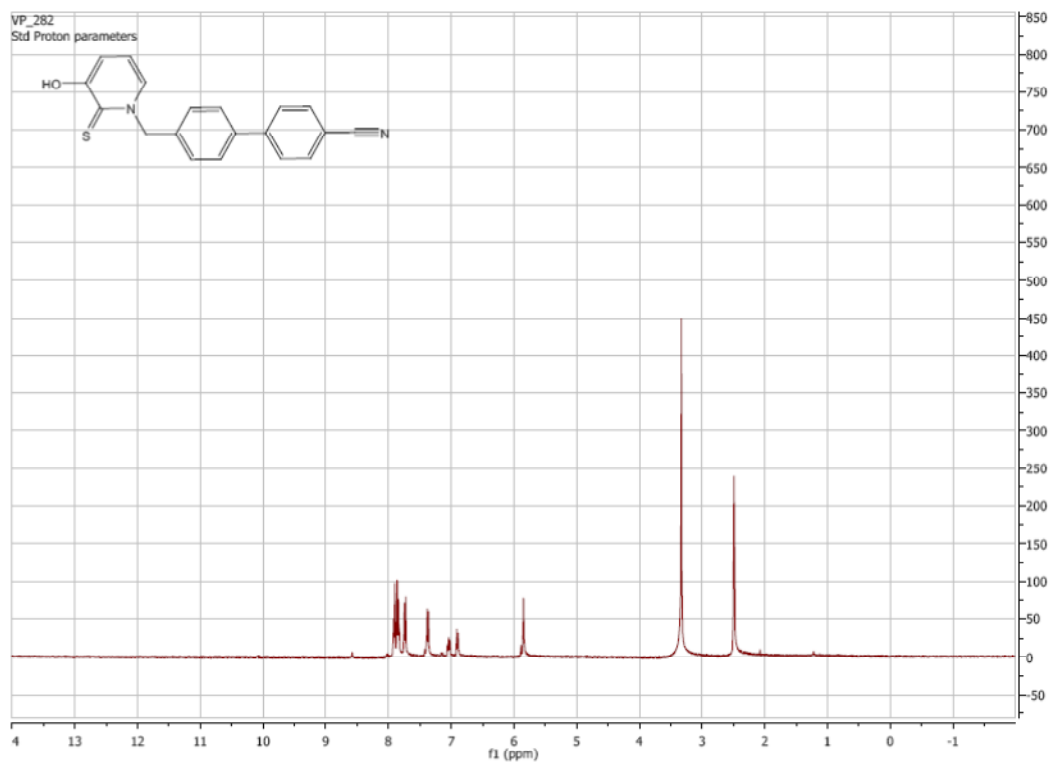
¹H NMR of **11i**:



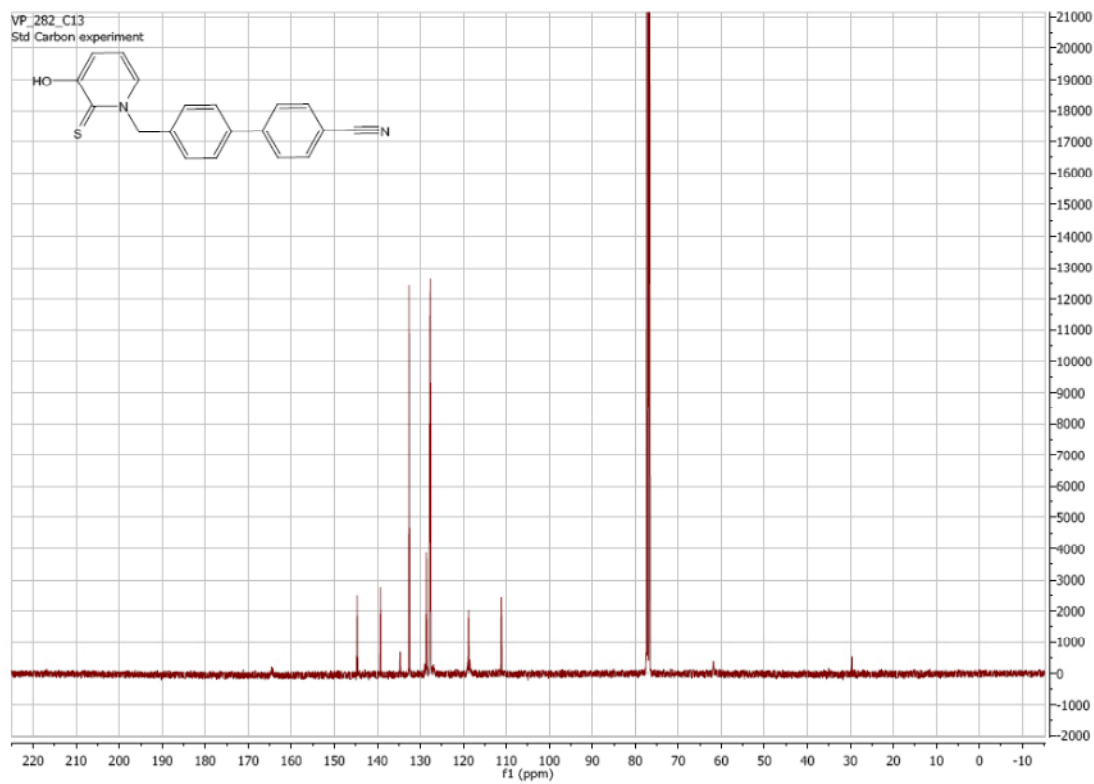
^{13}C NMR of **11i**:



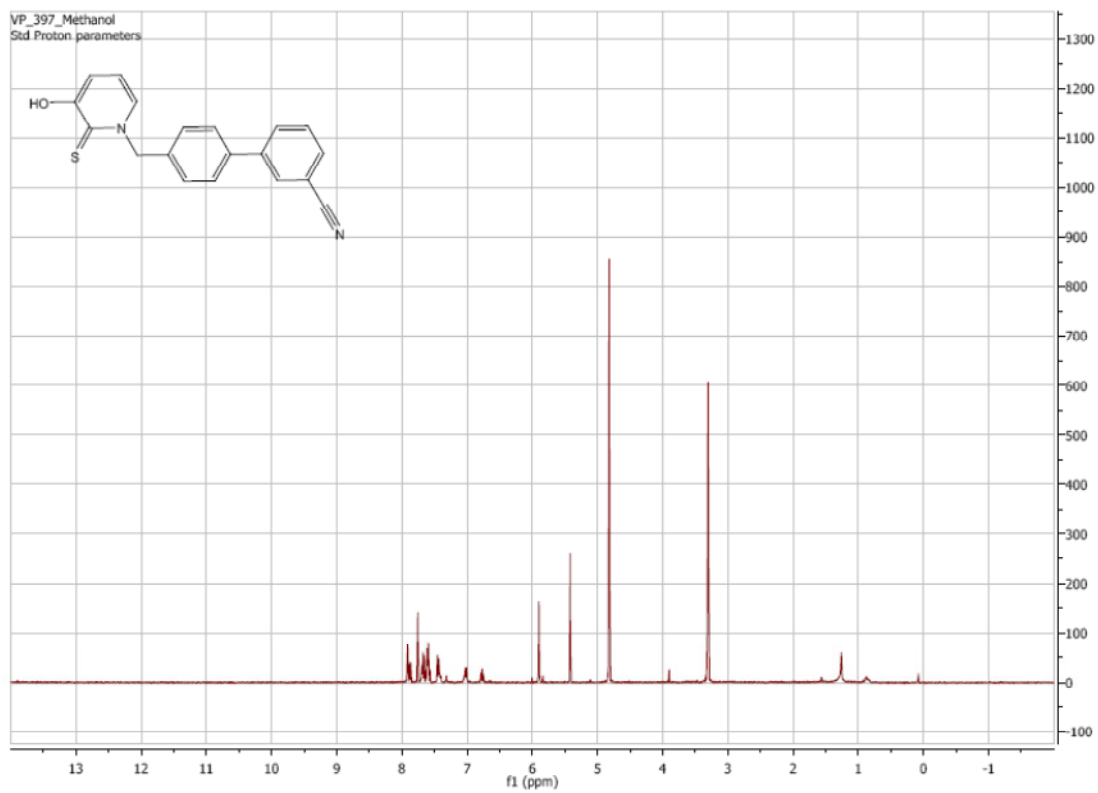
^1H NMR of **12a**:



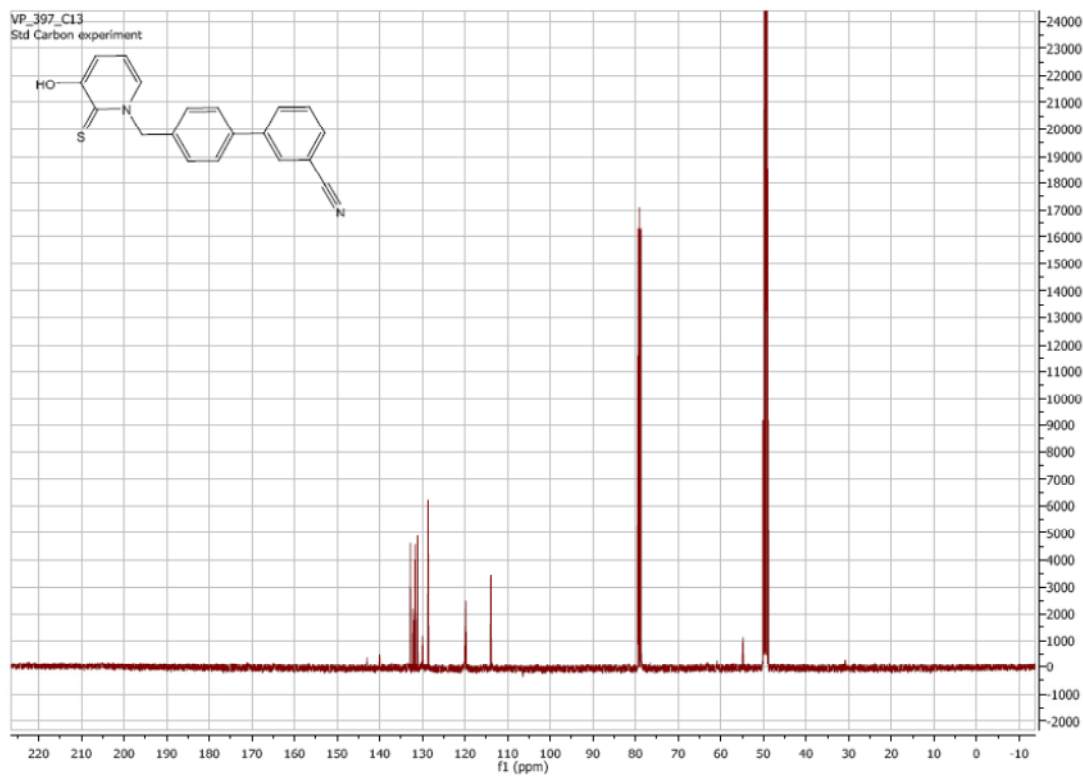
¹³C NMR of **12a**:



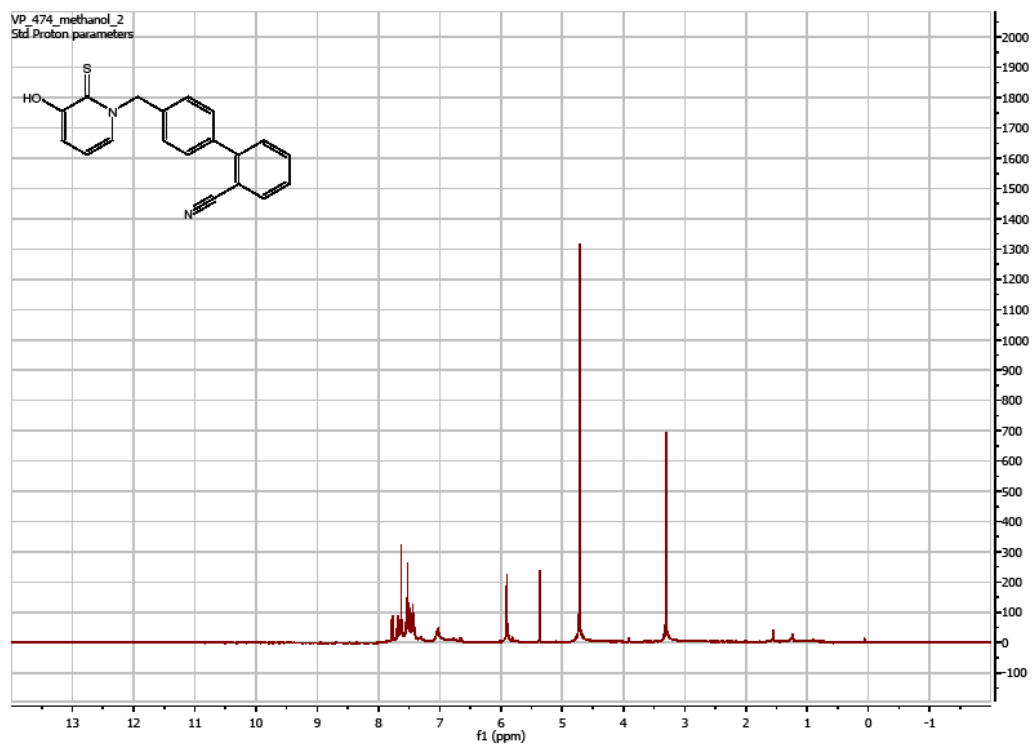
¹H NMR of **12b**:



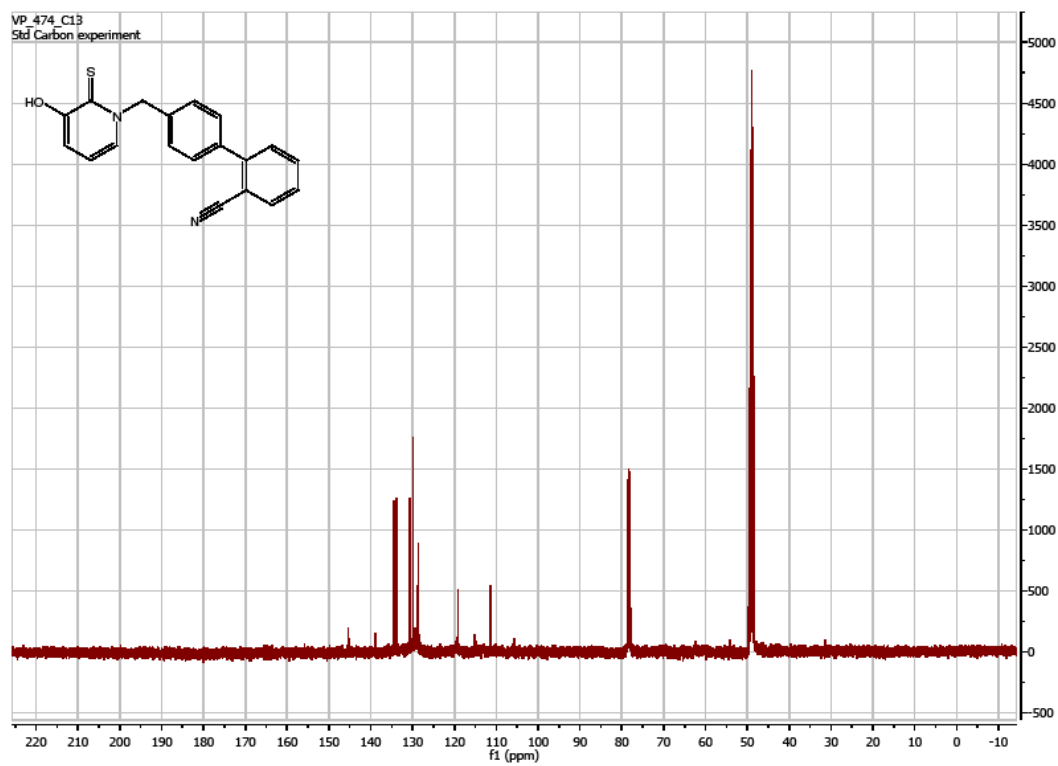
^{13}C NMR of **12b**:



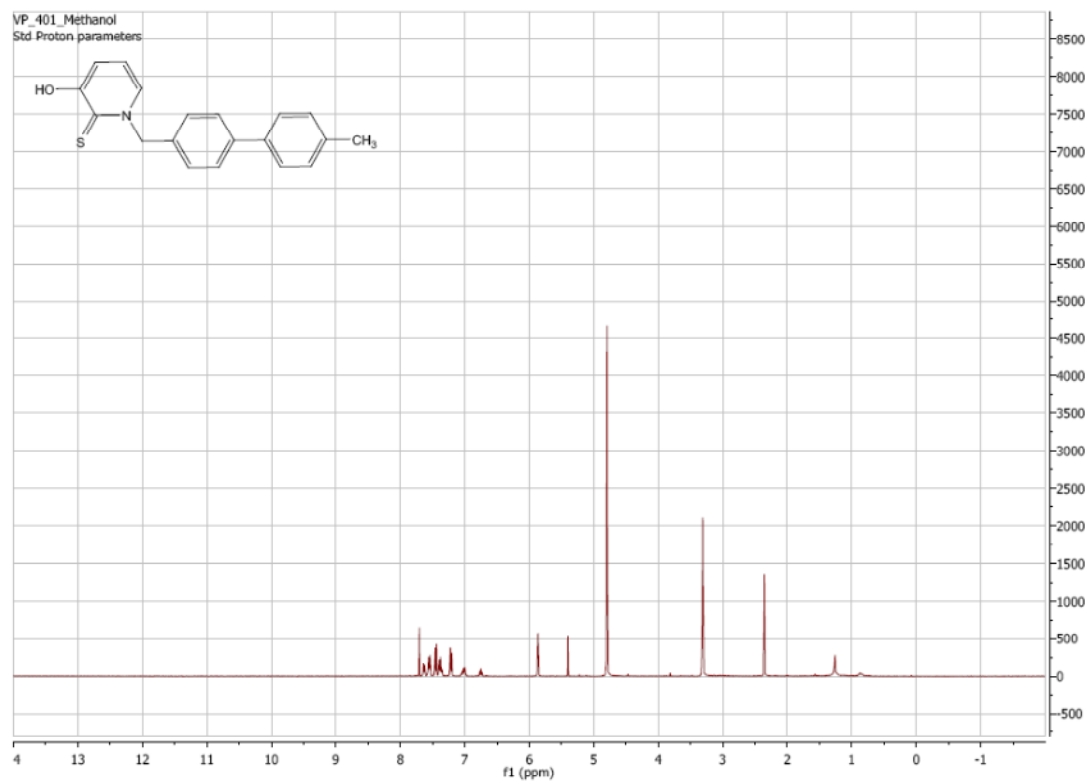
^1H NMR of **12c**:



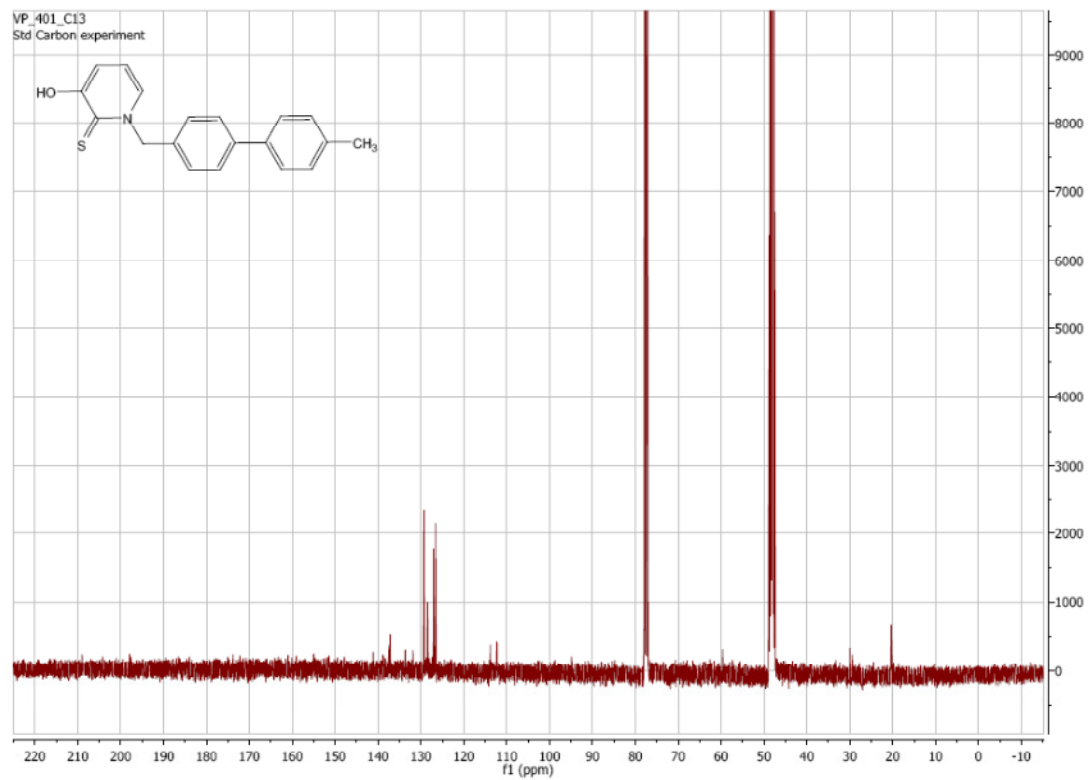
^{13}C NMR of 12c:



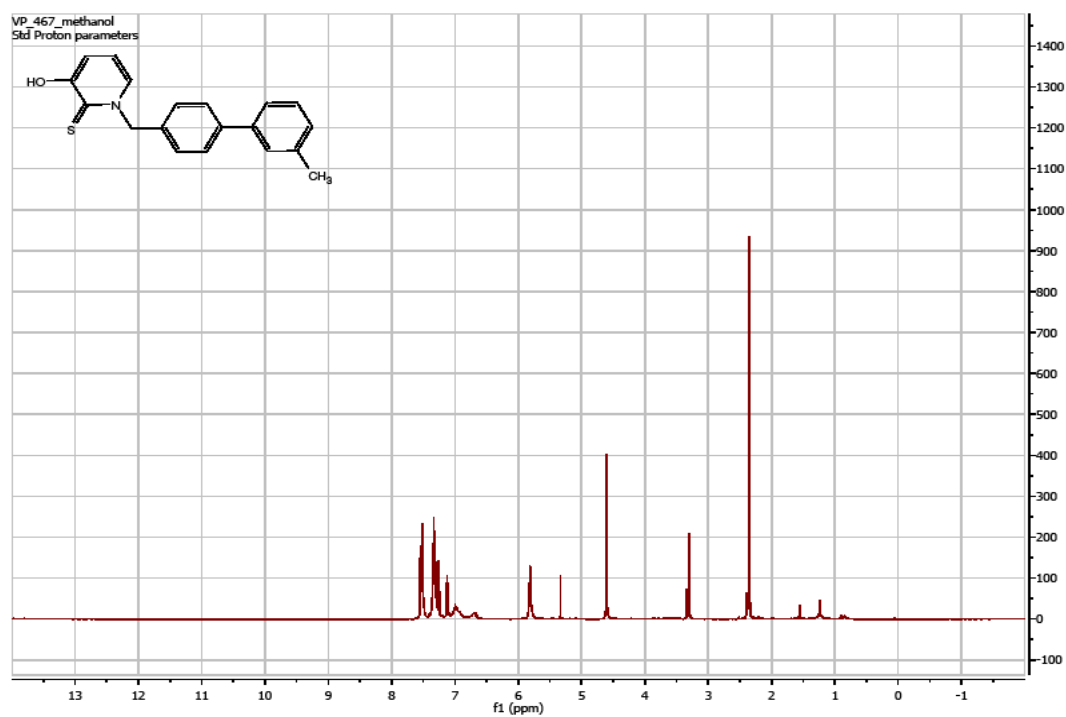
^1H NMR of 12d:



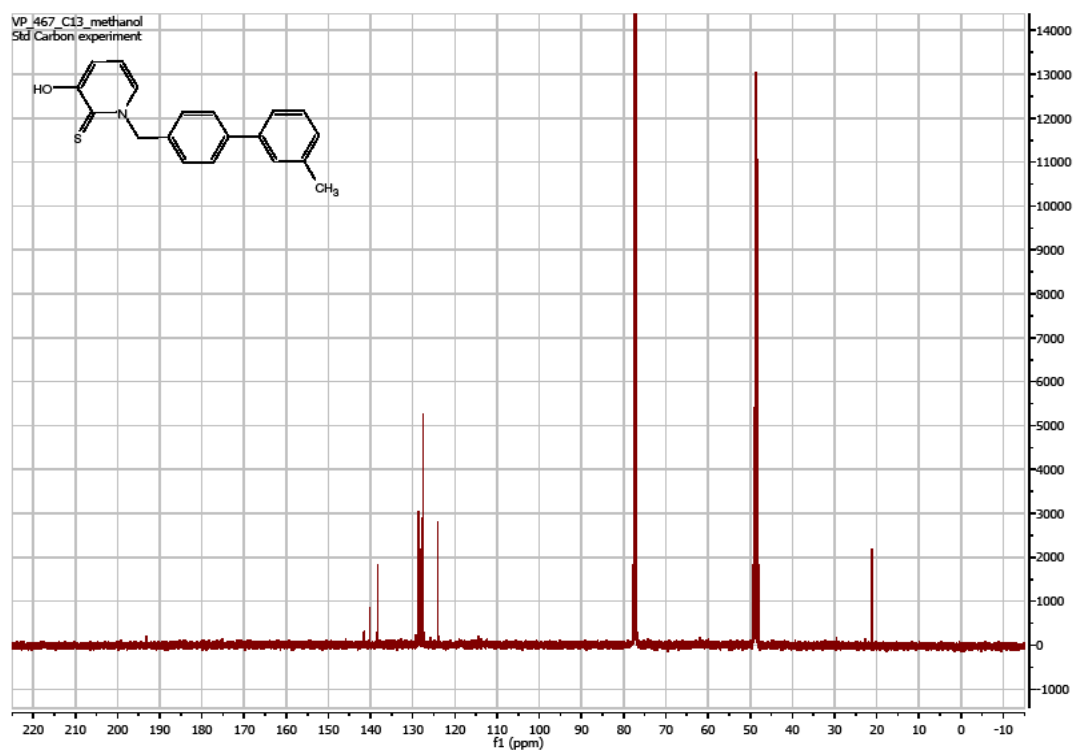
¹³C NMR of **12d**:



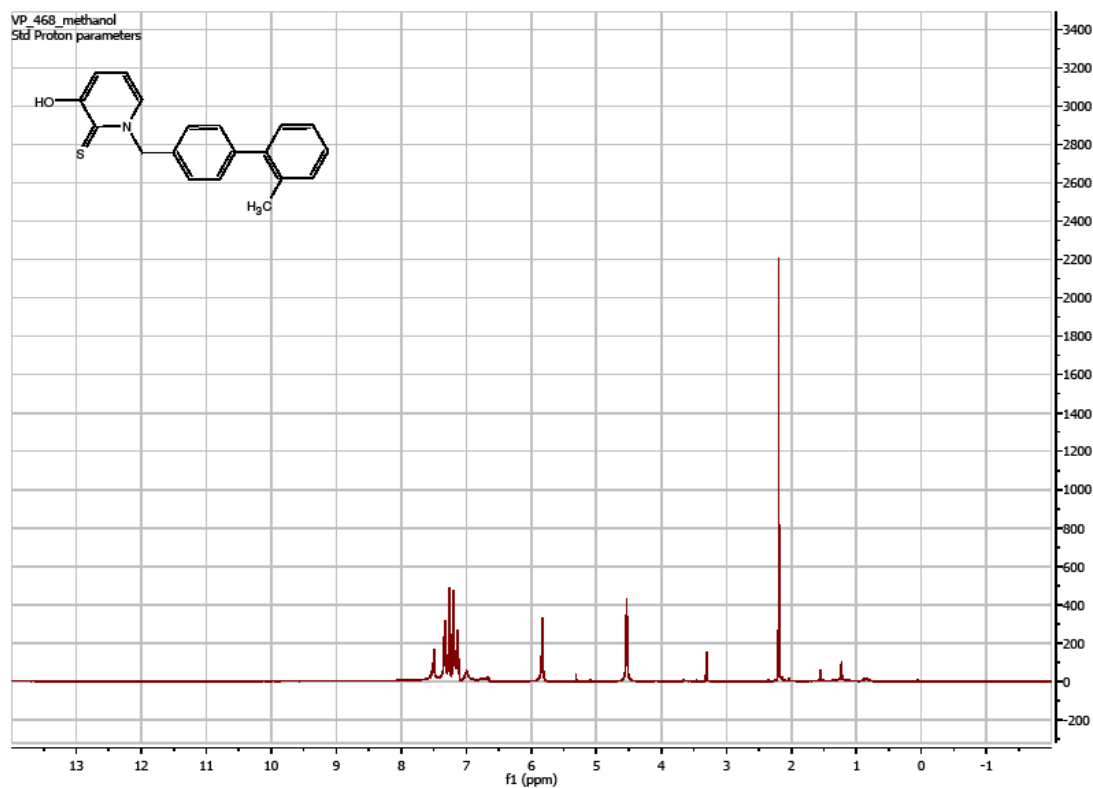
^1H NMR of **12e**:



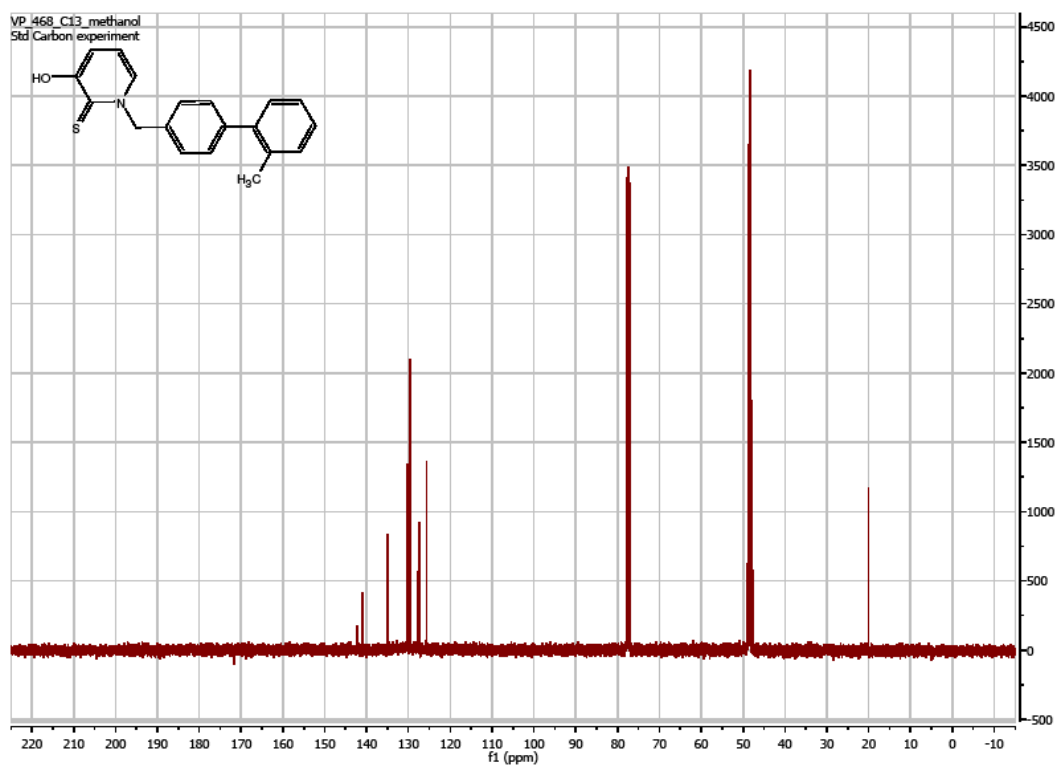
^{13}C NMR of **12e**:



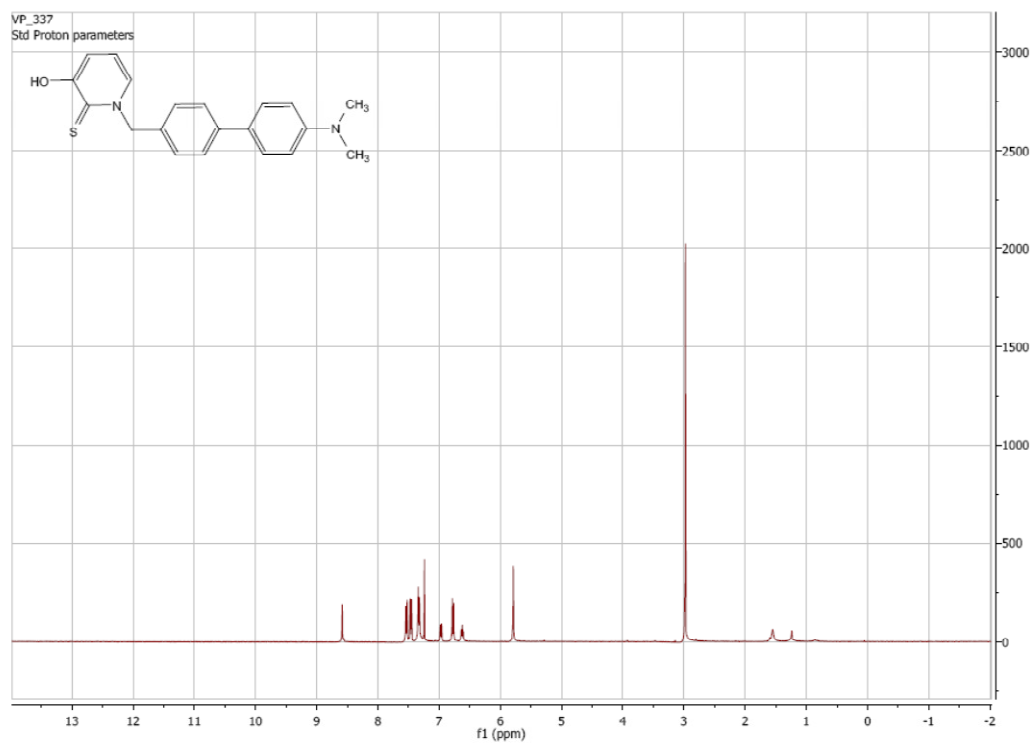
^1H NMR of **12f**:



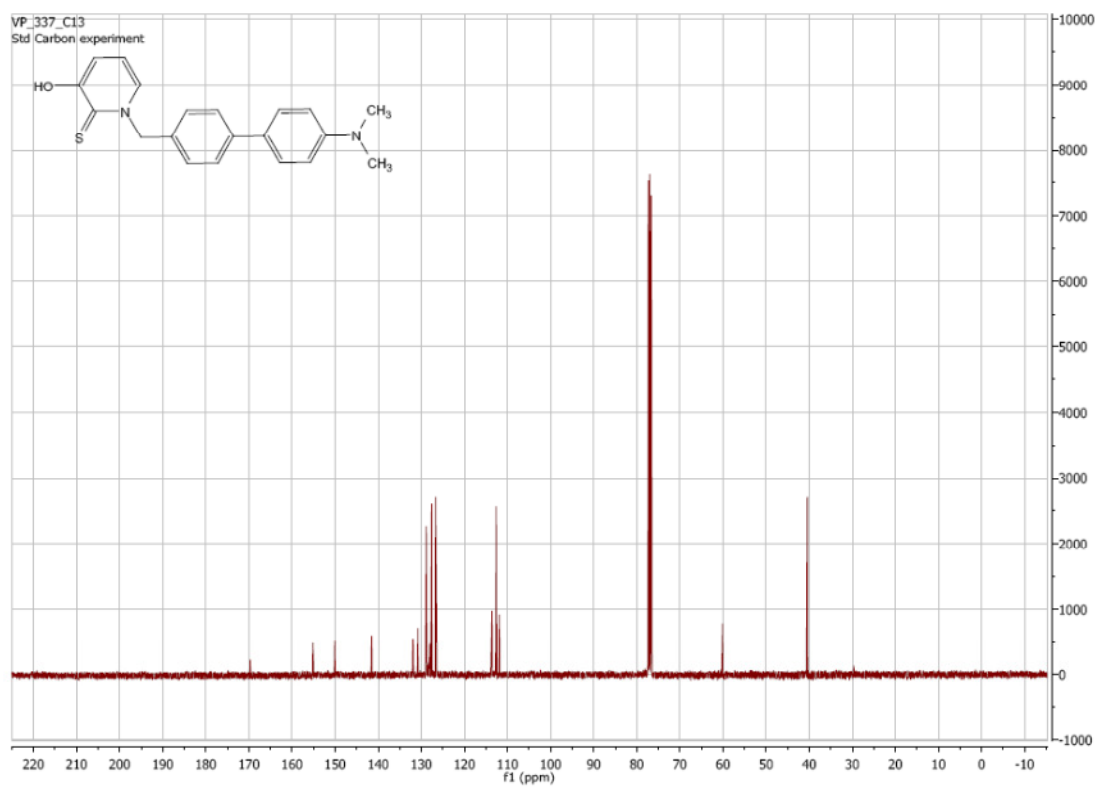
¹³C NMR of 12f:



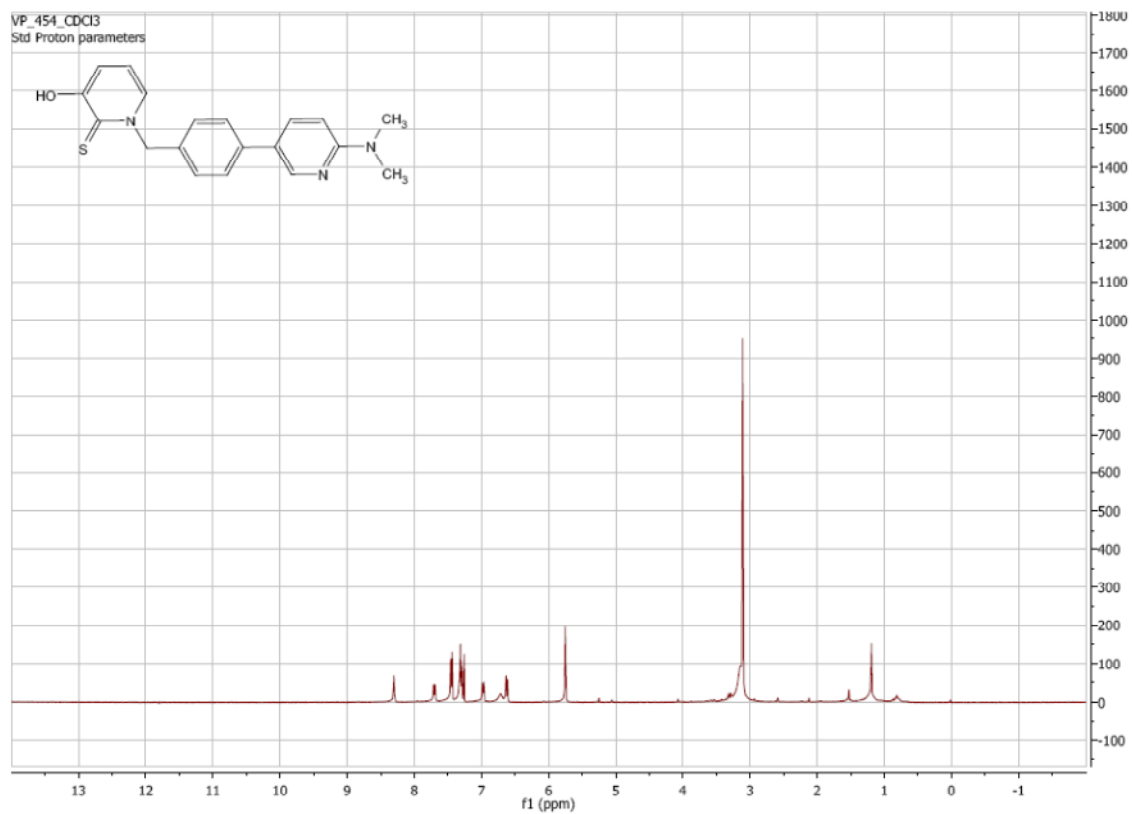
¹H NMR of 12g:



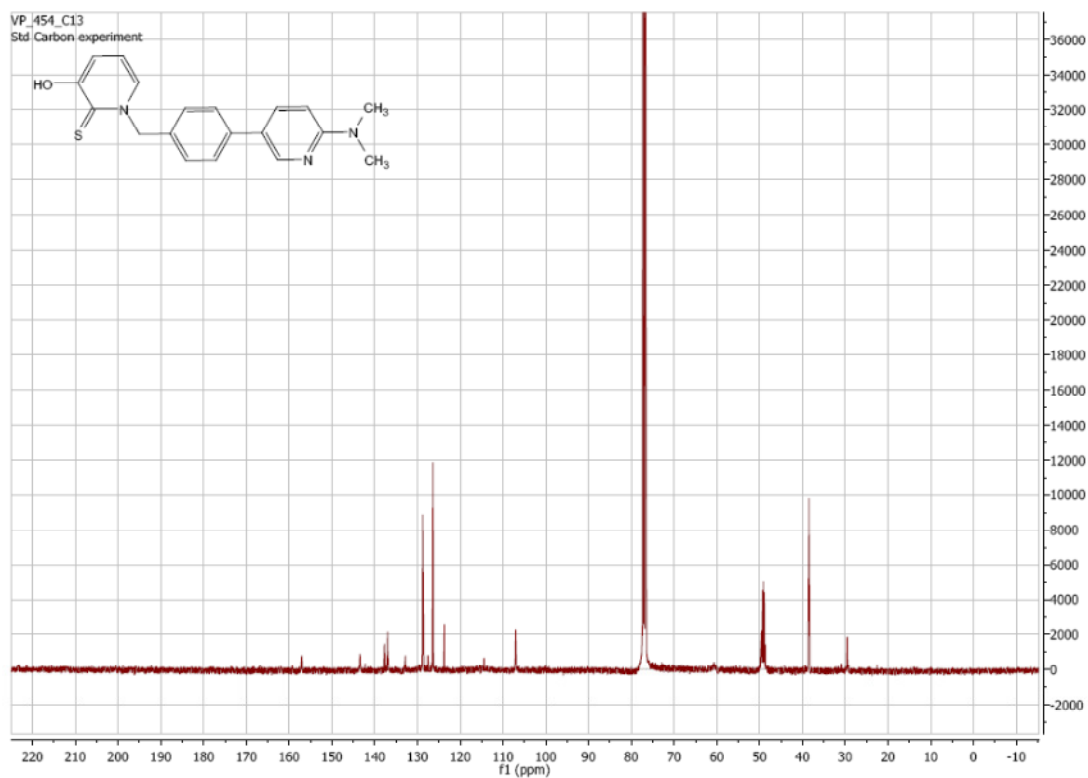
¹³C NMR of **12g**:



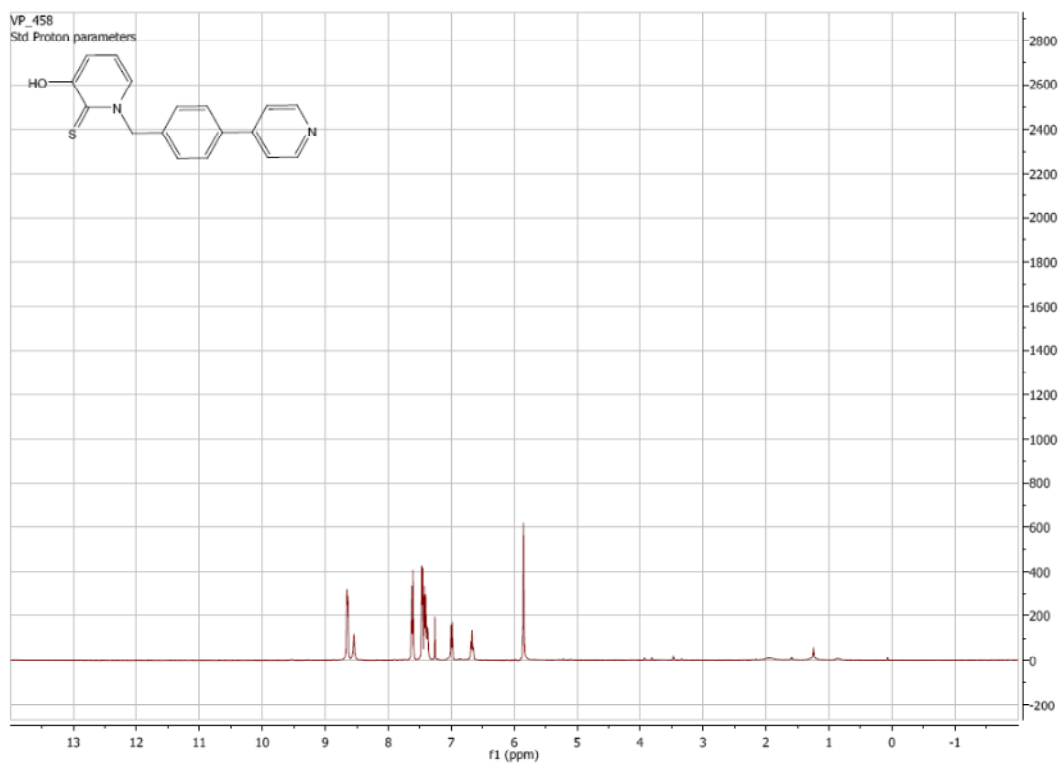
¹H NMR of **12h**:



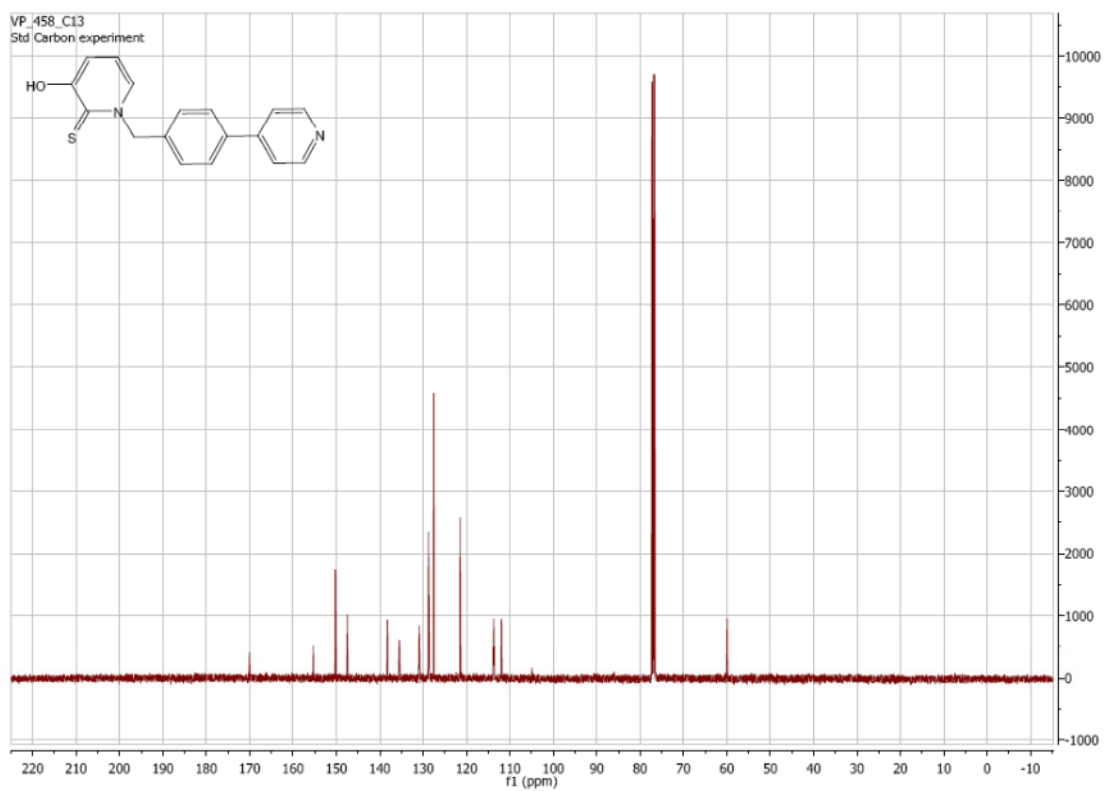
¹³C NMR of **12h**:



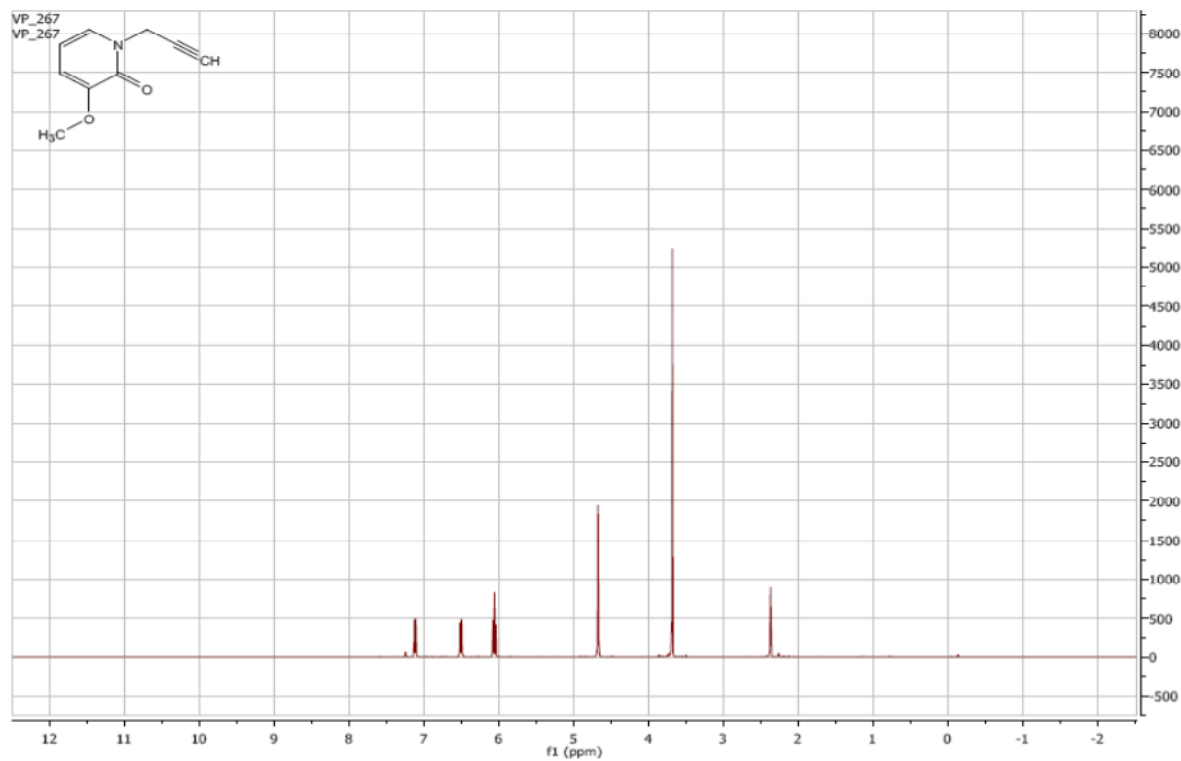
¹H NMR of **12i**:



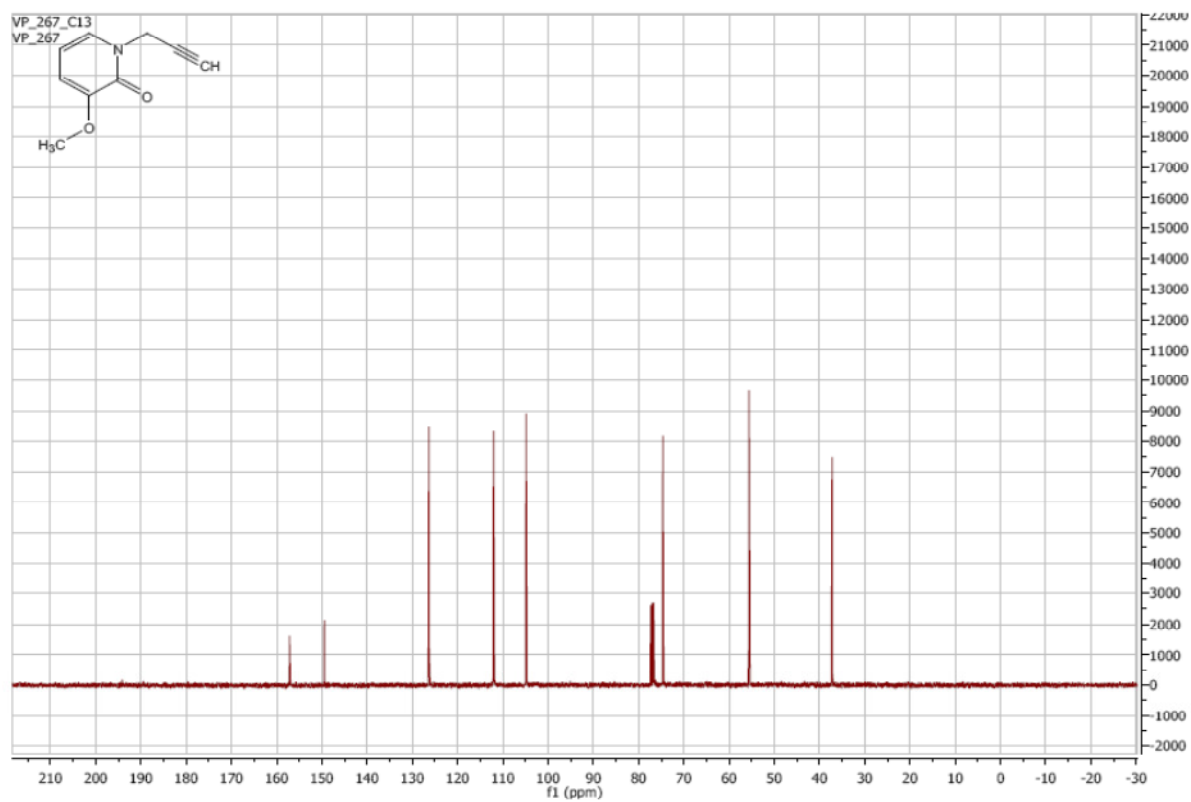
¹³C NMR of **12i**:



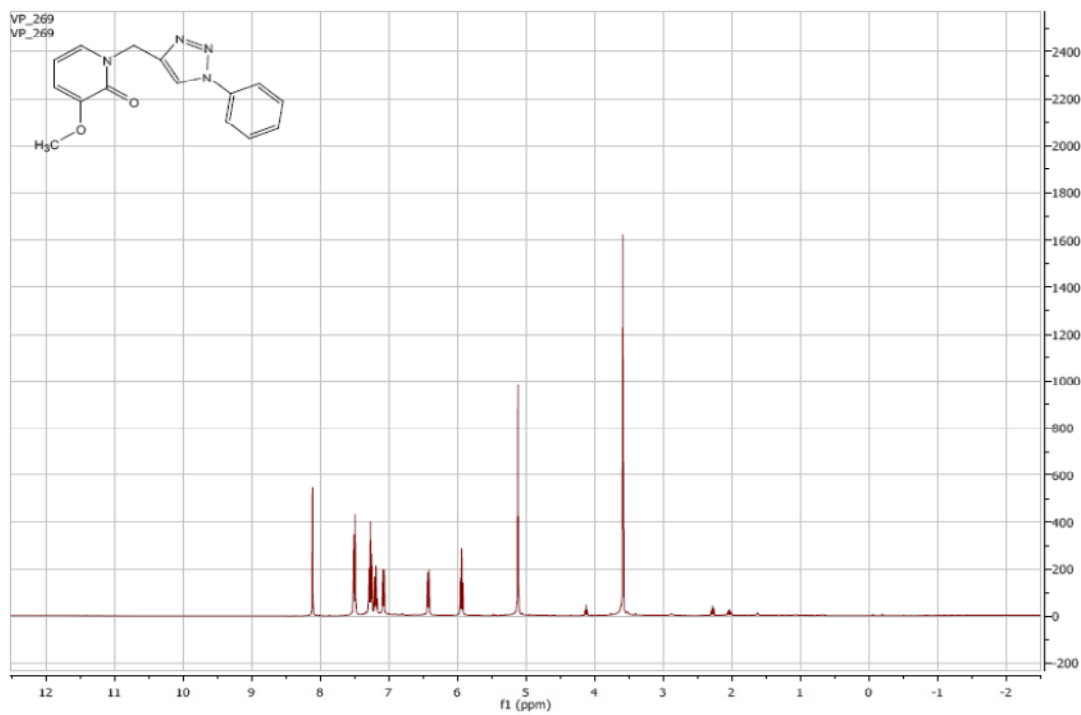
¹H NMR of **13**:



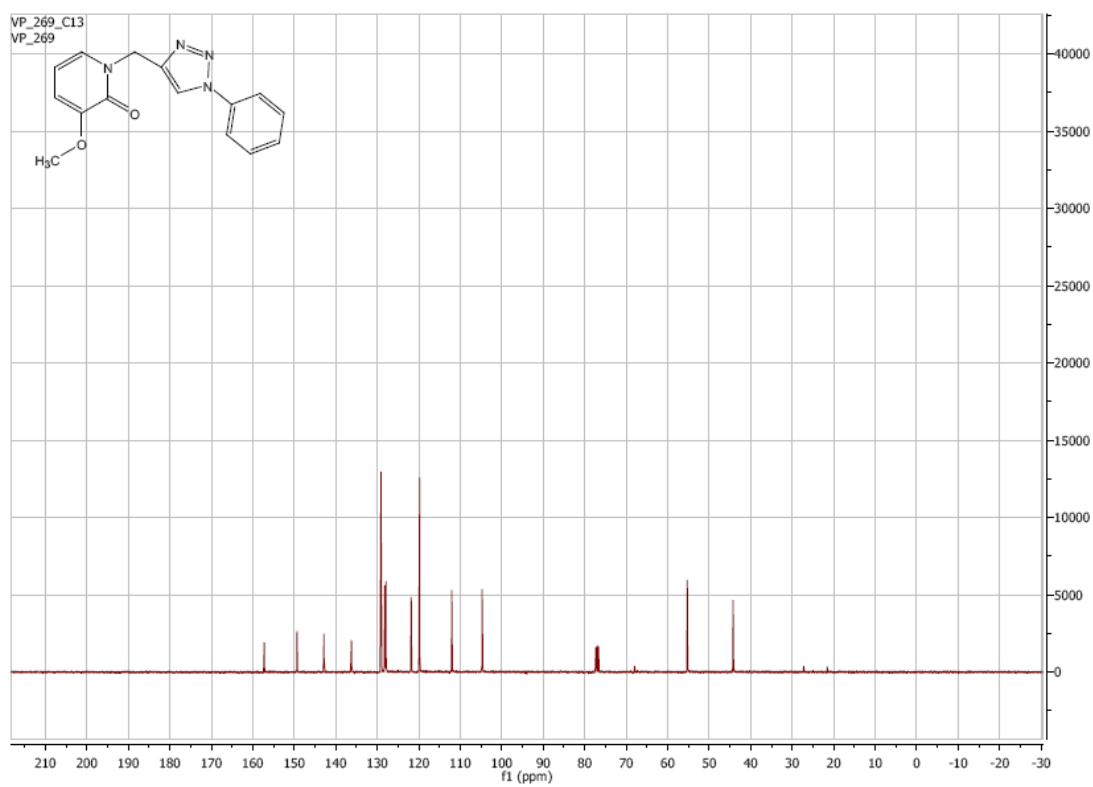
^{13}C NMR of **13**:



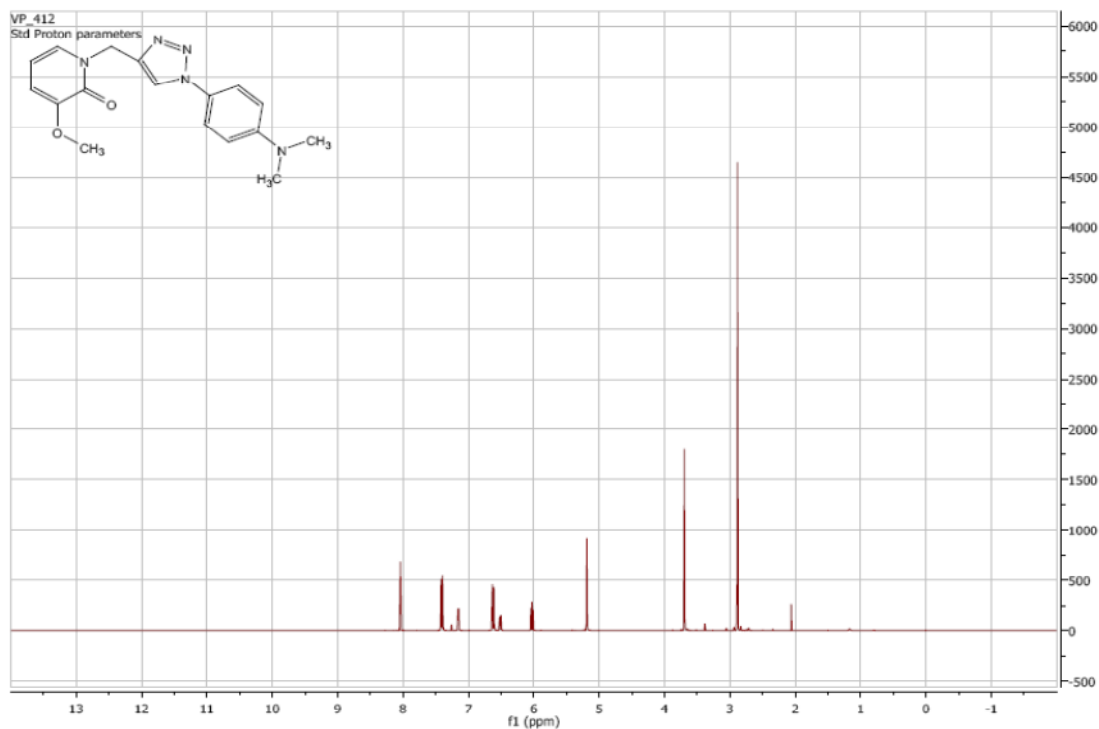
^1H NMR of **14a**:



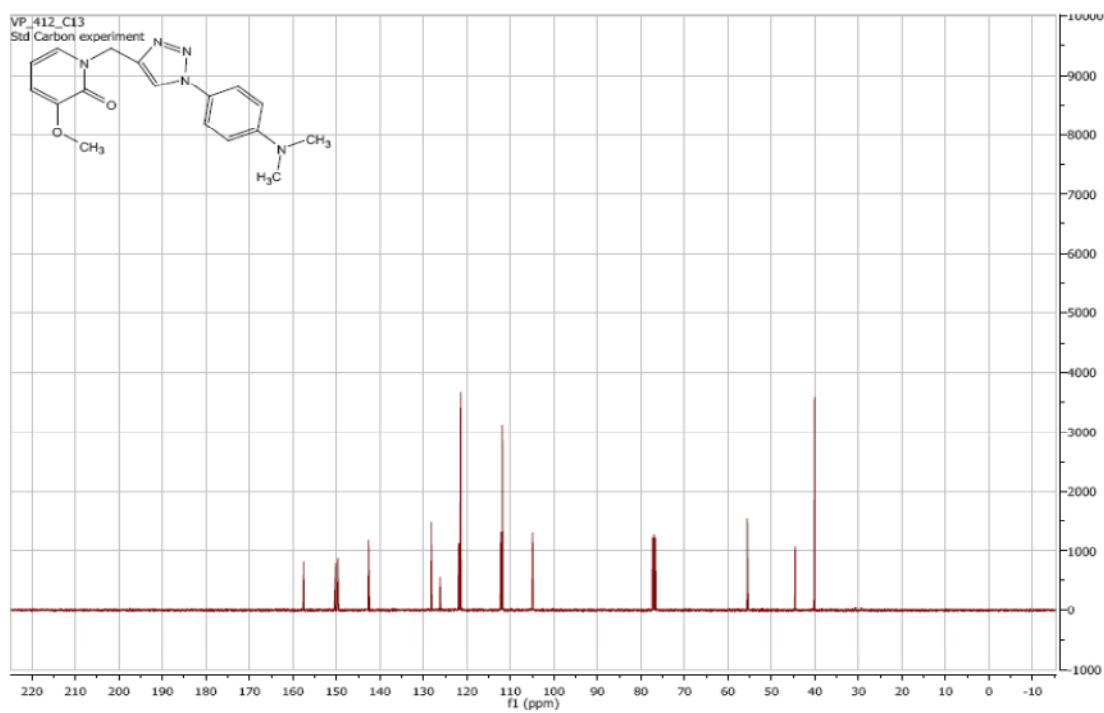
¹³C NMR of **14a**:



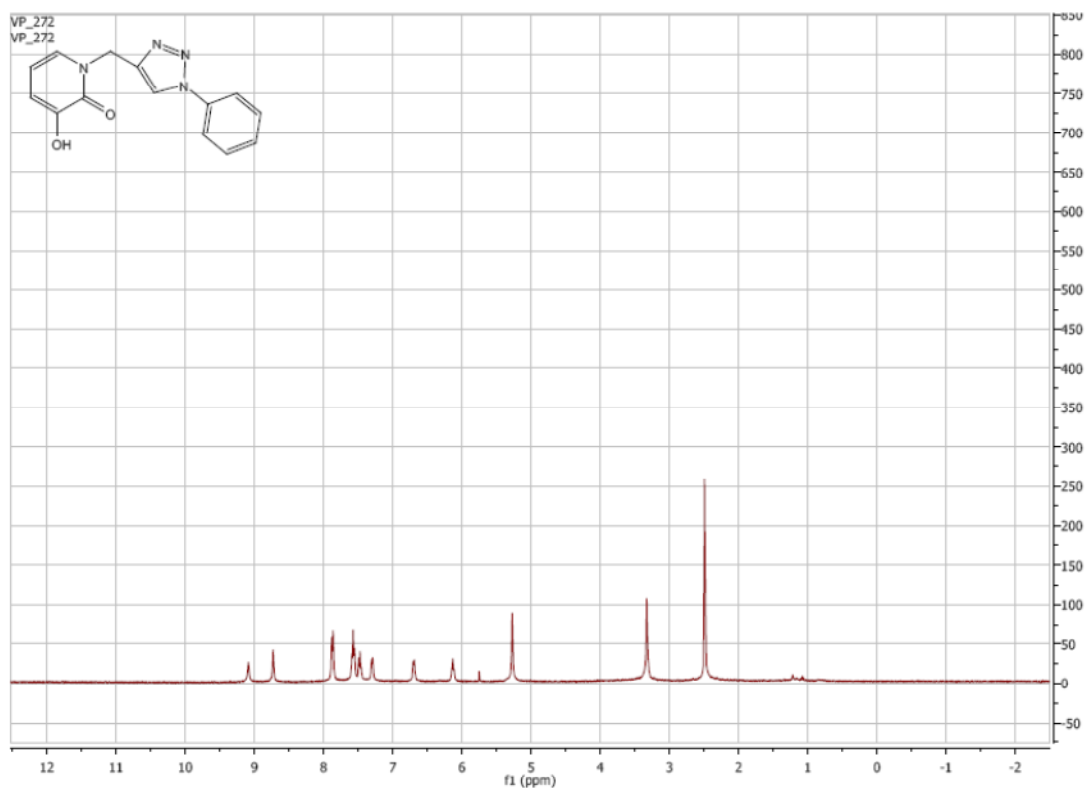
¹H NMR of **14b**:



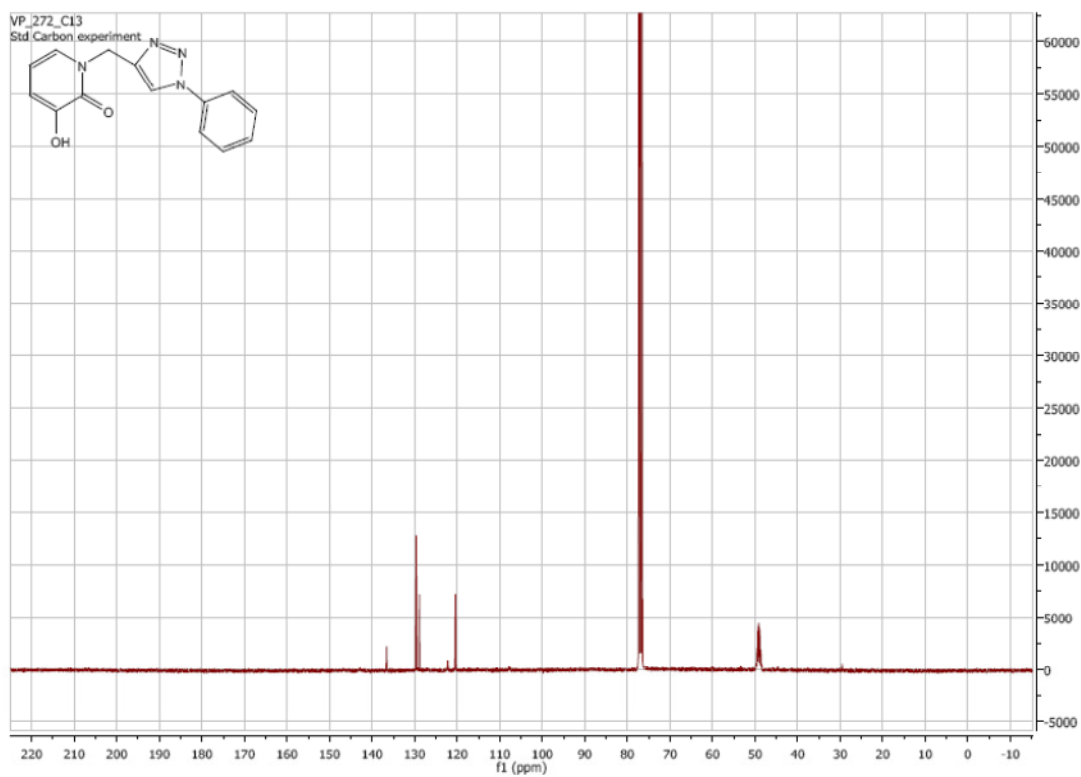
¹³C NMR of **14b**:



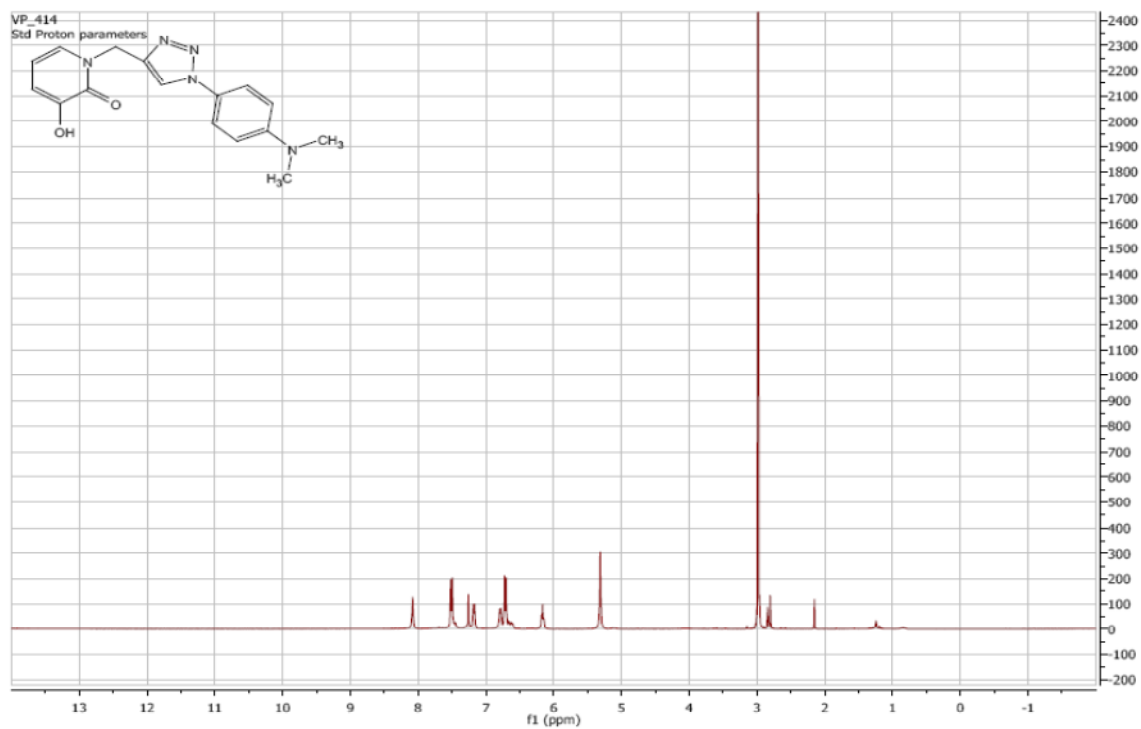
¹H NMR of **15a**:



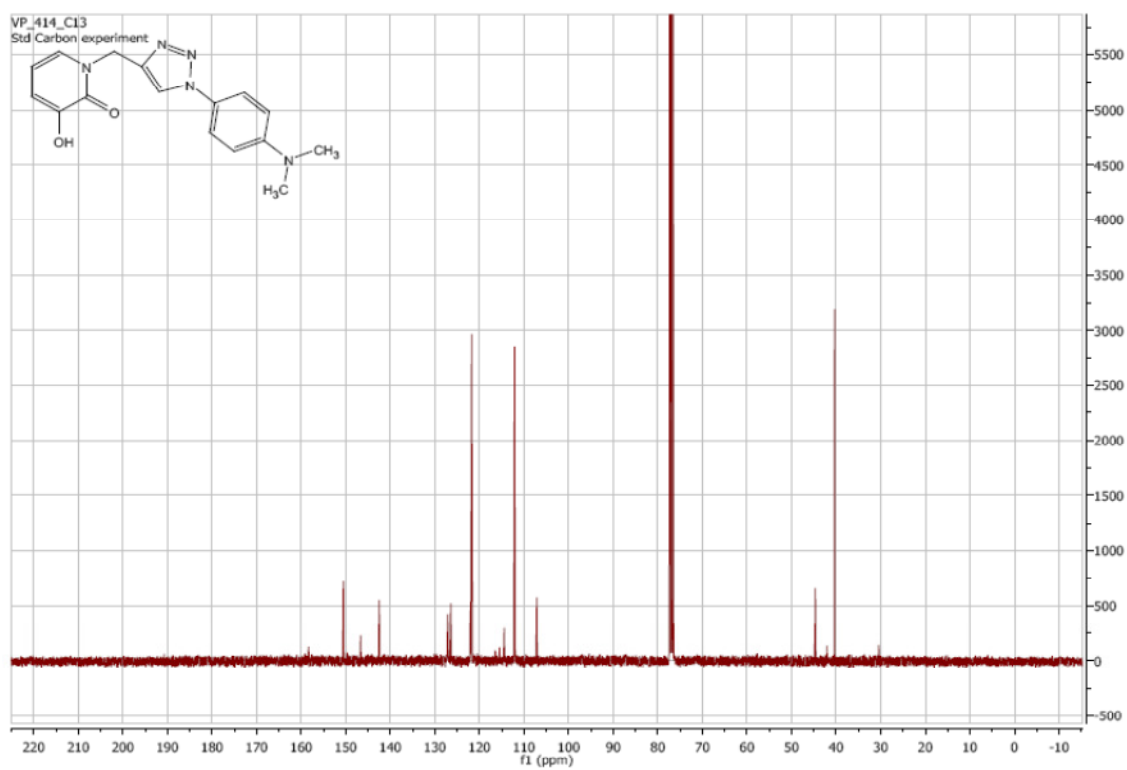
^{13}C NMR of **15a**:



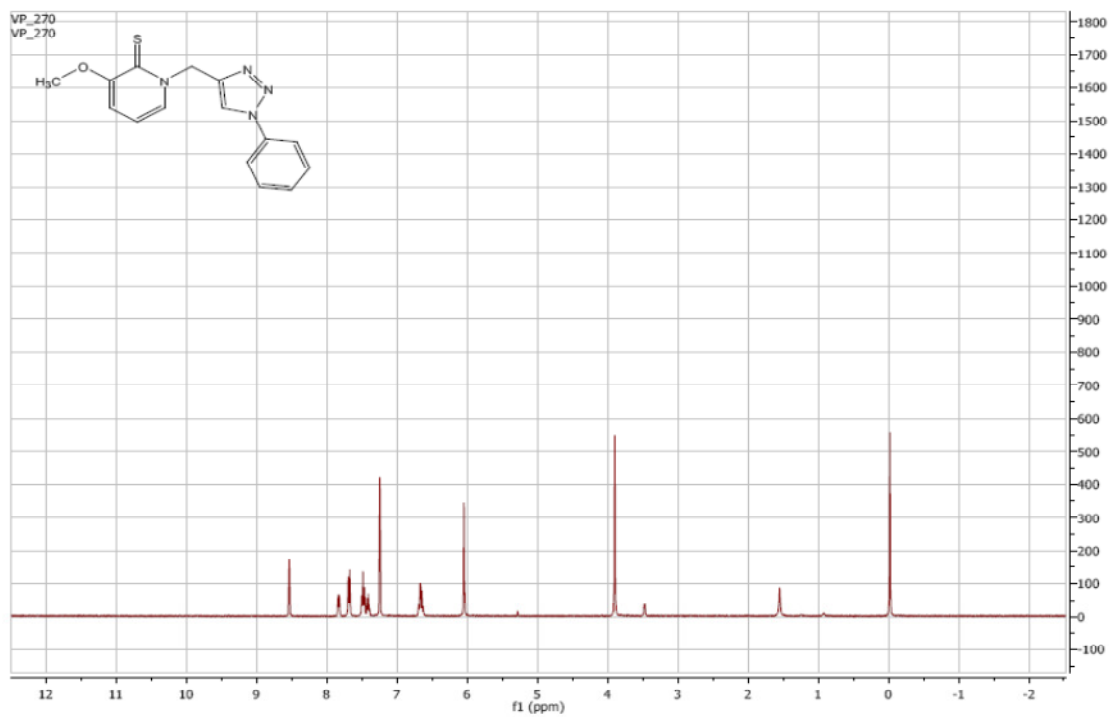
^1H NMR of **15b**:



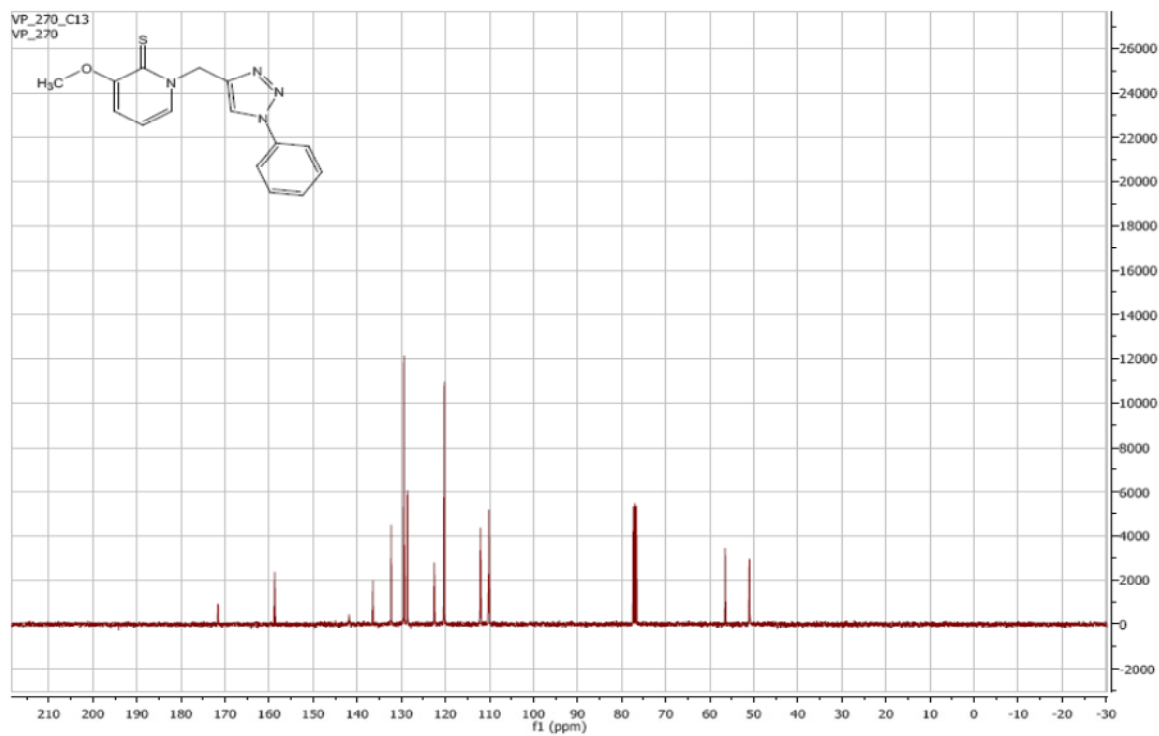
¹³C NMR of **15b**:



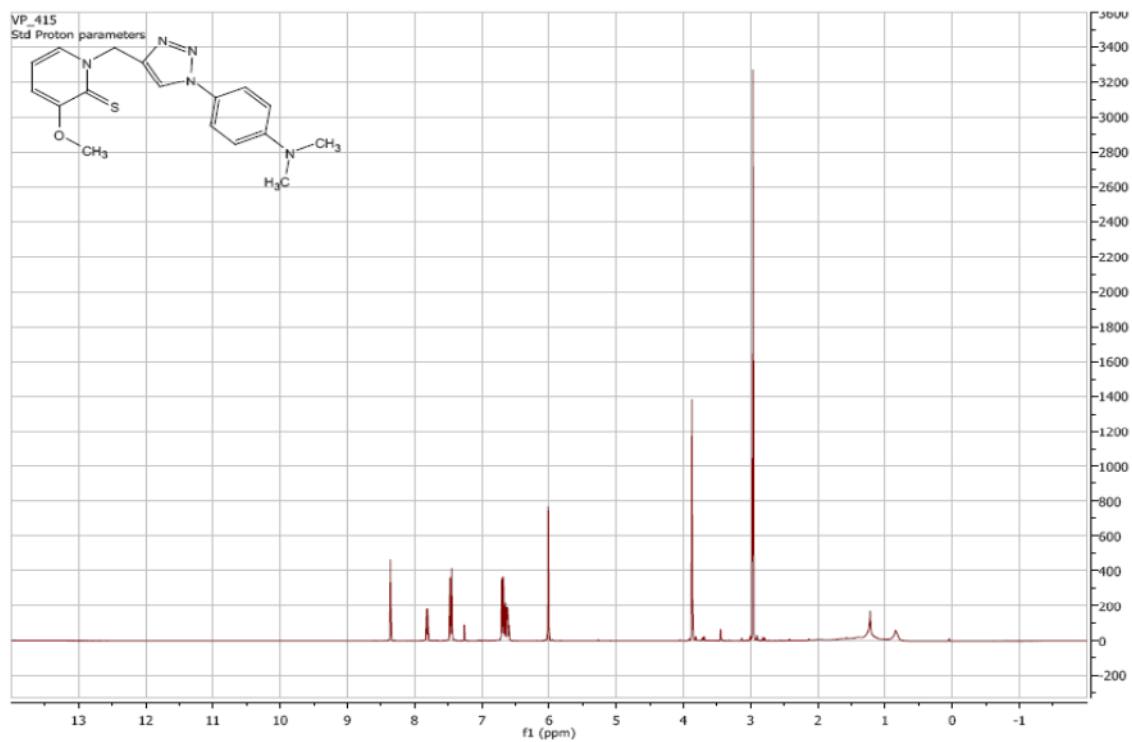
¹H NMR of **16a**:



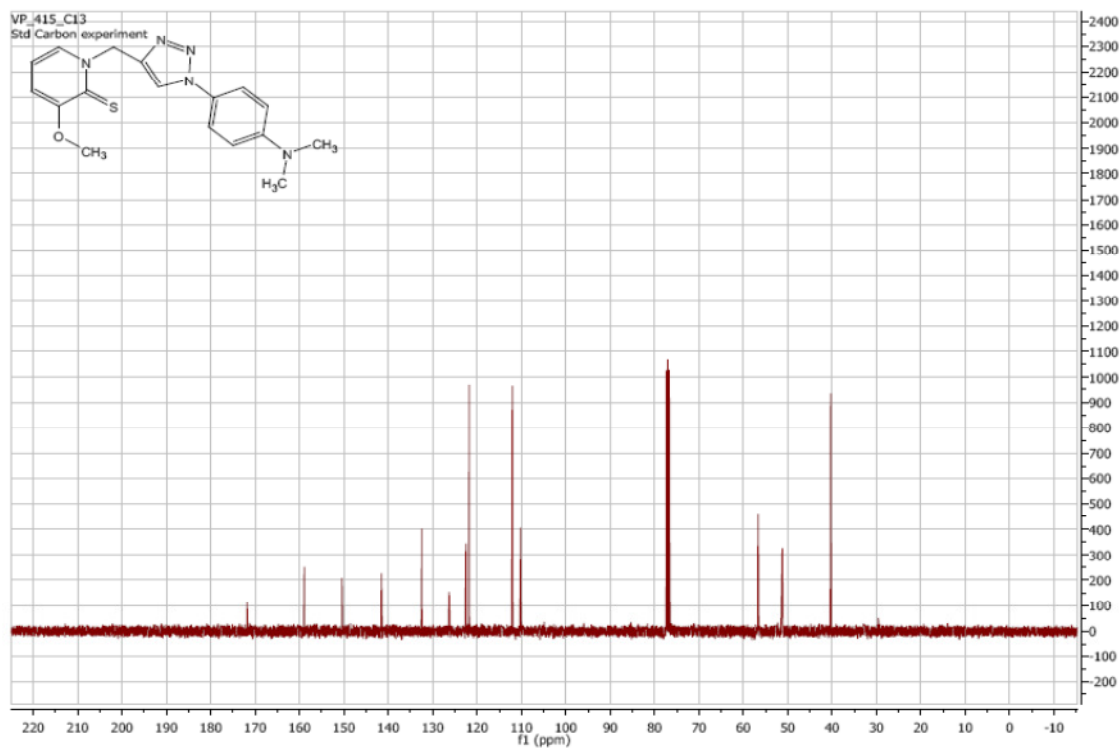
^{13}C NMR of **16a**:



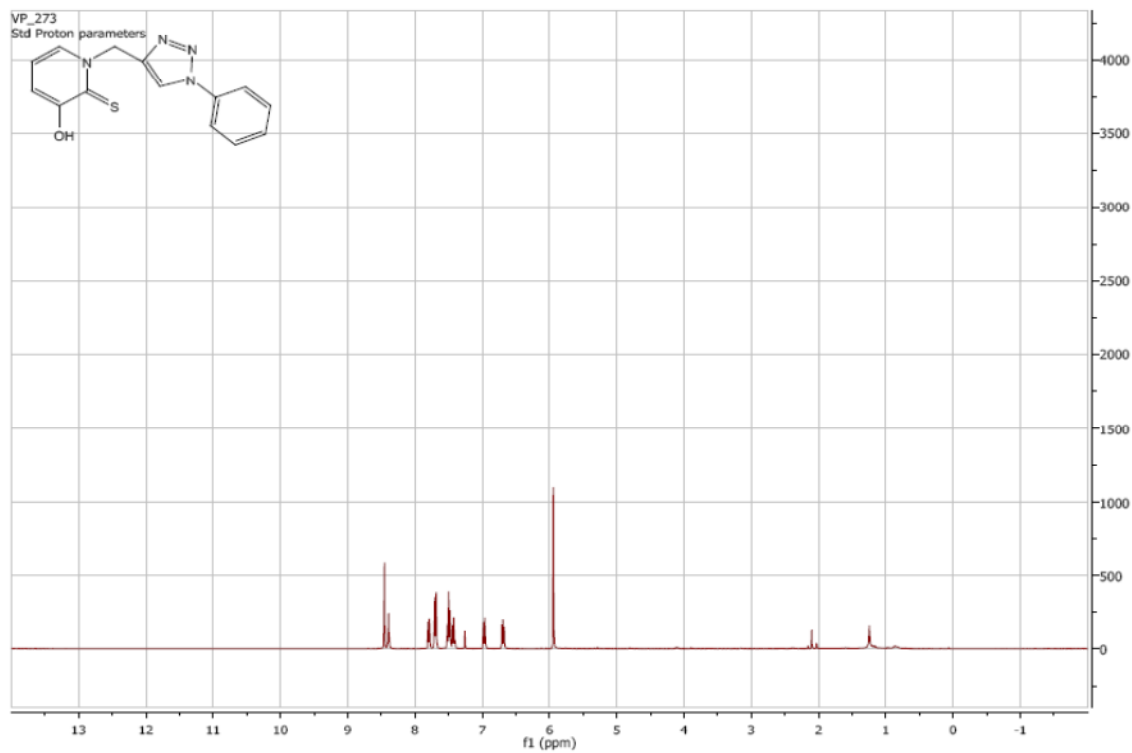
^1H NMR of **16b**:



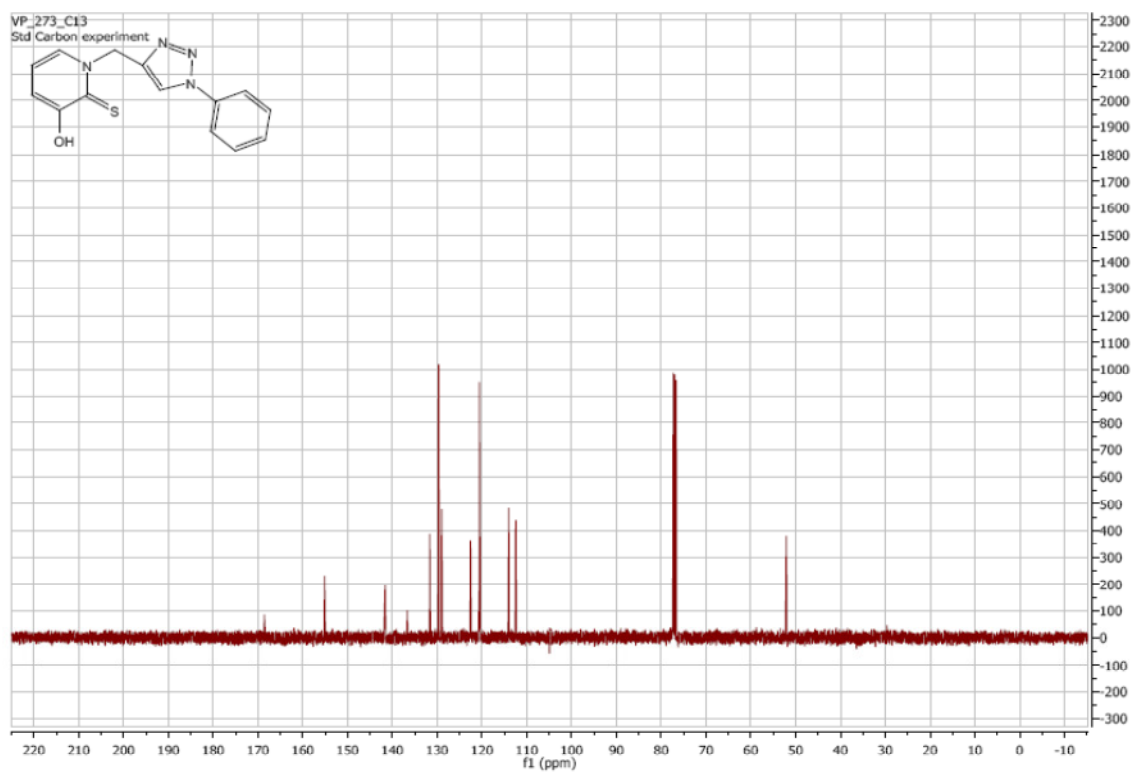
¹³C NMR of **16b**:



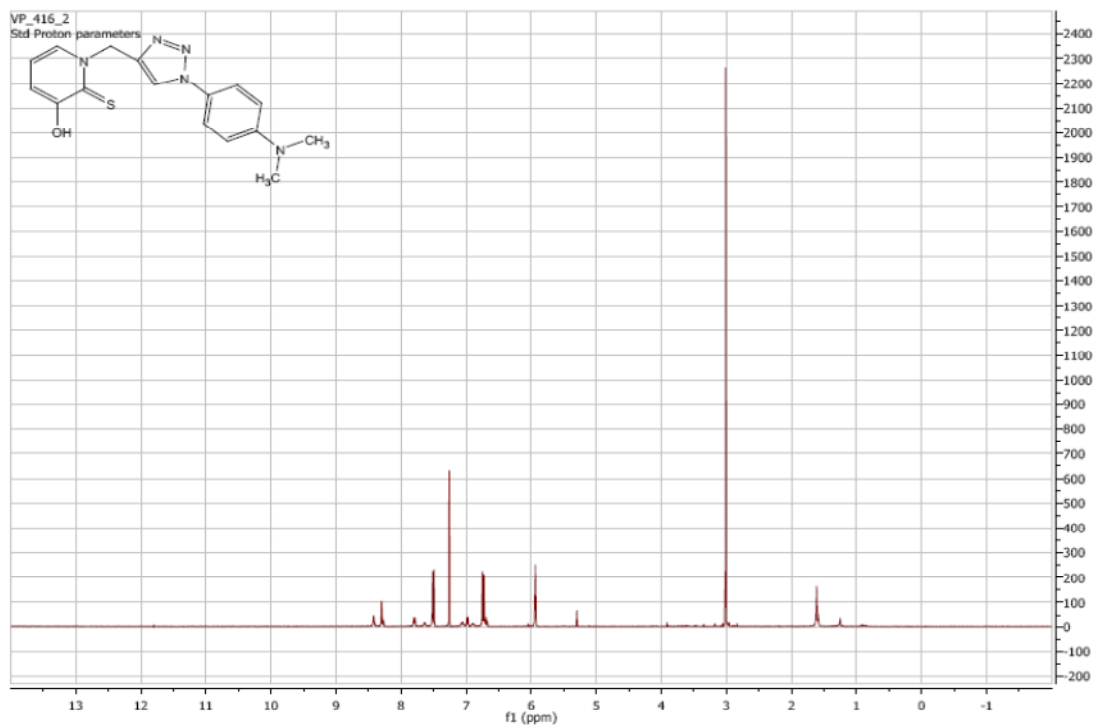
¹H NMR of **17a**:



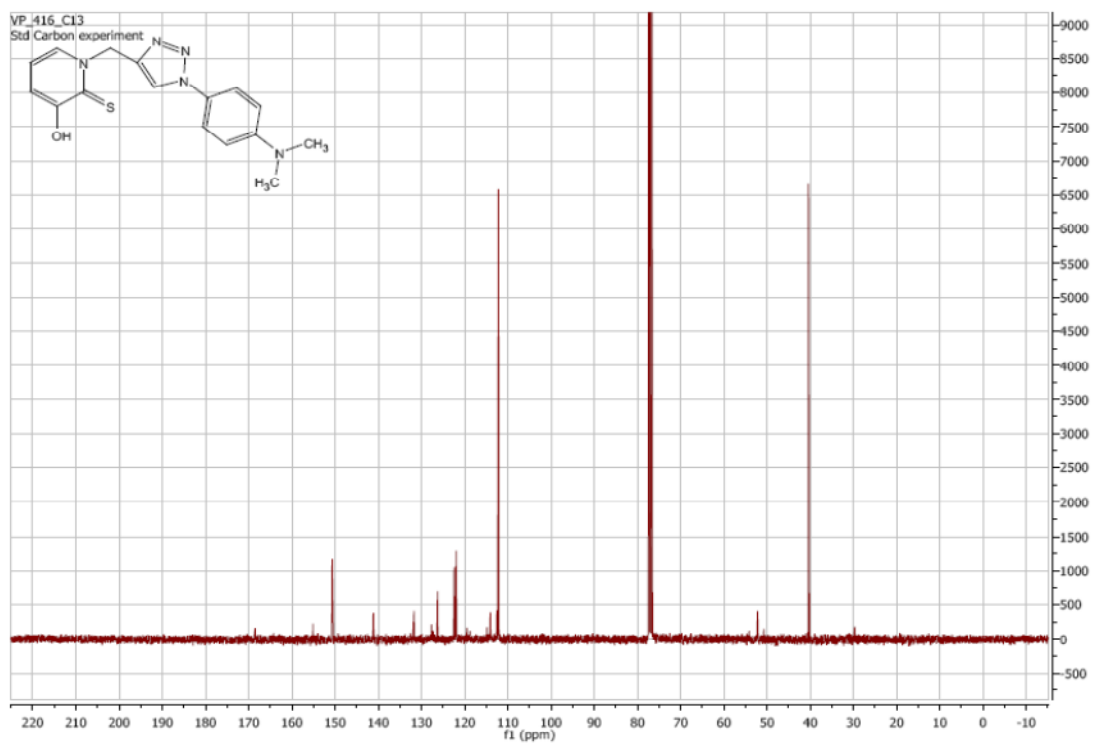
¹³C NMR of 17a:



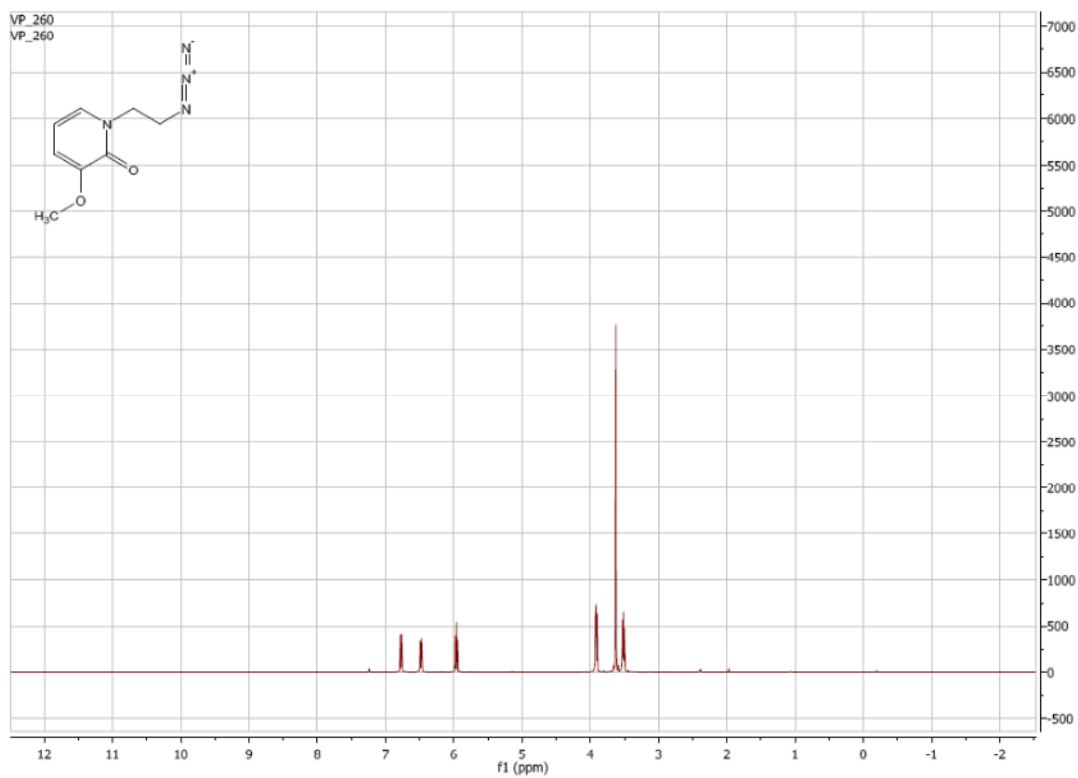
¹H NMR of 17b:



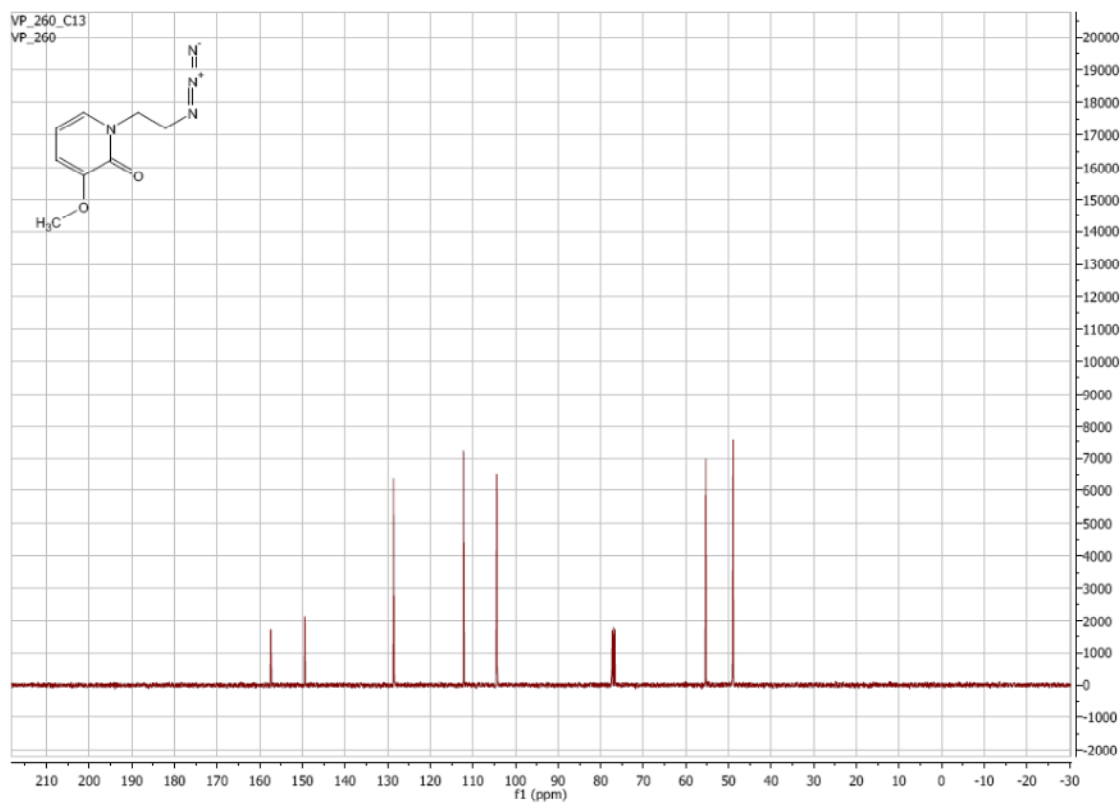
¹³C NMR of **17b**:



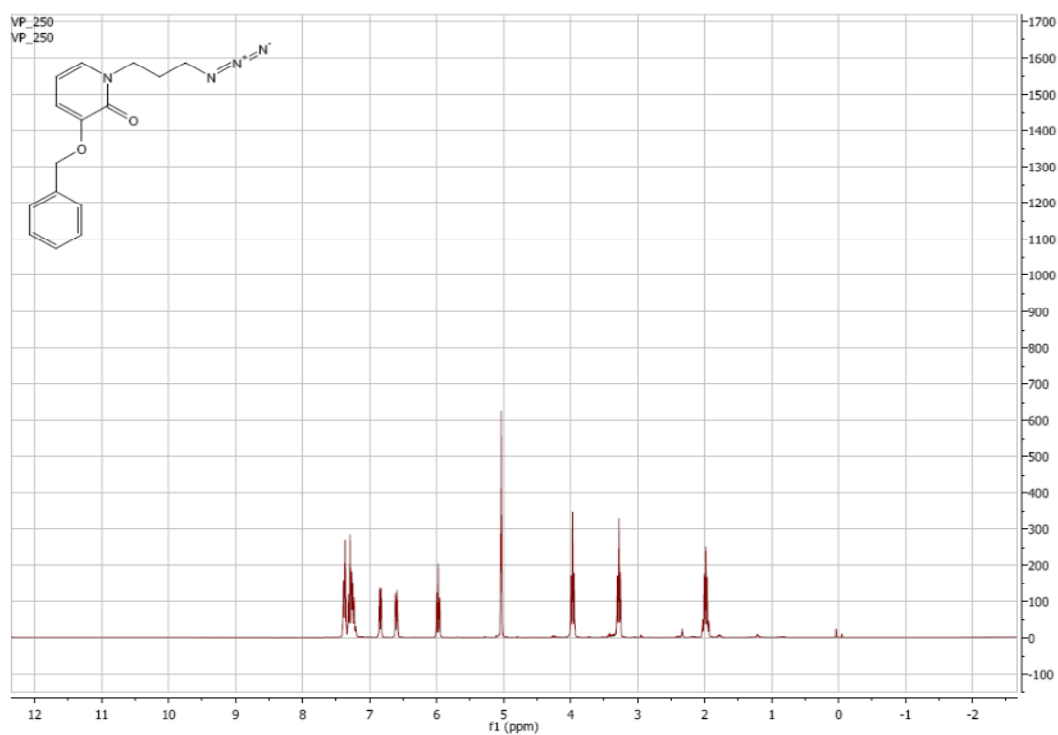
¹H NMR of **20a**:



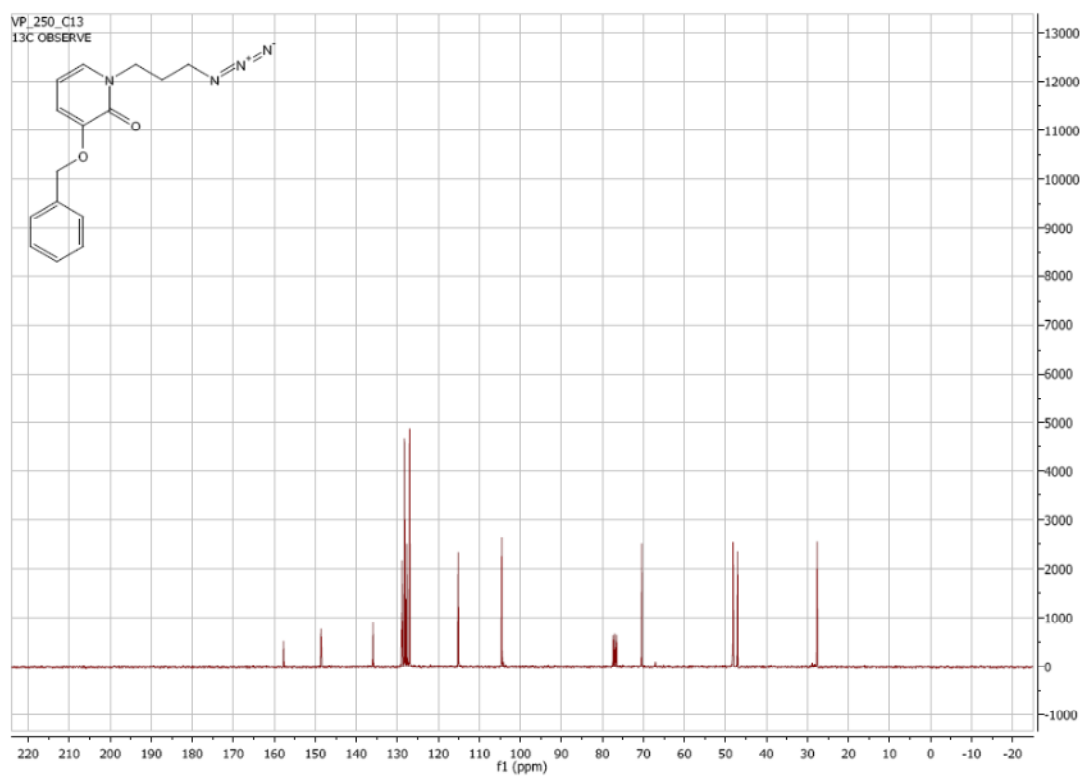
¹³C NMR of **20a**:

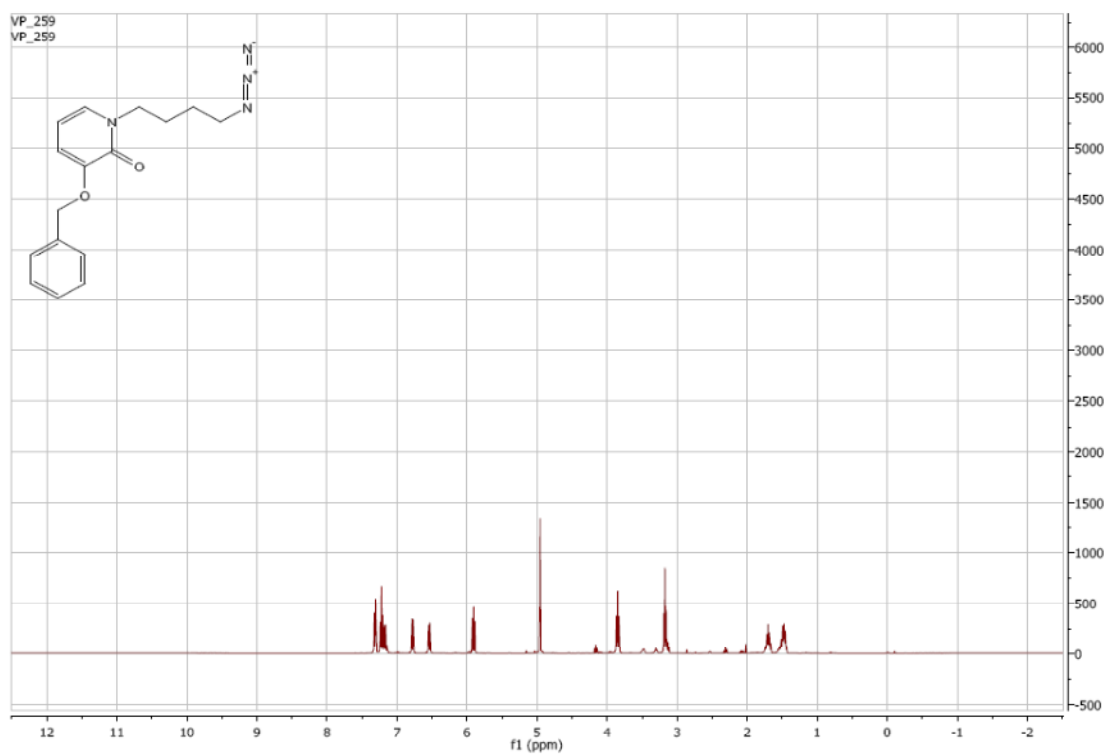
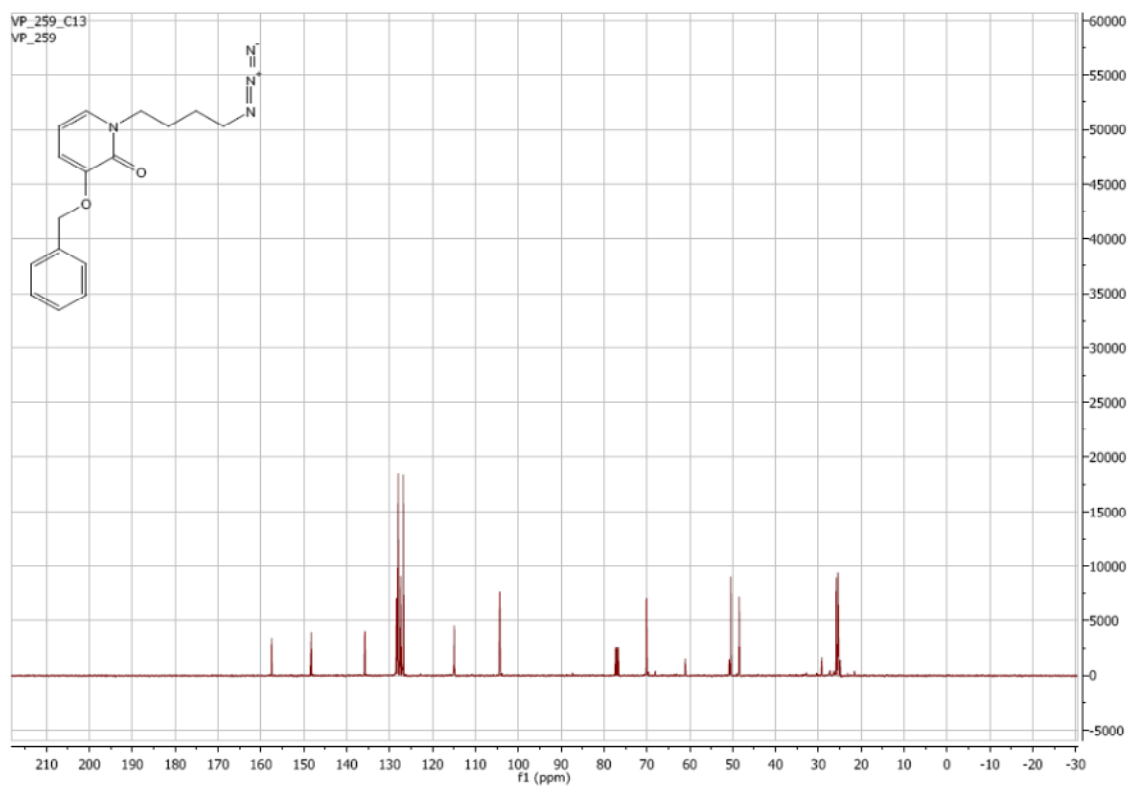


¹H NMR of **20b**:

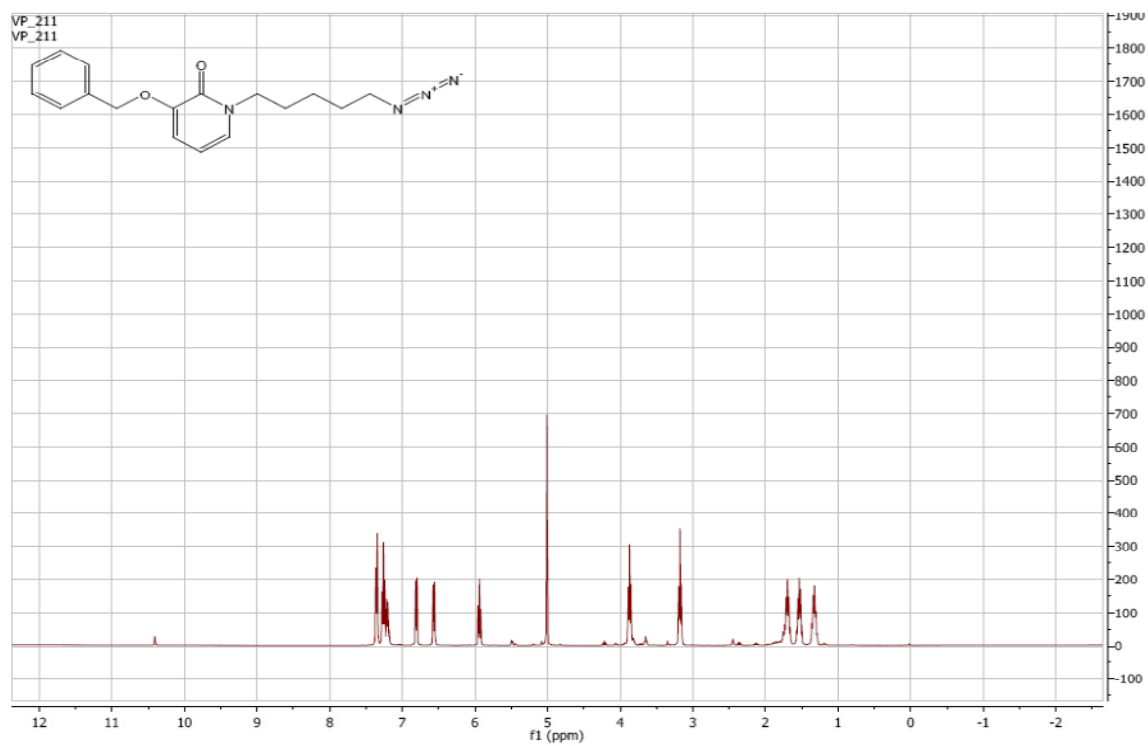


¹³C NMR of **20b**:

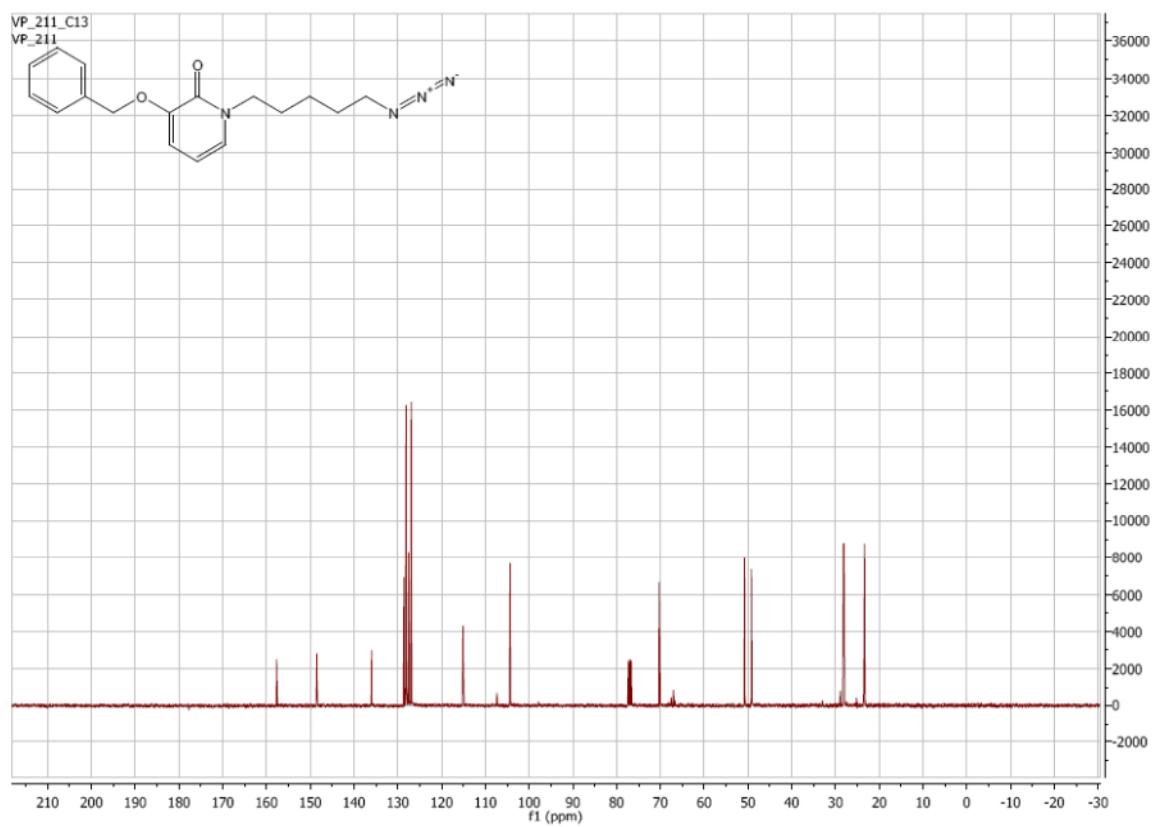


¹H NMR of **20c**: ^{13}C NMR of **20c**:

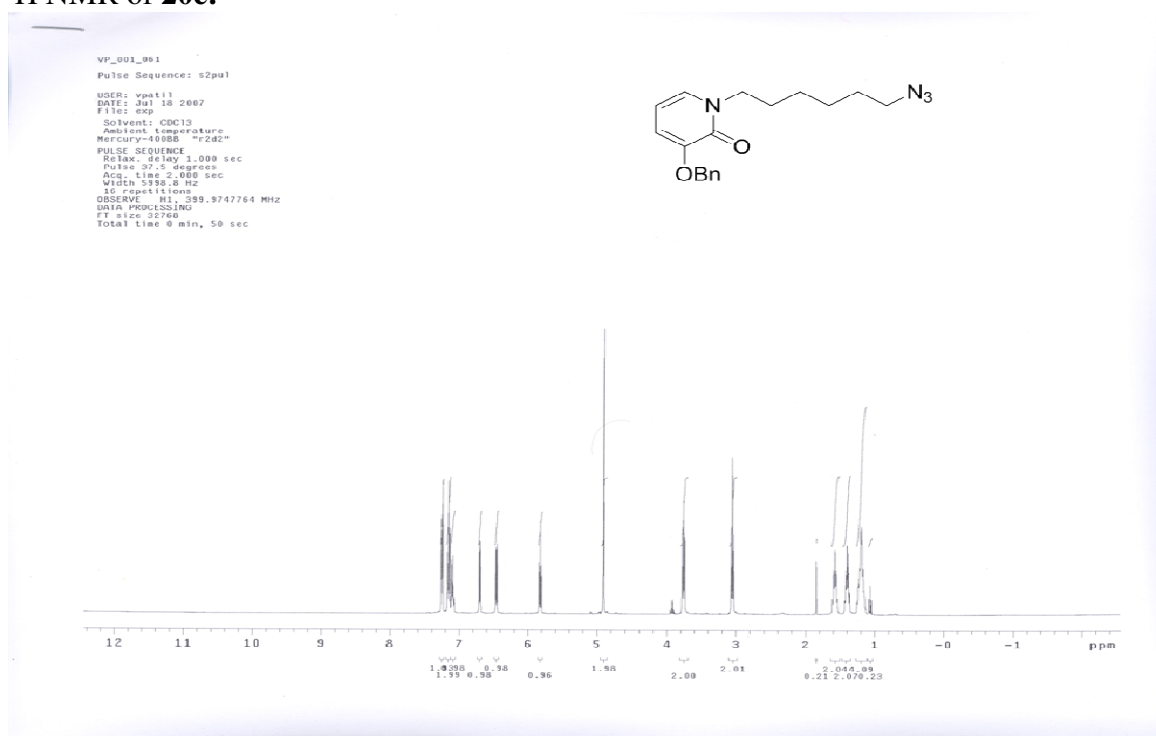
¹H NMR of **20d**:



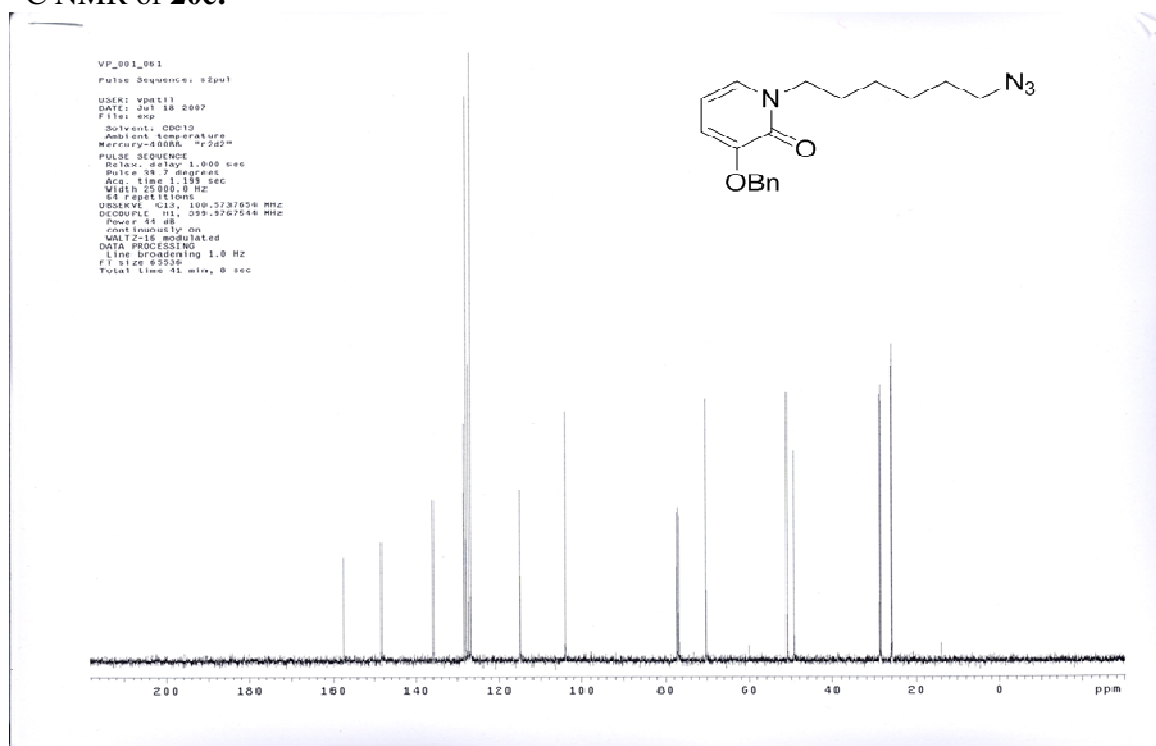
¹³C NMR of **20d**:



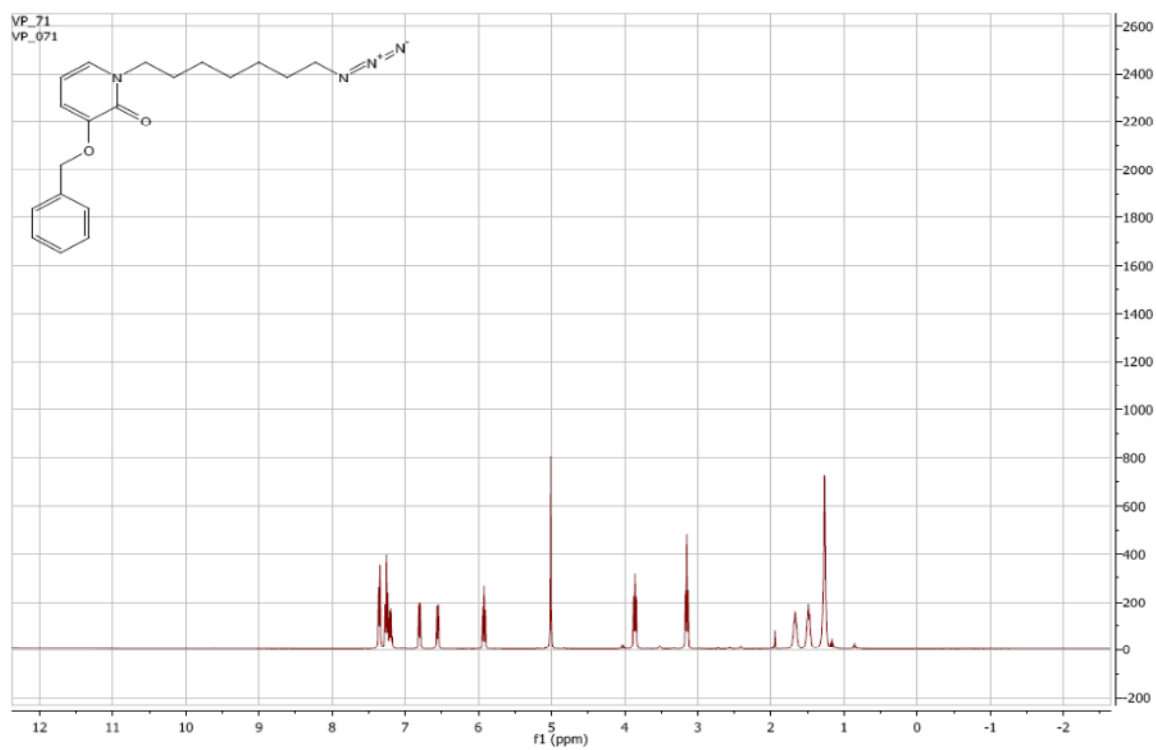
¹H NMR of 20e:



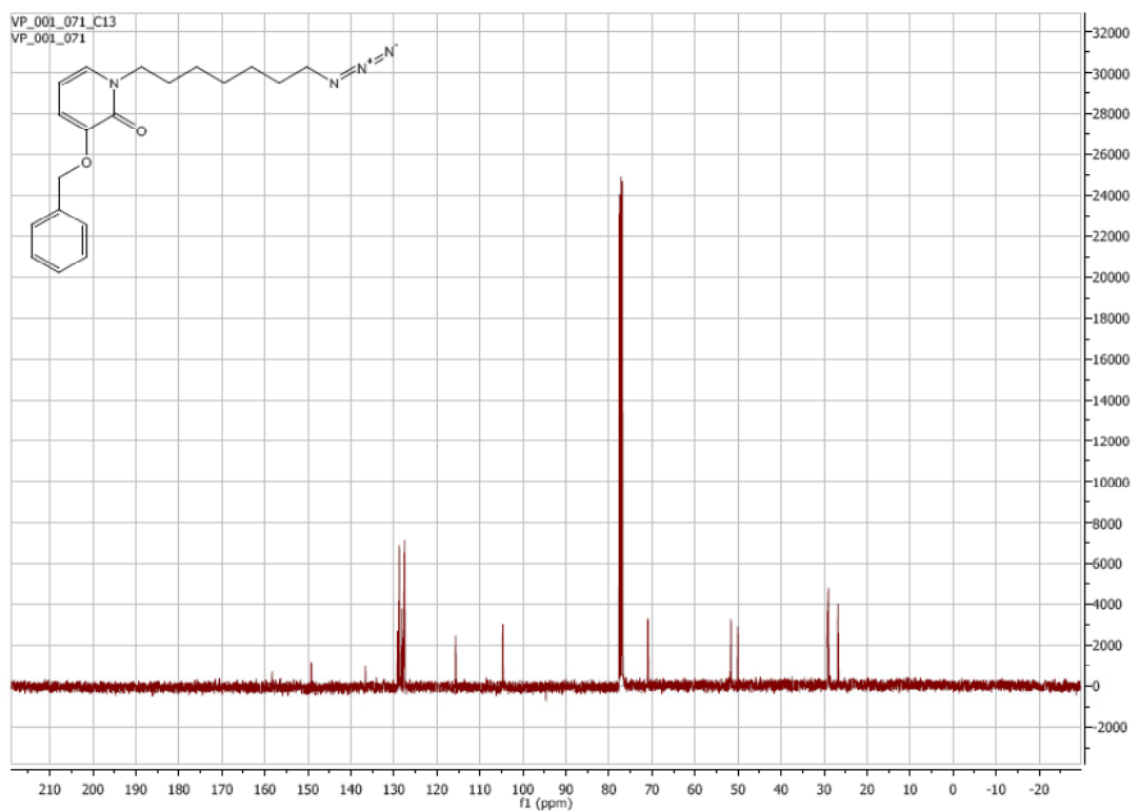
¹³C NMR of 20e:



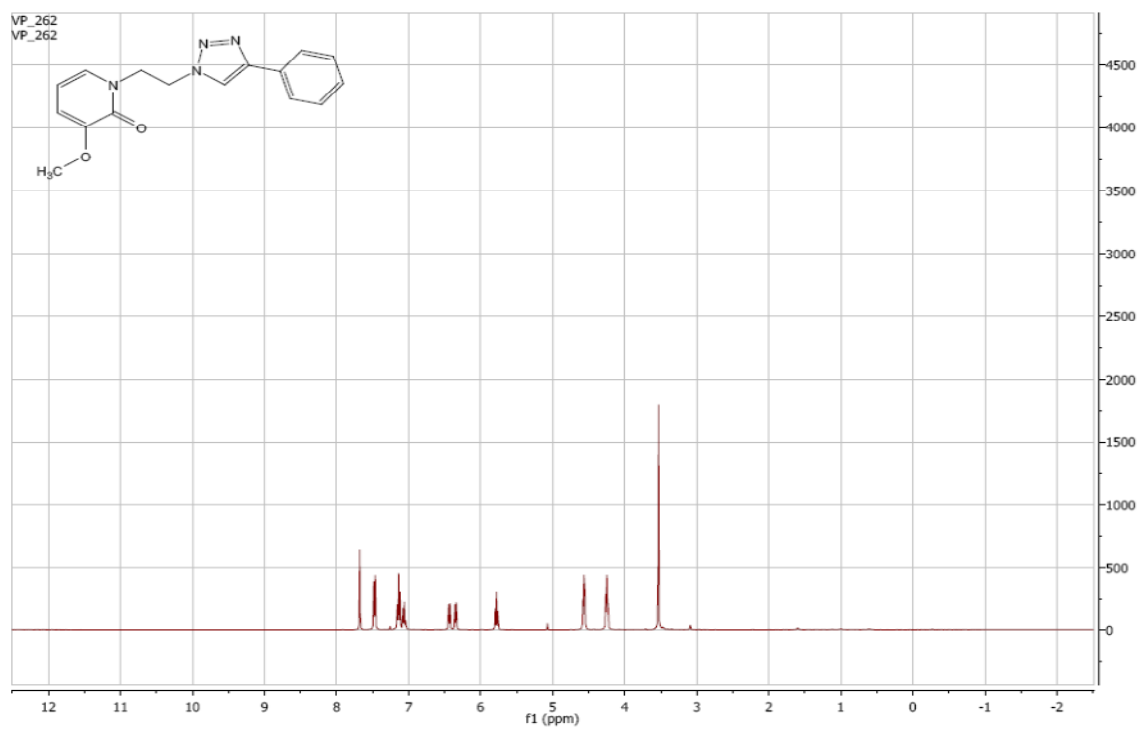
¹H NMR of **20f**:



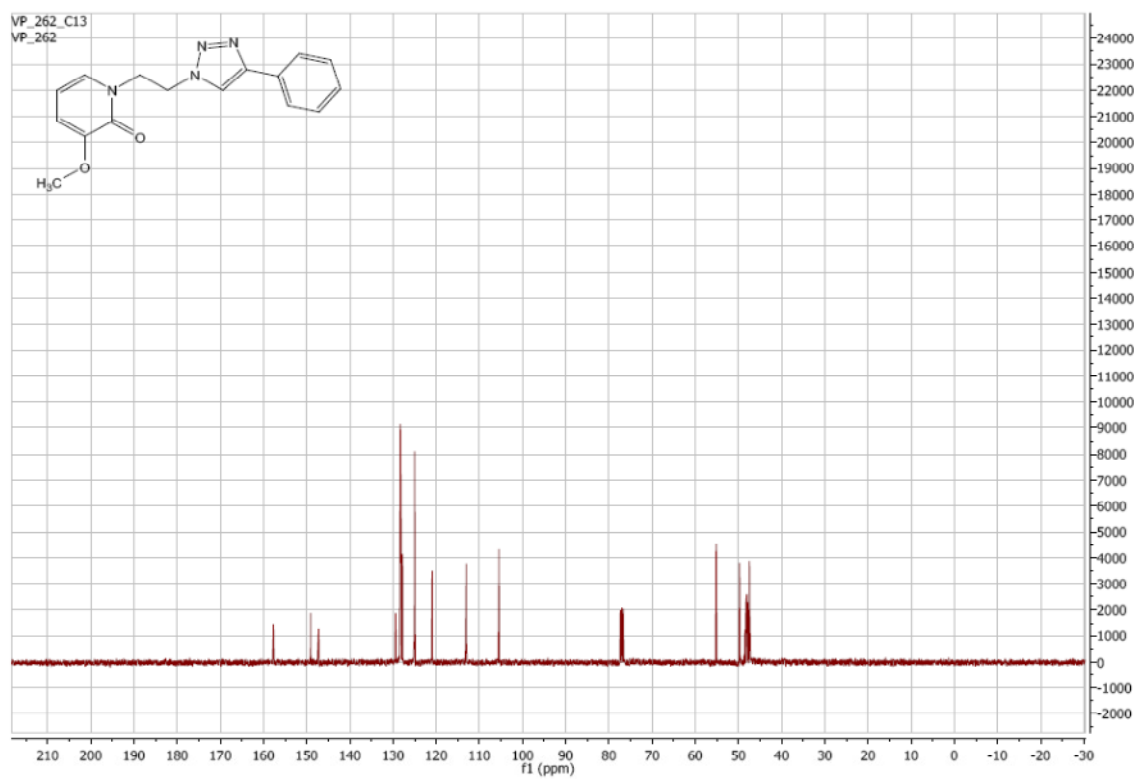
¹³C NMR of **20f**:



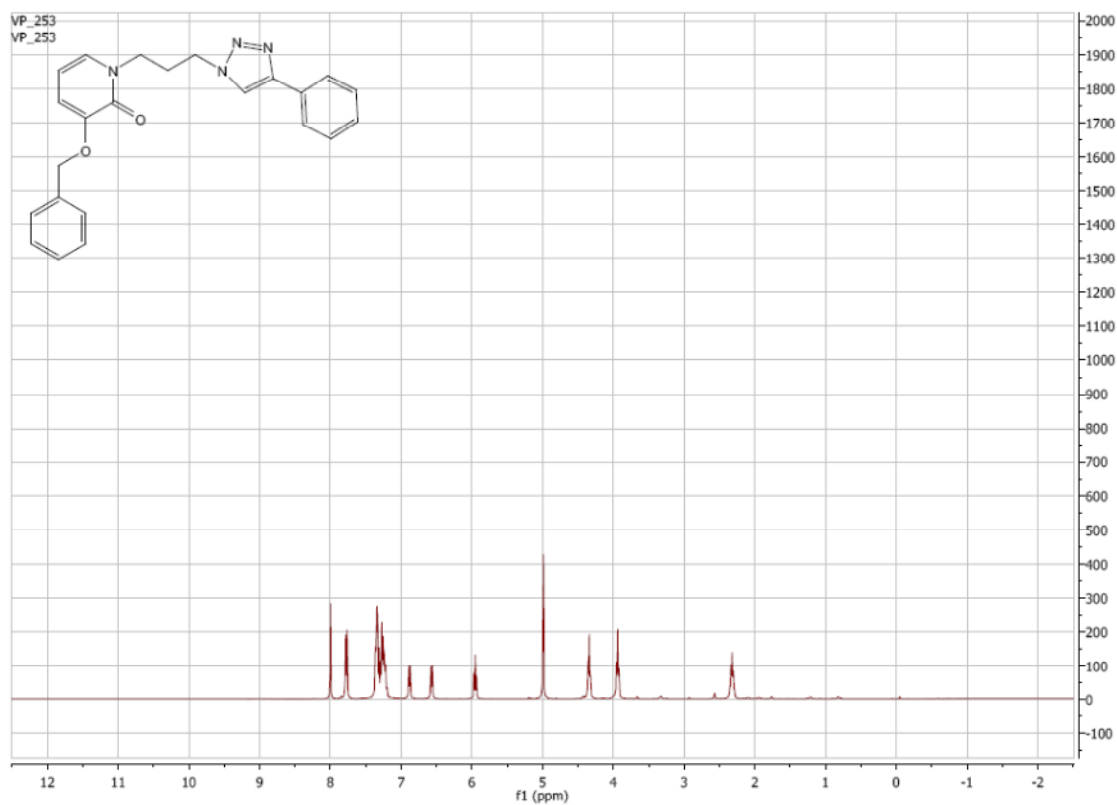
¹H NMR of **21a**:



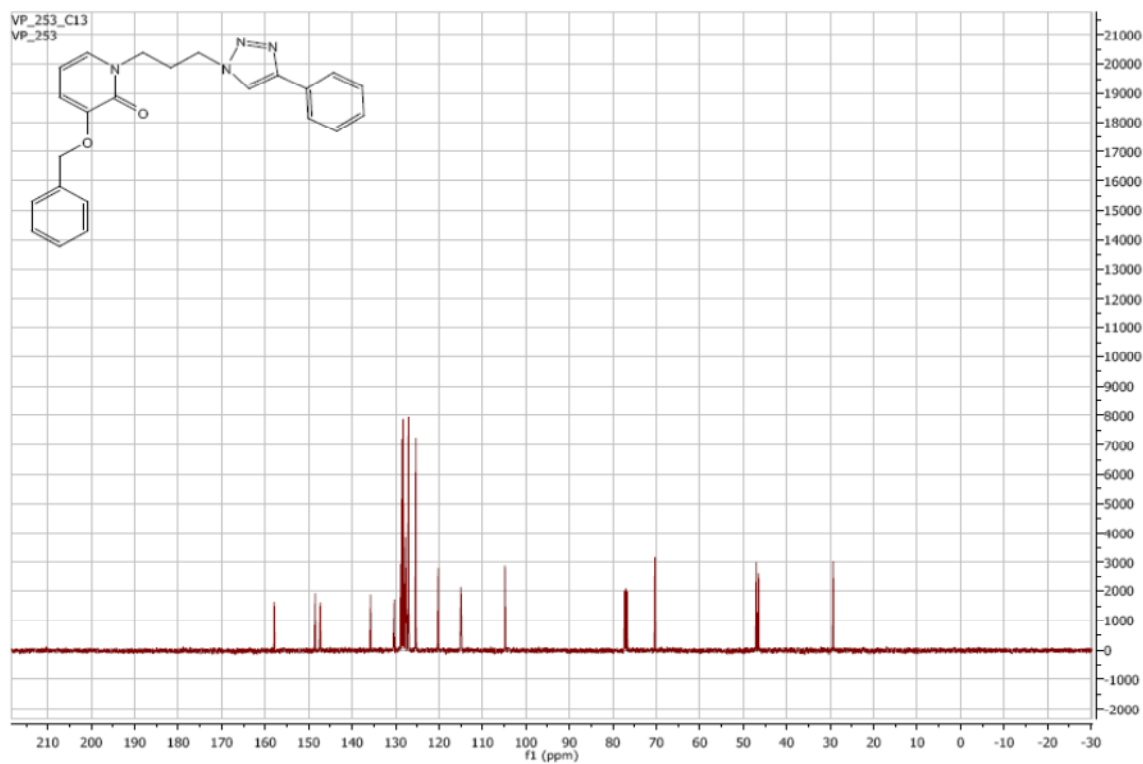
¹³C NMR of **21a**:



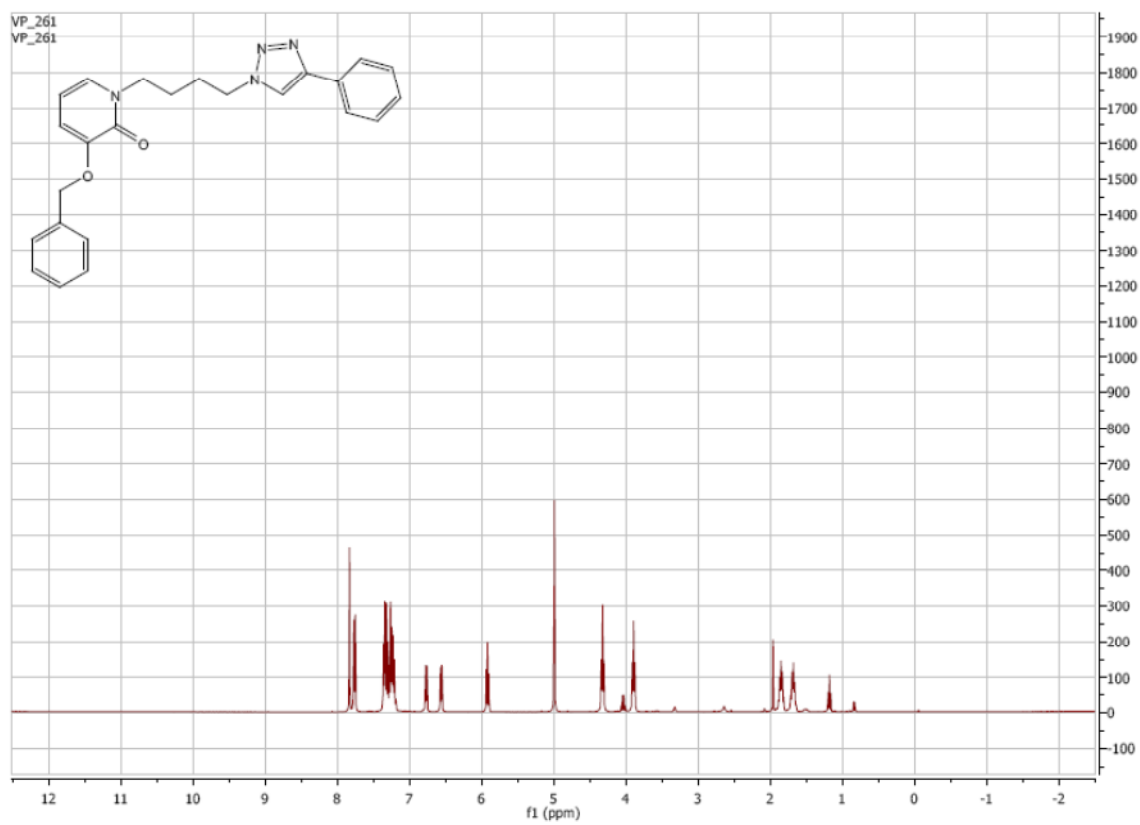
¹H NMR of **21b**:



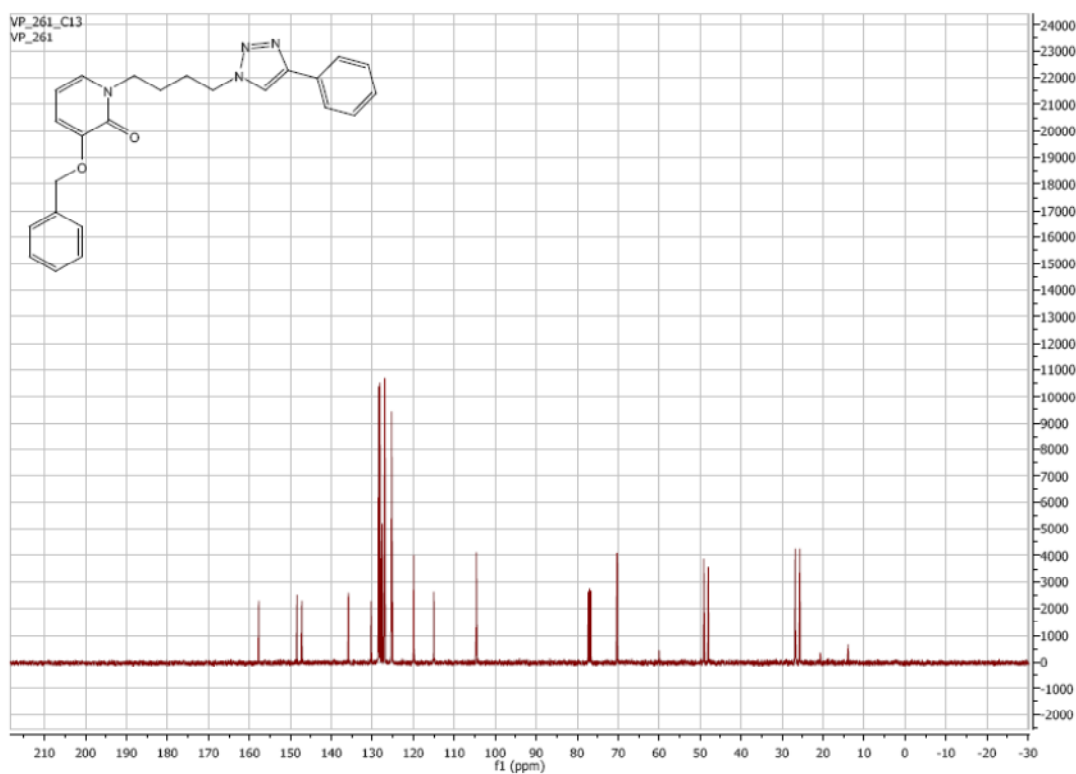
¹³C NMR of **21b**:



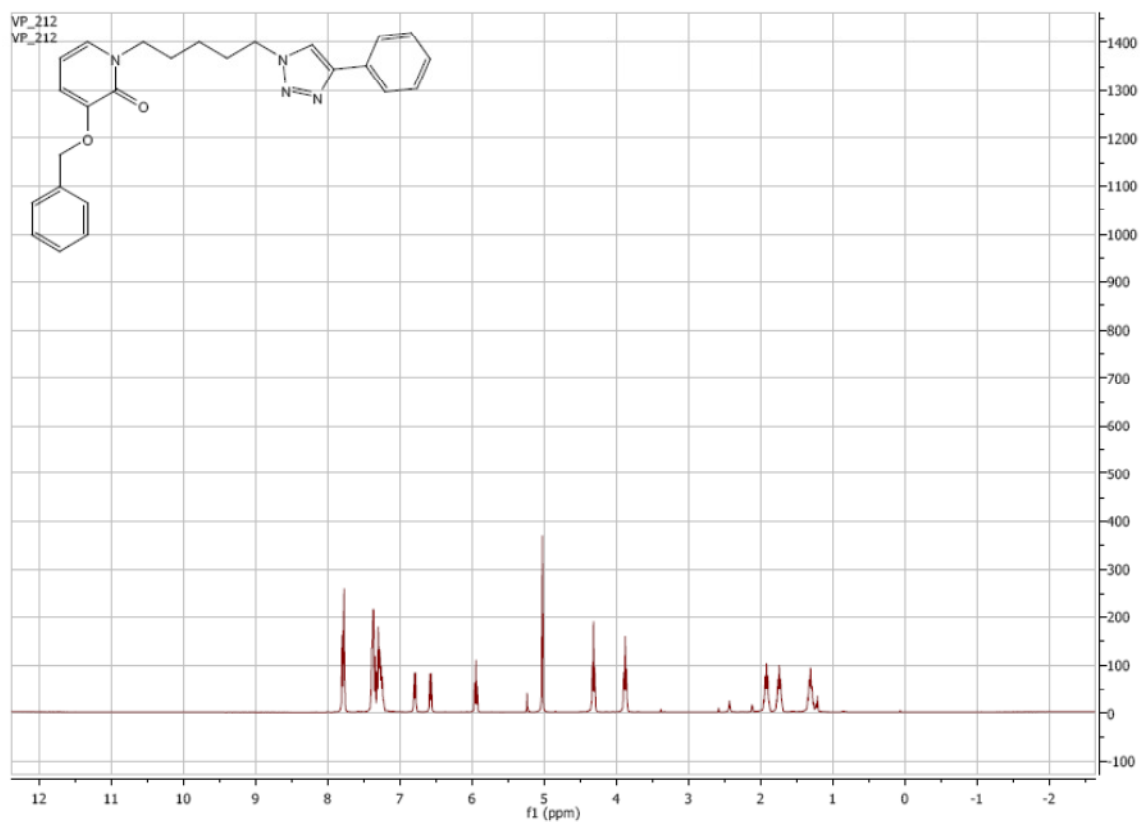
¹H NMR of **21c**:



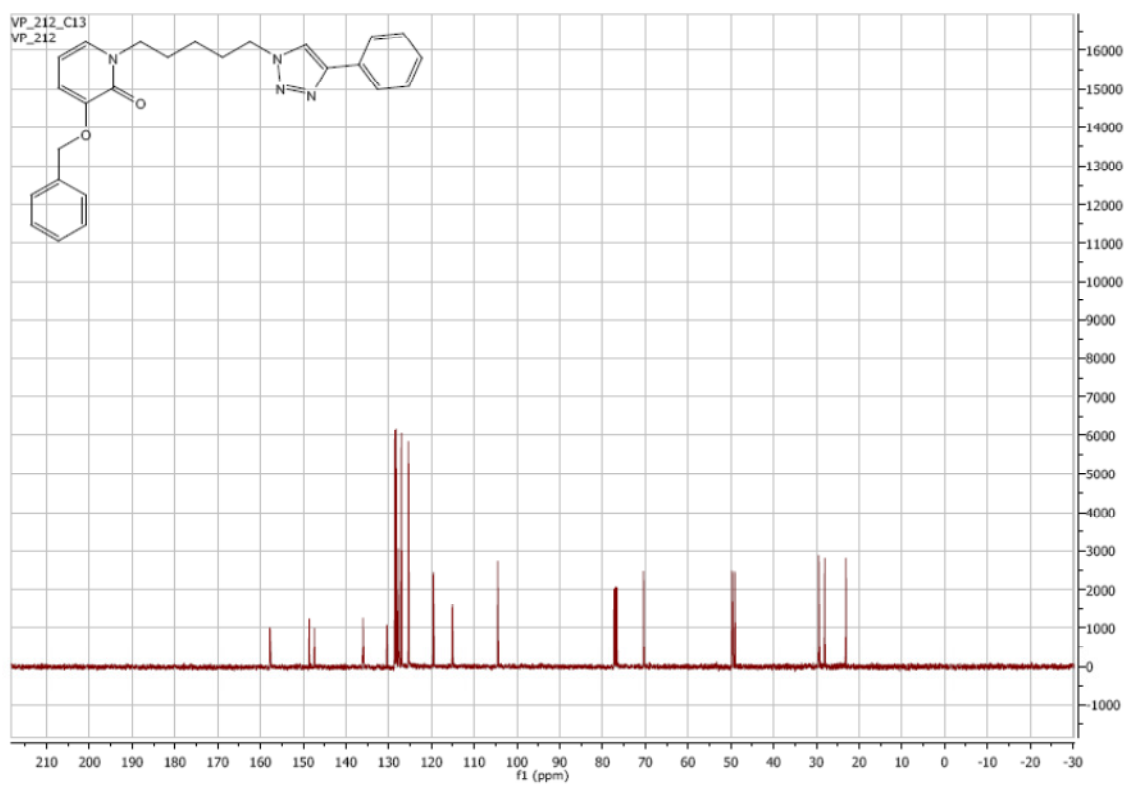
¹³C NMR of **21c**:



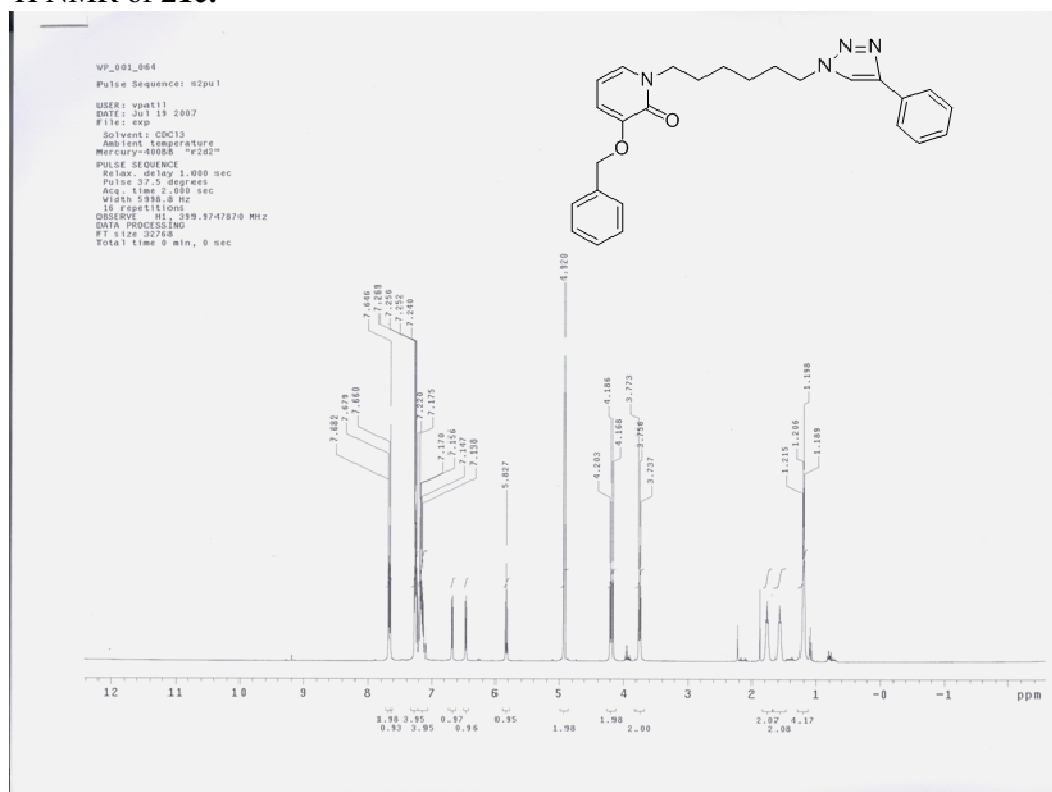
¹H NMR of **21d**:



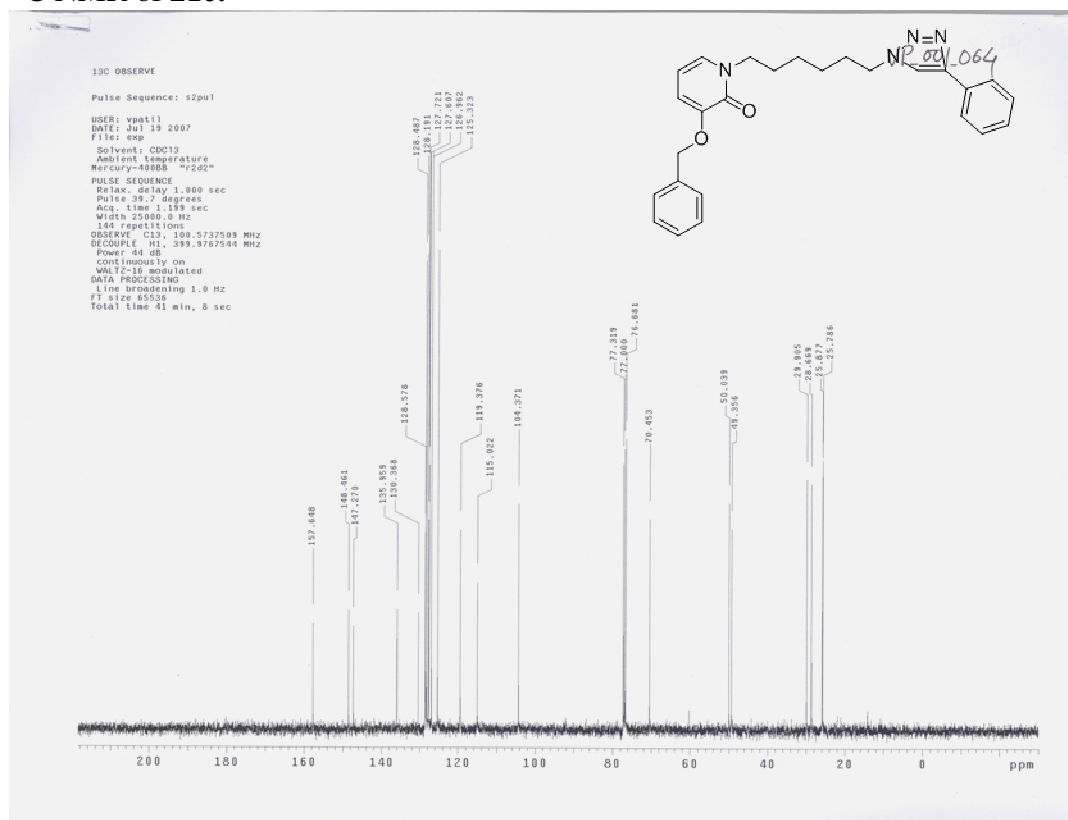
¹³C NMR of **21d**:



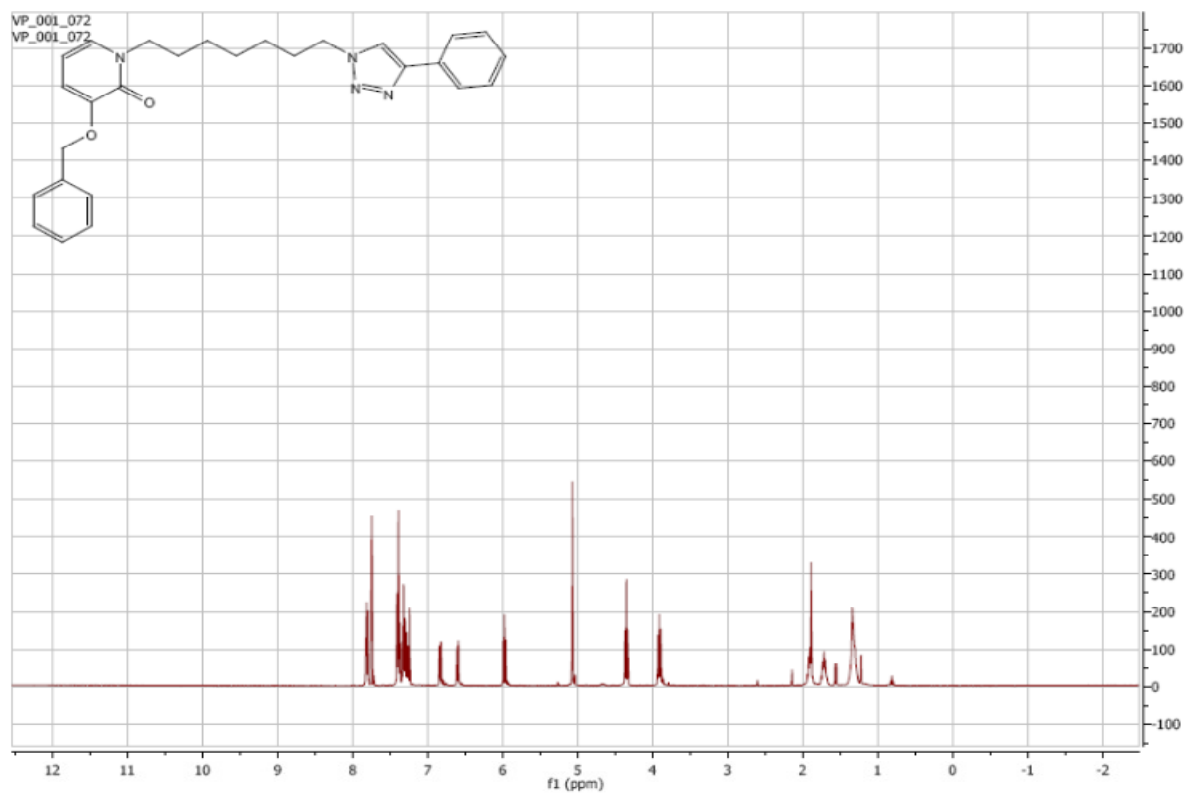
¹H NMR of 21e:



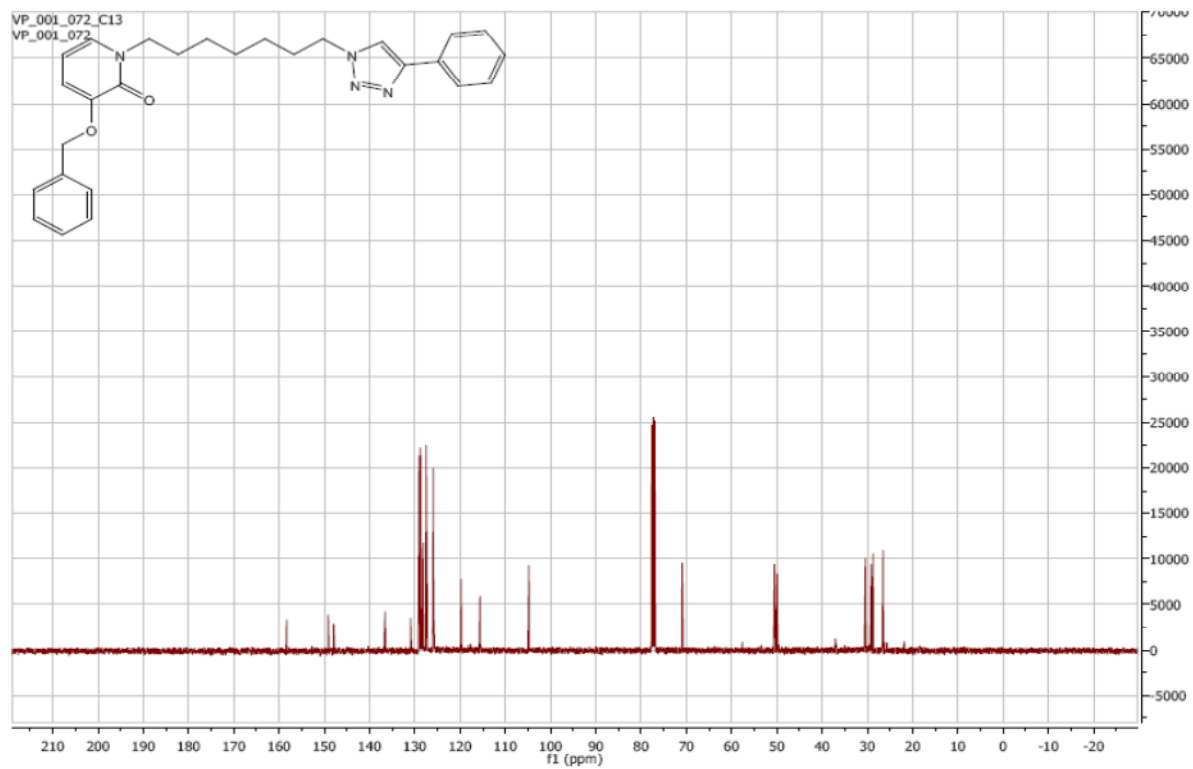
¹³C NMR of 21e:



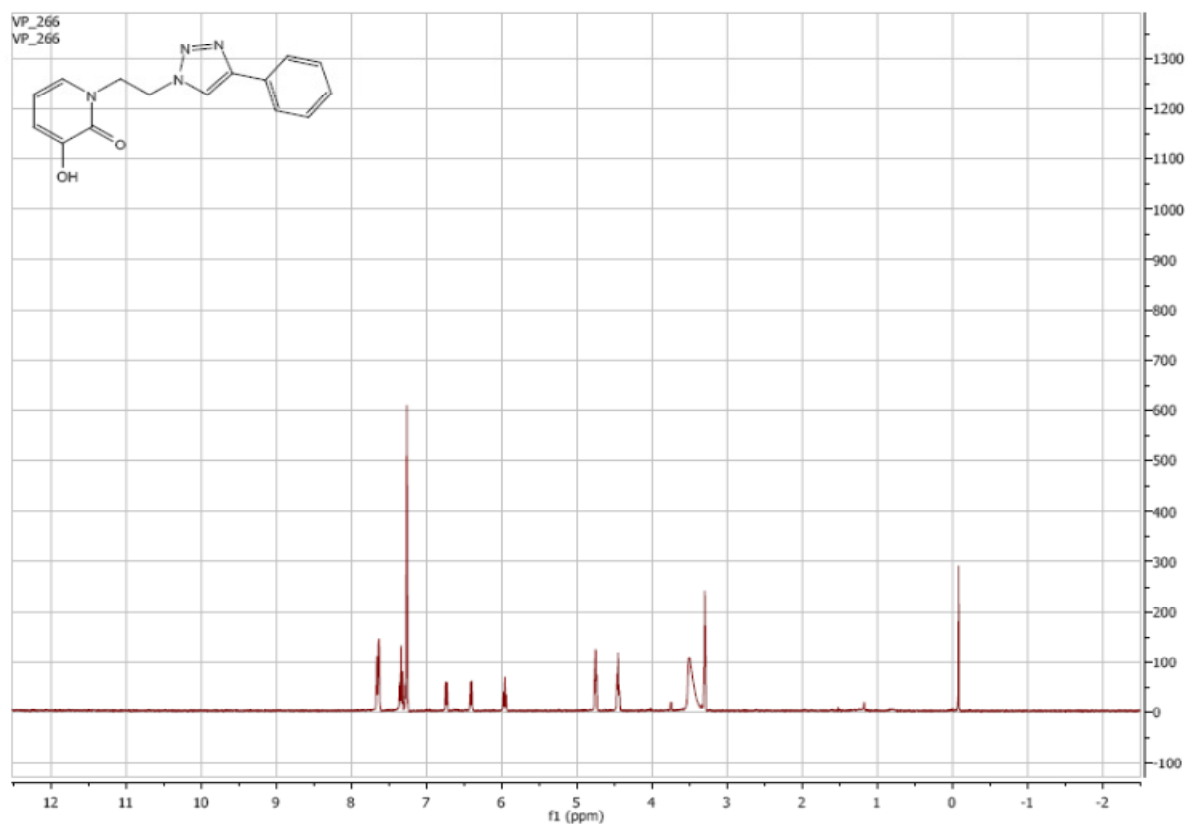
¹H NMR of **21f**:



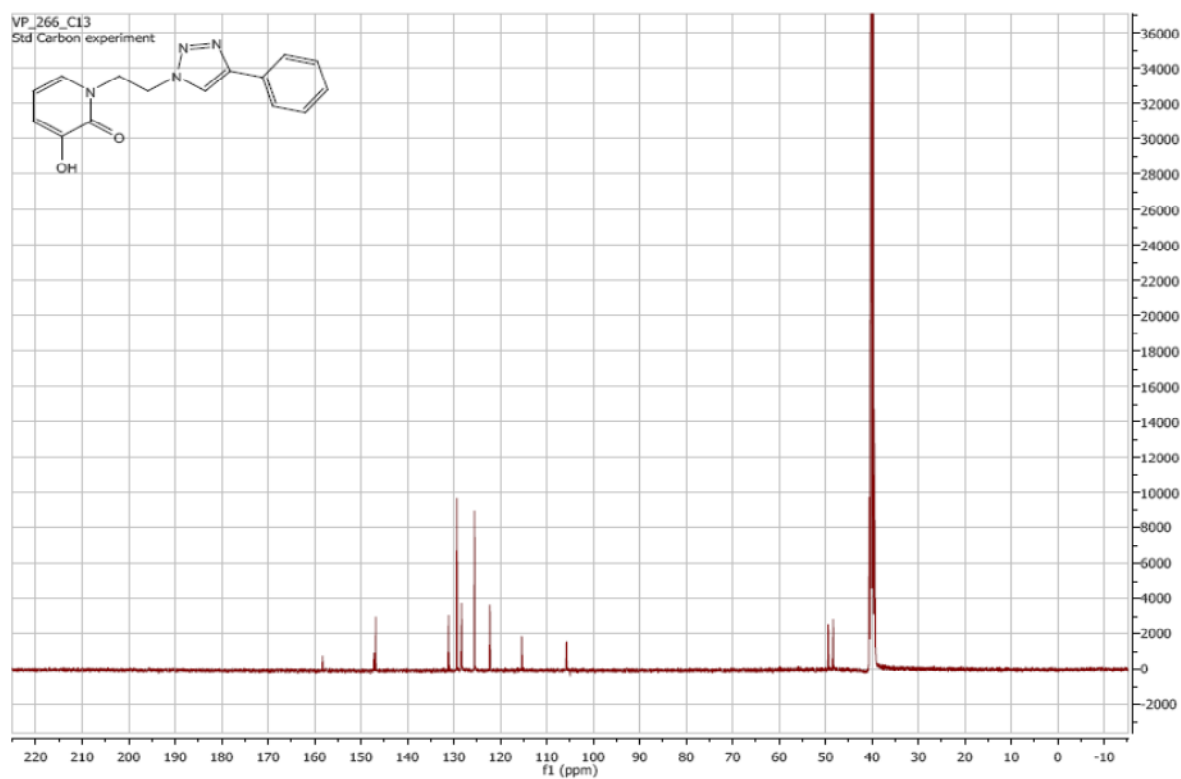
¹³C NMR of **21f**:



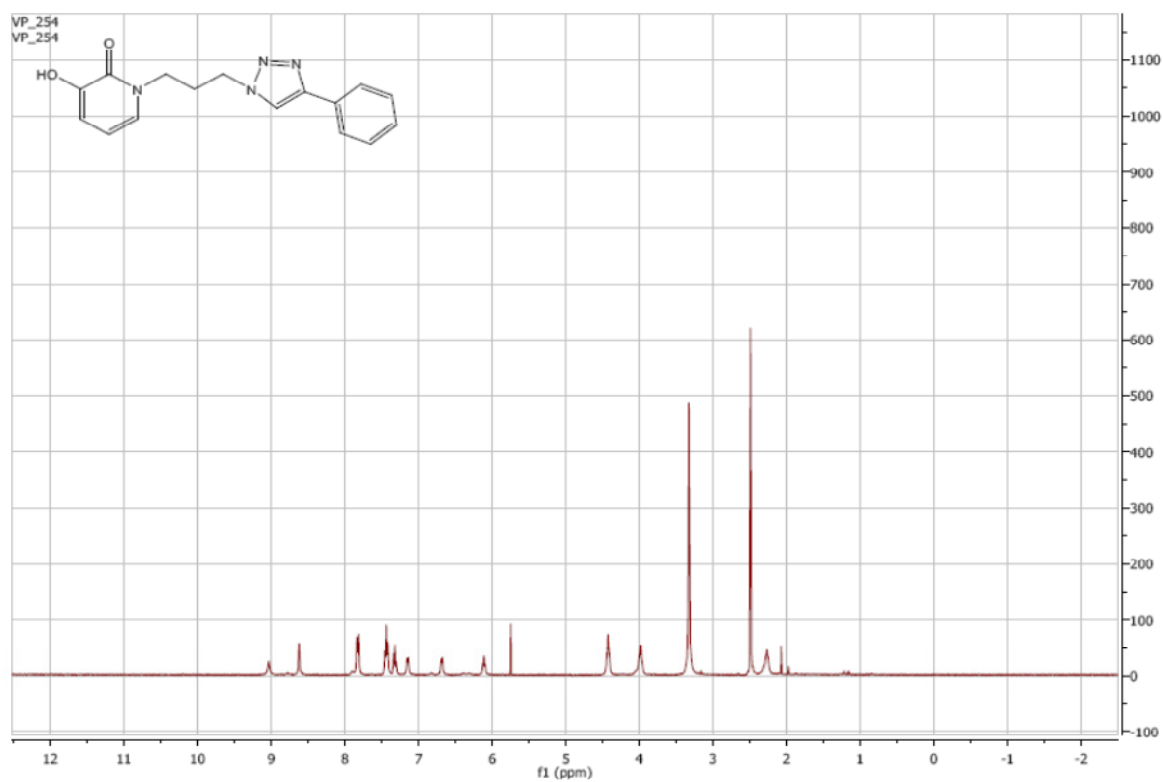
¹H NMR of **22a**:



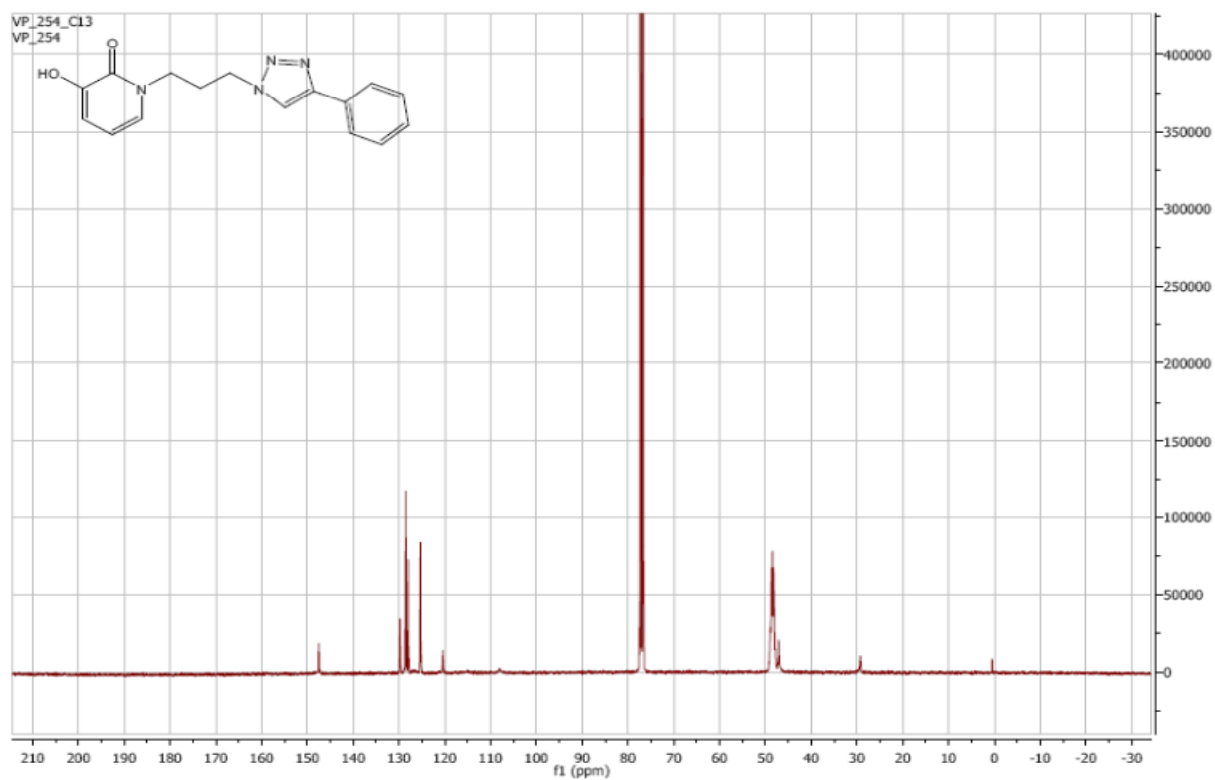
¹³C NMR of **22a**:



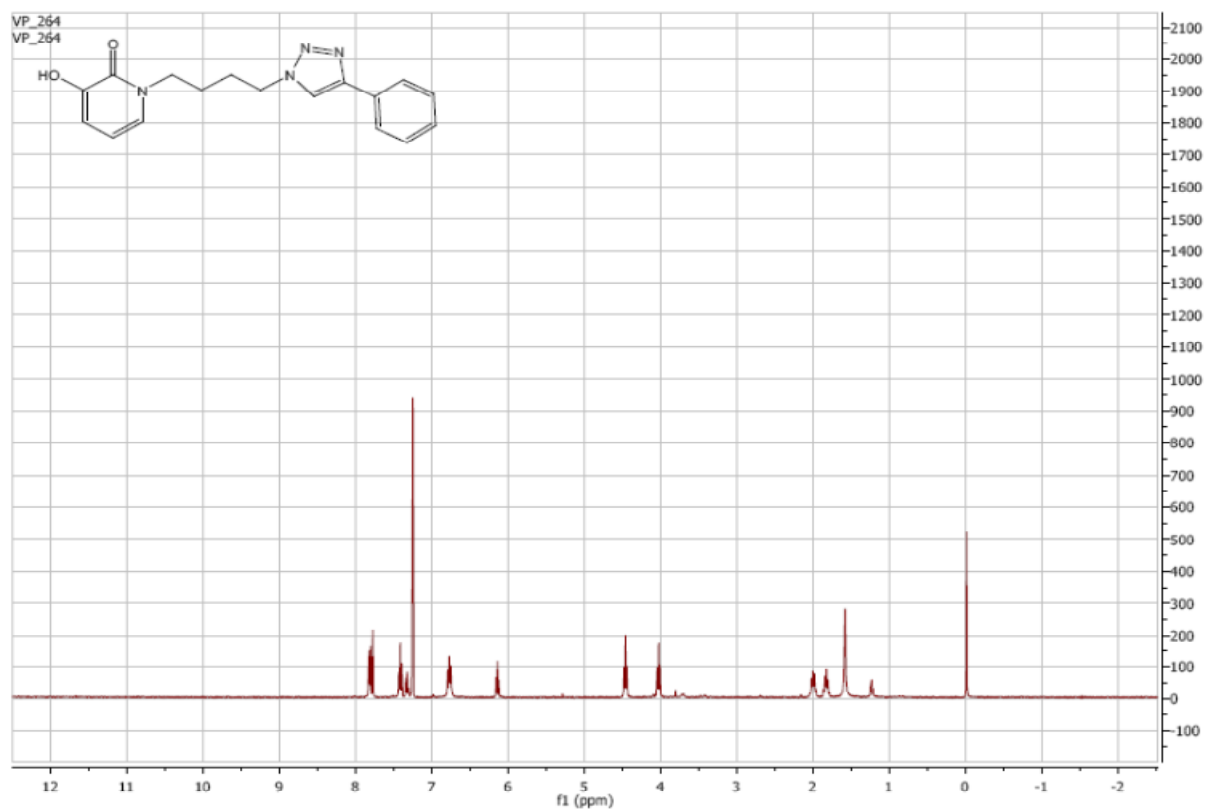
¹H NMR of **22b**:



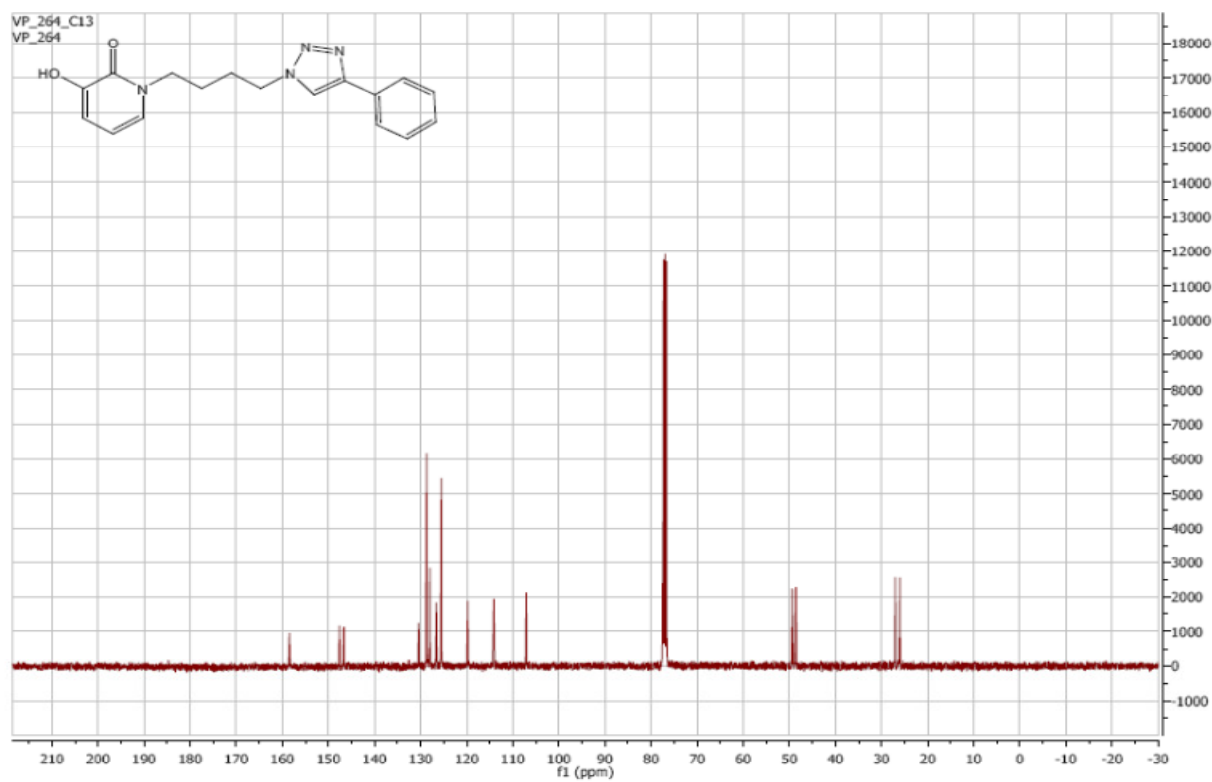
¹³C NMR of **22b**



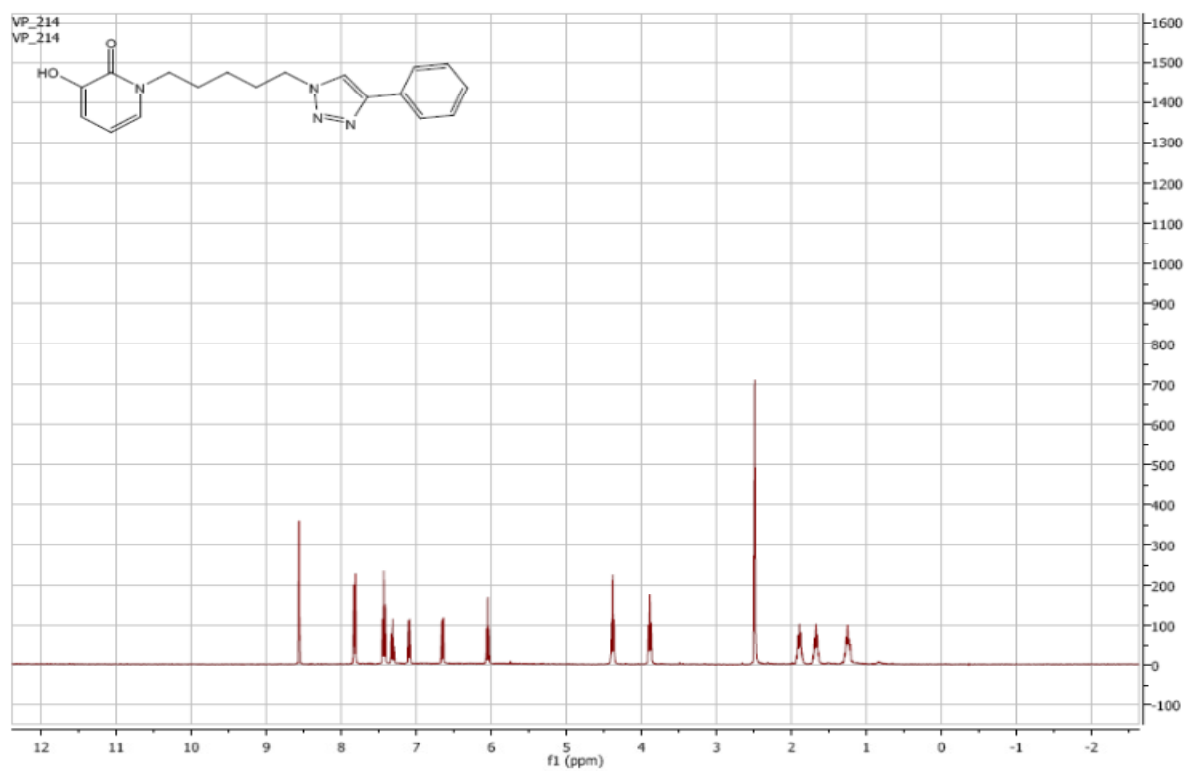
¹H NMR of **22c**:



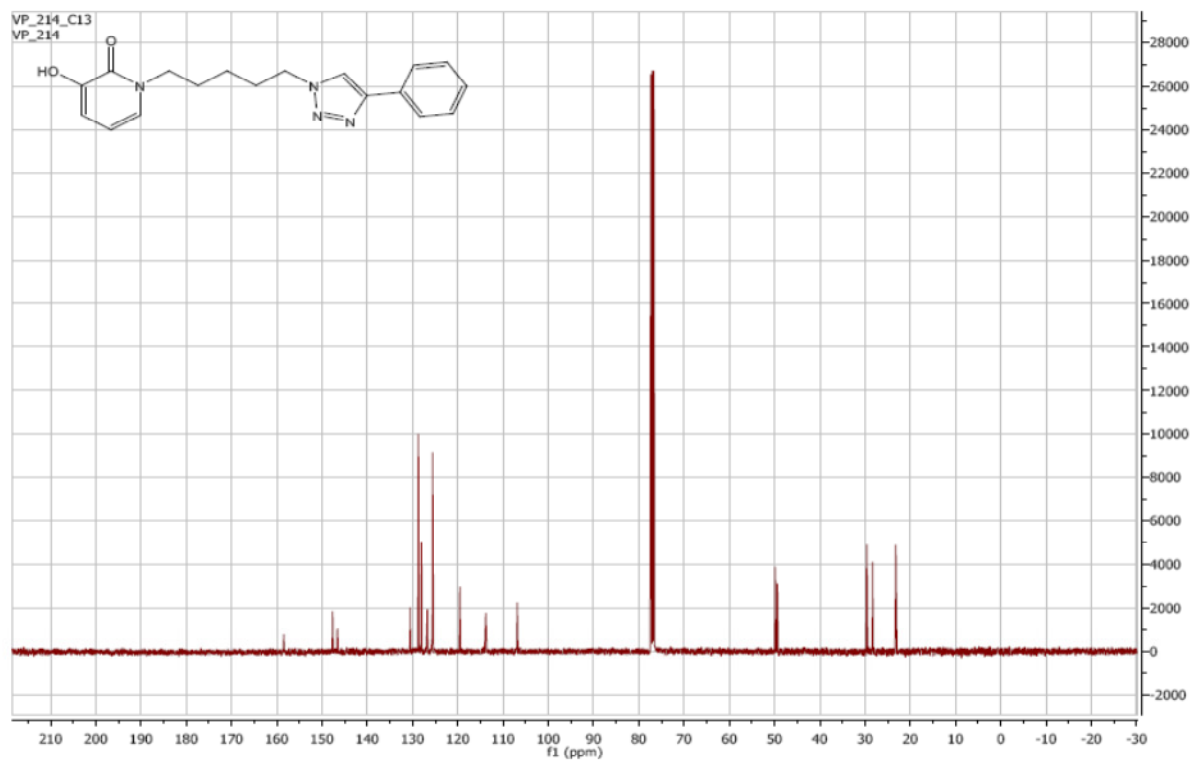
¹³C NMR of **22c**:



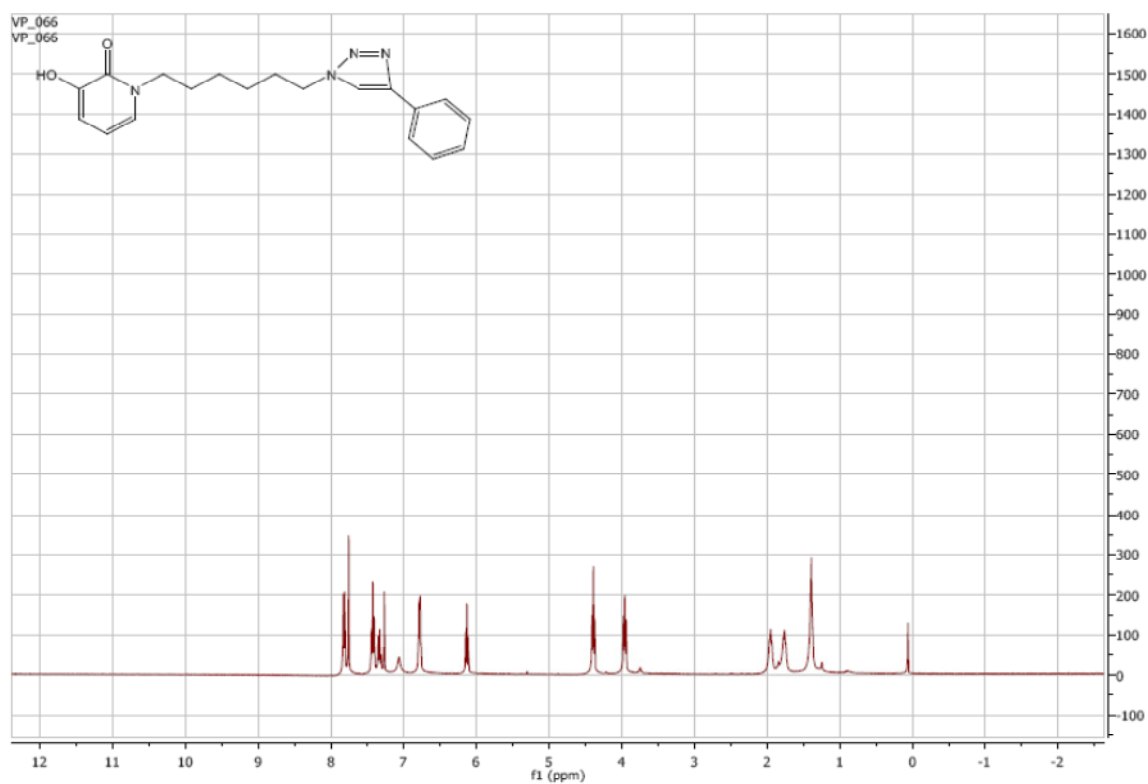
^1H NMR of **22d**:



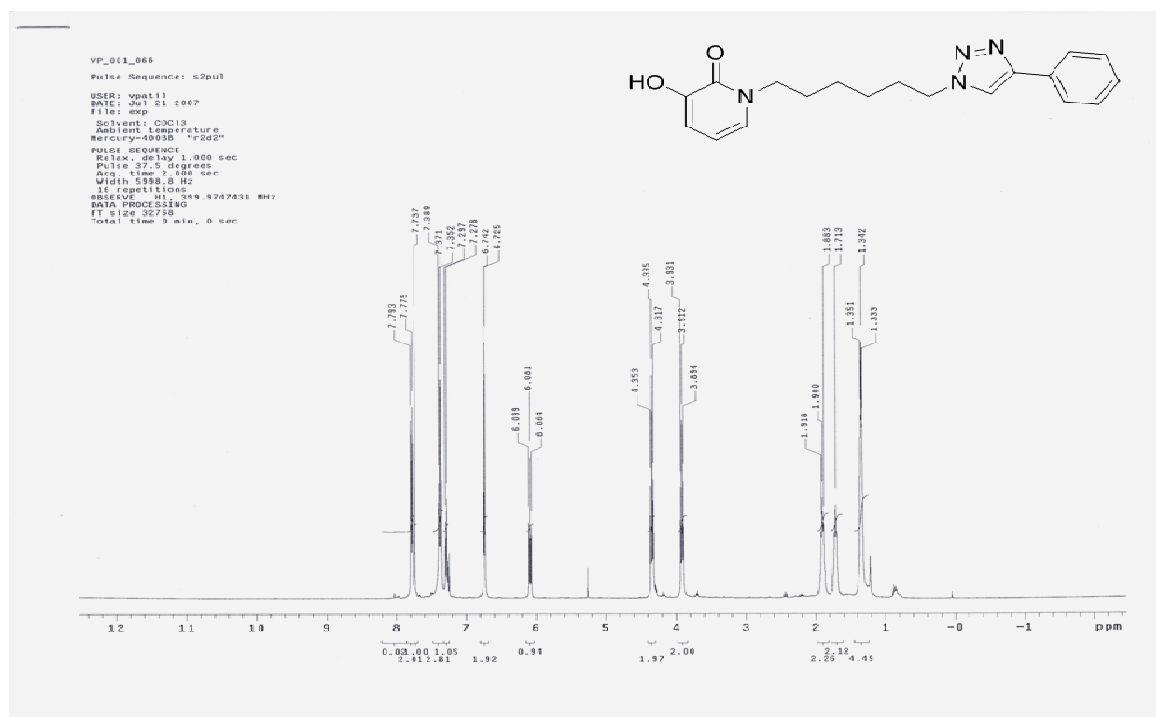
^{13}C NMR of **22d**:



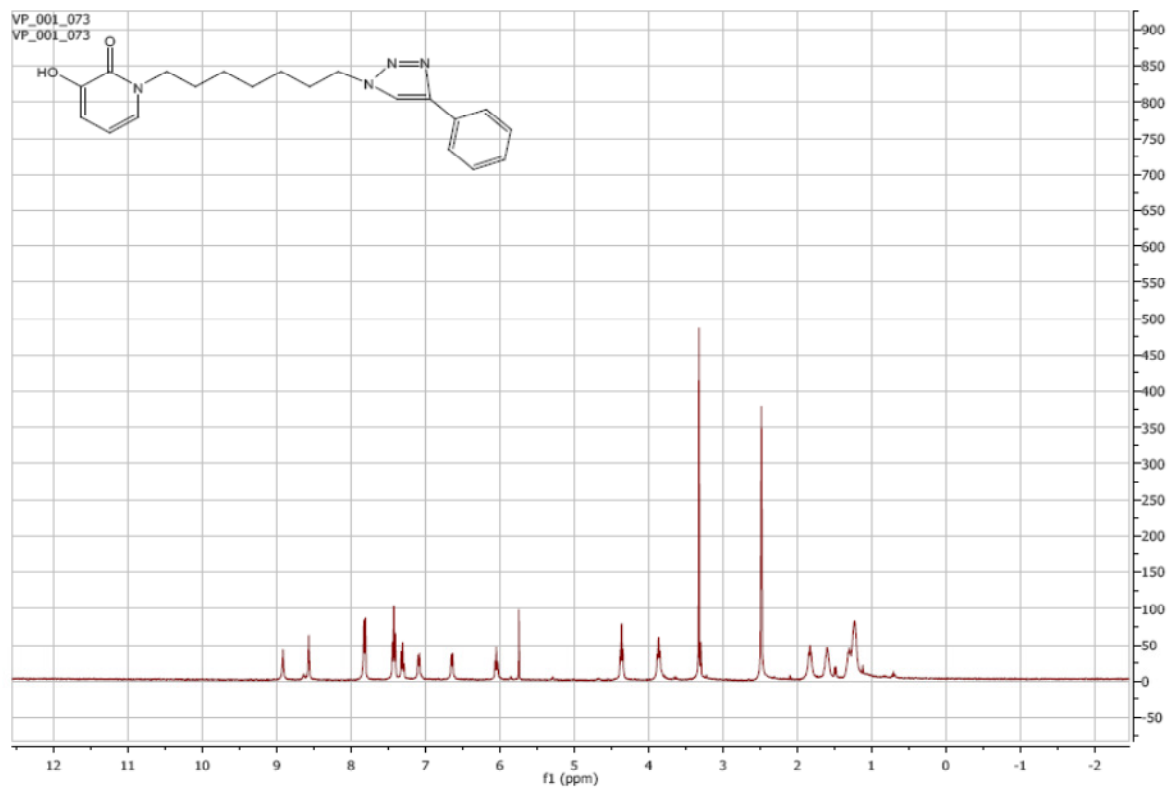
¹H NMR of **22e**:



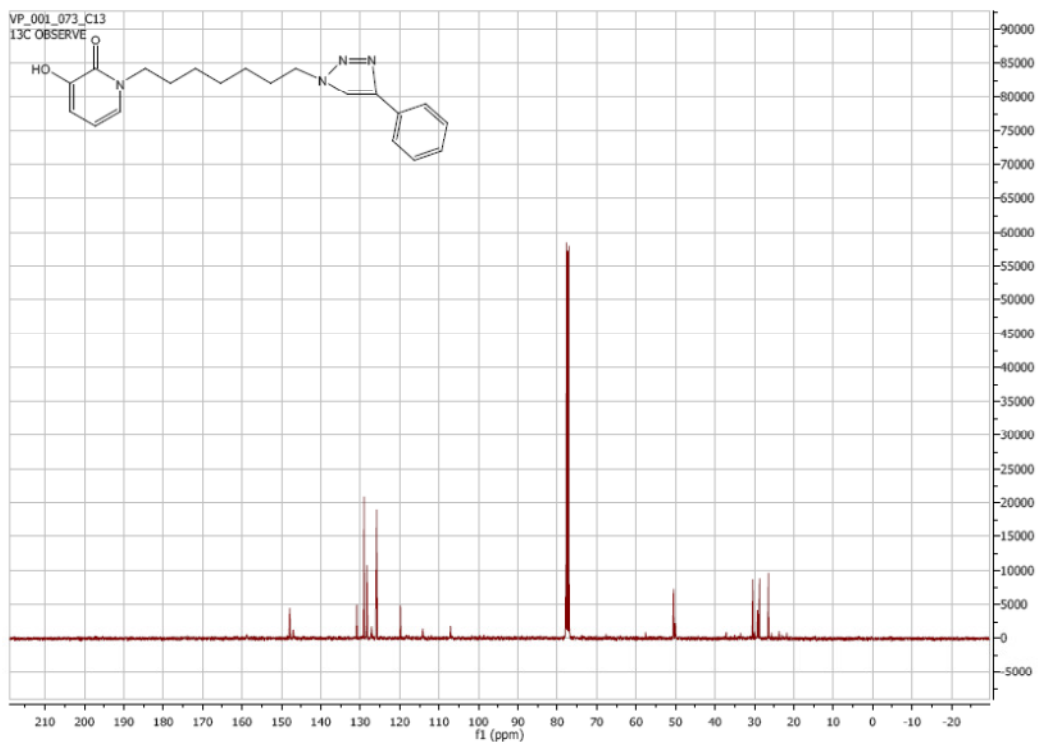
¹³C NMR of **22e**:



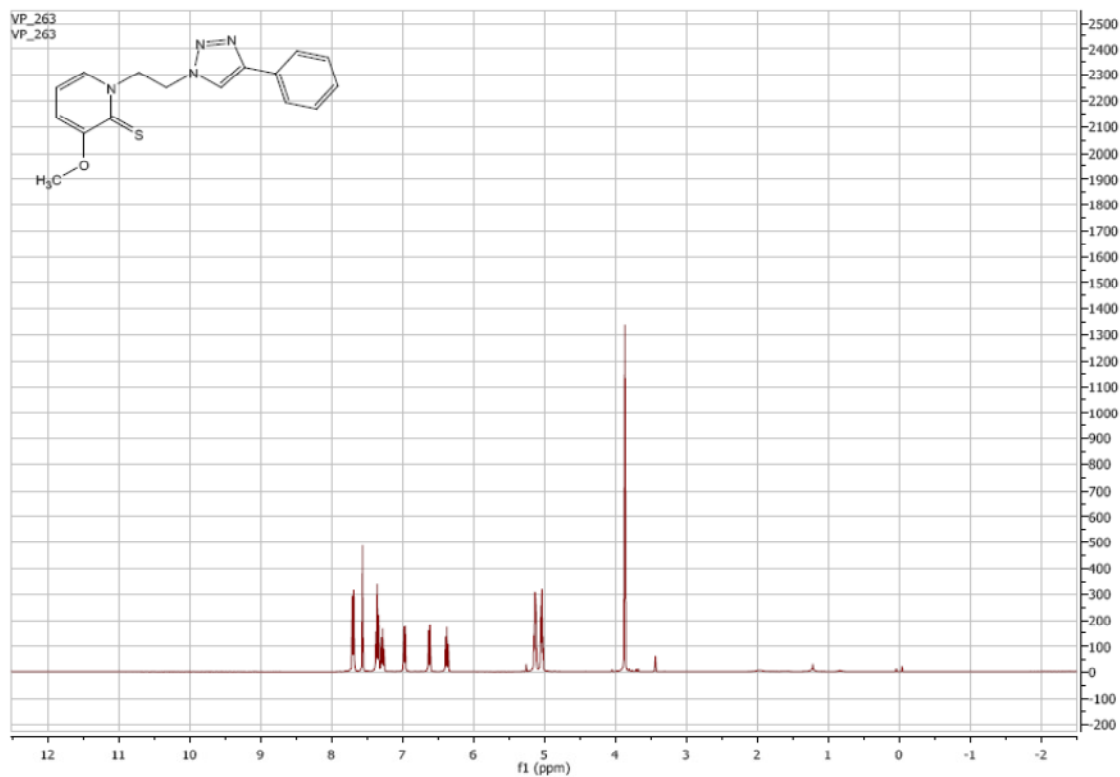
¹H NMR of **22f**:



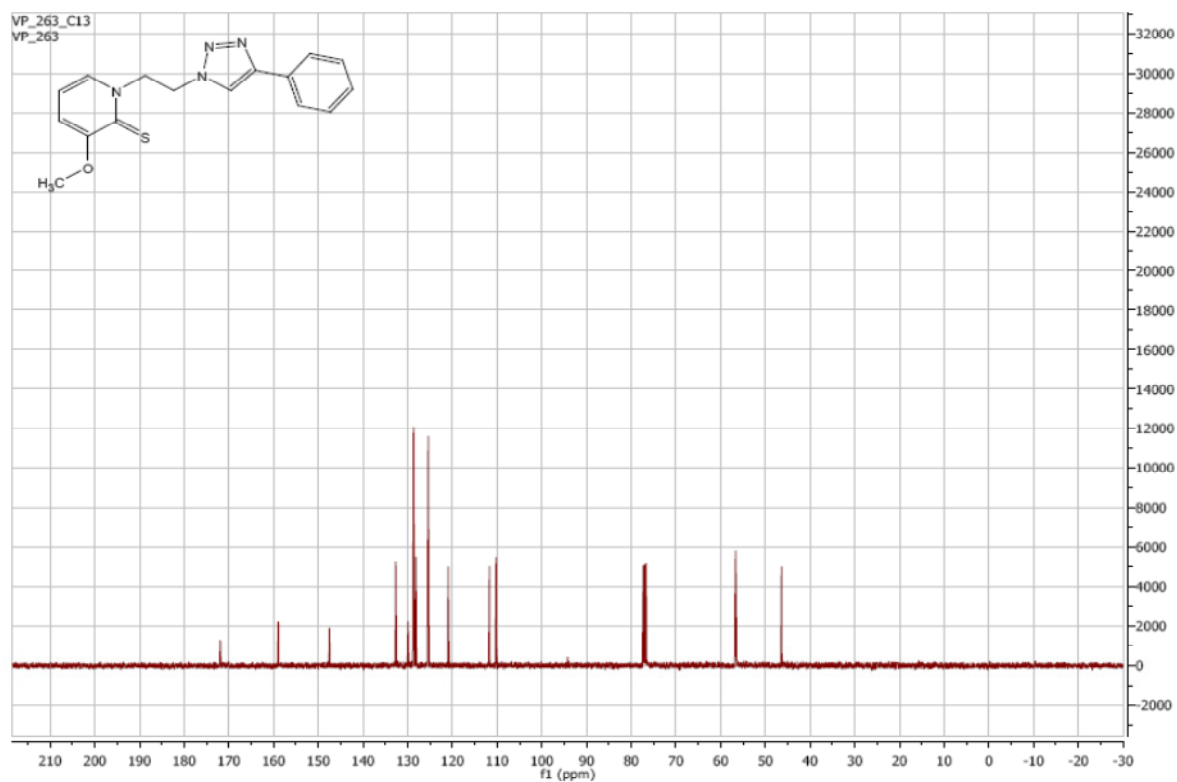
¹³C NMR of **22f**:



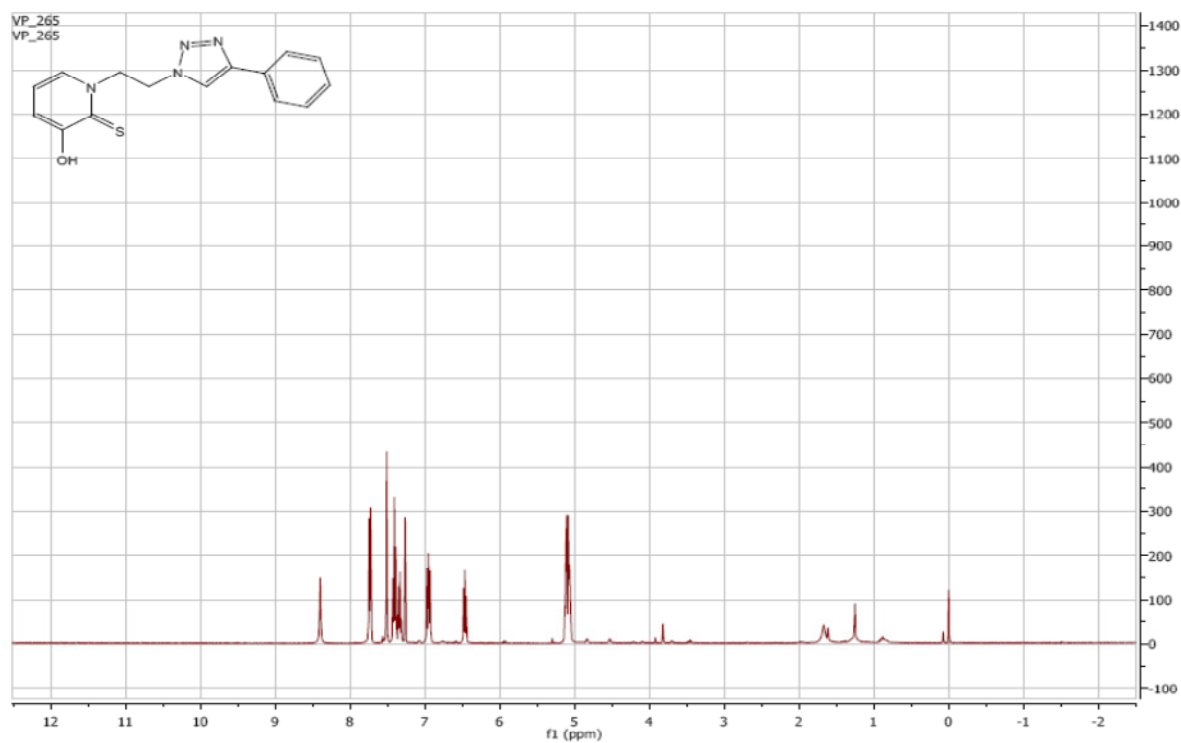
¹H NMR of **23**:



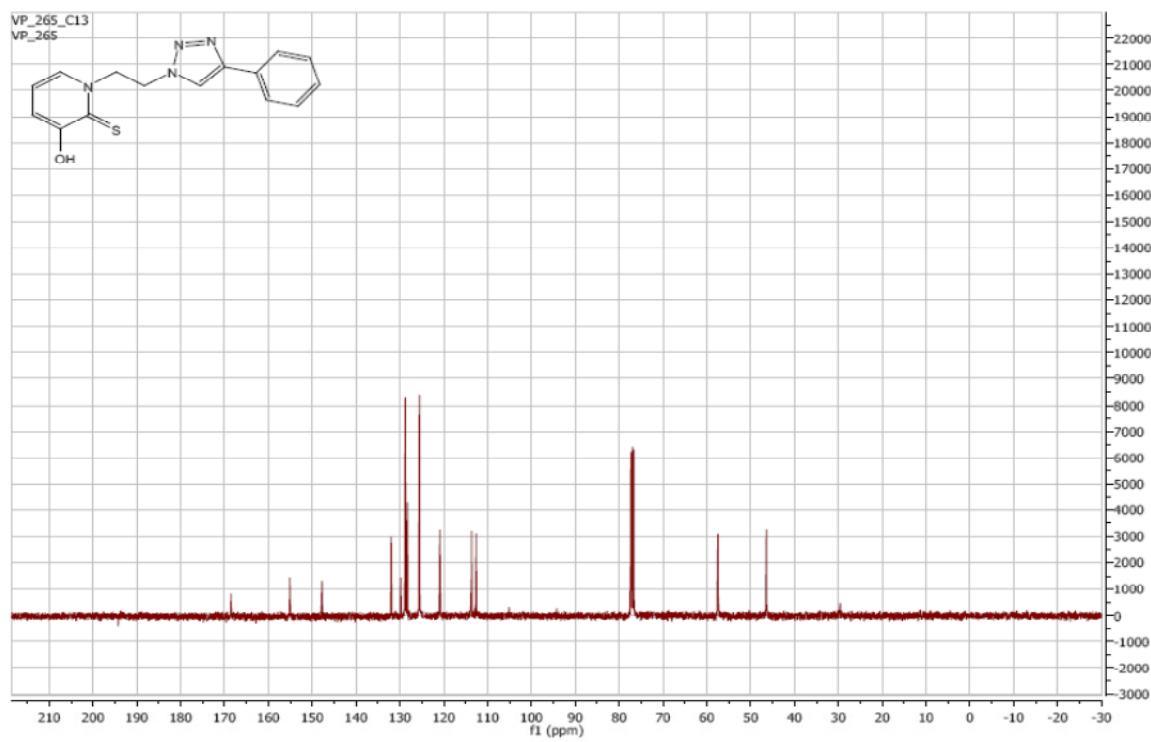
¹³C NMR of **23**:



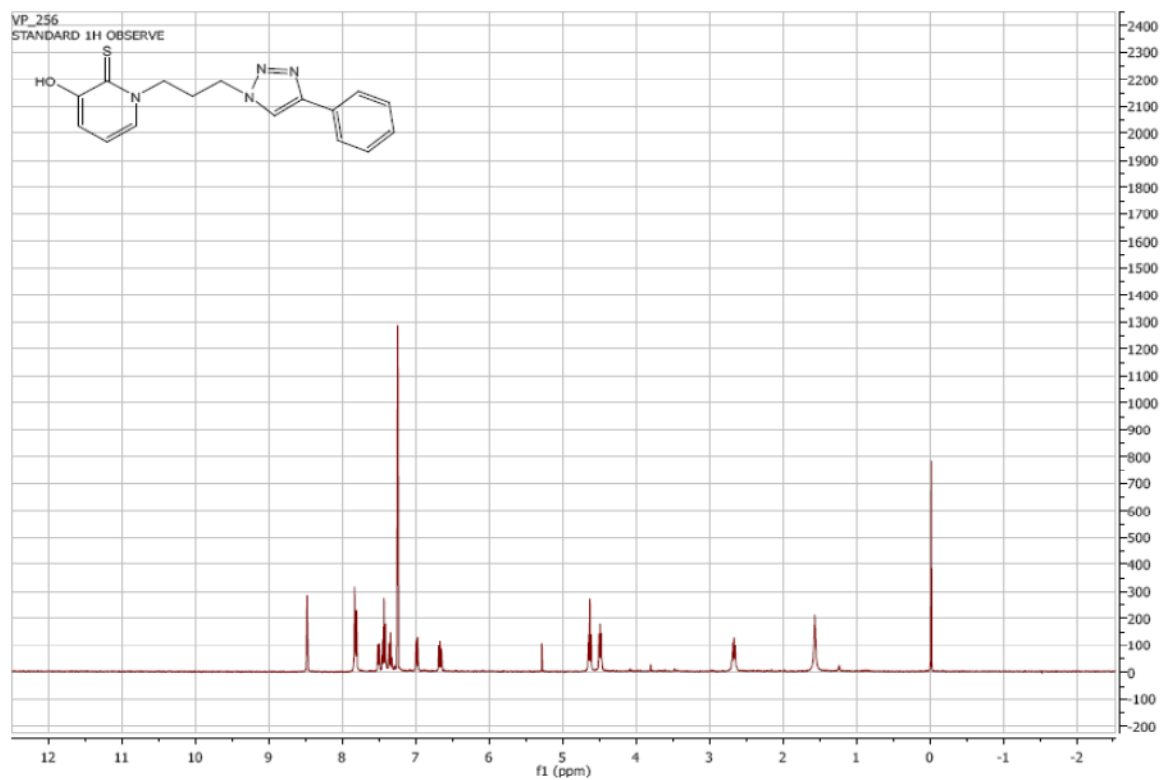
¹H NMR of **24**:



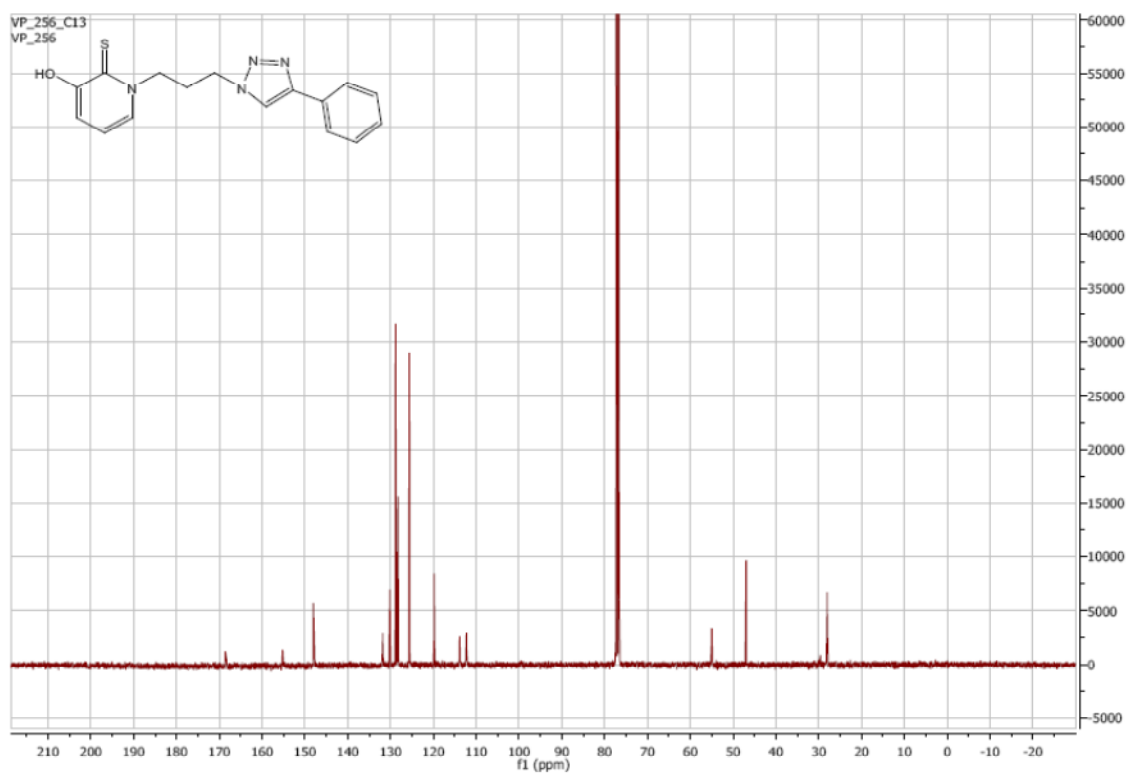
¹³C NMR of **24**:



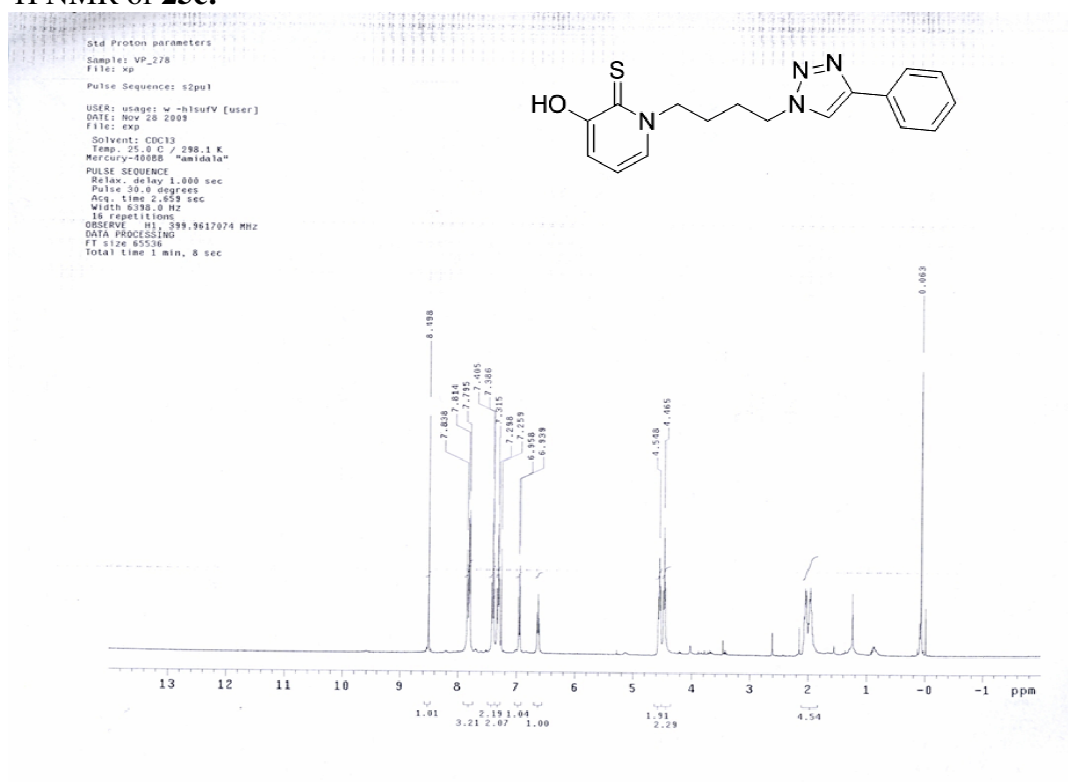
^1H NMR of **25b**:



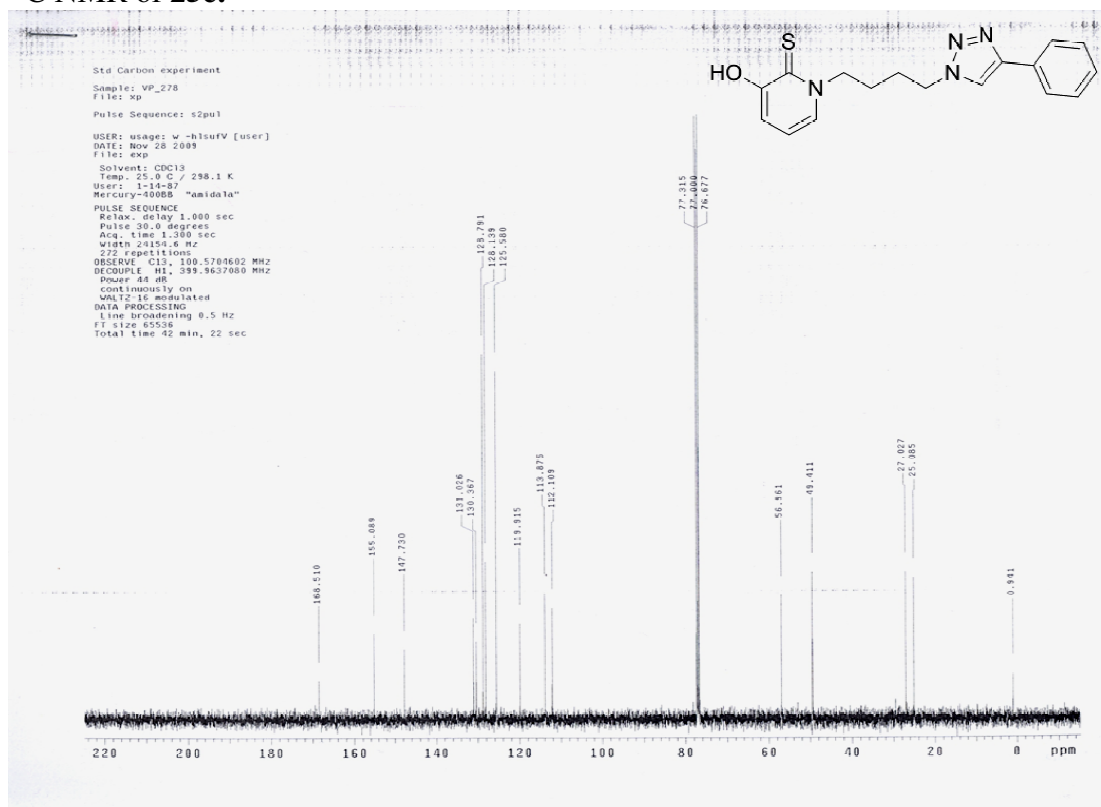
^{13}C NMR of **25b**:



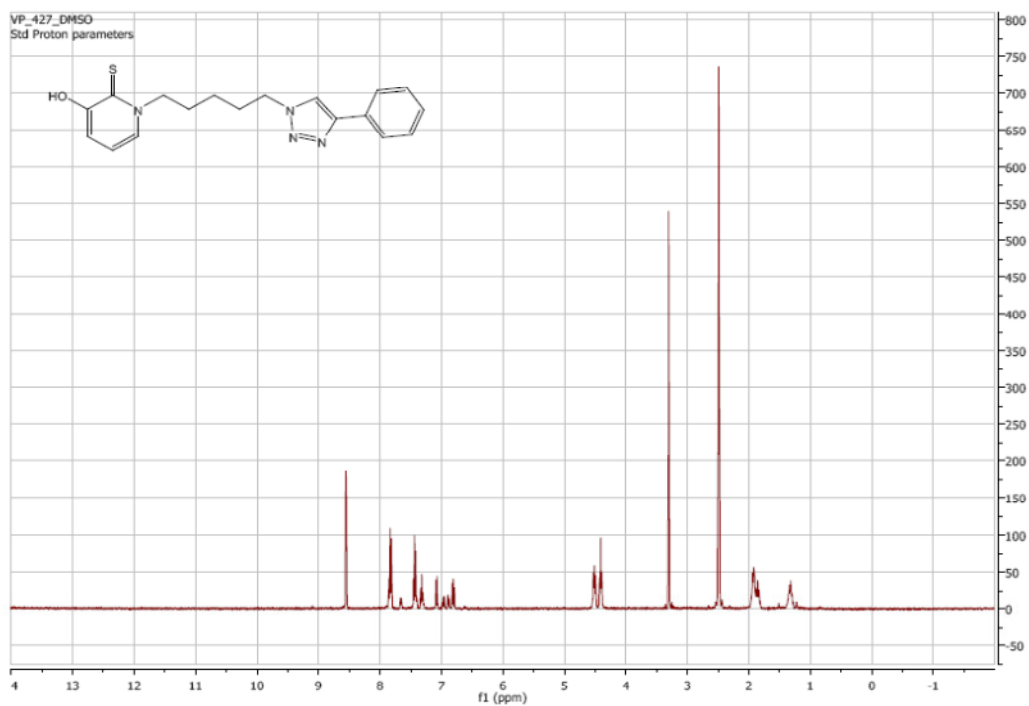
¹H NMR of 25c:



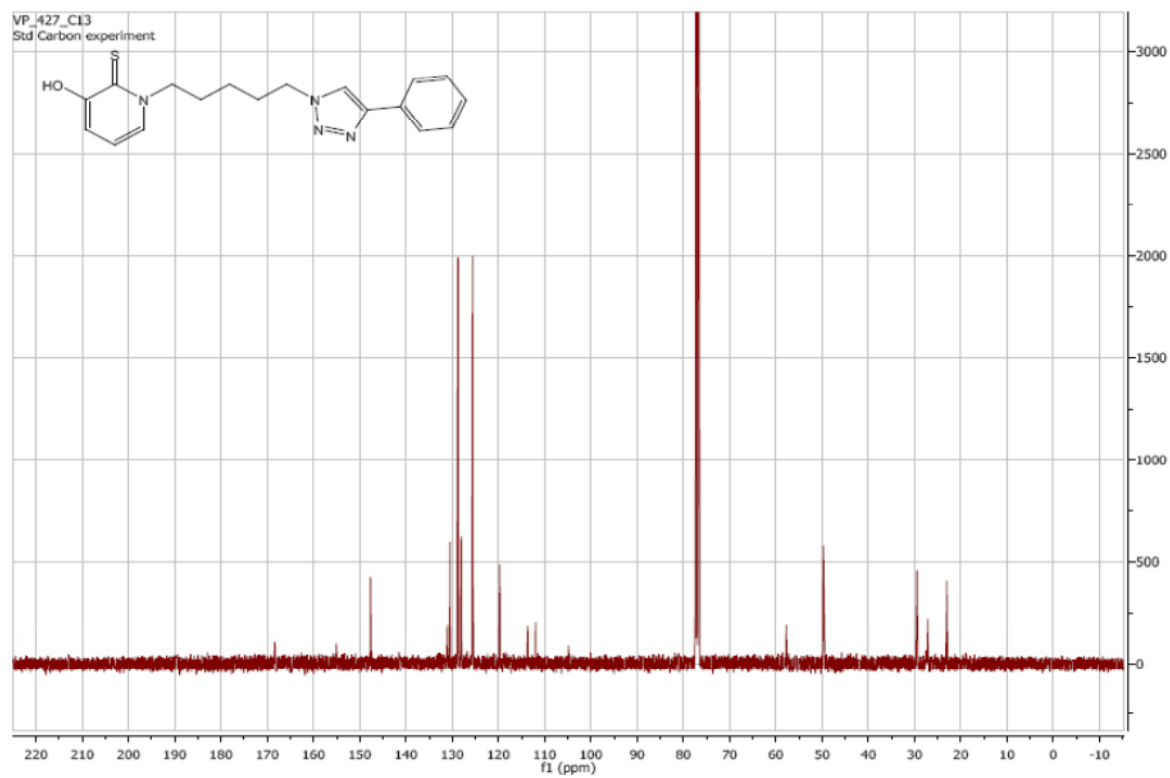
¹³C NMR of 25c:



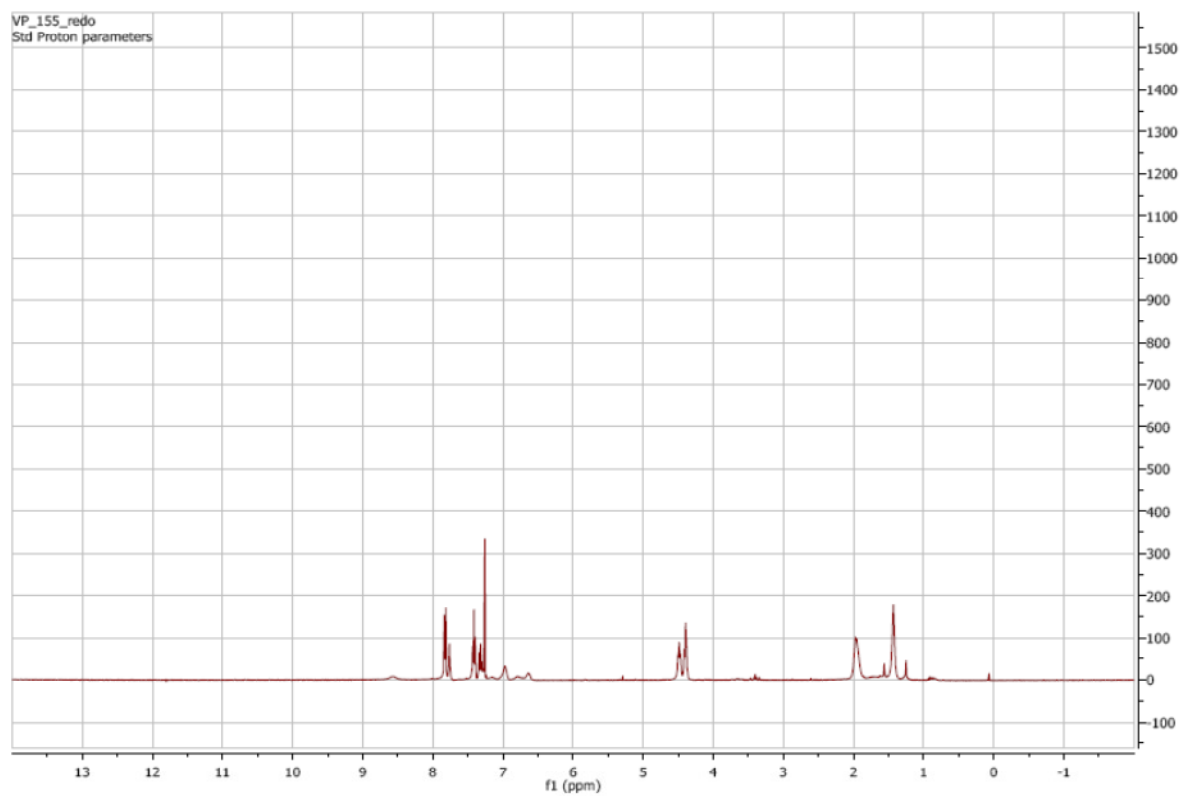
¹H NMR of **25d**:



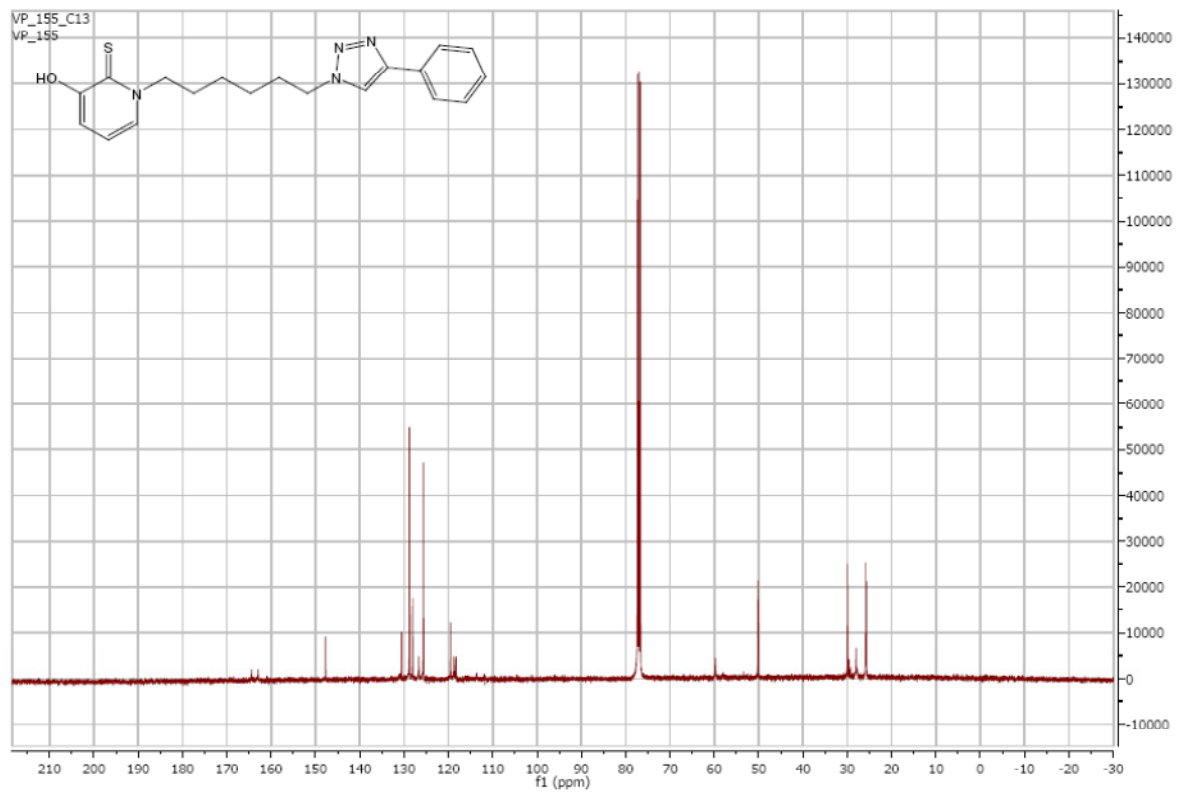
¹³C NMR of **25d**:



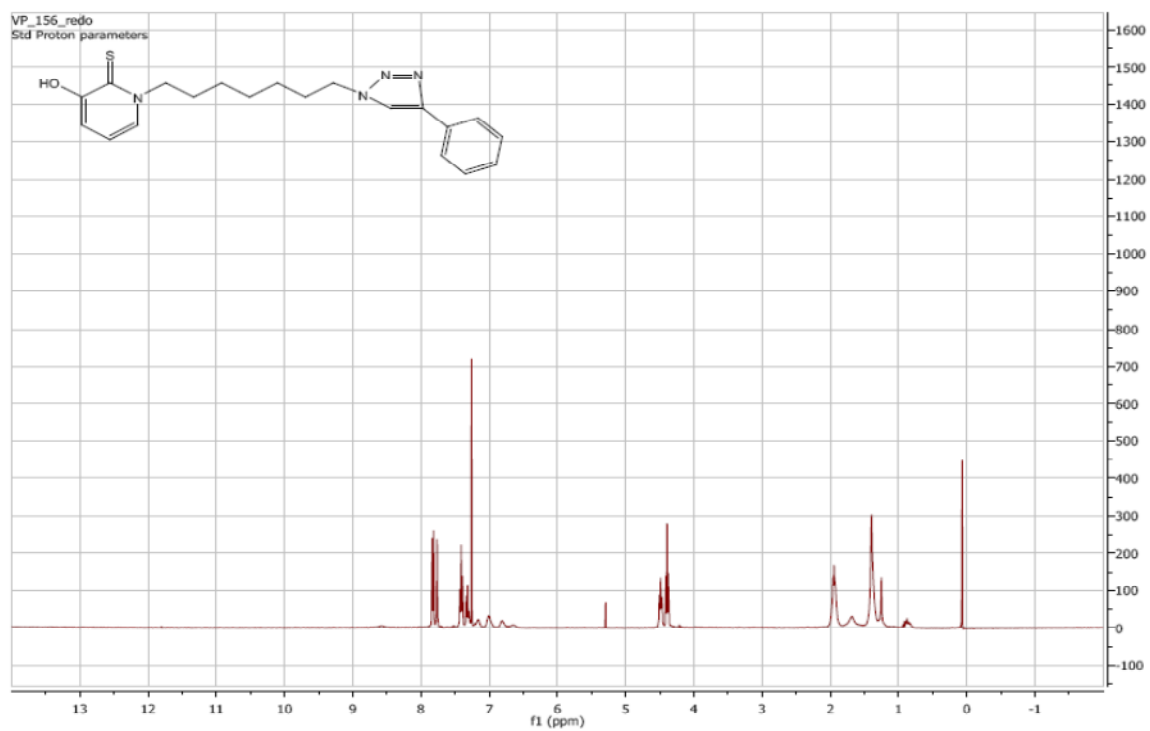
¹H NMR of **25e**:



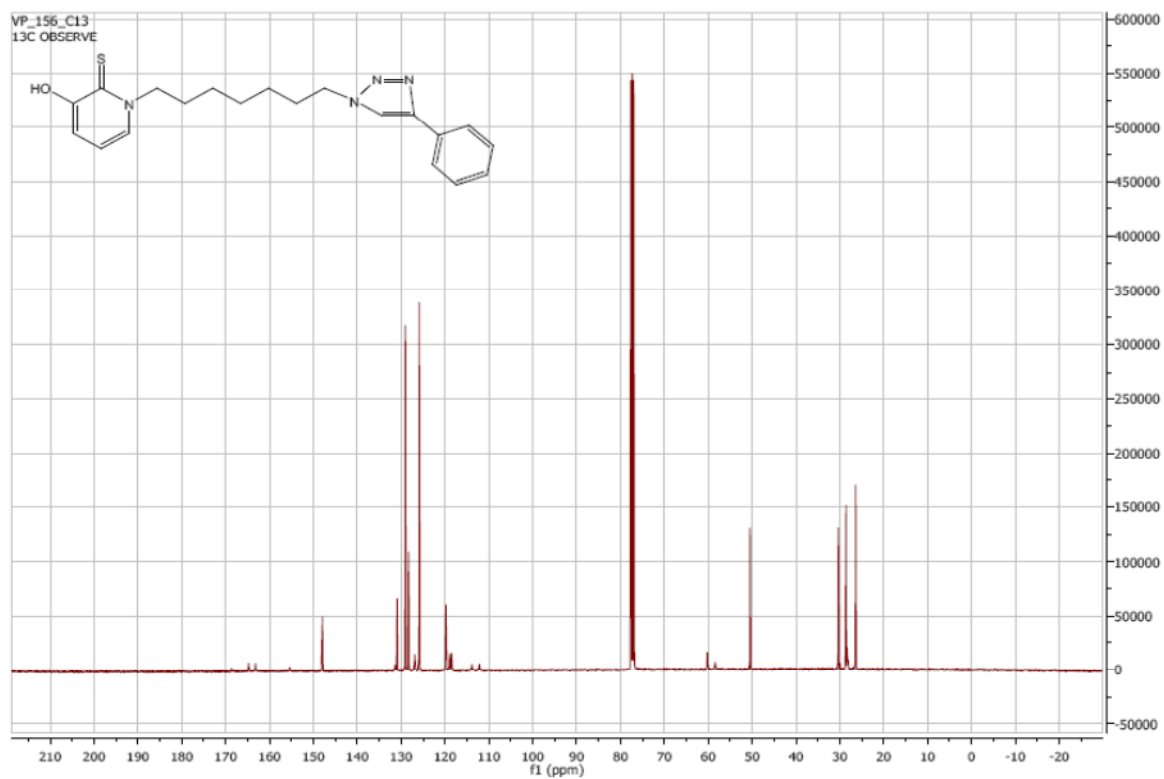
¹³C NMR of **25e**:



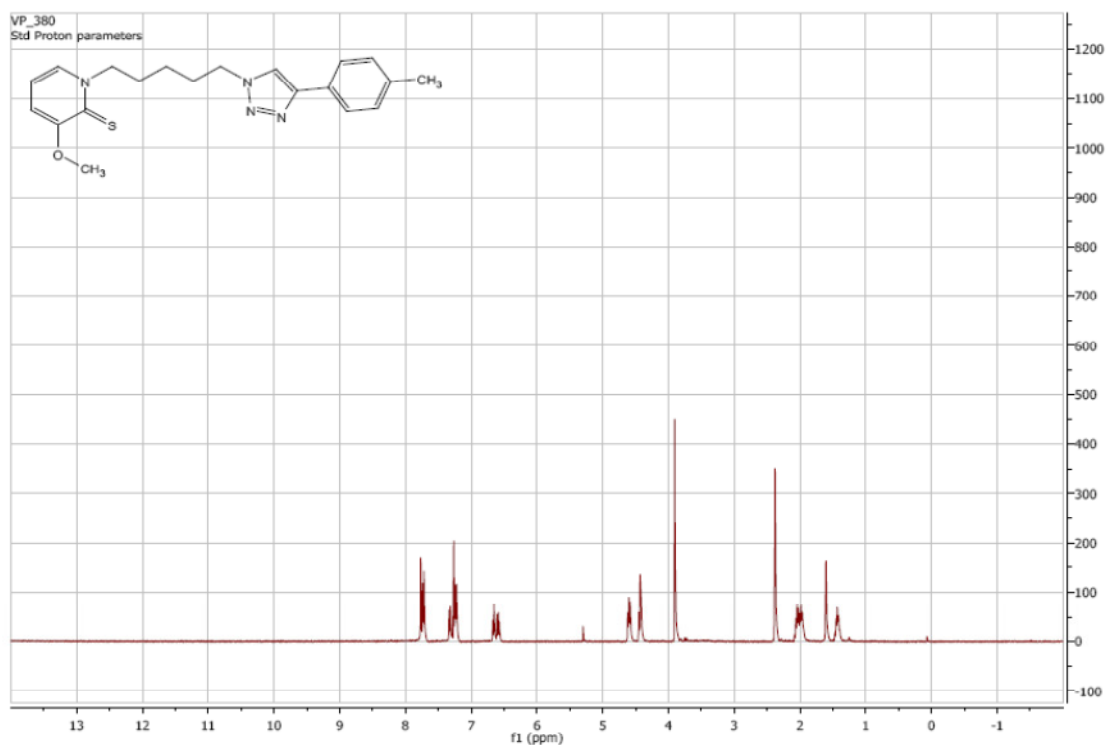
^1H NMR of **25f**:



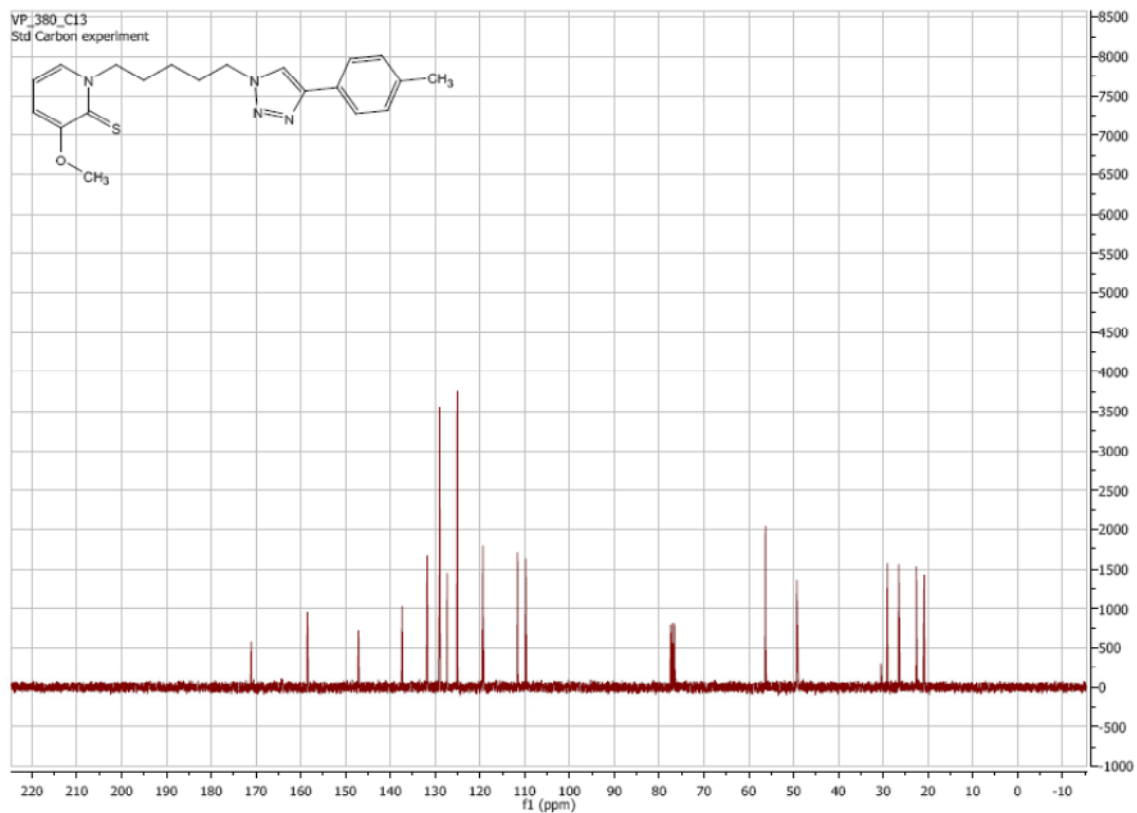
^{13}C NMR of **25f**:



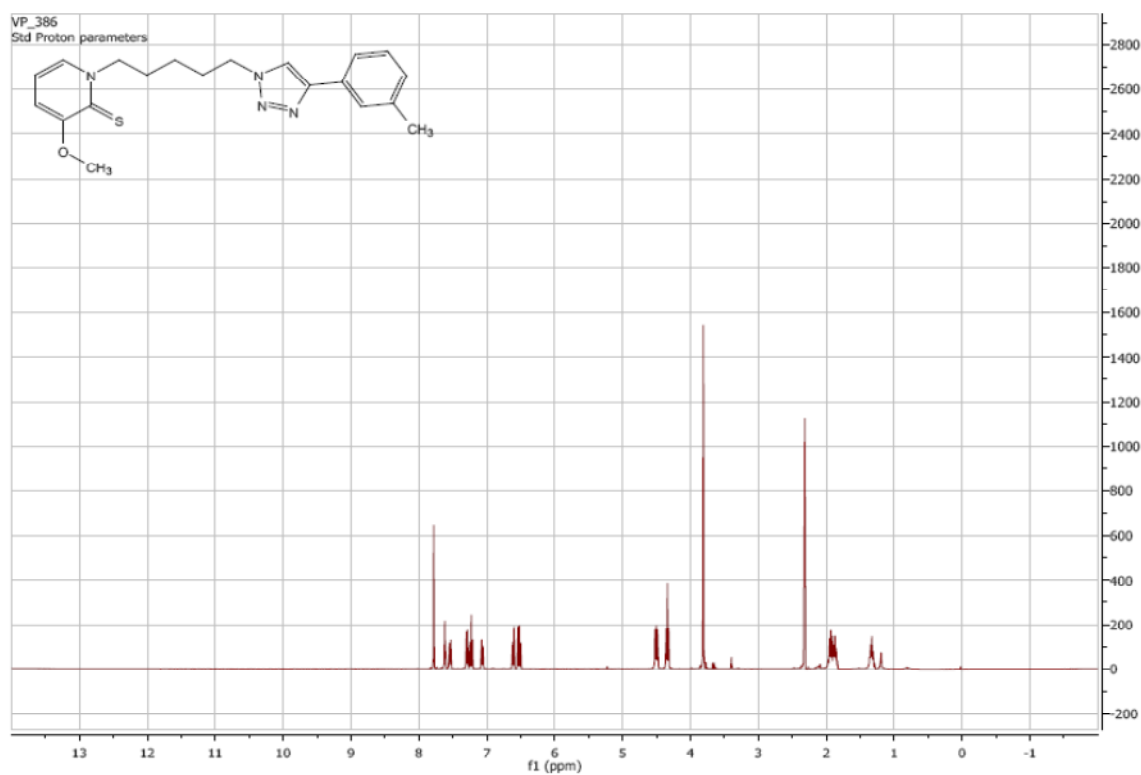
¹H NMR of **28a**:



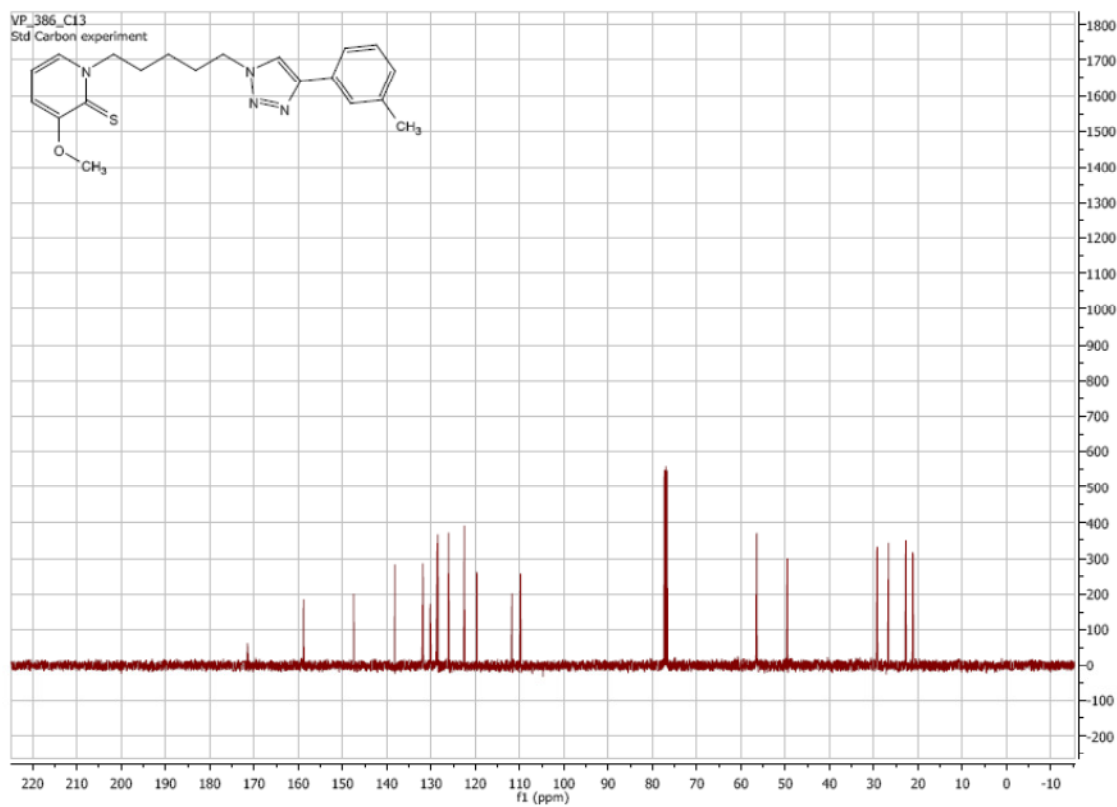
¹³C NMR of **28a**:



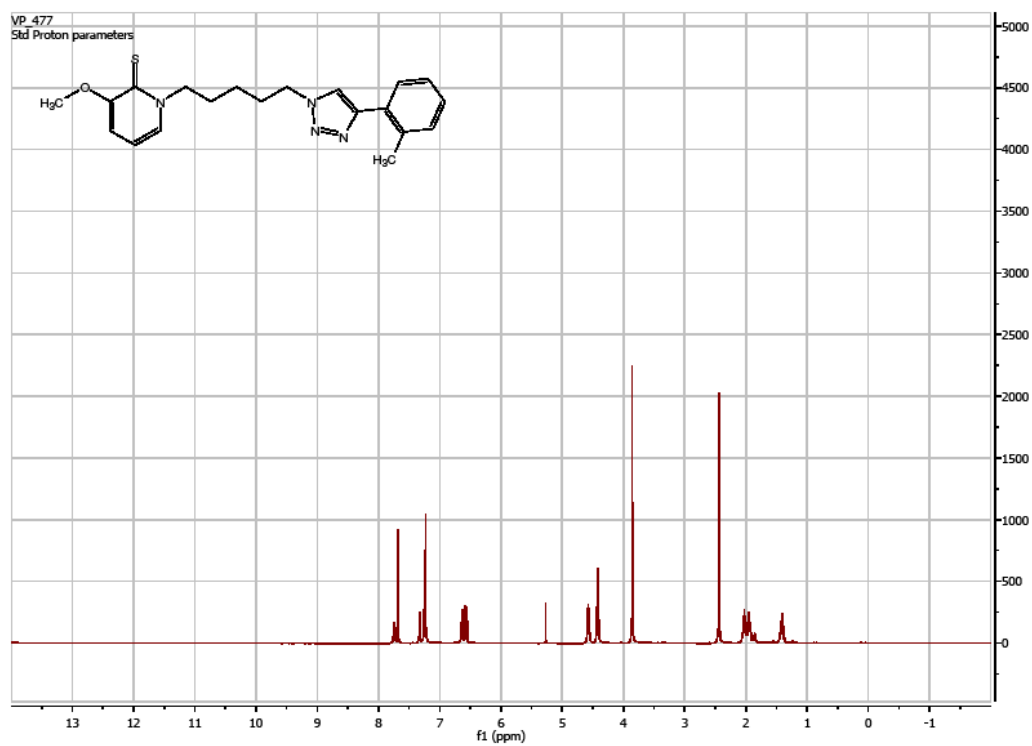
¹H NMR of **28b**:



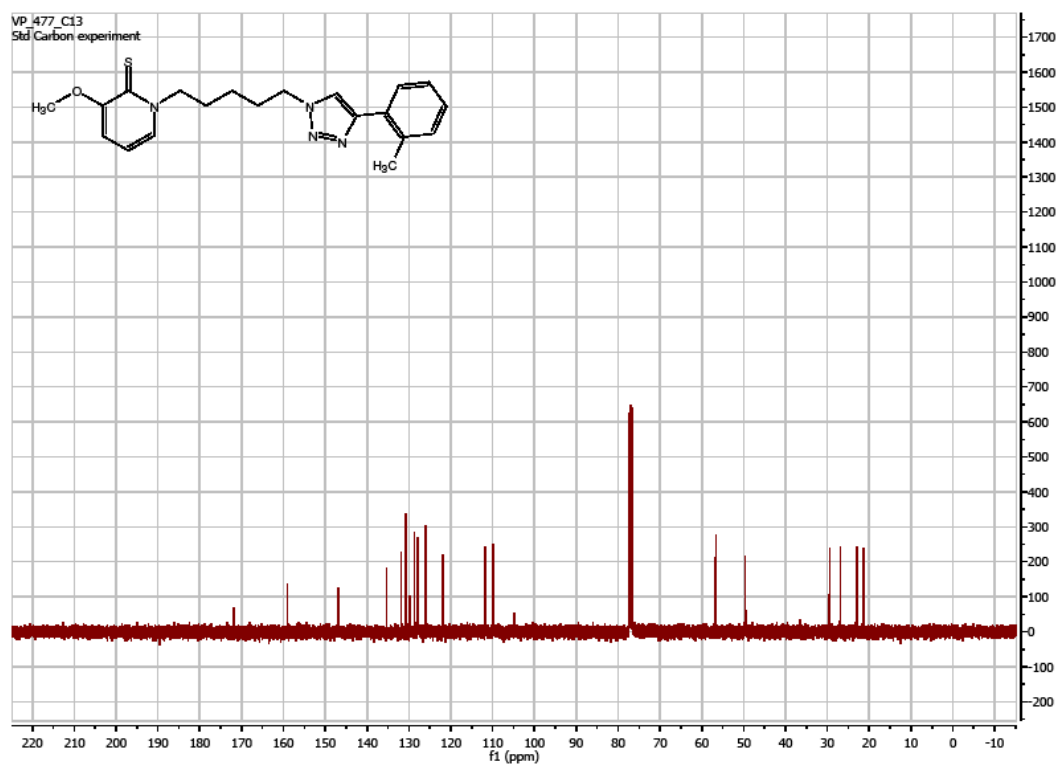
¹³C NMR of **28b**:



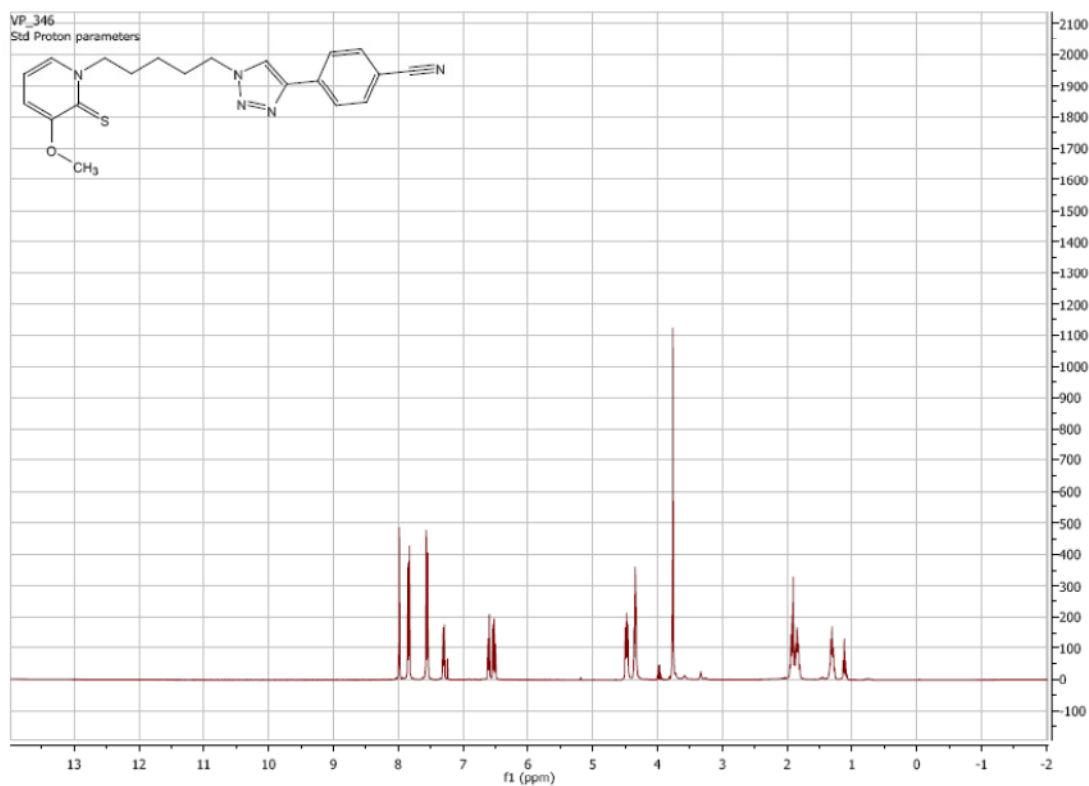
¹H NMR of **28c**:

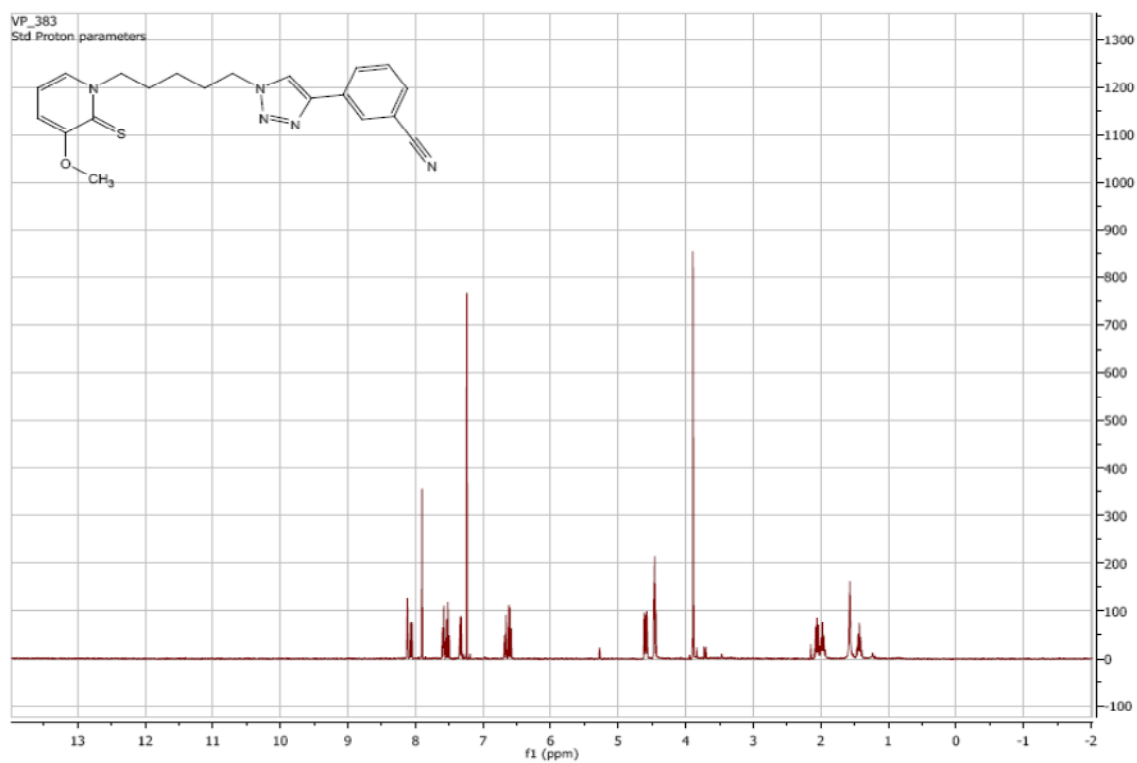
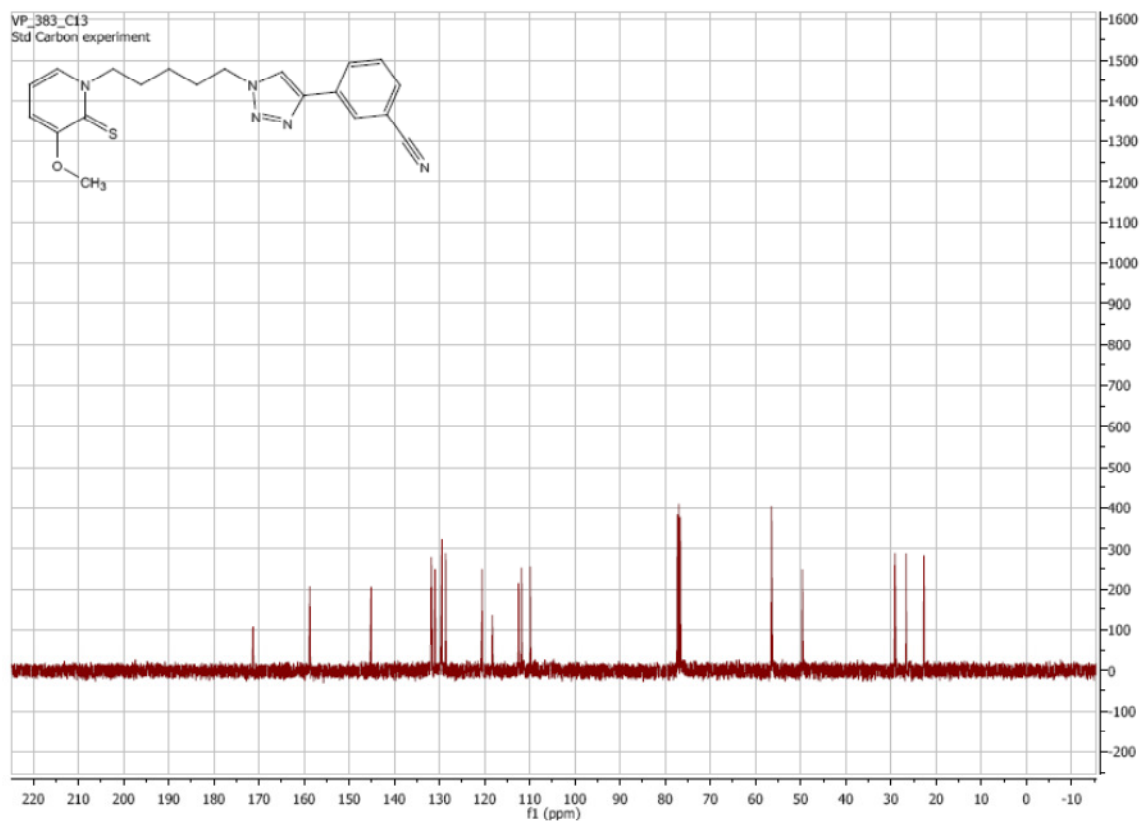


¹³C NMR of **28c**:

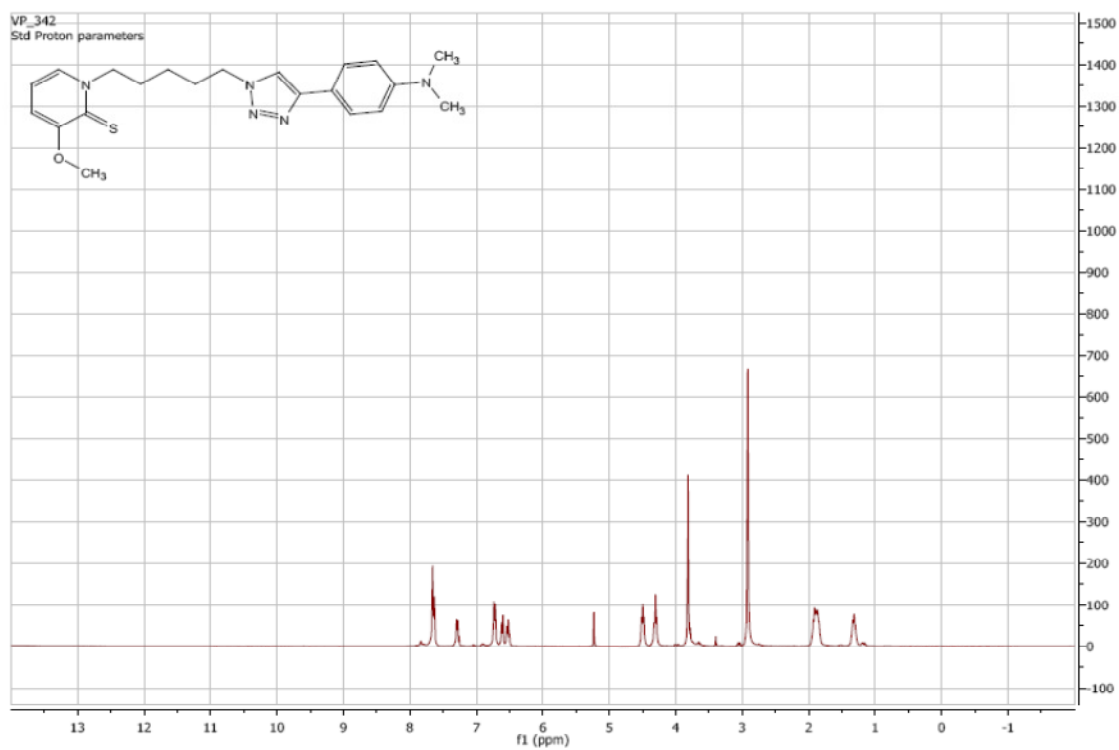


¹H NMR of **28d**:

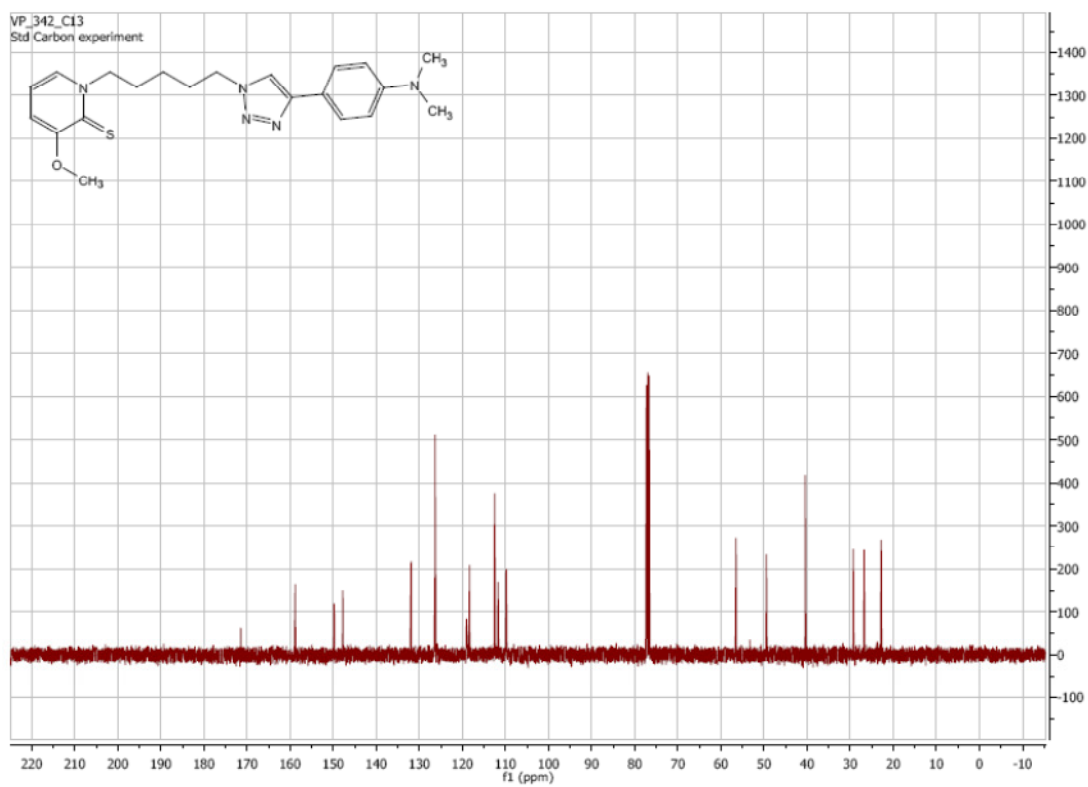


¹H NMR of **28e**: ^{13}C NMR of **28e**:

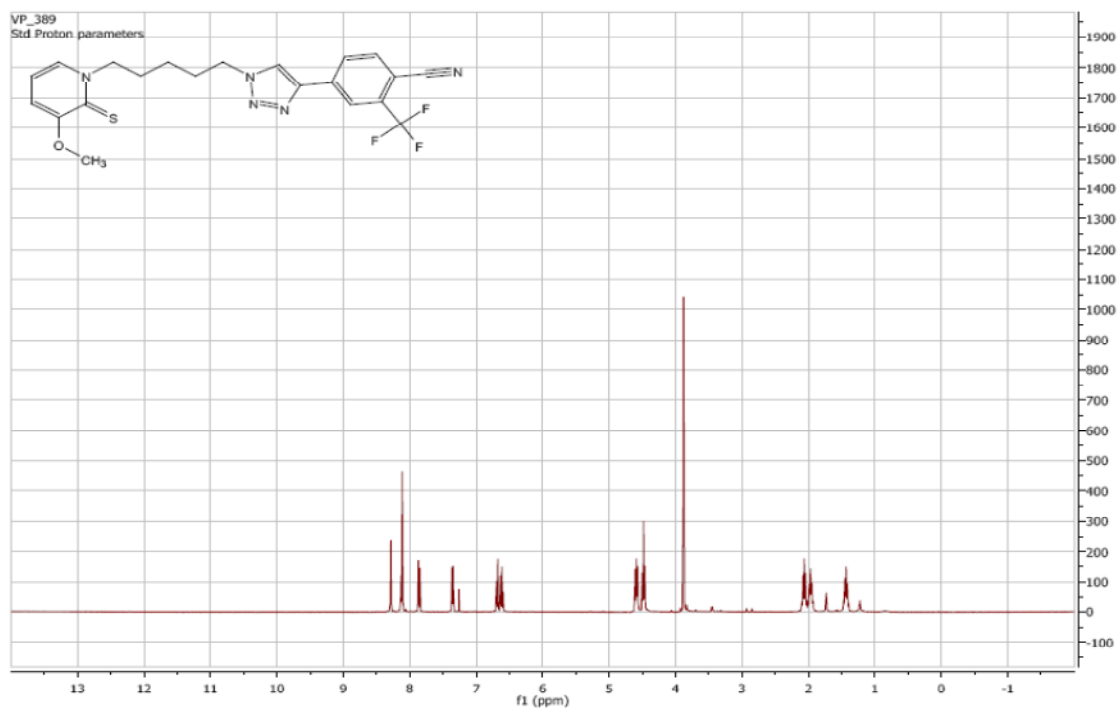
^1H NMR of **28f**:



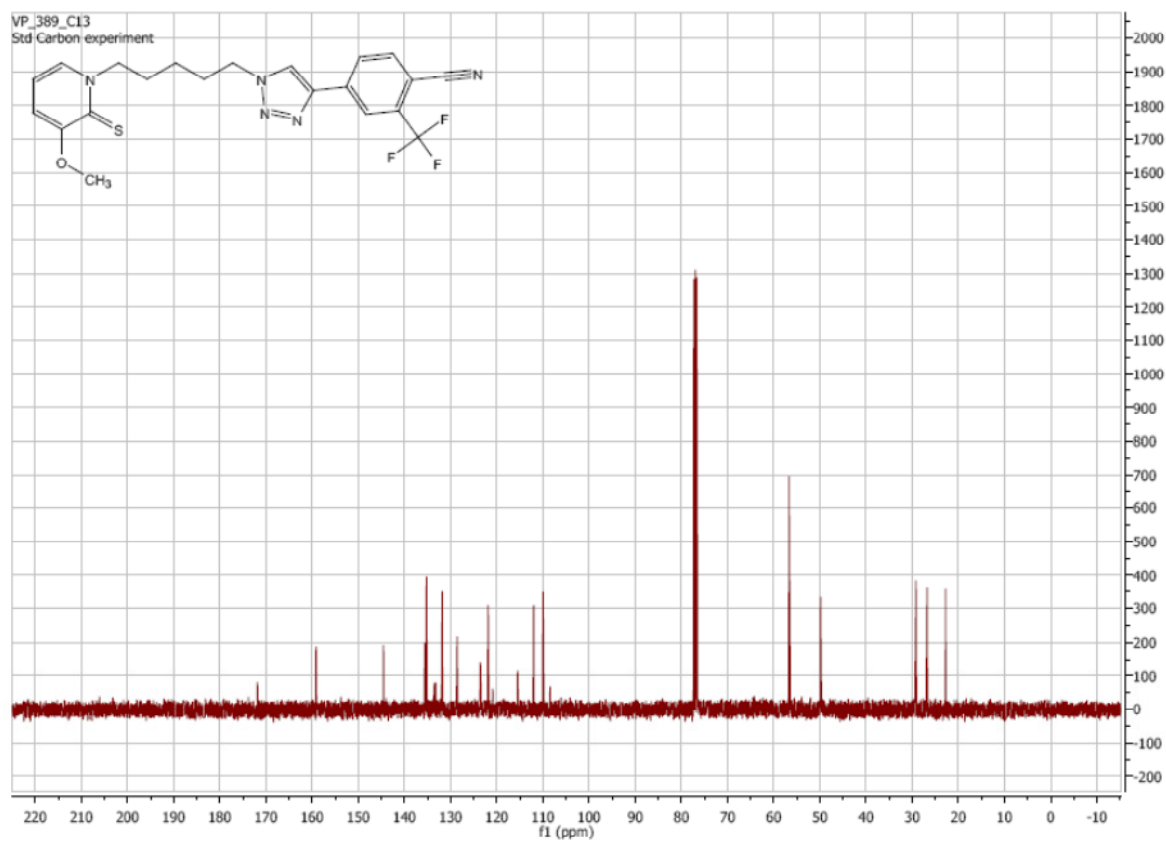
^{13}C NMR of **28f**:



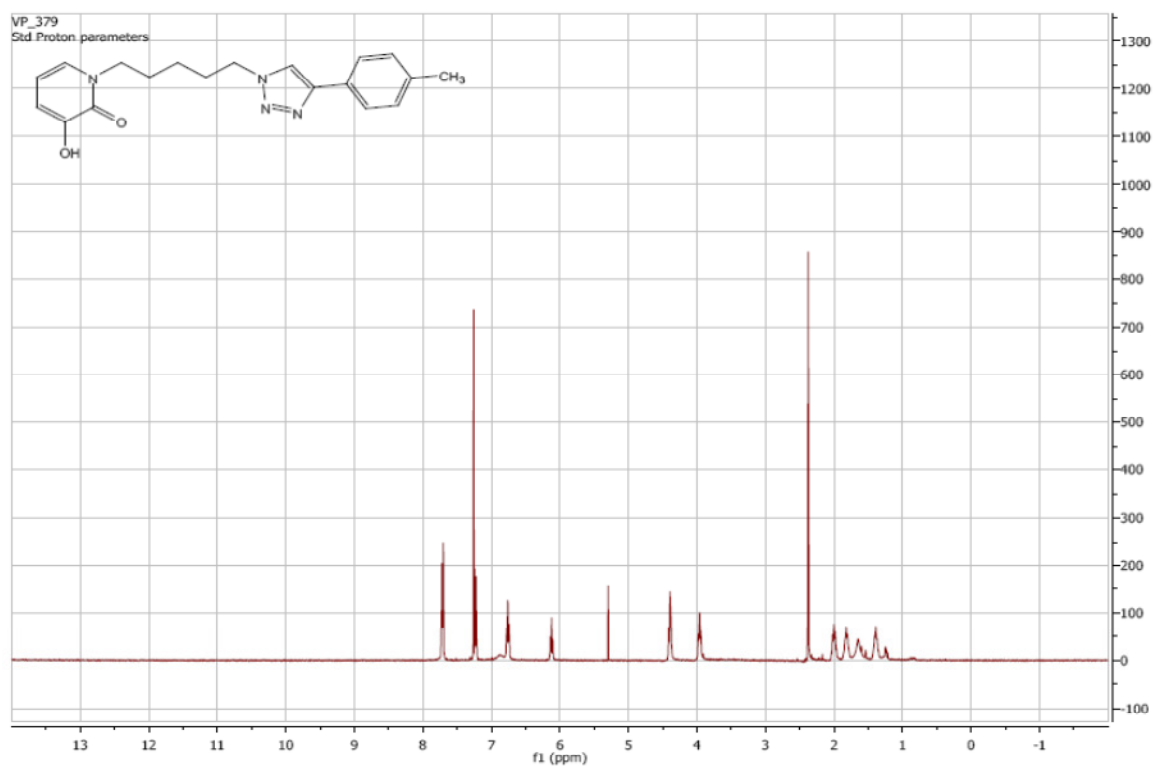
¹H NMR of **28g**:



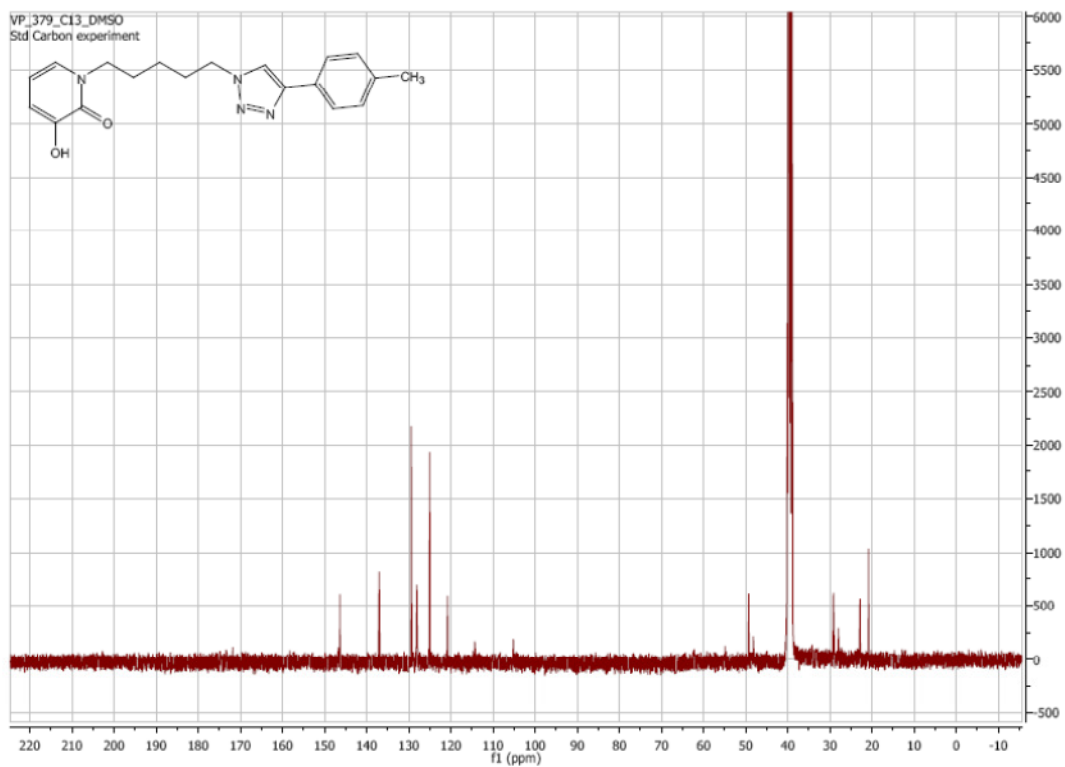
¹³C NMR of **28g**:



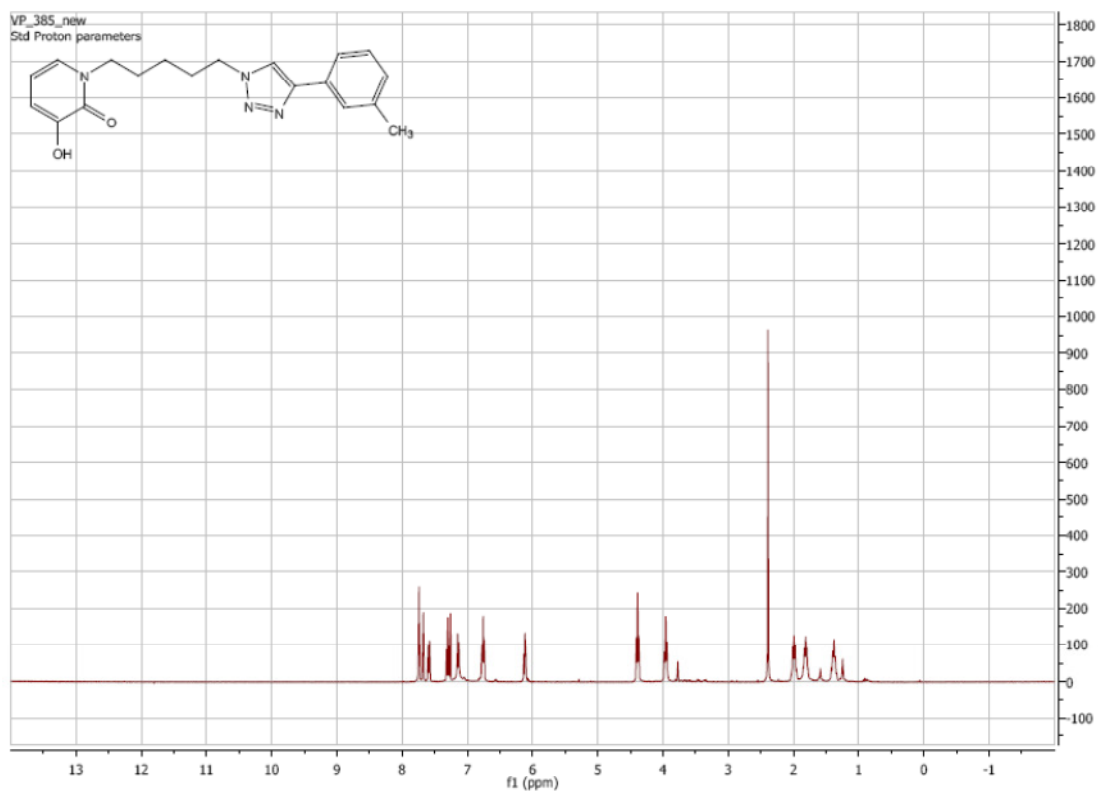
¹H NMR of **29a**:



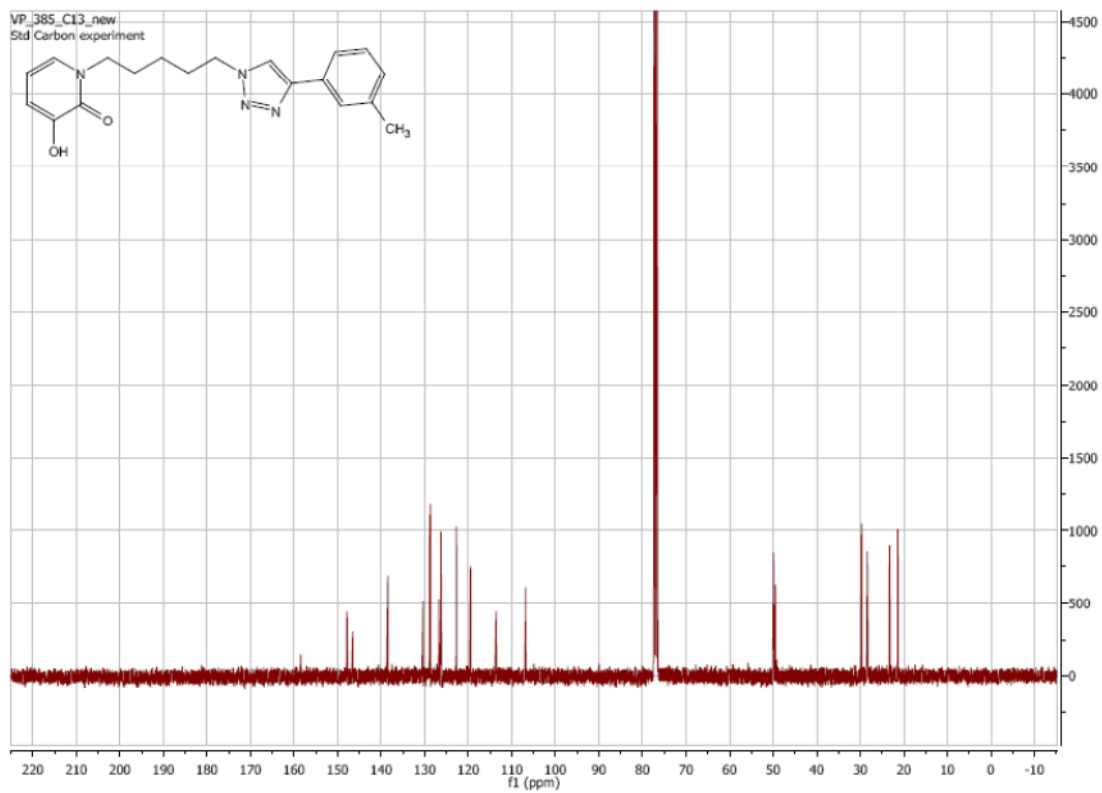
¹³C NMR of **29a**:



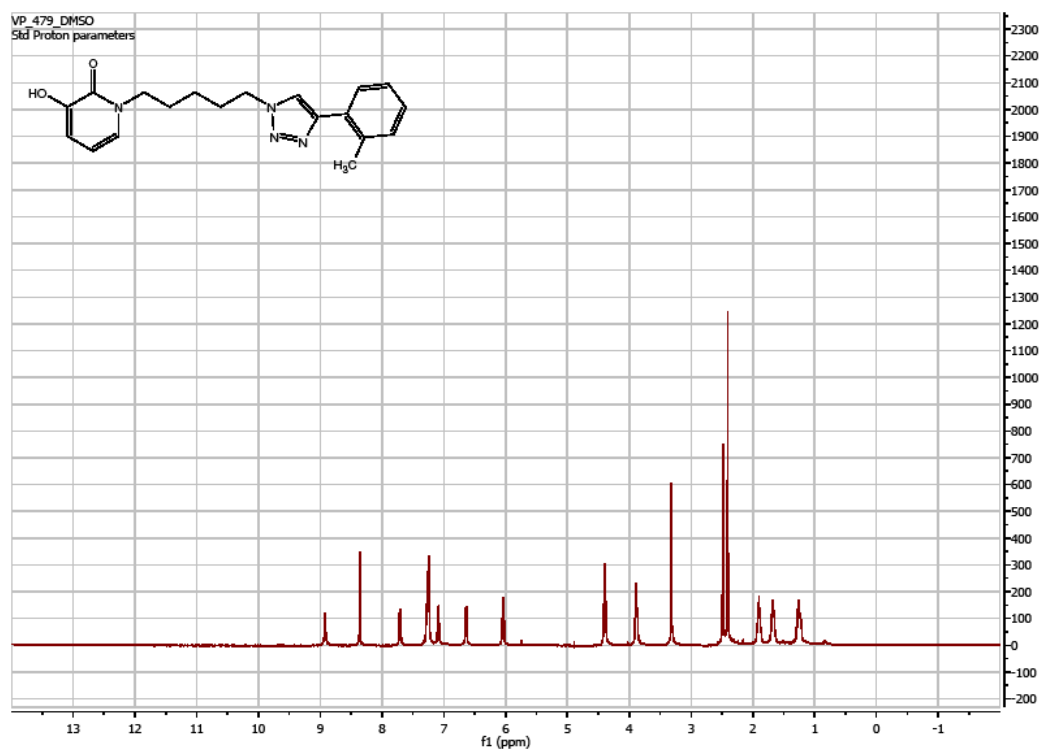
¹H NMR of **29b**:



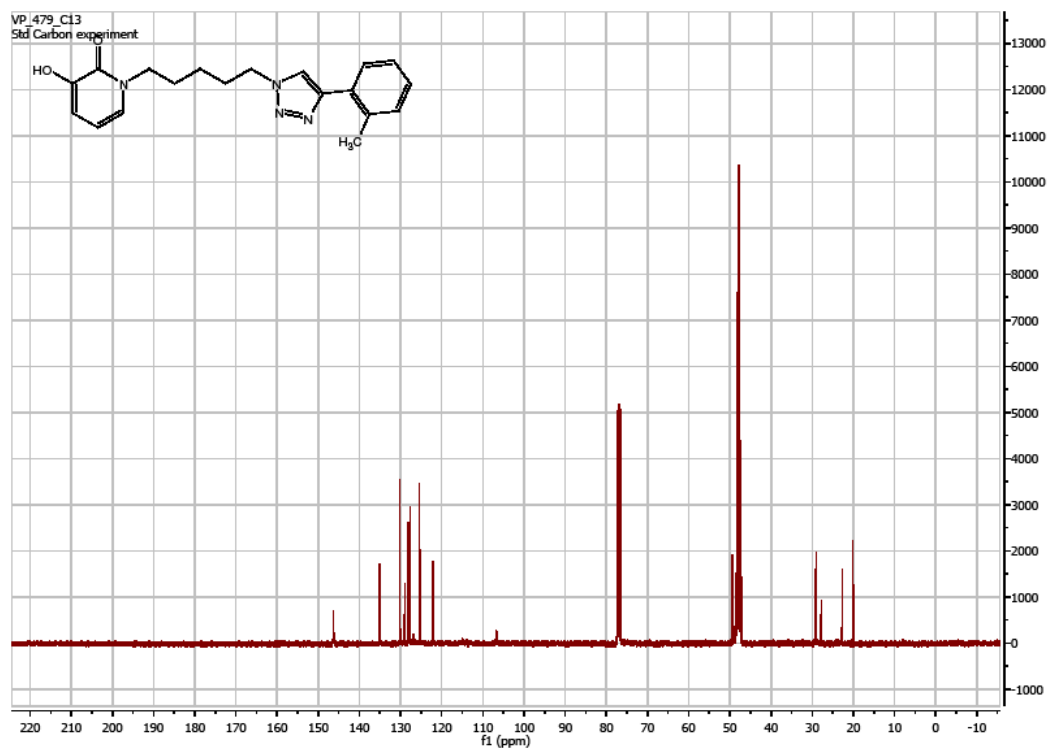
¹³C NMR of **29b**:



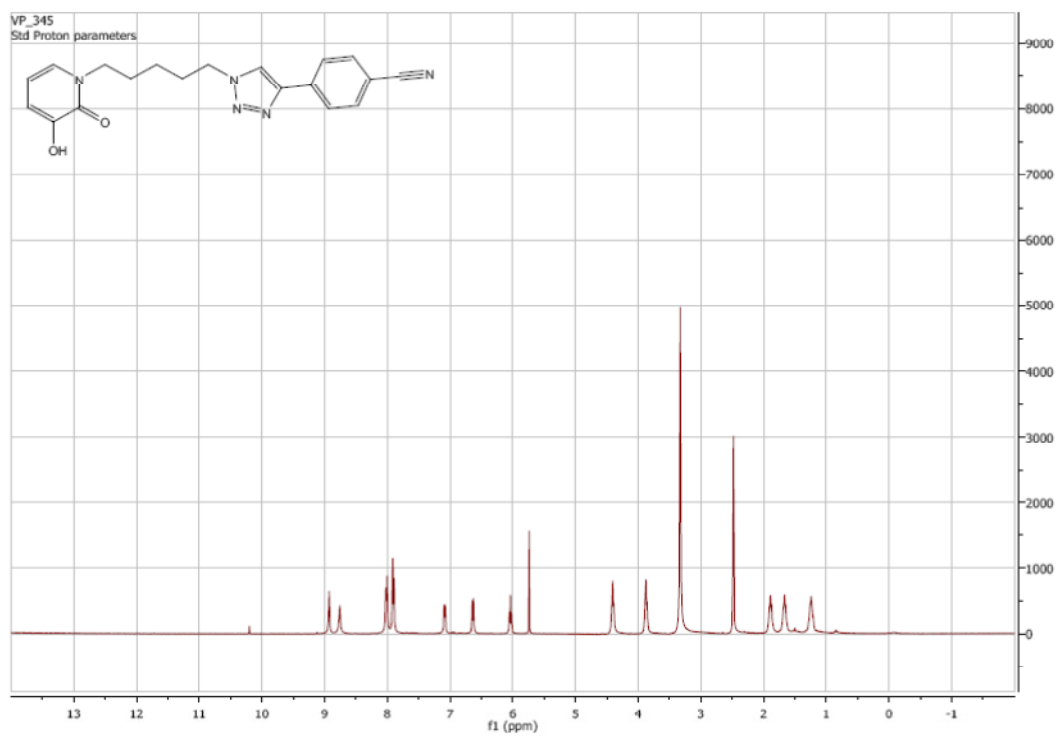
¹H NMR of **29c**:



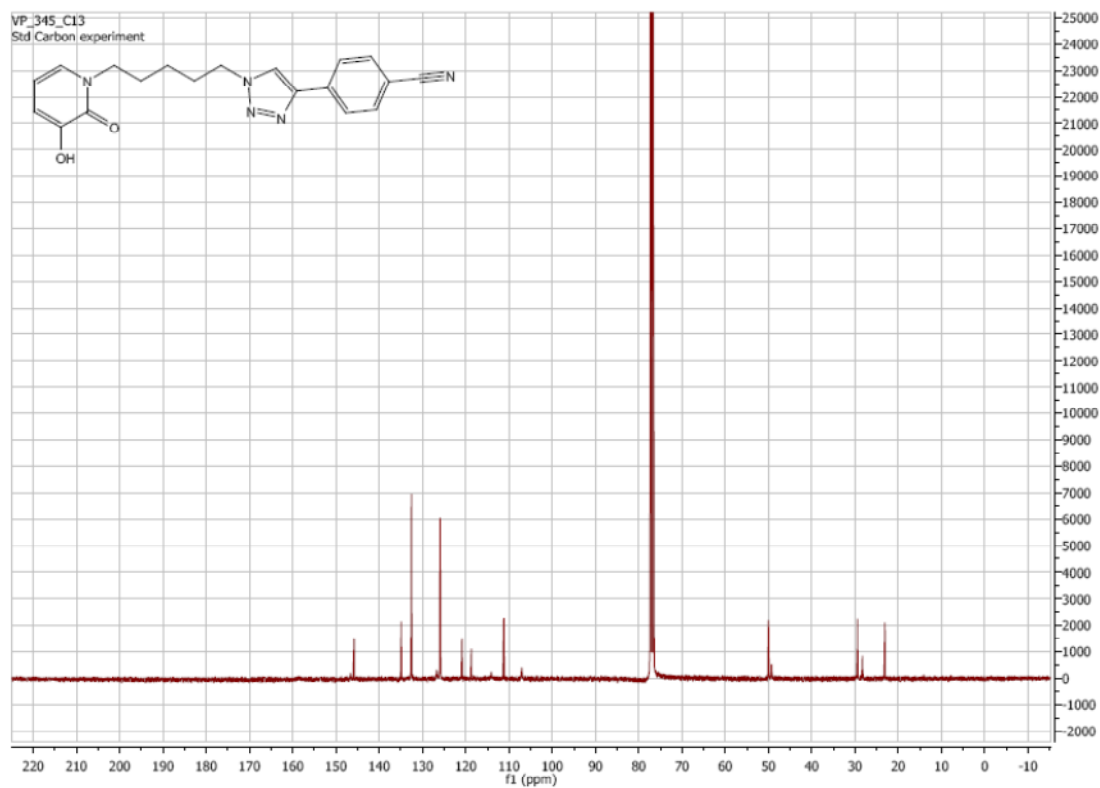
¹³C NMR of **29c**:



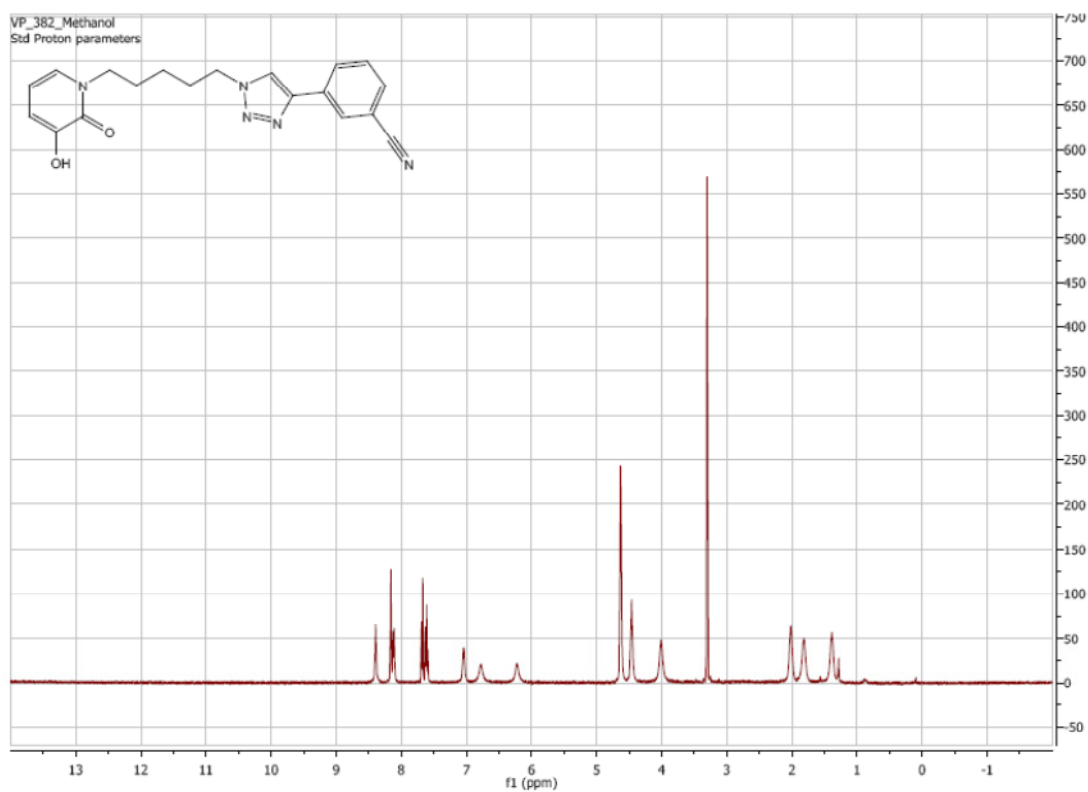
^1H NMR of **29d**:



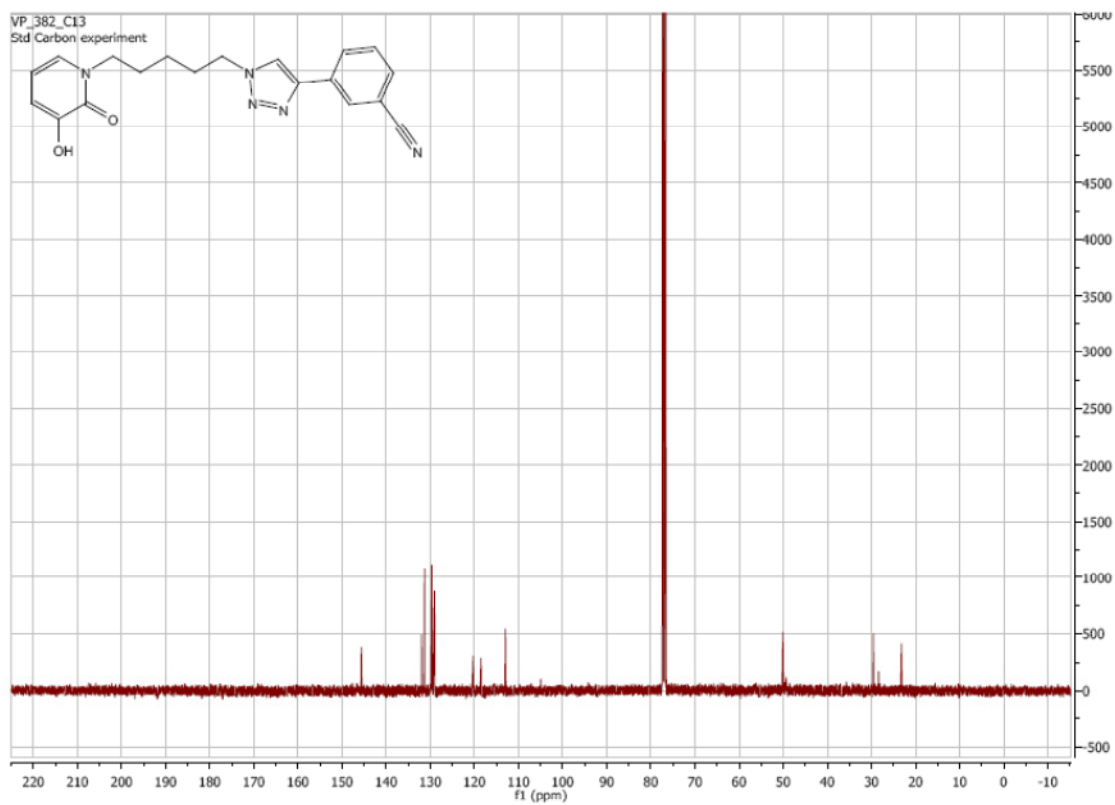
^{13}C NMR of **29d**:



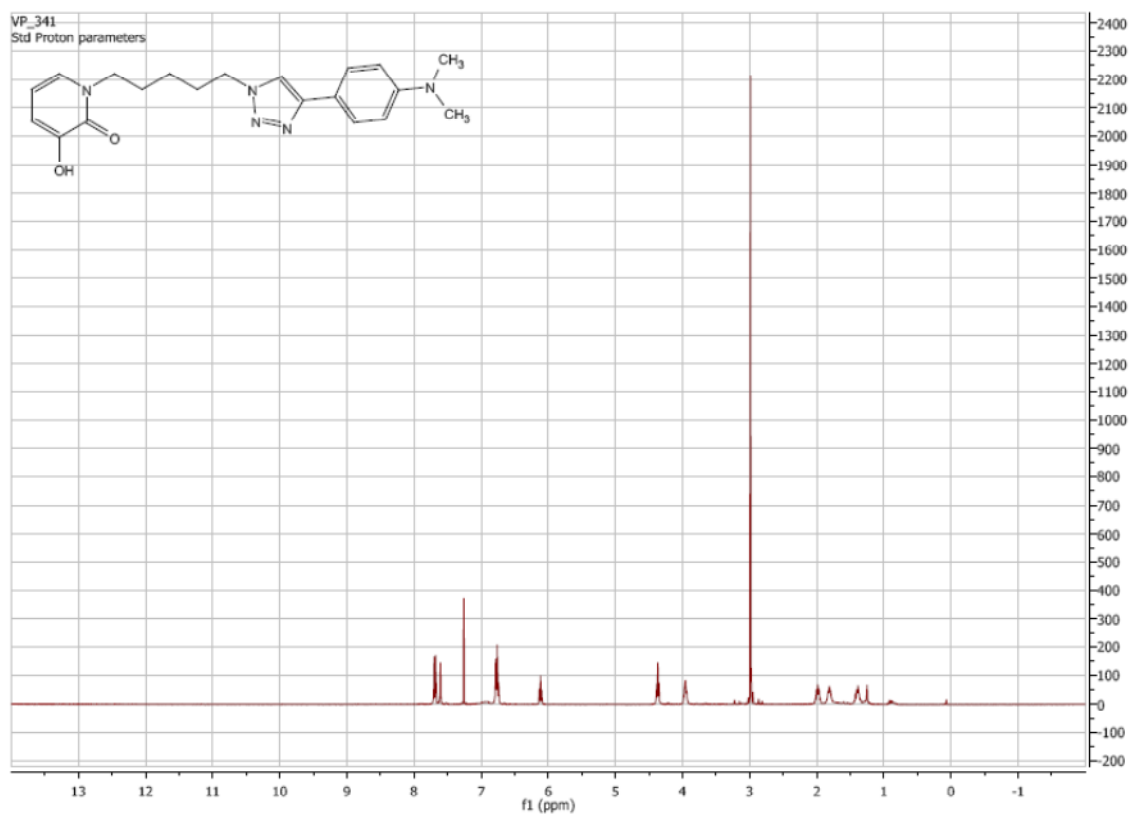
¹H NMR of **29e**:



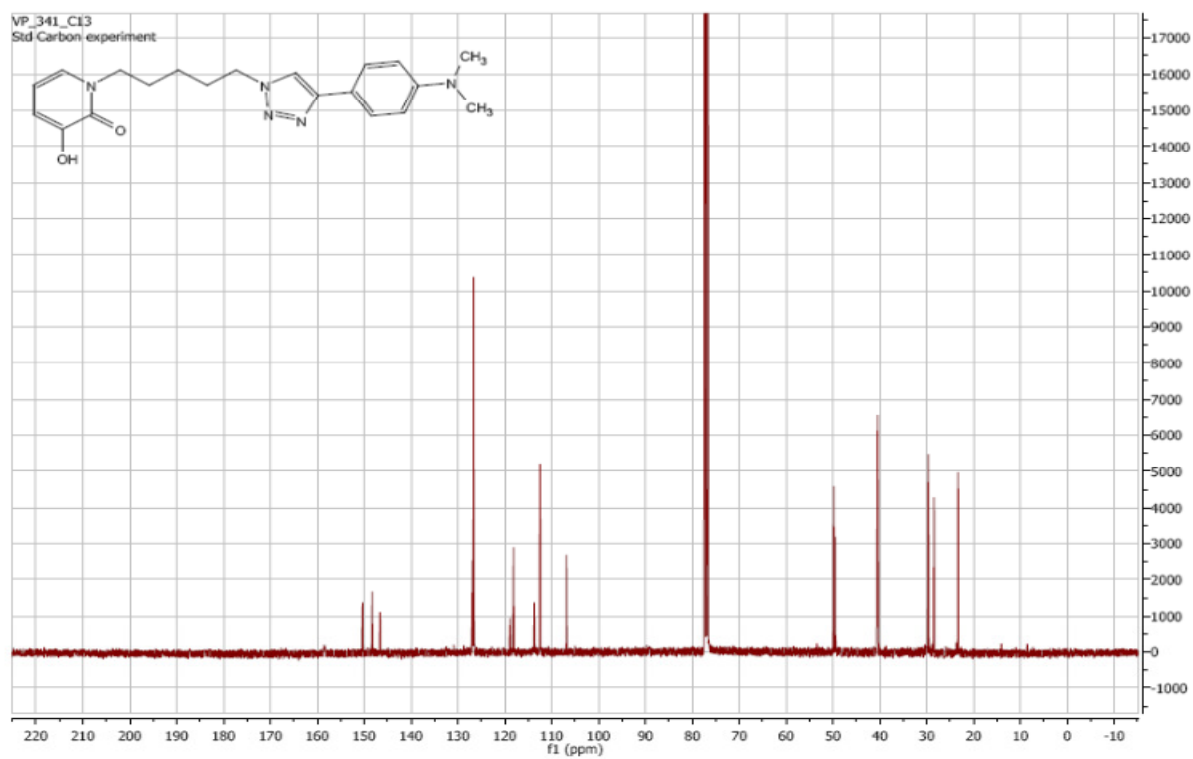
¹³C NMR of **29e**:

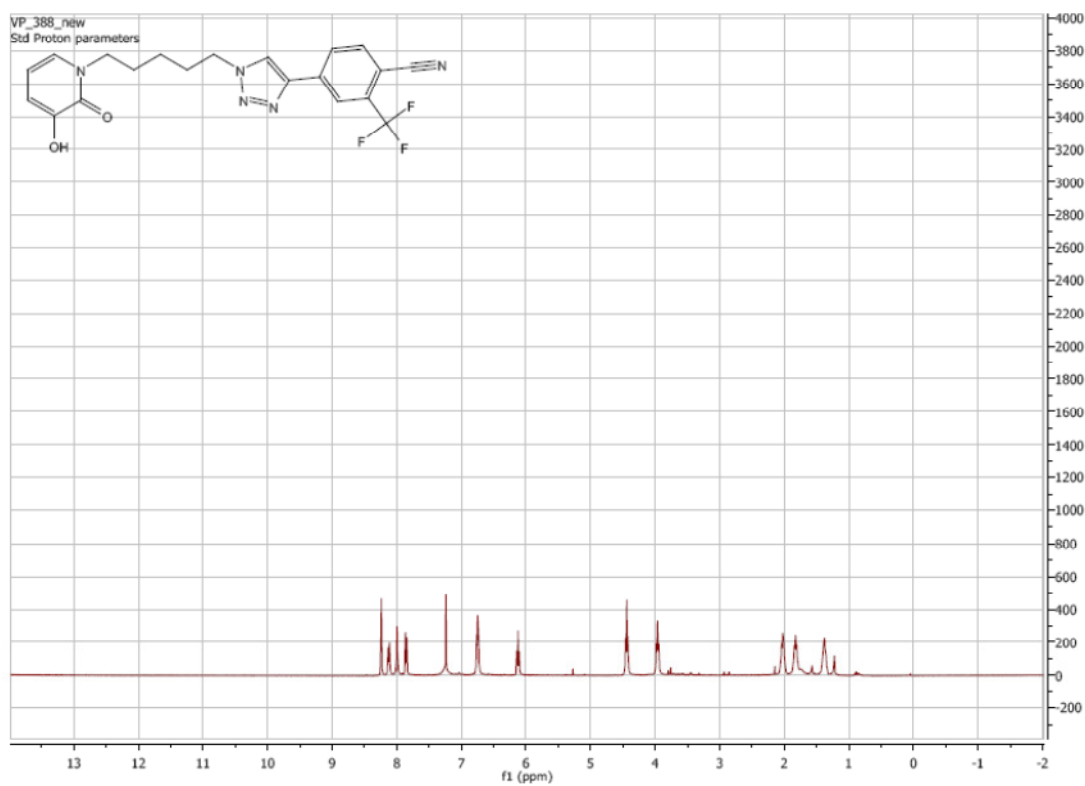
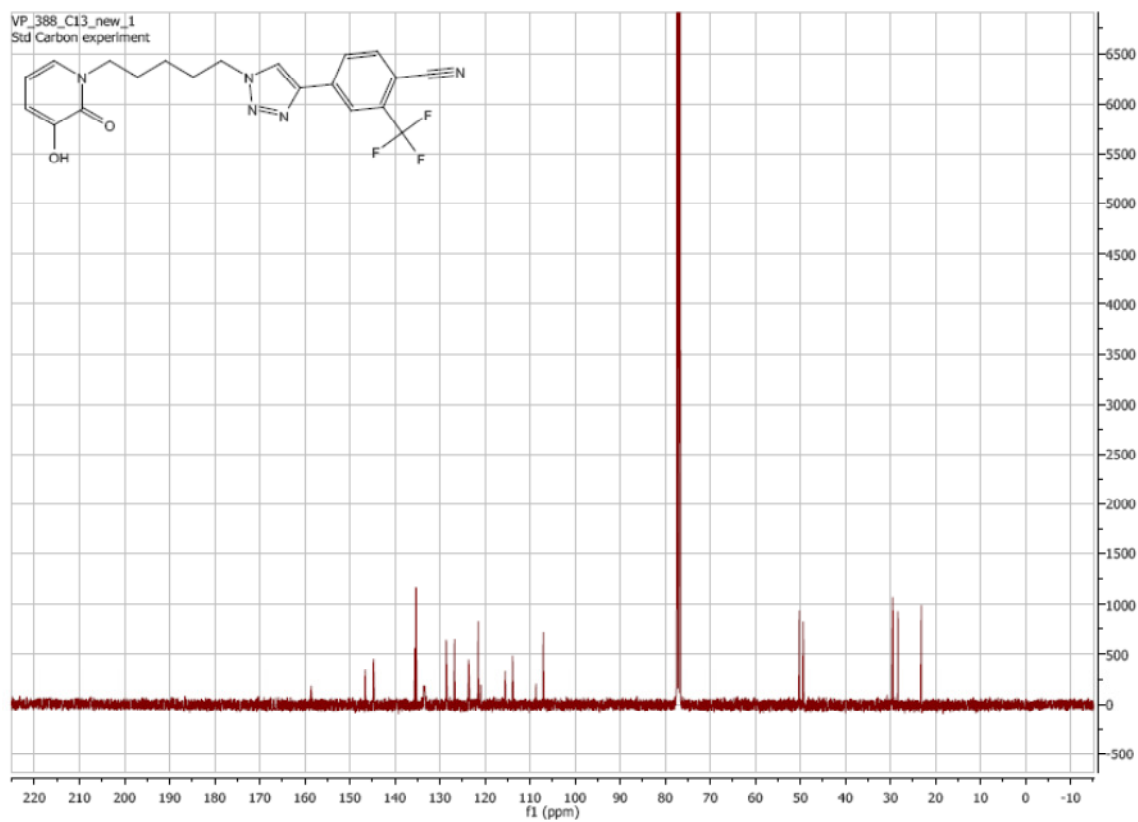


¹H NMR of **29f**:

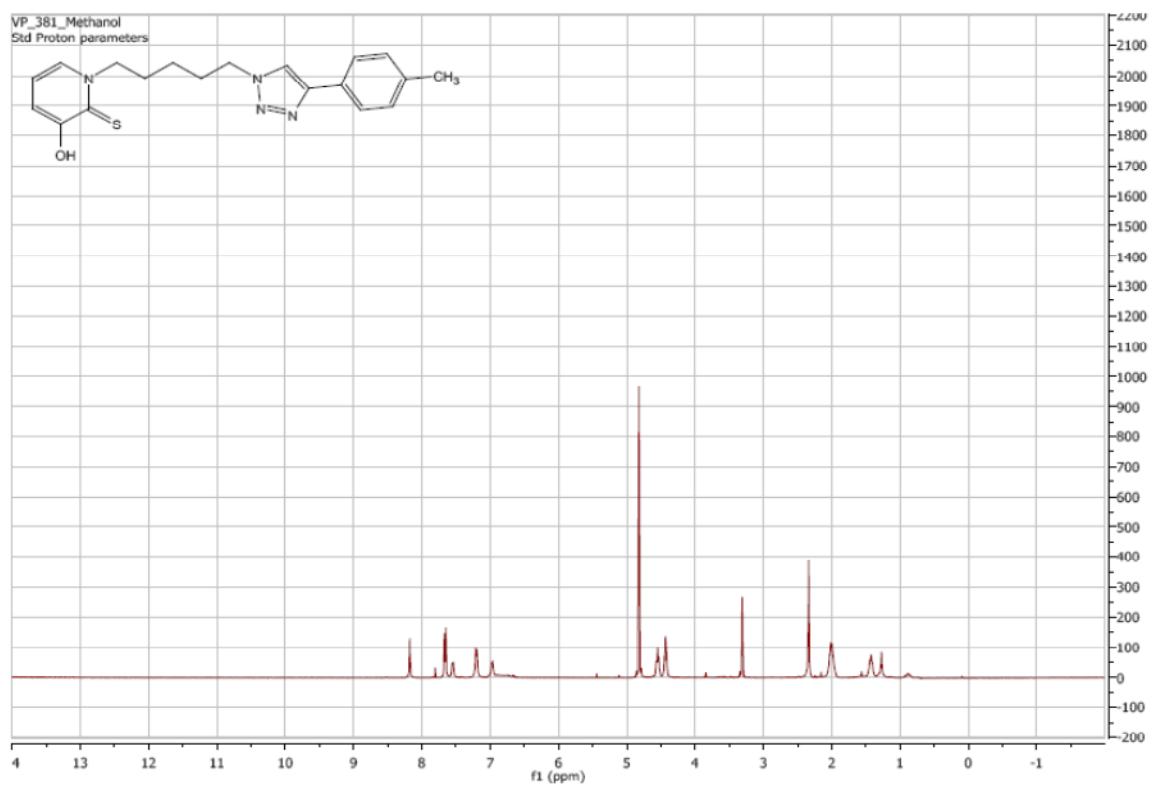


¹³C NMR of **29f**:

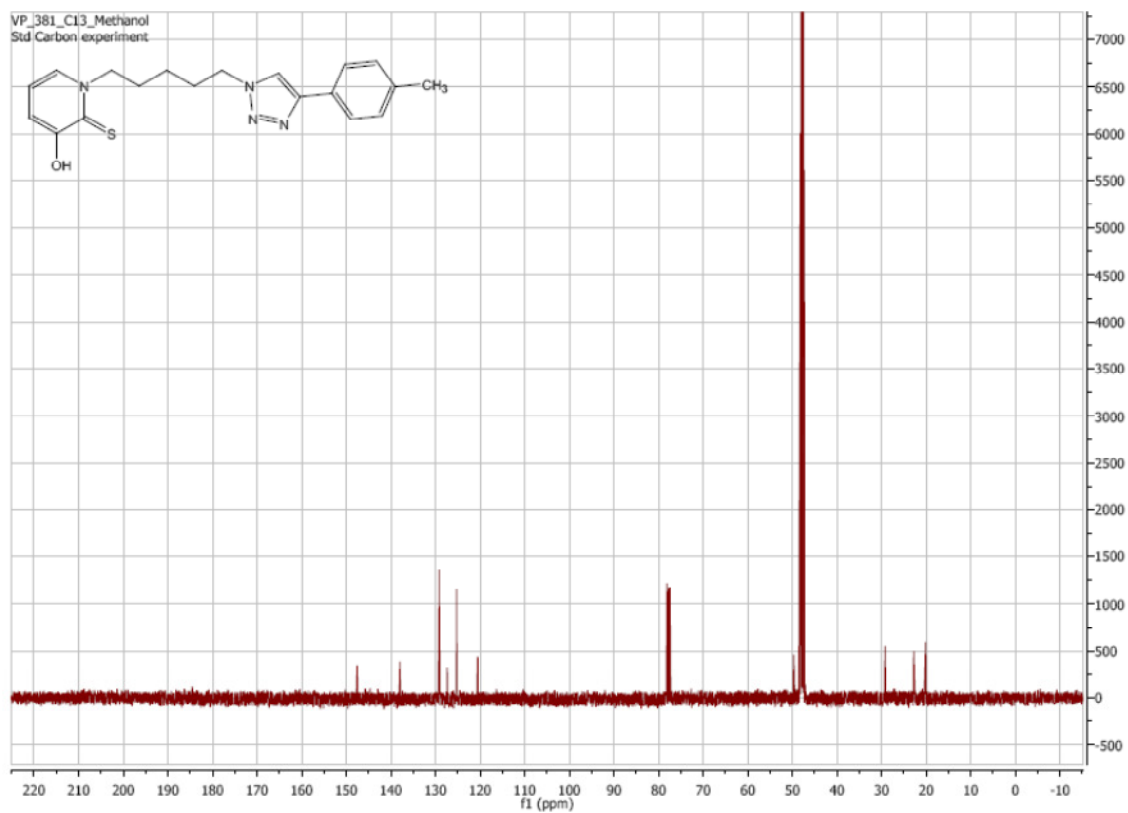


¹H NMR of **29g**: ^{13}C NMR of **29g**:

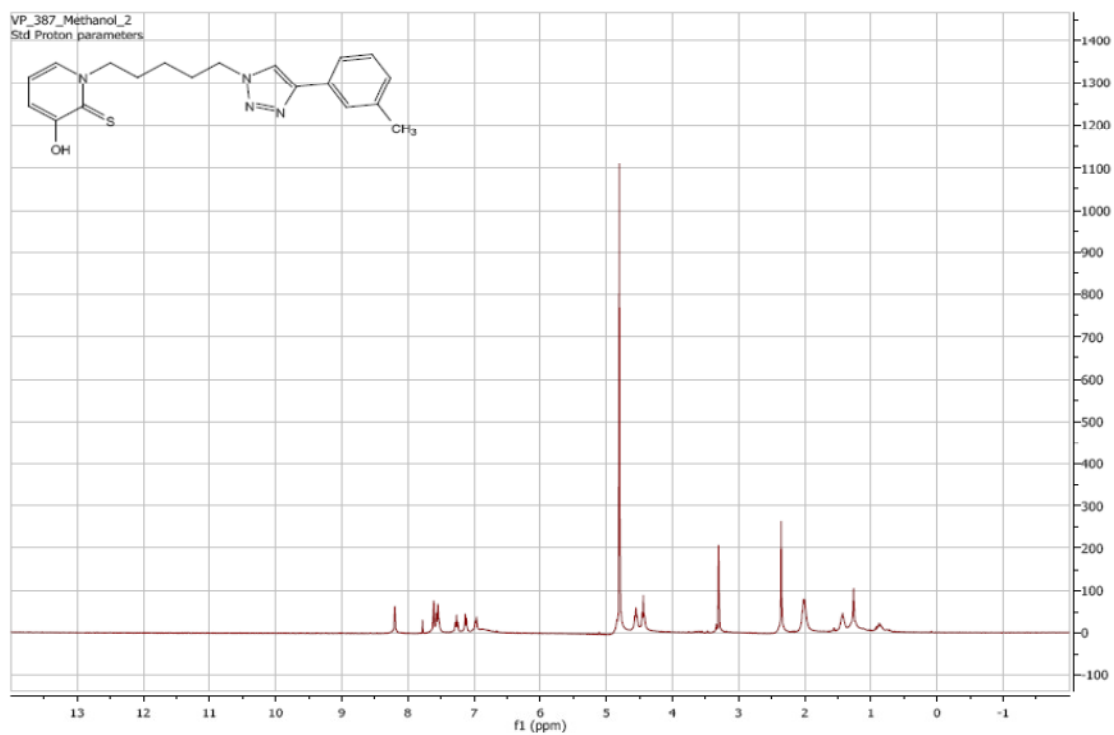
¹H NMR of **30a**:



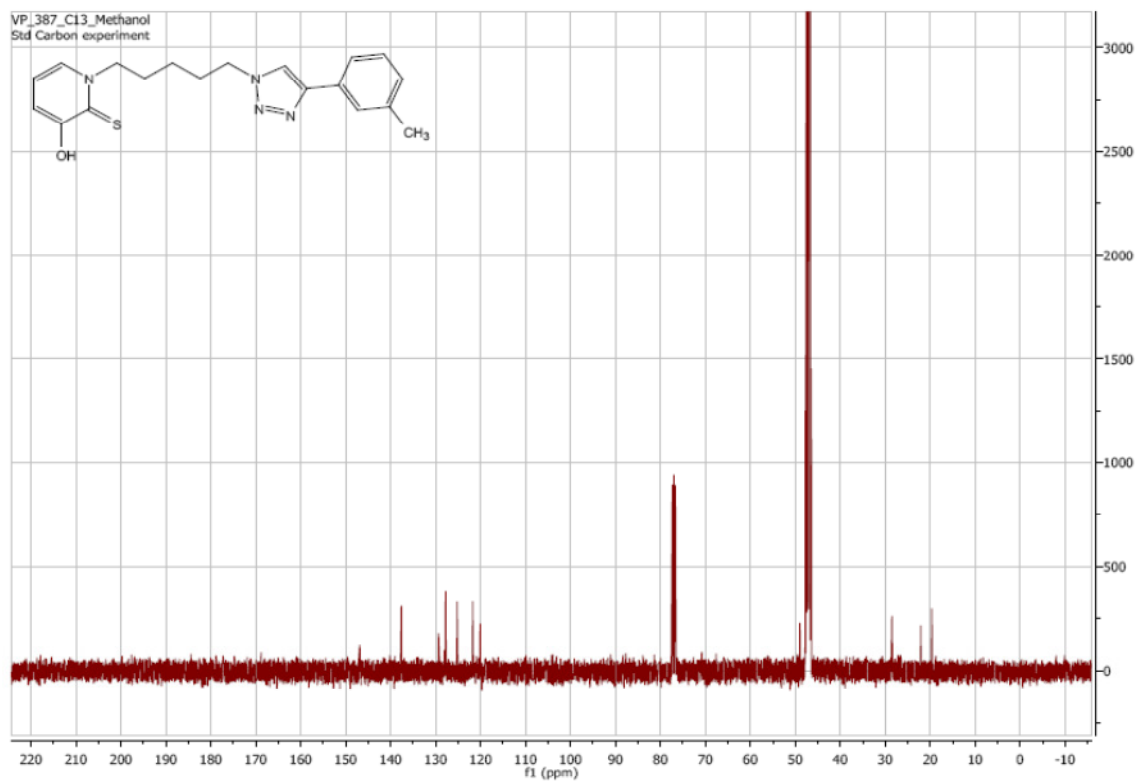
¹³C NMR of **30a**:



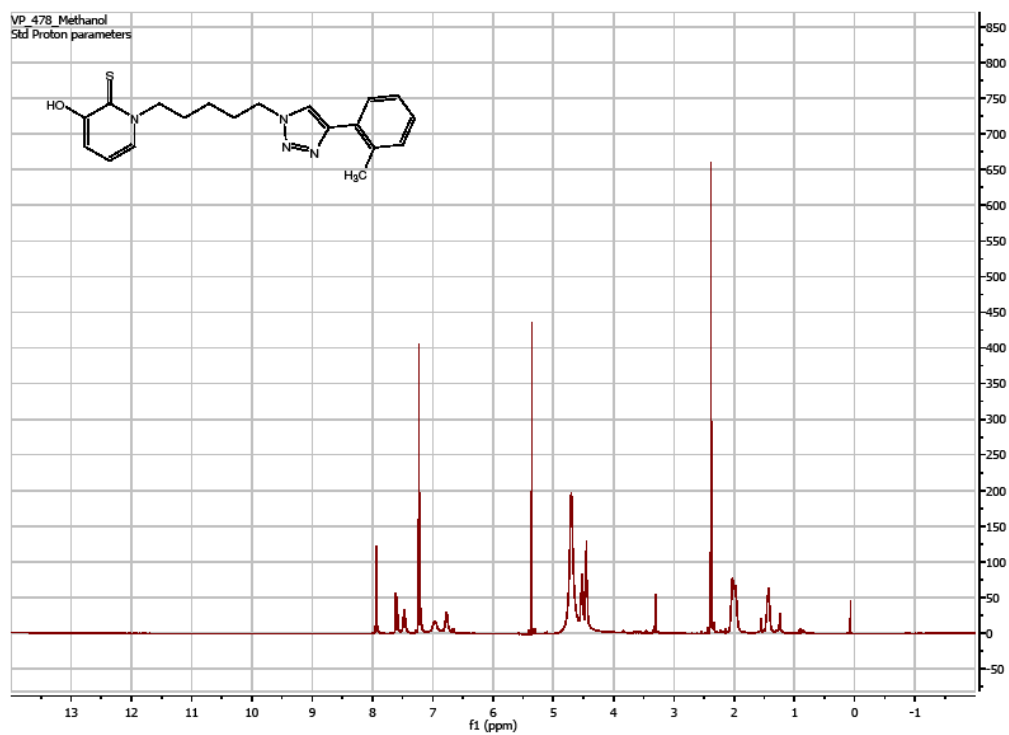
¹H NMR of **30b**:



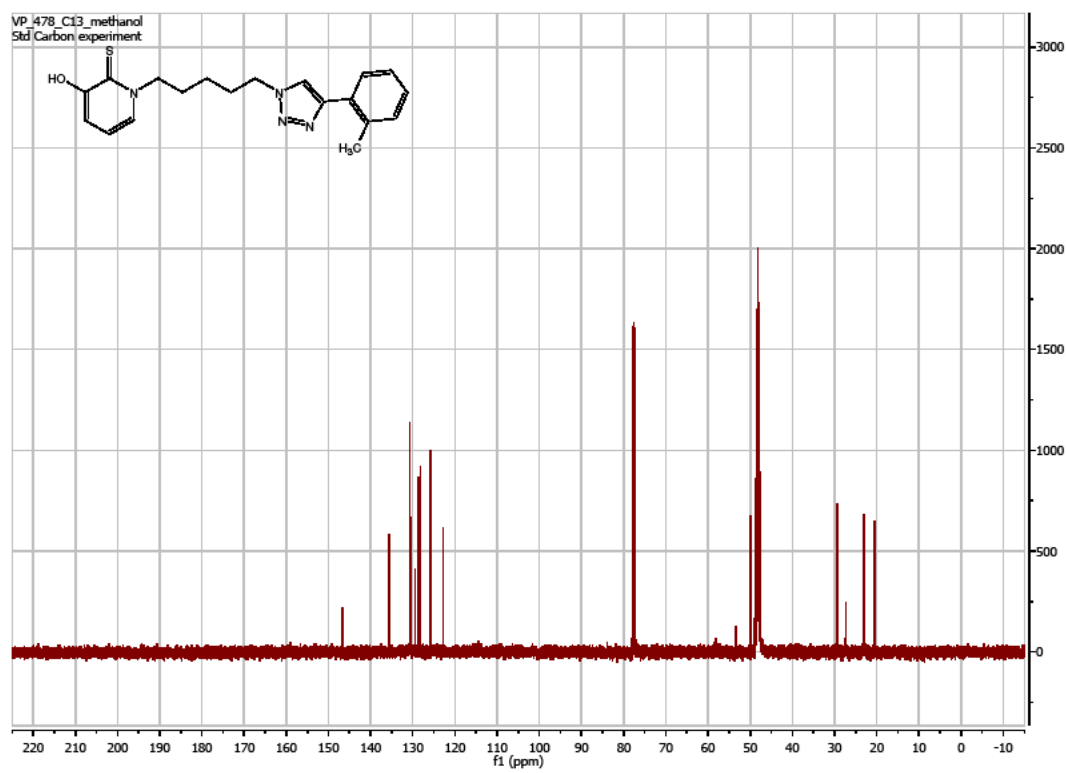
¹³C NMR of **30b**:



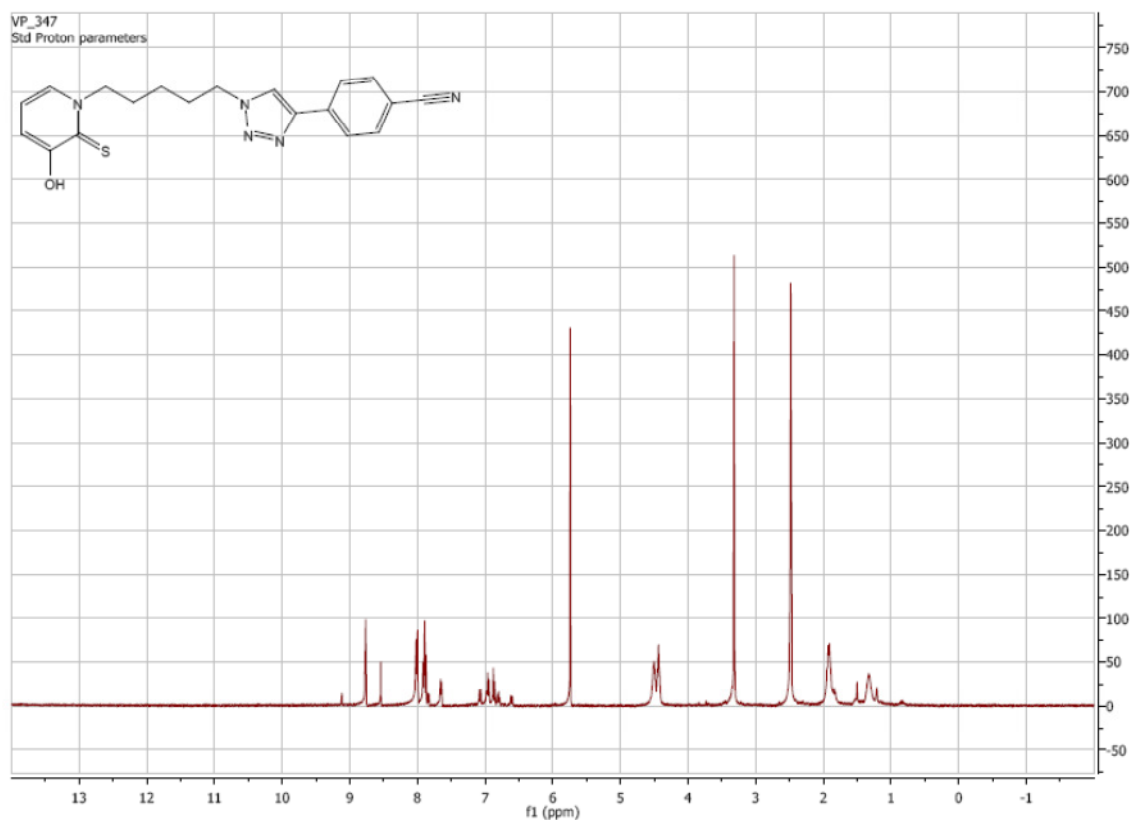
¹H NMR of **30c**:



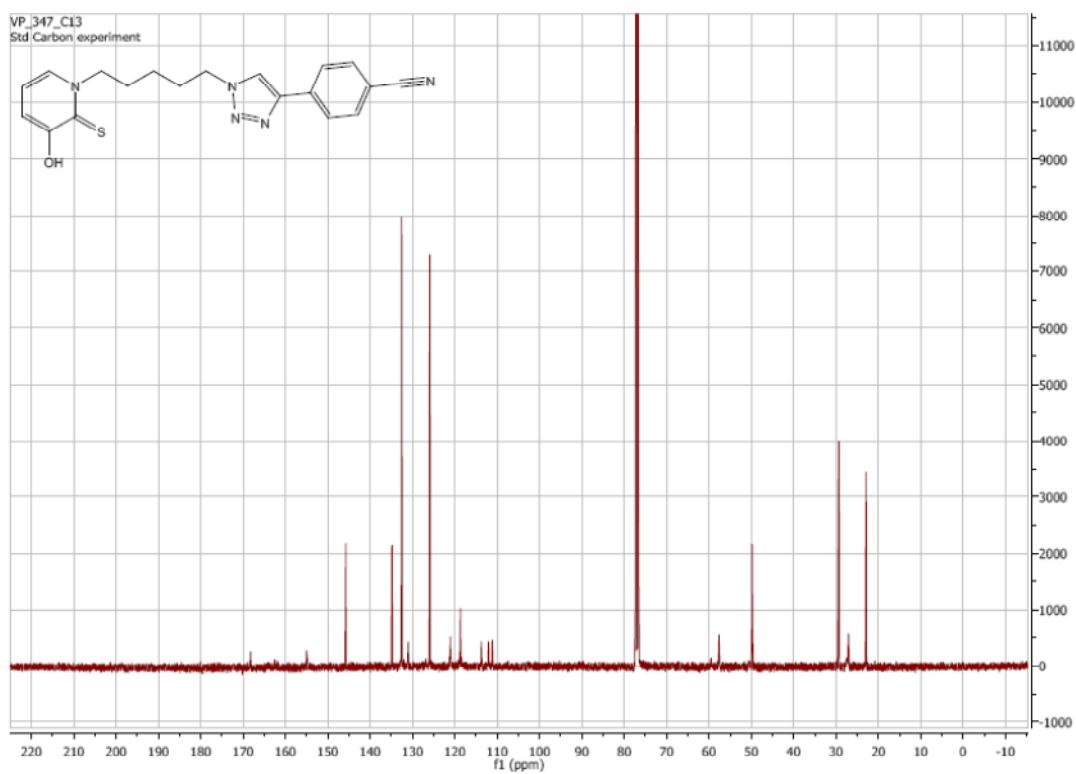
¹³C NMR of **30c**:



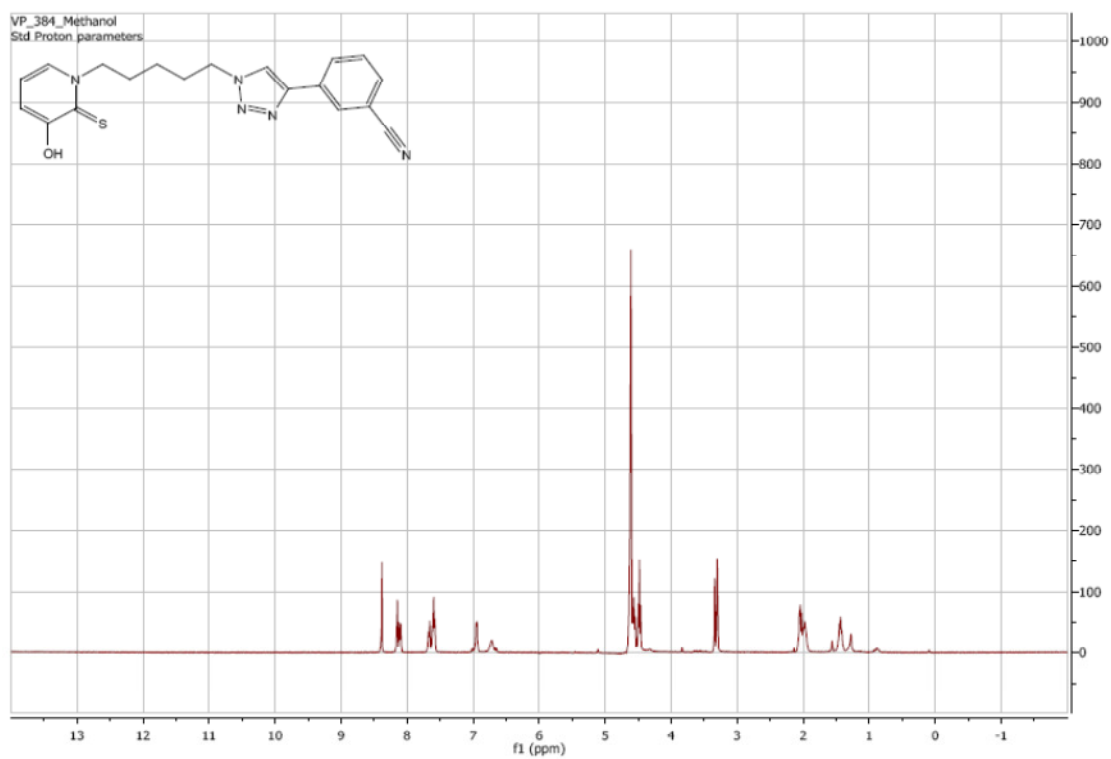
^1H NMR of **30d**:



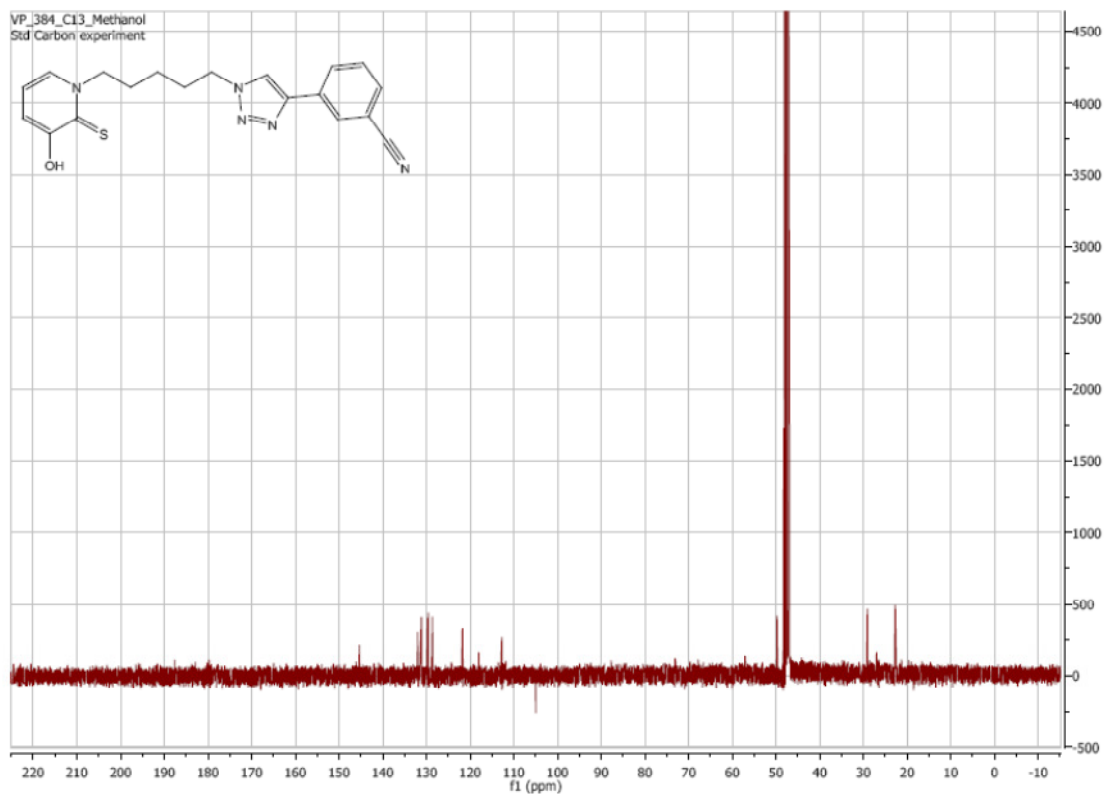
^{13}C NMR of **30d**:



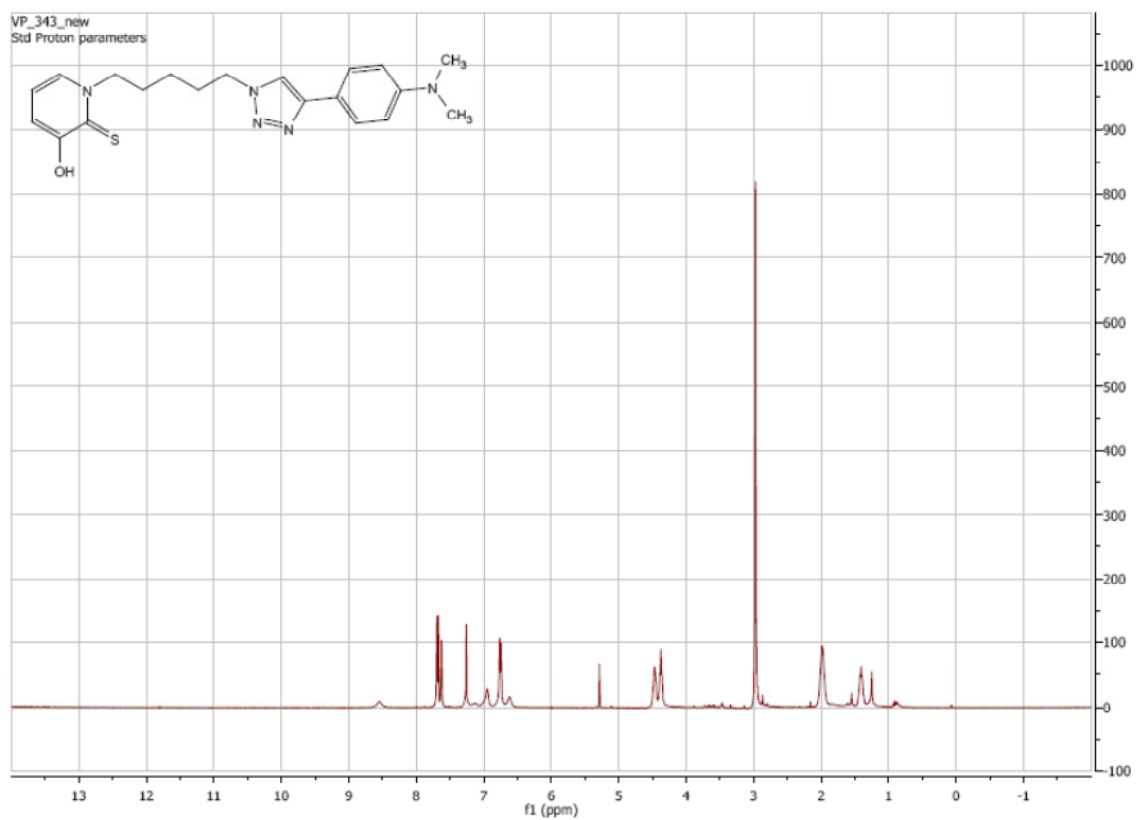
¹H NMR of **30e**:



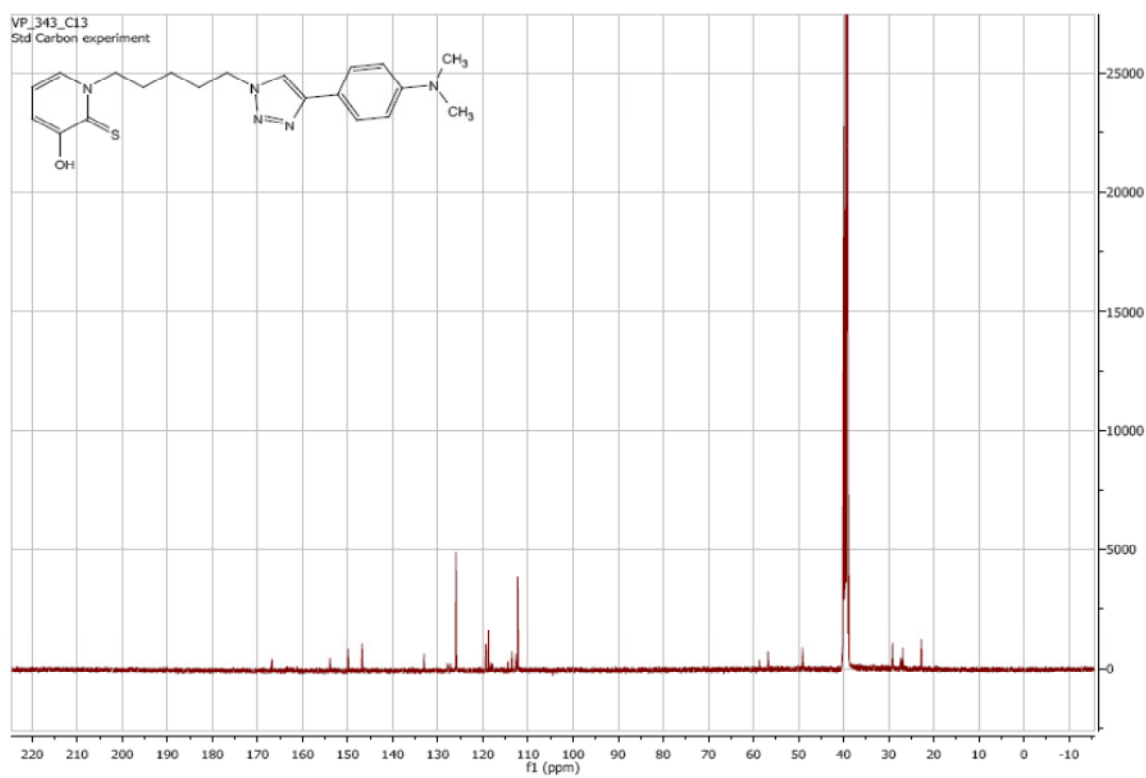
¹³C NMR of **30e**:



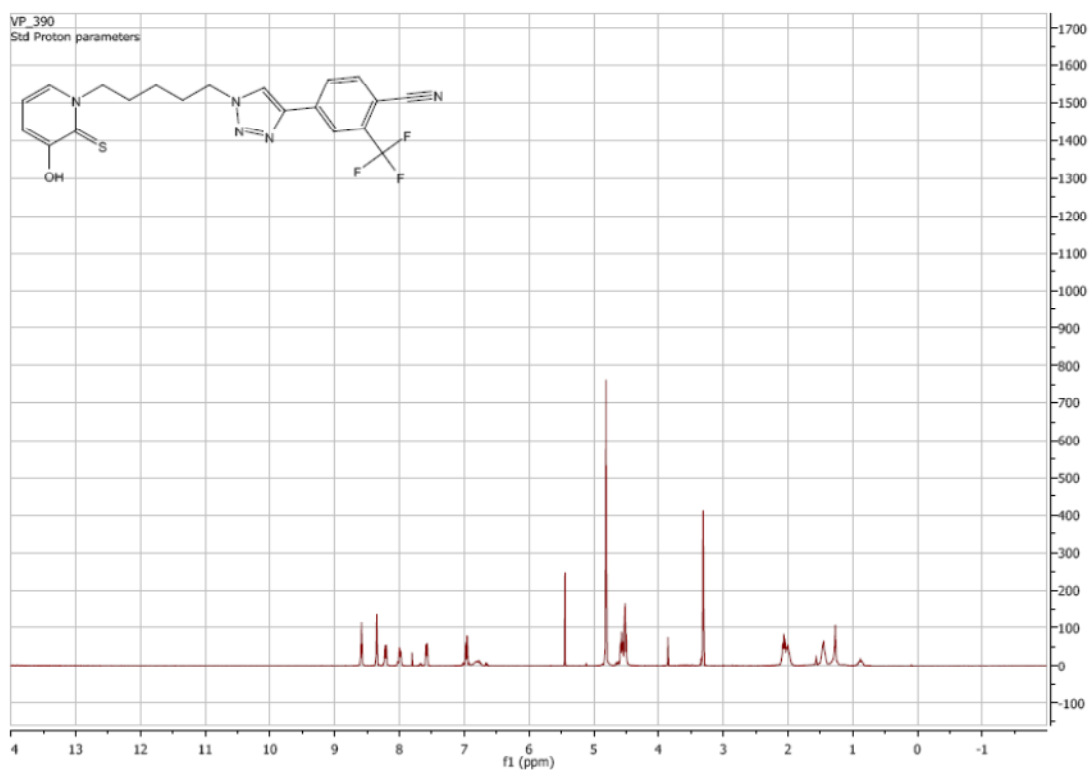
¹H NMR of **30f**:



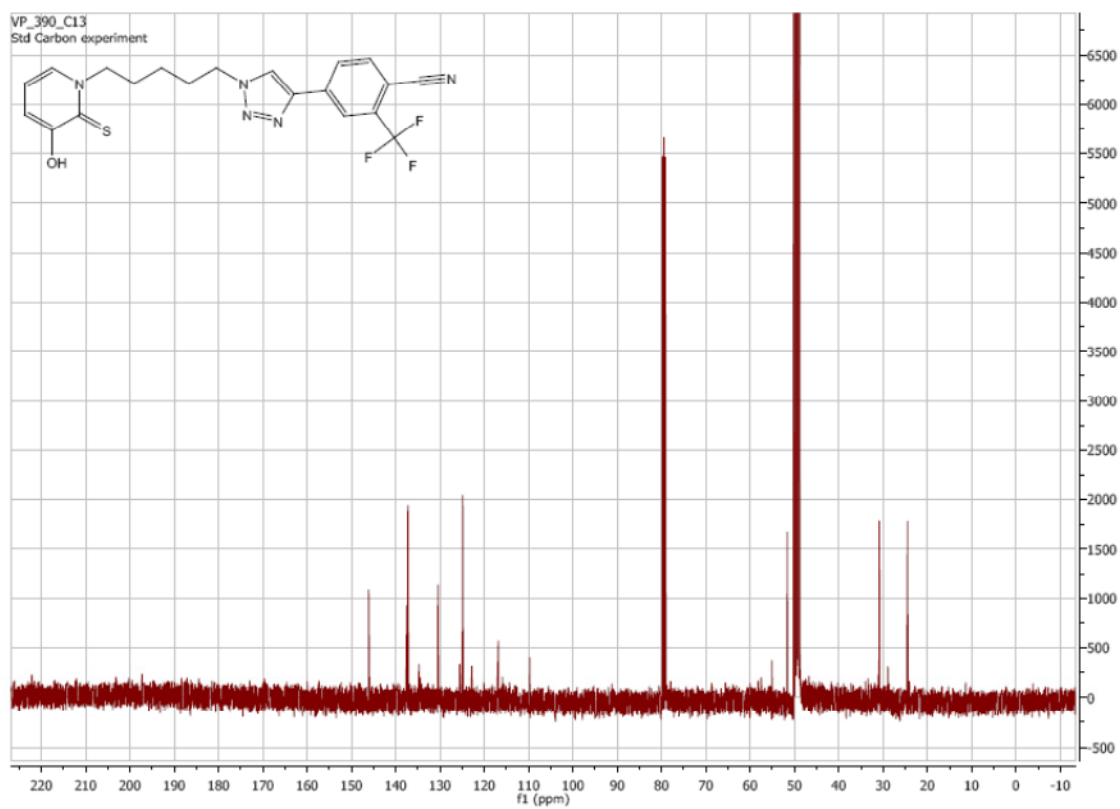
¹³C NMR of **30f**:



^1H NMR of **30g**:



^{13}C NMR of **30g**:



VITA

Vishal Patil

Vishal Patil was born in small town Takli (P.D.) near Chalisgaon, Maharashtra, India. He spent bulk of his childhood in Takli before moving to Mumbai, India to attend Institute of Chemical Technology, Mumbai to complete his undergraduate education. He earned his undergraduate degree in Chemical Technology in 2005. In January of 2006, Vishal joined Georgia Institute of Technology, Atlanta for his graduate studies. During his PhD, he worked on multiple projects involving drug design and synthesis. He received his Ph.D. in Organic Chemistry in August 2011 from Georgia Institute of Technology under the guidance of Dr. Adegboyega (Yomi) Oyelere.